INFORMATION TO USERS

This manuscript has been reproduced from the microfilm master. UMI films the text directly from the original or copy submitted. Thus, some thesis and dissertation copies are in typewriter face, while others may be from any type of computer printer.

The quality of this reproduction is dependent upon the quality of the copy submitted. Broken or indistinct print, colored or poor quality illustrations and photographs, print bleedthrough, substandard margins, and improper alignment can adversely affect reproduction.

In the unlikely event that the author did not send UMI a complete manuscript and there are missing pages, these will be noted. Also, if unauthorized copyright material had to be removed, a note will indicate the deletion.

Oversize materials (e.g., maps, drawings, charts) are reproduced by sectioning the original, beginning at the upper left-hand corner and continuing from left to right in equal sections with small overlaps.

Photographs included in the original manuscript have been reproduced xerographically in this copy. Higher quality 6" x 9" black and white photographic prints are available for any photographs or illustrations appearing in this copy for an additional charge. Contact UMI directly to order.

ProQuest Information and Learning
300 North Zeeb Road, Ann Arbor, MI 48106-1346 USA
800-521-0600

THE NEANDERTHAL PROBLEM:
3-D GEOMETRIC MORPHOMETRIC MODELS OF CRANIAL SHAPE VARIATION WITHIN AND AMONG SPECIES

by

KATERINA HARVATI

A dissertation submitted to the Graduate Faculty in Anthropology in partial fulfillment of the requirements for the degree of Doctor of Philosophy,
The City University of New York

2001

This manuscript has been read and accepted for the Graduate Faculty in Anthropology in satisfaction of the dissertation requirement for the degree of Doctor of Philosophy.

6/25/01 — Eric Delson

Date — Chair of Examining Committee: Eric Delson

6/26/01 — Louise D Lennihan

Date — Executive Officer: Louise Lennihan

Supervisory Committee:

Leslie F. Marcus

Ian Tattersall

Michelle Singleton

THE CITY UNIVERSITY OF NEW YORK

Abstract

THE NEANDERTHAL PROBLEM:
3-D GEOMETRIC MORPHOMETRIC MODELS OF CRANIAL SHAPE VARIATION WITHIN AND AMONG SPECIES

by

KATERINA HARVATI

Adviser: Professor Eric Delson

The taxonomic position of Neanderthals as a separate species or subspecies of *H. sapiens* is a matter of wide disagreement and has implications for modern human origins. Both morphological and genetic evidence suggest a wide separation between Neanderthals and modern humans. However, the interpretation of the genetic data has been questioned, while several authors see evidence for continuity or interbreeding between Neanderthals and Upper Paleolithic Europeans. The objectives of this study include: a) the quantitative evaluation of Neanderthal features which are usually described qualitatively, achieved with the use of geometric morphometrics; and b) the development of models of both intra- and inter-specific variation, to be applied to a comparison between Neanderthals and modern humans, in order to clarify the Neanderthal taxonomic position. Two such models were developed, based on modern human populations and on chimpanzee species and subspecies.

Geometric morphometrics enables the quantification of features that are difficult to measure with traditional caliper measurements. Landmarks were digitized on the temporal and occipital bone, and ridge curves along the posterior cranial profile. The data were processed using Generalized Procrustes Analysis, and the fitted coordinates were analyzed using multivariate statistical methods, including Principal Components, Canonical Variates and Discriminant Function analyses.

The temporal bone landmarks separate Neanderthals from modern humans most strongly. Some overlap exists in the posterior cranial profile, and extensive overlap is observed in the occipital bone landmarks. Neanderthals are consistently more distant from modern humans than the two chimpanzee species or subspecies, or any two recent human populations, are from each other. No morphological affinities were detected between Neanderthals and Upper Paleolithic Europeans. The latter are often quite distant from recent populations, probably due to high levels of cranial robusticity, but also very distant from Neanderthals. Limited similarities were found between Neanderthals and individual Central European Upper Paleolithic specimens. The Qafzeh/Skhul specimens are very distant from both Neanderthals and modern humans, probably due to retentions of primitive characters.

These findings support the hypothesis that Neanderthals represent a separate species from modern humans, although not unequivocally. Further investigation of the position of the Upper Paleolithic and Skhul/Qafzeh specimens is warranted.

Στους Γονεις μου

ACKNOWLEDGEMENTS

I thank the members of my dissertation committee, Professor Eric Delson, Professor Leslie Marcus, Dr. Ian Tattersall and Dr. Michelle Singleton for their input and advice during the writing of this thesis. Their comments and suggestions have added greatly to the value of this manuscript.

Professor Eric Delson, my curriculum and dissertation supervisor, greatly supported this project both during both the research and the writing stages. Furthermore, I thank Dr. Delson for his invaluable support and guidance throughout the course of my graduate studies, without which this research would not have been possible.

Professor Leslie Marcus was instrumental in providing insightful advice on statistics and geometric morphometrics that only he could provide. Any errors that may remain are entirely my own. Dr. Ian Tattersall kindly provided access to the skeletal and cast collection of the Anthropology Department of the American Museum of Natural History, as well as his invaluable perspective on the pattern of human evolution. Dr. Michelle Singleton provided much-needed and extensive help during data analysis and early writing stages. Her help is greatly appreciated.

In addition to my dissertation committee members, several people were instrumental in developing the ideas that led to this project: Dr. William Howells, who graciously provided his notes; Dr. Frederick Szalay and Dr.Timothy Bromage, who also guided me through the early years of my graduate career; and Dr. William Kimbel and Dr. Yoel Rak, who advised me extensively during the early stages of this research.

I also owe gratitude to David Reddy, whose help with the arduous data processing and analysis was indispensable, and whose good spirits and gentle personality helped me through many a crisis throughout the last year and a half.

I thank the curators of several institutions, who kindly allowed me to study the fossil and recent collections in their care. Without their help this study would not have been possible: Dr. Chris Stringer, Dr. Louise Humphry and Rob Kruszynski, British Museum (Natural History), London; Dr. Yoel Rak, University of Tel Aviv; Dr. George Koufos, Aristotle University of Thessaloniki; Dr. Jakov Radovcic, Croatian Museum of Natural History, Zagreb; Dr. Henry de Lumley, Dr. Marie-Antoinette de Lumley and Dr. Dominique Grimaud-Hervé, Institut de Paléolontologie Humaine, Paris; Dr. Gabriella

Spedini and Dr. Giorgio Manzi, Università La Sapienza, Rome; Dr. Roberto Macchiarelli and Dr. Luca Bondioli, Museo Pigorini, Rome; Dr. Patrick Semal, Institut Royale des Sciences Naturelles, Brussels; Dr. Reinhard Ziegler, Staatliches Museum für Naturkunde, Stuttgart; Dr. Maria Teschler, Naturhistorisches Museum, Vienna; Dr. André Langaney and Mario Chech, Musée de l'Homme, Paris; Dr. Horst Seidler and Dr. Sylvia Kirchengast, Uiversity of Vienna; Dr. Niels Lynnerup, University of Copenhagen; Dr. Wim van Neer, Royal Museum of Central Africa, Tervuren; Dr. Ross MacPhee, Department of Mammalogy , American Museum of Natural History, New York; Dr. Ian Tattersall, Gary Sawyer and Ken Mowbray, Department of Anthropology, American Museum of Natural History, New York. I also thank Dr. J. J. Hublin, who rescued my research in Paris at a crucial moment by lending me his laboratory's microscribe.

I would like to acknowledge here the help, guidance, knowledge and inspiration offered me throughout the years of my graduate studies by the CUNY and the NYCEP faculty. Thank you. Special thanks also go to all my colleagues and friends at NYCEP and elsewhere who provided moral and material support in the course of this project, and especially to Steven Frost, John Krigbaum, Eric Sargis, Larissa Swedell, Hartley Odwak, Bessie Skoures, and Mike Harvatis.

This research was supported by several institutions in its various stages: by a National Science Foundation Dissertation Improvement Grant, an American Museum of Natural History predoctoral fellowship, an Onassis Foundation predoctoral fellowship, and a CUNY/NYCEP dissertation write-up fellowship. A small grant was also awarded by the CARE Foundation for Archaeological Research in Israel. During the first two years of my graduate study, fellowships were granted me by the City University of New York.

Finally, and most importantly, I would like to thank my mother for her continuous support and encouragement despite the great distance that separates us; my father for being a source of inspiration; and Elias Papatheodorou, whose love and support gave me the strength to accomplish this feat.

TABLE OF CONTENTS

Contents

Contents

Contents

Contents

Contents

TABLE LISTING

FIGURE LISTING

CHAPTER 1

Introduction

The problem of species recognition is a central one in evolutionary biology. Great difficulties are encountered in assigning taxa to the species category among living organisms (Mayr 1970, 1976; Van Valen 1976; Cracraft 1983), which become even more serious when the species concept is applied to paleontology (Simpson 1951; Wiley 1978; Bock 1986; Willmann 1989; Szalay 1993). Paleoanthropology is no exception to these problems (see for example Adrews 1984; Wood 1992; Rightmire 1995), and the species issue has recently been at the core of discussion about human evolution in the Pleistocene. This study addresses the issues of species recognition and of the pattern of distribution of morphological variation in the hominid fossil record of the Pleistocene of Western Eurasia.

The number of hominid species present in Western Eurasia over the last one million years, as well as their role in the evolution of anatomically modern humans, is a matter of wide disagreement. Some workers recognize *Homo neanderthalensis* (Tattersall 1986, 1992, 2000; Stringer and Andrews 1988a; Rak 1993; Stringer 1994), *H. heidelbergensis* (Tattersall 1986, 1992, 2000; Stringer 1994), *H. antecessor* (Bermudez de Castro et al. 1997; Tattersall 2000), and even perhaps *H. steinheimensis* (Tattersall 1986), as separate species. In this view, the fossil evidence indicates numerous speciation events during the middle Pleistocene, while the diversity represented by the fossil record of the genus *Homo* is underestimated (Tattersall 1986, 1992; Schwartz and Tattersall 2000). Others subsume *H. erectus* into *H. sapiens* and consider morphological change during the Pleistocene the result of anagenetic evolution. In the latter view, these groups represent local populations of *H. sapiens*, linked by gene flow throughout their evolution (Wolpoff 1989, 1992; Wolpoff et al. 1994, 1997; Wolpoff and Caspari 1997).

The recognition of Neanderthals as a separate species implies negligible or no contribution on their part to the subsequent evolution of *H. sapiens*. This view is supported by genetic studies of living humans (Cann et al 1987; Armour et al 1996; Tischkoff et al. 1996; Harpending and Relethford 1997; Harpending et al. 1998), by the recent recovery of distinctive mitochondrial DNA from three Neanderthal specimens (Krings et al. 1997, 1999, 2000; Ovchinnikov et al. 2000), and by metric and non-metric

studies of the morphological distance between Neanderthals and modern humans (Stringer 1974a, 1989, 1992; Howells 1989; Lahr 1996; Schwartz and Tattersall 1996 a, b; Turbón et al. 1997; Bräuer and Broeg 1998; Pearson 2000). However, the interpretation of the genetic evidence as supporting the replacement hypothesis has recently been questioned (Oxnard 1997; Templeton 1997; Adcock et al. 2001; Relethford 2001a, b), while several authors see evidence of continuity or interbreeding between Neanderthals and early modern humans in the fossil material (Smith 1982, 1984, 1992; Smith et al. 1989; Wolpoff 1989, 1992; Frayer et al. 1993; Duarte et al. 1999; Churchill and Smith 2000; Wolpoff et al. 2001).

This project is the first comprehensive attempt to compare degrees of morphological diversity among these fossil hominid groups to the morphological variation present in modern humans and in another living primate taxon, the chimpanzee. Both interspecific and intraspecific patterns of variation were evaluated, in order to help resolve the problem of the taxonomic position of the Neanderthals and the other Middle and Late Pleistocene European fossil groups. Such an approach has been advocated strongly by several workers (Delson 1989; Shea et al. 1993), but has not been systematically undertaken until now, as the multivariate analyses comparing Neanderthals to modern humans published up to the present have been limited to the study of intra-specific variation. Very recently (June 2001), a study appeared which applied a model of interspecific variation based on macaque species to a comparison between Neanderthals and Upper Paleolithic Europeans (Schillaci and Froelich 2001). Schillaci and Froelich, however, included no measure of intra- or sub-specific variation. The present comprehensive research will contribute significantly to the resolution of these problem, which have important implications for the understanding of the pattern of human evolution and of the origin of modern humans.

The Case of the Neanderthals

The discovery of the Neanderthal type specimen from the Feldhofer cave in 1856 marked the beginning of a heated debate in paleoanthropology that continues to this day. It roughly coincided in time with the publication of Darwin's work 'The Origin of Species' in 1859, and with maturing ideas about evolution, which were just beginning to

be applied to humanity. Neanderthals were assigned to a different species from living humans, *Homo neanderthalensis*, as early as 1864 (King 1864). Once their status as archaic predecessors of modern humans was established, the place of this hominid group in the human evolutionary tree and its relationship to modern Europeans began to be intensely debated. Different authors emphasized either their differences from, or their similarities to, modern humans. The predominant view in the 1910s and '20s was represented by Boule and Keith, who were among the most influential scholars in placing Neanderthals in a separate species and rejecting any ancestral role for them in modern human evolution. Boule pointed out, their 'primitiveness' and inferiority, while Keith supported the Pre-sapiens theory of human evolution in Europe, becoming involved in the search for ancient modern-looking human remains and in the Piltdown scheme (Boule 1911-1913; Boule and Vallois 1957; Trinkaus and Shipman 1992, 1993).

The perception of Neanderthals and other fossil hominid finds began to change during the 1930s. A re-arrangement and 'pruning' of the tangled hominid taxonomy was undertaken in the 1940s and '50s by Mayr, Simpson and Dobzhansky, in accordance with the principles of the New Synthesis (Mayr 1970; Trinkaus and Shipman 1992, 1993; Tattersall 2000). In this revision, Neanderthals and the other Middle Pleistocene European fossil specimens were placed in *Homo sapiens,* and anagenetic evolution was emphasized. Speciation in the human lineage was considered impossible, as a single species of human was thought to occupy all available ecological niches. This revision of the Neanderthal position has been criticized as having been made without serious consideration of the fossil evidence in question, but was soon adopted by the anthropological community. Although Neanderthals were not accepted as modern human ancestors by all authors, they were assigned subspecific status within *H. sapiens*, and their morphological and behavioral similarities to modern humans were emphasized (Trinkaus and Shipman 1992, 1993; Tattersall 2000).

In the 1970s and '80s, however, more intensive and detailed study of the Neanderthal fossil evidence revealed profound morphological and behavioral differences from modern humans (Trinkaus and Shipman 1992, 1993). During this time period, the increasing influence of the theory of punctuated equilibrium, rather than phyletic gradualism, as the predominant pattern of evolution, and the eventual application of

cladistic methodology in paleoanthropology, began to change again the perspective on human evolution and modern human origins (Tattersall 2000). An increased number of species began to be recognized once again in the hominid fossil record, and the single-species hypothesis as a cause for precluding speciation in humans was rejected. Additionally, two technological advances were instrumental in reshaping the predominant view on modern human origins: the advent of genetic studies of modern humans, eventually to be extended to the extraction of ancient DNA from three Neanderthal specimens, which suggested a recent and African origin for modern humans; and the development of improved chronometric dating techniques, particularly thermoluminescence and electron spin resonance, which allowed the dating of the controversial fossils from the Levant, revealing the very early presence of anatomically modern humans in that region (Mellars and Stringer 1989).

The present debate centers on the possible contribution of Neanderthals to the evolution of modern humans, as well as on whether they can be accommodated within *H. sapiens* or should be assigned to a separate species, *H. neanderthalensis*. Proponents of the replacement theory of modern human origins consider Neanderthals to have had little or no contribution to the evolution of modern humans, and tend to view this group as a separate species (Stringer et al. 1984; Stringer and Andrews 1988; Stringer 1989, 1992, 1994; Tattersall 1986, 1992, 2000). They emphasize the great morphological, and genetic distance, as well as behavioral differences, between Neanderthals and modern humans (Stringer 1974a, 1989, 1992; Cann et al 1987; Howells 1989; Mellars 1989; Armour et al 1996; Lahr 1996; Schwartz and Tattersall 1996 a, b; Tischkoff et al. 1996; Harpending and Relethford 1997; Krings et al. 1997, 1999, 2000; Turbón et al. 1997; Bräuer and Broeg 1998; Ovchinnikov et al. 2000; Harpending et al. 1998; Pearson 2000). Supporters of the multiregional model of modern human origins see Neanderthals as at least partial ancestors of the Upper Paleolithic and modern Europeans (Wolpoff 1989, 1992; Wolpoff et al. 1994, 1997; Wolpoff and Caspari 1997). These authors emphasize Neanderthal-like features found in some Upper Paleolithic European specimens, as well as what they see as trends for modernization in some late Neanderthal samples (Smith 1982, 1984, 1992; Smith et al. 1989; Wolpoff 1989, 1992; Frayer et al. 1993; Duarte et al. 1999; Churchill and Smith 2000; Wolpoff et al. 2001). Several intermediate positions

have also been formulated, including replacement with limited gene flow from Neanderthals (Bräuer 1981, 1984, 1989, 1992), as well as a subspecific Neanderthal status without contribution to the modern human gene pool (Delson 1989; Dean et al. 1998).

The Species Problem

Little agreement exists among systematists on the definition of the species category, as well as on the criteria to be used to delimit species taxa. According to the biological species definition (Mayr 1940; Bock 1986), species are groups of actually or potentially interbreeding populations in nature which are reproductively isolated from other such groups; they are genetic, reproductive and ecological units. The species category defined in this way is the only taxonomic category that is not arbitrary (Simpson 1951; Mayr 1976). Biological species of living organisms are thought to be real entities, cohesive reproductive groups with isolated gene pools, and as such they are often considered the units of evolution. Other species definitions, such as the specific mate recognition system definition, which is based on the existence of a fertilization system shared exclusively by all members of a species (Paterson 1985), as well as the ecological definition (Van Valen 1976), are often thought to represent aspects of the biological species definition (Delson 1989; Eldredge 1993; Szalay 1993).

The biological species definition is based on the testable criterion of reproductive isolation. However, this criterion concerns the relationship between populations in sympatry and synchrony, and can only be applied directly in such cases. Problems arise with the application of the biological species concept when the populations examined become separated in space and time. Mayr 's (1957) multidimensional, or polytypic, species concept, concerns populations that may be separated in space, but can potentially interbreed, and therefore should be assigned to a single species. As the criterion of reproductive isolation in nature can no longer be applied directly, decisions about potential ability to interbreed are made based on degrees of morphological, behavioral and genetic similarity. Simpson's (1951) evolutionary species definition accounts for the extension of the biological species in time. According to this definition, species are phyletic lineages, or sequences of ancestral-descendent populations, which evolve

independently from other such lineages and have their own evolutionary roles and tendencies. Since in paleontology decisions about relationships between fossil samples of extinct populations must be made on the basis of morphological information of fossilized tissues alone, evolutionary species are delimited through evaluation of the morphological variation within and between fossil samples (Simpson 1951). Wiley (1978) noted that according to the evolutionary species definition, different species may or may not show morphological differences, and the number of evolutionary species may be over- or underestimated as a result. Willmann (1989) was also concerned with the extension of biological species in time, but disagreed with Simpson's and Wiley's definitions of the evolutionary species, which he considered arbitrary. According to his view, biological species, as defined by the criterion of reproductive isolation, are individuals which originate by speciation and terminate either by speciation or by extinction. However, recognition of biospecies in the fossil record again must rely on morphological criteria.

The phylogenetic species as defined by Eldredge and Cracraft (1980) is a diagnosable cluster of individuals that share a parental pattern of ancestry and descent. Species are delimited on the basis of uniquely derived traits. Eldredge and Cracraft consider this criterion superior to, but consistent with, the criterion of reproductive isolation. The phylogenetic species definition emphasizes the importance of morphological differentiation, but it assumes that most of this differentiation takes place at speciation, or branching, events. Once established, species are believed to change very little through time in their morphology (Eldredge 1971, 1993). Under this assumption the phylogenetic species is analogous to the biological species, since the criterion of morphological diagnosibility is thought to indicate reproductive isolation by speciation. The phylogenetic species concept, however, can lead to an overestimated number of species, since any geographical or temporal variation within a biological species will be interpreted as reflecting speciation events. The pattern of distribution of morphological variation within and between groups of organisms, and its relationship to reproductive isolation, bears directly on this problem.

Most authors agree that assignment of fossil samples to species taxa must involve analogy to living biological species. Szalay (1993) proposed that this can be

accomplished through the careful evaluation of the patterns of morphological variation in well-established biospecies. These models of variation must be based on living species that are phylogenetically, geographically and ecologically similar to the fossil organisms studied. Their application to the fossil samples can guide decisions about species recognition. Several authors agree that such an approach must be undertaken in order to clarify the alpha taxonomy of the hominid fossil record (Delson 1989; Albrecht and Miller 1993; Shea et al. 1993). The range of morphological variation within living species must be evaluated, so that a measure of the geographic, sexual and ontogenetic variation to be expected in a fossil sample can be obtained. However, the morphological difference between closely related species must also be studied, since it is often thought that closely related primate species cannot be differentiated on the basis of bony morphology alone (Tattersall 1986, 1992, 1993; Cope 1993; Kimbel and Rak 1993). Tattersall (1986, 1992, 1993) in particular has suggested that bony morphology does not reflect species diversity. According to this view, two closely related species will overlap in most morphological traits, leaving very few differences between them. Therefore, if differences in osteology can be discerned, they must represent differentiation at the species level at least. Distinct, readily recognizable 'morphs' separated by consistent differences in fossil samples are thought to represent species. As Tattersall (1986) stresses, it is imperative that the variation between, as well as within, species, be assessed when assigning fossil samples to species taxa.

Objectives

The objectives of this study were two-fold: 1) to quantitatively evaluate proposed Neanderthal traits which are usually described qualitatively; and 2) to develop models of inter- and intra- specific variation in cranial morphology, in order to obtain a measure of morphological difference within and between species which could be applied to a comparison between Neanderthals and modern humans.

To address the first objective, three anatomical regions were examined, including the temporal bone, the occipital bone, and the midsagittal posterior cranial profile. Several features proposed to differentiate Neanderthals from modern humans are found in these areas: the small mastoid process relative to the large juxtamastoid eminence (Boule

and Vallois 1957; Vallois 1969; Santa Luca 1978; Stringer et al. 1984; Stringer 1985; Hublin 1988; Condemi 1991, 1992; Elyaqtine 1996; Dean et al. 1998; Minugh-Purvis et al. 2000); the origin of the petrotympanic crest and the orientation of the tympanic plate (Vallois 1969; Trinkaus 1983; Vandermeersch 1985; Condemi 1992; Elyaqtine 1996; Schwartz and Tattersall 1996; Martínez et al. 1997; Minugh-Purvis et al. 2000); the elevated position of the external auditory meatus (Vallois 1969; Stringer et al. 1984; Vandermeersch 1985; Elyaqtine 1995b); the wide, shallow, and medially closed-off glenoid fossa (Vallois 1969); the robusticity of the zygomatic process and the supramastoid crest (Boule and Vallois 1957; Vallois 1969; Heim 1976); the occipital 'bun' (Boule 1911-1913; Thoma 1965; Hublin 1978b, 1988b; Stringer et al. 1984; Sergi 1991; Condemi 1991; Lieberman 1995; Dean et al. 1998); the strong occipital torus and suprainiac fossa (Santa Luca 1978; Hublin 1978, 1988a, b; Stringer and Trinkaus 1981; Trinkaus 1983; Stringer et al. 1984; Condemi 1991, 1992; Lieberman 1995; Bräuer and Broeg 1998); the medio-laterally broad and supero-inferiorly short occipital plane (McCown and Keith 1937; Heim 1974; Thoma 1975; Hublin 1988; Wolpoff et al. 2001); and a relatively flat cranial base (Laitman and Heimbuch 1982; Lieberman 1989).

There is some disagreement on the usefulness of these features in discriminating Neanderthals from modern humans. The occipital 'bun', the presence of a prominent occipitomastoid crest and the presence of a suprainiac fossa have all been disputed as Neanderthal features (Trinkaus and Le May 1982; Spitery 1985; Frayer 1992; Schwartz and Tattersall 1996b; Yaroch 1996). Furthermore, as these traits are difficult to measure in terms of traditional distance measurements, they are usually described qualitatively (Ducros 1967; Martínez et al 1997; Dean et al. 1998) and have not been the subject of rigorous quantitative analysis. The use of geometric morphometrics allowed for a quantitative description of these features and for an assessment of their presence and variability in middle and late Pleistocene fossils, as well as in recent humans.

The second objective of this study was to develop models of inter- and intra-specific variation in cranial morphology at different hierarchical levels, in order to obtain a measure of morphological difference within a single species and between two closely related species. This measure could then be applied to a comparison between Neanderthals and other European fossils and modern humans, with the purpose of

clarifying the taxonomic status of these fossils groups within the genus *Homo*. Two such models were developed, based on modern humans and chimpanzees.

Modern human model: The first model was based on nine populations of modern humans spanning the extremes of their geographical range, as well as a time depth back to the Epipaleolithic. As modern humans represent the closest living relatives of fossil hominids, they provide the best model for comparisons to them. However, this model can only provide a measure of intraspecific variation.

Chimpanzee model: A measure of both intra- and inter-specific variation was obtained from the model based on the genus *Pan*. This taxon is often considered to be the closest living relative to humans, and has been used as a model for early fossil humans (see discussion in Shea et al 1993), although it is probably not the most appropriate model ecologically for Pleistocene hominids. *Pan* is differentiated into two species, *P. troglodytes* and *P. paniscus,* and *P. troglodytes* is further subdivided into three subspecies, *P .t. verus, P. t. schweinfurthii* and *P. t. troglodytes*. The alpha taxonomy of this genus is not completely resolved; recent genetic evidence from mitochondrial DNA has questioned the number of species and subspecies present in *P. troglodytes* (Morin et al. 1994; Gonder et al. 1997). This study, however, accepts the two commonly recognized species of *Pan* and the three subspecies of *P. troglodytes* and included samples from both species and two subspecies of *P. troglodytes*.

Hypotheses and Testable Predictions

Two hypotheses were derived from the literature, and their predictions tested.

Hypothesis A. Neanderthals represent a distinct species that did not contribute to the subsequent evolution of modern humans in Europe (e.g. Tattersall 1986, 1992, 2000; Stringer 1994). If hypothesis *A* is true, then one would expect the amount of variation among the three fossil groups and modern humans to exceed that present between any two modern human populations. It would also exceed the variation present between the two *Pan troglodytes* subspecies. It would be roughly equivalent to the differences present between *Pan troglodytes* and *Pan paniscus*. Furthermore, no morphological affinities would be observed between Neanderthals and Upper Paleolithic or recent Europeans.

Hypothesis B. Neanderthals represent a geographic population of *H. sapiens* and did contribute to the evolution of modern humans in Europe (e.g. Smith 1982, 1984, 1992; Frayer et al. 1993; Wolpoff et al. 1994b, 1997). If hypothesis *B* is true, then one would expect the amount of variation between Neanderthals and modern humans to be less than that present between *Pan troglodytes* and *Pan paniscus*. It would be roughly equivalent to that present between pairs of modern human geographical populations, or between the subspecies of *Pan troglodytes*. Furthermore, morphological affinities would be observed between Neanderthals and Upper Paleolithic or recent Europeans.

Morphological Methods and Geometric Morphometrics

Morphological variation in modern humans, fossil hominids and non-human primates has been studied quantitatively in the past through the use of multivariate statistical analyses of linear measurements (Howells 1973, 1989; Stringer 1974a, 1989, 1992; Albrecht and Miller 1993; Van Vark 1995). Such studies have used intra-landmark distances, angles and indices to describe the shape of the objects studied. Traditional morphometrics, as these methods have been labeled (Marcus 1990), have helped quantify morphological differences as reflected by the measurements used, but they have many limitations. The true shape of the object cannot be captured in these analyses, since the relative positions of the landmarks used to obtain the measurements cannot be taken into account. Traditional multivariate analyses often treat the different measurements used as separate variables, even though they belong to one single geometric framework (Rohlf and Marcus 1993; Yaroch 1996; Zollikofer et al. 1998). Furthermore, this approach cannot quantify morphological variation that cannot be measured directly linearly. Traits that are variable in their expression and cannot be measured linearly are subject only to qualitative scrutiny, which results in wide disagreement among researchers as to the evaluation of character states (Dean 1993).

Some of these problems can be surmounted with the use of geometric morphometrics. In this kind of analysis the geometry of the object studied is better preserved in the data, which are collected as coordinates of morphological landmarks in either two or three dimensions. The original form can be recovered better from the coordinates of the landmarks recorded, and far less information is lost about the original

material studied. These techniques therefore allow one to identify the landmarks where shape variation occurs, as well as the relative levels of variation at each landmark (Rohlf and Marcus 1993; Yaroch 1996; O'Higgins 2000). An additional great advantage of geometric morphometrics is that they provide a way of quantifying shape differences, and therefore differences in character states, of variable traits which cannot be directly linearly measured (Dean 1993). Finally, geometric methods can readily provide illustrations of the shape changes between specimens in specimen space (Rohlf and Marcus 1993; Lynch et al. 1996).

This study applied geometric morphometrics to the complex anatomy of the temporal, occipital and parietal bones. Both landmark and ridge curve data were used, which were processed using a Procrustes superimposition method and analyzed using an array of multivariate statistical methods, including Principal Components Analysis, Canonical Variates Analysis and Mahalanobis D^2 analysis. The use of geometric morphometrics also allowed direct comparisons of the posterior cranium among specimens. Both these approaches were used to evaluate morphological similarities and incidence of particular traits among recent and fossil human specimens, as well as among chimpanzee species and subspecies, and between humans and chimpanzees. Particular attention was paid to the direct comparisons between Neanderthals and the Upper Paleolithic European and Skhul-Qafzeh specimens. The Mahalanobis distance matrices, as well as cluster and minimum spanning tree analyses, were used to evaluate the morphological distance and relationships among groups. The measures of morphological distance between the two chimpanzee species and subspecies, as well as those among the modern human populations, were compared to the distances between Neanderthals and Upper Paleolithic, as well as recent, Europeans.

The materials and methods used in this study are described in detail in Chapter 2. Analysis of the temporal bone landmarks and brief discussion of the results was undertaken in Chapter 3. Analysis of the occipital bone landmarks and discussion of the results is presented in Chapter 4, while the analysis of the posterior sagittal cranial profile and discussion of the results is presented in Chapter 5. The results of the three analyses are integrated and summarized in Chapter 6.

CHAPTER 2

Materials and Methods

In this chapter I will describe the modern human, primate, and fossil hominid specimens digitized; I will give the definitions of the landmarks and ridge curves digitized and explain the reasons for their choice; and, finally, I will discuss geometric morphometrics methods and the multivariate statistical methods used in the analysis of the data.

A. Samples

This study included a comparative sample of nine modern human populations and three chimpanzee taxa, including two species and two subspecies. The fossil sample comprised several Middle and Late Pleistocene hominid specimens.

1. Modern humans

Nine modern human populations were measured, each consisting of approximately 30 individuals, comprising a total of two hundred seventy individuals (see Table 2.1). Following Howells' (1973, 1989) seminal study, each population was chosen to represent a biological population limited in space and time. When possible, subsamples of Howells' populations were used, as in the case of the Andamanese, the Berg, the Dogon, the Greenland Eskimo, the San-Hottentot and the Tolai. The Australian population included here is not based on the sample used by Howells, as the Australian cranial collection from Adelaide used by Howells has been repatriated. Two additional populations not represented by Howells' groups were included here: the Epipaleolithic samples from Afalou and Taforalt, which were merged to represent one sample and a mixed European population represented by samples of six individuals each from five localities across Western Eurasia. The Epipaleolithic group was included in order to give a time-dimension in the comparative sample. It was also included in the Howell's later analysis (1989). The mixed European sample was included so as to better represent a larger sample of Western Eurasian populations that would simulate the variation in the fossil sample drawn from multiple populations.

Table 2.1: List of specimens by population and sex for the comparative modern human and chimpanzee samples.

Group		Male	Female	Undetermined	Total
Modern Humans		143	126	1	270
Andamanese	(And. Islands, India)	13	17	---	30
Australians	(New S. Wales, South Australia)	19	11	---	30
Berg	(Austria)	15	15	---	30
Dogon	(Mali, West Africa)	15	15	---	30
Epipaleolithic	(Morocco and Algeria)	18	12	---	30
Inugsuk	(Greenland)	15	15	---	30
European mixed	(Egypt, Dalmatia, Greece, Italy, Germany)	17	12	1	30
San-Hottentot	(South Africa)	16	14	---	30
Tolai	(New Britain, Melanesia)	15	15	---	30
Chimpanzees		52	40	2	94
Pan paniscus	(Zaire)	16	19	---	35
Pan t. schweinfurthii	(Zaire)	18	12	---	30
Pan t. troglodytes	(Zaire, Cameroon)	18	9	2	29

The sample was limited to adult crania as determined by a fully erupted adult dentition. Sex was unknown in most cases and was assessed by inspection during study. For specimens measured by Howells his sexing assignments were taken into consideration and were found almost always to agree with the author's assessment. Where possible, equal samples for males and females were measured, but this was not always achieved. It is noted that a bias toward females exists in relatively small-bodied populations, such as the Andamanese, while a male bias is present in the relatively large-bodied populations, such as the Epipaleolithic population. As sex was assessed by inspection, it is possible that, in generally small-bodied and gracile populations some males were misidentified as females, while in large-bodied and more robust populations some females were misidentified as males. This problem may have been exacerbated where available samples were limited and small, as the full range of variation present would not be adequately assessed.

Andaman Islanders, British Museum (Natural History), London: Thirty-five specimens were measured, including twenty-six crania measured by Howells (see Howells 1989, p. 115), and nine additional crania present in the same collection. As Howells notes, this population probably represents a cohesive group since it remained hostile to outsiders and quite isolated until the mid-1800s. The Andamanese studied are very homogeneous in their cranial morphology. They are easily identified from their small size and characteristic cranial morphology, as well as from their funerary custom of decorating skulls with red ochre (Sullivan 1918; Radcliffe-Brown 1948; Howells 1989).

Australians, British Museum (Natural History), London: Thirty crania from the Australian aborigine collection of the British Museum (Natural History) were digitized. These did not include any specimens measured by Howells. This collection does not represent a real biological population, as it included specimens from several Australian localities. This was necessary as no single locality was represented by a large enough sample in this collection. The sample used here was limited to specimens from New South Wales and South Australia. It probably represents several tribes from this large geographical area.

Berg, Carinthia, Austria, American Museum of Natural History, New York: Thirty specimens were measured, all of them included in Howells' study. As described in

Howells (1989, p.91), this collection of 496 individuals was obtained from a charnel house. It probably represents as many as five generations of the population of the very small and relatively isolated mountain village of Berg. The remarkable homogeneity observed among the specimens studied here is consistent with a small isolated population.

Dogon, Mali Republic, West Africa, Musée de l'Homme, Paris: Thirty-four crania were digitized, all of them included in Howells (1973, 1989). As reported in Howells (1989, p.93), the collection originates from burial caves located in the territory of the Dogon tribe. Some questions have been raised as to whether one or two different populations are represented in this collection. This study follows Howells in treating them as one population.

Inugsuk Eskimo, Greenland, Anthropological Laboratory, University of Copenhagen: Thirty specimens, all included in Howell's work, were measured from the collection of the pre-colonial Inugsuk of Greenland.

San-Hottentot, South Africa, Anthropological Laboratory, University of Vienna: Thirty specimens were measured from the Pöch collection of the University of Vienna, the largest collection of San-Hottentot outside South Africa. This collection includes San and Hottentot individuals, as well as individuals of mixed or uncertain ancestry, as reported in the collection catalog. It was also studied by Howells, representing part of his San-Bushman sample. Specimens of mixed ancestry or of dubious cranial morphology were excluded.

Epipaleolithic population from Northern Africa, Institut de Paléontologie Humaine, Paris: Nineteen individuals from the Epipaleolithic site of Afalou-Bou-Rhummel, Algeria, and eleven individuals from the Taforalt site, Morocco, were digitized. These sites are dated to 14-8.5 ka (Lahr 1994). The two samples represent distinct populations separated not only in space but probably also in time. They were included in the same group here as they are closer to each other than to any other population studied. Extensive similarities between the two groups have been noted by Ferembach (1962), who found them to differ primarily in the lesser degree of robusticity of the Taforalt relative to the Afalou. As these specimens are not well preserved, many landmarks and ridge curves are missing on several of the crania.

European mixed population, American Museum of Natural History, New York: This population comprises small subsamples (six individuals each) from five localities in Western Eurasia and is designed to simulate the Neanderthal fossil record in its geographic range and separation of specimens in space and time. The five subsamples include Beduins from Mt. Sinai, Greeks, Italians, Dalmatians and Northern Germans. The six Northern German individuals were found to show mild artificial cranial deformation. They were not included in the analysis of the posterior cranial profile.

2. Chimpanzees

Three samples representing two species, the pygmy (*Pan paniscus*) and common (*Pan troglodytes*) chimpanzee, and two subspecies of the latter *(P. t. troglodytes* and *P. t. schweinfurthi*), were digitized (Table 2.1). All adult specimens available were measured and therefore the chimpanzee samples do not include equal numbers of males and females. More bonobo females than males are represented, while fewer females than males are included in both common chimpanzee samples. As in some human populations, the relatively small size of bonobos, as well as their reduced canine dimorphism, probably resulted in misidentification of males as females. In common chimpanzees, however, this bias probably reflects a field collection bias toward male skulls. No zoo specimens were included.

Pan paniscus, Musée Royal de l'Afrique Centrale, Tervuren: Thirty-five specimens of pygmy chimpanzee were digitized, including sixteen males and nineteen females.

Pan troglodytes, Musée Royal de l'Afrique Centrale, Tervuren, and American Museum of Natural History, New York: Two populations of common chimpanzee were included, representing two subspecies: *P. t. troglodytes*, twenty-nine specimens, nineteen males and ten females; and *P. t. schweinfurthii*, thirty specimens, eighteen males and twelve females.

Table 2.2: List of fossil specimens measured.

	Specimen	Sex	Institution[1]
Neanderthals	Amud 1	Male	University of Tel Aviv
	Gibraltar 1	Female	BM(NH), London
	Circeo 1	Male	Museo Pigorini
	Krapina C	Female	MNH, Zagreb
	Krapina 5	Unknown	MNH, Zagreb
	Krapina 6	Unknown	MNH, Zagreb
	Krapina 10	Unknown	MNH, Zagreb
	Krapina 16	Unknown	MNH, Zagreb
	Krapina 38-1	Unknown	MNH, Zagreb
	Krapina 38-2	Male?	MNH, Zagreb
	Krapina 38-7	Male?	MNH, Zagreb
	Krapina 38-12	Female?	MNH, Zagreb
	Krapina 38-13	Male?	MNH, Zagreb
	Krapina 38-1	Unknown	MNH, Zagreb
	Krapina 39-1	Female?	MNH, Zagreb
	Krapina 39-6	Unknown	MNH, Zagreb
	Krapina 39-13	Unknown	MNH, Zagreb
	Krapina 39-15	Unknown	MNH, Zagreb
	Krapina 39-16	Unknown	MNH, Zagreb
	La Chapelle	Male	AMNH, cast
	La Ferrassie 1	Male	AMNH, cast
	La Quina 5	Female?	AMNH, cast
	La Quina 27	Unknown	IPH, Paris
	Saccopastore 1	Female?	La Sapienza, Rome
	Saccopastore 2	Male?	La Sapienza, Rome

[1] Abbreviations of institutional names: AMNH: American Museum of Natural History; AUT: Aristoteleion University of Thessaloniki; BM(NH): British Museum (Natural History); CNHM: Croatian Natural History Museum; IPH: Institut de Paléontologie Humaine; IRSN: Institut Royale des Sciences Naturelles; NHM: Naturhistorisches Museum; SMN: Staatliches Museum für Naturkunde

Table 2.2: List of fossil specimens measured (cont.d).

	Specimen	Sex	Institution
Neanderthals	Shanidar 1	Male	AMNH, cast
	Spy 1	Female?	IRSN, Brussels
	Spy 2	Male	IRSN, Brussels
	Tabun 1	Female	BM(NH), London
Early Neanderthals	Biache	Unknown	AMNH, cast
	Reilingen	Male?	SMN, Stuttgart
	Steinheim	Female?	SMN, Stuttgart
	Swanscombe	Unknown	BM(NH), London
Archaic *H. sapiens*	Kabwe	Male	BM(NH), London
	Petralona	Male	AUT, Thessaloniki
	Singa	Male	BM(NH), London
H. erectus	Ceprano	Unknown	La Sapienza, Rome
	Sambungmachan 3	Female?	AMNH
Early modern humans	Qafzeh 9	Female	University of Tel Aviv
	Qafzeh 6	Male	IPH, Paris
	Skhul 5	Male	AMNH, cast
	Skhul 9	Male?	University of Tel Aviv
Late Paleolithic humans	Cro Magnon 1	Male	AMNH, cast
	Cro Magnon 2	Female	AMNH, cast
	Ein Gev	Male	University of Tel Aviv
	Koonalda	Male	BM(NH), London
	Mladec 1	Female	NHM, Vienna
	Mladec 2	Female	NHM, Vienna
	Predmosti 3	Male	AMNH, cast
	Predmosti 4	Female	AMNH, cast

3. Fossil hominid specimens

This sample comprised Middle Pleistocene hominids from Africa and Europe; Neanderthal specimens from Europe and the Near East; Late Pleistocene early anatomically modern humans from the Near East; and Late Paleolithic anatomically modern humans from Europe (Table 2.2). Where the original fossils were unavailable, casts from the Anthropology Department of the American Museum of Natural History were measured. Sexing of the fossil specimens was assigned using a variety of sources from the literature (McCown and Keith 1937; Genoves 1954; Boule and Vallois 1957; Jelinek 1969; Oakley et al. 1971; Smith 1980; Vandermeersch 1981; Radovcic et al. 1988; Delson et al. 2001).

According to the accretion hypothesis, as formulated most recently by Dean *et al.* 1998, the Neanderthal lineage evolved in Europe in isolation from other archaic populations since the early Middle Pleistocene and led to the evolution of the classic Neanderthals through various stages. According to this model, Middle Pleistocene and later European hominids show an accumulation of Neanderthal traits through time and can be sorted into four stages. Stage one and two include pre-Neanderthal fossils from isotope stages 12 and 9-11 respectively, labeled here as 'archaic *Homo sapiens*'. The Neanderthal sample comprises specimens from stages three and four. Stage three includes early Neanderthals dated to isotope stages 7-5 (Saccopastore, Krapina), and stage four includes 'classic' Neanderthal specimens dated to isotope stages 4 and 3. Specimens from the Near East, such as Amud 1 and Shanidar 1, were also included in this sample, although there are some problems regarding their placement with European Neanderthals (Dean et al. 1998). Earlier specimens with Neanderthal affinities were labeled 'early Neanderthals', as per the accretion hypothesis. In addition to these fossils, two late *H. erectus* were also measured (Ceprano and Sm-3), as well as several early anatomically modern human specimens. The specimens included in the fossil sample are listed in Table 2.2.

Table 2.3: Landmark definitions and types. For standard osteological landmarks definitions follow Howells (1973).

1. Inion (III)
2-3. Asterion right and left (I)
4. Lambda (I)
5. Opisthion (II)
6. Basion (II)
7-8. Point on posterior edge of the occipital condyle, 2 cm from the midline, right and left (III)
9. Hormion (I)
10. Staphylion (I)
11-12. Stylomastoid foramen right and left (I)
13-14. Most antero-medial point of the jugular fossa right and left (II)
15-16. Most postero-lateral point of the jugular fossa right and left (II)
17-18. Most lateral point of the vaginal plate of the styloid process, right and left (II)
19-20. Most medial point of the vaginal plate of the styloid process, at its juncture with the carotid canal, right and left (I)
21-22. Porion, right and left (II)
23-24. Auriculare, right and left (III)
25-26. Parietal Notch, right and left (II)
27-28. Mastoidiale, right and left (II)
29-30. Tip of the juxtamastoid eminence (Hublin 1978a) right and left (II)
31-32. Deepest point on the lateral margin of the articular eminence (root of the articular eminence), right and left (II)
33-34. Root of the zygomatic process, right and left (III)
35-36. Suture between the temporal and zygomatic bones, inferior aspect of zygomatic process, right and left (I)
37-38. Suture between the temporal and zygomatic bones, superior aspect of zygomatic process, right and left (I)
39-40. Frontomalare posterior, right and left (I)
41-42. Lateral end of the inferior nuchal line, right and left (anterior end of the antero-inferior branch, between the insertions for the rectus capitis posterior major and the superior oblique, Hublin 1978a) (II)
43-44. Lateral end of the superior nuchal line, right and left (the most lateral extent of the splenius capitis scar on the occipital bone, Dean 1993) (II)
45-46. Most inferior point on the entoglenoid pyramid, right and left (II)
47-48. Pterygoid canal right and left (I)
49-50. Suture between maxilla and sphenoid bone, right and left (I)
51. Bregma (I)
52. Glabella (II)
53. Nasion (I)
54. Prosthion (I)
55-56. Infraorbital foramen, right and left (I)
57-58. Anterior pterion, right and left (I)

B. Methods

1. Landmarks and Ridge Curves

The data were collected in the form of three-dimensional coordinates of landmarks and ridge curves using the Microscribe 3DX digitizer. Specimens were placed in the Frankfurt horizontal plane. Fifty-eight landmarks were digitized (see Table 2.2). Of these, ten lie on or near the midline sagittal plane and are therefore unique, while the rest represent pairs of right and left homologues. Thirty-four of them are standard osteological landmarks (Howells 1973); the remaining twenty-four were selected to capture the morphology of specific bony structures. Forty-two ridge curves were also digitized (Table 2.3); four of these lie on the midline sagittal plane. The remaining thirty-eight are pairs of right and left homologues. While both right and left side landmarks were always collected, ridge curves were collected on both sides only for the fossil specimens. For the modern human and primate samples only midline and right-side ridge curves were digitized, with the exception of the Andamanese and the Epipaleolithic populations. As these populations were digitized first, all ridge curves were collected. In the remaining comparative groups, left-side ridge curves were digitized only when they were better preserved than their right-side homologues. All data were collected by the author.

Not all landmarks and ridge curves digitized were used in this analysis. Only landmarks on the temporal and occipital bones were used, while only three line segments from bregma to opisthion on the midline were analyzed.

Definitions: In geometric morphometrics, landmarks are defined as homologous points that can be reliably and repeatedly located in all specimens under study. There are several kinds of landmarks as defined by Bookstein (1990) and by Valeri et al. (1998). Type I landmarks (Bookstein 1990; Dean 1993) are located at the juxtaposition of types of tissues, such as the meeting point of three structures, an intersection of sutures, or the center of small convex enclosures or foramina. Type I landmarks are usually traditional osteometric landmarks. Most landmarks used here are of this type, and are either traditional landmarks or were selected to capture the morphology of specific structures. Type II landmarks are points on curvature maxima, such as tips of bulging structures or the deepest points of invaginations. Some traditional osteometric landmarks are of this

type, and several type II landmarks were used here. Type III landmarks are extremal points, or points defined by reference to other landmarks, and are commonly used to extract data from planes, such as the planes describing the curves of bony structures. As such they are used here as the points along ridge curves (but not the ridge curve end points, which are usually type I or type II landmarks (Dean 1996; see also Delson et al. 2001). A final category is that of 'fuzzy' landmarks, as defined by Valeri et al. (1998). Fuzzy landmarks represent areas of biological significance that are exactly delimited, but which correspond to an area larger than a point. Such landmarks were used here only to orient the ridge curve describing the curve of the parietals from bregma to asterion through the parietal boss, which is a fuzzy landmark. Table 2.3 gives the landmark definitions and types.

A ridge curve is defined as 'a three-dimensional curving line on the surface of a biological structure' (Dean 1993, p.xiii; see also Dean 1996). It is delineated by a series of type III landmarks that are local curvature maxima on the surface. Ridge curves can also be defined by midline planes, by the edges of bony structures, by sutures or by muscle attachment markings. The definitions of the ridge curves digitized are listed in Table 2.4.

2. Analysis

Most of the fossils included in this study, as well as some of the Epipaleolithic specimens, do not preserve all of the landmarks and ridge curves. Because morphometrics does not accommodate missing data it was found necessary to proceed in the following ways: a) to introduce levels of analysis in which subsets of landmarks were considered and b) to reconstruct data by reflecting right and left sides.

Levels of Analysis: In addition to the separate analysis of landmarks and ridge curves, and in order to include fragmentary fossils in the sample, several levels, or steps, were introduced in the analysis of the data. First the data were subdivided into three anatomically defined sets, so as to maximize the number of fossil specimens in each set: temporal bone landmarks, occipital bone landmarks and midline ridge curve segments of the posterior cranial profile. Within these data sets several levels of analysis were undertaken, beginning with all landmarks and only complete specimens and

Table 2.4: Definitions of ridge curves

1. Lambda to Inion (midline)
2-3. Lambda to Inion parasagittal right and left, parallel to Lambda to Inion 2 cm lateral
4. Inion to Opisthion
5. Basion to Hormion
6-7. Inion to Opisthion parasagittal right and left, parallel to Inion to Opisthion 2 cm lateral
8-9. Porion to Mastoidiale, outline mastoid from porion to mastoidiale, right and left
10-11. Mastoidiale to Stylomastoid foramen, outline of the digastric notch, right and left
12-13. Parietal notch to Mastoidiale, right and left
14-15. Mastoidiale to Posterior Occipital Condyle, right and left
16-17. Postero-lateral point of jugular fossa to asterion, outline of occipito-mastoid suture, right and left
18-19. Asterion to tip of entoglenoid pyramid, outline of squamosal suture, right and left
20-21. Medial vaginal plate to lateral vaginal plate end, rim of the vaginal plate of the styloid process, right and left
22-23. Closed outline of the glenoid fossa, right and left
24-25. From root of articular eminence to inferior zygomatico-temporal suture, right and left
26-27. From inferior zygomatico-temporal suture to the root of the zygomatic process, right and left
28-29. From auriculare to superior sygomatico-temporal suture, right and left
30-31. From superior sygomatico-temporal suture to frontomalare posterior, right and left
32-33. From lateral end of the inferior nuchal line to midpoint, along the inferior nuchal line, right and left
34-35. From lateral end of the superior nuchal line to inion, along the superior nuchal line, right and left
36-37. From asterion to lambda, along the lambdoid suture, right and left
38. From bregma to lambda, along the sagittal suture
39-40. From bregma to asterion, passing through the parietal boss, right and left
41-42. From bregma to anterior pterion, right and left

successively increasing the number of specimens by decreasing the number of landmarks (see Table 2.5). Results from the different levels of analysis were compared.

Data Reconstruction: Minimal reconstruction was allowed during data collection for specimens where very little damage in a particular area of interest was observed. However, as the majority of fossil specimens still exhibited many missing landmarks, data were reconstructed by mirror imaging for right-left homologous landmarks. In the temporal bone analysis, the right temporal bone was used as routine. However, when the left temporal was more complete it was used instead, using mirror image reflection. In both these instances, reflection was performed in GRF-ND, which automatically reflects right-left mirror image configurations. The process of reflection has the unfortunate effect of eliminating variation due to asymmetry for the landmarks concerned. Nevertheless, the noticeable increase in the fossil sample size that mirror imaging produced justified its use. Reconstruction for each landmark by other methods is also possible, but was not performed here.

Geometric Morphometrics Methods: The landmark coordinate data collected for this study were analyzed with the use of the Procrustes methods of superimposition, which superimpose the landmark coordinates configurations of the specimens and scale them for size, so that the differences they exhibit are due to 'shape' (Rohlf 1990; Rohlf and Marcus 1993; Slice 1996). The Procrustes methods have been shown to have the highest statistical power among alternative geometric morphometric approaches (Rohlf 2000).

Superimposition was performed using the software GRF-ND and Morpheus (Slice 1992, 1994-1999). The specimen configurations are translated to common origin, scaled to unit centroid size (the square root of the sum of squared distances of all landmarks to the centroid of the object, the measure of size used here) and rotated according to a best-fit criterion, here the generalized procrustes analysis. A consensus configuration is calculated by computing the mean of all specimens for each landmark. As noted above, reflection of right and left side was allowed in the temporal bone landmark analyses, as most fossil specimens did not preserve both right and left side completely, allowing fossil specimens preserving different sides to be combined in one sample.

Table 2.5: Number of landmarks and specimens in each level of analysis for each dataset.

Dataset: Temporal Landmarks

	Landmarks	Modern Humans	Chimpanzees	Neanderthals	AMH	Other
Step 1	15	257	91	Saccopastore 2 La Chapelle La Ferrassie 1 Shanidar 1 Circeo 1 Amud 1	Skhul 5 Cro Magnon 1 Predmosti 3	Kabwe
Step 2	13	263	92	Saccopastore 1 La Chapelle La Ferrassie 1 Shanidar 1 Circeo 1 Amud 1 La Quina 27 Gibraltar 1 Krapina C Krapina 39-1 Spy 1 Spy 2	Skhul 5 Cro Magnon 1 Predmosti 3 Predmosti 4 Mladec 2 Qafzeh 9	Kabwe Reilingen

Table 2.5 (cont.d): Number of landmarks and specimens in each level of analysis for each dataset.

Dataset: Occipital Landmarks

	Landmarks	Modern Humans	Chimpanzees	Neanderthals	AMH	Other
Step 1	17	238	90	Saccopastore 1	Skhul 5 Cro Magnon 1 Predmosti 3 Predmosti 4 Mladec 1 Ein Gev	Kanalda Kabwe
Step 2	16	250	90	Saccopastore 1 La Chapelle La Ferrassie 1 Shanidar 1	Skhul 5 Cro Magnon 1 Predmosti 3 Predmosti 4 Mladec 1 Ein Gev	Kanalda Kabwe Biache
Step 3	8	267	92	Saccopastore 1 La Chapelle La Ferrassie 1 Shanidar 1 Amud 1 Circeo 1 La Quina 5 Tabun C1 Spy 2	Skhul 5 Cro Magnon 1 Predmosti 3 Predmosti 4 Mladec 1 Ein Gev Qafzeh 9	Kanalda Kabwe Biache Petralona Reilingen

Table 2.5 (cont.d): Number of landmarks and specimens in each level of analysis for each dataset.

Dataset: Midline Ridge Curves

	Landmarks	Semilandmarks	Modern Human	Chimpanzees	Neanderthals	AMH	Other
Step 1	4 (Inion, Lambda, Opisthion, Bregma)	27	245	91	Saccopastore 1 La Chapelle La Ferrassie 1 Shanidar 1	Skhul 5 Cro Magnon 1 Predmosti 3 Predmosti 4 Ein Gev	Kanalda Petralona Biache Singa
Step 2	3 (Inion, Lamdba, Opisthion)	15	251	92	Saccopastore 1 La Chapelle La Ferrassie 1 Shanidar 1 Gibraltar 1	Skhul 5 Cro Magnon 1 Predmosti 3 Predmosti 4 Ein Gev	Kanalda Petralona Biache Singa
Step 3	3 (Inion, Lambda Bregma)	25	249	92	Saccopastore 1 La Chapelle La Ferrassie 1 Shanidar 1 Amud 1 Circeo 1 La Quina 5 Tabun C1 Spy 1	Skhul 5 Cro Magnon 1 Predmosti 3 Predmosti 4 Ein Gev Cro Magnon 2 Mladec 1 Skhul 9	Kanalda Petralona Biache Singa Reilingen

The fitted coordinate configurations resulting from these procedures were thought to lie in Kendall's shape space (Rohlf 1996; O'Higgins 2000). Recently, however, Slice (2001) found that instead they lie in a hemispherical variant of this shape space. As in both cases shape space is non-Euclidean, a projection of these coordinates to tangent space is usually recommended. However, biological data are restricted in their variation and the shape space coordinates are almost identical to their projections in tangent space (Slice 2001). This assumption was tested in the three regional datasets using TPSSMALL (Rohlf 1998), which compares the Procrustes distances to the Euclidean distances. In all three cases the correlation between the two distances is very strong (temporal bone landmarks: correlation 0.9998 and root MS error 0.0004; occipital bone landmarks: 0.9999 and 0.0005; and midline ridge curves: 0.9999 and 0.00003).

Differences in centroid size between the specimens can be studied separately from differences in shape. Shape differences between specimens and between group means are visualized graphically in the form of displacement vectors of each landmark for each specimen or group mean from the consensus configuration in Morpheus. These displacement vectors show where most of the morphological variation occurs, allowing one to identify the landmarks where shape differences lie, as well as the magnitude of difference at each landmark. Multivariate statistical analysis was undertaken on the fitted coordinates of the specimen configurations (see below).

The ridge curve data were analyzed using the same principles of Procrustes fitting. Before fitting, however, each ridge curve was resampled so as to produce an equal number of homologous semi-landmarks and line segments for each ridge curve of each specimen. The semi-landmarks were then superimposed according to a least squares criterion and analysis of their fitted coordinates proceeded in the same way as in the landmarks analysis (see Delson et al. 2001). Again, shape differences along each ridge curve can be visualized graphically.

Statistical Methods The groups were labeled by genus, species and population. Neanderthals were designated to a species different from modern humans, and this designation was used to look for significance at the species level in the Principal Components Analysis (PCA). The remaining human fossil specimens were placed in an 'Unknown' species category, with the exception of the early anatomically modern and

Upper Paleolithic specimens, which were included in *H. sapiens* and assigned to their own population. However, species membership information was not used in the CVA, in order not to bias the results. This analysis was performed on the populations. All statistics were performed using the SAS statistical software package. Visualization of results was performed in GRF-ND and Morpheus, and the plots were obtained using SAS and Statistica. The analysis was conducted in the following steps.

Centroid size was analyzed first, in order to assess differences in size between Neanderthals and the other fossil specimens included here and modern human populations. An Analysis of Variance (ANOVA, SAS PROC GLM) was conducted on centroid size to determine whether there are significant differences in centroid size between groups and between males and females. In order to assess the degree of sexual dimorphism in each species, the female mean centroid size was subtracted from the male mean centroid size and divided by the standard deviation. The fitted coordinate configurations of the specimens were analyzed using Principal Components Analysis (PCA, SAS PROC PRINCOMP), in order to explore how variation is partitioned within and among the samples, as well as to achieve data reduction. An Analysis of Variance (SAS PROC GLM) was performed on the PCA scores to determine the significance of population, sex and interaction effects along each component. A one-way ANOVA was also performed to test for significant differences between genera and species along each principal component. Furthermore, the shape differences along the components separating Neanderthals, or other fossils, from modern humans were explored. The influence of each landmark on each principal component cannot be easily assessed by inspection of the eigenvectors of each variable for that component, as is normally done, as each landmark is represented by three variables (coordinates). In order to assess the influence of each landmark on each principal component, the squared root of the sum of squares for the eigenvector coefficients of the three coordinates of each landmark was calculated. The landmarks with the highest values were interpreted as driving the variation along each component. The shape variation at each landmark along each axis was visualized in GRF-ND by plotting the eigenvectors for each PC on the consensus configurations. This allows visualization of a hypothetical configuration at the extremes of each PC (Slice 1996). These hypothetical configurations are used here to illustrate

shape changes along a PC. A correlation analysis with centroid size was performed for the scores of each PC (SAS PROC CORR), in order to determine the significance of centroid size variation in the variation along that component and to identify allometric effects.

A Canonical Variates Analysis (CVA, SAS PROC CANDISC) was conducted on the principal component scores, in order to maximize the separation between groups and to evaluate the shape differences that best separate them. Unlike the PCA, this analysis uses group membership information. The group information used here was population membership rather than species or genus information, so as not to bias the results toward separation of pre-designated species. The CVA was performed on the principal component scores rather than on the coordinates in order to reduce the number of variables analyzed. However, the first 30 principal components were used, accounting for more than 95 % of the total variance, as it was determined that the results changed with inclusion of fewer components. The shape differences along each canonical variate were also visualized in GRF-ND. The scores of each canonical variate were regressed on the fitted coordinates and the coefficients replaced the eigenvector coefficients in GRF-ND and plotted on the fitted configurations in the same way as the principal components eigenvectors. This allows visualization of hypothetical specimen configurations along each canonical variate, and was used to illustrate shape differences. As with the principal components, a correlation analysis with centroid size was performed, in order to determine how much of the variation along that canonical variate can be explained by variation in centroid size.

A discriminant analysis was conducted (SAS PROC DISCRIM), treating the non-Neanderthal fossil specimens as unknown specimens to be classified in one of the pre-defined groups (at the population level) by posterior probability. The robustness of this analysis was further tested by conducting a cross-validation test on the entire dataset, using the CROSSVALIDATE option in the PROC DISCRIM procedure. The discriminant analysis is forced to classify all specimens into one of the predefined groups used. As some of these specimens do not belong to any of these groups (such as Kabwe or Petralona), their placement into one or the other group should not be interpreted as a meaningful classification. Rather, these results are only of interest in indicating

morphological similarities. Of particular interest are the results of the assignment of the early anatomically modern humans, who cannot be placed within any of the recent human populations included here, as well as of specimens such as Reilingen and Biache, which are generally considered to be early representatives of the Neanderthal lineage (see e.g. Dean et al. 1998).

Mahalanobis D^2 matrices were obtained for the groups included in the analysis correcting for unequal sample sizes (Sarmiento and Marcus 2000). Non-significant D^2 values, as well as those significant to the 0.05, 0.01 and 0.001 levels, were reported in the matrix tables. These matrices were used to produce cluster (UPGMA) and minimum spanning trees, using the NTSYS program (Rohlf 1986-1998). When performing a Mahalanobis distance analysis, the position of singletons and groups comprising very few specimens relative to other groups can be misleading due to misrepresentation of the variation in their groups. In order to test for this effect, false singleton situations were produced by randomly taking specimens out of the modern human sample and treating them as singletons. In one out of the three trials conducted, the specimen exhibited very a large D^2 value to its own population, although the two other false singletons showed very small D^2 values to their groups and clustered closely with them in the cluster analysis. The Mahalanobis distances between singletons and other groups or specimens, may therefore be overestimated.

The above series of analyses was performed three times for each level of analysis of each anatomically defined dataset. The analysis was performed on the combined human and chimpanzee sample first. It was repeated on the human sample alone, so as to better resolve shape differences among human groups and among human fossil specimens. Finally, each anatomically defined analysis was repeated on the chimpanzee sample alone. This was done because the distances among the chimpanzee taxa may be underestimated in the combined sample analysis, due to the greater variation in the human sample, thus biasing the results. Since this last step of analysis was conducted in order to test the consistency of the chimpanzee model, and not to investigate shape differences among the chimpanzee taxa, it focused on the Mahalanobis distances calculated rather than on the results of the PCA and CVA, as with the combined sample and human sample analyses.

CHAPTER 3

Temporal Bone Landmarks

The temporal bone is one of the most diagnostic anatomical areas for Neanderthals, as it is the location of several traits thought to differentiate this fossil group from modern humans (Trinkaus and Smith 1985; Vandermeersch 1985; Condemi 1991; Elyaqtine 1996). These include the small size of the mastoid process relative to the large juxtamastoid eminence, a proposed derived feature (Boule and Vallois 1957; Vallois 1969; Santa Luca 1978; Stringer et al. 1984; Stringer 1985; Hublin 1988; Condemi 1991, 1992; Arsuaga et al. 1993; Elyaqtine 1996; Dean et al. 1998; Minugh-Purvis et al. 2000); the supero-inferiorly low and antero-posteriorly short squama (Boule and Vallois 1957; Vallois 1969; Heim 1976); the origin of the petrotympanic crest at the most inferiorly projecting part of the tympanic (Vallois 1969; Vandermeersch 1985; Elyaqtine 1996; Schwartz and Tattersall 1996; Minugh-Purvis et al. 2000); the coronal orientation of the tympanic plate (Trinkaus 1983; Condemi 1992; Martínez et al. 1997); the elevated position of the external auditory meatus relative to the zygomatic process and the floor of the glenoid fossa (Vallois 1969; Stringer et al. 1984; Vandermeersch 1985; Elyaqtine 1995b); a wide, shallow and medially closed-off glenoid fossa (Vallois 1969); the robusticity and lateral projection of the zygomatic process and the strong supramastoid crest (Boule and Vallois 1957; Vallois 1969; Heim 1976); the more medial position of the stylomastoid foramen (Vallois 1969); and an anteriorly closed digastric fossa (Vallois 1969; Vandermersch 1985; Martínez et al. 1997; Minugh-Purvis et al. 2000). Aside from the height and length of the squama and the height of the mastoid, these characteristics are difficult to measure directly and, as a consequence, have not been subject to rigorous quantitative analysis.

Fifteen temporal landmarks were selected so as to best represent these traits. Most are standard osteological landmarks (Howells 1973), but other landmarks are also included and their definitions given in Table 3.1. As most fossil and some modern human specimens were incomplete, analysis was undertaken in two steps varying in their number of landmarks and in the fossil sample included, so as to include as many landmarks and as many specimens as possible (see Chapter 2, also Table 3.2).

Table 3.1: Landmarks collected on the temporal bone.

1. Asterion	(Steps 1 and 2)
2. Stylomastoid Foramen	(Steps 1 and 2)
3. Most medial point of the jugular fossa	(Steps 1 and 2)
4. Most lateral point of the jugular fossa	(Steps 1 and 2)
5. Lateral origin of the petro-tympanic crest	(Steps 1 and 2)
6. Most medial point of the petro-tympanic crest at the level of the carotid canal	(Steps 1 and 2)
7. Porion	(Steps 1 and 2)
8. Auriculare	(Steps 1 and 2)
9. Parietal Notch	(Steps 1 and 2)
10. Mastoidiale	(Steps 1 and 2)
11. Most inferior point on the juxtamastoid crest (following Hublin 1978a)	(Steps 1 and 2)
12. Deepest point of the lateral margin of the articular eminence (root of the articular eminence)	(Steps 1 and 2)
13. Suture between the temporal and zygomatic bones on the inferior aspect of the zygomatic process	(Step 1)
14. Suture between the temporal and zygomatic bones on the superior aspect of the zygomatic process	(Step 1)
15. Most inferior point on the entoglenoid pyramid	(Steps 1 and 2)

Table 3.2: Number of landmarks and specimens in each level of analysis.

	Landmarks	Modern Humans	Chimpanzees	Neanderthals	AMH	Other
Step 1	15	257	91	Saccopastore 2 La Chapelle La Ferrassie 1 Shanidar 1 Circeo 1 Amud 1	Skhul 5 Cro Magnon 1 Predmosti 3	Kabwe
Step 2	13 (minus the 2 landmarks on the superior and inferior aspects of the zygomatic suture)	263	92	Saccopastore 2 La Chapelle La Ferrassie 1 Shanidar 1 Circeo 1 Amud 1 La Quina 27 Gibraltar 1 Krapina C Krapina 39-1 Spy 1 Spy 2	Skhul 5 Cro Magnon 1 Predmosti 3 Predmosti 4 Mladec 2 Qafzeh 9	Kabwe Reilingen

As outlined in Chapter 2, within these steps there were four additional levels of analysis: A) performed on the combined chimpanzee and human samples; B) on the human sample alone; C) on the chimpanzee sample only.

Step 1

This step includes all landmarks, thus limiting the number of fossil specimens that can be included as most of them are incomplete even after data reconstruction. Only six Neanderthals preserve all fifteen landmarks: La Ferrassie 1, La Chapelle-aux-Saints, Circeo 1, Saccopastore 2 and the two Near Eastern specimens Amud 1 and Shanidar 1 (Table 3.2). Among the other fossil specimens only Kabwe, Skhul 5, Cro-Magnon 1 and Predmosti 3 were included. The modern human and chimpanzee samples were also somewhat restricted due to missing data, most notably the Epipaleolithic population from North Africa (21 specimens out of a total of 30).

Centroid Size: An analysis of variance (ANOVA) was conducted on centroid size to investigate genus, species, population and sex effects. Species, population and sex were all found to be highly significant (p 0.0001), but no genus or interaction effects were detected.

Centroid size for the temporal bone landmarks is very similar in *Homo* and *Pan* (Table 3.3, Fig. 3.1). The means of the two samples are not significantly different between the genera. Centroid size differences are also relatively small between males and females, although there is a significant overall sex effect. Means are smaller for females in both humans and chimpanzees, human females, however, also have a smaller standard deviation than human males. The standard deviation of chimpanzee females is almost identical to that of males. Within the chimpanzee sample, bonobos are significantly different from both common chimpanzee subspecies in their smaller means, although a sex bias in the chimpanzee samples might be influencing this result (19 out of the 35 bonobos and only 21 out of the 59 common chimpanzees are female). The two common chimpanzee subspecies are not significantly different from each other.

Common chimpanzees show equivalent levels of sexual dimorphism to humans in their temporal landmarks centroid size. Bonobos are less sexually dimorphic than either modern humans or common chimpanzees.

Table 3.3: Centroid size listed by species, sex and population (Step 1).

	Mean	Range	St. Deviation	N
Homo	**10.88**	**9.44-12.82**	**0.75**	**267**
Males	11.15	9.43-12.82	0.72	148
Females	10.51	9.45-12.02	0.61	118
Modern	10.85	9.44-12.82	0.74	160
Males	11.14	9.44-12.82	0.72	141
Females	10.51	9.45-12.33	0.61	118
Neanderthal	11.80	11.28-12.19	0.31	6
Kabwe	12.25	---	---	1
Skhul 5	11.29	---	---	1
Cro Magnon 1	12.61	---	---	1
Predmosti 3	12.69	---	---	1
Andamanese	9.94	9.44-10.85	0.35	30
Australian	10.67	9.83-11.29	0.44	30
Berg	10.67	9.85-11.72	0.47	28
Dogon	10.56	9.69-11.55	0.50	28
Epipaleolithic	11.89	10.43-12.71	0.56	21
Eskimo	11.74	10.92-12.82	0.45	30
European (mixed)	10.75	9.73-11.83	0.46	30
San	10.46	9.80-11.48	0.47	30
Tolai	11.12	10.02-11.88	0.50	30
Pan	**10.82**	**8.93-12.94**	**0.86**	**91**
Males	11.07	9.48-12.94	0.82	49
Females	10.46	8.93-12.15	0.80	40
P. paniscus	9.98	8.93-10.88	0.38	35
Males	10.13	9.48-10.88	0.36	16
Females	9.86	8.93-10.41	0.37	19
P. troglodytes	11.34	9.94-12.93	0.64	56
Males	11.53	10.20-12.94	0.54	33
Females	11.00	9.94-12.32	0.69	21
P. t. schweinfurthii	11.30	9.94-12.94	0.73	28
P. t. troglodytes	11.37	10.14-12.21	0.55	28

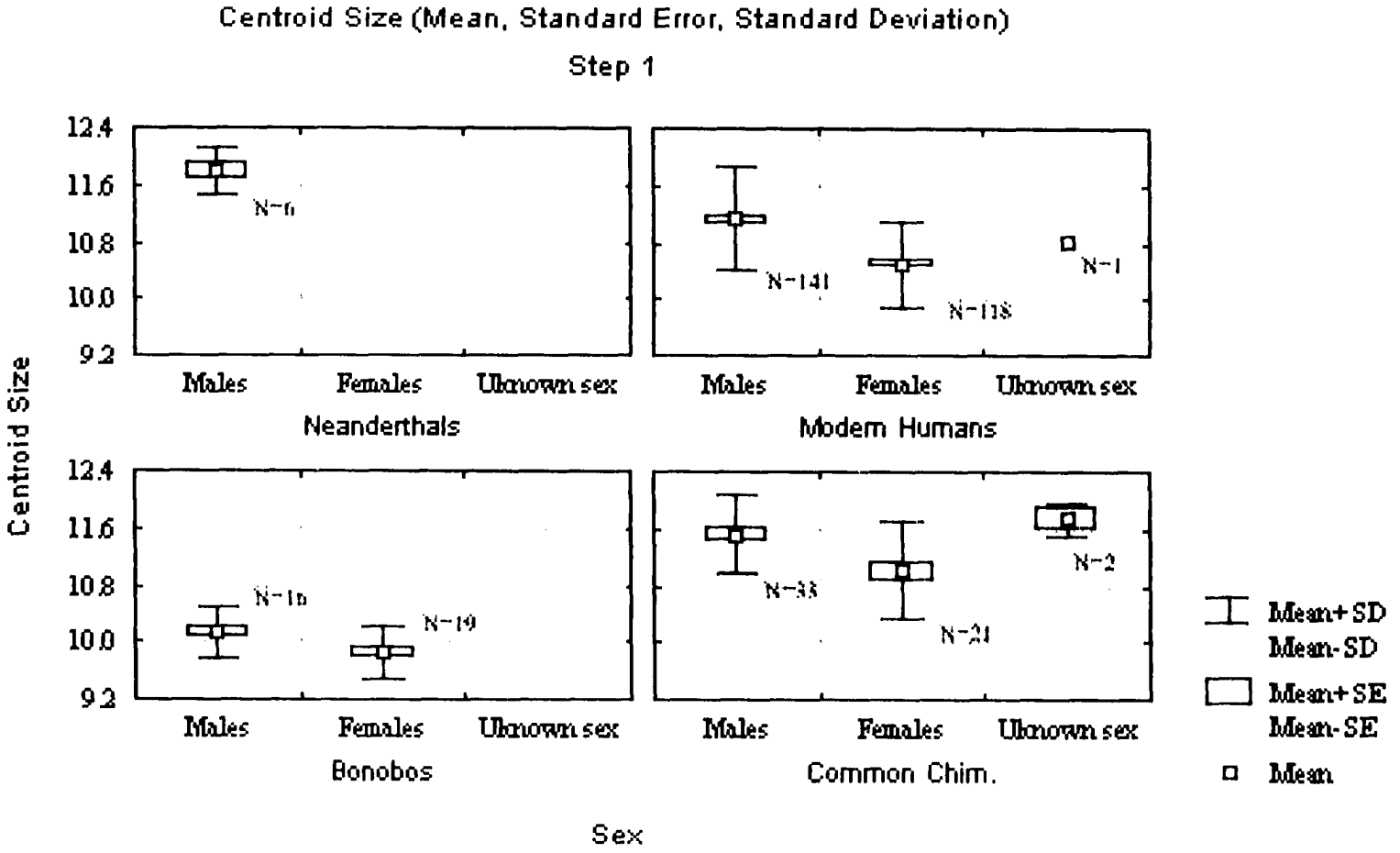

Figure 3.1: Centroid size mean, standard error and standard deviation, labeled by species and sex (Step 1).

In the human sample, Neanderthals fall within the range of modern humans but in its upper part, and are not significantly different from the Epipaleolithic and the Eskimo, the two populations with the highest mean centroid size values here. The Neanderthal sample, however, is very small and does not include any female specimens. Kabwe also falls near the upper limit of the modern human variation, as does Skhul 5 to a lesser extent. Both of these specimens are considered male. The Upper Paleolithic group, comprising here only two male specimens, Cro Magnon 1 and Predmosti 3, is found here to be significantly larger in centroid size than any other group, including Neanderthals. Among recent human populations, the Epipaleolithic and the Eskimo are the largest, differing significantly from all other recent groups. The robusticity and large size of these populations have been noted in the past (Ferembach 1962; Lahr 1996). The Andamanese are significantly smaller than all other recent groups with the exception of the San. The reduced stature and cranial dimensions of these populations are also well documented (Broom 1912; Sullivan 1921; Howells 1973; Lahr 1996) The human geographic populations are much more differentiated in temporal bone centroid size compared to the chimpanzee subspecies, reflecting the much wider geographic and body size range in modern humans.

Step 1A - Combined human and chimpanzee sample

Principal Components Analysis: A principal components analysis was undertaken on the variance-covariance matrix of the 45 coordinates. The results are summarized in Table 3.4. An analysis of variance (ANOVA) was conducted on the principal components to test for significant population and sex effects along each principal component. A Bonferroni pairwise test was conducted on the mean scores of the populations to test for significant differences at this level. A correlation analysis was performed with centroid size on each principal component, in order to determine whether any of them are highly correlated with centroid size. The results are also reported in Table 3.4. None of the principal components in this analysis was found to be highly correlated with centroid size, including the ones that separate modern humans from Neanderthals and human males from human females. No adjustment for centroid size-related shape differences was therefore undertaken.

In evaluating the shape differences along each principal component, the squared root of the sum of squares of the three eigenvector coefficients for each landmark was calculated, so as to facilitate the interpretation of the eigenvector loadings for each principal component. These values are presented in Table 3.5, and the highest few of them for each principal component can be interpreted as driving the separation along that component. The shape differences at each landmark along the principal component axes were then visualized in GRF-ND, and the effects were magnified as needed for purposes of better visualization.

The first principal component (Fig. 3.2) accounts for 41.07 % of the variance and is highly significant for population at the 0.0001 level and sex effects at the 0.01 level, but not for interaction effects. It separates humans from chimpanzees, as well as Neanderthals from modern humans. Chimpanzees are significantly different from modern humans along this component, while Neanderthals are significantly different from both chimpanzees and all the human populations, including the Upper Paleolithic specimens, Kabwe and Skhul 5. The means for males and females are also significantly different from each other. Chimpanzees form a distinct cloud on the negative side of PC 1 and modern humans cluster on the positive side. Neanderthals fall between the modern human and chimpanzee groups but closer to the former, and overlap slightly with the negative extreme of the modern human range. Amud 1 is the only specimen that falls within the modern human range. Kabwe falls near the center of the modern human range, as do Skhul 5, Cro Magnon 1 and Predmosti 3. PC 1 does not separate modern human populations, although the Eskimo tend to be more positive and the Epipaleolithic more negative, the other populations falling between them. When PC 1 is labeled by sex, a weak tendency is observed for females to have more negative scores than males. This tendency is stronger in humans. It does not apply to Neanderthals, as they fall outside the negative extreme of the modern human range even though they are all thought to be male. Figure 3.3 shows the means of the scores of each principal component for males and females by population.

The landmarks driving the separation along PC 1 (Table 3.5) are, in order of magnitude, the tip of the mastoid (10), the tip of the juxtamastoid eminence (11), the lateral end of the petro-tympanic crest (5), and to a lesser extent the medial end of the

Table 3.4: Summary of the PCA results, ANOVA and Correlation Analysis for PCs 1-15, Step 1A.

	Principal Components Analysis			ANOVA, Pr > F			Correlation with Centroid Size	
	Eigenvalue	Proportion	Cumulative	Popul.	Sex	Interaction	Rho	Pr > F
PC 1	0.008066	0.410753	0.410753	0.0001	0.0051	0.5821	0.01743	0.7425
PC 2	0.001327	0.067571	0.478324	0.0001	0.0049	0.7264	0.22936	0.0001
PC 3	0.001243	0.063274	0.541598	0.0001	0.71	0.2858	-0.23515	0.0001
PC 4	0.001025	0.052203	0.593801	0.0001	0.3711	0.1062	0.40149	0.0001
PC 5	0.000777	0.03956	0.633362	0.0001	0.0260	0.9238	-0.11851	0.0249
PC 6	0.000719	0.036605	0.669967	0.0001	0.6705	0.3308	-0.10641	0.0442
PC 7	0.00065	0.033111	0.703078	0.0001	0.0001	0.4723	0.22919	0.0001
PC 8	0.000503	0.025632	0.72871	0.0001	0.9332	0.6181	0.17302	0.001
PC 9	0.00047	0.023913	0.752623	0.0001	0.6492	0.5108	0.24071	0.0001
PC 10	0.000441	0.022441	0.775064	0.1170	0.6740	0.0484	0.24071	0.3324
PC 11	0.000401	0.020406	0.79547	0.0001	0.2328	0.5008	-0.01096	0.8362
PC 12	0.000349	0.017764	0.813234	0.0001	0.8629	0.3622	-0.15128	0.0041
PC 13	0.000325	0.016572	0.829806	0.0001	0.0059	0.52	0.17214	0.0011
PC 14	0.000296	0.015065	0.84487	0.0001	0.5931	0.2940	0.02140	0.6865
PC 15	0.000284	0.014477	0.859348	0.0001	0.4717	0.3171	-0.00092	0.9861

Table 3.5: Square roots of the sum of squares of the eigenvector coefficients for the three coordinates of each landmark, PCs 1-10, 15. Step 1A.

	PC 1	PC 2	PC 3	PC 4	PC 5	PC 6	PC 7	PC 8	PC 9	PC 10	PC 15
1. Asterion	0.21	**0.56**	0.15	**0.43**	**0.30**	**0.33**	**0.43**	**0.32**	0.27	**0.59**	0.22
2. Stylom. F.	0.14	0.07	0.14	0.07	0.16	0.12	0.20	0.11	0.10	0.12	0.12
3. Md. Jug.	**0.25**	0.02	0.23	0.16	0.17	0.16	0.27	**0.37**	**0.45**	0.10	**0.38**
4. Lt. Jug.	0.24	0.07	0.08	0.15	0.19	0.19	0.10	0.12	0.16	0.19	0.15
5. Lt. Petro-Tym. Cr.	**0.39**	0.19	0.08	0.05	0.15	**0.50**	**0.47**	0.28	0.15	0.21	**0.54**
6. Md. Petro-Tym. Cr.	0.24	0.07	0.18	0.25	0.23	0.12	0.20	0.22	**0.34**	0.19	0.05
7. Porion	0.23	0.06	0.08	0.21	0.11	0.17	0.19	**0.34**	0.25	0.08	0.15
8. Auriculare	0.19	0.08	0.12	0.23	0.13	0.12	0.16	0.28	**0.36**	0.06	0.25
9. Parietal N.	0.19	0.26	**0.65**	**0.36**	**0.51**	0.20	0.18	**0.38**	0.08	**0.58**	0.11
10. Mastoid	**0.41**	**0.53**	0.24	0.23	**0.27**	**0.49**	**0.37**	0.23	0.20	0.12	0.25
11. Juxt. Em.	**0.40**	**0.33**	**0.48**	0.30	**0.44**	**0.29**	**0.38**	0.16	0.12	0.10	**0.41**
12. Artic. Em.	0.23	0.07	0.15	0.15	0.13	0.19	0.15	0.28	**0.30**	0.09	0.10
13. Zyg. Sut.Inf.	0.10	**0.33**	0.23	**0.33**	0.23	0.15	0.15	0.16	0.11	**0.27**	0.22
14. Zyg. Sut. Sup.	0.17	0.22	0.20	**0.41**	0.21	0.26	0.06	0.25	**0.35**	0.14	0.23
15. Entogl. Pyr.	**0.25**	0.11	0.10	0.15	0.25	0.15	0.07	0.11	0.27	0.21	0.18

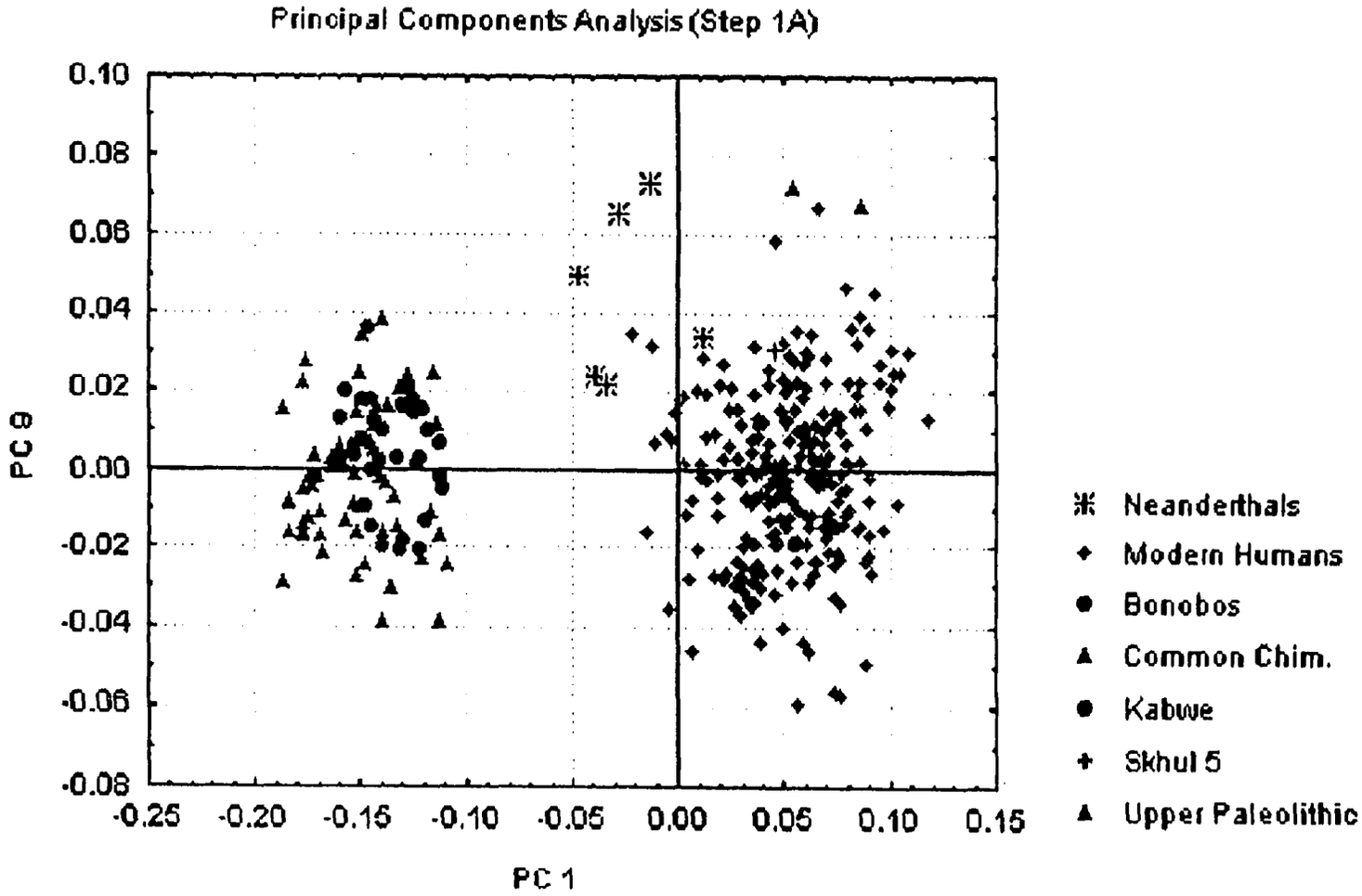

Figure 3.2: Principal Components Analysis (Step 1A), PCs 1 and 9.

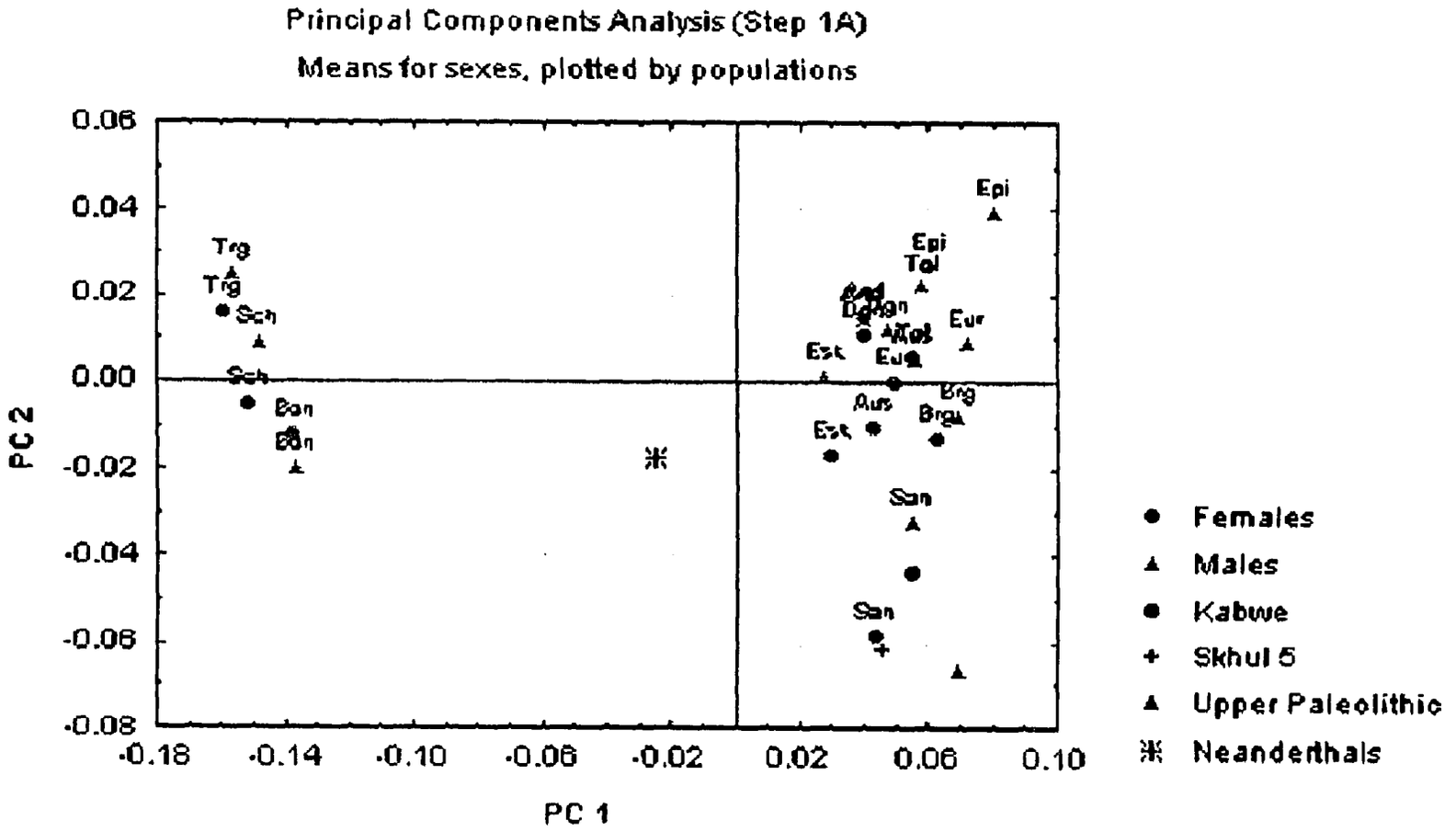

Figure 3.3: Principal Components Analysis (Step 1A), means for sexes by population. PCs 1 and 2.

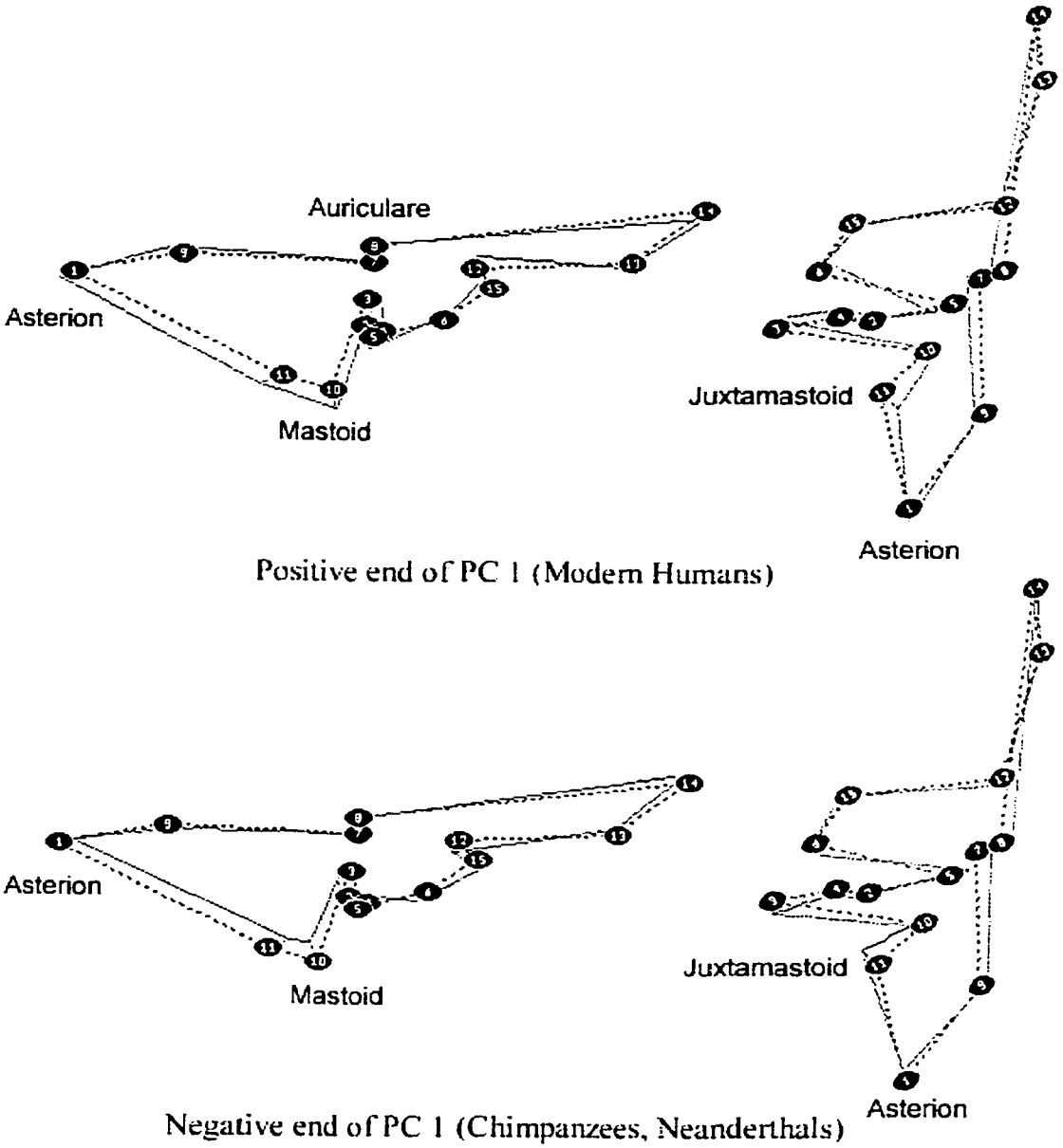

Figure 3.4: Shape variation along PC 1 (Step 1A), right lateral (left) and right ventral (right) views. The dotted line represents the consensus configuration.

jugular fossa (3) and the entoglenoid pyramid (15). Figure 3.4 shows the shape variation at each landmark along PC 1 in both ventral and lateral views. The most important shape differences along this axis are the following: the tip of the mastoid process (10) and of the juxtamastoid eminence (11) are placed more inferiorly on the positive side of PC 1 and more superiorly on the negative side, reflecting their larger of both structures in humans compared to the apes, but particularly of the mastoid process. These two points are also positioned more laterally in the positive (human) end of PC 1, as seen in ventral view. The medial end of the petro-tympanic crest (6) is placed more anteriorly, while the lateral end (5) is placed more posteriorly in the positive (human) end of PC 1, reflecting a more sagittal orientation of this structure in humans and a more coronal orientation in chimpanzees. The medial end of the jugular fossa (3) is more anterior in the positive end of this component, as is its lateral end (4). In ventral view, the tip of the entoglenoid pyramid (15) is more lateral in the positive end of this axis and more medial in the negative.

In all of these structures Neanderthals differ from modern humans in the same direction as chimpanzees, but to a lesser degree. Furthermore, human females also tend to differ from males in similar ways as chimpanzees and Neanderthals, indicating a tendency for females to have smaller mastoid processes and juxtamastoid eminences. These shape differences are consistent with both the described Neanderthal morphology (Vallois 1969; Hublin 1978; Santa Luca 1978; see above), and the normal pattern expected for human sexual dimorphism (see Steele and Bramblett 1988; White and Folkens 1991). As noted above, Kabwe falls within the range of modern humans in these characteristics and differs from Neanderthals in the same ways as modern humans do, as do also Skhul 5, Cro Magnon 1 and Predmosti 3. PC 1 is not correlated with centroid size (Table 3.4).

Neanderthals are partially separated from modern humans in two additional components, PCs 9 and 15. These are also the principal components along which Neanderthals are significantly different from modern humans at the species level. PC 9 (2.4 %, Fig. 3.2) is significant for population effects but not for sex or interaction effects. Along PC 9 the Upper Paleolithic specimens are significantly different from all human groups except Neanderthals. Neanderthals are significantly different from most modern

human groups, including the Berg, Europeans, Andamanese, Australians and Dogon. When treated at the species rather than the population level, Neanderthals are significantly different from modern humans and from the two chimpanzee species along PC 9.

The Upper Paleolithic specimens cluster at the positive end of PC 9, as do Neanderthals, who overlap with the positive extreme of the modern human variation. La Ferrassie 1, Shanidar 1 and Circeo 1 are better separated from modern humans, while Amud 1, but particularly La Chapelle and Saccopastore 2 overlap more with the modern human cloud. Skhul 5 also falls on the positive part of the modern human variation but well within the modern human sample. Kabwe falls within the modern range of variation on the negative side. Among modern human populations, PC 9 tends to separate the Eskimo, Tolai, Andamanese and Epipaleolithic on the positive end of the modern human range from the San, Dogon and Australians on the negative end, with the two European populations roughly in the middle.

The shape variation along this axis (Fig. 3.5) includes, in the positive end, the more anterior placement of the medial end of the jugular fossa (3); the more lateral position of auriculare (8); the more posterior and inferior position of the root of the articular eminence (12); the more medial position of the superior aspect of the zygomatic suture (14); and the elevated position of the me dial end of the petro-tympanic crest (6). The shape differences that characterize Neanderthals and the two Upper Paleolithic specimens compared to most modern humans, therefore, can be described as an anterior placement of the antero-medial end of the jugular fossa, a stronger supramastoid crest, a posteriorly placed articular eminence and shallower glenoid fossa, a more elevated medial end of the petro-tympanic crest and perhaps a more antero-posteriorly curved zygomatic process. PC 9 is not correlated with centroid size (Table 3.4).

PC 15 (1.4 %, Fig. 3.6) is significant for population effects but not for sex or interaction effects. Along this component Neanderthals are significantly different from all groups except the Eskimo and the San. When the ANOVA was repeated at the species rather than the population level, Neanderthals are found to be significantly different from modern humans and from the two chimpanzee species along PC 15.

Neanderthals cluster on the negative extreme of PC 15. Three specimens, La

Ferrassie 1, Circeo 1 and Saccopastore 2 fall outside the modern human range, while La Chapelle and Shanidar 1 overlap with its negative fringe. As in PC 1, however, Amud 1 falls within the modern human cloud and is in this case widely removed from the other Neanderthal specimens, including Shanidar 1, which clusters with the Neanderthal sample although it has the most positive score among them. Skhul 5 is placed at the positive extreme of the modern human range along this axis, while the two Upper Paleolithic specimens fall near its center. Among modern human populations, the Eskimo group tends to be more negative, although modern human populations almost completely overlap. Kabwe falls almost exactly at the center of the modern human range.

The landmarks driving the separation along PC 15 are listed in Table 3.5. The shape differences along this axis (Fig. 3.7) include, in the negative end, the more anterior and medial placement of the lateral origin of the petro-tympanic crest (5); the more inferior projection of the juxtamastoid eminence (11); and the more medial position of the medial end of the jugular fossa (3). These differences tend to characterize Neanderthals relative to modern humans, with the exception of Amud 1, and can be described as an anterior origin and more coronal orientation of the petro-tympanic crest, a large juxtamastoid eminence relative to the smaller mastoid process, and a more medially placed antero-medial end of the jugular fossa. The opposite shape traits (a more sagittal orientation of the petro-tympanic crest, a small juxtamastoid eminence and a lateral position of the medial end of the jugular fossa) characterize Skhul 5 at the positive extreme of the modern human range. PC 15 is not correlated with centroid size (Table 3.4).

Kabwe is separated from the rest of the human sample along PC 5 (3.96 %. Fig. 3.8), where it falls on the negative extreme and is significantly different from all other human groups. PC 5 is significant for population effects to the 0.0001 level, as well as for sex effects to the 0.05 level. This axis does not separate Neanderthals from modern humans, or bonobos from common chimpanzees, and modern human populations overlap completely on this component. When PC 5 is labeled by sex, females tend to have more positive scores than males, but this tendency is much stronger among chimpanzees.

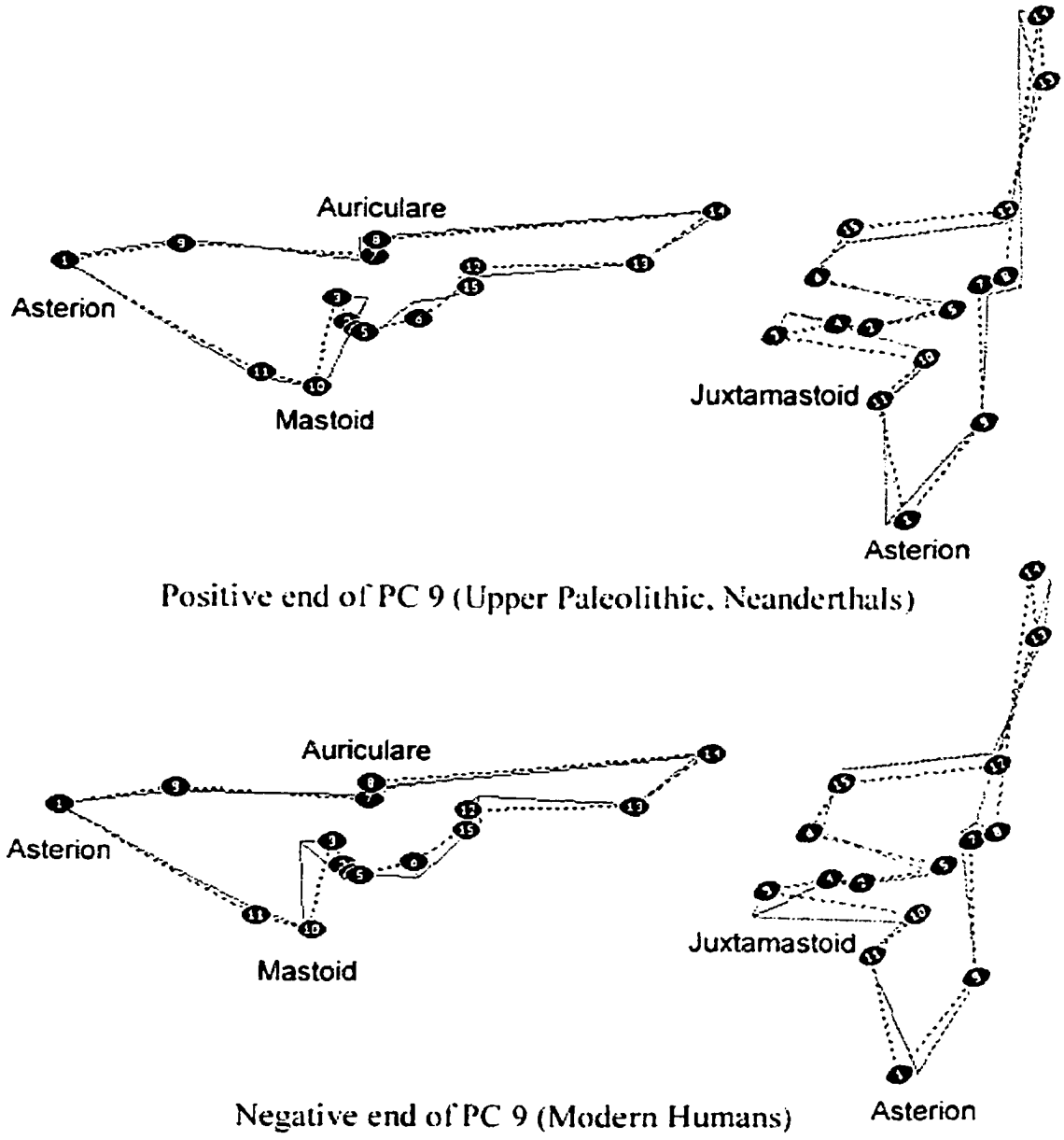

Figure 3.5: Shape variation along PC 9 (Step 1A), right lateral (left) and right ventral (right) views. The dotted line represents the consensus configuration.

The shape differences along PC 5 are shown in Fig. 3.9. In the negative end, where Kabwe falls, the parietal notch (9) is depressed and posteriorly placed, while asterion (1) is more anteriorly placed, reflecting an antero-posteriorly short mastoid portion of the temporal bone. The tip of the juxtamastoid eminence is also more posteriorly, inferiorly and laterally placed, and the tip of the mastoid process (10) is more laterally and slightly more superiorly positioned. Kabwe is therefore separated from modern humans and Neanderthals by the combination an antero-posteriorly short mastoid portion of the temporal, a relatively large juxtamastoid eminence, and laterally placed mastoid process and juxtamastoid eminence. No correlation is observed between PC 5 and centroid size (Table 3.4).

Two more components are significant for sex effects, PC 2 (0.01) and PC 7 (0.0001). Along PC 2 (6.8 %) the mean value for males is significantly different from that of females, males tending to be more positive than females. When the means for each modern human population are labeled by sex, the means for males are more positive than the female means in most modern human populations except for the Andamanese and the Dogon, where the means for the two sexes are almost identical. This trend is also present in the two common chimpanzee subspecies, but not in bonobos, where it is reversed. The shape differences along this axis include, in the positive end, a superiorly and anteriorly placed asterion, a more inferiorly placed tip of the mastoid process and juxtamastoid eminence, and more posteriorly placed zygomatic suture landmarks. These differences tend to characterize modern human and common chimpanzee males relative to females, and bonobo females relative to males.

PC 7 (3.3 %) is significant for sex and population effects to the 0.0001 level. Among modern human populations, the Epipaleolithic tend to cluster in the positive axis and the Andamanese in the negative. These two populations are significantly different from each other along this component. In the human sample, females tend to have more negative scores than males along this axis, although the two sexes overlap widely. When the means for sexes are plotted by population (Fig. 3.10), the mean values for males are more positive than the female values in all modern human populations. This trend is not present in chimpanzees, with the exception of *P. t. troglodytes*.

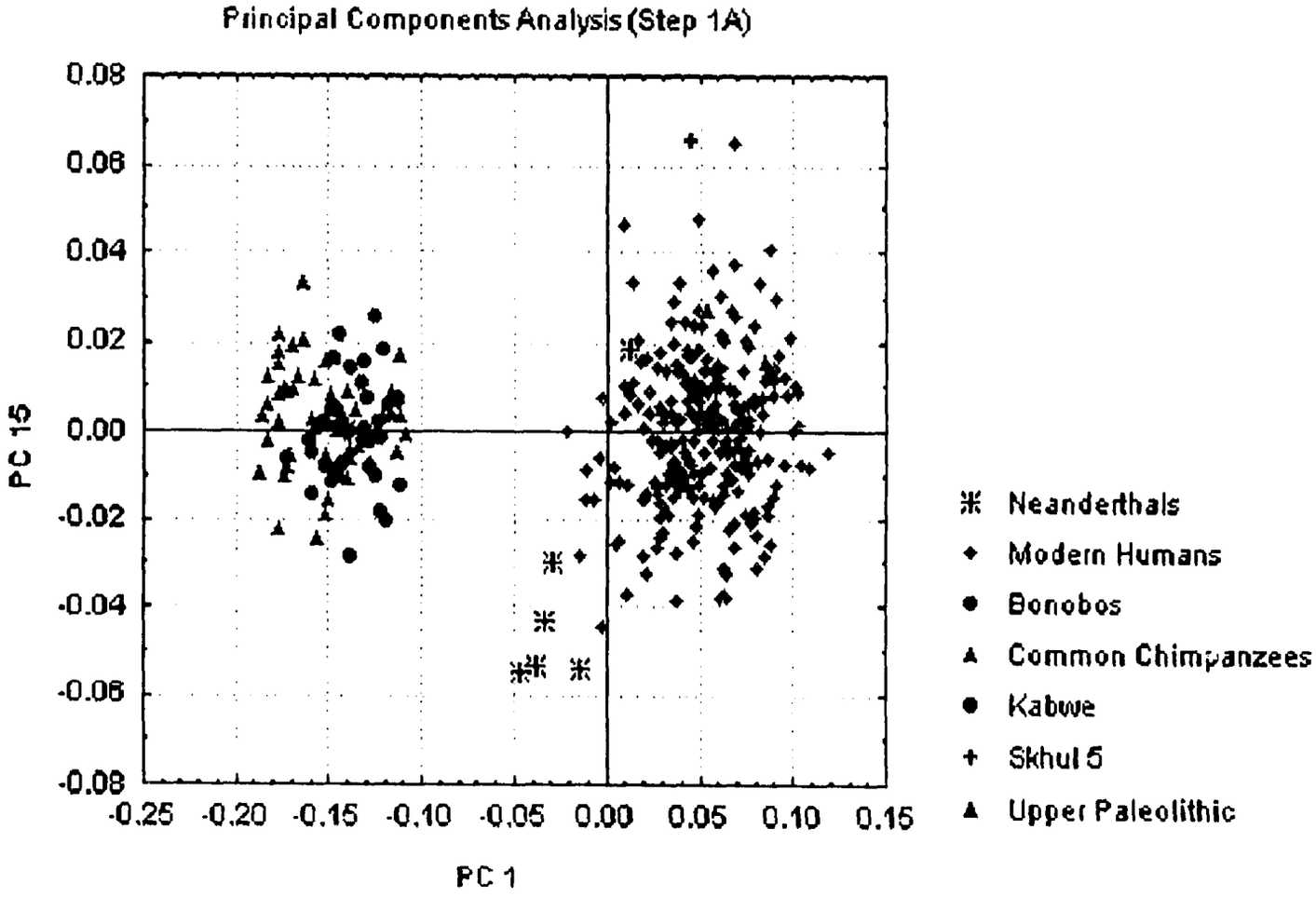

Figure 3.6: Principal Components Analysis (Step 1A), PCs 1 and 15.

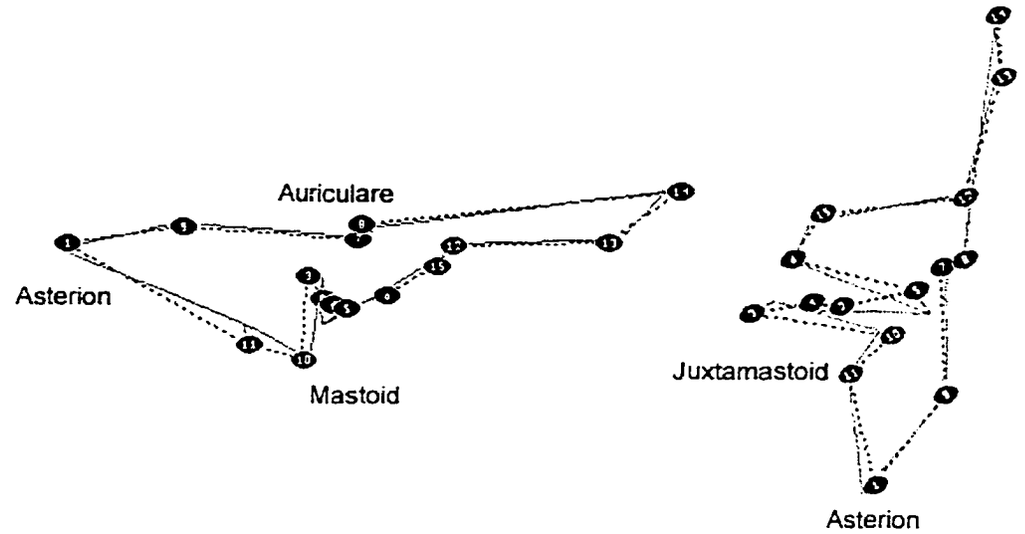

Positive end of PC 15 (Modern Humans)

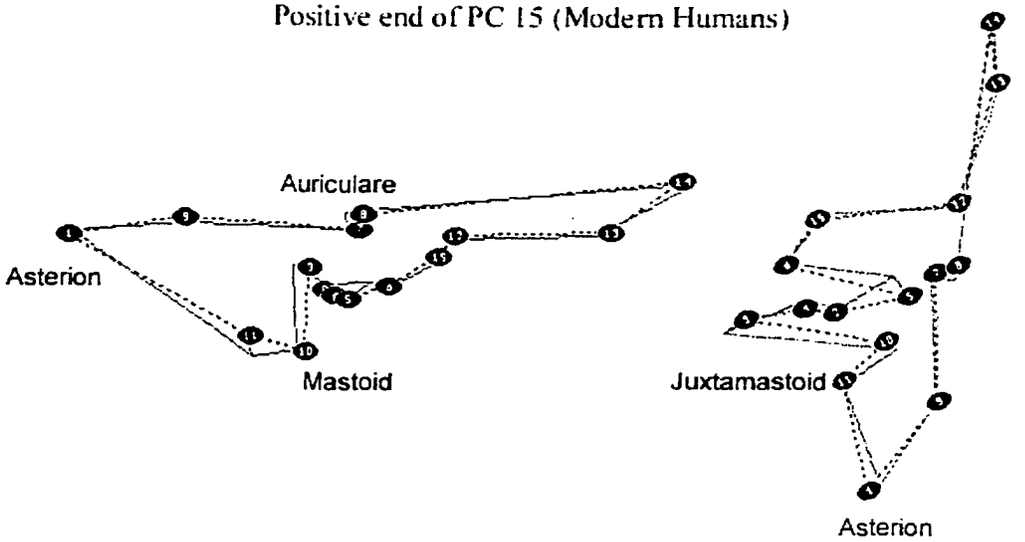

Negative end of PC 15 (Neanderthals)

Figure 3.7: Shape variation along PC 15 (Step 1A), right lateral (left) and right ventral (right) views. The dotted line represents the consensus configuration.

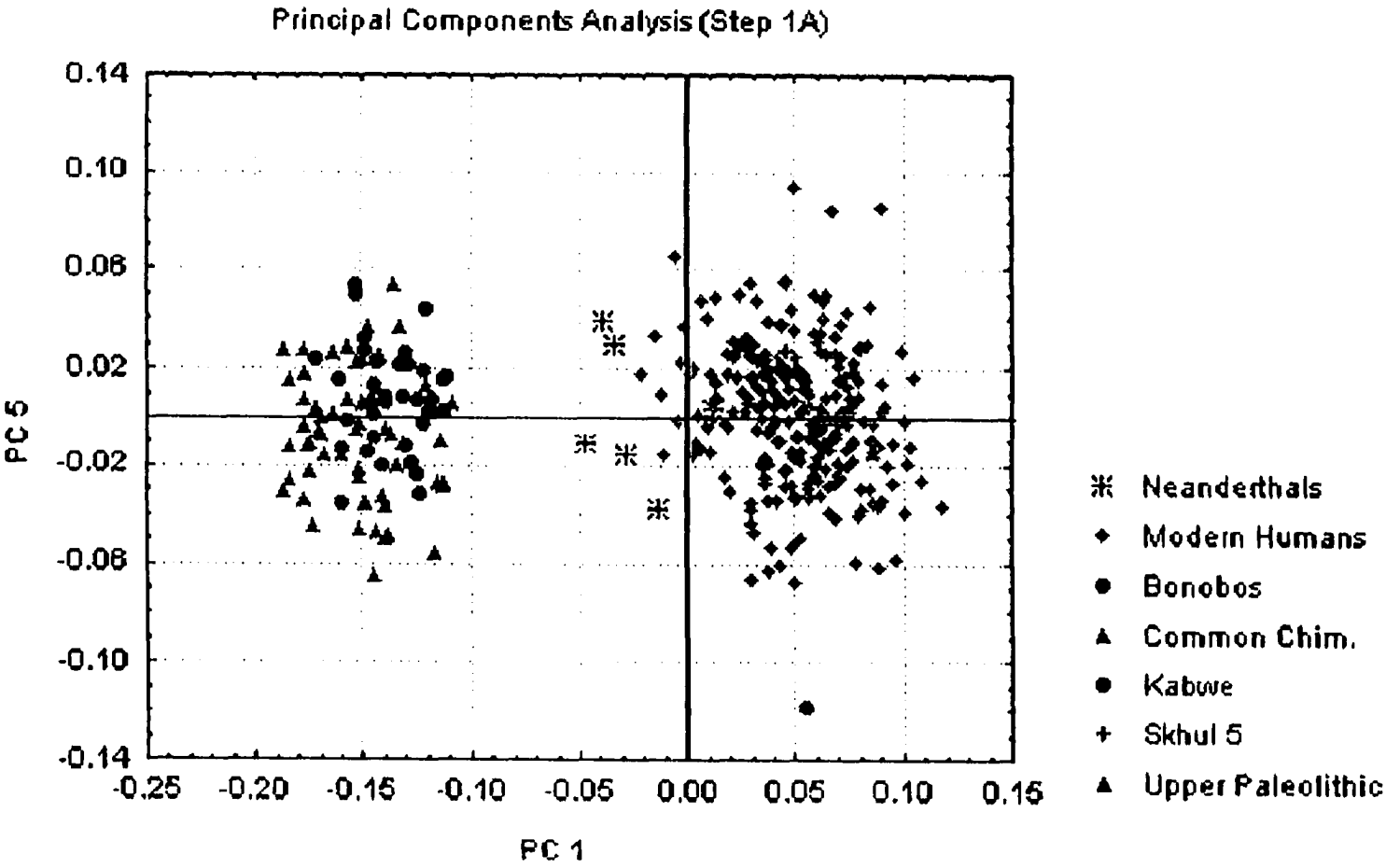

Figure 3.8: Principal Components Analysis (Step 1A), PCs 1 and 5.

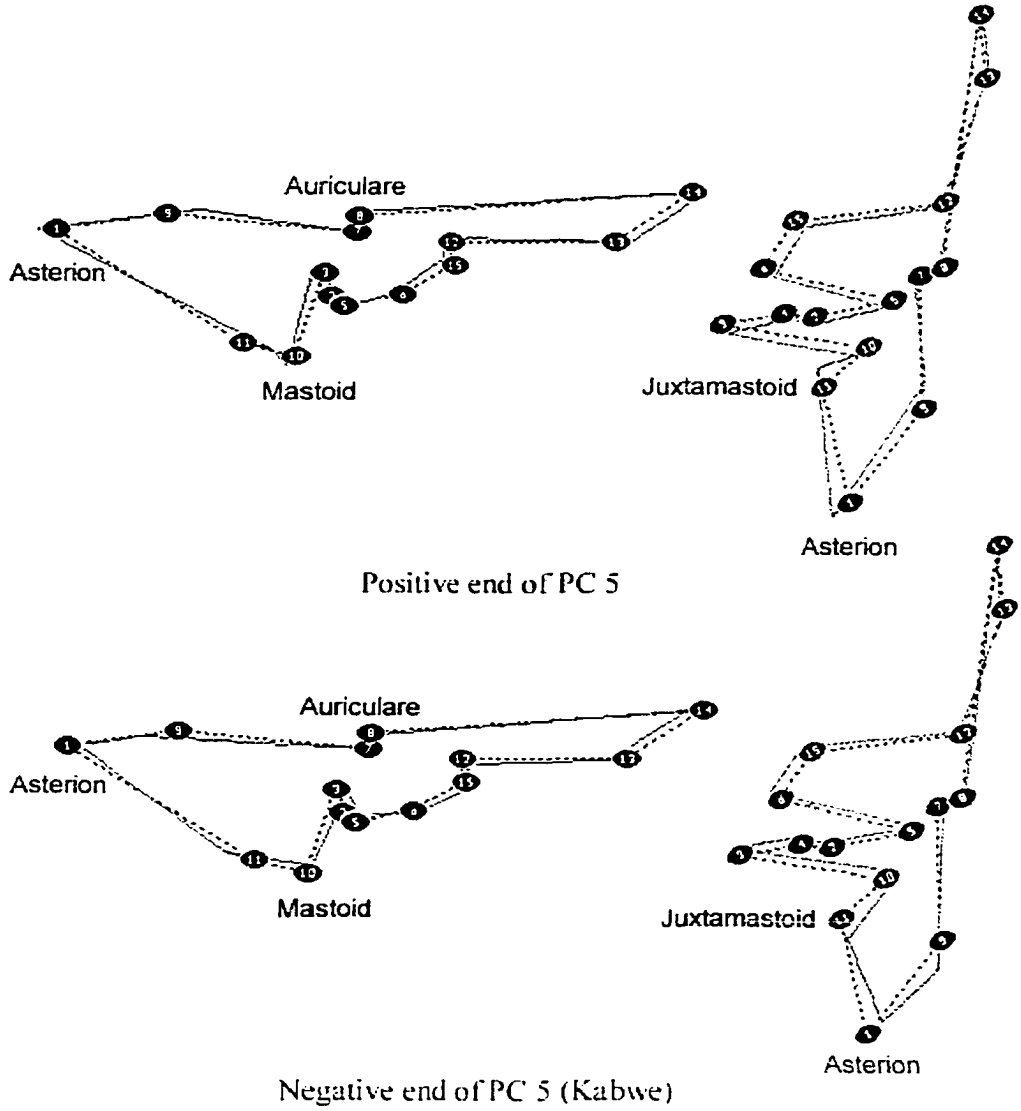

Figure 3.9: Shape variation along PC 5 (Step 1A), right lateral (left) and right ventral (right) views. The dotted line represents the consensus configuration.

The shape variation along this component (Fig. 3.11) includes, in the positive end, and anterior and more lateral placement of the lateral origin of the petro-tympanic crest (5); a medial position of asterion (1); and a more inferior placement of the mastoid tip (10) and the juxtamastoid eminence (11), which are also more widely separated from each other in the antero-posterior dimension. These differences can be described as a more coronally oriented petro-tympanic crest, probably related to the larger and more antero-posteriorly bulging mastoid process, a larger juxtamastoid eminence and an antero-posterior curvature of the temporal bone. They characterize males relative to females, as well as the populations that lie on the positive side of PC 7 (Epipaleolithic, San, Dogon) compared to those that cluster on the negative side (Eskimo, mixed Europeans). In both cases, however, there is considerable overlap and these shape differences do not separate either populations or sexes completely. PC 7 is not correlated with centroid size (Table 3.4).

Canonical Variates Analysis: A canonical variates analysis was performed using the first 30 principal components (97.9 % of the total variance) at the population level (Table 3.6). An ANOVA was performed on the CV scores at the population level. As with PC 1, chimpanzees are significantly different from humans along CaV 1, while Neanderthals are significantly different from chimpanzees and all modern human populations. Neanderthals are clearly separated from modern humans along this canonical axis, which also separates humans from chimpanzees (68.9 % of the total variance, mostly influenced by PC 1, Fig. 3.12).

Neanderthals cluster on the negative side along CaV 1, between the chimpanzees on the negative side and the modern humans on the positive side. All Neanderthal specimens fall outside the modern human range along this axis and outside the 95 % confidence ellipses of all modern human populations along CaVs 1 and 3, except Amud 1, which again falls within the range of variation of modern humans. Kabwe falls near Amud 1, near the negative end of the modern human range. Skhul 5 and the two Upper Paleolithic specimens are not separated from modern humans. The two chimpanzee species tend to diverge slightly along CaV 1, bonobos placing slightly more positive and hence closer to the human cloud. This axis does not differentiate between modern human groups or chimpanzee subspecies, and is not correlated with centroid size (Table 3.6).

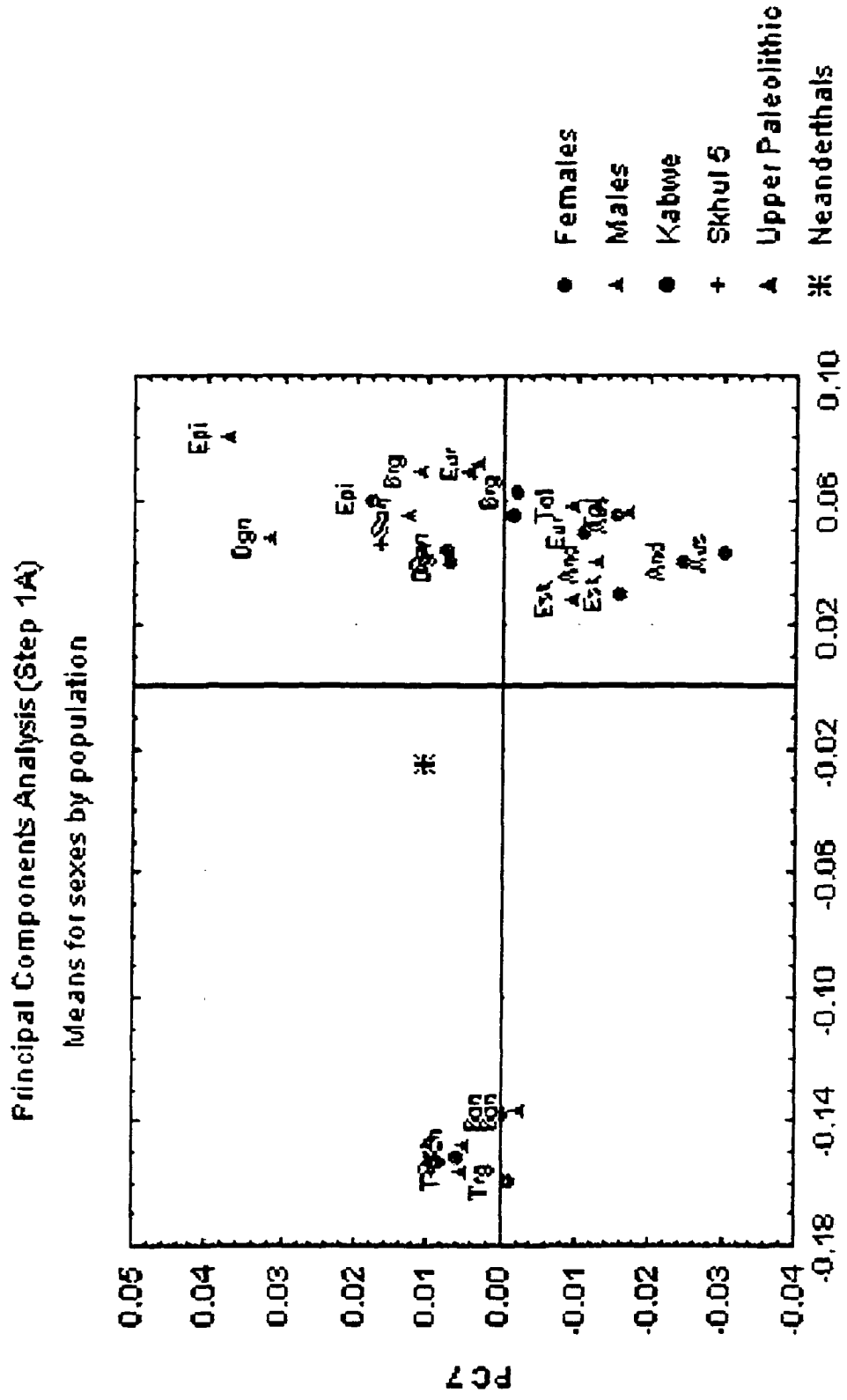

Figure 3.10: Principal Components Analysis (Step 1A), means for sexes by population. PCs 1 and 7.

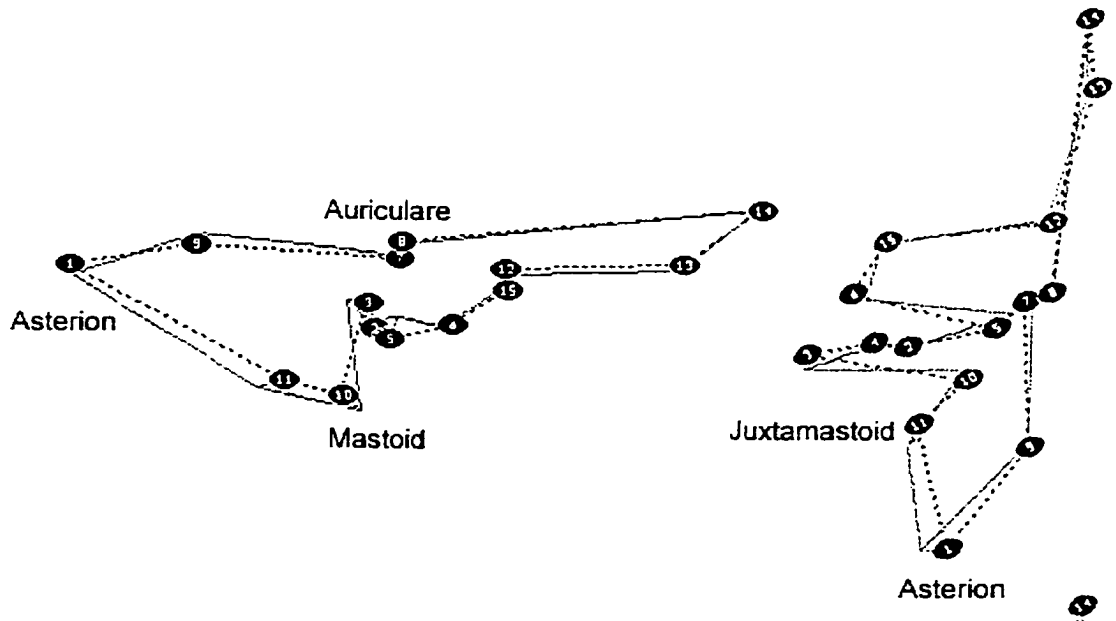

Positive end of PC 7 (Males)

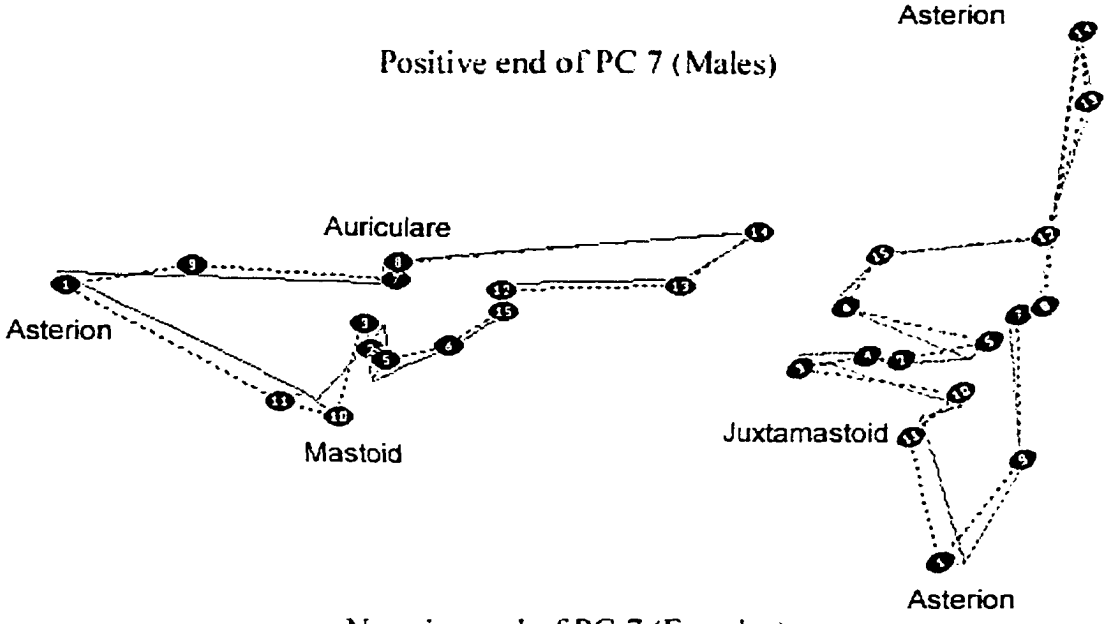

Negative end of PC 7 (Females)

Figure 3.11: Shape variation along PC 7 (Step 1A), right lateral (left) and right ventral (right) views. The dotted line represents the consensus configuration.

Table 3.6: Summary of the CVA results and Correlation Analysis, CaVs 1-5, Step 1A.

	Canonical Variates Analysis			Correlation with Centroid Size	
	Eigenvalue	Proportion	Cumulative	Rho	Pr > F
CaV 1	24.1714	0.6895	0.6895	0.00367	0.9448
CaV 2	2.1065	0.0601	0.7496	0.01036	0.8451
CaV 3	1.9899	0.0568	0.8064	0.23399	0.0001
CaV 4	1.4857	0.0424	0.8488	-0.11889	0.0245
CaV 5	1.4404	0.0411	0.8899	0.60484	0.0001

The shape variation along CaV 1 (Fig. 3.13) is similar to that described for PC 1. In the negative end, where chimpanzees and Neanderthals fall relative to modern humans, the tip of the mastoid process (10) is elevated; the juxtamastoid eminence (11) is more medially placed; the lateral origin of the petro-tympanic crest is more anterior and its medial end more posterior; asterion (1) is anteriorly positioned; and auriculare (8) is more lateral. These shape differences characterize chimpanzees and, to a lesser extent, Neanderthals, relative to modern humans. They can be described as a smaller mastoid process which is more widely separated from the juxtamastoid eminence, a more coronal orientation of the petro-tympanic crest, an antero-posteriorly shorter mastoid portion of the temporal bone, and a stronger supramastoid crest.

CaV 2 summarizes 6 % of the variance. It separates the chimpanzee species, the majority of bonobos falling on its negative side, although the difference between them is not significant. Among modern humans, CaV 2 completely separates the Andamanese in the positive end from the San in the negative end, the mean scores of these two populations being significantly different from each other along this canonical axis. All other modern human populations fall in between these two, with the Dogon closer to the San and between the San and the other modern human groups. Neanderthals fall entirely within the modern human range, as do Kabwe and the three early anatomically modern humans. CaV 2 is mostly influenced by PCs 2 and 3. The shape differences along this axis include, on the positive extreme, an elevated and more anterior asterion, a more inferior the tip of the mastoid, an elevated and more posterior zygomatic suture, and a more medial placement of the medial end of the petro-tympanic crest and the entoglenoid pyramid. These differences characterize the Andamanese compared to the San. Although this canonical axis appears to be separating large-bodied populations from small-bodied ones, it is not correlated with centroid size.

CaV 3 (5.7 %, Fig. 3.13) separates bonobos from common chimpanzees, the former clustering on its positive side. Skhul 5 and the two Upper Paleolithic specimens fall at the positive extreme of this axis. The mean score for the Upper Paleolithic specimens the latter group being significantly different from most human populations except Neanderthals and the Berg. These specimens fall at the extreme of the 95 % confidence ellipses for modern human populations along CaV 3. Neanderthals span the

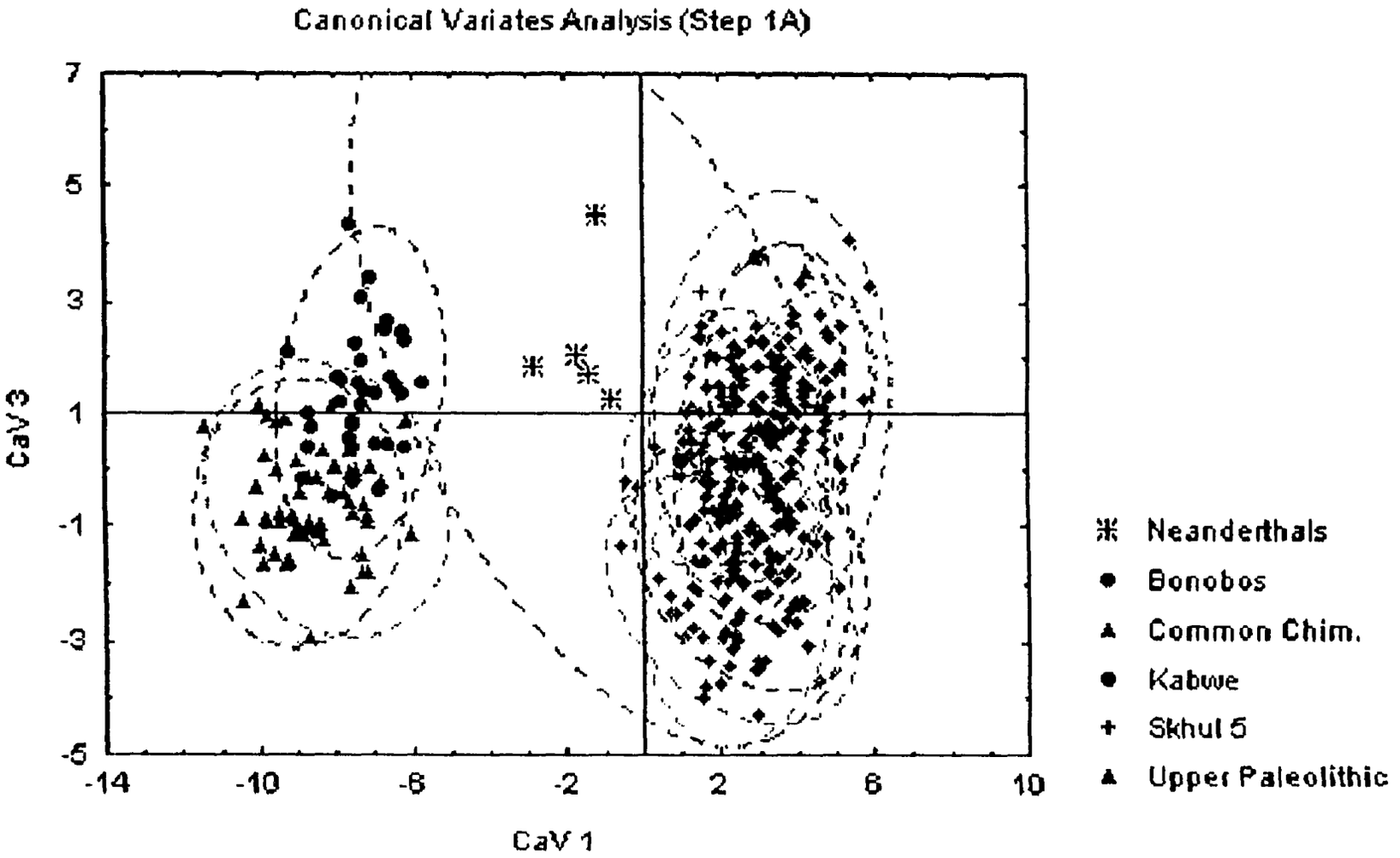

Figure 3.12: Canonical Variates Analysis (Step 1A), CaVs 1 and 3. Dotted lines represent the 95 % confidence ellipses for each group.

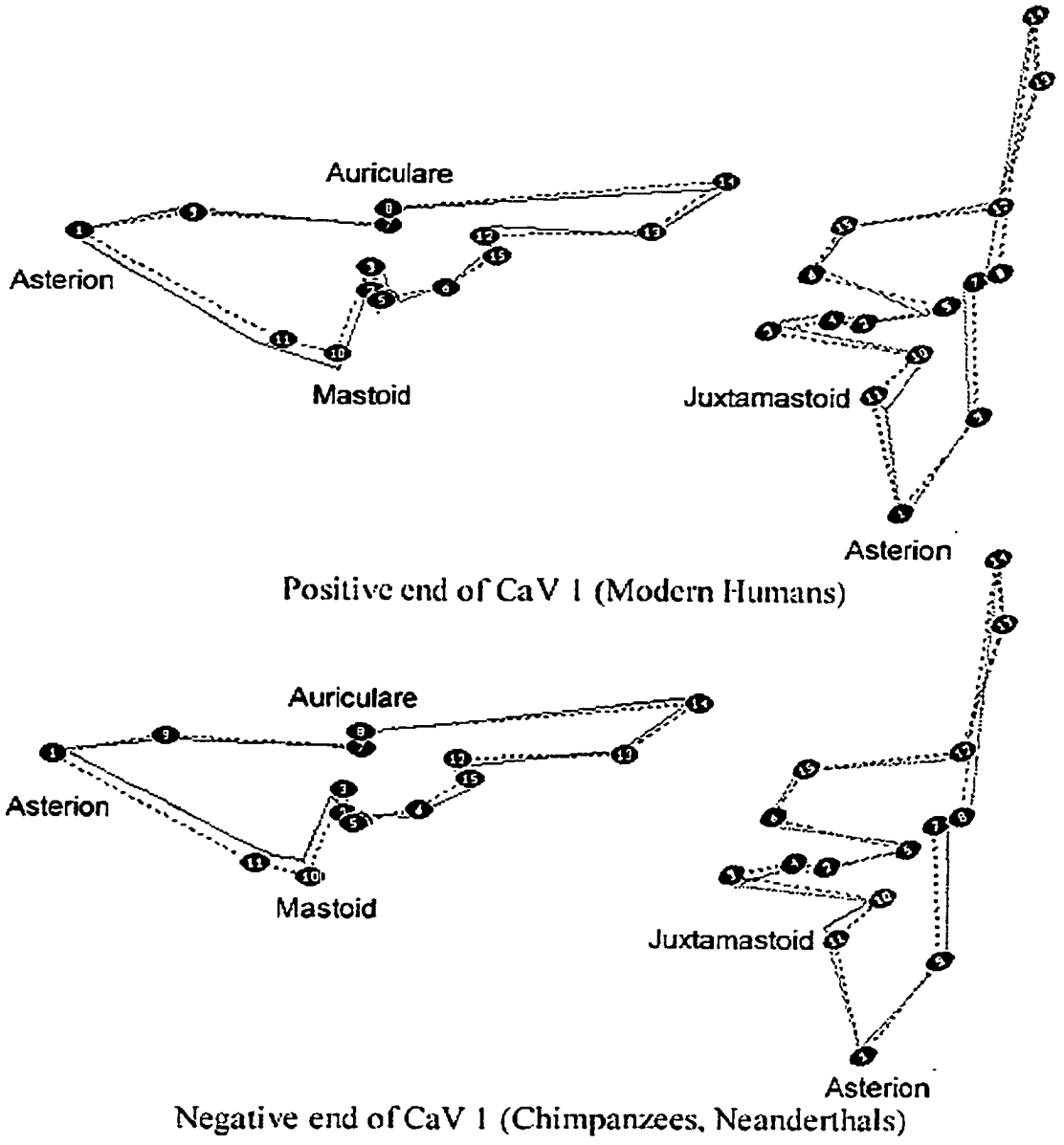

Figure 3.13: Shape variation along CaV 1 (Step 1A), right lateral (left) and right ventral (right) views. The dotted line represents the consensus configuration.

positive side of the modern human range, with La Ferrassie 1 falling outside its positive end and Amud 1 falling near its center, while Kabwe falls close to the center of the modern human cloud. CaV 3 also partially separates the San, the Dogon and the Andamanese on the negative side from the Australians, the Eskimo, the Tolai, the Epipaleolithic group, the Berg and the mixed European population on the positive. The Andamanese are significantly different from all other human groups except the Dogon along this axis.

CaV 3 is mostly influenced by PCs 8 and 9. The shape variation along it (Fig. 3.14) includes, in the positive end, more medially placed zygomatic suture (13, 14) and asterion (1); a more laterally and inferiorly placed root of the articular eminence (12); and elevated and laterally placed porion and auriculare. These shape differences can be described as a wider glenoid and tympanic area, a relatively shallow glenoid fossa and an elevation of the auditory meatus relative to the zygomatic process and the floor of the glenoid fossa. They characterize La Ferrassie 1, Skhul 5, Cro Magnon 1, Predmosti 3 and, to some extent, the other Neanderthal specimens except Amud 1, relative to most modern humans. They also characterize bonobos relative to common chimpanzees.

CaV 4 (4.2 %, mostly influenced by PCs 16, 7 and 3) separates the two chimpanzee species, but also places Neanderthals and Kabwe at the positive end of the modern human range. When the ANOVA is performed at the species level, Neanderthals are found to be significantly different from modern humans as a whole along this axis. At the population level, they are significantly different from most modern human groups, but not from the Epipaleolithic, the Berg and the Andamanese. Skhul 5 and the two Upper Paleolithic specimens fall near the center of the modern human sample along this axis. Among modern humans, the Epipaleolithic fall at the positive end overlapping with the Neanderthals and Kabwe, while the Eskimo fall at the negative end. The shape differences at the positive end of this axis include a lateral placement of auriculare relative to porion, indicating a strong supramastoid crest, a more inferior tip of the juxtamastoid eminence, indicating a larger size for this structure, and a slightly shorter zygomatic process antero-posteriorly. CaV 4 is not correlated with centroid size (Table 3.6).

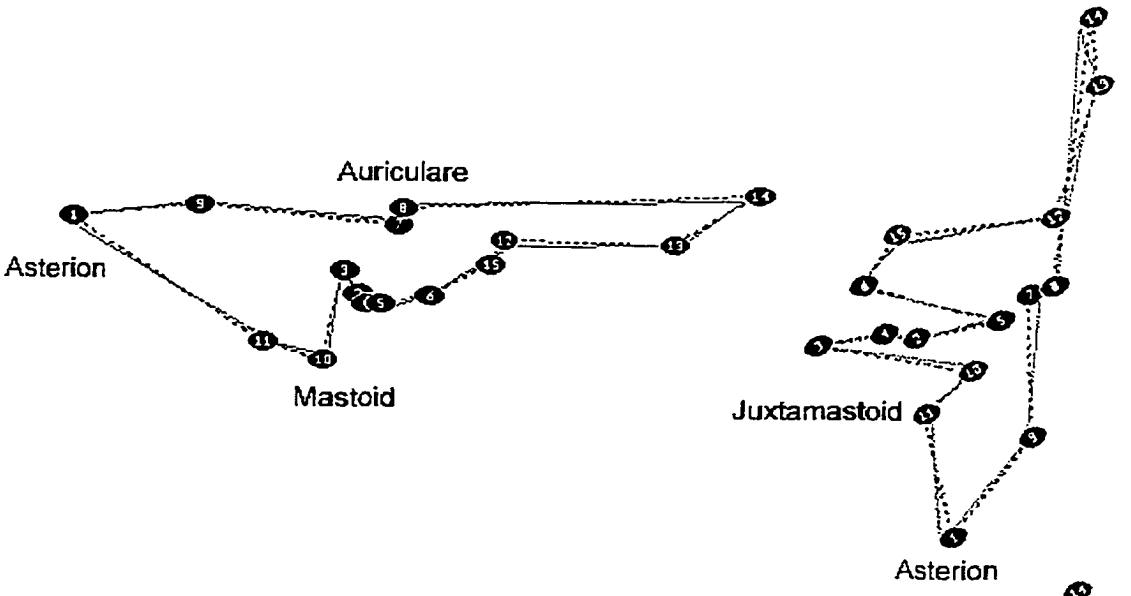

Positive end of CaV 3 (Upper Paleolithic, Neanderthals)

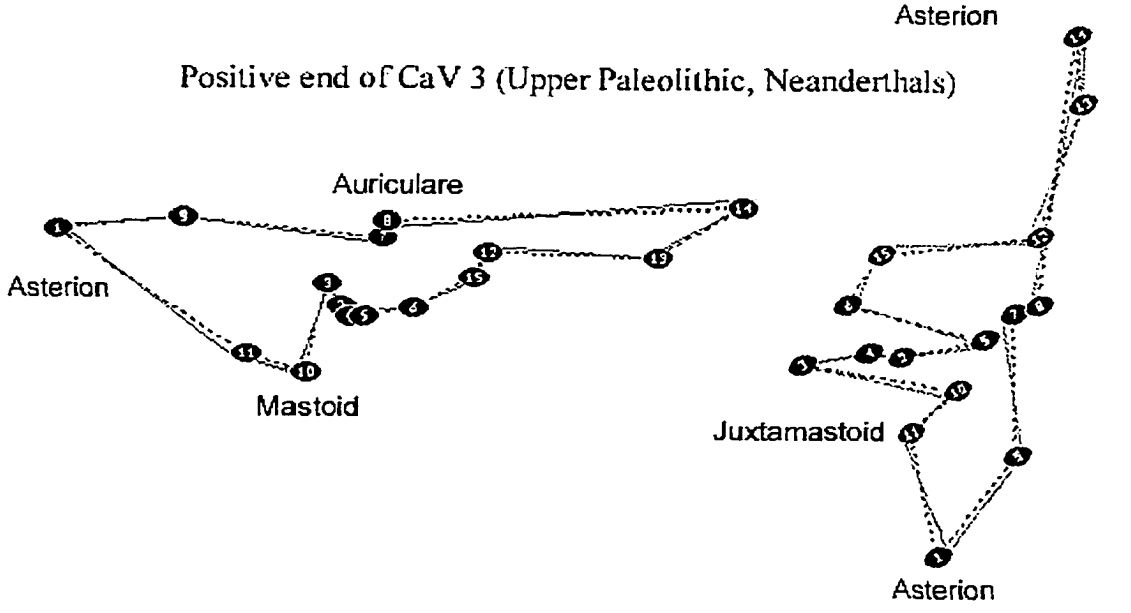

Negative end of CaV 3

Figure 3.14: Shape variation along CaV 3 (Step 1A), right lateral (left) and right ventral (right) views. The dotted line represents the consensus configuration.

Classification: A discriminant analysis was performed excluding Kabwe, Skhul 5, Cro Magnon 1 and Predmosti 3, which were treated as unknowns to be classified into one of the other groups by posterior probability. Skhul 5 and Predmosti 3 were classified as Berg, with a posterior probability of 0.8 and 0.74 respectively, while Cro Magnon was classified as European (0.4). Kabwe was classified as Australian (0.63). A cross-validation classification was obtained for the entire dataset and the results are summarized in Table 3.7. Classification success varied. No human was misclassified as chimpanzee and vice versa. In the human sample, no modern human was misclassified as Neanderthal, although one Neanderthal, Amud 1, was misclassified as a modern human (Epipaleolithic). Of the two Upper Paleolithic specimens, Cro Magnon 1 is classified correctly while Predmosti 3 is misclassified as Berg. The highest classification success overall were achieved by the Andamanese (96.67 %), the bonobos (94.29 %) and the San (93.33 %). The success rates of these two modern human groups reflect their distinctiveness among the modern human populations included here. The lowest success rate was 43.33 % for the mixed European group. As expected, a very large proportion of the Berg (25 %) were misclassified as European and vice versa (26.77 %). Furthermore, as the mixed European group is not a population in the biological sense, but includes specimens from widely separate geographic localities, European specimens were also misclassified as Andamanese, Australian, Epipaleolithic and Eskimo. In the chimpanzee sample, only 1 out of 35 bonobos was misclassified as *P .t. schweinfurthii* and 1as *P. t. troglodytes*. The two common chimpanzee subspecies show high levels of misclassification among themselves (higher than 30 % for both). One *P.t. schweinfurthii* but no *P. t. troglodytes,* were misclassified as bonobos.

Mahalanobis D^2, Cluster Analysis and Minimum Spanning Tree: The unbiased Mahalanobis distances between pairs of groups were calculated (Table 3.8). Neanderthals are more distant from chimpanzees than they are from modern humans. They are more distant from modern humans than the two chimpanzee species and subspecies are from each other. They are also more distant from the modern human groups than any modern human population is from another. The group that is closest to Neanderthals is the Eskimo population, and the one that is most distant from them is the Andamanese population. The two European groups are not close to Neanderthals, the

Berg being the second most removed modern human group from them. The Andamanese also appear very widely separated from all human groups. The distances between modern human populations are much greater than that between the two common chimpanzee subspecies, and are also much greater than the distance between the chimpanzee species. The smallest distance among the modern human groups is that between the Berg and the European, while the greatest is that between the San and the Andamanese. All modern human populations are closest neighbors with their geographic neighbors in this analysis (European, Australo-Melanesian and sub-Saharan African pairs). The Upper Paleolithic specimens are quite distant from the recent human populations, being closest to the Berg and most distant from the Andamanese. They are also very distant from the Neanderthals, the distance between them being the highest one among all human groups. Kabwe appears almost equidistant from modern humans and Neanderthals. The great distances observed between the two Upper Paleolithic European specimens and other groups may be overestimated due to the very small sample size which probably underestimates the variation in this population.

A cluster analysis (UPGMA) and a minimum spanning tree analysis were performed on the squared root of the D^2 (Fig. 3.15). The two chimpanzee species cluster on a separate branch from the human sample, with the two common chimpanzee subspecies clustering very close to each other. Neanderthals are outliers to all other human groups. They are greatly separated from modern humans, with a distance that is almost twice as great as that among recent human populations. The two Upper Paleolithic specimens are outliers to all other recent human populations, reflecting the great distance of this group to the recent groups. The two European populations, as well as the Australians and the Tolai, cluster close together within a larger European-Asian-Melanesian branch, which also includes the Eskimo and the Epipaleolithic from N. Africa. The two sub-Saharan African groups, the San and the Dogon, cluster together on a separate branch with a deeper split, reflecting a greater distance between these two populations. The Andamanese are placed on their own branch, relatively distant from all other recent groups. Modern human populations, therefore, cluster geographically in their temporal bone morphology. The position of the Andamanese as the most distinct group may be due to the isolation of this island population, and the separate sub-Saharan

African branch with its deep splitting indicates a large amount of morphological distance compared to the other geographically related groups, the two European and the two Australian-Melanesian populations.

The minimum spanning tree (Fig. 3.15) shows that Neanderthals are widely separated from the modern human groups. They are linked to the Eskimo as their closest neighbors, although this distance is very large and probably does not reflect any substantial similarity. The Upper Paleolithic specimens are linked to the Berg population from Austria and also appear quite distant from the recent human groups.

Step 1B – Human sample only

Principal Components Analysis: In this analysis Neanderthals are less clearly separated from modern humans in the first few principal components than in Step 1A. They cluster on the positive side along PC 3, and are more clearly separated along PC 9. PC 3 (8.7 %, Fig. 3.16) is significant for population effects to the 0.0001 level and for sex effects at the 0.001 level. Neanderthals are significantly different from some modern human populations, including the Epipaleolithic, San, Berg and Upper Paleolithic specimens. When the ANOVA is conducted at the species level, Neanderthals are significantly different from modern humans along this component. Neanderthals cluster near the positive end of this axis, Saccopastore 2 falling outside the modern human range, and La Ferrassie 1 overlapping most with it. Kabwe is also separated from modern humans on the negative end of PC 3. Skhul 5 and the two Upper Paleolithic specimens fall very close together near the center of the modern human range. Among modern human groups, PC 3 separates the Eskimo on its positive side from the Berg, the mixed European population and the Epipaleolithic on the negative side. When PC 3 is labeled by sex, a weak tendency is observed for most females to have more positive scores than most males. When the means for the sexes are plotted by population (Fig. 3.17), a weak tendency is observed for the female means to be more positive along this component than the male mean values.

The shape variation along PC 3 (Table 3.10, Fig. 3.18) in the negative end of PC 3, where Kabwe falls, includes a more inferiorly placed asterion (1); a more posteriorly, inferiorly and laterally placed juxtamastoid eminence (11) and a more laterally placed

Table 3.7: Cross-validation classification summary, Step 1A (percentages for each population in bold).

	And	Aus	Brg	Dgn	Epi	Esk	Eur	San	Tol	UP	Bon	Nea	Sch	Trg	Total
And	30	0	0	0	0	0	0	0	0	0	0	0	0	0	30
%	**100**	0	0	0	0	0	0	0	0	0	0	0	0	0	100
Aus	1	22	1	0	0	3	1	0	2	0	0	0	0	0	30
%	3.33	**73.33**	3.33	0	0	10	3.33	0	6.67	0	0	0	0	0	100
Brg	0	0	20	0	0	0	7	0	1	0	0	0	0	0	28
%	0	0	**71.43**	0	0	0	25	0	3.57	0	0	0	0	0	100
Dgn	0	1	0	22	0	3	0	2	0	0	0	0	0	0	28
%	0	3.57	0	**78.57**	0	10.71	0	7.14	0	0	0	0	0	0	100
Epi	0	0	0	1	19	0	1	0	0	0	0	0	0	0	21
%	0	0	0	4.76	**90.48**	0	4.76	0	0	0	0	0	0	0	100
Esk	0	0	0	1	0	25	3	0	1	0	0	0	0	0	30
%	0	0	0	3.33	0	**83.33**	10	0	3.33	0	0	0	0	0	100
Eur	3	1	8	0	2	0	13	0	3	0	0	0	0	0	30
%	10	3.33	26.67	0	6.67	0	**43.33**	0	10	0	0	0	0	0	100
San	0	1	0	1	0	0	0	28	0	0	0	0	0	0	30
%	0	3.33	0	3.33	0	0	0	**93.33**	0	0	0	0	0	0	100
Tol	0	6	0	0	1	2	0	0	21	0	0	0	0	0	30
%	0	20	0	0	3.33	6.67	0	0	**70**	0	0	0	0	0	100
UP	0	0	1	0	0	0	0	0	0	1	0	0	0	0	2
%	0	0	50	0	0	0	0	0	0	**50**	0	0	0	0	100
Bon	0	0	0	0	0	0	0	0	0	0	33	0	1	1	35
%	0	0	0	0	0	0	0	0	0	0	**94.29**	0	2.86	2.86	100
Nea	0	0	0	0	1	0	0	0	0	0	0	5	0	0	6
%	0	0	0	0	16.67	0	0	0	0	0	0	**83.33**	0	0	100
Sch	0	0	0	0	0	0	0	0	0	0	1	0	17	10	28
%	0	0	0	0	0	0	0	0	0	0	3.57	0	**60.71**	35.71	100
Trg	0	0	0	0	0	0	0	0	0	0	0	0	9	19	28
%	0	0	0	0	0	0	0	0	0	0	0	0	32.14	**67.86**	100
Total	34	31	30	25	23	33	25	30	28	1	34	5	27	30	356
%	9.55	8.71	8.43	7.02	6.46	9.27	7.02	8.43	7.87	0.28	9.55	1.4	7.58	8.43	100

Table 3.8: Unbiased Mahalanobis D^2, Step 1A. All distances 0.001 significance level except: NS = non-significant, * = 0.05 level, ** = 0.01 level.

	And	Aus	Brg	Dgn	Epi	Esk	Eur	Kbw	San	Skh5	Tol	UP	Bon	Nea	Sch	Trg
And	0.00	24.73	30.20	25.83	33.84	31.23	27.41	67.72	39.59	100.42	25.71	74.78	116.51	85.01	123.87	138.10
Aus	24.73	0.00	16.45	20.43	24.95	14.20	10.45	57.09	22.69	81.42	5.72	52.93	106.71	73.68	116.92	132.46
Brg	30.20	16.45	0.00	26.37	18.45	25.02	4.83	64.18	29.73	75.60	15.68	41.67	131.80	80.42	147.71	166.87
Dgn	25.83	20.43	26.37	0.00	21.73	18.39	16.40	67.23	14.13	108.44	22.50	73.39	113.91	69.09	117.29	131.66
Epi	33.84	24.95	18.45	21.73	0.00	27.50	14.34	68.78	33.94	93.21	23.62	46.73	137.57	65.86	152.29	168.95
Esk	31.23	14.20	25.02	18.39	27.50	0.00	17.50	80.74	27.63	106.27	13.98	41.77	103.12	56.73	114.02	129.45
Eur	27.41	10.45	4.83	16.40	14.34	17.50	0.00	63.74	24.52	78.85	11.11	45.67	120.30	73.20	134.57	151.72
Kbw	67.72	57.09	64.18	67.23	68.78	80.74	63.74	0.00	58.35	125.41	75.99	96.68	118.40	75.38	148.73	152.17
San	39.59	22.69	29.73	14.13	33.94	27.63	24.52	58.35	0.00	107.97	24.05	68.96	115.75	76.60	135.22	151.04
Skh5	100.42	81.42	75.60	108.44	93.21	106.27	78.85	125.41	107.97	0.00	85.24	71.26**	159.48	144.74	173.30	188.77
Tol	25.71	5.72	15.68	22.50	23.62	13.98	11.11	75.99	24.05	85.24	0.00	48.54	117.28	76.43	128.57	146.51
UP	74.78	52.93	41.67	73.39	46.73	41.77	45.67	96.68	68.96	71.26**	48.54	0.00	163.25	86.14	179.41	196.35
Bon	116.51	106.71	131.80	113.91	137.57	103.12	120.30	118.40	115.75	159.48	117.28	163.25	0.00	86.81	20.47	22.43
Nea	85.01	73.68	80.42	69.09	65.86	56.73	73.20	75.38	76.60	144.74	76.43	86.14	86.81	0.00	103.23	115.14
Sch	123.87	116.92	147.71	117.29	152.29	114.02	134.57	148.73	135.22	173.30	128.57	179.41	20.47	103.23	0.00	2.16**NS**
Trg	138.10	132.46	166.87	131.66	168.95	129.45	151.72	152.17	151.04	188.77	146.51	196.35	22.43	115.14	2.16**NS**	0.00

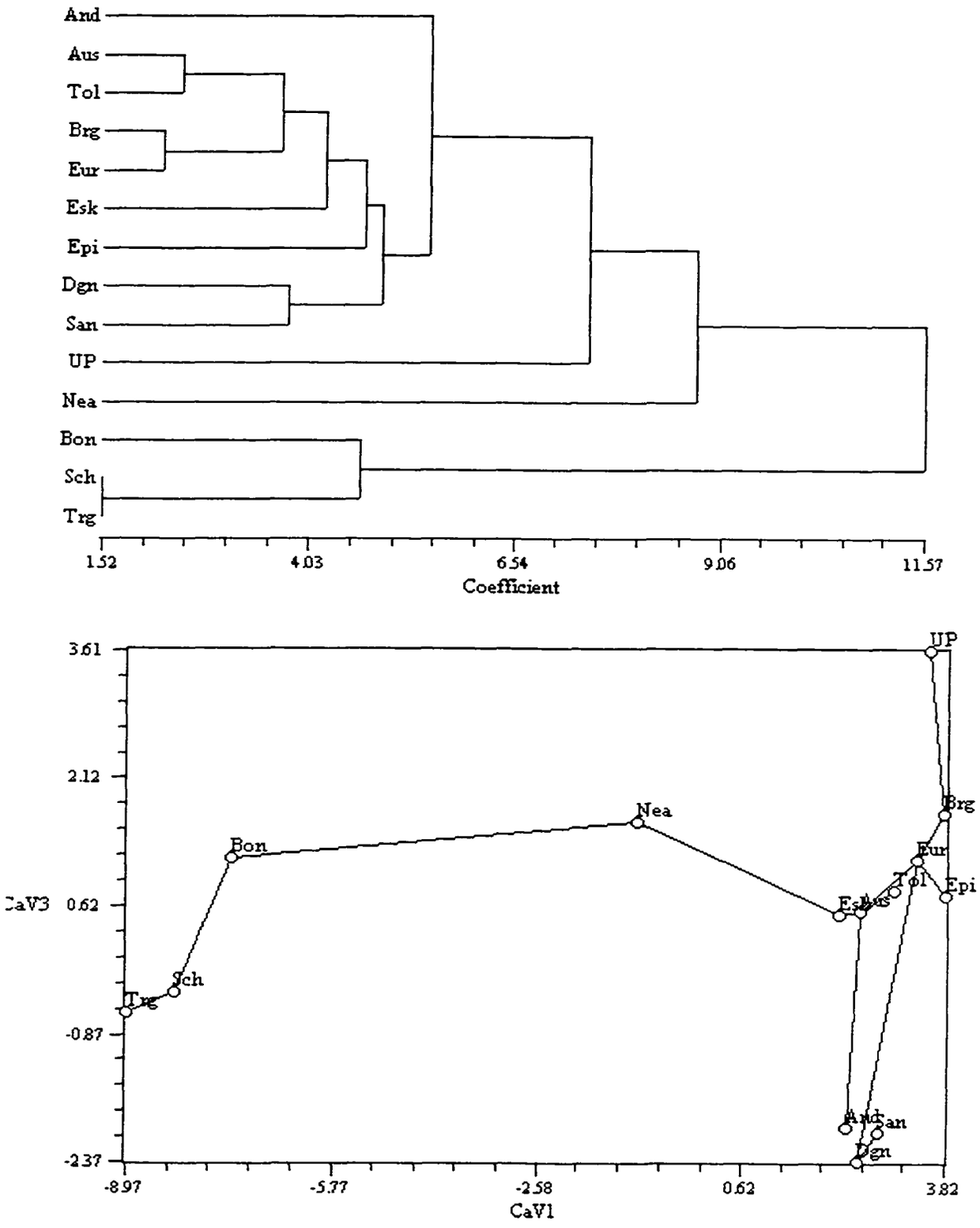

Figure 3.15: Cluster analysis (UPGMA, top) and minimum spanning tree (bottom), excluding singletons (Step 1A), based on Mahalanobis distances (D).

mastoid process (10); and a depressed zygomatic suture (14, 13). These shape traits characterize Kabwe relative to all modern humans and Neanderthals, and some of them are similar to the shape differences found in PC 5 of Step 1A. The opposite shape differences, an elevated asterion, a more anterior and medial placement of the juxtamastoid and the mastoid process tip and an elevated zygomatic suture characterize Saccopastore, and, to a lesser degree, the other Neanderthal specimens relative to most modern humans. PC 3 is not correlated with centroid size (Table 3.9).

PC 9 (4 % of the total variance, Fig. 3.16) is significant population effects (0.0001), and along it Neanderthals are significantly different from all modern human populations. It separates Neanderthals on its positive end from modern humans, with the exception of Amud 1, which falls well within the modern human range. Kabwe and Predmosti 3 fall on near the positive end of the modern human range, while Skhul 5 and Cro Magnon 1 fall near its center. Among modern human populations the Europeans, Berg and Epipaleolithic tend to be more positive, and the San, Dogon and Andamanese more negative.

The shape differences at the positive end of PC 9 (Table 3.10, Fig. 3.19) include a more anterior and lateral placement of the lateral origin of the petro-tympanic crest (5); a lateral and superior placement of both porion (7) and auriculare (8); a posterior position of the entoglenoid pyramid; and a more inferior and lateral placement of the root of the articular eminence. These differences can be described as an anterior origin and coronal orientation of the petro-tympanic crest, a wide tympanic and glenoid area, a shallow glenoid fossa with a posteriorly placed entoglenoid pyramid, and an elevated porion relative to both the zygomatic suture and the floor of the glenoid fossa. PC 9 is not strongly correlated with centroid size (Table 3.9).

An additional principal component, PC 1 is significant for sex effects at the 0.001 level. Along this axis females tend to have more negative scores than males. When the mean scores of each sex for PC 1 are plotted by population (Fig. 3.17), a strong tendency is observed for the female mean values to be more negative than males across all populations. PC 1 also separates the San on the negative side from the Epipaleolithic on the positive and these two populations are significantly different from each other. Neanderthals, Kabwe, Skhul 5 and the two Upper Paleolithic specimens, both male, fall

well within the modern human range but on the negative side. The shape differences in the negative end include a small mastoid process and juxtamastoid eminence, an antero-posteriorly long and supero-inferiorly short mastoid portion of the temporal bone, and an antero-posteriorly elongated zygomatic process. These shape differences characterize females relative to males, as well as the San relative to the Epipaleolithic, and are similar to those found in Step 1A. They are not related to centroid size differences.

Canonical Variates Analysis: The CVA (Table 3.11) was performed on the first 30 principal components (97.1 % of the total variance). Neanderthals are best separated along CaV 3, but also cluster at the extremes of the modern human range along CaVs 2 and 5. The first canonical axis (22 %) separates the sub-Saharan African populations on its negative side from the remaining modern human groups on the positive side, while Neanderthals also fall on the negative side overlapping with the San.

Neanderthals are separated from modern humans on the positive extreme of CaV 3 (16 % of the total variance, mostly influenced by PC 3, Fig. 3.20). They overlap only with the positive fringe of the modern human range, Amud 1 falling within the 95 % confidence ellipse of the Eskimo along CaVs 1 and 3. They are significantly different from all modern human populations in their mean score on CaV 3. Kabwe and the early modern human specimens fall near the center of the human range. This axis also separates the Eskimo on the positive side from the remaining modern human groups. The shape variation at the positive end of CaV 3 (Fig, 3.21) includes an elevated position of the superior aspect of the zygomatic suture (14); a more superior and lateral placement of auriculare (8); an inferior position of the root of the articular eminence (12); an anterior lateral origin of the petro-tympanic crest (5); and an elevated and posteriorly placed asterion (1). They can be described as a supero-inferiorly thick zygomatic process, a shallow glenoid fossa, a coronally oriented petro-tympanic crest, a more robust supramastoid crest and a shorter mastoid portion of the temporal bone. CaV 3 is only weakly correlated with centroid size.

Neanderthals also cluster at the positive end of CaV 2 (18.8 %, most strongly influenced by PCs 2 and 9, Fig. 3.20). Neanderthals are significantly different from all modern human populations except the Berg, Epipaleolithic and Upper Paleolithic group.

Table 3.9: Summary of the PCA results, ANOVA and Correlation Analysis for PCs 1-10, Step 1B.

	Principal Components Analysis			ANOVA, Pr > F			Correlation with Centroid Size	
	Eigenvalue	Proportion	Cumulative	Popul.	Sex	Interaction	Rho	Pr > F
PC 1	0.001591	0.122274	0.122274	0.0001	0.0003	0.8948	0.0933	0.1284
PC 2	0.00144	0.110705	0.232979	0.0001	0.1347	0.2022	0.26868	0.0001
PC 3	0.001141	0.087679	0.320658	0.0001	0.0054	0.8162	0.13496	0.0275
PC 4	0.000796	0.061211	0.381869	0.0001	0.1485	0.3119	0.08558	0.1632
PC 5	0.000777	0.059702	0.441571	0.0011	0.2049	0.9082	-0.34569	0.0001
PC 6	0.00073	0.056131	0.497702	0.0001	0.1813	0.1543	0.17158	0.0049
PC 7	0.000629	0.048324	0.546026	0.0001	0.0985	0.2802	0.13114	0.0322
PC 8	0.000548	0.042136	0.588161	0.0001	0.7687	0.0751	0.18868	0.002
PC 9	0.000527	0.040471	0.628632	0.0001	0.0640	0.9366	0.3306	0.0001
PC 10	0.00046	0.035373	0.664005	0.3689	0.8019	0.1098	-0.00632	0.9181

Table 3.10: Squared roots of the sum of squares of the eigenvector coefficients for the three coordinates of each landmark. – Step 1B.

	PC 1	PC 2	PC 3	PC 4	PC 5	PC 6	PC 7	PC 8	PC 9	PC 10
1. Asterion	**0.41**	0.20	**0.39**	**0.48**	**0.30**	0.25	0.22	**0.27**	0.27	**0.64**
2. Stylom. F.	0.06	0.17	0.15	0.20	0.03	0.17	0.11	0.12	0.17	0.14
3. Md. Jug.	0.06	**0.27**	0.20	**0.31**	0.10	0.24	0.17	**0.54**	0.27	**0.29**
4. Lt. Jug.	0.05	0.10	0.18	0.23	0.05	0.14	0.12	0.21	0.23	0.18
5. Lt. Petro-Tym. Cr,	0.23	0.11	0.10	0.26	0.31	**0.42**	**0.51**	0.16	**0.41**	0.10
6. Md. Petro-Tym. Cr.	0.08	0.18	0.25	0.21	0.08	**0.32**	0.04	**0.39**	0.18	0.17
7. Porion	0.12	0.08	0.22	0.06	0.15	0.09	0.22	0.18	**0.33**	0.09
8. Auriculare	0.14	0.11	0.23	0.04	0.16	0.13	**0.28**	0.19	**0.30**	0.15
9. Parietal N.	**0.30**	**0.63**	0.11	**0.49**	**0.41**	0.16	**0.44**	**0.33**	0.24	**0.43**
10. Mastoid	**0.57**	0.21	**0.27**	**0.37**	**0.36**	**0.43**	0.27	0.19	0.26	0.11
11. Juxt. Em.	**0.30**	**0.45**	**0.45**	0.18	**0.57**	**0.36**	**0.30**	0.20	0.19	0.08
12. Artic. Em.	0.09	0.15	0.24	0.11	0.24	0.10	0.20	0.22	**0.28**	0.15
13. Zyg. Sut.Inf.	**0.38**	0.21	0.26	0.13	0.08	0.16	0.24	0.02	0.05	**0.29**
14. Zyg. Sut. Sup.	0.21	**0.26**	**0.36**	0.14	0.18	**0.31**	0.20	0.21	0.16	0.23
15. Entogl. Pyr.	0.14	0.13	0.19	0.04	0.17	0.22	0.11	0.24	**0.33**	0.15

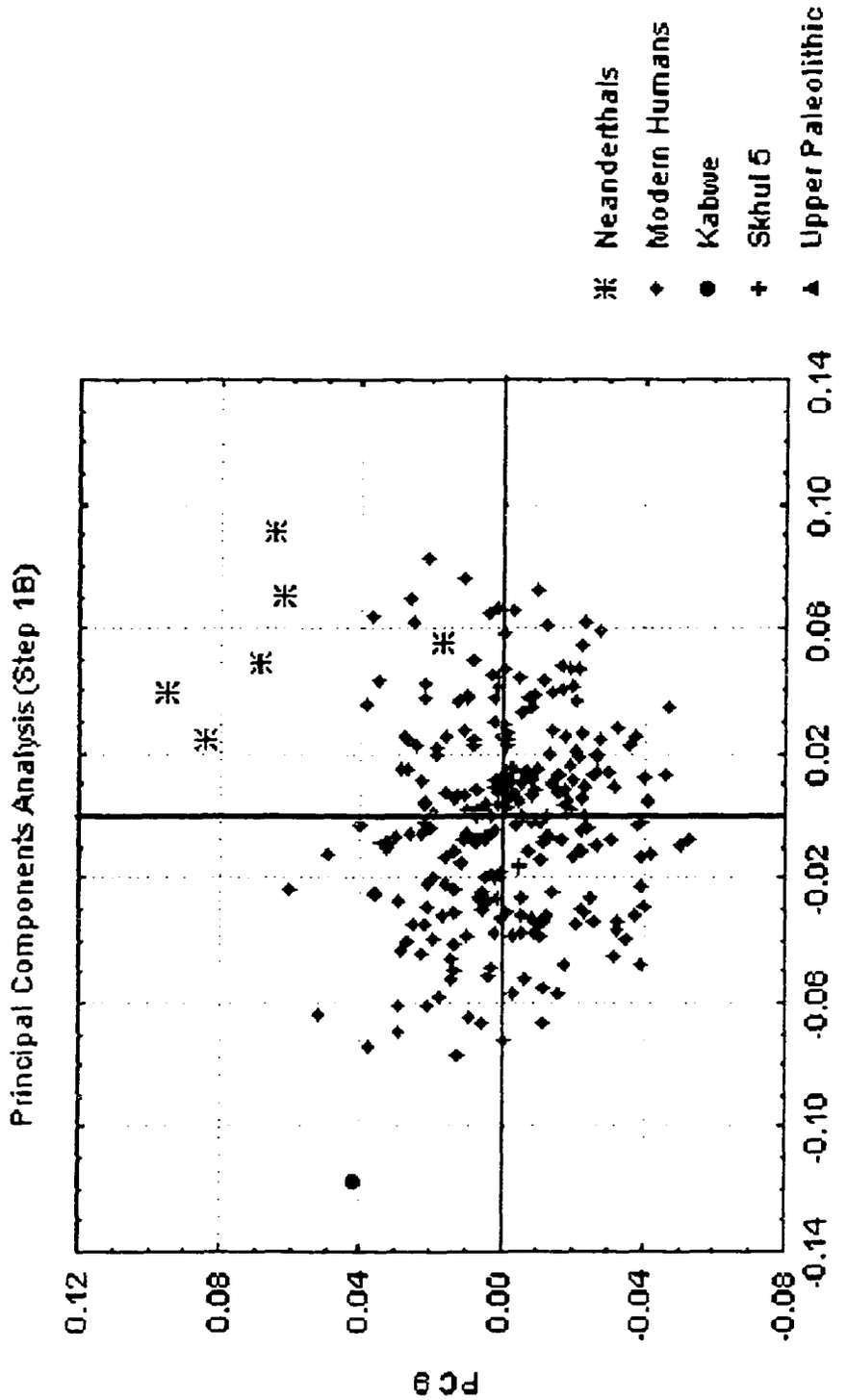

Figure 3.16: Principal Components Analysis (Step 1B), PCs 3 and 9.

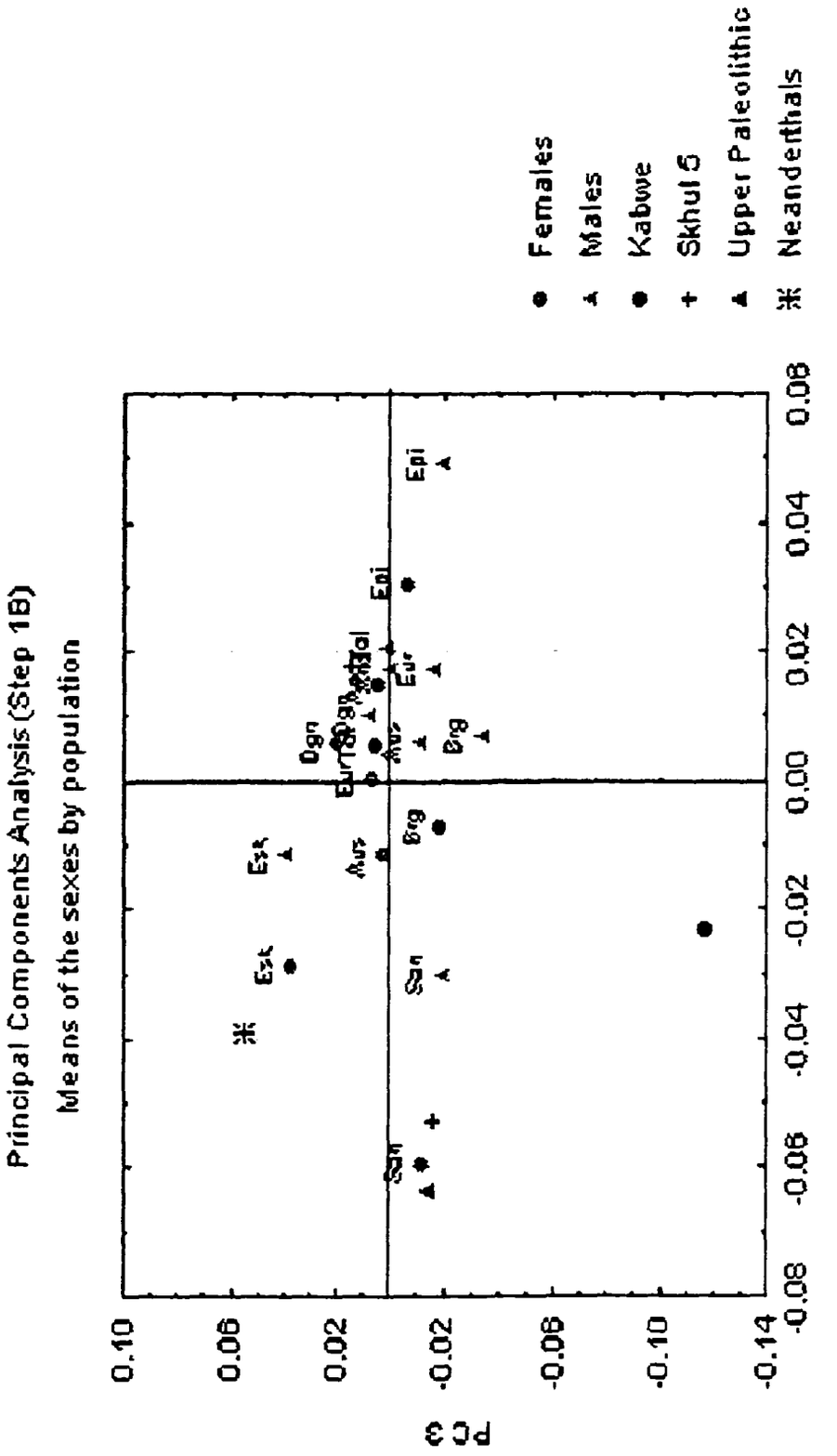

Figure 3.17: Principal Components Analysis (Step 1B), means for sexes by population. PCs 1 and 3.

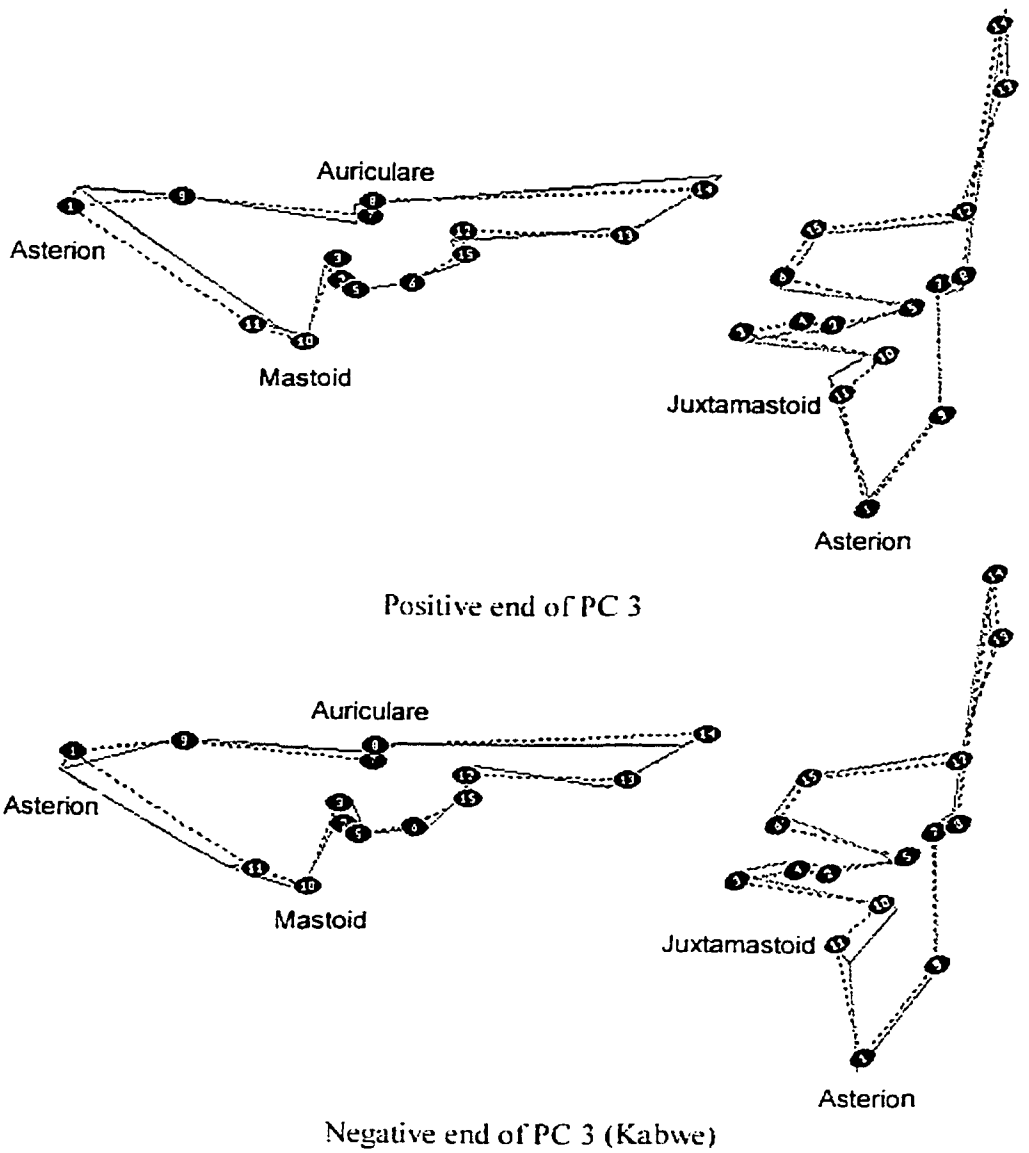

Figure 3.18: Shape variation along PC 3 (Step 1B), right lateral (left) and right ventral (right) views. The dotted line represents the consensus configuration.

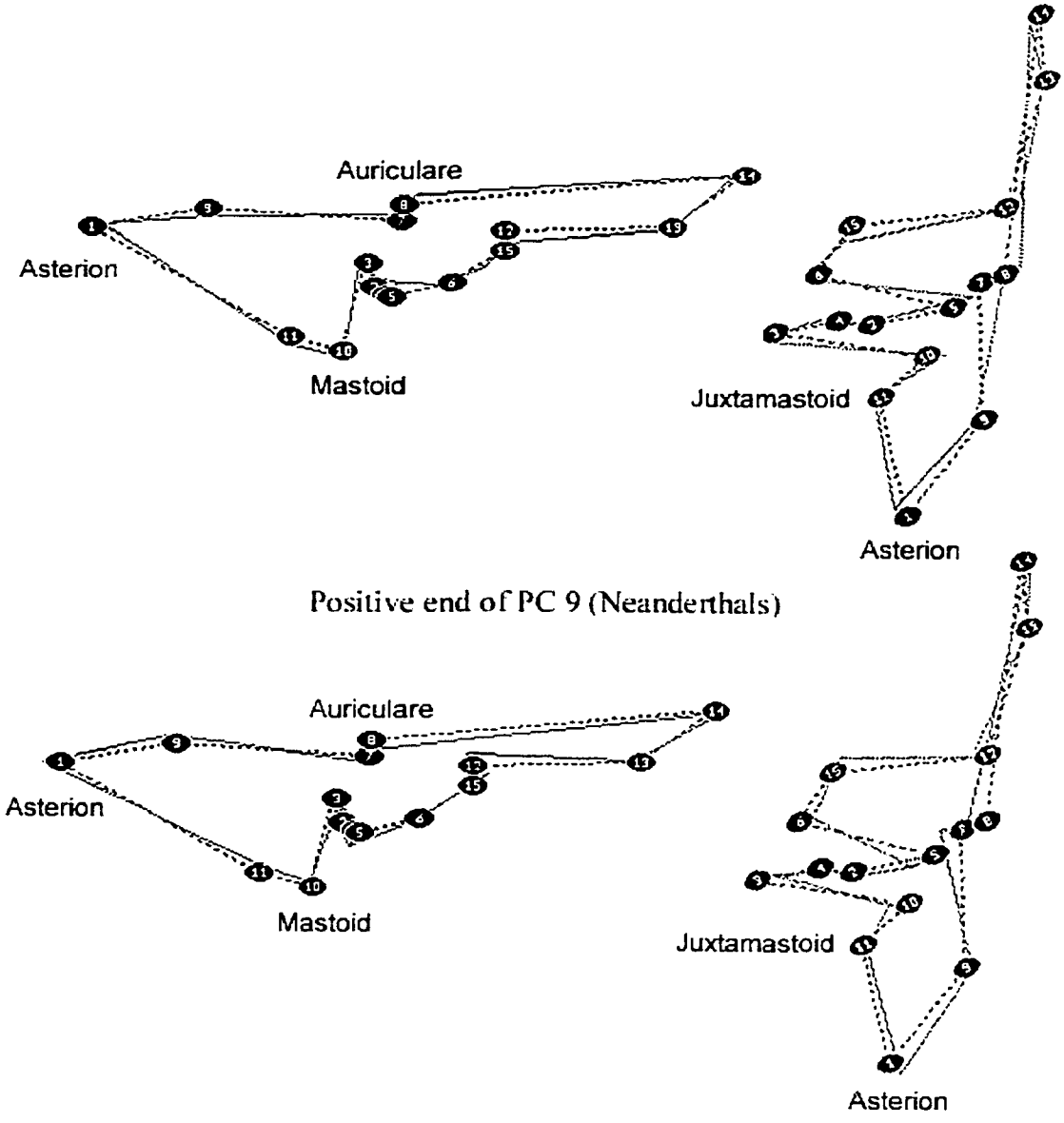

Figure 3.19: Shape variation along PC 9 (Step 1B), right lateral (left) and right ventral (right) views. The dotted line represents the consensus configuration.

Only La Ferrassie 1 falls outside the modern human range along this axis, the other Neanderthal specimens falling at its positive end. The two Upper Paleolithic specimens also fall at the positive end of the modern human cloud, Predmosti 3 falling just outside it. Kabwe and Skhul 5 fall near its center. Among modern human groups, the Andamanese are separated on the negative end of CaV 2 from the remaining populations. The shape differences at the positive end of CaV 2 (Fig. 3.22) include a more inferior placement of the articular eminence, indicating a shallow glenoid fossa; a more medial position of asterion (1) and of the zygomatic suture (14, 13), indicating perhaps an antero- posteriorly curved temporal bone; and a posterior placement of the parietal notch (9), suggesting an antero-posteriorly short mastoid portion of the temporal. CaV 3 is only weakly correlated with centroid size (Table 3.11).

Neanderthals also fall at the positive extreme of CaV 4 (14.2 %, most strongly influenced by PCs 14 and 9, Fig. 3.23). Circeo 1 falls outside the modern human range, while the other Neanderthal specimens fall at its positive extreme, where they overlap with the Epipaleolithic. The shape differences at the positive end of this axis include a larger and more medially placed juxtamastoid eminence relative to the mastoid process and a more anterior medial end of the jugular fossa. CaV 4 is only very weakly related to centroid size (Table 3.11).

CaV 5 (8.3 %, most strongly influenced by PCs 26 and 4, Fig. 3.23) separates Kabwe, Skhul 5, and partially also Neanderthals, from modern humans on its negative end. Shanidar 1 and La Ferrassie 1 fall outside the modern human cloud, while the other Neanderthal specimens fall near its negative end. The two Upper Paleolithic specimens fall near the center of this axis. The shape differences at the negative end of CaV 5 include a small mastoid process, an inferiorly placed asterion, a more lateral root of the articular eminence and more medial end of the petro-tympanic crest, indicating medio-laterally wider tympanic and glenoid fossa areas. CaV 5 is also only weakly related to centroid size (Table 3.11).

Classification: The results of this analysis were very similar to those described in Step 1A. Here, however, Cro Magnon 1 was classified as Eskimo (0.7) rather than as European. The results of the cross-validation classification (Table 3.12) were also similar to those of Step 1A. Again, no modern human was misclassified as Neanderthal,

Table 3.11: Summary of the CVA results and Correlation Analysis, CaVs 1-5, Step 1B.

	Canonical Variates Analysis			Correlation with Centroid Size	
	Eigenvalue	Proportion	Cumulative	Rho	Pr > F
CaV 1	3.0254	0.2206	0.2206	0.0278	0.9639
CaV 2	2.5805	0.1881	0.4087	0.54555	0.0001
CaV 3	2.1932	0.1599	0.5686	0.24936	0.0001
CaV 4	1.9506	0.1422	0.7108	0.12604	0.0396
CaV 5	1.1377	0.0829	0.7937	0.20191	0.0009

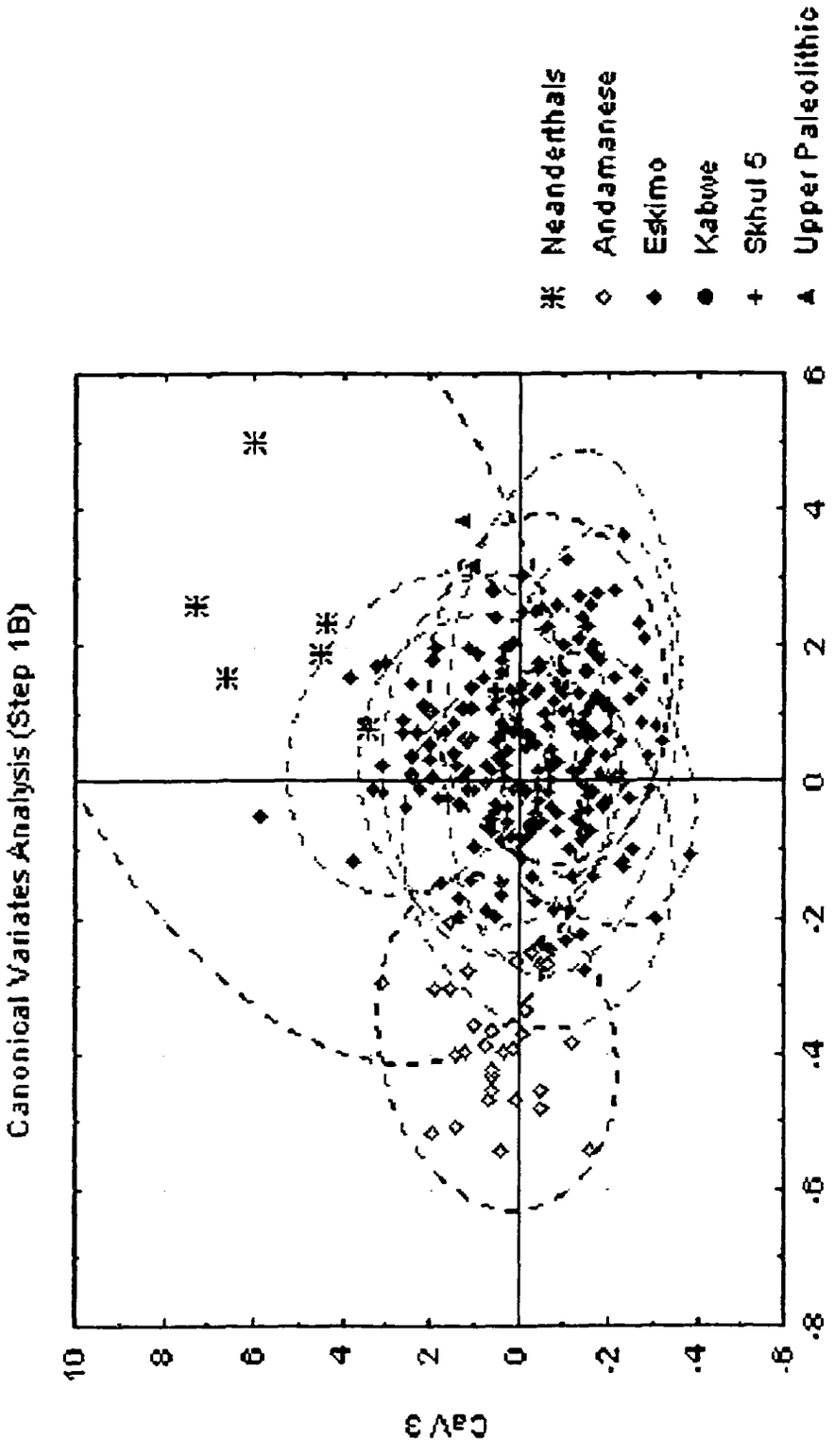

Figure 3.20: Canonical Variates Analysis (Step 1B), CaVs 2 and 3. Dotted lines represent the 95% confidence ellipses for each group.

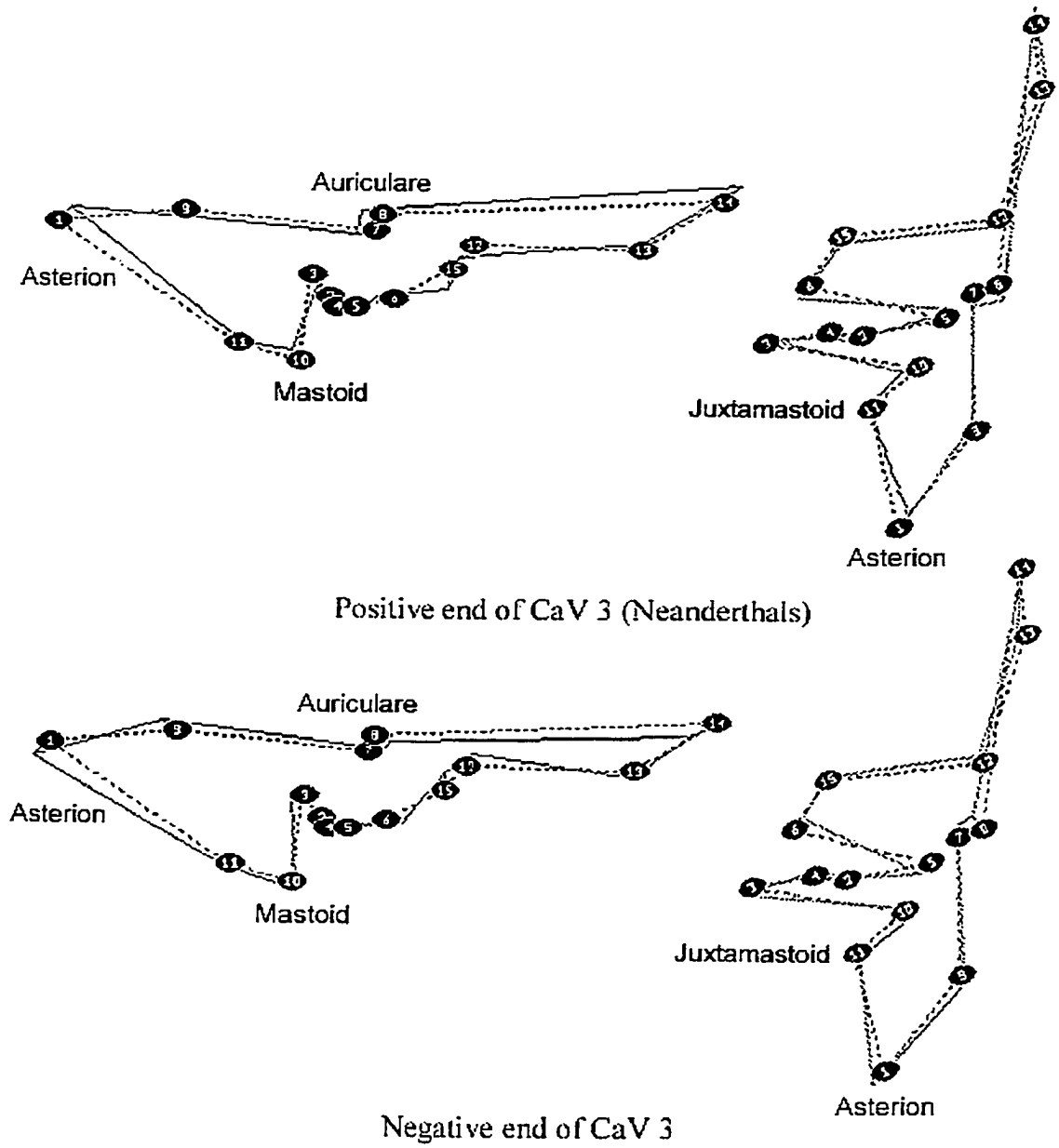

Figure 3.21: Shape variation along CaV 3 (Step 1B), right lateral (left) and right ventral (right) views. The dotted line represents the consensus configuration.

although Amud 1 was misclassified as Dogon. Unlike Step 1A, however, both Upper Paleolithic specimens are misclassified, Cro Magnon as Eskimo and Predmosti 3 as Berg. The Andamanese and the San showed the highest correct classification percentages for modern human populations and the lowest rates of successful classification was shown by the mixed European population.

Mahalanobis D^2, Cluster Analysis and Minimum Spanning Tree: As in Step 1A, the Mahalanobis D^2 matrix was calculated (Table 3.13). Results are very similar to Step 1A. The Upper Paleolithic specimens are slightly closer to the Eskimo population than to the Berg, unlike Step 1A. The cluster diagrams are very similar to those in Step 1A, differing only with respect to the position of the Eskimo, who now cluster ore tightly with the Australian-Melanesian pair. The minimum spanning tree differs from that obtained in Step 1A in that the Upper Paleolithic group is now linked to the Eskimo rather than the Berg population.

Step 1C – Chimpanzee sample only

In order to test the consistency of the chimpanzee model, the analysis was repeated on the chimpanzee sample. As the primary concern here is the consistency of the distances among these taxa, the discussion will focus on the discriminant and Mahalanobis D^2 analyses, rather than on the PCA or CVA.

Classification: As in the previous steps, a discriminant analysis was performed on the chimpanzee sample and a cross-validation classification obtained (Table 3.14). Only one bonobo is misclassified as a common chimpanzee, as a *P. t. troglodytes*, while no common chimpanzees were misclassified as bonobos, a higher classification success than in the combined sample analysis (Step 1A), where two bonobos and one common chimpanzee were misclassified. The misclassification levels between the two chimpanzee subspecies are quite high (approximately 30 % in both). These values are similar to those obtained in Step 1A.

Mahalanobis D^2: The unbiased Mahalanobis D^2 matrix was calculated in the same way as in the previous steps (Table 3.15). Bonobos are much more widely removed from the two common chimpanzee subspecies than these two groups are from each other, as in Step 1A. Furthermore, the distances between bonobos and both subspecies of

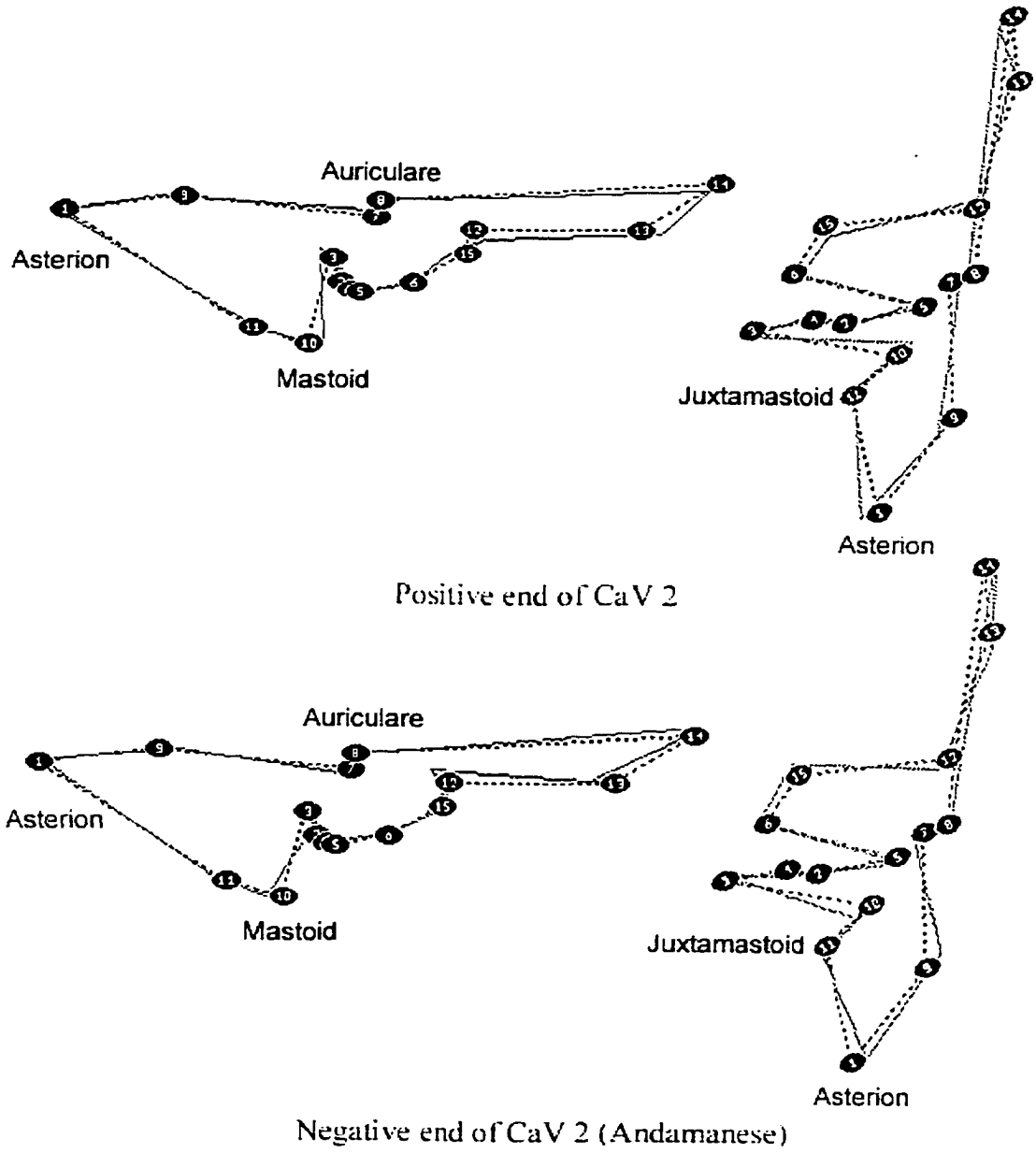

Figure 3.22: Shape variation along CaV 2 (Step 1B), right lateral (left) and right ventral (right) views. The dotted line represents the consensus configuration.

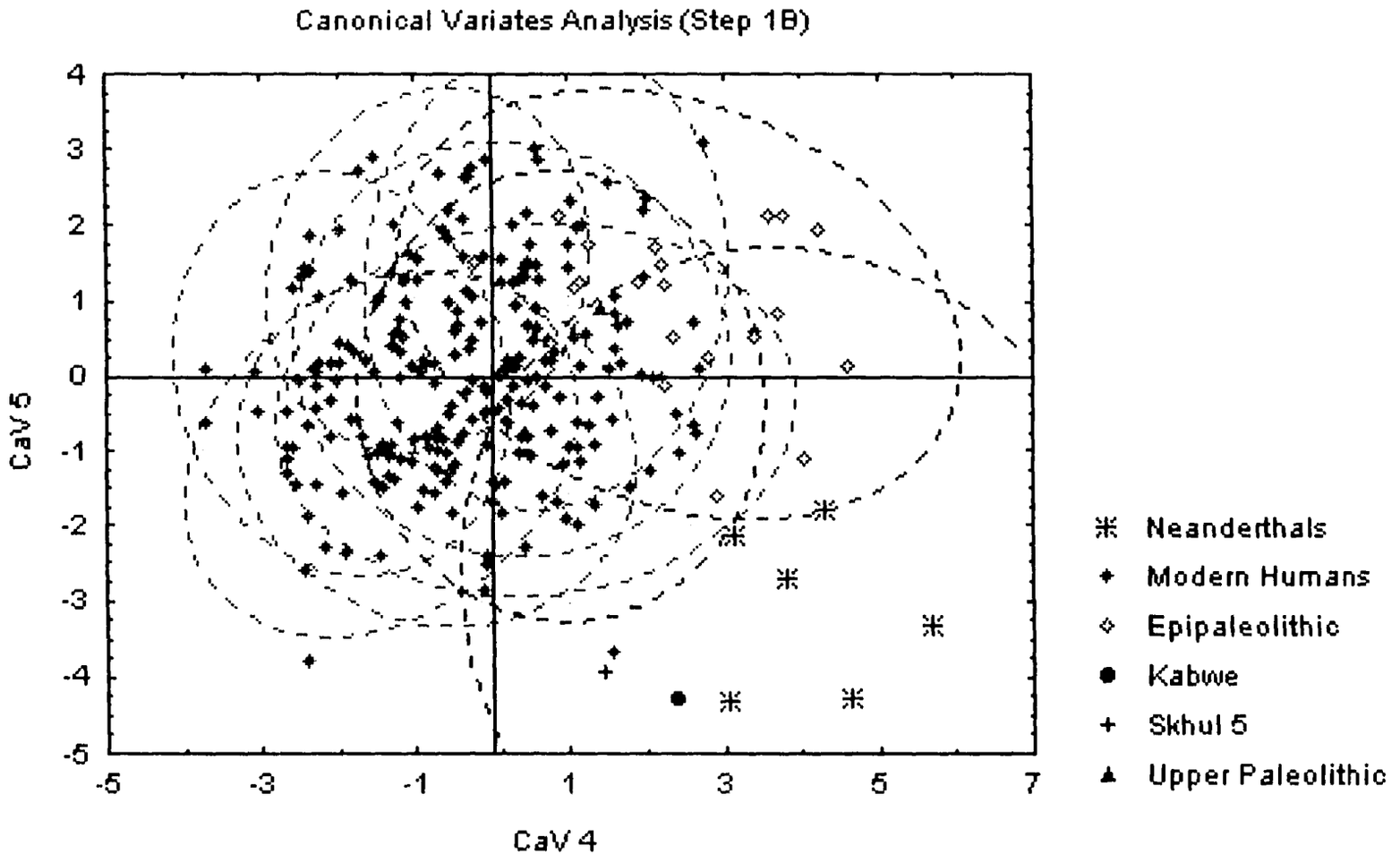

Figure 3.23: Canonical Variates Analysis (Step 1B), CaVs 4 and 5. Dotted lines represent the 95% confidence ellipses for each group.

Table 3.12: Cross-validation classification summary, Step 1B (percentages for each population in bold).

	And	Aus	Brg	Dgn	Epi	Esk	Eur	San	Tol	UP	Nea	Total
And	28	2	0	0	0	0	0	0	0	0	0	30
%	**93.33**	6.67	0	0	0	0	0	0	0	0	0	100
Aus	1	22	1	0	0	3	1	0	2	0	0	30
%	3.33	**73.33**	3.33	0	0	10	3.33	0	6.67	0	0	100
Brg	0	0	20	0	0	0	7	0	1	0	0	28
%	0	0	**71.43**	0	0	0	25	0	3.57	0	0	100
Dgn	0	1	0	20	0	4	1	2	0	0	0	28
%	0	3.57	0	**71.43**	0	14.29	3.57	7.14	0	0	0	100
Epi	0	1	0	0	18	0	0	0	1	1	0	21
%	0	4.76	0	0	**85.71**	0	0	0	4.76	4.76	0	100
Esk	0	0	0	1	0	26	3	0	0	0	0	30
%	0	0	0	3.33	0	**86.67**	10	0	0	0	0	100
Eur	2	2	9	0	2	0	13	0	2	0	0	30
%	6.67	6.67	30	0	6.67	0	**43.33**	0	6.67	0	0	100
San	0	1	0	2	0	0	0	27	0	0	0	30
%	0	3.33	0	6.67	0	0	0	**90**	0	0	0	100
Tol	0	3	0	0	1	2	0	0	24	0	0	30
%	0	10	0	0	3.33	6.67	0	0	**80**	0	0	100
UP	0	0	1	0	0	1	0	0	0	0	0	2
%	0	0	50	0	0	50	0	0	0	**0**	0	100
Nea	0	0	0	1	0	0	0	0	0	0	5	6
%	0	0	0	16.67	0	0	0	0	0	0	**83.33**	100
Total	31	32	31	24	21	36	25	29	30	1	5	265
%	11.7	12.08	11.7	9.06	7.92	13.58	9.43	10.94	11.32	0.38	1.89	100

Table 3.13: Unbiased Mahalanobis D^2, Step 1B. All distances 0.001 significance level except: NS = non-significant, * = 0.05 level, ** = 0.01 level.

	And	Aus	Brg	Dgn	Epi	Esk	Eur	Kbw	San	Skh5	Tol	UP	Nea
And	0.00	24.34	29.32	26.23	35.30	31.53	26.99	59.38	40.68	113.59	25.90	73.45	94.34
Aus	24.34	0.00	16.70	21.56	24.73	13.44	11.67	51.57**	23.62	93.91	6.98	53.79	74.45
Brg	29.32	16.70	0.00	27.88	18.35	25.13	4.64	58.17**	30.72	93.30	17.14	38.88	87.72
Dgn	26.23	21.56	27.88	0.00	23.88	18.29	17.69	58.45**	14.57	124.93	23.47	71.68	73.18
Epi	35.30	24.73	18.35	23.88	0.00	26.61	14.90	60.23	32.66	108.36	24.97	41.96	73.10
Esk	31.53	13.44	25.13	18.29	26.61	0.00	17.41	72.52	28.05	118.37	13.51	39.22	62.65
Eur	26.99	11.67	4.64	17.69	14.90	17.41	0.00	57.54**	25.32	98.69	11.73	43.88	80.18
Kbw	59.38	51.57**	58.17**	58.45**	60.23	72.52	57.54**	0.00	53.15**	140.73	68.83	97.98	76.84
San	40.68	23.62	30.72	14.57	32.66	28.05	25.32	53.15**	0.00	130.55	25.76	66.86	83.59
Skh5	113.59	93.91	93.30	124.93	108.36	118.37	98.69	140.73	130.55	0.00	108.87	89.03	149.93
Tol	25.90	6.98	17.14	23.47	24.97	13.51	11.73	68.83	25.76	108.87	0.00	47.59	84.71
UP	73.45	53.79	38.88	71.68	41.96	39.22	43.88	97.98	66.86	89.03	47.59	0.00	92.35
Nea	94.34	74.45	87.72	73.18	73.10	62.65	80.18	76.84	83.59	149.93	84.71	92.35	0.00

common chimpanzee are considerably larger than those found in the combined analysis, being almost doubled. However, they are still much smaller than those between Neanderthals and modern human populations, both in the combined and in the human sample analyses. It is now greater than almost all distances among modern human groups and is only equivalent to the distance between the San and Andamanese, the largest among modern human populations. The distance between the two common chimpanzee subspecies is also almost doubled, but it is still quite small and still not significant, as in Step 1A. It is now equivalent to the smallest distances among modern human groups.

Table 3.14: Cross-validation classification summary, Step 1C (percentages for each population in bold).

	Bon	Sch	Trg	Total
Bon	34	0	1	35
	97.14	0	2.86	100
Sch	0	19	9	28
	0	**67.86**	32.14	100
Trg	0	10	18	28
	0	35.71	**64.29**	100

Table 3.15 Unbiased Mahalanobis D^2, chimpanzee sample, Step 1C. All distances 0.001 significance level except: NS = non-significant, * = 0.05 level, ** = 0.01 level.

	Bon	Sch	Trg
Bon	0.00	38.10	36.08
Sch	38.10	0.00	4.78**NS**
Trg	36.08	4.78**NS**	0.00

Step 2

This step includes only 13 of the 15 temporal bone landmarks. The omission of the two landmarks on the zygomatic suture made possible the inclusion of six additional Neanderthal specimens: Gibraltar 1, Spy 1 and 2, La Quina 27, Krapina C and Krapina 39-1 (see Table 3.2, p.3). The pre-Neanderthal specimen from Reilingen was also included, as was the early modern human specimen Qafzeh 9 and the European Upper Paleolithic specimens Mladec 2 and Predmosti 4. The total Neanderthal sample was therefore increased to twelve, the early modern human sample from the Near East to two, and the European Upper Paleolithic sample to four, while the recent human and chimpanzee samples were also somewhat increased. The two early anatomically modern human specimens from Israel, Skhul 5 and Qafzeh 9, were placed in a separate population (EAM), as were also the Upper Paleolithic specimens (UP).

Centroid Size: The removal of the two landmarks of the zygomatic suture reduces the magnitude of centroid size across taxa, as expected. While the mean centroid size in the two genera was almost identical in the previous analysis, here the mean for *Homo* is slightly higher (Table 3.16, Fig. 3.24). Although when the analysis of variance is conducted at the genus level, a significant genus effect is detected (0.01), when this analysis is performed at the level of populations, the chimpanzee populations are not significantly different from the human groups. The standard variation in humans is only slightly higher than that in chimpanzees. As in Step 1, the mean value and the standard deviation of males is larger than that of females in both genera.

Within the chimpanzee sample, bonobos are still smaller than common chimpanzees, but only significantly smaller than one of the common chimpanzee subspecies, *P. t. schweinfurthii*. Bonobos show a lower degree of sexual dimorphism than both common chimpanzees and modern humans, even less so than in Step 1. Common chimpanzees show an equivalent, and even slightly higher degree of sexual dimorphism than modern humans. As in Step 1, the two common chimpanzee subspecies are not significantly different from each other.

In the humans sample, Neanderthals fall well within the range of modern humans, but show slightly higher mean values. They are not significantly different in their mean

Table 3.16: Centroid size listed by genus, sex, species and population

	Mean	Range	St. Deviation	N
Homo	**8.07**	**6.84-9.89**	**0.59**	**283**
Males	8.31	6.84-9.81	0.57	150
Females	7.79	6.86-9.14	0.47	127
Modern	8.06	6.84-9.75	0.59	269
Males	8.32	6.84-9.75	0.57	141
Females	7.77	6.86-9.14	0.47	124
Neanderthals	8.17	7.41-8.86	0.48	12
Males	8.37	7.71-8.86	0.41	7
Females	7.77	7.55-8.00	0.32	3
Unknown sex	7.76	7.41-8.12	0.50	2
Kabwe	9.81	---	---	1
Reilingen	7.77	---	---	1
Skhul 5	8.23	---	---	1
Qafzeh 9	7.60	---	---	1
Upper Paleolithic	8.74	7.96-9.34	0.58	4
Andamanese	7.40	6.84-8.18	0.34	30
Australian	7.95	7.24-8.61	0.40	30
Berg	8.05	7.39-8.98	0.39	30
Dogon	7.78	6.97-8.64	0.40	29
Epipaleolithic	9.01	7.49-9.75	0.46	24
Eskimo	8.50	7.96-9.32	0.40	30
European (mixed)	8.05	7.27-9.97	0.47	30
San	7.69	6.86-8.58	0.46	30
Tolai	8.27	7.29-8.98	0.43	30
Pan	**7.89**	**6.80-9.30**	**0.56**	**92**
Males	8.07	7.10-9.30	0.56	51
Females	7.61	6.79-9.00	0.43	39
P. paniscus	7.42	6.79-7.89	0.25	35
Males	7.49	6.17-7.88	0.21	16
Females	7.35	6.79-7.89	0.27	19
P. troglodytes	8.17	7.10-9.30	0.50	57
Males	8.34	7.10-9.30	0.46	35
Females	7.85	7.12-9.00	0.41	20
P. t. schweinfurthii	8.07	7.10-9.30	0.56	29
P. t. troglodytes	8.27	7.54-9.22	0.41	28

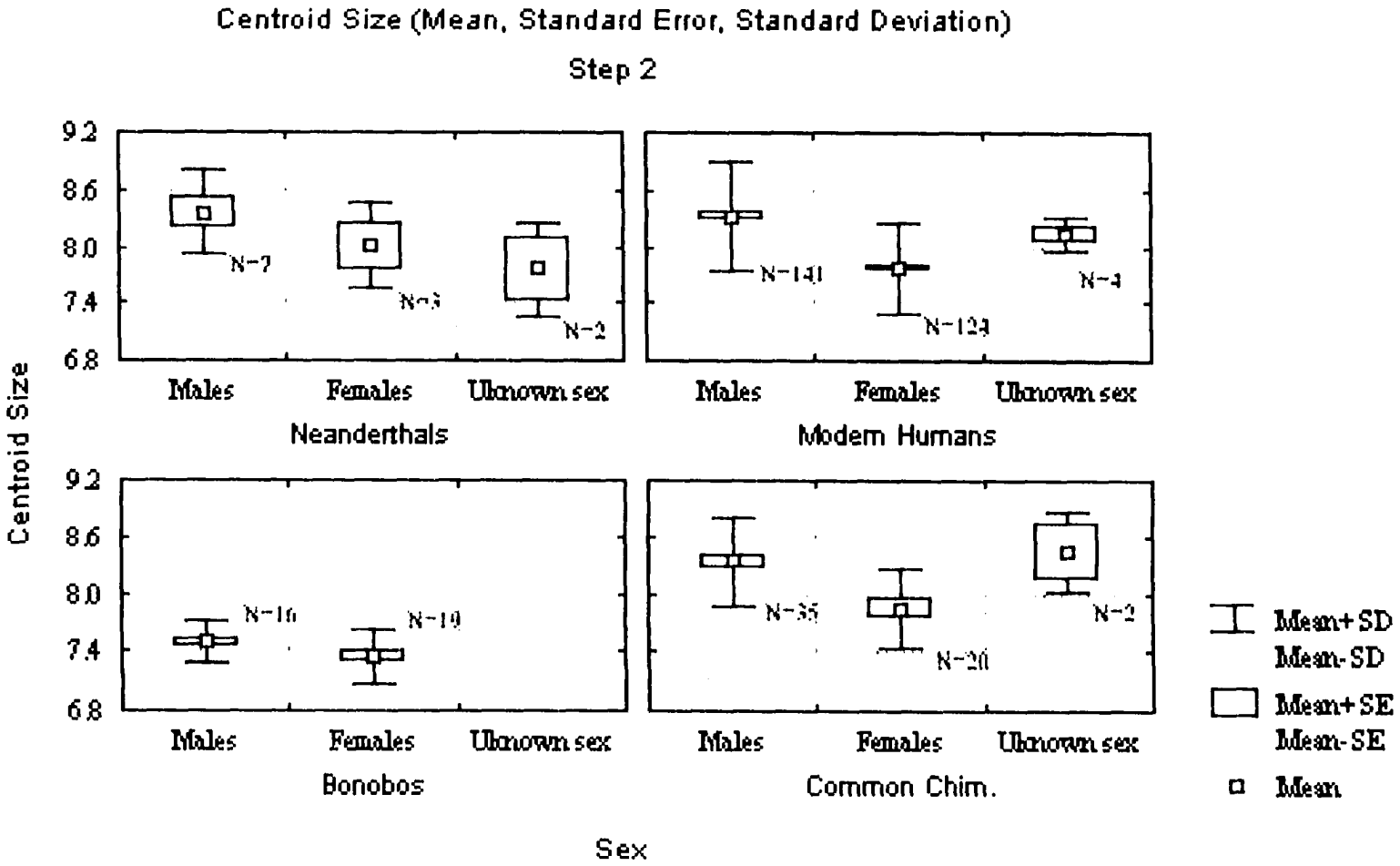

Figure 3.24: Centroid size mean, standard error and standard deviation, labeled by species and sex (Step 2).

centroid size than most modern human populations. The standard deviation for Neanderthals is smaller than that of modern humans. Although the number of Neanderthal specimens is very small, and their sex assignment uncertain, the degree of sexual dimorphism in this taxon appears equivalent to that of modern humans. The differences in centroid size among modern human populations observed in Step 1 are reduced here. Only Kabwe is significantly larger than all other human groups, except the Epipaleolithic. Although the Epipaleolithic and the Eskimo still show the largest mean centroid size values. The Epipaleolithic are significantly larger than most human groups except the Eskimo, Upper Paleolithic, Tolai and Neanderthals. The Eskimo are only significantly larger than the Andamanese, who show the smallest mean value, as are also the Neanderthals.

Step 2A – Combined human and chimpanzee sample

Principal Components Analysis: Neanderthals are separated from modern humans along PC 1, and partially also PC 10. PC 4 separates Kabwe from modern humans. As in Step 1, PC 1 (43.8 %, significant for population (0.0001) and sex (0.01) effects, Table 3.17, Fig. 3.25) separates humans from chimpanzees, with Neanderthals falling in between. Along this component, all the chimpanzee taxa are significantly different in their mean scores from all the human populations, and Neanderthals are significantly different from all modern human populations, including the Upper Paleolithic and the early anatomically modern human groups. As in Step 1, Amud 1 is the only Neanderthal to fall well within the modern human range. Along this component there is also a strong trend in the modern human sample, but not in the chimpanzee sample, for females to have more positive scores than males. When the mean scores of the two sexes for PC 1 are plotted by population (Fig. 3.26), the female mean values are slightly more positive than the male ones in humans, including Neanderthals and the early modern humans, but not in chimpanzees.

The shape differences at the positive end of this axis (Table 3.18, Fig, 3.27), include a smaller mastoid process (10), a medially placed juxtamastoid eminence (11), an elevated and anteriorly placed lateral origin of the petro-tympanic crest (5), and a laterally projecting porion (7). These shape differences characterize chimpanzees relative

to humans, Neanderthals relative to modern humans, and modern human females relative to males. PC 1 is not strongly correlated to centroid size differences (Table 3.17).

PC 10 (2.2 %, significant for population effects at the 0.0001 level, Fig. 3.25), separates Neanderthals partially from modern humans on its negative end, Shanidar 1, La Ferrassie 1, Gibraltar 1 and Circeo 1 falling outside the modern human range. The specimens that fall furthest within the modern human cloud are La Quina 27, Spy 2 and Amud 1. The shape variation along this axis (Fig. 3.28) includes, at its negative end, a more anterior lateral origin of the petro-tympanic crest (5), a depressed parietal notch (9), a more anterior and lateral root of the articular eminence (12) and a more posteriorly placed entoglenoid pyramid (13). PC 10 is also not strongly correlated with centroid size (Table 3.17).

PC 4 (4.8 %, significant for population effects at the 0.0001 level) separates Kabwe from the remaining human sample. This specimen falls just outside the positive end of the human range along this axis. The shape differences that characterize the positive end of PC 4 include the more anterior placement of asterion, the more inferior and posterior placement of the parietal notch, a larger juxtamastoid eminence, and a slightly more anterior placement of the lateral origin of the petro-tympanic crest. In addition to PC 1, one other principal component, PC 5 (4.2 %) is significant for sex effects (0.001). Human females tend to have more positive scores than males along this axis. When the mean scores are plotted for the sexes by population (Fig. 3.26), a relatively strong tendency is observed for the female means to be more positive than the males among modern human populations, but not in Neanderthals or in chimpanzees. PC 5 also separates Reilingen at its negative end from the rest of the human sample. The shape differences that characterize the negative end of this axis include a larger mastoid process with a more anteriorly placed tip, a more medial placement of asterion, a more anterior medial end of the jugular fossa, a more anterior lateral origin of the petro-tympanic crest, and a larger juxtamastoid eminence. PC 5 is only weakly correlated with centroid size.

Canonical Variates Analysis: In this analysis, Neanderthals are separated from modern humans along both CaV 1 and 2. As in Step 1, CaV 1 (69.6 % of the total variance, most strongly influenced by PC 1, Fig. 3.29) separates the human from the

Table 3.17: Summary of the PCA results, ANOVA and Correlation Analysis for PCs 1-10, Step 2A.

	Principal Components Analysis			ANOVA, Pr > F			Correlation with Centroid Size	
	Eigenvalue	Proportion	Cumulative	Popul.	Sex	Interaction	Rho	Pr > F
PC 1	0.012897	0.437714	0.437714	0.0001	0.0052	0.5343	-0.1957	0.0002
PC 2	0.002231	0.075709	0.513423	0.0001	0.0785	0.6977	0.33794	0.0001
PC 3	0.001744	0.059203	0.572626	0.0001	0.8878	0.4508	-0.00874	0.8661
PC 4	0.001426	0.048401	0.621027	0.0001	0.1822	0.5799	0.23436	0.0001
PC 5	0.001238	0.042013	0.66304	0.0001	0.0004	0.8223	-0.26446	0.0001
PC 6	0.001057	0.035859	0.698899	0.0001	0.9687	0.5887	0.15212	0.0031
PC 7	0.000926	0.031428	0.730327	0.0001	0.0785	0.316	0.15481	0.0026
PC 8	0.000838	0.028449	0.758776	0.0001	0.5602	0.9429	0.19668	0.0001
PC 9	0.000703	0.023854	0.782629	0.0003	0.0306	0.0429	-0.1016	0.0493
PC 10	0.000639	0.02169	0.804319	0.0001	0.3243	0.8752	-0.16322	0.0015

Table 3.18: Squared roots of the sum of squares of the eigenvector coefficients for the three coordinates of each landmark, PCs 1-10, Step 2A.

	PC 1	PC 2	PC 3	PC 4	PC 5	PC 6	PC 7	PC 8	PC 9	PC 10
1. Asterion	0.15	**0.40**	0.26	**0.51**	**0.41**	**0.35**	**0.32**	**0.41**	**0.37**	0.24
2. Stylom. F.	0.12	0.06	0.06	0.10	0.23	0.15	0.11	0.17	0.03	0.13
3. M. Jug. OFS.	0.26	0.21	0.15	0.11	**0.35**	0.17	**0.35**	**0.39**	0.25	0.22
4. L. Jug. Fos.	0.24	0.09	0.05	0.12	0.17	0.09	0.12	0.22	0.09	0.15
5. Lat. Petro-Tym. Cr.	**0.46**	0.13	0.22	**0.34**	**0.39**	**0.38**	0.15	**0.27**	**0.54**	**0.48**
6. Med. Petro-Tym. Cr.	0.21	0.14	0.06	0.04	0.29	0.20	**0.31**	0.24	0.21	0.24
7. Porion	**0.27**	0.03	0.16	0.06	0.12	0.22	0.12	**0.27**	0.09	0.11
8. Auriculare	0.22	0.09	0.22	0.03	0.12	**0.34**	0.15	0.19	0.18	0.14
9. Parietal N.	0.18	**0.54**	**0.43**	**0.52**	0.17	0.22	**0.58**	0.21	**0.34**	**0.35**
10. Mastoid	**0.42**	**0.35**	**0.59**	0.14	**0.44**	**0.51**	0.22	**0.41**	**0.31**	0.23
11. Juxtam. Em.	**0.44**	**0.55**	**0.30**	**0.49**	**0.32**	**0.28**	0.20	0.16	0.16	0.29
12. Artic. Em.	0.14	0.12	**0.36**	0.08	0.20	0.20	**0.28**	0.23	**0.36**	**0.35**
13. Entogl. Pyr.	0.20	0.06	0.16	0.18	0.01	0.16	**0.29**	0.24	0.24	**0.38**

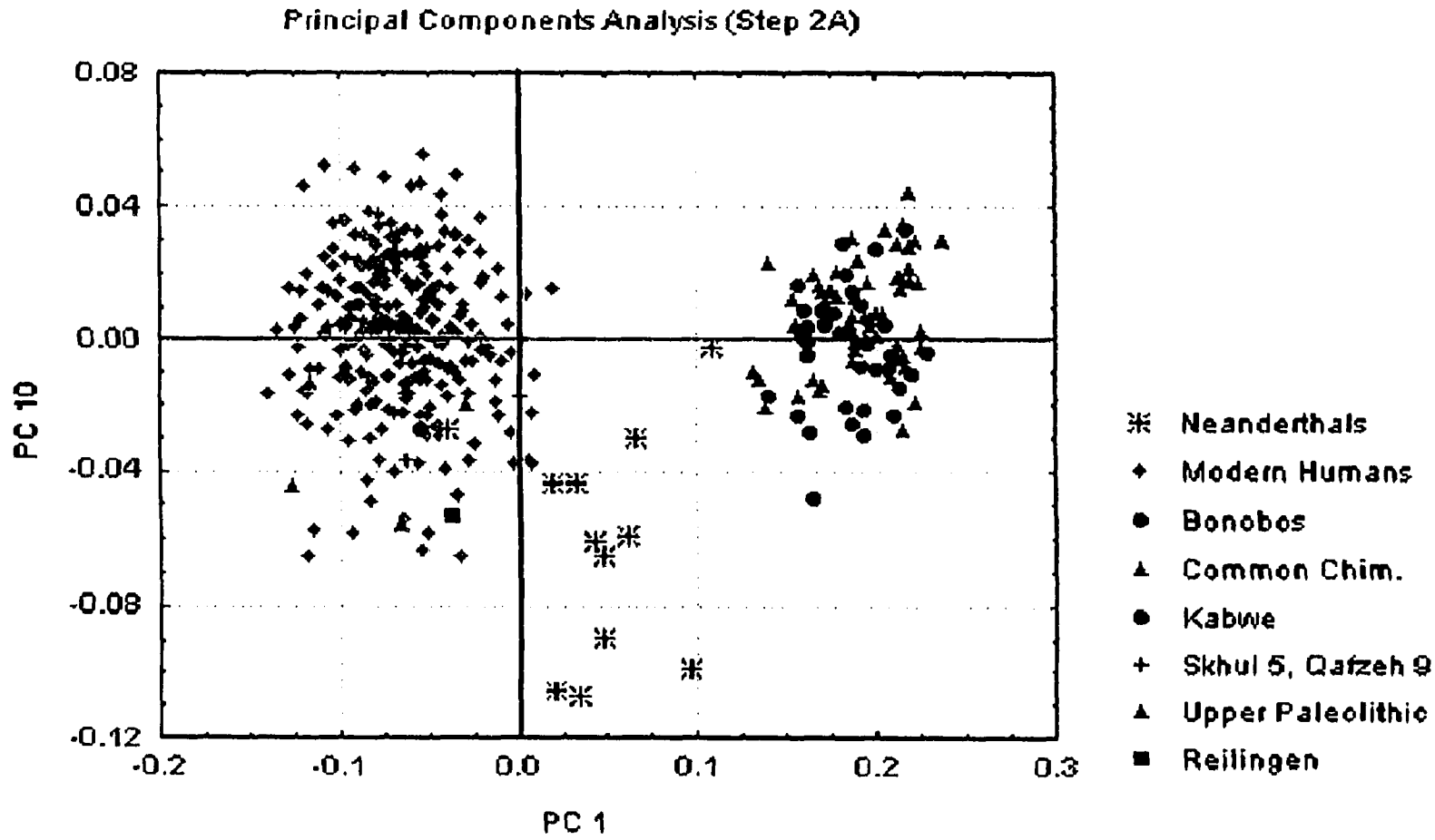

Figure 3.25: Principal Components Analysis (Step 2A), PCs 1 and 10.

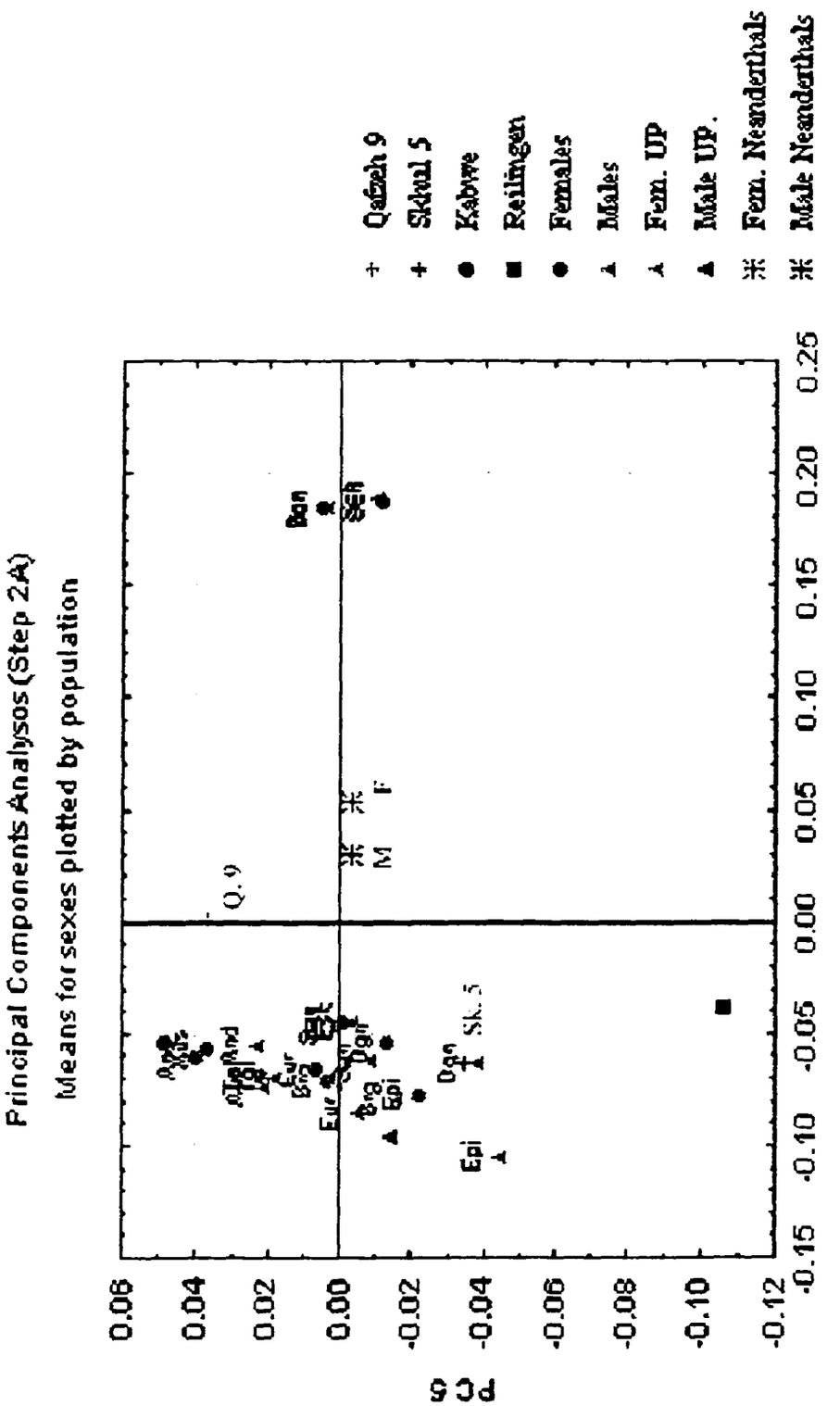

Figure 3.26: Principal Components Analysis (Step 2A), mean scores for sexes labeled by population, PCs 1 and 5.

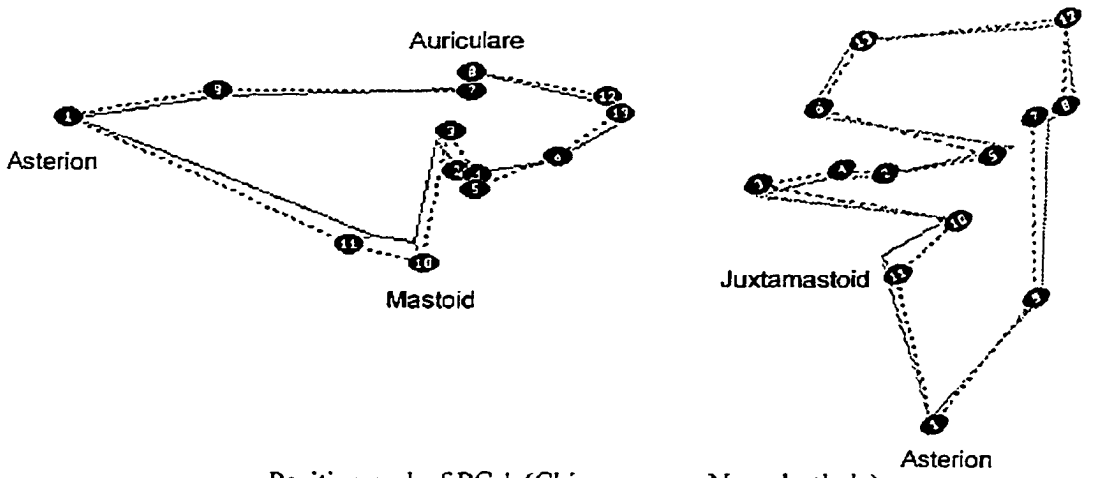

Positive end of PC 1 (Chimpanzees, Neanderthals)

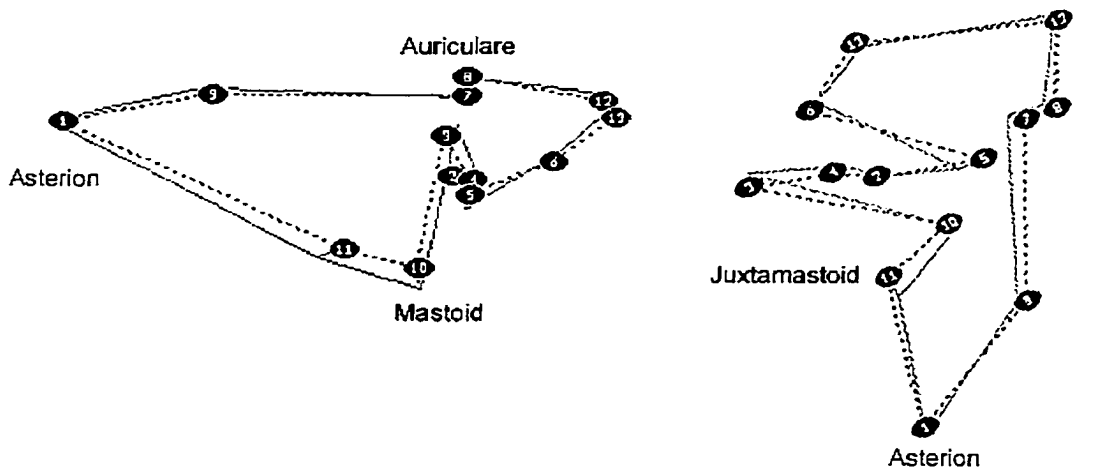

Negative end of PC 1 (Modern Humans)

Figure 3.27: Shape variation along PC 1 (Step 2A), right lateral (left) and right ventral (right) views. The dotted line represents the consensus configuration.

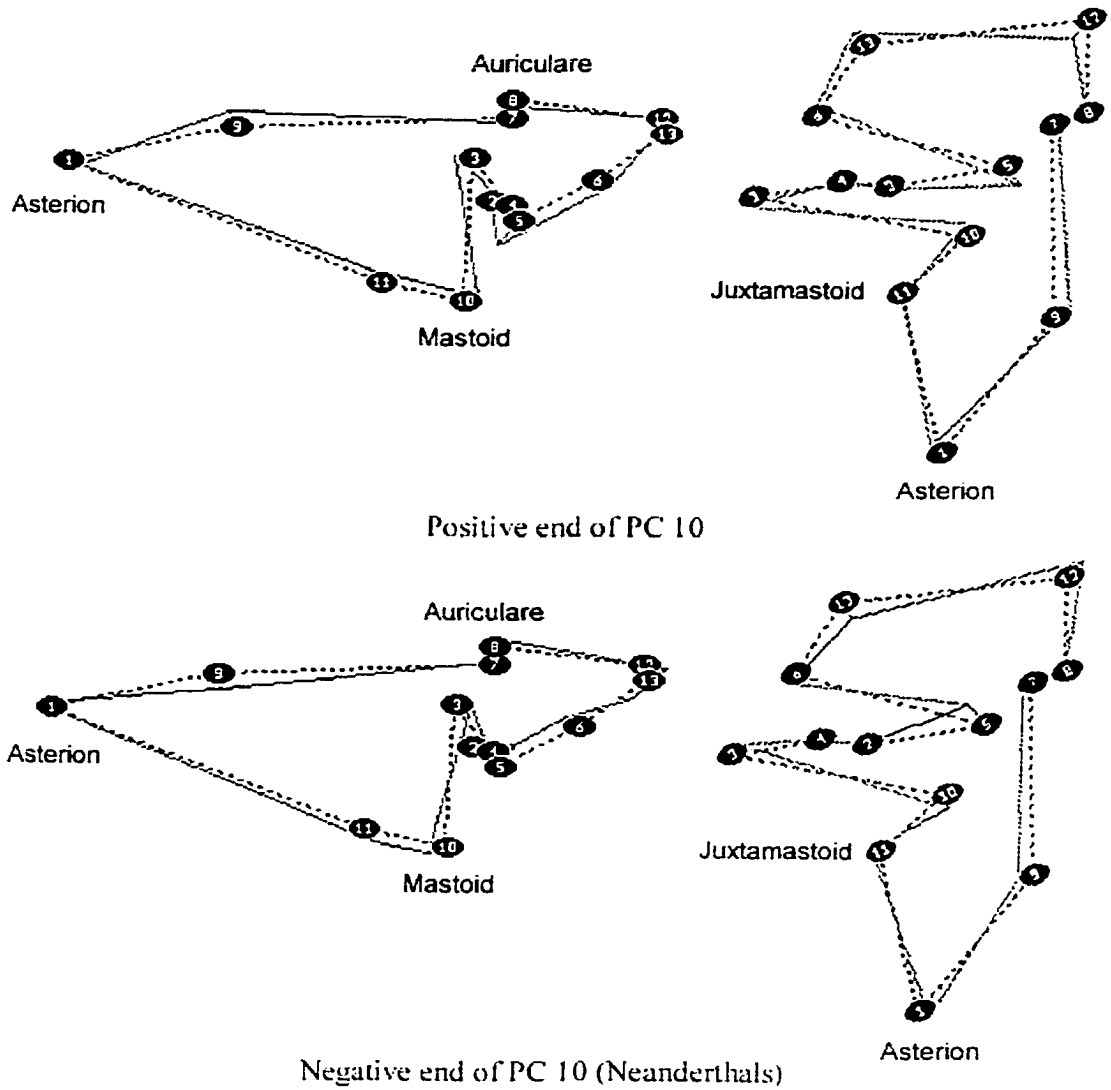

Fig. 3.28: Shape variation along PC 10 (Step 2A), right lateral (left) and right ventral (right) views. The dotted line represents the consensus configuration.

chimpanzee sample. It also partially separates Neanderthals from modern humans, although the ranges of these two groups overlap. The chimpanzee populations are significantly different from the modern human groups along this axis, and Neanderthals are significantly different from both. As in the previous analyses, Amud 1 is the Neanderthal specimen that falls furthest within the modern human range along this axis, and is separated from the rest of the Neanderthal sample, including Shanidar 1, the other Eastern specimen included here. Kabwe falls close to the positive end of the modern human range and within the region of overlap between Neanderthals and modern humans along CaV 1. Reilingen falls very close to Amud 1. The shape variation along this axis (Fig. 3.30) is similar to that described for PC 1. It includes at its positive end a smaller mastoid process (10) and a more medially placed juxtamastoid eminence (11), a more anterior and superior placement of the lateral origin of the petro-tympanic crest (5) and a more lateral porion (7) and auriculare (8). These shape differences characterize chimpanzees relative to humans and, to a lesser extent, Neanderthals relative to modern humans. CaV 1 is very weakly related to centroid size.

Neanderthals are completely separated from modern humans on the negative side of CaV 2 (6.5 %, most strongly influenced by PCs 10, 7 and 5, Fig. 3.29), falling entirely outside the 95 % confidence ellipse of all modern human populations along CaVs 1 and 2. They are significantly different from all modern human populations along this axis. Amud 1 is the specimen that is closest to the modern human cloud, but still outside the confidence ellipse of modern human populations. Reilingen is also widely separated from modern humans and falls at the edge of the Neanderthal confidence ellipse. The other fossil specimens fall well within the modern human range. In the negative end of this axis, the lateral origin of the petro-tympanic crest (5) is elevated and more anterior, the mastoid process (10) is small and the juxtamastoid eminence (11) is large and more medially placed. The root of the articular eminence (12) is more laterally, anteriorly and inferiorly placed and the entoglenoid pyramid (13) is more posterior and inferior, indicating a medio-laterally wide and medially closed-off glenoid fossa with a shallow floor (Fig. 3.31). CaV 2 is not strongly correlated with centroid size (Table 3.19).

CaV 3 (6 %, most strongly influenced by PCs 6, 13 and 3) separates Qafzeh 9

Table 3.19: Summary of the CVA results and Correlation Analysis, CaVs 1-5, Step 2A.

	Canonical Variates Analysis			Correlation with Centroid Size	
	Eigenvalue	Proportion	Cumulative	Rho	Pr > F
CaV 1	25.0135	0.6962	0.6962	-0.14936	0.0037
CaV 2	2.3299	0.0648	0.7611	-0.15537	0.0026
CaV 3	2.163	0.0602	0.8213	-0.00228	0.9649
CaV 4	1.5781	0.0439	0.8652	0.32289	0.0001
CaV 5	1.3633	0.0379	0.9031	0.37393	0.0001

from modern humans. Among modern human populations it also separates the Andamanese on its positive end from the San on its negative end. Kabwe, Reilingen and the Neanderthals fall near the center of the modern human range, as do all the Upper Paleolithic specimens. Skhul 5 falls near the center of the Andamanese cloud, while Qafzeh 9 falls at the positive extreme of CaV 3, outside even of the Andamanese 95 % confidence ellipse. The shape differences along CaV 3 include, at its positive end, a very lateral placement of auriculare, a more posterior placement of the root of the articular eminence, a more anterior placement of the medial end of the jugular fossa, and a more medial position of the medial end of the petro-tympanic crest and the entoglenoid pyramid. These shape differences characterize Qafzeh 9 relative to rest of the human sample, as well as Skhul 5 and the Andamanese relative to other modern humans and fossil specimens. The opposite shape changes characterize the San relative to the other modern human groups. CaV 3 does not reflect size-related shape variation (Table 3.19).

Classification: As in Step 1A, Kabwe was classified as Australian (posterior probability of 0.52). Reilingen was classified as Neanderthal (0.99), Qafzeh 9 as Andamanese (1.0) and Skhul 5 as Berg (0.97). Predmosti 3 and Cro Magnon 1 were also classified as Berg (0.62 and 0.52 respectively), Mladec 2 as Eskimo (0.76) and Predmosti 4 as Andamanese (0.63).

A cross-validation classification was obtained for the rest of the dataset and the results summarized in Table 3.20. Results are similar to those obtained in Step 1. No human was misclassified as a chimpanzee and vice versa. Furthermore, no modern human was misclassified as Neanderthal, although one Neanderthal, Amud 1, was misclassified as a modern human, this time as an Epipaleolithic individual rather than a Dogon. All other Neanderthal specimens were correctly classified. The highest success rate overall was achieved by the Andamanese (100 %), and the lowest by the Europeans (40 %). As in Step 1, a large proportion of the European (16.67 %) were misclassified as Berg and vice versa (23.33 %), and European specimens were also misclassified as Andamanese, Australian, Dogon, Epipaleolithic, Eskimo and Tolai. Only one Upper Paleolithic specimen was classified correctly, while the other three were classified as Andamanese, Berg and Eskimo. Skhul 5 was classified as Upper Paleolithic, while

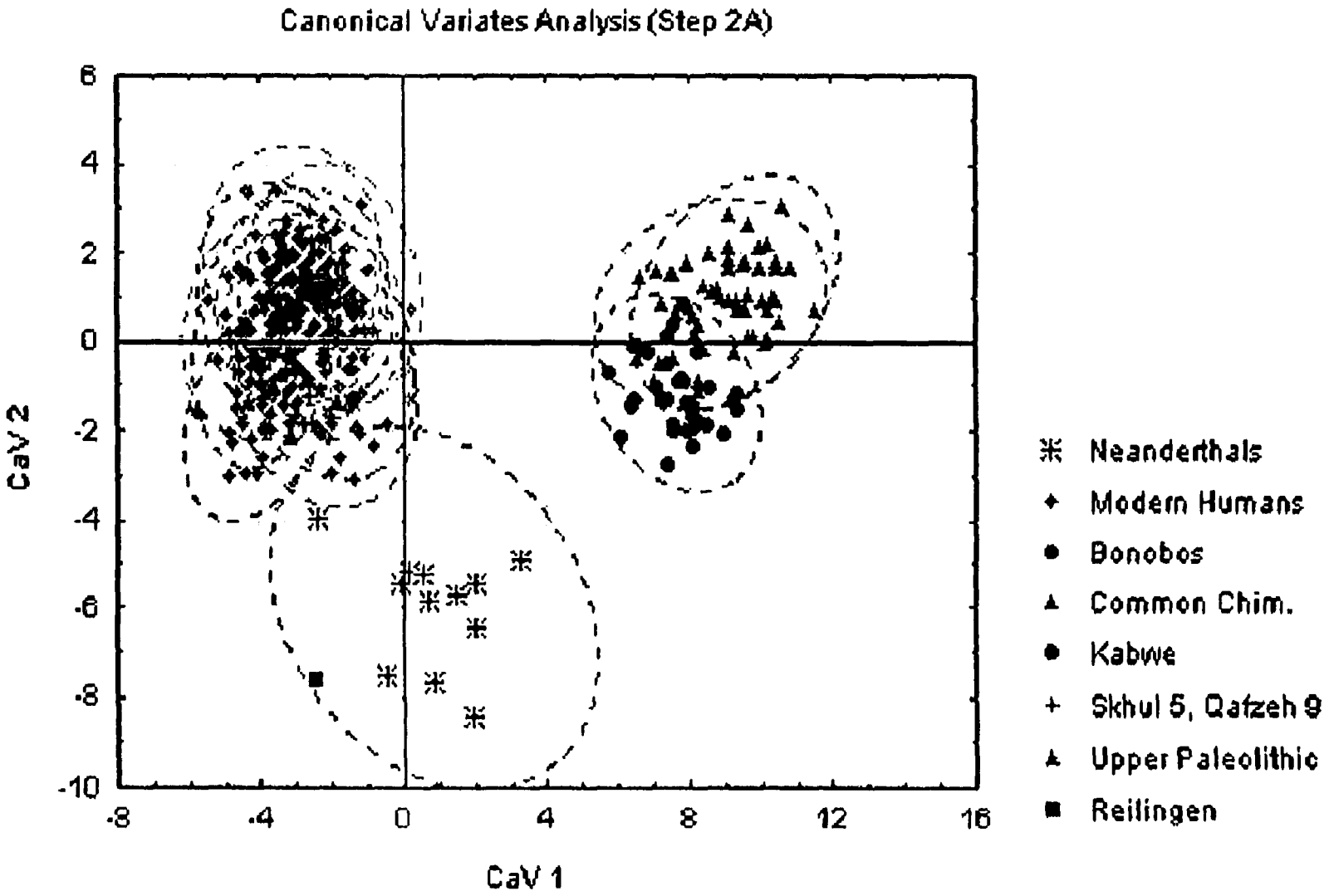

Figure 3.29: Canonical Variates Analysis (Step 2A), CaVs 1 and 2. Dotted lines represent the 95% confidence ellipses for each group.

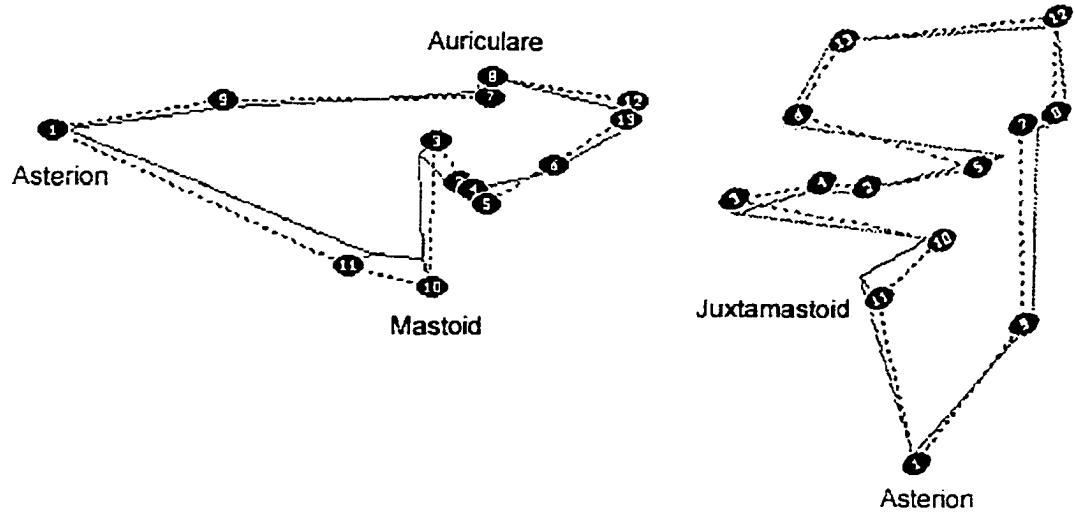

Positive end of CaV 1 (Chimpanzees, Neanderthals)

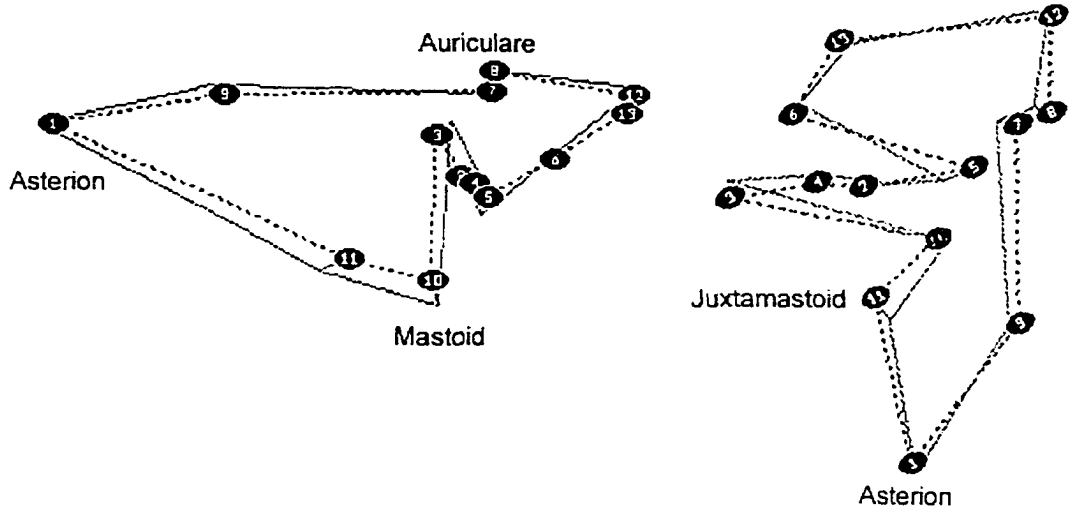

Negative end CaV 1 (Modern Humans)

Fig. 3.30: Shape variation along CaV 1 (Step 2A), right lateral (left) and right ventral (right) views. The dotted line represents the consensus configuration.

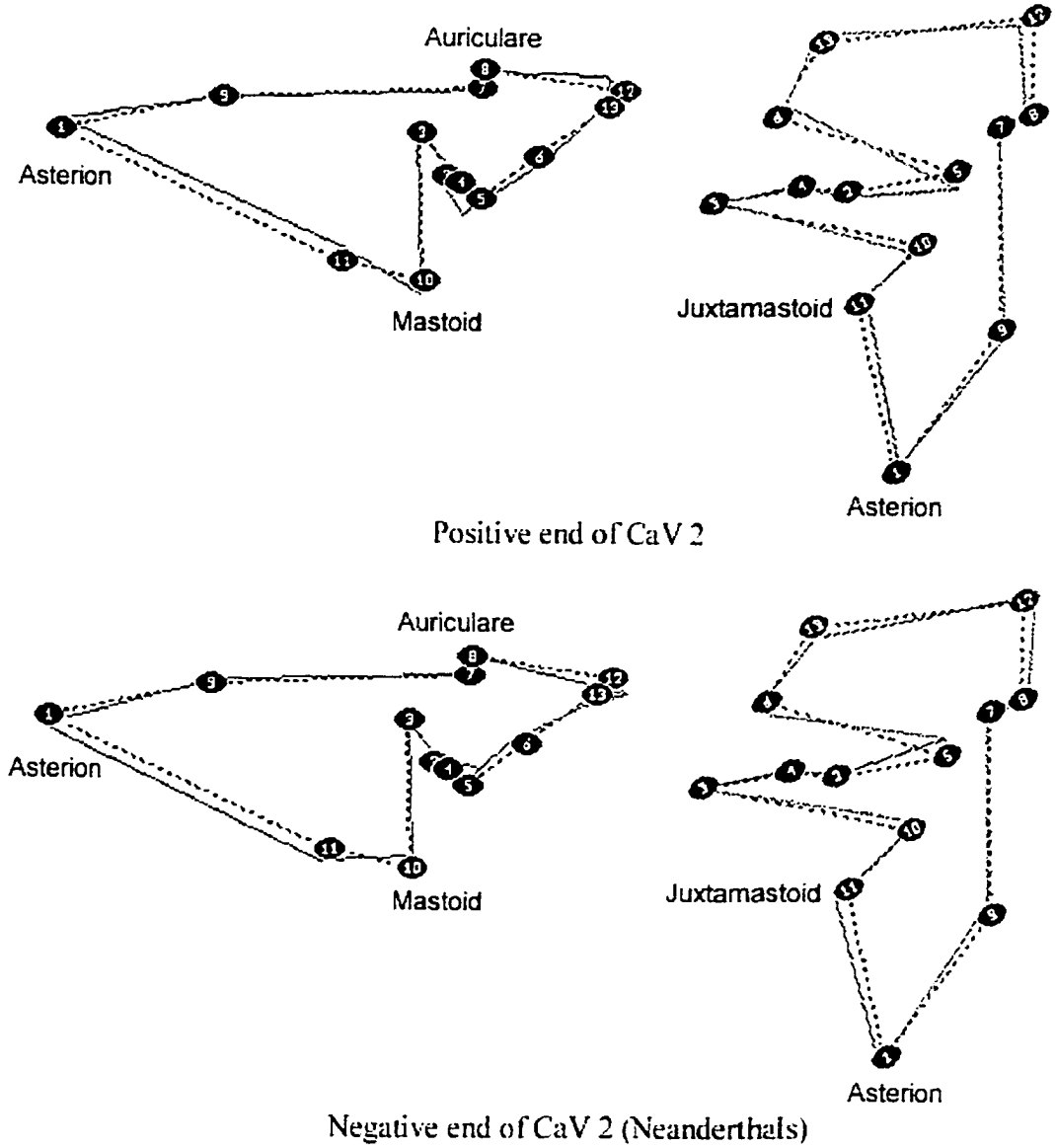

Figure 3.31: Shape variation along CaV 2 (Step 2A), right lateral (left) and right ventral (right) views. The dotted line represents the consensus configuration.

Qafzeh 9 was classified as Andamanese. In the chimpanzee sample, the two common chimpanzee subspecies show high levels of misclassification among themselves, while one *P. t. troglodytes*, but no *P.t. schweinfurthii,* were misclassified as bonobos. One bonobo was misclassified as *P.t. schweinfurthi.*

Mahalanobis D^2, Cluster Analysis and Minimum Spanning Tree: The unbiased Mahalanobis D^2 matrix was calculated (Table 3.21). Results are similar to those obtained in Step 1. Neanderthals are very distant from modern humans, the smallest distance between them and any modern human group (the Eskimo) being greater than the greatest distance between any pair of modern human populations (between the San and the Andamanese). Neanderthals are most distant from the Andamanese. The Upper Paleolithic group is closest to the Berg and most distant to the Neanderthals. As also found previously, the two common chimpanzee subspecies are much closer to each other than any modern human groups, while the two chimpanzee species are as distant from each other as some modern human populations. Among the latter, all three geographic pairs still show the smallest distances to each other.

The cluster diagram (Fig. 3.32) is similar to that obtained in Step 1A. Neanderthals are still outliers to all other human groups, the Andamanese are outliers to modern humans and the modern human geographic pairs still cluster together. The Upper Paleolithic specimens, however, now fall within the larger branch of the modern human populations, rather than being outliers to them as in Step 1. Furthermore, the position of the Epipaleolithic has changed. Instead of falling within the Asian-Australian-Melanesian branch, as in Step 1A, this group now falls on its own branch, being outliers to all recent human groups except the Andamanese. The minimum spanning tree (Fig. 3.33) shows the Upper Paleolithic specimens linked to the Berg, while the Neanderthals are joined to the Eskimo, as in Step 1A. The populations in the three geographic pairs are all closest neighbors to each other.

Table 3.20: Cross-validation classification summary, Step 2A (percentages for each population in bold).

	And	Aus	Brg	Dgn	EAM	Epi	Esk	Eur	San	Tol	UP	Bon	Nea	Sch	Trg	Total
And	30	0	0	0	0	0	0	0	0	0	0	0	0	0	0	30
%	**100**	0	0	0	0	0	0	0	0	0	0	0	0	0	0	100
Aus	0	23	1	1	0	0	1	1	0	3	0	0	0	0	0	30
%	0	**76.67**	3.33	3.33	0	0	3.33	3.33	0	10	0	0	0	0	0	100
Brg	1	0	21	0	0	2	0	5	0	1	0	0	0	0	0	30
%	3.33	0	**70**	0	0	6.67	0	16.67	0	3.33	0	0	0	0	0	100
Dgn	0	1	0	24	0	0	2	1	0	1	0	0	0	0	0	29
%	0	3.45	0	**82.76**	0	0	6.9	3.45	0	3.45	0	0	0	0	0	100
EAM	1	0	0	0	0	0	0	0	0	0	1	0	0	0	0	2
%	50	0	0	0	**0**	0	0	0	0	0	50	0	0	0	0	100
Epi	0	0	2	0	0	20	0	1	0	0	1	0	0	0	0	24
%	0	0	8.33	0	0	**83.33**	0	4.17	0	0	4.17	0	0	0	0	100
Esk	0	1	0	1	0	0	25	1	0	2	0	0	0	0	0	30
%	0	3.33	0	3.33	0	0	**83.33**	3.33	0	6.67	0	0	0	0	0	100
Eur	3	1	7	1	0	1	0	12	1	4	0	0	0	0	0	30
%	10	3.33	23.33	3.33	0	3.33	0	**40**	3.33	13.33	0	0	0	0	0	100
San	0	1	0	1	0	0	0	0	28	0	0	0	0	0	0	30
%	0	3.33	0	3.33	0	0	0	0	**93.33**	0	0	0	0	0	0	100
Tol	0	6	1	0	0	0	2	1	0	20	0	0	0	0	0	30
%	0	20	3.33	0	0	0	6.67	3.33	0	**66.67**	0	0	0	0	0	100
UP	1	0	1	0	0	0	1	0	0	0	1	0	0	0	0	4
%	25	0	25	0	0	0	25	0	0	0	**25**	0	0	0	0	100
Bon	0	0	0	0	0	0	0	0	0	0	0	34	0	1	0	35
%	0	0	0	0	0	0	0	0	0	0	0	**97.14**	0	2.86	0	100
Nea	0	0	0	0	0	1	0	0	0	0	0	0	11	0	0	12
%	0	0	0	0	0	8.33	0	0	0	0	0	0	**91.67**	0	0	100
Sch	0	0	0	0	0	0	0	0	0	0	0	0	0	17	12	29
%	0	0	0	0	0	0	0	0	0	0	0	0	0	**58.62**	41.38	100
Trg	0	0	0	0	0	0	0	0	0	0	0	1	0	10	17	28
%	0	0	0	0	0	0	0	0	0	0	0	3.57	0	35.71	**60.71**	100
Total	36	33	33	28	0	24	31	22	29	31	3	35	11	28	29	373
%	9.65	8.85	8.85	7.51	0	6.43	8.31	5.9	7.77	8.31	0.8	9.38	2.95	7.51	7.77	100

Table 3.21: Unbiased Mahalanobis D^2, Step 2A. All distances 0.001 significance level except: NS = non-significant, * = 0.05 level, ** = 0.01 level.

	And	Aus	Brg	Dgn	EAM	Epi	Esk	Eur	Kbw	Rei	San	Tol	UP	Bon	Nea	Sch	Trg
And	0.00	29.02	25.61	23.95	71.83	33.96	31.06	22.74	40.83**	157.73	42.32	25.86	33.80	121.58	74.59	136.41	151.37
Aus	29.02	0.00	13.40	18.65	97.51	26.81	14.22	9.01	27.85NS	117.74	22.12	5.98	26.57	110.28	61.78	123.59	138.59
Brg	25.61	13.40	0.00	17.78	77.51	14.36	20.43	4.61	39.77**	110.35	26.29	11.95	18.06	138.08	66.49	150.34	169.80
Dgn	23.95	18.65	17.78	0.00	98.22	18.66	18.02	10.55	38.77*	106.22	15.12	16.08	34.19	116.95	62.67	124.93	140.98
EAM	71.83	97.51	77.51	98.22	0.00	89.78	101.09	86.39	116.38	199.64	124.06	98.72	82.26	187.39	103.12	207.78	224.26
Epi	33.96	26.81	14.36	18.66	89.78	0.00	29.00	12.71	40.10**	91.31	33.94	23.23	22.40	144.11	58.69	163.61	180.23
Esk	31.06	14.22	20.43	18.02	101.09	29.00	0.00	15.36	42.60**	97.66	31.51	14.67	19.63	104.95	46.50	124.24	138.63
Eur	22.74	9.01	4.61	10.55	86.39	12.71	15.36	0.00	37.77*	109.99	24.06	7.27	22.53	124.67	66.80	137.22	154.08
Kbw	40.83**	27.85NS	39.77**	38.77*	116.38	40.10**	42.60**	37.77*	0.00	121.62	28.35NS	36.90*	24.47NS	106.01	45.60**	124.98	138.69
Rei	157.73	117.74	110.35	106.22	199.64	91.31	97.66	109.99	121.62	0.00	119.01	125.06	110.27	198.31	72.91	225.10	251.38
San	42.32	22.12	26.29	15.12	124.06	33.94	31.51	24.06	28.35NS	119.01	0.00	22.04	39.95	119.77	70.51	140.40	156.49
Tol	25.86	5.98	11.95	16.08	98.72	23.23	14.67	7.27	36.90*	125.06	22.04	0.00	25.26	114.74	71.86	130.25	144.82
UP	33.80	26.57	18.06	34.19	82.26	22.40	19.63	22.53	24.47NS	110.27	39.95	25.26	0.00	134.10	57.92	154.19	169.53
Bon	121.58	110.28	138.08	116.95	187.39	144.11	104.95	124.67	106.01	198.31	119.77	114.74	134.10	0.00	81.06	15.69	19.63
Nea	74.59	61.78	66.49	62.67	103.12	58.69	46.50	66.80	45.60**	72.91	70.51	71.86	57.92	81.06	0.00	105.56	120.06
Sch	136.41	123.59	150.34	124.93	207.78	163.61	124.24	137.22	124.98	225.10	140.40	130.25	154.19	15.69	105.56	0.00	1.29NS
Trg	151.37	138.59	169.80	140.98	224.26	180.23	138.63	154.08	138.69	251.38	156.49	144.82	169.53	19.63	120.06	1.29NS	0.00

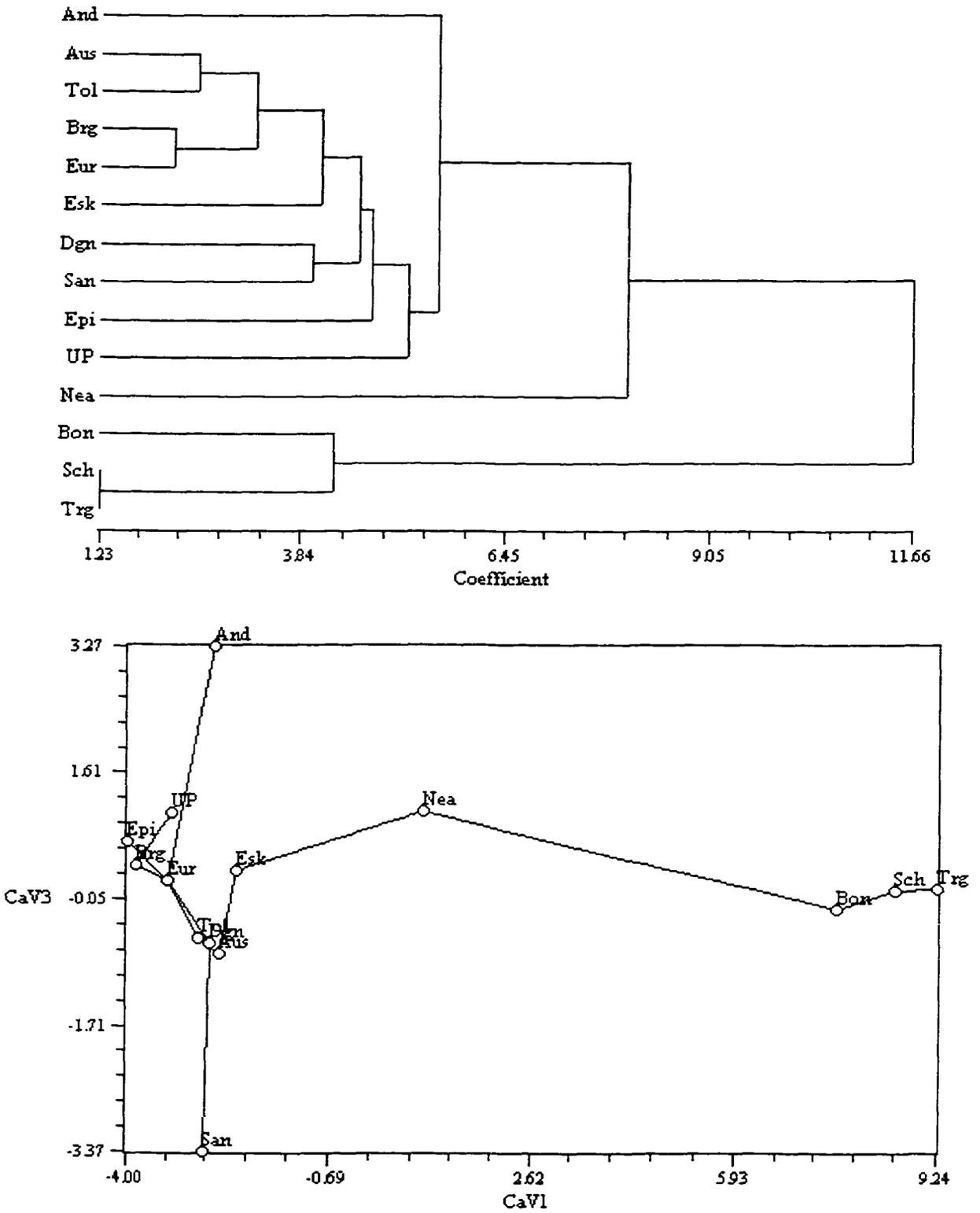

Fig. 3.32: Cluster analysis (UPGMA, top) and minimum spanning tree (Step 2A).

Step 2B – Human sample only

Principal Components Analysis: In this step Neanderthals are separated from modern humans along PC 5, and to a lesser extent, PC 3. PC 5 (6.3 % of the total variance, significant for population effects at the 0.0001 level, Table 3.22, Fig. 3.33) is the axis that best separates this fossil group from modern humans, although this separation is not complete. Neanderthals are significantly different in their mean score from most modern human populations, except the Upper Paleolithic specimens, the Epipaleolithic, the Eskimo and the Andamanese. When the ANOVA was conducted at the species level, Neanderthals are significantly different in their mean score from modern humans as a whole. Spy 2 and, to a lesser extent, La Quina 27, fall well within the modern human range, while several other specimens fall at its positive fringe. Shanidar 1, La Ferrassie 1 and Circeo 1 fall outside the modern human cloud on the positive end of this axis. Reilingen falls very close to La Quina 27 at the negative end of the Neanderthal range and within the modern human one and Kabwe also falls in the overlap area between the modern humans and Neanderthals. The Upper Paleolithic specimens, with the exception of Predmosti 3, also fall at the positive end of the modern human range. Predmosti 3 and the two early modern human specimens fall near the center of the modern human range.

The shape variation along this axis (Fig. 3.34, see also Table 3.23) includes, in the positive end, the anterior placement of the lateral origin of the petro-tympanic crest (5); the anterior placement of asterion (1); the anterior position of the tip of the mastoid process (10); the more inferior and posterior placement of the juxtamastoid eminence (11); and the more posteriorly placed parietal notch. PC 5 is only weakly correlated with centroid size.

PC 3 (8.7 %, Fig. 3.33) is significant for population (0.0001) and sex effects (0.05). It partially separates Neanderthals from modern humans, the former clustering on the negative side of this axis and overlapping with the positive end of the modern human range. As with PC 5, the mean Neanderthal score is significantly different from the modern human one, but when compared with the modern human populations, it is only significantly different from the Australians, Europeans, Berg, Epipaleolithic, San and Upper Paleolithic populations. Gibraltar 1 and Saccopastore 2 fall outside the modern

Table 3.22: Summary of the PCA results, ANOVA and Regression on Centroid Size PCs 1-10, Step 2B.

	Principal Components Analysis			ANOVA, Pr > F			Regression on Centroid Size	
	Eigenvalue	Proportion	Cumulative	Popul.	Sex	Interaction	Rho	Pr > F
PC 1	0.002541	0.132182	0.132182	0.0001	0.0302	0.6986	0.33190	0.0001
PC 2	0.002107	0.109617	0.241799	0.0001	0.0841	0.6880	0.03766	0.5281
PC 3	0.001682	0.087472	0.329271	0.0001	0.017	0.51	0.23939	0.0001
PC 4	0.001437	0.074742	0.404013	0.0001	0.0135	0.6861	-0.16134	0.0065
PC 5	0.001208	0.062811	0.466824	0.0001	0.3298	0.8317	0.30696	0.0001
PC 6	0.001176	0.061156	0.527979	0.0001	0.0461	0.2274	0.02007	0.7368
PC 7	0.001028	0.053457	0.581436	0.0001	0.2115	0.079	0.07272	0.2227
PC 8	0.000967	0.050306	0.631742	0.0001	0.0735	0.7596	0.29052	0.0001
PC 9	0.00074	0.038482	0.670224	0.0313	0.1908	0.0156	0.14144	0.0173
PC 10	0.000634	0.032994	0.703218	0.0043	0.9541	0.8883	0.12090	0.0421

Table 3.23: Squared roots of the sum of squares of the eigenvector coefficients for the three coordinates of each landmark, Step 2B, PCs 1-10.

	PC 1	PC 2	PC 3	PC 4	PC 5	PC 6	PC 7	PC 8	PC 9	PC 10
1. Asterion	**0.37**	0.15	0.17	**0.50**	**0.36**	0.29	**0.32**	**0.41**	**0.45**	0.16
2. Stylom. F.	0.08	0.06	0.10	0.25	0.09	0.15	0.08	0.22	0.07	0.12
3. M. Jug. Fos.	0.20	0.31	0.20	0.32	0.25	0.03	0.45	0.27	**0.35**	**0.35**
4. L. Jug. Fos.	0.12	0.07	0.16	0.20	0.11	0.11	0.15	0.27	0.10	0.12
5. Lat. Petro-Tym. Cr.	0.24	0.21	0.22	0.27	**0.51**	**0.62**	0.16	0.16	0.29	**0.56**
6. Med. Petro-Tym. Cr.	0.14	0.12	0.19	0.25	0.25	0.15	0.27	0.23	**0.34**	0.20
7. Porion	0.05	0.12	0.18	0.06	0.13	0.19	0.19	0.25	0.10	0.12
8. Auriculare	0.09	0.11	**0.34**	0.08	0.24	**0.30**	0.14	0.15	0.15	0.18
9. Parietal N.	**0.42**	**0.37**	**0.44**	**0.43**	**0.30**	0.22	**0.60**	0.20	**0.44**	0.14
10. Mastoid	**0.47**	**0.54**	0.20	**0.37**	**0.35**	**0.33**	0.21	**0.47**	0.19	**0.34**
11. Juxtam. Em.	**0.50**	**0.45**	**0.60**	0.20	**0.32**	**0.42**	0.14	0.12	0.20	0.09
12. Artic. Em.	0.14	0.33	**0.25**	0.18	0.18	0.08	0.24	0.26	**0.32**	**0.45**
13. Entogl. Pyr.	0.18	0.21	0.09	0.03	0.21	0.13	0.17	**0.36**	0.23	0.27

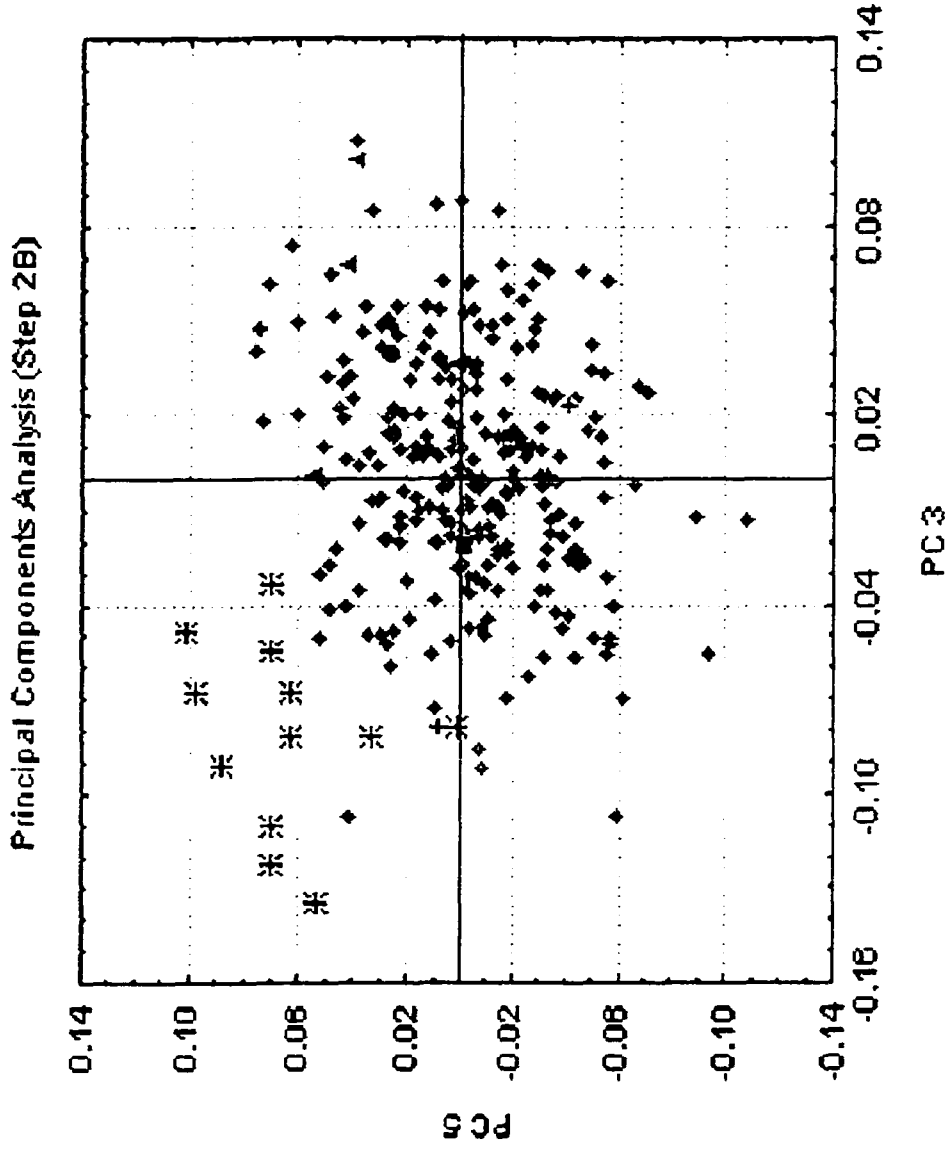

Figure 3.33: Principal Components Analysis (Step 2B), PCs 3 and 5.

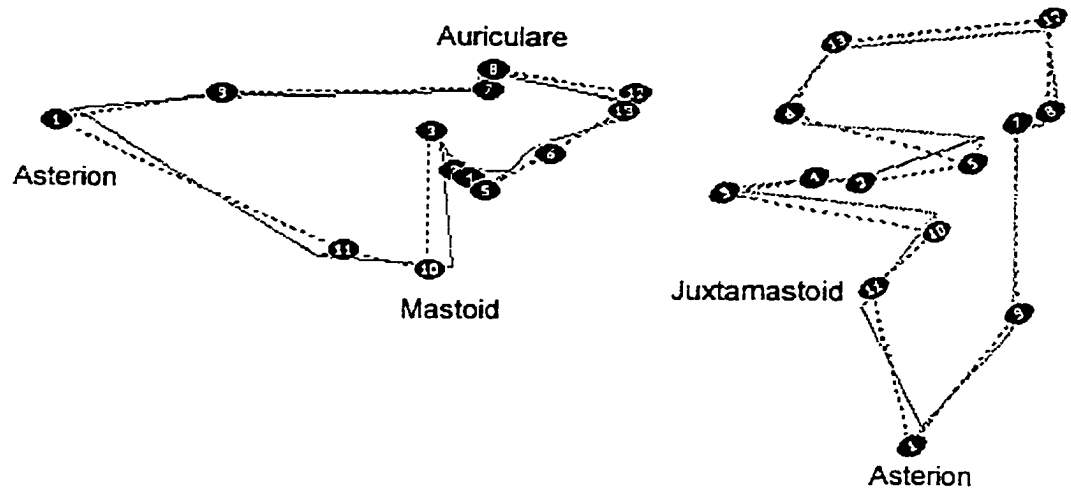

Positive end of PC 5 (Neanderthals)

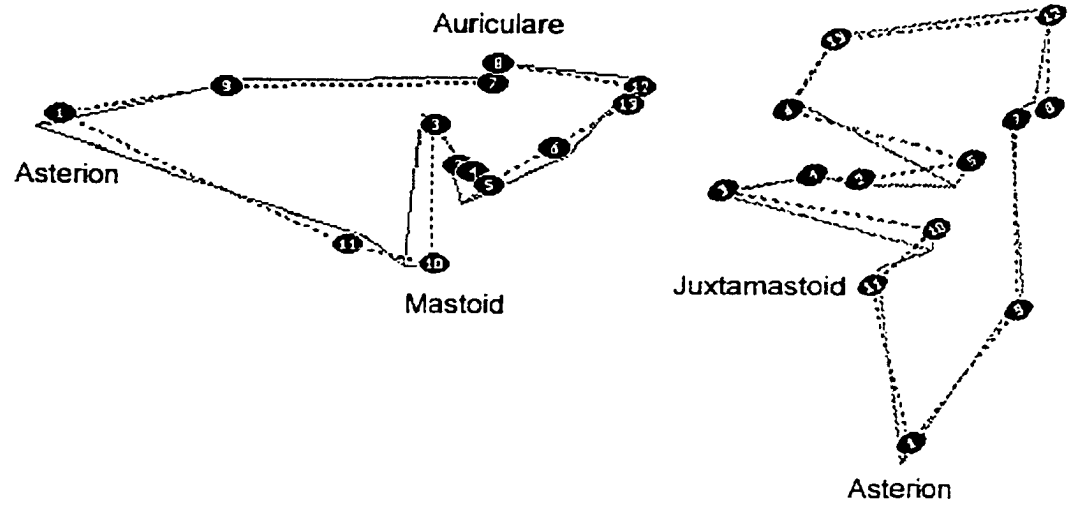

Negative end of PC 5

Figure 3.34: Shape variation along PC 5 (Step 2B), right lateral (left) and right ventral (right) views. The dotted line represents the consensus configuration.

human cloud. Kabwe falls well within the modern human range and on its negative side, as do the Upper Paleolithic specimens and Skhul 5. Qafzeh 9 falls at the positive extreme of the modern human range and within the range of overlap with Neanderthals. Reilingen falls near the center of the modern human range. Among modern human populations, PC 3 partially separates the Eskimo, Andamanese and Dogon, who fall mostly on the positive side, from the Epipaleolithic, San and Berg, who fall mostly on the negative. When PC 3 is labeled by sex, a tendency is observed for males to have more positive scores than females. The mean scores for males for most populations, including Neanderthals and the Upper Paleolithic specimens, are more positive than the mean scores for females (Fig. 3.35). In the Andamanese and the Berg male and female mean scores are almost identical, while females have a more positive mean score in the Eskimo.

The shape variation among this component (Fig. 3.36) includes, at the negative end, a medially and anteriorly placed juxtamastoid eminence (11); a more anterior placement of the parietal notch (9); a more lateral and slightly elevated auriculare (8); and a more laterally and posteriorly placed root of the articular eminence (12). These shape differences tend to characterize Neanderthals relative to most modern humans, and females relative to males. A small (5.7 %) but significant component of this axis reflects centroid size-related shape variation. PC 3 is only weakly correlated with centroid size.

Kabwe falls just outside the modern human range at the negative end of PC 1 (13.2 %, significant for population (0.0001) and sex (0.05) effects, Fig. 3.37). Neanderthals also tend to fall on the negative side of this axis, and Circeo 1, Spy 1 and La Quina 27 fall outside the modern human range and close to Kabwe. All other fossil specimens fall well within the modern human range. The mean scores for males are more positive than the mean scores for females in Neanderthals and in most modern human populations, except in the Dogon, where the mean value for males is more negative, and in the Andamanese, where the male and female mean scores are almost identical (Fig. 3.38).

The shape differences at the negative end of PC 1 include a postero-medially placed juxtamastoid eminence, a small mastoid process, an anteriorly and inferiorly

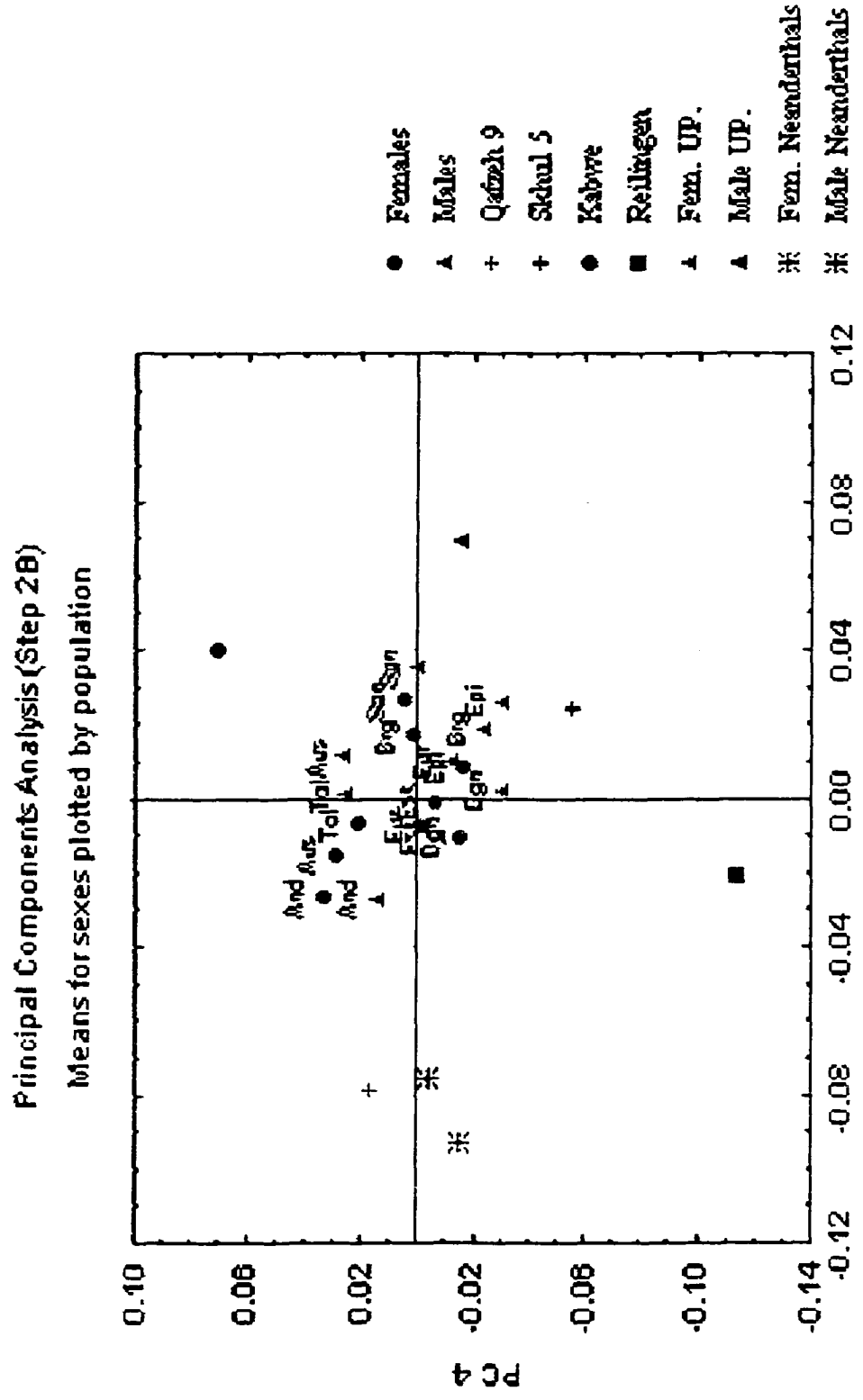

Figure 3.35: Principal Components Analysis (Step 2B), mean scores for sexes plotted by population, PCs 3 and 4.

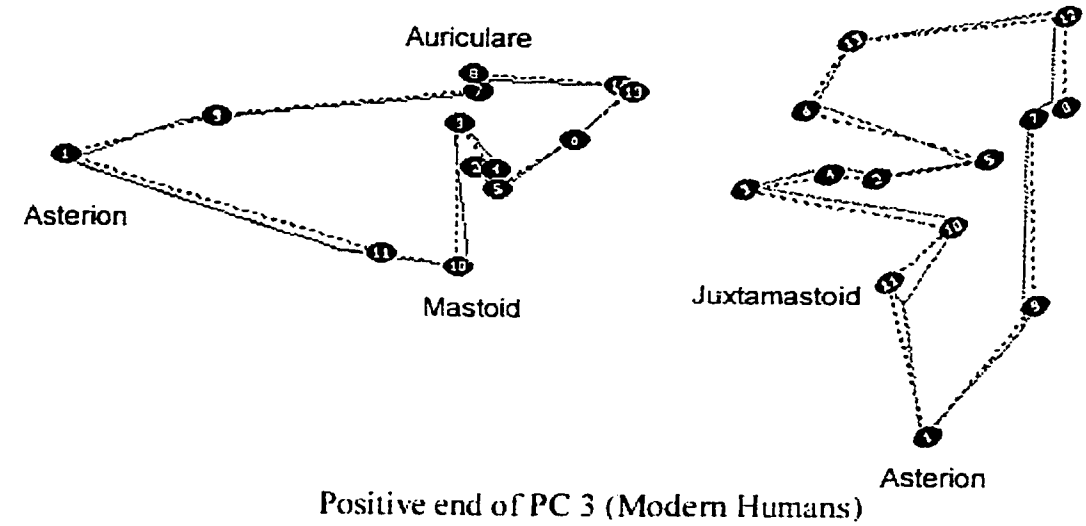

Positive end of PC 3 (Modern Humans)

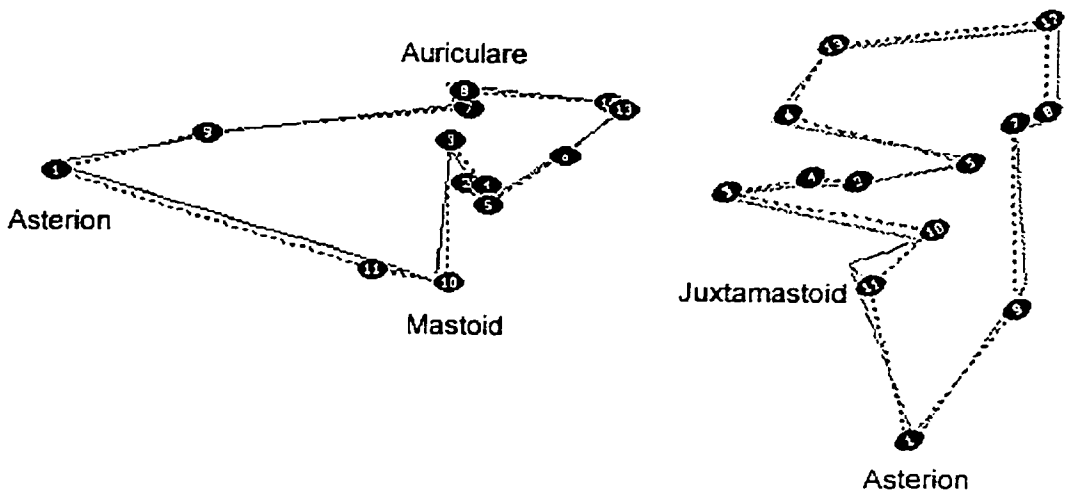

Negative end of PC 3 (Neanderthals)

Figure 3.36: Shape variation along PC 3 (Step 2B), right lateral (left) and right ventral (right) views. The dotted line represents the consensus configuration.

placed parietal notch, and a more inferiorly placed asterion. They characterize Kabwe relative to modern humans, as well as most females relative to males. PC 1 is weakly correlated with centroid size.

PC 4 (7.5 %, Fig. 3.37) is significant for population (0.0001) and sex effects (0.05). PC 4 separates Reilingen from modern humans, this specimen falling on its negative end and outside the modern human range. Neanderthals span the entire modern human range along this component, with La Quina 27 falling outside it on the negative end and near Reilingen. Kabwe falls at the positive extreme of the modern human cloud, but within it. The early anatomically modern human and the Upper Paleolithic specimens fall well within the modern human range. When PC 4 is labeled by sex, a slight tendency is observed for females to be more positive than males. The male mean scores by population are more negative than the female ones in most populations, except the Australians, where they are almost identical, and in Neanderthals, where this trend is reversed (Fig. 3.35).

The shape differences at the negative end of PC 4 include a more medial placement of asterion, superiorly and anteriorly placed parietal notch, and an anterior placement of the tip of the mastoid process. These shape differences characterize Reilingen and La Quina 27 relative to the rest of the human sample as well as most modern human males relative to females. The opposite shape differences characterize Kabwe relative to most modern humans and Neanderthals. PC 4 is only very weakly correlated with centroid size (Table 3.22).

***Canonical Variates Analysis*:** In this analysis, and unlike Step 1B, Neanderthals are completely separated from modern humans along the first canonical axis (Fig. 3.39). CaV 1 explains 25.4 % of the total variance and is most strongly influenced by PCs 5, 3 and 10. Neanderthals fall on its positive side and outside the 95 % ellipses of all modern human groups along CaVs 1 and 2. They are significantly different in their mean score value from all modern human groups. Amud 1 is closest to the modern human cloud, but still outside the modern human confidence ellipses. Reilingen falls at the positive end of CaV 1 and within the Neanderthal sample. Kabwe falls within the modern human range but near its positive end, while the other fossil specimens fall well within the range of modern human variation along this axis.

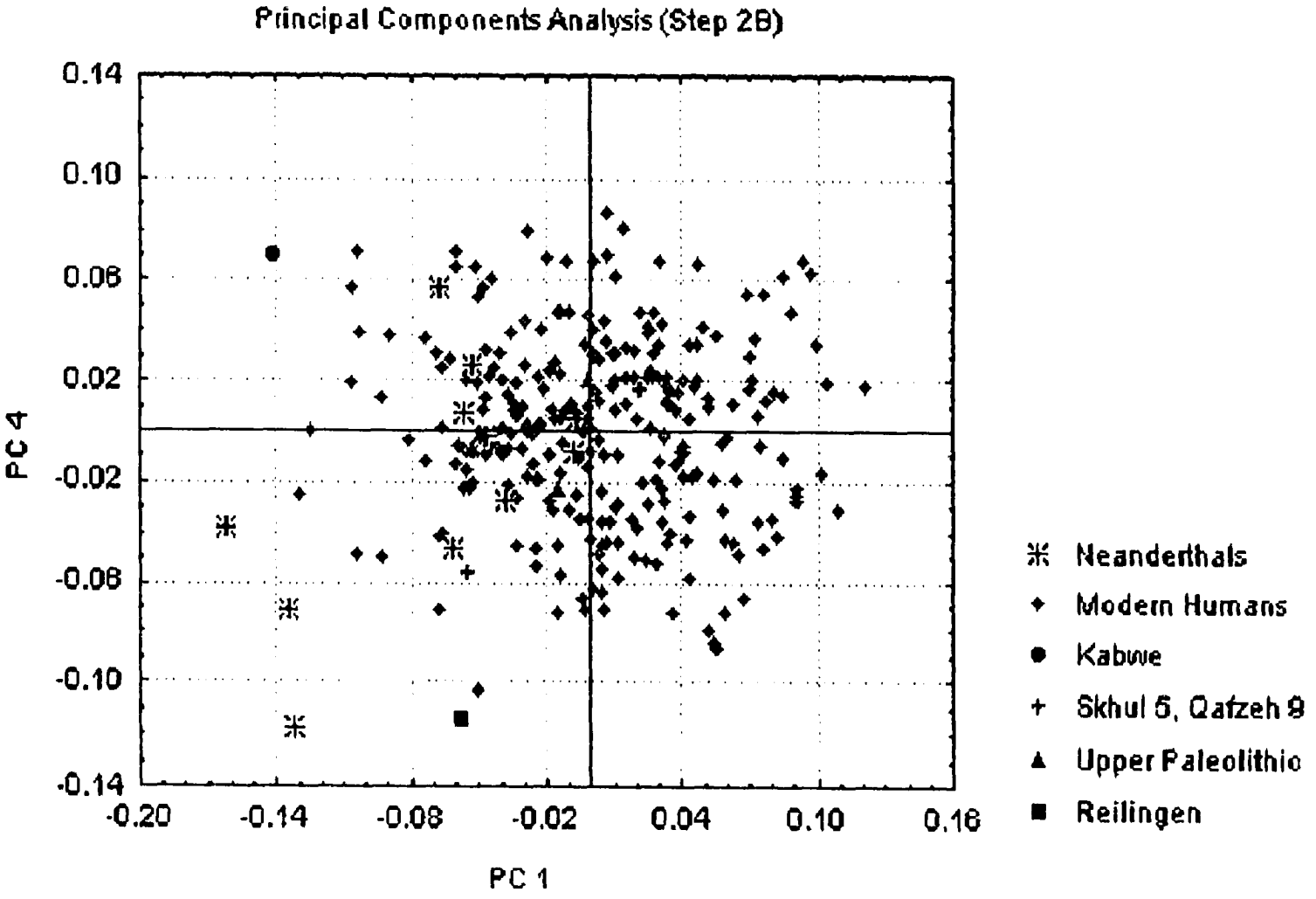

Figure 3.37: Principal Components Analysis (Step 2B), PCs 1 and 4.

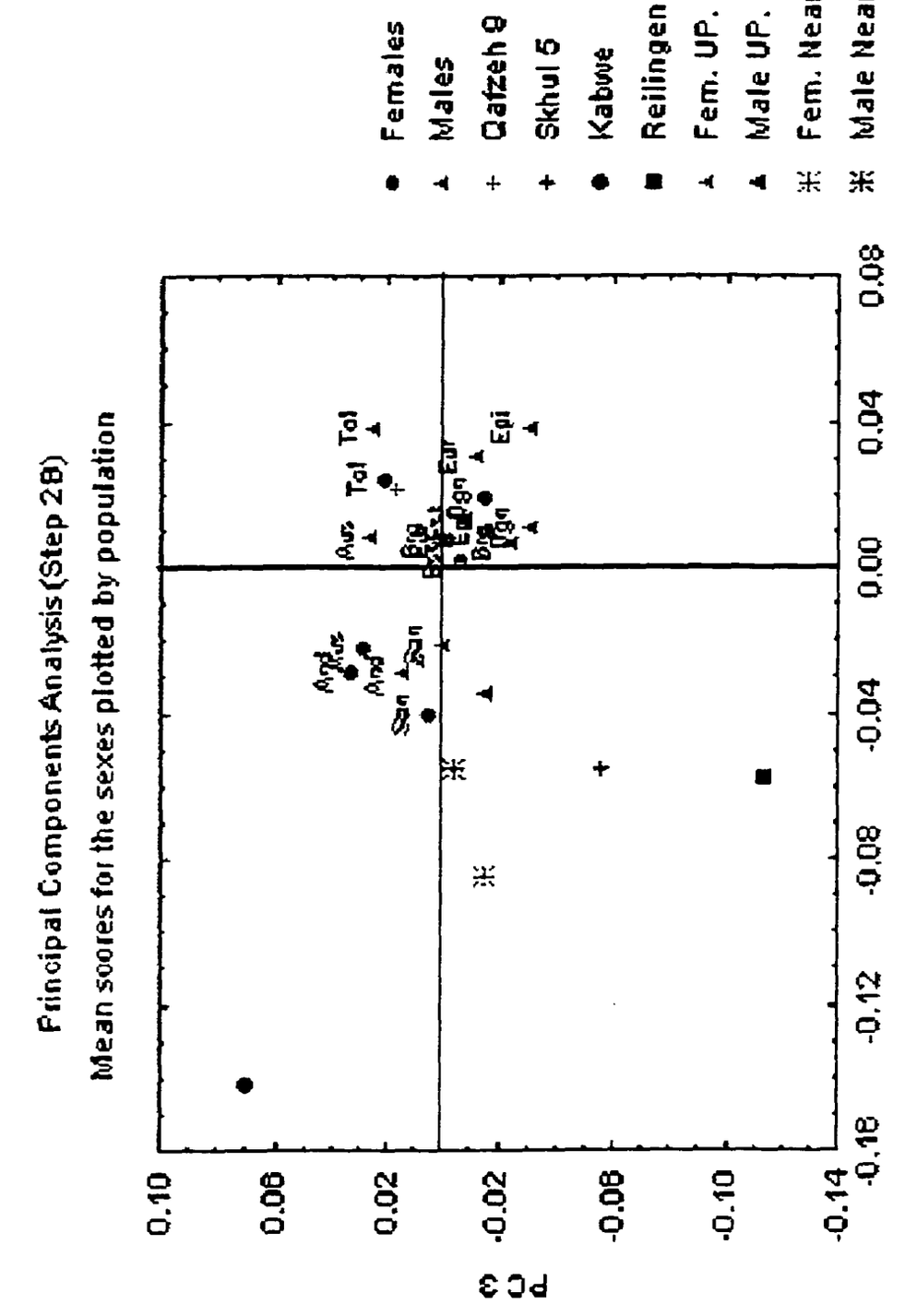

Figure 3.38: Principal Components Analysis (Step 2B), mean scores for sexes labeled by population, PCs 1 and 3.

The shape differences along CaV 1 (Fig. 3.40) include, at its positive end, an anterior placement of the lateral origin of the petro-tympanic crest (5), a small mastoid process (10), which is approximately as large as the juxtamastoid eminence (11), a medially placed juxtamastoid eminence (11), and a more lateral auriculare (8) and porion (7). CaV 1 is weakly correlated with centroid size (Table 3.24).

CaV 2 (18.8 %, Fig. 3.39) separates the Andamanese on the positive end of the modern human range from the San on the negative, with the remaining populations falling in between around the zero axis and overlapping extensively with each other. The Andamanese are significantly different from most other modern human groups in their mean score, with the exception of the Epipaleolithic, the Berg and the Upper Paleolithic groups. Qafzeh 9 also falls at the positive extreme of this axis and outside the 95 % confidence ellipse of all modern human groups, including the Andamanese, while Skhul 5 falls well within the modern human cloud, but near its positive end and overlapping with the Andamanese. These two specimens are significantly different from all other human groups in their mean score. The Upper Paleolithic specimens cluster close together near the center of the modern human range, where Kabwe also falls.

The shape differences (Fig. 3.41) that characterize Qafzeh 9, and to a lesser extent, the Andamanese and Skhul 5, include a laterally placed auriculare (8), a posteriorly positioned root of the articular eminence (12), a medially placed medial end of the petro-tympanic crest (6), and an anterior placement of the medial end of the jugular fossa (3). These differences are similar to those described for CaV 3, Step 2A. CaV 2 is not correlated with centroid size (Table 3.24).

Classification: The UP and EAM were included here as populations. As in Step 2A, Reilingen was classified as Neanderthal (1.00). Kabwe, however, was classified as Upper Paleolithic (0.52). All the Upper Paleolithic, early modern human and Neanderthal specimens were placed in their groups. The cross-validation classification results (Table 3.25) were similar to those in Step 2A. Here, however, none of the Upper Paleolithic specimens was successfully classified. Three of them were placed with the Berg and one with the Epipaleolithic modern human population.

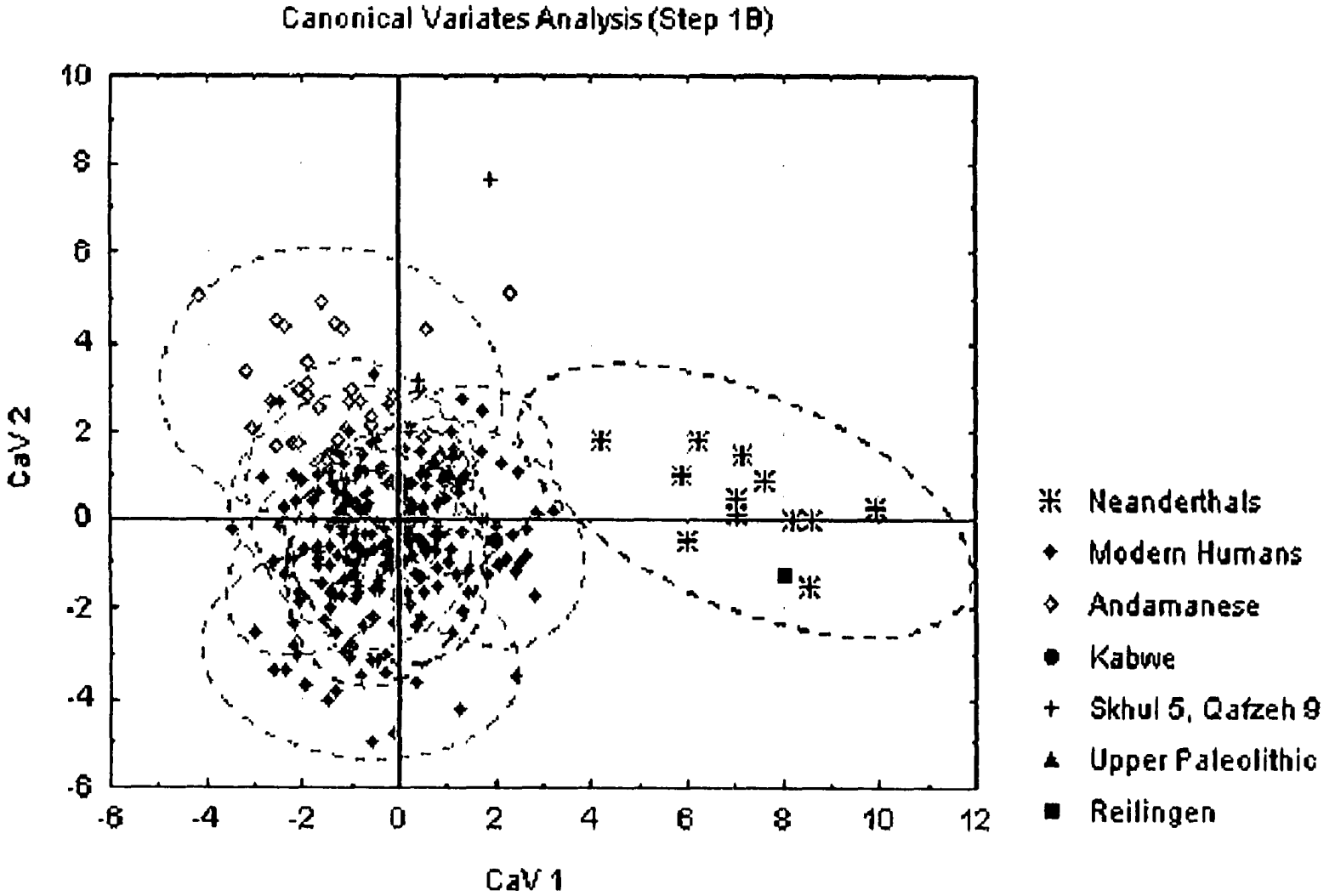

Figure 3.39: Canonical Variates Analysis (Step 2B), CaVs 1 and 2.

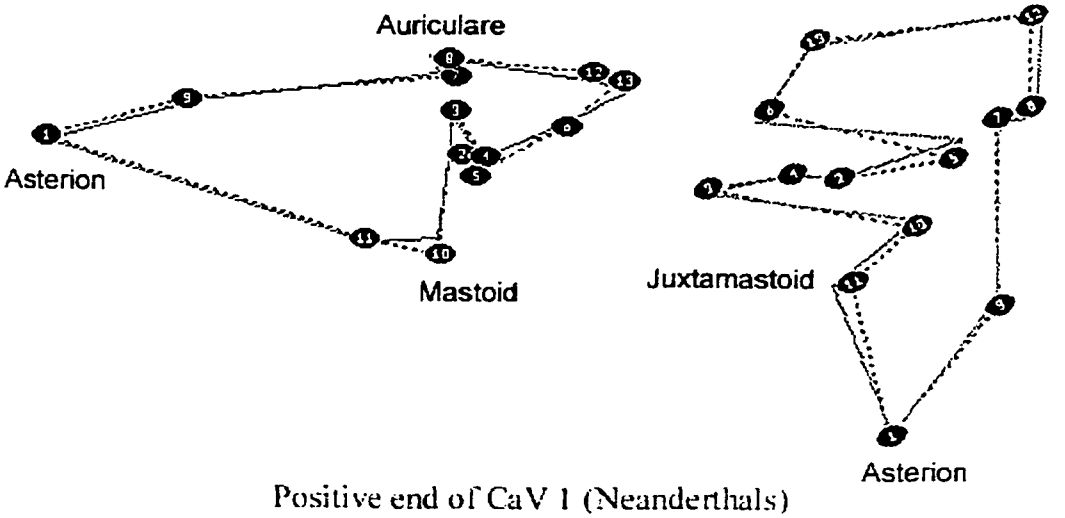

Positive end of CaV 1 (Neanderthals)

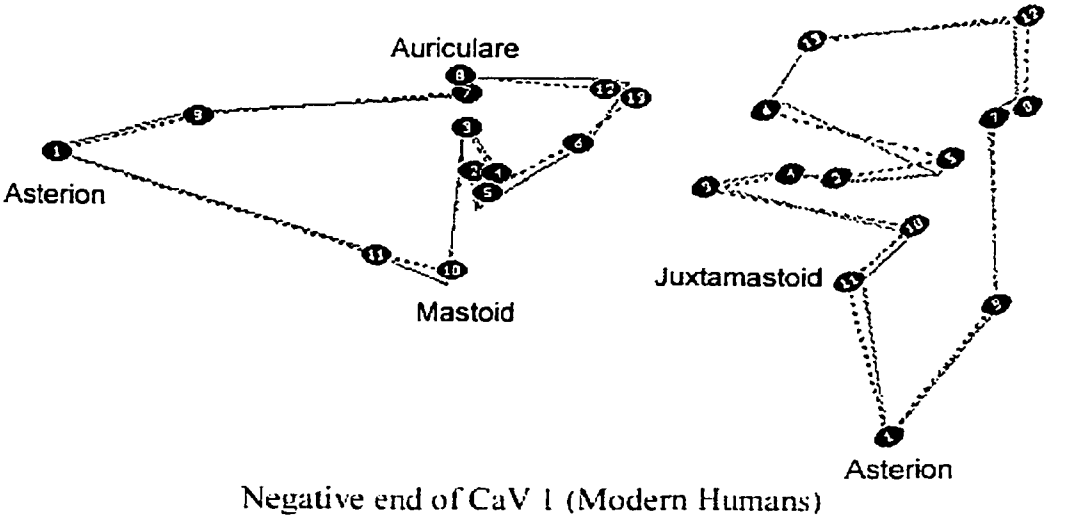

Negative end of CaV 1 (Modern Humans)

Figure 3.40: Shape variation along CaV 1 (Step 2B), right lateral (left) and right ventral (right) views. The dotted line represents the consensus configuration.

Table 3.24: Summary of the CVA results and Correlation Analysis, CaVs 1-5, Step 2B.

	Canonical Variates Analysis			Correlation with Centroid Size	
	Eigenvalue	Proportion	Cumulative	Rho	Pr > F
CaV 1	3.5329	0.2543	0.2543	0.23019	0.0001
CaV 2	2.6122	0.188	0.4423	-0.0525	0.93
CaV 3	2.0635	0.1485	0.5908	0.25513	0.0001
CaV 4	1.9833	0.1427	0.7335	0.47904	0.0001
CaV 5	1.1382	0.0819	0.8155	-0.12350	0.0379

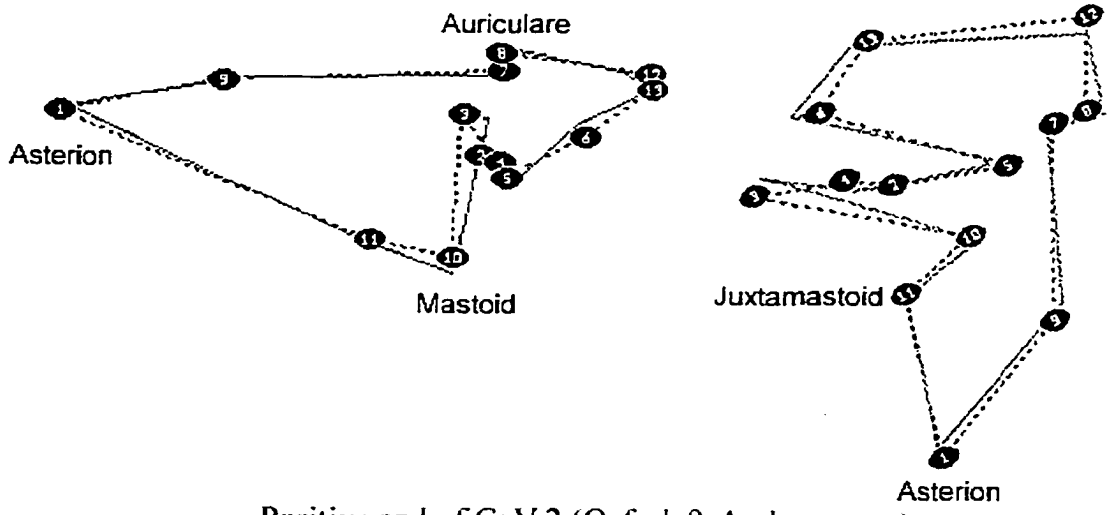

Positive end of CaV 2 (Qafzeh 9, Andamanese)

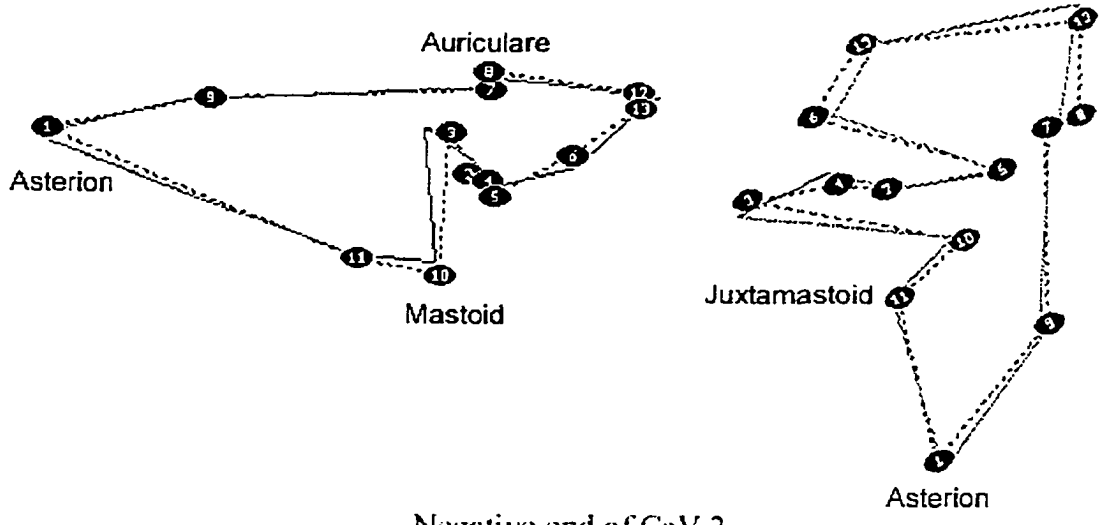

Negative end of CaV 2

Figure 3.41: Shape variation along CaV 2 (Step 2B), right lateral (left) and right ventral (right) views. The dotted line represents the consensus configuration.

Table 3.25: Cross-validation classification summary, Step 2B (percentages for each population in bold).

	And	Aus	Brg	Dgn	EAM	Epi	Esk	Eur	San	Tol	UP	Nea	Total
And	27	0	0	0	0	1	2	0	0	0	0	0	30
%	**90**	0	0	0	0	3.33	6.67	0	0	0	0	0	100
Aus	0	26	1	1	0	0	1	0	0	1	0	0	30
%	0	**86.67**	3.33	3.33	0	0	3.33	0	0	3.33	0	0	100
Brg	1	1	19	0	0	2	0	6	0	1	0	0	30
%	3.33	3.33	**63.33**	0	0	6.67	0	20	0	3.33	0	0	100
Dgn	0	1	0	24	0	0	2	1	0	1	0	0	29
%	0	3.45	0	**82.76**	0	0	6.9	3.45	0	3.45	0	0	100
EAM	1	0	1	0	0	0	0	0	0	0	0	0	2
%	50	0	50	0	**0**	0	0	0	0	0	0	0	100
Epi	0	0	2	0	0	20	0	1	0	0	1	0	24
%	0	0	8.33	0	0	**83.33**	0	4.17	0	0	4.17	0	100
Esk	0	0	0	1	0	0	26	1	0	2	0	0	30
%	0	0	0	3.33	0	0	**86.67**	3.33	0	6.67	0	0	100
Eur	3	1	7	1	0	1	0	11	0	6	0	0	30
%	10	3.33	23.33	3.33	0	3.33	0	**36.67**	0	20	0	0	100
San	0	1	0	1	0	0	0	0	28	0	0	0	30
%	0	3.33	0	3.33	0	0	0	0	**93.33**	0	0	0	100
Tol	0	6	1	0	0	0	2	1	0	20	0	0	30
%	0	20	3.33	0	0	0	6.67	3.33	0	**66.67**	0	0	100
UP	0	0	3	0	0	1	0	0	0	0	0	0	4
%	0	0	75	0	0	25	0	0	0	0	**0**	0	100
Nea	0	0	0	0	0	1	0	0	0	0	0	11	12
%	0	0	0	0	0	8.33	0	0	0	0	0	**91.67**	100
Total	32	36	34	28	0	26	33	21	28	31	1	11	281
%	11.39	12.81	12.1	9.96	0	9.25	11.74	7.47	9.96	11.03	0.36	3.91	100

Table 3.26: Unbiased Mahalanobis D^2, Step 2B. All distances 0.001 significance level except: NS = non-significant, * = 0.05 level, ** = 0.01 level.

	And	Aus	Brg	Dgn	EAM	Epi	Esk	Eur	Kbw	Rei	San	Tol	UP	Nea
And	0.00	28.22	22.33	23.26	71.29	34.28	31.43	20.93	41.06*	172.97	38.04	24.24	33.13	79.57
Aus	28.22	0.00	14.34	18.46	95.32	28.58	14.16	9.86	28.83NS	135.77	22.43	6.56	27.66	63.02
Brg	22.33	14.34	0.00	17.65	76.48	15.82	21.15	4.38	39.50*	131.86	24.92	11.48	17.53	73.07
Dgn	23.26	18.46	17.65	0.00	96.98	19.53	17.55	10.42	36.50*	124.12	15.05	15.96	32.11	64.85
EAM	71.29	95.32	76.48	96.98	0.00	92.89	100.78	84.87	116.06	211.18	116.28	94.66	84.36	103.90
Epi	34.28	28.58	15.82	19.53	92.89	0.00	27.89	13.15	34.95NS	101.39	33.69	24.16	20.41	60.08
Esk	31.43	14.16	21.15	17.55	100.78	27.89	0.00	15.00	39.99*	111.42	31.38	14.31	18.87	49.74
Eur	20.93	9.86	4.38	10.42	84.87	13.15	15.00	0.00	36.40*	126.89	23.14	7.31	20.48	69.74
Kbw	41.06*	28.83NS	39.50*	36.50*	116.06	34.95NS	39.99*	36.40*	0.00	125.37	31.89NS	37.87*	25.41NS	44.66*
Rei	172.97	135.77	131.86	124.12	211.18	101.39	111.42	126.89	125.37	0.00	142.18	145.88	117.77	80.41
San	38.04	22.43	24.92	15.05	116.28	33.69	31.38	23.14	31.89NS	142.18	0.00	20.82	39.16	75.83
Tol	24.24	6.56	11.48	15.96	94.66	24.16	14.31	7.31	37.87*	145.88	20.82	0.00	24.77	75.73
UP	33.13	27.66	17.53	32.11	84.36	20.41	18.87	20.48	25.41NS	117.77	39.16	24.77	0.00	63.11
Nea	79.57	63.02	73.07	64.85	103.90	60.08	49.74	69.74	44.66*	80.41	75.83	75.73	63.11	0.00

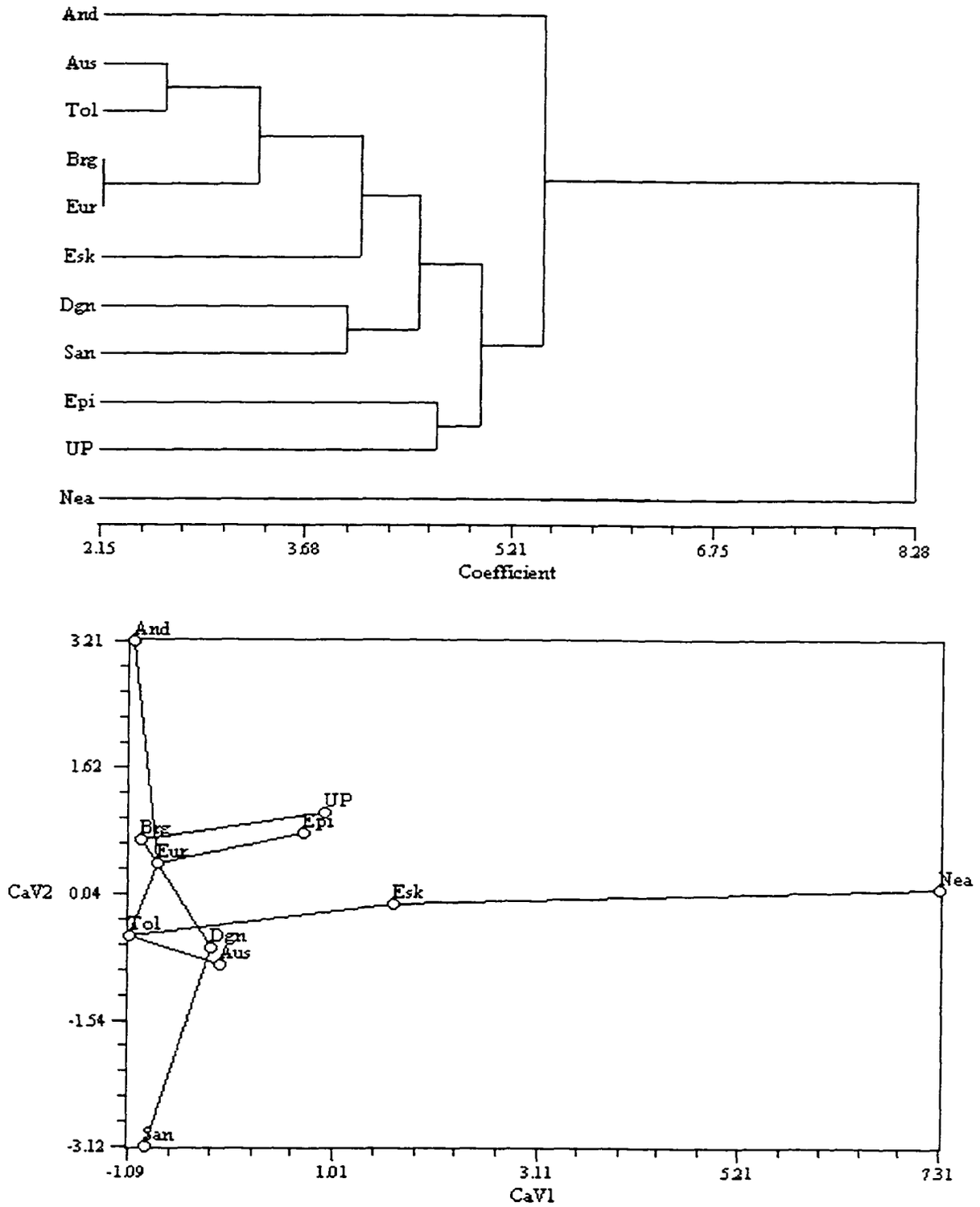

Figure 3.42: Cluster analysis (UPGMA, top) and minimum spanning tree (Step 2B).

Mahalanobis D^2, Cluster Analysis and Minimum Spanning Tree: The unbiased Mahalanobis D^2 matrix was calculated (Table 3.26) and results were similar to those in the previous steps. Neanderthals are still very far from modern human populations, showing the smallest distance to the Eskimo. This distance is greater than the greatest distance among modern human groups (San and Andamanese). Neanderthals are not close to the Upper Paleolithic or the modern European groups. As in Steps 1 and 2A, the Upper Paleolithic are closest to the Berg and farthest from the Andamanese among modern human groups, although they are most distant overall from the Neanderthals.

The cluster analysis (Fig. 3.42) is also similar to that in Step 2A. Here, however, the Upper Paleolithic specimens cluster with the Epipaleolithic in a deep splitting branch. Neanderthals are still outliers to all other human groups, while the Andamanese are outliers to all other modern human groups. All three geographic pairs preserve their clustering. The minimum spanning tree (Fig. 3.43) shows the Upper Paleolithic to be closest to the Berg, while the Epipaleolithic are linked to the European group. Neanderthals are linked to the Eskimo, but are very far from all modern human groups.

Step 2C – Chimpanzee sample only

As in Step 1, the analysis was repeated on the chimpanzee sample alone, in order to test for the consistency of the chimpanzee model. As in Step 1C, only the results of the discriminant analysis and the Mahalanobis D^2 analysis will be discussed here.

Classification: A discriminant analysis was performed and a cross-validation classification was obtained for the chimpanzee sample (Table 3.27). In this case no bonobos were misclassified as common chimpanzees or vice versa. This is a better result than that obtained in Step 2A, where one bonobo and one common chimpanzee specimen were misclassified. The misclassification rates between the two common chimpanzee subspecies are also slightly lower than in Step 1.

Mahalanobis D^2: In the unbiased Mahalanobis D^2 analysis (Table 3.28), bonobos are much more widely separated from both common chimpanzee subspecies than the two subspecies are from each other. As in Step 1E, the distances between bonobos and the two common chimpanzee subspecies are almost doubled compared to those found in Step 2A. However, they are still considerably smaller than those between Neanderthals and

modern humans, and are now equivalent to the largest distances among modern human groups. The distance between the two common chimpanzee subspecies is also greatly increased, but it is still quite small and not significant, as in Steps 2A, 1A and 1E. It is now equivalent, rather than smaller than, the smallest distances among modern human groups.

Table 3.27: Cross-validation classification summary, Step 2C (percentages for each population in bold).

	Bon	Sch	Trg	Total
Bon	35	0	0	35
	100	0	0	100
Sch	0	19	10	29
	0	**65.52**	34.48	100
Trg	0	8	20	28
	0	28.57	**71.43**	100

Table 3.28: Unbiased Mahalanobis D^2, chimpanzee sample, Step 2C. All distances 0.001 significance level except: NS = non-significant, * = 0.05 level, ** = 0.01 level.

	Bon	Sch	Trg
Bon	0.00	27.87	33.97
Sch	27.87	0.00	4.42NS
Trg	33.97	4.42NS	0.00

Discussion

Modern humans: The modern human mean configuration shows a medio-laterally narrower tympanic area and glenoid fossa, a more sagittal orientation of the petro-tympanic crest and a larger mastoid process relative to both chimpanzees and Neanderthals. Modern humans show consistent geographic clustering in their temporal bone landmarks configurations. The groups in all three geographic pairs are closest neighbors with their geographic neighbors and cluster together all the analyses of both Steps 1 and 2.

Modern human males were found to differ from females in their temporal bone landmark configurations. These differences include larger and more laterally placed mastoid processes and juxtamastoid eminences, antero-posteriorly long and supero-inferiorly short mastoid portions of the temporal bone, and an antero-posteriorly elongated zygomatic process with an inferiorly placed zygomatic suture. There is, however, considerable overlap between males and females. Examination of the mean scores for males and females by population shows that the pattern of sexual dimorphism is consistent across the modern human groups included in this analysis. The shape differences observed are in agreement with the general principles for sex estimation based on cranial features (e.g. Steele and Bramblett 1988; White and Folkens 1991), which indicate a greater overall robusticity and larger mastoid processes in males relative to females. These differences are often attributed to greater size in males. However, none of the principal components separating males from females are strongly correlated with centroid size.

Chimpanzees: The chimpanzee mean configuration differs from the mean modern human configuration in having a more laterally placed porion and auriculare, and a more medially and inferiorly placed entoglenoid pyramid and medial end of the petro-tympanic crest, indicating a strong and laterally projecting supramastoid crest and a medio-laterally wider glenoid fossa and tympanic area. It is also characterized by a much more coronal orientation of the petro-tympanic crest, whose lateral origin is more lateral; a more posterior placement of both the medial and the lateral end of the jugular fossa; a smaller and more medially placed mastoid process and juxtamastoid eminence; a more inferiorly placed root of the articular eminence; a more inferior and anterior placement of

the parietal notch and asterion; and an elevated superior aspect of the zygomatic suture. These shape differences are consistent with the differences between great ape and human basicrania described by Olson (1981). Olson found that great apes differ from modern humans in their strong and more laterally projecting supramastoid crest, their small and medially positioned mastoid process, and their wide and shallow digastric fossa with a small and medially placed juxtamastoid eminence at its medial border.

The same shape differences also separate humans from chimpanzees along the first principal component and first canonical axis of all the analyses of the combined human and chimpanzee sample (Steps 1A, 1C, 2A and 2C). Chimpanzees were found to differ from humans in their medio-laterally wider tympanic area, their coronally oriented petro-tympanic crest, their smaller mastoid process, and their smaller and more medially placed juxtamastoid eminence.

Neanderthals: Neanderthals differ from chimpanzees in the same ways as modern humans do, and these differences are reflected in their intermediate placement between modern humans and chimpanzees on PC 1 and CaV 1 of all the combined sample analyses. The mean Neanderthal configuration is much more similar to the modern human than to the chimpanzee mean configuration. In a comparison between the Neanderthal and modern human mean configurations, Neanderthals differ from the modern humans in many of the same shape features that separate modern humans from chimpanzees. These include a more laterally placed auriculare and porion; a more coronal orientation of the petro-tympanic crest; a smaller mastoid process and more medially placed juxtamastoid eminence; an inferiorly placed entoglenoid pyramid an articular eminence; an antero-posteriorly shorter mastoid portion; and an elevated superior aspect of the zygomatic suture. However, Neanderthals do not show smaller juxtamastoid eminences than modern humans, as chimpanzees do. In the Neanderthal mean configuration the juxtamastoid eminence appears only slightly more inferiorly placed, but it is at the same height, or even lower, than the Neanderthal mastoid process. Compared to Kabwe, the mean Neanderthal configuration shows a more anteriorly placed mastoid process and juxtamastoid eminence; a more anterior lateral origin of the petro-tympanic crest and more coronal orientation of that crest; a more laterally placed auriculare and root of the articular eminence; and an antero-posteriorly larger mastoid

portion.

The shape differences that were found to separate Neanderthals from modern humans in the PCA and CVA include the more coronal orientation of the petro-tympanic crest; the lateral placement of porion and auriculare; the posterior position of the entoglenoid pyramid; a more inferior and lateral placement of the root of the articular eminence; a more anteriorly placed asterion, indicating an antero-posteriorly shorter mastoid portion; an elevated superior aspect of the zygomatic suture and a more inferiorly placed juxtamastoid eminence relative to the mastoid process (Step 1B, PCs 9 and 3, CaVs 3, 2 and 4). In Step 2B (PCs 3 and 5, CaV 1), after removing the two landmarks on the zygomatic process and increasing the Neanderthal sample from six to twelve, the shape characteristics that separate Neanderthals from modern humans include a small mastoid process; a relatively large and medially placed juxtamastoid eminence; a more laterally placed root of the articular eminence; and a more laterally placed auriculare and porion. None of these axes are strongly correlated with centroid size.

These differences support previous descriptions of Neanderthal temporal bone as characterized by a small mastoid process relative to the large juxtamastoid eminence (Vallois 1969; Santa Luca 1978; Smith 1982; Stringer 1985; Hublin 1988; Condemi 1991, 1992; Elyaqtine 1995a, 1996; Dean et al. 1998; Minugh-Purvis et al. 2000). This analysis found the size of the mastoid process to be more important in separating this fossil group than the size of the juxtamastoid eminence. The equal height of the two structures therefore appears to be due to the reduction of the height of the mastoid process rather than the increased height of the juxtamastoid eminence. This finding disagrees with Trinkaus (1983), who, measuring the mastoid process from the Frankfurt plane, concluded that the size of the Neanderthal mastoid process largely overlaps with that of modern humans, and that it is the increase in the height of the juxtamastoid eminence that results in the diagnostic morphology of this area in Neanderthals. This landmark analysis, by being orientation free, may provide a better means of assessing relative contributions of different structures to a morphological pattern (see also Martínez et al. 1997).

The anteriorly placed lateral origin of the petro-tympanic crest (Vallois 1969; Vandermeersch 1985; Elyaqtine 1996; Schwartz and Tattersall 1996; Minugh-Purvis et

al. 2000) and the coronal orientation of this crest (Trinkaus 1983; Martínez et al. 1997) were also very important in driving the separation between Neanderthals and modern humans. These traits are both considered primitive retentions from *H. erectus*, the opposite conditions being derived traits of modern humans (Martínez et al. 1997; Schwartz and Tattersall 1997; Dean et al. 1998). The robusticity of the zygomatic process and the strong supramastoid crest (Boule and Vallois 1957; Vallois 1969; Heim 1976; Elyaqtine 1995) are reflected in the lateral projection of auriculare and the elevated position of the superior aspect of the zygomatic suture. The described Neanderthal wide, shallow and medially closed-off glenoid fossa (Vallois 1969) is reflected in the lateral and inferior placement of the root of the articular eminence and the posterior position of the entoglenoid pyramid. However, this shape difference was only found to be important in separating the two groups in Step 1, before removal of the zygomatic suture landmarks and before the addition of further Neanderthal specimens.

The proposed Neanderthal condition of an elevated external auditory meatus relative to the zygomatic process and the floor of the glenoid fossa (Vallois 1969; Vandermeersch 1985; Elyaqtine 1995b) is also best assessed when the landmarks of the zygomatic process are present. Porion itself was not found to be elevated, but the floor of the glenoid cavity, as represented by the root of the articular eminence, as well as the inferior aspect of the zygomatic suture, were found to be lower in Neanderthals compared to modern humans. The relative position of porion with regard to these structures, therefore, appears elevated. These results are consistent with the findings of Yaroch (1996), who also noted that porion is not superiorly positioned in Neanderthals, but rather that the zygomatic arch appeared more inferiorly placed. As Yaroch noted, this shape difference may best be described in terms of the relationship between the face and the neurocranium, rather than the position of the external auditory meatus. Although not among the strongest shape differences separating Neanderthals from modern humans, this feature did differentiate Neanderthals from modern humans. The more medial position of the Neanderthal stylomastoid foramen suggested by Vallois (1969; Vandermersch 1985), was not found.

In the Mahalanobis D^2 analysis, Neanderthals were always very widely removed from all modern human groups, including the Upper Paleolithic specimens. They were

closest to the Eskimo in all analyses, although this distance was too large to reflect any substantial similarities between the two. When the mean Eskimo configuration is compared to the mean Neanderthal configuration and the mean modern human configuration, it is found to be almost identical to the mean modern human configuration, and to be similar to Neanderthals only in its more posterior placement of porion and auriculare and the inferior placement of the parietal notch. Neanderthals do not show any affinities in this analysis to either of the two recent European groups, or to the Upper Paleolithic European specimens. They are the outliers to all other human groups in all cluster analyses, and are placed very far from the modern human groups, although joined to the Eskimo, in all minimum spanning trees. All specimens, except for one (Amud 1) were always correctly classified, and no modern human specimen was ever misclassified as Neanderthal.

These results are in agreement with previous multivariate analysis of cranio-facial measurements (Stringer 1974a, 1989, 1992; Bräuer and Rimbach 1990; Bräuer 1992; Turbón et al 1997), which found Neanderthals to be widely separated from modern humans, including the Upper Paleolithic specimens. No morphological affinities between Neanderthals and the Upper Paleolithic European specimens were found. Previous claims of a phylogenetic relationship between these two groups, suggested both from multivariate analyses of cranial measurements (Simmons and Smith 1991; Kidder et al. 1992) and from morphological observations focusing mainly on the occipital and frontal bone (Jelinek 1969; Smith 1982, 1984, 1992; Smith et al. 1989; Frayer 1992; Churchill and Smith 2000; Wolpoff et al. 2001), are therefore not supported by the present analysis.

Amud 1 is the only specimen that overlaps with modern humans or is closest to the modern human range along the axes that separate Neanderthals from modern humans in the CVA, although a slightly greater overlap is observed between the modern human and the Neanderthal ranges in the PCA of the human sample only. Amud 1 is consistently misclassified as modern human. Although it shows such Neanderthal features as the more coronal orientation of the petro-tympanic crest, the shallow glenoid fossa, the supero-inferiorly tall zygomatic process at the suture and the superior placement of asterion, and a somewhat elevated porion relative to the modern human mean configuration, it is intermediate between modern humans and Neanderthals in all of

these traits. Furthermore, and perhaps most importantly, it shows a large mastoid process with an anteriorly positioned tip, and in this characteristic it is almost identical to the modern human mean configuration. These characteristics have been noted also by Suzuki (1970) in his description of this specimen. This author finds the mastoid process of Amud 1 to be of average size for modern humans, as do also Stringer and Trinkaus (1981). Suzuki also notes that its glenoid fossa is deeper than the European Neanderthals, although shallower than in modern humans, as also observed here, and that the morphology of its tympanic crest falls within the modern human range of variation. The other Eastern Neanderthal included in this analysis, Shanidar 1, does show similarities with Amud 1 or with modern humans in these characteristics. This pattern is consistent with a mosaic view of human evolution in the Late Pleistocene of Western Asia (Trinkaus 1984; Trinkaus and Smith 1985).

The early specimens from Krapina and Saccopastore included here share the typical temporal landmark configuration that distinguishes Neanderthals from modern humans. The Neanderthal character of the temporal bone of Saccopastore 2 was noted by Condemi (1991, 1992). The Krapina remains have been described as possessing a wide range of variation in temporal, and particularly mastoid, morphology, but still possessing a Neanderthal pattern (Smith 1982; Minugh-Purvis 2000). The sample in Step 2 included only two specimens from Krapina, Krapina C and 39-1, thus not reflecting the entire range of variation in this group, as many of the Krapina temporal bones were too fragmentary to be included. These specimens, however, conformed with the pattern observed in the other Neanderthals, confirming previous observations of their essential resemblance to the Western European Neanderthal sample (Smith 1982).

Reilingen: This specimen was only included in Step 2. Compared to the mean modern human configuration, it differs in having a smaller mastoid process, a much larger juxtamastoid eminence, a very laterally placed auriculare, a posteriorly placed entoglenoid pyramid, and a more coronal orientation of the petro-tympanic crest, which mostly reflects the more anterior position of the medial end of this crest. In all of these features it is similar to Neanderthals. However, compared to the Neanderthal mean configuration, this specimen differs in its more posterior placement of the lateral origin of the petro-tympanic crest and a relatively larger mastoid process, in these respects being

more similar to modern humans. It differs from both in the anterior placement of the root of the articular eminence. When compared to the configuration of Kabwe, Reilingen differs in the more coronal orientation of the petro-tympanic crest (although the two specimens share a relatively posterior lateral origin of this crest, in its larger and more anteriorly placed mastoid process and juxtamastoid eminence, its antero-posteriorly longer mastoid portion, and, again, its anteriorly placed root of the articular eminence. The unusual anterior placement of the root of the articular eminence in this specimen may be due to the reconstruction, as the lateral rim of the glenoid fossa is slightly broken and this landmark's position was estimated during data collection.

The temporal bone morphology of Reilingen has been previously descibed as resembling archaic specimens more than the classic Neanderthals (Dean et al. 1998). However, the Reilingen temporal bone landmarks configuration appears to differ least from the Neanderthal mean configuration. It is intermediate between Neanderthals and modern humans in its mastoid process development, although the tip of the mastoid is broken off and its position was estimated during data collection. The difference between this observation and that of Dean et al. (1998) is due perhaps to the lack of measurements on the squamous portion of the temporal bone, which was found by these authors to be similar to pre-Neanderthal specimens such as Steinheim and different from the classic Neanderthal pattern.

In all Mahalanobis D^2 analyses Reilingen is closest to Neanderthals and relatively removed from Kabwe. Reilingen is also always classified as a Neanderthal with very high posterior probabilities. However, this may be also be due to the lack of a more appropriate group to classify this specimen.

Kabwe: This specimen falls mostly within the range of modern human variation in both the PCA and CVA of the temporal bone landmarks analysis. Compared to the modern human mean configuration, however, several differences are observed, including a smaller mastoid process, a more posteriorly placed and slightly larger juxtamastoid eminence, and an antero-posteriorly and supero-inferiorly shorter mastoid portion. These shape differences place it in the area of overlap between modern humans and Neanderthals in the PCA, as, for example, in PC 5 of Step 2B. Kabwe also differs from the mean Neanderthal configuration in having a more posteriorly placed mastoid process

and juxtamastoid eminence, a more medially placed auriculare relative to porion, a more posterior lateral origin of the petro-mastoid crest and a more sagittal orientation of this crest. It differs from both in its posteriorly placed zygomatic suture.

The absence of lateral projection of auriculare relative to porion is somewhat surprising, as this specimen is considered to show a stronger lateral projection of the supramastoid crest over the external acoustic meatus than Neanderthals (Dean et al. 1998). However, in this analysis it appears similar to modern humans in this respect and shows less of a lateral projection of auriculare, measured on the supramastoid crest, relative to porion. A weak supramastoid crest, however, has previously been described for this specimen (Elyaqtine 1995). Furthermore, Kabwe is found to share with modern humans the more sagittal orientation of the petro-tympanic crest and the more posterior position of the lateral origin of this crest, both considered derived traits of modern humans (Schwartz and Tattersall 1996; Martínez et al. 1997; Dean et al. 1998). The more sagittal orientation of this crest was also found by Martínez et al. (1997) in Kabwe and other Middle Pleistocene specimens and modern humans, but not Neanderthals, *H. erectus* or the Middle Pleistocene specimens from Sima de los Huesos, who instead exhibit the primitive coronal orientation.

These differences from both modern humans and Neanderthals place this specimen at an approximately equal distances from the two groups in the Mahalanobis D^2 analyses. This is similar to the findings of Stringer (1974) based on a multivariate analysis of cranio-facial measurements, where Kabwe and Petralona were found to be approximately equally removed from both modern humans and Neanderthals. Kabwe always shows the smallest distances to the Australian modern human population (Steps 1A, 1B and 2C) and to the Upper Paleolithic sample (Steps 2A-2B). These distances, however, are still very large and probably do not indicate particular similarities. It is most widely separated from Skhul 5 (Step 1), and Reilingen and the EAM group (Step 2). Kabwe is classified by posterior probability as Australian (Steps 1A and 1B) and Upper Paleolithic (Step 2B). These classification results, however, do not reflect true affinities, as Kabwe most probably does not belong to any of the defined populations in this analysis.

Skhul 5 and Qafzeh 9: Skuhl 5 is similar to the mean modern human

configuration in having a posteriorly placed lateral origin of the petro-tympanic crest, a sagittal orientation of this crest, and a large mastoid process which is much larger than its substantial juxtamastoid eminence. It differs from modern humans and is similar to Neanderthals only in the inferior placement of the root of its articular eminence. It differs from both modern human and Neanderthal mean configurations in showing an antero-posteriorly long mastoid portion of the temporal bone, and a more medially placed entoglenoid pyramid. The similarities to modern humans observed here are consistent with the descriptions of McCown and Keith (1937), who found the temporal bone morphology of this specimen to be modern. Skhul 5 falls within the modern human range in the PCA and the CVA. It is, however, very distant from all groups in the Mahalanobis D^2 analyses (Step 1), being most removed from Neanderthals and Kabwe, and closest to the Upper Paleolithic specimens, although this distance is also quite large. Similar large distances from both archaic and modern humans have been noted before for the Qafzeh/Skhul sample. Skhul 5 is classified as Berg in all analyses.

Qafzeh 9 is similar to the modern human mean configuration in having a large mastoid and a very small juxtamastoid eminence. It differs from it in having a medio-laterally wider glenoid fossa, in this respect resembling Neanderthals, as well as a posteriorly placed root of the articular eminence. It differs from Neanderthals in its very small juxtamastoid eminence and its large mastoid process. Furthermore, it is intermediate between the two in the orientation of its petro-tympanic crest, and it differs from both in the large medio-lateral distance between auriculare and porion, indicating a strong and laterally projecting supramastoid crest. Finally, it differs from Skhul 5 in having an antero-posteriorly shorter mastoid portion, a more coronally oriented petro-tympanic crest, and a stronger supramastoid crest.

Vandermeersch (1981) noted the large supramastoid crest of Qafzeh 9 relative to both Skhul 5 and modern humans. However, he found this specimen to conform to the modern human pattern of temporal bone morphology. In the present analysis Qafzeh 9 does not fall with Neanderthals either in the PCA or the CVA. It is, however, separated from all other human specimens in the CVA (CaV 3 of Step 2A and CaV 2 of Step 2B). The same axes separate the Andamanese from the other modern human populations, Skhul 5 falling within the range of this modern human group. The shape differences that

separate Qafzeh and the Andamanese from other modern humans include a large mastoid process, a laterally projecting auriculare, a medio-laterally long petro-tympanic crest, and a posterior placement of the root of the articular eminence. When the mean configuration for this population was compared to that of the remaining human groups, it differed in the lateral placement of auriculare and the medial placement of porion, resulting in a large medio-lateral distance between the two landmarks, as well as in the posterior placement of the root of the articular eminence. Both these differences also characterize Qafzeh 9.

With the addition of Qafzeh 9 in Step 2, these two specimens were considered together as one group (EAM) in the Mahalanobis D^2 analysis. As in Step 1, where Skhul 5 was considered alone, this group is very distant again from all groups, although slightly closer to the modern rather than the archaic specimens. It is closest to the Andamanese, although this distance is still very large, and most distant from Reilingen, Kabwe and the Neanderthals. Qafzeh 9 was classified as Andamanese in all steps.

These results are consistent with previous findings of retentions of pleisiomorphous morphology in these specimens which separates them from modern humans (Stringer 1974a, 1989, 1992; Kidder et al. 1992; Turbón et al. 1997)

Upper Paleolithic specimens: This analysis included two Upper Paleolithic specimens in Step 1 (Cro Magnon 1 and Predmosti 3) and four in Step 2 (additionally Predmosti 4 and Mladec 2). The mean configuration for these specimens is very similar to that of modern humans, exhibiting a large mastoid process, small juxtamastoid eminence, posteriorly placed lateral origin and sagittal orientation of the petro-tympanic crest and an antero-posteriorly long mastoid portion. In all of these respects they are different from Neanderthals. They differ from the mean modern human configuration in having a somewhat inferiorly placed root of the articular eminence, like Neanderthals. Among these specimens, Mladec 2 shows some similarities to the Neanderthal configuration, in having a juxtamastoid eminence that is larger than the mastoid process. This specimen also shows a strong lateral projection of auriculare, as in Neanderthals, and a posteriorly placed lateral origin and sagittal orientation of the petro-tympanic crest, as in modern humans. The mixture of modern human and Neanderthal-like morphology in this specimen may lend some support to the claims for limited gene flow between Neanderthals and early modern Europeans, as has been claimed by several authors

particularly for the Central European Upper Paleolithic sample (Jelinek 1969; Smith 1982, 1984, 1992; Smith et al. 1989; Frayer 1992; Churchill and Smith 2000; Wolpoff et al. 2001). However, this specimen was never separated from modern humans in either the PCA or CVA, nor was it misclassified as Neanderthal.

These specimens are not separated from modern humans in the PCA or CVA. However, in Step 1, and perhaps due to the sample size of only two individuals, they appear very distant from other modern human groups in the Mahalanobis distance. They are much closer to the recent human populations in Step 2, after the removal of the zygomatic process landmarks and the addition of two specimens. In order to test the relative contribution of these two factors to the different results, the analysis was repeated using the Upper Paleolithic sample of Step 1 (2 specimens) and the landmark set of Step 2 (13 landmarks). In this analysis the Upper Paleolithic specimens were again very distant from modern human populations, as in Step 1, strongly suggesting that it is the increase in sample size that resulted in the reduced Mahalanobis distances between this group and modern humans in Step 2.

In all analyses the Upper Paleolithic specimens are much closer in Mahalanobis D^2 to modern humans than to Neanderthals. They show the shortest distance to the Berg, and are most distant from Neanderthals. They are almost always classified as Berg. These results are in agreement with previous multivariate analyses of cranio-facial measurements (Stringer 1974, 1989, 1992; Bräuer and Rimbach 1990; Bräuer 1992; Turbón et al 1997) that find these specimens to be widely separated from Neanderthals despite claims for some degree of continuity between the two (Jelinek 1969; Smith 1982, 1992; Smith et al. 1989; Frayer 1992; Kidder et al. 1992). However, as these claims are usually centered on Central European specimens, it is interesting to note the partial similarity of the occipito-mastoid region of Mladec 2 to the Neanderthal configuration.

In summary, the temporal bone landmarks analysis separates Neanderthals widely from modern humans. This analysis supports most previously described Neanderthal temporal bone features. The Upper Paleolithic specimens are found to be very close to modern humans, and to cluster with modern Europeans. Skhul 5 and Qafzeh 9 are similar to modern humans, but appear to have retained some primitive conditions, which contribute to the relatively large distance of these specimens from the recent human

groups. Finally, recent human populations show consistent geographic clustering in all analyses of the temporal bone.

CHAPTER 4

Occipital Bone Landmarks

Several Neanderthal traits are located on the occipital bone. These include the occipital 'bun' and the high convexity of the occipital plane (Boule 1911-1913; Thoma 1965; Hublin 1978b, 1988b; Stringer et al. 1984; Sergi 1991; Condemi 1991; Lieberman 1995; Dean et al. 1998), the strong occipital torus with a suprainiac fossa and no external occipital protuberance (Santa Luca 1978; Hublin 1978, 1988a, b; Stringer and Trinkaus 1981; Trinkaus 1983; Stringer et al. 1984; Condemi 1991, 1992; Lieberman 1995; Bräuer and Broeg 1998), a medio-laterally broad and supero-inferiorly short occipital plane with a depressed lambda and superiorly placed inion (McCown and Keith 1937; Heim 1974; Thoma 1975; Hublin 1988; Wolpoff et al. 2001), and a relatively flat cranial base (Laitman and Heimbuch 1982; Lieberman 1989). Some authors have proposed, however, that many of these features fall within the range of modern human variation. Trinkaus and LeMay (1982) found that the occipital bun is not unique to Neanderthals and that it is related to developmental factors, while Spitery (1985) found that the occipital plane curvature and proportions fall with the modern human range.

Seventeen landmarks were recorded on this bone, designed to capture these traits as best as possible (Table 4.1). Most are standard osteological landmarks (Howells 1973), but other landmarks are also included, and their definitions are given in Table 1. Hormion is also included, although located on the sphenoid bone. A weakness of this analysis is the lack of appropriate landmarks on the occipital squama, which makes quantification of many of these features difficult. As most fossil and some modern human specimens were incomplete, analysis was undertaken in steps so as to include as many landmarks and as many specimens as possible. As explained in Chapter 2, minimal reconstruction was undertaken during data collection, and landmarks missing only on one side were reconstructed by mirror imaging.

The Steps followed in this chapter are as follows (Table 4.2): Step 1 inlcudes all 17 landmarks, but only one Neanderthal specimen, Saccopastore 1. Step 2 includes 16 landmarks, excluding hormion, and four Neanderthal specimens. Finally, Step 3 includes 12 landmarks and 9 Neanderthals. As before, in each step the analysis was repeated A) on the combined chimpanzee and human sample; B) on the human sample only; and C) on

Table 4.1: Landmarks collected on the occipital bone

1.	Inion	(Steps 1-3)
2.	Asterion (Right)	(Steps 1-3)
3.	Asterion (Left)	(Steps 1-3)
4.	Lambda	(Steps 1-3)
5.	Opisthion	(Steps 1-2)
6.	Basion	(Steps 1-2)
7-8.	Points at the posterior end of the occipital condyle, 2 cm from midline, on the lip of the foramen magnum (Right and Left)	(Steps 1-2)
9.	Hormion	(Step 1)
10.	Most antero-medial point of the jugular fossa (Right)	(Steps 1-2)
11.	Most postero-lateral point of the jugular fossa (Right)	(Steps 1-2)
12.	Most antero-medial point of the jugular fossa (Left)	(Steps 1-2)
13.	Most postero-lateral point of the jugular fossa (Left)	(Steps 1-2)
14-15.	Lateral end of the inferior nuchal line (anterior end of the antero-inferior branch, between the insertions for the rectus capitis posterior major and the superior oblique, Hublin 1978) (Right and Left)	(Steps 1-3)
16-17.	Lateral end of the superior nuchal line (the most lateral extent of the splenius capitis scar on the occipital bone, Dean 1993) (Right and Left)	(Steps 1-3)

Table 4.2: Number of landmarks and specimens in each level of analysis.

	Landmarks	Modern Humans	Chimpanzees	Neanderthals	AMH	Other
Level 1	17	238	90	Saccopastore 1	Skhul 5 Cro Magnon 1 Predmosti 3 Predmosti 4 Mladec 1 Ein Gev	Kanalda Kabwe
Level 2	16	250	90	Saccopastore 1 La Chappele La Ferrassie 1 Shanidar 1	Skhul 5 Cro Magnon 1 Predmosti 3 Predmosti 4 Mladec 1 Ein Gev	Kanalda Kabwe Biache
Level 3	8	267	92	Saccopastore 1 La Chappele La Ferrassie 1 Shanidar 1 Amud 1 Guattari La Quina 5 Tabun C1 Spy 2	Skhul 5 Cro Magnon 1 Predmosti 3 Predmosti 4 Mladec 1 Ein Gev Qafzeh 9	Kanalda Kabwe Biache Petralona Reilingen

Table 4.3: Centroid size listed by genus, species, sex and population, Step 1

	Mean	Range	St. Deviation	N
Homo	**19.02**	**16.18-22.16**	**1.01**	**247**
Males	19.43	16.56-22.16	0.96	129
Females	18.56	16.18-20.86	0.87	117
Modern	19.01	16.18-22.16	1.00	245
Males	19.42	16.56-22.16	0.95	128
Females	18.55	16.18-20.86	0.87.	116
Saccopastore 1	19.70	---	---	1
Kabwe	21.31	---	---	1
Skhul 5	20.24	---	---	1
Upper Paleolithic	20.47	19.71-20.86	0.46	5
Kanalda	20.84	---	---	1
Andamanese	17.44	16.18-18.26	0.56	29
Australian	18.95	17.42-20.39	0.73	30
Berg	19.42	18.10-21.33	0.80	30
Dogon	18.59	17.04-19.67	0.58	29
Epipaleolithic	19.92	19.36-20.53	0.58	3
Eskimo	19.99	19.10-22.16	0.72	30
European (mixed)	19.41	18.43-21.06	0.74	28
San	18.84	17.24-20.59	0.75	30
Tolai	18.94	17.74-20.18	0.64.	29
Pan	**15.05**	**13.40-16.72**	**0.74**	**90**
Males	15.26	13.83-16.72	0.80	48
Females	14.76	13.40-15.86	0.58	40
P. paniscus	14.37	13.40-15.13	0.37	33
Males	14.36	13.83-15.07	0.36	15
Females	14.40	13.40-15.13	0.39	18
P. troglodytes	15.43	13.99-16.72	0.61	57
Males	15.68	13.99-16.72	0.56	33
Females	15.06	14.24-15.87	0.53	22
P. t. schweinfurthii	15.28	13.99-16.72	0.66	29
P. t. troglodytes	15.59	14.24-16.52	0.53	28

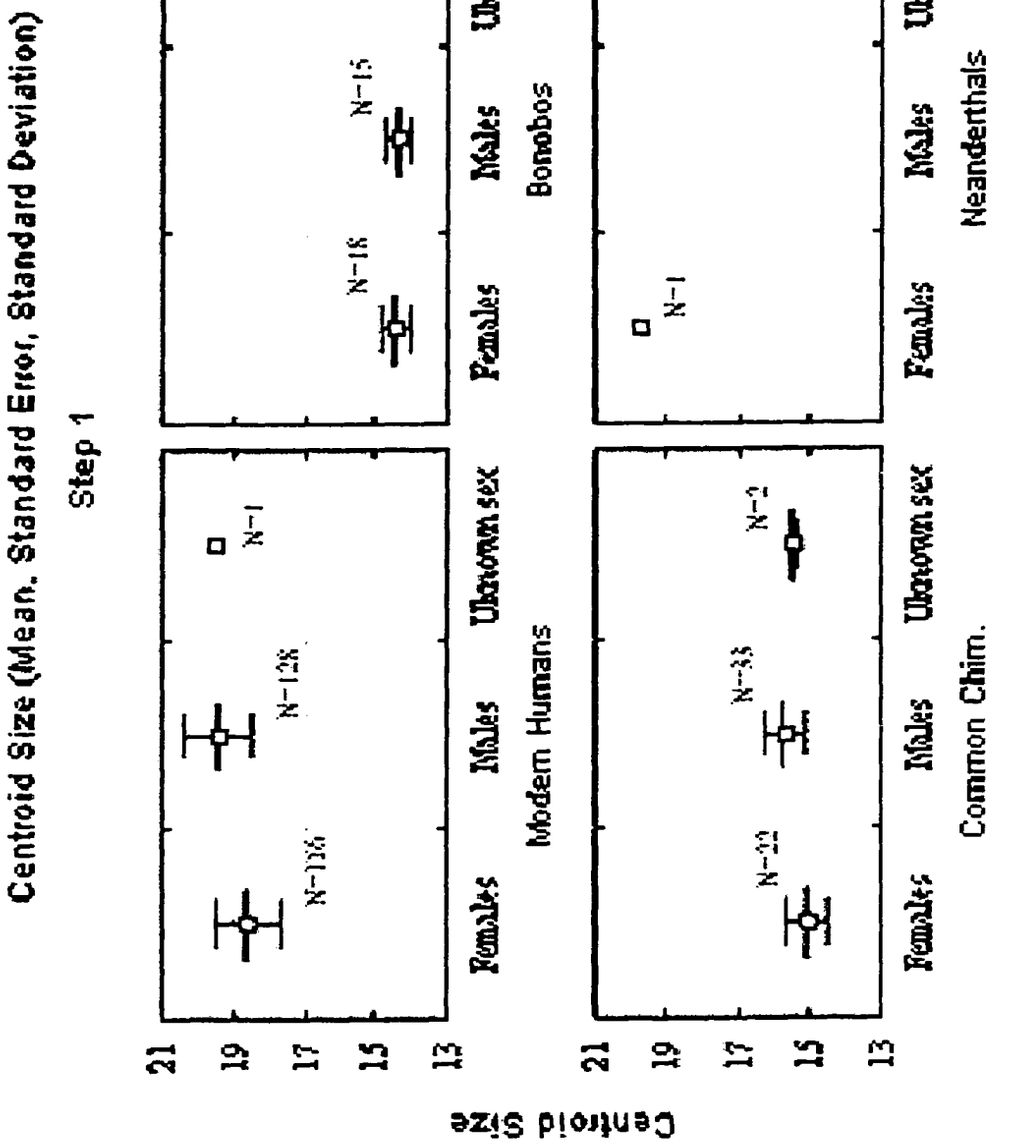

Figure 4.1: Centroid size mean, standard error and standard deviation, labeled by species and sex (Step 1).

the chimpanzee sample only.

Step 1

All 17 of the landmarks listed in Table 1 were used. The only Neanderthal that is complete enough to be included here is Saccopastore 1. Among the other fossil material, Kabwe, Predmosti 3 and 4, Mladec 1, Ein Gev, Cro Magnon 1 and Skhul 5 are also included. The Epipaleolithic population is represented only by three specimens.

Centroid Size: An analysis of variance (ANOVA) was conducted on centroid size to investigate genus, species, population and sex. Sex and population were found to be highly significant (p 0.0001). An interaction effect, significant to the 0.01 level, was also found. Both the mean centroid size value and the standard deviation in *Homo* is greater than in *Pan* (see Table 4.3, Fig. 4.1). All three chimpanzee taxa are significantly smaller in their mean centroid size values for the occipital bone landmarks from all modern human populations. Both human and chimpanzee females have smaller means and standard deviations than males, although the difference between male and female standard deviations is greater in chimpanzees.

When the samples are separated by species, bonobos show a smaller mean centroid size value and standard deviation than common chimpanzees. The three chimpanzee taxa, however, are not significantly different from each other in their mean centroid sizes. Male and female bonobos have very similar mean centroid size values and standard deviations, females showing slightly higher values for both. Male common chimpanzees, on the other hand, have a higher mean centroid size than females, but equivalent standard deviations. There is almost no sexual dimorphism in occipital bone landmark centroid size in bonobos, females being slightly larger than males. Common chimpanzees, on the other hand, show very high degrees of sexual dimorphism, males being larger than females. These results are similar to those obtained in the temporal landmarks analysis, but the pattern is stronger here.

In the human sample, the centroid size of Saccopastore 1, the only Neanderthal specimen here, and a female, is close to the modern human mean, although it is higher than the female mean. The centroid size for Kabwe is much higher than the modern human mean and it is relatively close to the upper limit of the modern human range.

Skhul 5 and Kanalda are smaller, but also in the upper part of the modern human range. The mean value of the Upper Paleolithic group is significantly different from all other modern human groups, with the exception of the Epipaleolithic and the Eskimo, the two human populations with the highest mean centroid size values here. All of these specimens, except Saccopastore 1, Mladec 1 and Predmosti 4, are considered male. Within modern humans, there is a relatively high degree of sexual dimorphism, males being larger than females, but lower than in common chimpanzees.

At the population level, *P. t. troglodytes* shows a slightly higher mean and somewhat smaller standard deviation than *P. t. schweinfurthii.* As in the temporal bone landmark analysis, the two subspecies are almost identical in their means and ranges. The human geographic populations, on the other hand, are much more differentiated in terms of both means and standard deviations in occipital bone centroid size. The Eskimo and the Epipaleolithic show the highest mean values, as in the temporal bone landmark analysis, but these populations are not significantly different in their means from the other modern human groups, with the exception of the Andamanese. The latter show the lowest mean values, also as in the temporal bone analysis, and are significantly smaller from all other human groups except the San and the Dogon.

Step 1A – Combined Sample Analysis

Principal Component Analysis: A PCA was conducted on the variance-covariance matrix of the 51 variables. An ANOVA was conducted on the principal component scores to test for significant population and sex effects on each principal component. A Bonferroni pairwise test was conducted on the mean scores of the populations to test for significant differences at this level. A correlation analysis was also performed for each principal component with centroid size, so as to determine whether they are highly correlated with centroid size. Table 4.4 shows the eigenvalues and proportions, as well as the results of the ANOVA and correlation analysis in summary for PCs 1 to 10. As in the temporal bone landmark analysis, in order to assess the contribution of each landmark to each principal component, the squared root of the sums of squares of the three eigenvectors for each landmark (three coordinates per landmark) was calculated (see Chapter 2). These values are show in Table 4.5 for the first ten

principal components. The landmarks with the highest values for each principal component are presented here in bold. They can be interpreted as driving the separation along that component.

Saccopastore 1, the only Neanderthal specimen included in this step is never separated from modern humans in this analysis. Humans are separated from chimpanzees only along PC 1 (Figure 4.2). This component summarizes 60.3 % of the total variance and is significant for population (0.0001) and sex (0.01) effects (Table 4.4). The mean scores for all three chimpanzee taxa are significantly different from those of all human groups. In the human sample, Saccopastore 1 is not separated from the modern humans, but Kabwe falls at the negative extreme of the modern human range, between humans and chimpanzees. Skhul 5, the Upper Paleolithic specimens and Kanalda all fall within the modern human range. Modern human populations are not well separated. None of the modern human groups are significantly different from the others in their mean scores for PC 1, including the Upper Paleolithic specimens. When PC 1 is labeled by sex, a tendency is observed for males to have more negative scores than females. When the mean scores for males and females are plotted by population (Fig. 4.3), the means for males are more negative than those for females in most human groups, but not in the Europeans and the Berg, where the trend are reversed, and not in the San, where the means for the two sexes are almost identical. The male means are also more negative among bonobos and *P. t. troglodytes*, but not in *P. t. schweinfurthii*.

The shape differences from one end of this component to the other are shown in Figure 4.4. In the positive end, where humans are located, lambda (4) is more superior, and inion (1) and the lateral ends of the superior nuchal lines (16 and 17) are more inferior, reflecting the greater height supero-inferiorly of the human occipital squama relative to that of chimpanzees, a difference which is due to a supero-inferior enlargement of the occipital plane and a shortening of the nuchal plane. Hormion (9) is more posterior, reflecting the antero-posteriorly shorter clivus in humans compared to chimpanzees. These shape differences also tend to characterize females relative to males in most, but not all, modern human populations. PC 1 is relatively strongly correlated

Table 4.4: Summary of PCA results, ANOVA and Correlation Analysis for PCs 1-10, Step 1A

	Principal Components Analysis			ANOVA : Pr > F			Correlation with Centroid Size	
	Eigenvalue	Proportion	Cumulative	Pop.	Sex	Interaction	Rho	Pr > F
PC 1	0.009891	0.603395	0.603395	0.0001	0.0071	0.1655	0.80636	0.0001
PC 2	0.000964	0.058807	0.662201	0.0001	0.9296	0.0084	-0.32064	0.0001
PC 3	0.000886	0.054026	0.716227	0.0001	0.2914	0.1071	0.13223	0.0151
PC 4	0.000659	0.040204	0.756431	0.0001	0.2156	0.441	-0.0094	0.8635
PC 5	0.000584	0.035635	0.792066	0.0001	0.5649	0.8686	0.1238	0.023
PC 6	0.000415	0.02533	0.817396	0.0001	0.2096	0.9264	-0.11995	0.0277
PC 7	0.000359	0.021882	0.839278	0.0001	0.0028	0.0229	-0.20942	0.0001
PC 8	0.000321	0.019552	0.85883	0.0001	0.2720	0.3762	0.05389	0.324
PC 9	0.000253	0.015453	0.874282	0.0013	0.0028	0.0018	0.03519	0.5197
PC 10	0.000204	0.012458	0.886741	0.0036	0.0734	0.3257	-0.01592	0.7569

Table 4.5: Squared roots of the sum of squares of the eigenvector coefficients for the three coordinates of each landmark. PCs 1-10, Step 1A.

	PC 1	PC 2	PC 3	PC 4	PC 5	PC 6	PC 7	PC 8	PC 9	PC 10
1. Inion	**0.33**	**0.29**	0.14	**0.38**	**0.31**	**0.26**	**0.67**	0.10	0.17	0.16
2. Asterion R	0.18	0.21	**0.27**	0.20	**0.25**	**0.31**	0.12	**0.50**	0.09	0.13
3. Asterion L	0.18	0.17	0.23	**0.22**	**0.25**	**0.28**	0.17	**0.51**	0.11	0.11
4. Lambda	**0.62**	**0.25**	**0.54**	0.09	**0.51**	0.26	0.09	**0.29**	**0.32**	0.12
5. Opisthion	0.00	0.10	0.10	**0.28**	0.19	0.18	**0.25**	**0.28**	**0.25**	0.06
6. Basion	0.02	0.08	0.23	0.13	0.09	0.17	0.15	0.03	0.11	0.12
7. Occ. Cond. R	0.11	0.12	0.22	0.20	0.15	0.26	**0.26**	0.11	0.09	**0.24**
8. Occ. Cond. L	0.12	0.11	0.20	0.20	0.15	0.26	**0.30**	0.12	0.16	**0.28**
9. Hormion	**0.35**	**0.31**	0.24	0.20	0.21	0.24	**0.30**	**0.26**	**0.35**	0.20
10. Jugular F. med. R	0.11	0.17	0.09	0.05	0.11	0.20	0.18	0.12	**0.48**	**0.21**
11. Jugular F. lat. R	0.15	0.04	0.07	0.12	0.15	0.17	0.19	0.07	**0.25**	0.06
12. Jugular F. med. L	0.13	0.17	0.11	0.06	0.10	0.20	0.19	0.11	**0.41**	0.18
13. Jugular F. lat. L	0.16	0.03	0.11	0.13	0.15	0.19	0.19	0.04	0.21	0.06
14. Inf. Nuchal Line R	0.11	0.13	**0.25**	**0.47**	**0.35**	0.20	0.10	0.21	0.19	**0.52**
15. Inf. Nuchal Line L	0.10	0.16	0.23	**0.46**	**0.29**	0.21	0.11	0.19	0.15	**0.57**
16. Sup. Nuchal Line R	**0.31**	**0.52**	**0.33**	0.19	0.25	**0.29**	0.06	0.23	0.19	0.18
17. Sup. Nuchal Line L	**0.32**	**0.52**	**0.30**	0.20	0.23	**0.35**	0.12	**0.27**	0.14	0.11

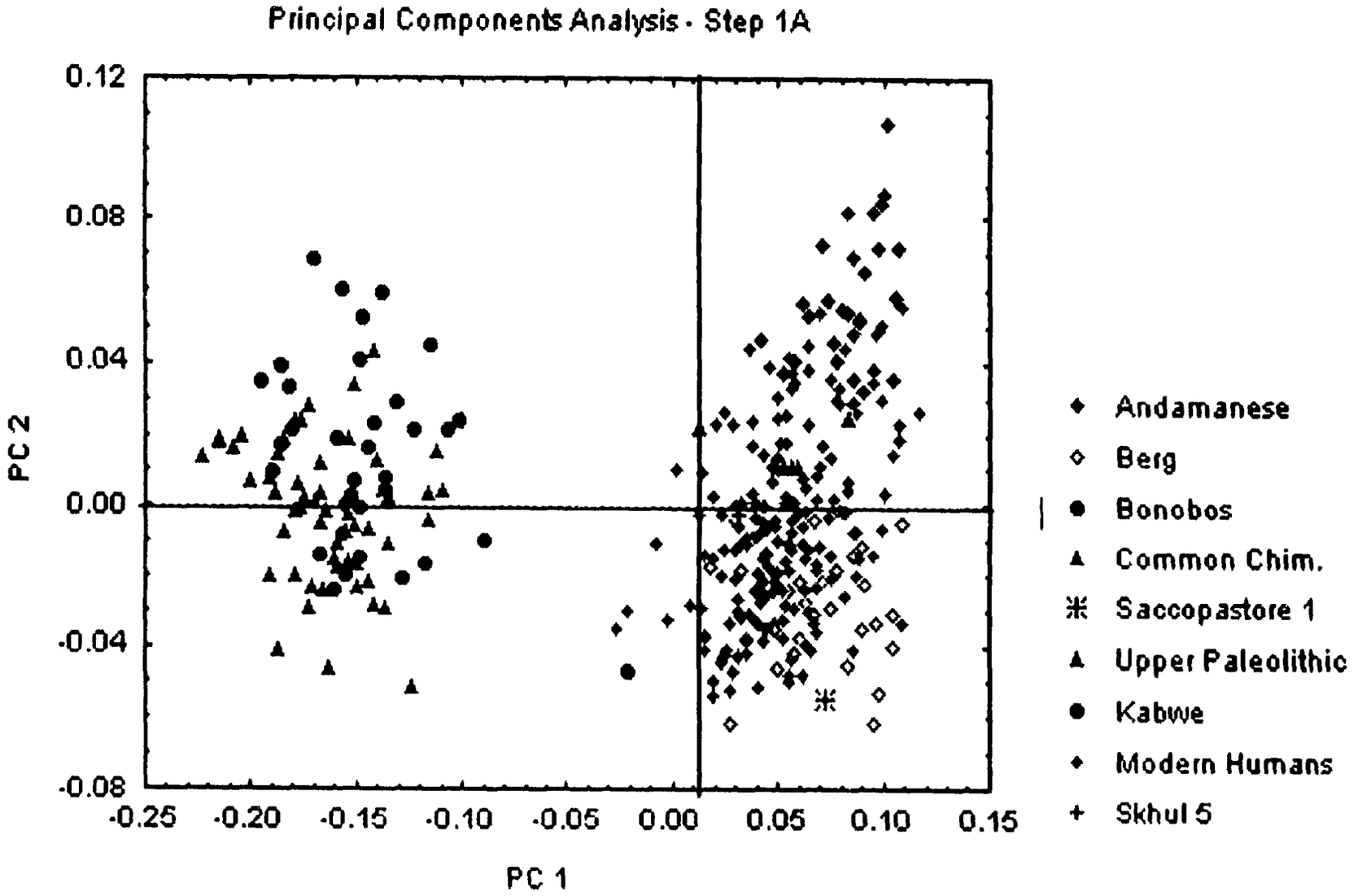

Figure 4.2: Principal Components Analysis, PCs 1 and 2 (Step 1A)

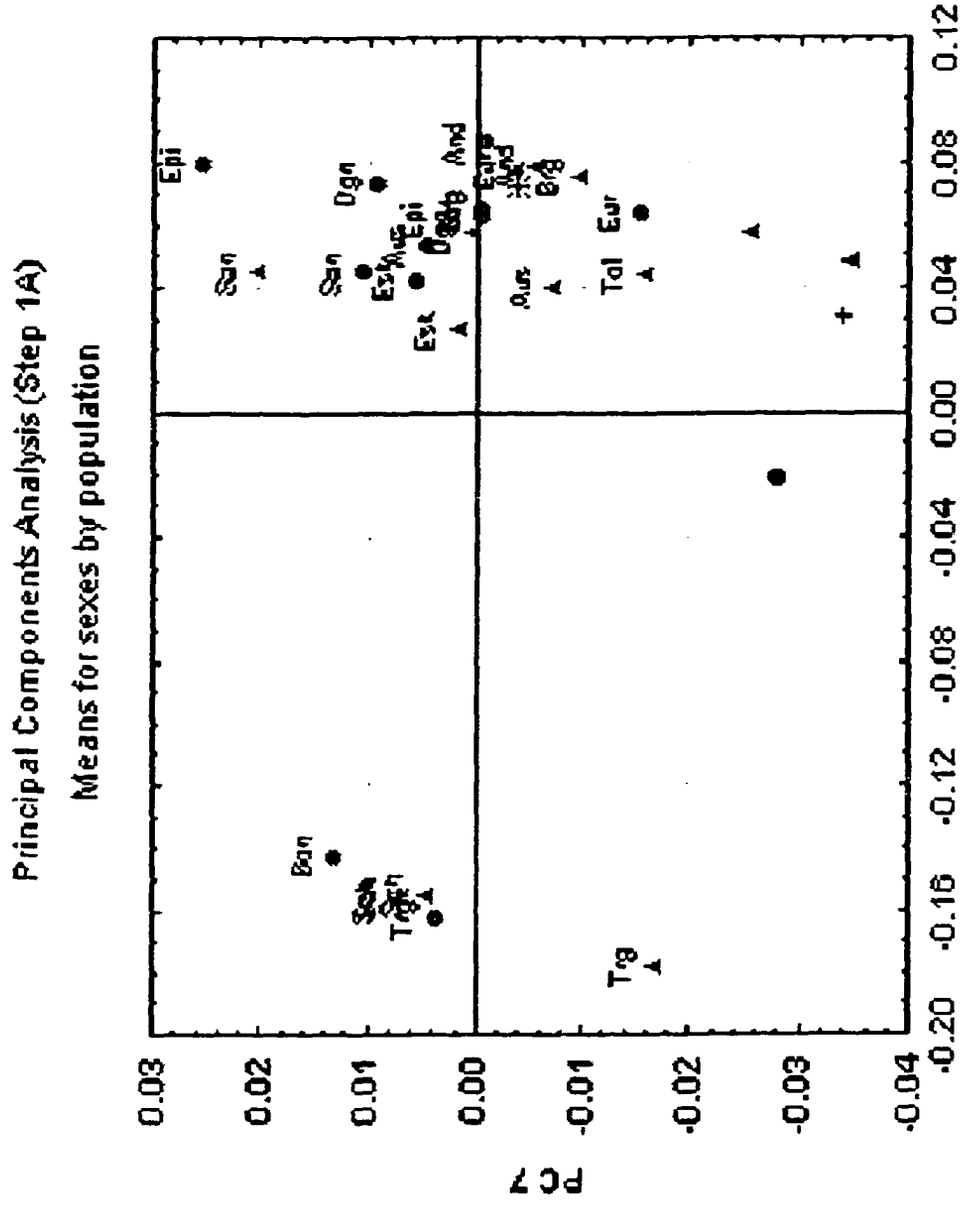

Figure 4.3: Principal Components Analysis (Step 1A), mean scores for the sexes plotted by population, PCs 1 and 7.

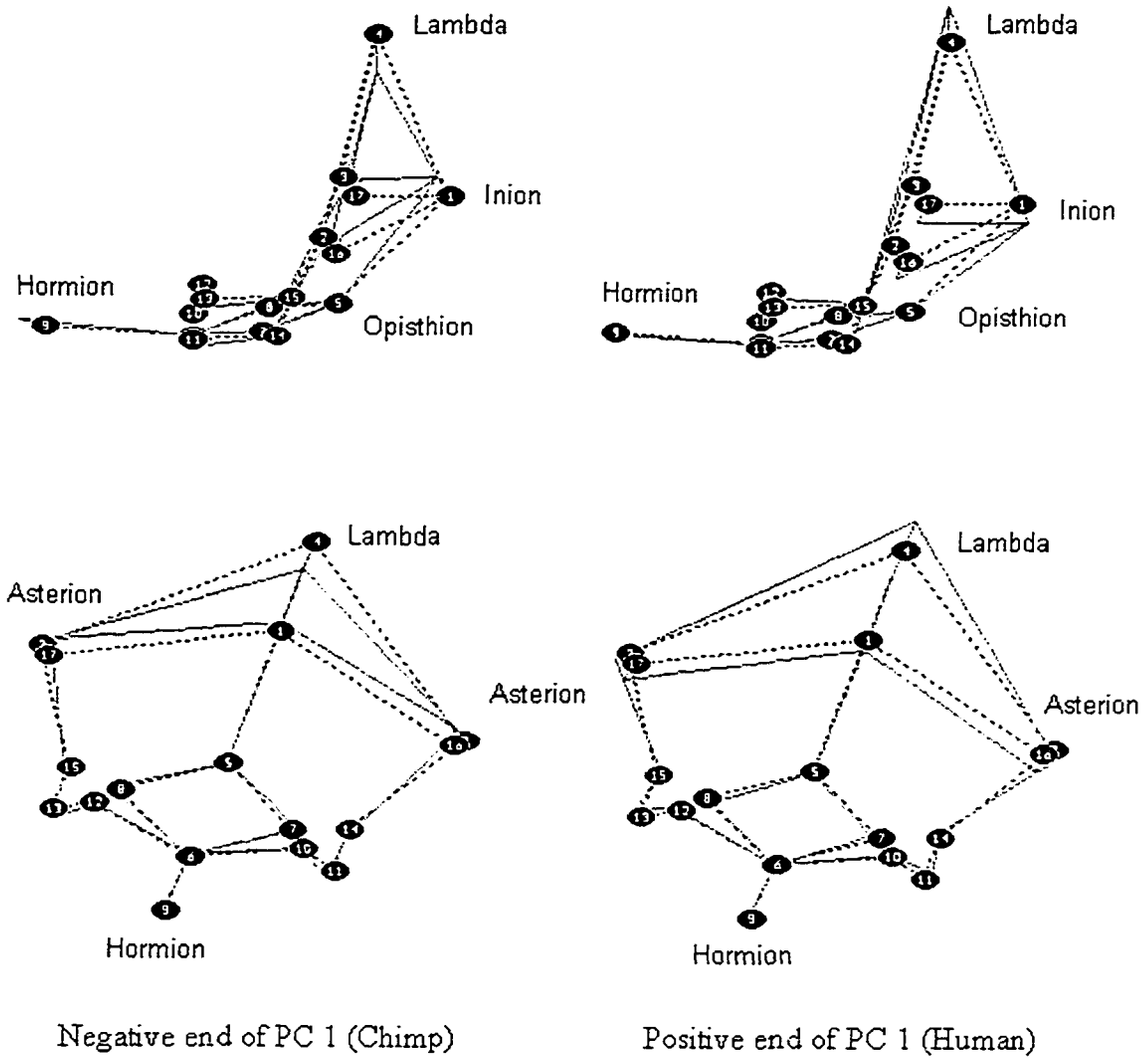

Negative end of PC 1 (Chimp)

Positive end of PC 1 (Human)

Figure 4.4: Shape variation along PC 1 (Step 1A). Lateral (top) and postero-ventral views. The dotted line represents the consensus configuration.

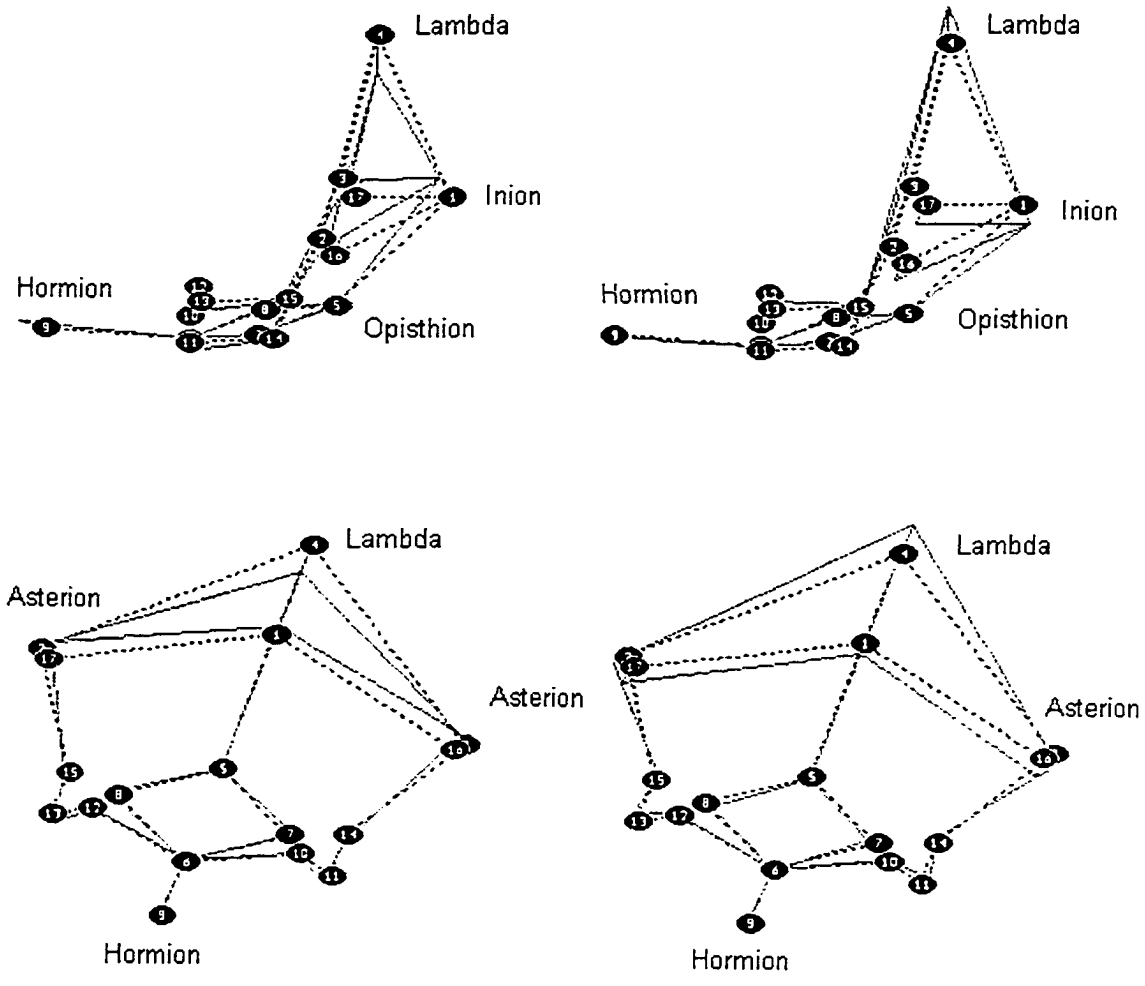

Figure 4.4: Shape variation along PC 1 (Step 1A). Lateral (top) and postero-ventral views. The dotted line represents the consensus configuration.

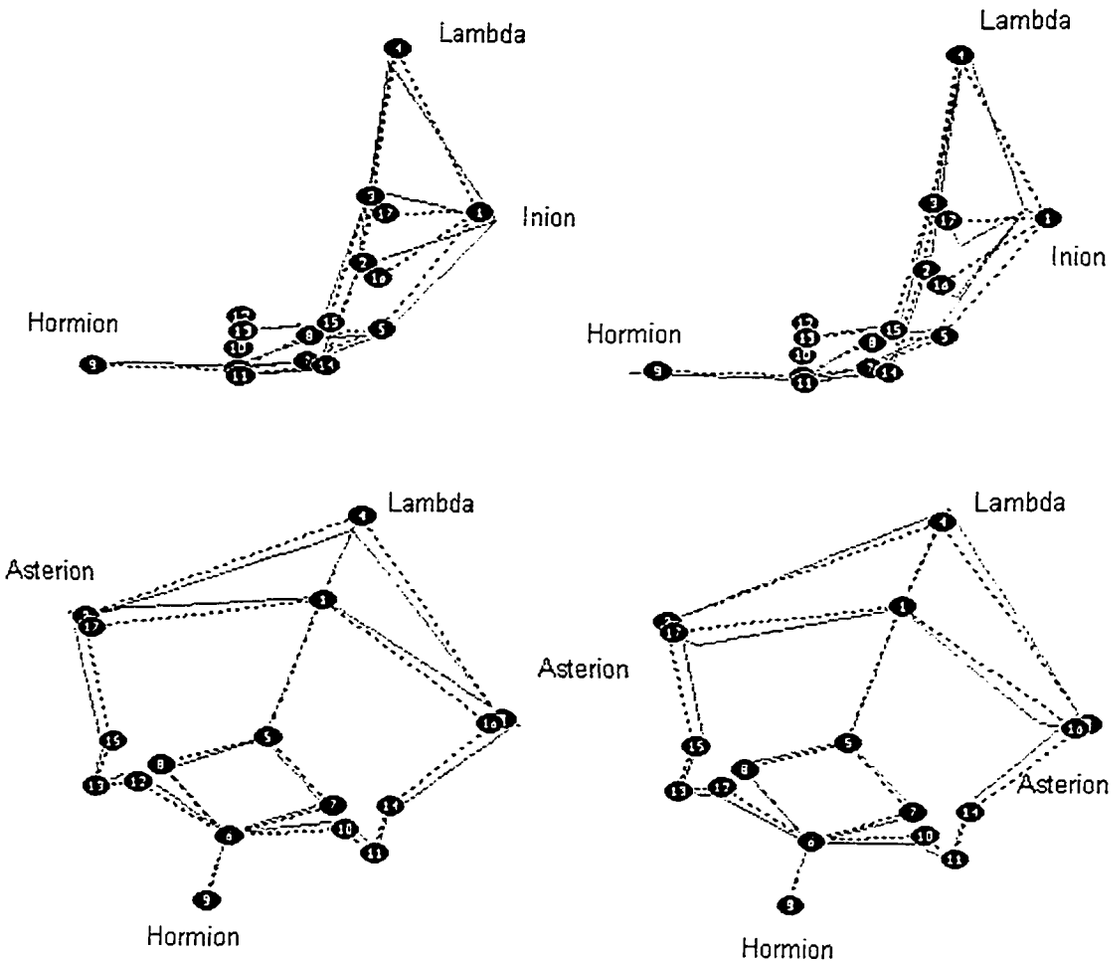

Negative end of PC 2 (Neand., Berg)

Positive end of PC 2 (Andam.)

Figure 4.6: Shape variation along PC 2 (Step 1A). Lateral (top) and postero-ventral views. The dotted line represents the consensus configuration.

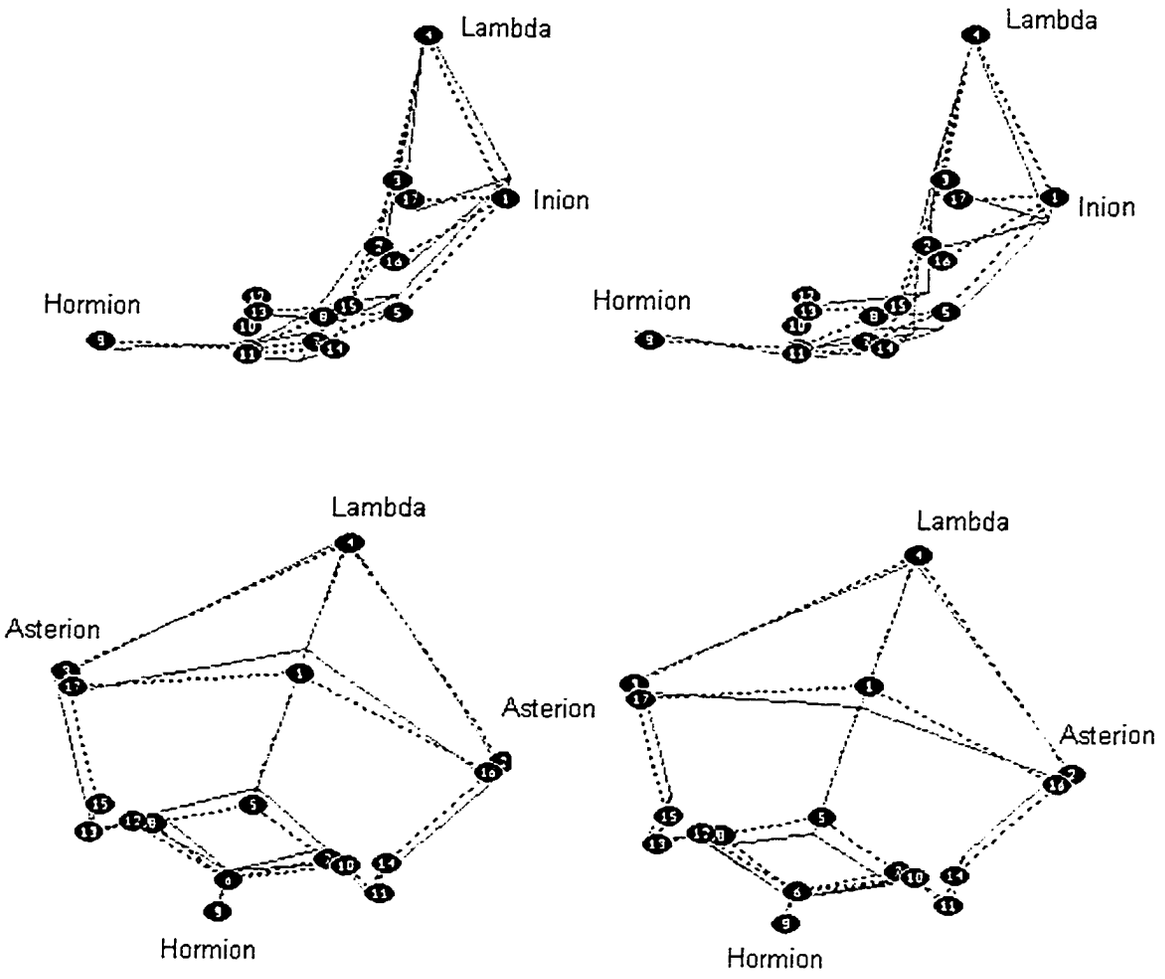

Negative end of PC 4 (Kabwe)

Positive end of PC 4

Figure 4.7: Shape variation along PC 4 (Step 1A). Lateral (top) and postero-ventral views. The dotted line represents the consensus configuration.

with centroid size (R=0.81, significant to the 0.0001 level). When plotted against centroid size and regression lines fitted for each population (Fig. 4.5), it can be seen that the regression slopes are not parallel across populations. As the groups behave differently across genera and across populations, no adjustment for centroid size differences can be undertaken. A large proportion of the shape differences that separate humans from chimpanzees are related to centroid size differences, but they are probably not related to allometry.

PC 2 (Fig. 4.2) summarizes 5.9 % of the total variance, and is significant for population effects at the 0.0001 level, as well as for interaction effects at the 0.01 level. PC 2 separates the two chimpanzee species somewhat, bonobos tending to have positive scores, although the mean scores for the three chimpanzee groups are not significantly different from each other. PC 2 is the only principal component in this step of analysis that places Saccopastore 1 at the negative extreme of the modern human range. Kabwe also falls in the negative end of the modern human range, but well within it. Skhul 5, the Upper Paleolithic specimens and Kanalda all fall near the center of the modern human variation. PC 2 separates modern human populations quite well. The Andamanese fall at its positive end and the Eskimo, San, Australians, Berg and Europeans at the negative end, with the Dogon, Tolai and the Epipaleolithic falling in between.

Figure 4.6 shows the shape changes along PC 2. In the negative end, where Saccopastore 1 falls, the lateral ends of the superior nuchal line (16, 17) as well as asteria (2, 3) are more lateral, reflecting a medio-laterally wider occipital. The lateral ends of the superior nuchal line are also more superior. Inion (1) is slightly more inferior and more posterior, reflecting the posterior protrusion of the Neanderthal occipital bone. Lambda (4) is more inferior and slightly more anterior, indicating a supero-inferiorly shorter and antero-posteriorly longer occipital plane, which is more steeply inclined. Hormion (9) is more posterior. These shape changes characterize the only Neanderthal included here relative to most humans, although this specimen overlaps with the extreme of the modern human range. PC 2 is weakly correlated with centroid size (Table 4.4).

PC 4 accounts for 4 % of the total variance and is significant for population effects (0.0001). It separates the two chimpanzee species. It doesn't separate Neanderthals, Skhul 5, the Upper Paleolithic specimens and Kanalda from modern

humans. Kabwe, however, falls on the negative end of PC 4, just outside the range of modern human variation. The shape variation in the negative end (Fig. 4.7) includes a more anterior placement of the lateral ends of the inferior nuchal line (14, 15), a more superior inion (1), and a more superior opisthion (5). These shape differences can be described as a relatively short occipital squama with an elevated nuchal plane, and an anteriorly placed inferior nuchal line. Kabwe is characterized by these shape differences relative to most modern humans, but it is not greatly removed from the end of the modern human range.

PC 6 summarizes 2.5 % of the total variance. It is significant for population effects at the 0.0001 level. It does not separate bonobos from common chimpanzees or the two chimpanzee subspecies. It does separate Kabwe from modern humans, Kabwe falling on the negative extreme of PC 6 outside the modern human range. At the fringe of this range are also Cro Magnon 1, Skhul 5, Ein Gev, Predmosti 3 and 4. Mladec 1, the other Upper Paleolithic specimen that is included, falls also on the negative end of the modern human range, but less removed, while Saccopastore 1 falls near the center of the modern human range.

In the negative end, where Kabwe and the Upper Paleolithic fall, lambda (4) is more anterior, inion (1) is more posterior, as are asteria and the lateral ends of the superior nuchal line (2, 3, 16, 17), while the landmarks around the foramen magnum (5-8) are elevated. These shape differences can be described as an antero-posteriorly elongated and posteriorly projecting occipital squama, with a sharper angle between the occipital and nuchal planes.

PCs 7 and 9 are significant for sex effects at the 0.01 level. PC 7 (2.2 %) is also significant for interaction effects (0.05). It shows a tendency for females in both samples to have more positive scores than males. When the mean scores for males and females are plotted by population (Fig. 4.3), the female means are more positive in most, but not all, modern human groups. The female means are more positive in the Epipaleolithic and the European populations. Among chimpanzees, the female means are more positive than the males, being more widely separated than in the human groups. This trend is the opposite of that observed in the human sample. The shape differences along PC 7 include, at the negative end, a more inferior inion (1) resulting in a supero-inferiorly taller

occipital plane; a more posterior opisthion (5) and more lateral occipital condyles (7, 8), reflecting an antero-posteriorly longer and medio-laterally wider foramen magnum; and a more inferior hormion (9), showing a relatively flat basioccipital. PC 7 is only weakly correlated with centroid size (Table 4.4).

Along PC 9 (1.5 %) a stronger separation between the male and female mean scores is observed in the chimpanzee taxa, where males are more positive than females. A similar, but weaker trend is observed among human groups, where in most populations, except in the Tolai, San and Europeans, the male mean is more positive than the female. This tendency is stronger in the chimpanzee sample. The shape differences in the positive end of PC 9 are a more inferior and posterior lambda (4), indicating a supero-inferiorly and antero-posteriorly short occipital plane, and an elevated and more posterior opisthion (5), showing a relatively large antero-posteriorly foramen magnum. The medial ends of the jugular fossae (10,11) are more lateral, anterior and inferior, while the lateral ends (12, 13) are more lateral, indicating jugular processes that more laterally projecting and jugular fossae that are both antero-medially wider and supero-inferiorly deeper in males. PC 9 is not correlated with centroid size (Table 4.4).

Canonical Variates Analysis: A canonical variates analysis was undertaken at the population level on the first 30 principal components (98.4 % of the total variance). The results are summarized in Table 4.6. CaV 1 (85.4 % of the total variance, most highly influenced by PC 1, Fig. 4.8) separates humans from chimpanzees, the mean scored for the three chimpanzee taxa being significantly different from the means of all human groups. It does not separate Saccopastore 1 or any of the fossil specimens from modern humans, nor does it separate the chimpanzee species or subspecies. The shape differences along CaV 1 are similar to those described by PC 1. In the positive end, where humans fall, inion (1) is more inferior and posterior, the lateral ends of the superior nuchal line (16, 17) are more inferior, and lambda (4) is more superior. Hormion (9) is more posterior, reflecting the shorter clivus of humans compared to chimpanzees. CaV 1 is strongly correlated with centroid size (R=0.89, significant to the 0.0001 level). When plotted against centroid size with regression lines fitted for each population, the situation is similar to that found for PC 1 (Fig. 4.9).

CaV 2 (4.1 %, most highly influenced by PC 2, Fig. 4.8) separates bonobos from common chimpanzees, the mean score value for bonobos being significantly different from those of the two common chimpanzee subspecies. CaV 2 also separates Kabwe from modern humans. This specimen falls at the negative extreme of CaV 2, outside the 95 % confidence ellipse of all modern human populations. Saccopastore 1 also falls on the negative end of CaV 2 and close to Kabwe, but overlapping with a few specimens at the negative fringe of the modern human range and within the 95 % ellipses of several modern human groups. CaV 2 also partially separates modern human populations, the Andamanese falling at the positive extreme and overlapping only with the Dogon at the negative part of their range, and the other groups falling mostly on the negative side of CaV 2. The Andamanese are significantly different in their mean score on this axis from all other human groups except the Dogon.

The shape differences along CaV 2 are shown in Fig. 4.10. In the negative end, where Kabwe and Saccopastore fall, lambda (4) is more inferior and anterior and inion (1) is more posterior, reflecting an antero-posterior elongation and posterior protrusion of the occipital plane. The lateral ends of the superior nuchal line (16, 17) are more superior and slightly more lateral, perhaps indicating a more horizontal rather than downcurved superior nuchal line. CaV 2 is only weakly correlated with centroid size.

CaV 3 (3.4 %, most highly influenced by PC 3, Fig. 4.11) separates the Berg, Upper Paleolithic specimens (except Predmosti 4), Skhul 5 and Saccopastore 1 on the negative end from the San, Dogon, Australians and Tolai on the positive end. The Upper Paleolithic group is significantly different in its mean score for CaV 3 from most modern human populations, but not for the Berg, the Andamanese, the Epipaleolithic and the European groups. The shape changes along CaV 3 (Fig. 4.12) include, in the negative end, where the Berg, Saccopastore 1, Skhul 5 and most of the Upper Paleolithic specimens fall, a more anterior lambda (4), resulting in a more posterior projection of the occipital bone. The lateral ends of the superior nuchal line (16, 17) are more posterior and superior. The landmarks around the foramen magnum (5-8) are elevated as is hormion (9), reflecting a more elevated nuchal plane relative to the occipital plane and a sharper angle between the two.

Table 4.6: Summary of the CVA results and Correlation Analysis, for CaV1-5, Step 1A

	Canonical Variates Analysis			Correlation with Centroid Size	
	Eigenvalue	Proportion	Cumulative	Rho	Pr > F
CaV 1	61.9209	0.8543	0.8543	0.89164	0.0001
CaV 2	2.969	0.041	0.8952	-0.31605	0.0001
CaV 3	2.456	0.0339	0.9291	-0.04569	0.4031
CaV 4	1.3485	0.0186	0.9477	-0.00297	0.9567
CaV 5	1.1196	0.0154	0.9631	-0.12422	0.0226

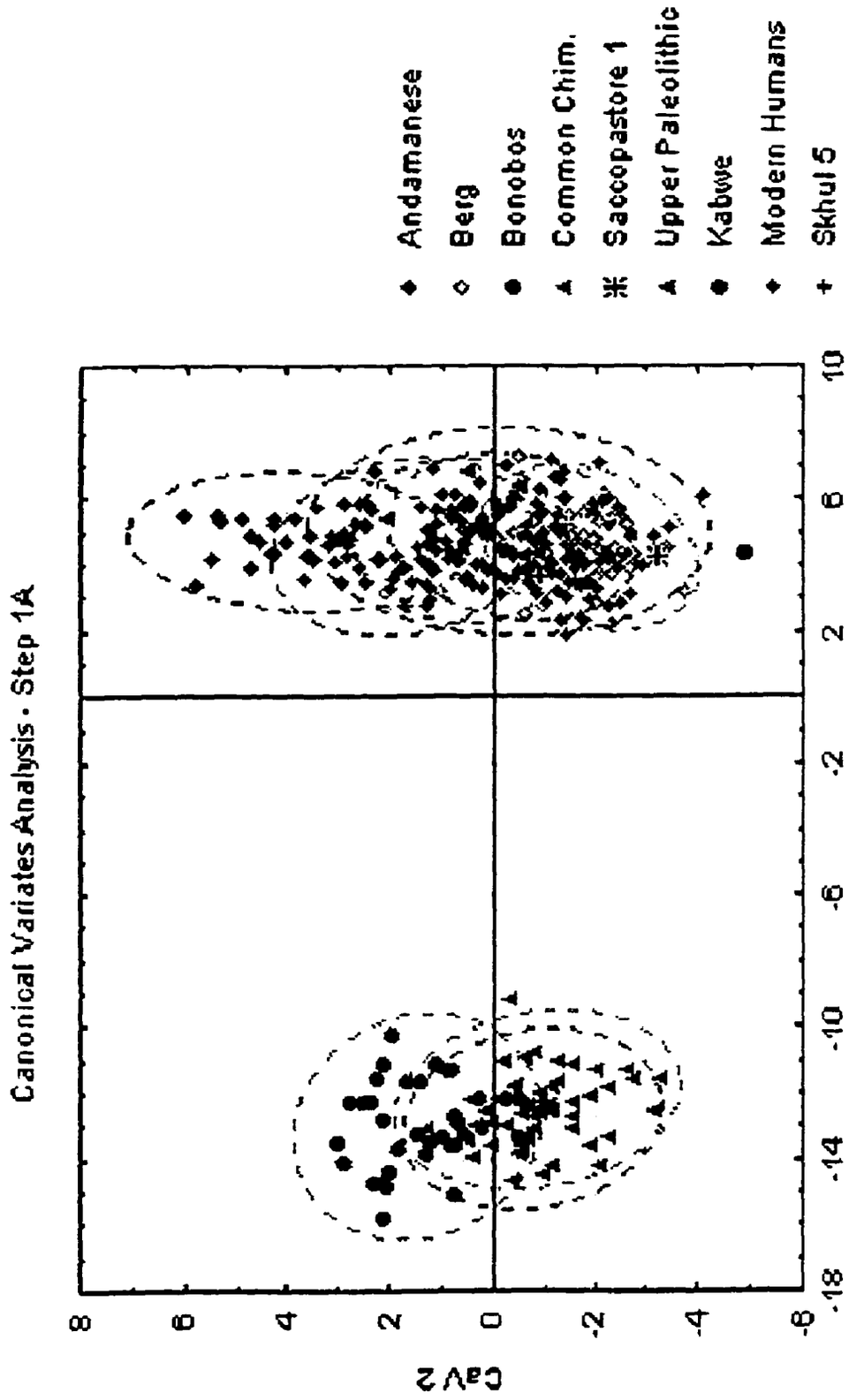

Figure 4.8: Canonical Variates Analysis, CaVs 1 and 2 (Step 1A). Dotted lines represent the 95 % confidence ellipses for each group.

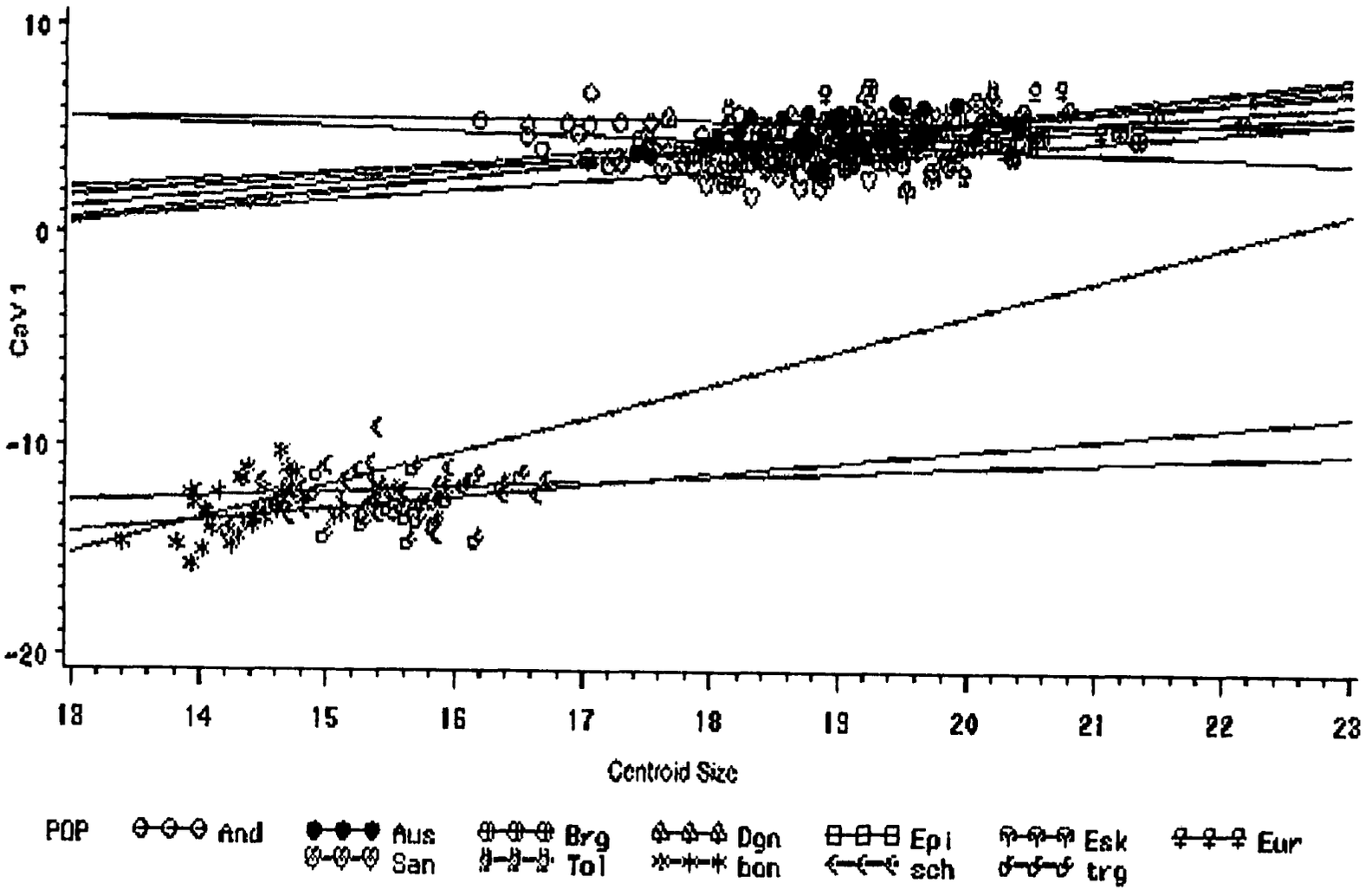

Figure 4.9: CaV 1 (Step 1A) plotted against centroid size with regression lines fitted for each population.

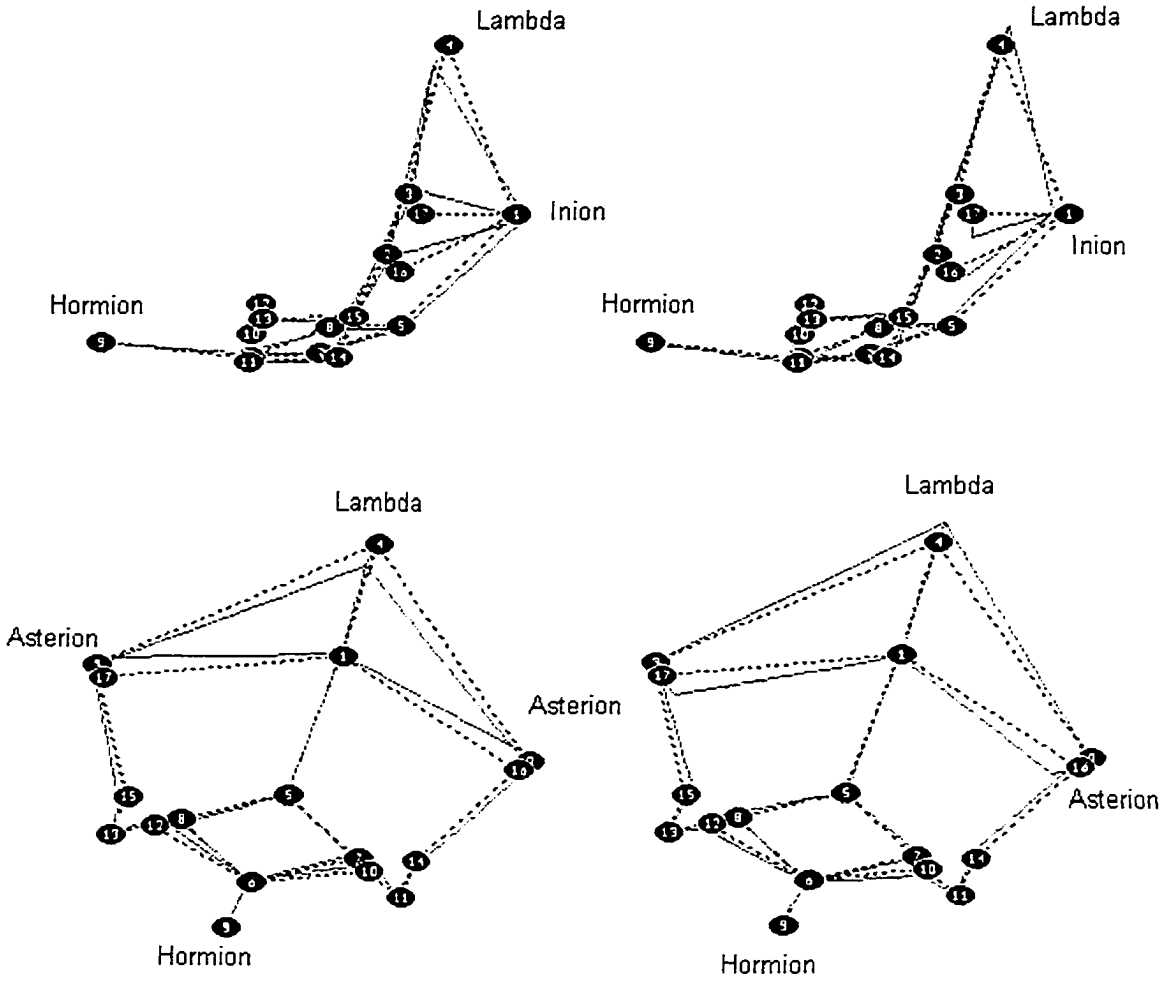

Negative end of CaV 2 (Kabwe, Sac 1)

Positive end of CaV 2 (Andam.)

Figure 4.10: Shape variation along CaV 2 (Step 1A). Lateral (top) and postero-ventral view. The dotted line represents the consensus configuration.

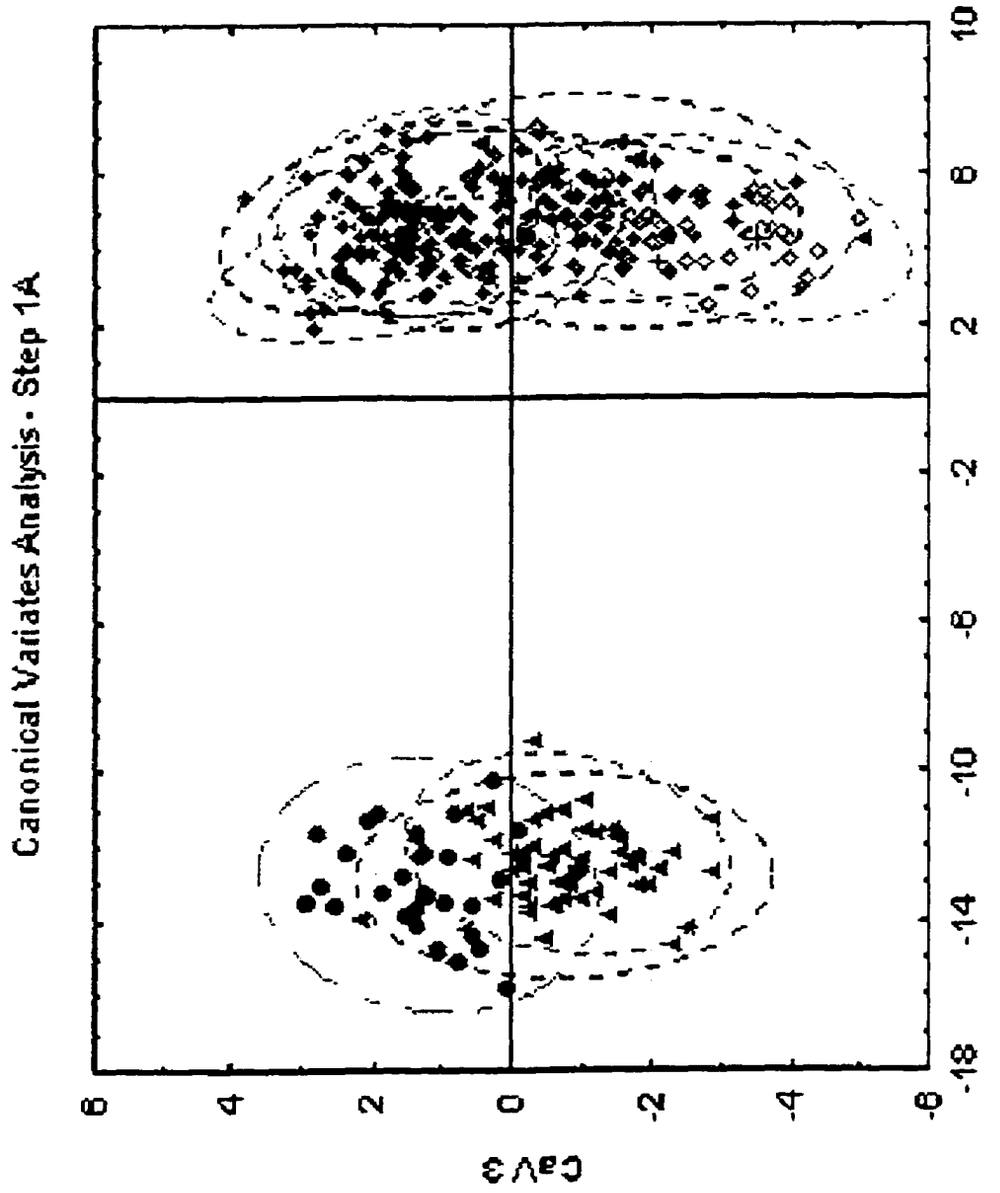

Figure 4.11: Canonical Variates Analysis, CaVs 1 and 3 (Step 1A). Dotted lines represent the 95 % confidence ellipses for each group.

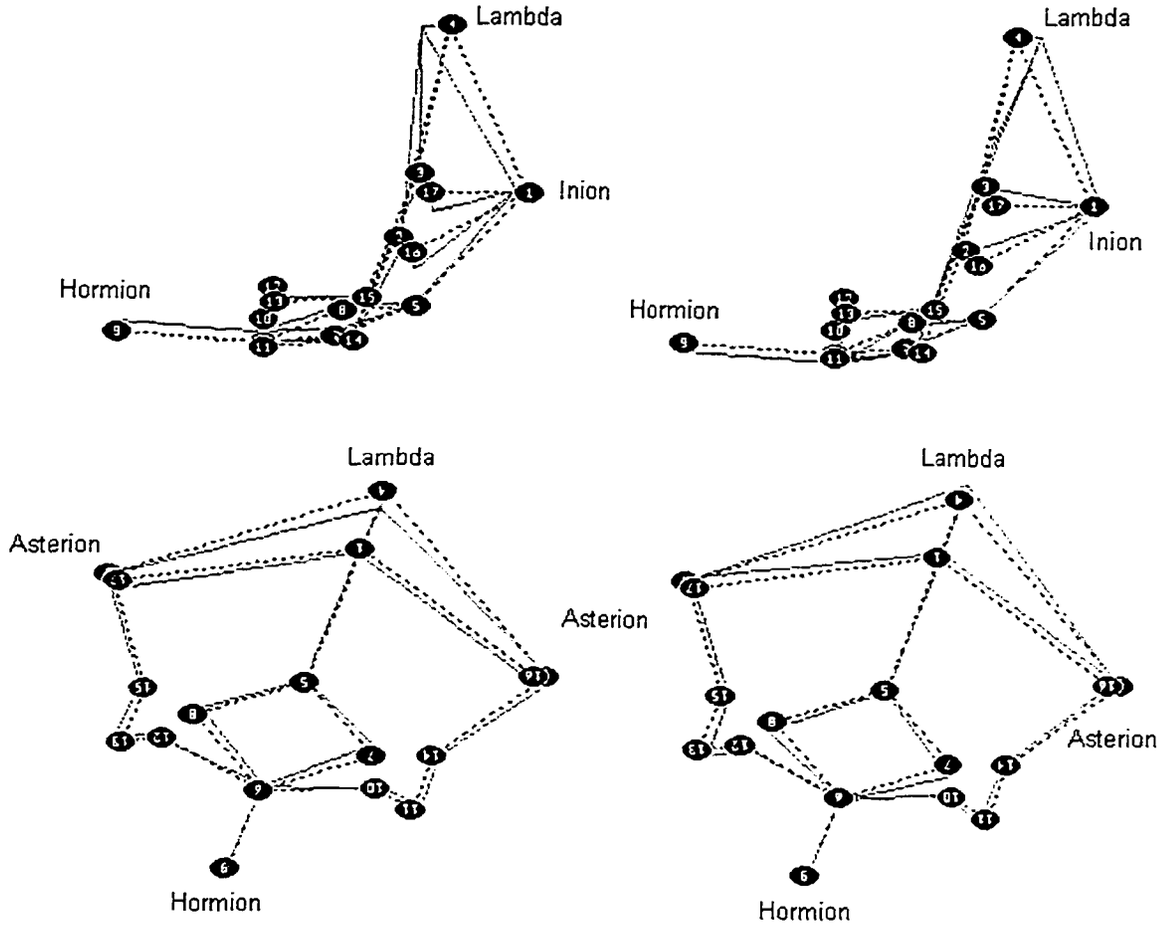

Negative end of CaV 3 (Sac. 1, Berg)

Positive end of CaV 3

Figure 4.12: Shape variation along CaV 3 (Step 1A). Lateral (top) and postero-ventral view. The dotted line represents the consensus configuration.

CaV 5 (1.5 %, influenced most by PCs 13, 6 and 10, Fig. 4.13) separates Kabwe and the Upper Paleolithic specimens from modern humans. The Upper Paleolithic specimens are significantly different from all other human groups except the Epipaleolithic. Kabwe and the Upper Paleolithic group fall outside the 95 % confidence ellipse of all modern human groups, with the exception of Mladec 1 and Predmosti 4, which fall at the fringe of the ellipses. Saccopastore 1 falls well within the modern human cloud. The shape changes at the negative end of CaV 5 include a supero-inferiorly short occipital plane and tall nuchal plane with an elevated inion and superior nuchal line, a medio-laterally short squama and anteriorly placed medial ends of the jugular fossae (Fig. 4.14).

Classification: A discriminant analysis was performed excluding Saccopastore 1, Kabwe, Skhul 5, Kanalda and the Upper Paleolithic specimens, which were treated as unknown to be classified into one of the other groups, and the posterior probabilities of these classifications were calculated. Saccopastore 1 was classified as Berg with a posterior probability of 0.999, Kabwe was classified as Eskimo (0.98), Kanalda as Tolai (0.75), and Skhul 5 as Berg (0.68). All Upper Paleolithic specimens were placed correctly in their group by posterior probability.

A cross-validation classification was obtained for the entire dataset and the results summarized in Table 4.7. Classification success varied. No human was misclassified as a chimpanzee and vice versa. The highest correct classification percentage overall was obtained by the bonobos, who were all classified correctly. Only two out of the five Upper Paleolithic specimens were classified correctly, the remaining three being classified as Tolai, Epipaleolithic and Australian. Among modern human populations the highest correct classification was achieved by the Dogon (89.66 %). The lowest rate of successful classification (33.33 %) was achieved by the Epipaleolithic, who comprise only 3 specimens in this analysis, and the mixed European populations (50 %). As in Chapter 3, a large proportion of the mixed Europeans (14.29 %) was misclassified as Berg, and vice versa (16.67 %). Also as in Chapter 3, specimens from the mixed European population were also misclassified as Andamanese, Epipaleolithic, Eskimo, San and Tolai. Finally, the two common chimpanzee subspecies show high levels of misclassification among themselves.

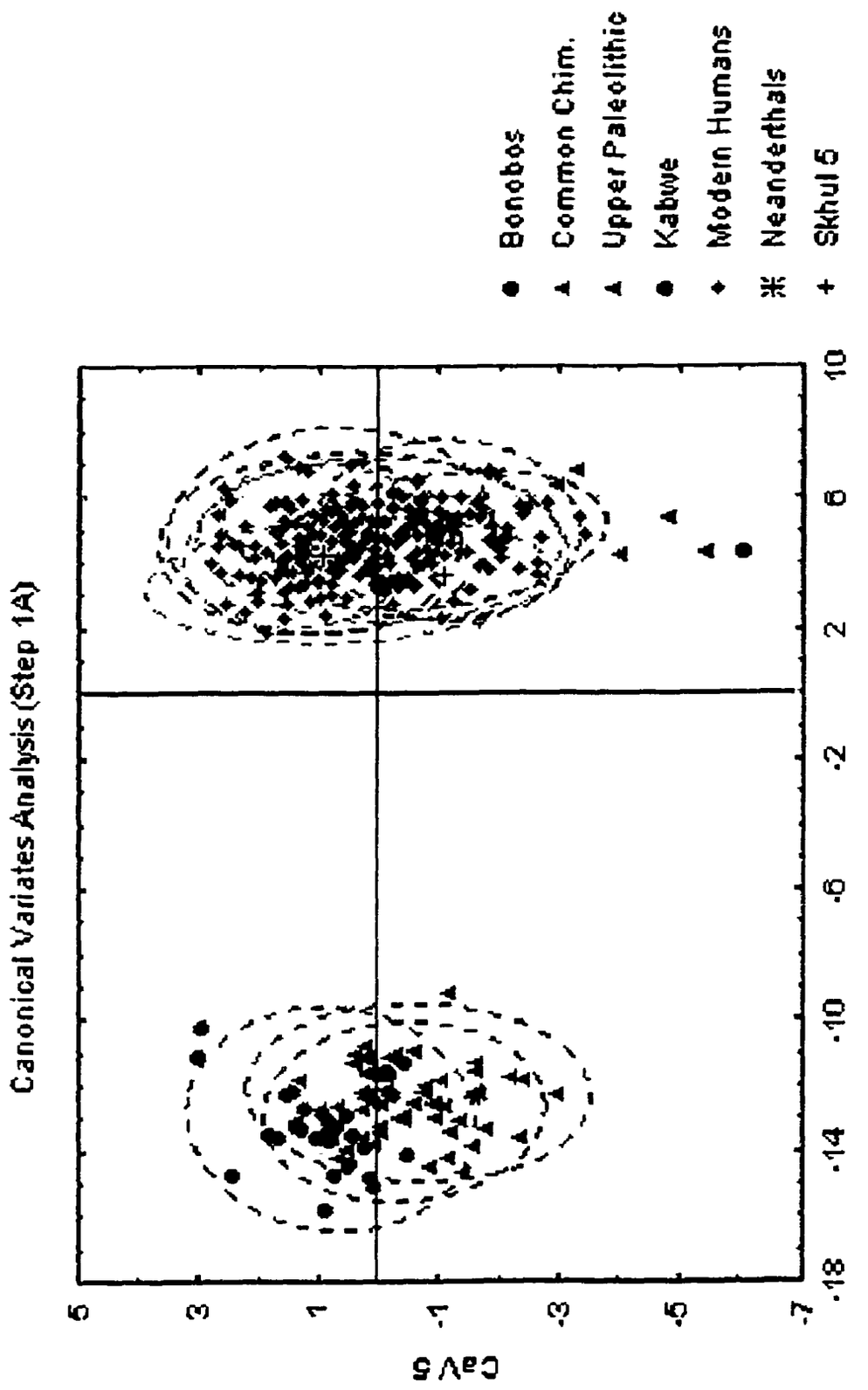

Figure 4.13: Canonical Variates Analysis (Step 1A). CaVs 1 and 5. Dotted lines represent the 95 % confidence ellipses for each group.

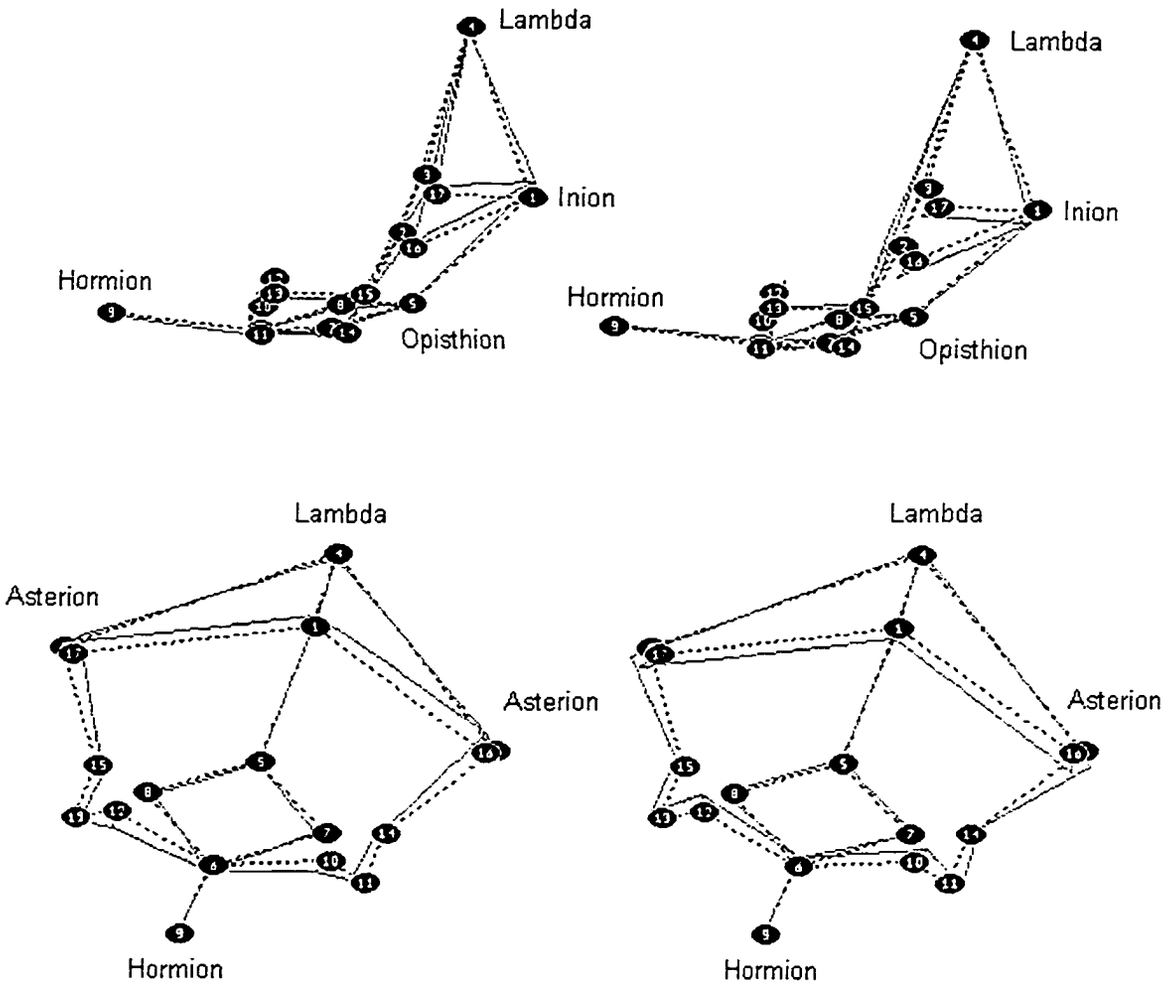

Figure 4.14: Shape variation along CaV 5 (Step1A). Lateral (top) and postero-ventral view. The dotted line represents the consensus configuration.

Mahalanobis D^2, Cluster Analysis and Minimum Spanning Tree: The unbiased Mahalanobis distances between pairs of groups were calculated (Table 4.8). Humans are widely separated from chimpanzees. The two common chimpanzee subspecies are very close to each other, with a D^2 distance equivalent to, but smaller than, the distance between the geographically closest modern human populations (Berg and European, Tolai and Australians), the pairs that show the smallest D^2 among modern human groups. The distance between the two chimpanzee species is equivalent to that between the more widely separated modern human populations (e.g. Australians and Dogon), but smaller than the greatest distance between a pair of modern human groups (San and Andamanese) and smaller than the distance between the Upper Paleolithic group and any modern human population. The Upper Paleolithic group is quite removed from the rest of the human sample. It is closest to the Epipaleolithic, and most distant from the Dogon. This is also the greatest distance observed in the human sample. Among modern human groups, out of the three geographic pairs (Berg and Europeans, Australians and Tolai, San and Dogon), only the first two show the smallest distance to each other.

A UPGMA analysis and a minimum spanning tree analysis (Fig. 4.15) were performed on the squared root of the unbiased D^2. The first cluster diagram shows the two chimpanzee species clustering in a separate branch from the human groups, with the two common chimpanzee subspecies clustering very close to each other. Among the human groups, the Upper Paleolithic is the outlier to the rest of the human sample. The clustering of modern human populations is different in this analysis from that obtained in Chapter 3. Some of the geographic clustering is preserved, as the two European populations, as well as the Australians and the Tolai, cluster close together within a larger branch, which also includes the Eskimo and the San. The Dogon are no longer placed with the San. In the minimum spanning tree, the Upper Paleolithic group is joined to the Epipaleolithic group. Modern human populations are far removed from the chimpanzees. The Berg and Europeans and the Australians and Tolai are linked here also, but not the San and the Dogon.

Table 4.7: Cross-validation classification summary (percentages for each population in bold). Step 1A.

	And	Aus	Brg	Dgn	Epi	Esk	Eur	San	Tol	UP	Bon	Sch	Trg	Total
And	23	2	0	0	3	0	1	0	0	0	0	0	0	29
%	**79.31**	6.9	0	0	10.34	0	3.45	0	0	0	0	0	0	100
Aus	0	26	0	0	0	2	1	1	0	0	0	0	0	30
%	0	**86.67**	0	0	0	6.67	3.33	3.33	0	0	0	0	0	100
Brg	0	0	25	0	0	0	5	0	0	0	0	0	0	30
%	0	0	**83.33**	0	0	0	16.67	0	0	0	0	0	0	100
Dgn	1	0	0	26	0	0	1	1	0	0	0	0	0	29
%	3.45	0	0	**89.66**	0	0	3.45	3.45	0	0	0	0	0	100
Epi	0	0	0	0	1	1	1	0	0	0	0	0	0	3
%	0	0	0	0	**33.33**	33.33	33.33	0	0	0	0	0	0	100
Esk	0	2	0	0	0	26	0	1	1	0	0	0	0	30
%	0	6.67	0	0	0	**86.67**	0	3.33	3.33	0	0	0	0	100
Eur	3	0	4	0	1	2	14	2	1	1	0	0	0	28
%	10.71	0	14.29	0	3.57	7.14	**50**	7.14	3.57	3.57	0	0	0	100
San	0	0	0	2	1	0	1	26	0	0	0	0	0	30
%	0	0	0	6.67	3.33	0	3.33	**86.67**	0	0	0	0	0	100
Tol	0	4	0	0	0	0	1	1	23	0	0	0	0	29
%	0	13.79	0	0	0	0	3.45	3.45	**79.31**	0	0	0	0	100
UP	0	1	0	0	1	0	0	0	1	2	0	0	0	5
%	0	20	0	0	20	0	0	0	20	**40**	0	0	0	100
Bon	0	0	0	0	0	0	0	0	0	0	33	0	0	33
%	0	0	0	0	0	0	0	0	0	0	**100**	0	0	100
Sch	0	0	0	0	0	0	0	0	0	0	0	22	7	29
%	0	0	0	0	0	0	0	0	0	0	0	**75.86**	24.14	100
Trg	0	0	0	0	0	0	0	0	0	0	1	4	23	28
%	0	0	0	0	0	0	0	0	0	0	3.57	14.29	**82.14**	100
Total	27	35	29	28	7	31	25	32	26	3	34	26	30	333
%	8.11	10.51	8.71	8.41	2.1	9.31	7.51	9.61	7.81	0.9	10.21	7.81	9.01	100

Table 4.8: Unbiased Mahalanobis D^2, Step 1A.. All distances 0.001 significance level except: NS = non-significant, * = 0.05 level, ** = 0.01 level.

	Kan	And	Aus	Brg	Dgn	Skh5	Epi	Esk	Eur	Kbw	San	Tol	UP	Bon	Sac1	Sch	Trg
Kan	0.00	70.61	48.88	70.38	71.47	101.99	55.70	61.96	63.19	132.81	72.55	47.41	63.86	364.76	143.40	339.74	362.67
And	70.61	0.00	32.51	38.34	16.81	58.80	22.02	39.22	22.55	127.24	40.62	22.11	37.07	316.19	74.94	293.15	313.08
Aus	48.88	32.51	0.00	28.84	19.06	45.32	25.62	12.09	13.98	90.35	11.71	9.32	37.97	311.12	58.40	289.50	307.25
Brg	70.38	38.34	28.84	0.00	32.02	42.67	28.44	25.30	7.37	98.32	26.91	24.62	39.88	319.05	23.39NS	275.52	296.61
Dgn	71.47	16.81	19.06	32.02	0.00	67.76	25.27	23.12	16.72	118.77	17.28	16.04	56.10	305.18	59.81	280.31	296.96
Skh5	101.99	58.80	45.32	42.67	67.76	0.00	66.95	64.42	47.65	94.35	53.43	53.17	52.14	320.75	61.81*	287.05	292.27
Epi	55.70	22.02	25.62	28.44	25.27	66.95	0.00	16.49	15.67	79.88	31.27	21.40	24.68	344.12	68.25	308.26	334.56
Esk	61.96	39.22	12.09	25.30	23.12	64.42	16.49	0.00	15.18	73.81	10.82	14.55	40.45	326.26	49.74	288.05	311.56
Eur	63.19	22.55	13.98	7.37	16.72	47.65	15.67	15.18	0.00	98.55	18.90	9.53	32.00	317.44	36.02*	286.74	307.09
Kbw	132.81	127.24	90.35	98.32	118.77	94.35	79.88	73.81	98.55	0.00	83.02	105.06	73.67	404.85	90.88	340.21	352.62
San	72.55	40.62	11.71	26.91	17.28	53.43	31.27	10.82	18.90	83.02	0.00	16.75	55.76	273.20	51.97	243.62	261.95
Tol	47.41	22.11	9.32	24.62	16.04	53.17	21.40	14.55	9.53	105.06	16.75	0.00	37.49	304.23	61.21	281.59	303.10
UP	63.86	37.07	37.97	39.88	56.10	52.14	24.68	40.45	32.00	73.67	55.76	37.49	0.00	362.36	54.70	323.08	347.12
Bon	364.76	316.19	311.12	319.05	305.18	320.75	344.12	326.26	317.44	404.85	273.20	304.23	362.36	0.00	343.23	17.85	20.15
Sac1	143.40	74.94	58.40	23.39NS	59.81	61.81*	68.25	49.74	36.02*	90.88	51.97	61.21	54.70	343.23	0.00	294.12	310.20
Sch	339.74	293.15	289.50	275.52	280.31	287.05	308.26	288.05	286.74	340.21	243.62	281.59	323.08	17.85	294.12	0.00	5.89
Trg	362.67	313.08	307.25	296.61	296.96	292.27	334.56	311.56	307.09	352.62	261.95	303.10	347.12	20.15	310.20	5.89	0.00

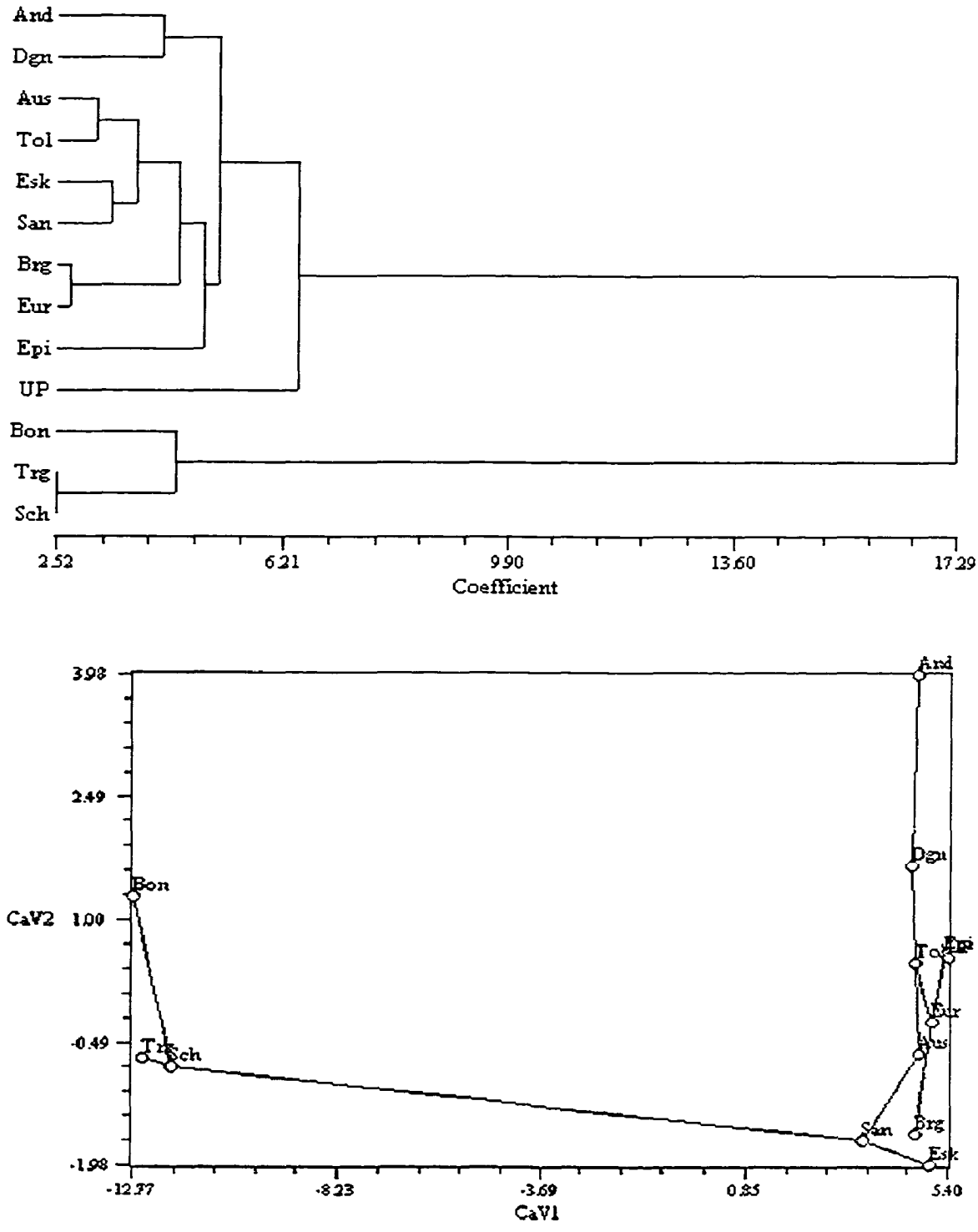

Figure 4.15: Cluster (UPGMA) analysis (top) and minimum spanning tree (bottom, Step 1A).

Step 1B – Human sample only

Principal Components Analysis: The results of the PCA are similar to those obtained in Step 1A (Table 4.9). Saccopastore 1 is not separated from modern humans. It falls at the negative end of PC 2 (14.9 % of the total variance) and overlapping with the Berg. This population is significantly different in its mean score from all other modern human groups except the mixed European population. The shape changes along this component are similar to those observed for PC 2 of Step 1A. In the negative end, where Saccopastore 1 and the Berg fall, they include a much more posteriorly projecting inion, a more inferiorly and anteriorly placed lambda, more laterally placed asteria, and a more superiorly placed basion and hormion. These differences indicate a medio-laterally wide occipital squama, with a supero-inferiorly short and antero-posteriorly elongated occipital plane. PC 2 is not strongly correlated with centroid size (Table 4.9).

PCs 4 (7 %) and 9 (3 %) are significant for sex effects to the 0.001 level. In both cases females tend to have more positive scores than males. When the means for males and females are plotted by population along PC 4 the female means are more positive in all populations except in the Europeans and the Eskimo. Along PC 9, the means for females are more positive than those for males in all populations except the Tolai. The shape differences in the positive end of these two components include a supero-inferiorly taller occipital plane, with a less posteriorly projecting inion, more posteriorly placed medial ends of the jugular fossae, a medio-laterally wide foramen magnum and more laterally placed lateral ends of the inferior nuchal lines. These changes are similar to those found to differentiate females from males in Step 1A. PC 4 and PC 9 are only weakly correlated with centroid size (Table 4.9).

Canonical Variates Analysis: In the CVA (Table 4.10), again Saccopastore 1 is not separated from modern humans, but falls at the negative end of the modern human range along CaV 2 (23.1 % of the total variance), overlapping with the Berg population. As with PC 2, the Berg are significantly different from all other modern human populations except for the Upper Paleolithic and European populations. The shape changes along this canonical axis are similar to those described for PC 2 and also for CaV 2 in Step 1A. CaV 2 is only weakly correlated with centroid size.

Kabwe is separated from modern humans along CaV 4 (8.8 %, most highly influenced by PCs 4, 6 and 9, Fig. 4.18). This specimen falls outside the 95 % confidence ellipses of all modern human populations along this axis. It is characterized by an inferiorly placed lambda, more steeply inclined occipital plane and elevated lateral ends of the superior nuchal line. CaV 4 is only weakly correlated with centroid size (Table 4.10).

The Upper Paleolithic specimens are partially separated from modern humans along CaV 3 (13.5 %) and CaV 4 on the negative sides of both (Fig. 4.16). Predmosti 3, Cro Magnon 1 and Ein Gev fall outside the 95 % confidence ellipses of all modern human populations along these two axes, while Mladec 1 and Predmosti 4 fall at their edges. The shape differences at the negative end of CaV 3 include a more posteriorly projecting inion, a more anteriorly placed lambda and more steeply inclined occipital plane, and a more inferiorly placed opisthion, indicating a relatively long nuchal plane. The negative end of CaV 4 is characterized by a depressed lambda and elevated lateral ends of the superior nuchal line. These shape differences are consistent with the morphology described for the Upper Paleolithic specimens, which includes a strong and posteriorly projecting occipital protuberance, a hemibun with a small lambdoidal depression, a long nuchal plane and strong cranial superstructures (Billy 1970; Genet-Varcin 1970; Vlcek 1970; Smith 1984; Gambier 1989; Churchill et al. 2000). Like CaV 4, CaV 3 is only weakly correlated with centroid size (Table 4.10).

Classification: The results of the classification by posterior probability are very similar to those obtained in Step 1A. Saccopastore 1 was classified as Berg (0.998), Kabwe as Eskimo (0.91), Kanalda as Tolai (0.83), as before. The only difference is in the classification of Skhul 5, which was here classified as European (0.63) rather than Berg. The results of the cross-validation classification were also very similar to those of Step 1A (Table 4.11).

Mahalanobis D^2, Cluster Analysis and Minimum Spanning Tree: The unbiased Mahalanobis D^2 matrix for Step 1B is reported in Table 4.12. The distance between the Epipaleolithic and the mixed European populations is only significant to the 0.05 level. The smallest distance observed is again that between the Berg and mixed European populations. This pair and the Australian-Melanesian pair show the smallest distances

Table 4.9: Summary of the PCA results, ANOVA and Correlation Analysis, for PCs 1-10, Step 1B

	Principal Components Analysis			ANOVA Pr > F			Correlation with Centroid Size	
	Eigenvalue	Proportion	Cumulative	Popul.	Sex	Interaction	Rho	Pr > F
PC 1	0.001547	0.211048	0.211048	0.0001	0.1021	0.0875	-0.43152	0.0001
PC 2	0.00109	0.14864	0.359688	0.0001	0.1158	0.1605	-0.38512	0.0001
PC 3	0.000646	0.088128	0.447816	0.0001	0.1298	0.7258	0.09044	0.1564
PC 4	0.000516	0.070325	0.518142	0.0001	0.001	0.1178	-0.16646	0.0088
PC 5	0.000446	0.060881	0.579022	0.0001	0.8484	0.3888	-0.12696	0.0462
PC 6	0.000381	0.052006	0.631028	0.0001	0.3333	0.8266	0.04611	0.4706
PC 7	0.000316	0.043086	0.674114	0.0001	0.3857	0.8297	-0.07335	0.2508
PC 8	0.00028	0.038152	0.712266	0.0001	0.4643	0.2186	0.08069	0.2063
PC 9	0.000218	0.029697	0.741964	0.0001	0.0003	0.3695	-0.25483	0.0001
PC 10	0.000178	0.024273	0.766237	0.0264	0.062	0.1893	-0.05189	0.4169

Table 4.10: Summary of the CVA results and Correlation Analysis, CaV 1-5, Step 1B

	Canonical Variates Analysis			Correlation with Centroid Size	
	Eigenvalue	Proportion	Cumulative	Rho	Pr > F
CaV 1	4.0332	0.3134	0.3134	-0.49844	0.0001
CaV 2	2.9696	0.2308	0.5442	-0.33435	0.0001
CaV 3	1.7343	0.1348	0.679	-0.24778	0.0001
CaV 4	1.1272	0.0876	0.7666	-0.24287	0.0001
CaV 5	0.8136	0.0632	0.8298	0.16259	0.0105

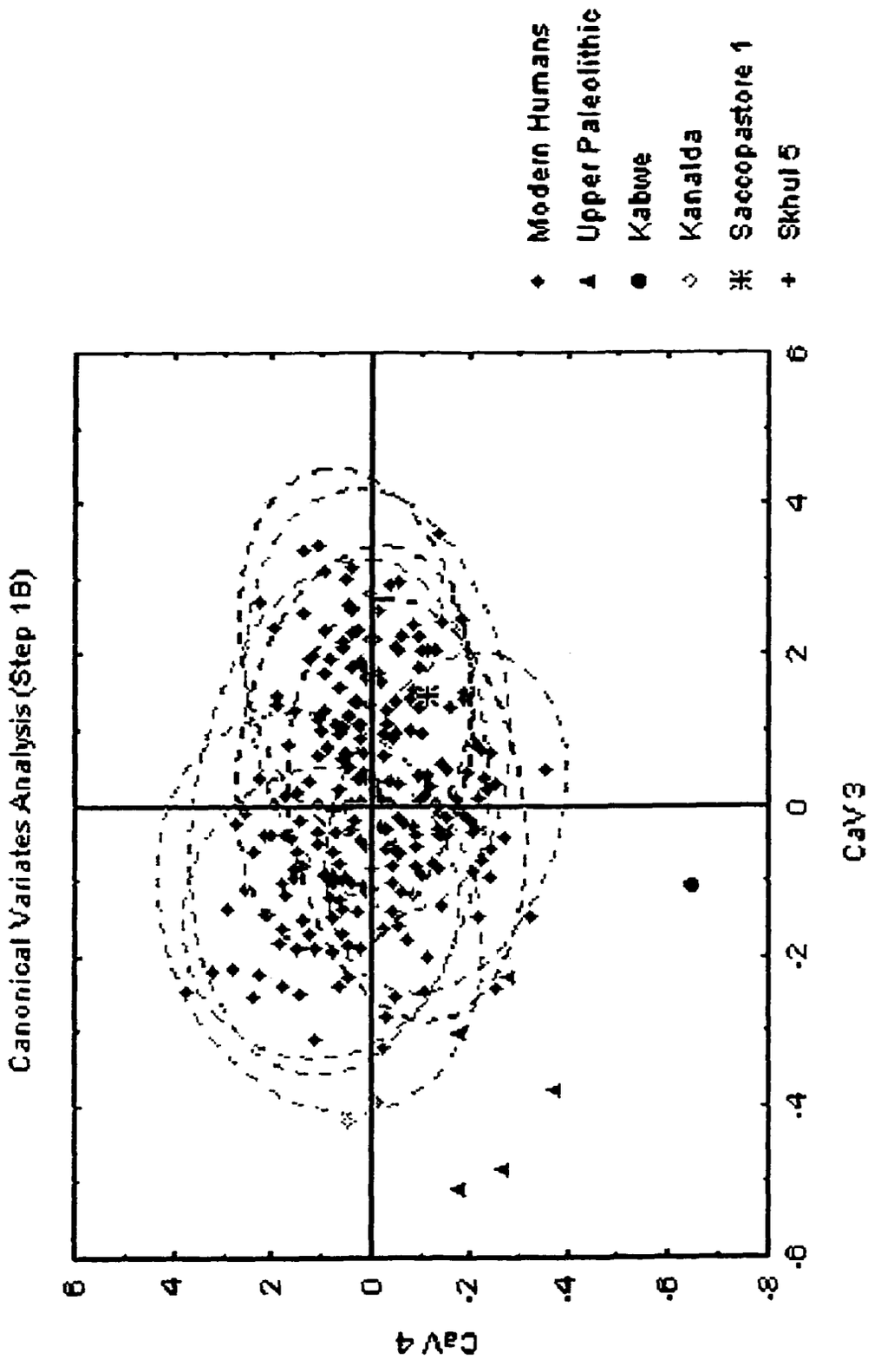

Figure 4.16: Canonical Variates Analysis (Step 1B), CaVs 3 and 4. Dotted lines represent the 95 % confidence ellipses for each group.

one to the other. Neither of the two groups in the third pair are closest neighbors to the other. The greatest distance is that between the Upper Paleolithic group and the San. As in Step 1A, the Upper Paleolithic specimens are quite distant from all recent human populations, and are closest to the Epipaleolithic. The UPGMA diagram and minimum spanning tree are very similar to those in Step 1A, the only difference being in the relative position of the Epipaleolithic population.

Table 4.11: Cross-validation classification summary (percentages for each population in bold), Step 1B.

	And	Aus	Brg	Dgn	Epi	Esk	Eur	San	Tol	UP	Total
And	24	0	0	2	1	0	2	0	0	0	29
%	**82.76**	0	0	6.9	3.45	0	6.9	0	0	0	100
Aus	0	24	0	0	0	2	2	0	2	0	30
%	0	**80**	0	0	0	6.67	6.67	0	6.67	0	100
Brg	0	0	26	0	0	0	4	0	0	0	30
%	0	0	**86.67**	0	0	0	13.33	0	0	0	100
Dgn	0	0	0	26	1	0	1	0	1	0	29
%	0	0	0	**89.66**	3.45	0	3.45	0	3.45	0	100
Epi	0	0	0	1	0	1	0	0	0	1	3
%	0	0	0	33.33	**0**	33.33	0	0	0	33.33	100
Esk	0	2	0	0	0	23	0	2	3	0	30
%	0	6.67	0	0	0	**76.67**	0	6.67	10	0	100
Eur	2	0	6	0	2	0	13	2	2	1	28
%	7.14	0	21.43	0	7.14	0	**46.43**	7.14	7.14	3.57	100
San	0	0	0	1	0	2	1	26	0	0	30
%	0	0	0	3.33	0	6.67	3.33	**86.67**	0	0	100
Tol	0	2	0	0	0	1	1	0	24	1	29
%	0	6.9	0	0	0	3.45	3.45	0	**82.76**	3.45	100
UP	0	1	0	0	1	0	0	0	1	2	5
%	0	20	0	0	20	0	0	0	20	**40**	100
Total	26	29	32	30	5	29	24	30	33	5	243
%	10.7	11.93	13.17	12.35	2.06	11.93	9.88	12.35	13.58	2.06	100

Table 4.12: Unbiased Mahalanobis D^2, Step 1B. All distances 0.001 significance level except: NS = non-significant, * = 0.05 level, ** = 0.01 level.

	Kan	And	Aus	Brg	Dgn	Skh5	Epi	Esk	Eur	Kbw	San	Tol	UP	Sac1
Kan	0.00	76.82	52.61	79.09	73.24	113.34	56.36*	68.10	68.11	126.69	76.50	50.31	62.61	151.93
And	76.82	0.00	33.99	36.89	16.67	74.69	24.41	39.50	23.21	126.87	42.02	22.22	37.12	81.74
Aus	52.61	33.99	0.00	29.27	21.25	68.82	33.00	12.65	15.09	93.58	12.46	10.28	39.48	59.21
Brg	79.09	36.89	29.27	0.00	30.31	65.46	28.75	24.86	7.79	104.75	27.00	25.08	39.22	29.81NS
Dgn	73.24	16.67	21.25	30.31	0.00	75.14	24.62	22.74	17.16	113.56	18.38	16.15	53.57	64.81
Skh5	113.34	74.69	68.82	65.46	75.14	0.00	80.23	85.47	64.02	123.01	69.56	71.07	78.72	99.56
Epi	56.36*	24.41	33.00	28.75	24.62	80.23	0.00	20.86	16.79	81.94	33.62	22.25	25.17	75.01
Esk	68.10	39.50	12.65	24.86	22.74	85.47	20.86	0.00	15.93	76.67	9.57	14.95	41.76	48.87
Eur	68.11	23.21	15.09	7.79	17.16	64.02	16.79	15.93	0.00	104.90	19.25	10.44	31.24	41.92*
Kbw	126.69	126.87	93.58	104.75	113.56	123.01	81.94	76.67	104.90	0.00	81.67	107.98	86.36	102.72
San	76.50	42.02	12.46	27.00	18.38	69.56	33.62	9.57	19.25	81.67	0.00	18.68	57.59	54.23
Tol	50.31	22.22	10.28	25.08	16.15	71.07	22.25	14.95	10.44	107.98	18.68	0.00	34.80	67.03
UP	62.61	37.12	39.48	39.22	53.57	78.72	25.17	41.76	31.24	86.36	57.59	34.80	0.00	64.53
Sac1	151.93	81.74	59.21	29.81NS	64.81	99.56	75.01	48.87	41.92*	102.72	54.23	67.03	64.53	0.00

Step 1C – Chimpanzee sample only

The analysis was repeated on the chimpanzee sample alone, in order to test for the consistency of the chimpanzee model. As in the temporal bone landmark analysis, only the results of the Mahalanobis D^2 analysis will be discussed here.

***Classification*:** As in the previous steps, a discriminant analysis was performed on the chimpanzee sample and a cross-validation classification was obtained (Table 4.13). Two bonobos were classified as *P. t. schweinfurthii* and one as *P. t. troglodytes*, and two of each subspecies of common chimpanzee were classified as bonobos. The classification success at the species level, therefore, is lower than in the temporal bone landmark analysis. The misclassification rates among the two common chimpanzee subspecies are quite high (approx. 25 % in both), as also found in the temporal bone analysis.

***Mahalanobis D^2*:** The unbiased Mahalanobis D^2 was calculated, as in the previous steps (Table 4.14). The distances between bonobos and the two common chimpanzee subspecies are slightly higher than in the combined sample analysis, but still equivalent to, or even smaller than, the distances between modern human populations obtained in both steps 1A and 1B. The distance between the subspecies of the common chimpanzee is approximately doubled, but it is still smaller most distances among modern human populations. It is only higher than the smallest distance between modern human groups, that between the European and Berg populations.

Table 4.13: Cross-validation classification summary (percentages for each population in bold), Step 1B.

	Bon	Sch	Trg	Total
Bon	30	2	1	33
%	**90.91**	6.06	3.03	100
Sch	2	20	7	29
%	6.9	**68.97**	24.14	100
Trg	2	7	19	28
%	7.14	25	**67.86**	100
Total	34	29	27	90
%	37.78	32.22	30	100

Table 4.14: Unbiased Mahalanobis D^2, excluding singletons, Step 1C. All distances significant to the 0.001 level, except NS = non-significant, * =0.05 and ** = 0.01.

	Bon	Sch	Trg
Bon	0.00	19.91	24.01
Sch	19.91	0.00	12.32
Trg	24.01	12.32	0.00

Step 2

The analysis was repeated with sixteen landmarks, excluding hormion, the landmark that is most often missing. The sample size of Neanderthals is increased to 4, and includes, in addition to Saccopastore 1, La Chapelle, La Ferrassie 1 and Shanidar 1. The fossil specimen Biache is also included in this increased sample, and the Epipaleolithic modern human group now includes sixteen specimens (see Table 4.2).

Centroid Size: As in Step 1, population and sex effects are significant to the 0.0001 level, while and interaction effect is also significant (0.01). All three chimpanzee taxa are significantly smaller in their mean centroid size values from all modern human populations. Centroid size for both genera is reduced with the removal of hormion, although slightly less so for the human sample than the chimpanzee sample. As in Step 1, both the mean and standard deviation for centroid size are greater in humans than in chimpanzees (see Table 4.15, Fig. 4.17). The male mean overall is significantly larger than the female one, the mean and standard deviation values for males being greater than the female values in both genera.

Bonobos show a lower mean and standard deviation than common chimpanzees. The two common chimpanzee subspecies show similar means and ranges of variation. The mean value for female bonobos is higher than that of bonobo males, while the standard deviation is equivalent for the two sexes in this species. Common chimpanzee males, on the other hand, have a higher mean and slightly greater standard deviations than females. Bonobos show very little sexual dimorphism, females tending to be larger than males, while sexual dimorphism is very strong in common chimpanzees, males being larger than females.

Modern human males have greater mean and standard deviation than females. Sexual dimorphism is much stronger in modern humans than in bonobos, but weaker than common chimpanzees. The pattern of sexual dimorphism, males being larger than females, is similar between modern humans and common chimpanzees. The Neanderthal mean centroid size is greater than the mean for modern humans, or even the mean for modern human males, while their standard deviation is equivalent. The centroid size of Saccopastore 1, the only female Neanderthal included here, is closer to the modern human mean, although it is larger than the mean for females. Kabwe is larger than the

Table 4.15: Centroid size listed by genus, species, sex and population, Step 2.

	Mean	Range	St. Deviation	N
Homo	**18.30**	**15.39-21.25**	**1.03**	**263**
Males	18.71	15.78-21.25	0.99	140
Females	17.81	15.39-20.06	0.86	121
Modern	18.26	15.39-21.25	1.00	257
Males	18.65	15.78-21.25	0.95	136
Females	17.78	15.39-20.06	0.86	120
Neanderthals	20.02	18.98-21.22	1.01	4
Males	20.37	19.42-21.22	0.90	3
Females	18.98	---	---	1
Kabwe	20.46	---	---	1
Biache	18.57	---	---	1
Skhul 5	19.47	---	---	1
Upper Paleolithic	19.61	18.91-20.06	0.45	5
Kanalda	19.97	---	---	1
Andamanese	16.65	15.39-17.45	0.54	29
Australian	18.18	16.70-19.56	0.71	30
Berg	18.67	17.29-20.42	0.77	30
Dogon	17.77	16.26-18.82	0.57	29
Epipaleolithic	19.29	18.49-20.38	0.64	15
Eskimo	19.10	18.12-21.25	0.73	30
European (mixed)	18.64	17.61-20.27	0.74	28
San	18.04	16.50-19.81	0.74	30
Tolai	18.14	17.00-19.33	0.62	29
Pan	**14.03**	**12.53-15.70**	**0.71**	**90**
Males	14.23	12.78-15.70	0.78	48
Females	13.76	12.53-14.81	0.54	40
P. paniscus	13.40	12.53-14.12	0.37	33
Males	13.34	12.78-13.96	0.37	15
Females	13.45	12.53-14.12	0.38	18
P. troglodytes	14.39	13.05-15.70	0.60	57
Males	14.64	13.05-15.70	0.55	33
Females	14.02	13.27-14.81	0.51	22
P. t. schweinfurthii	14.24	13.05-15.70	0.65	29
P. t. troglodytes	14.55	13.27-15.40	0.50	28

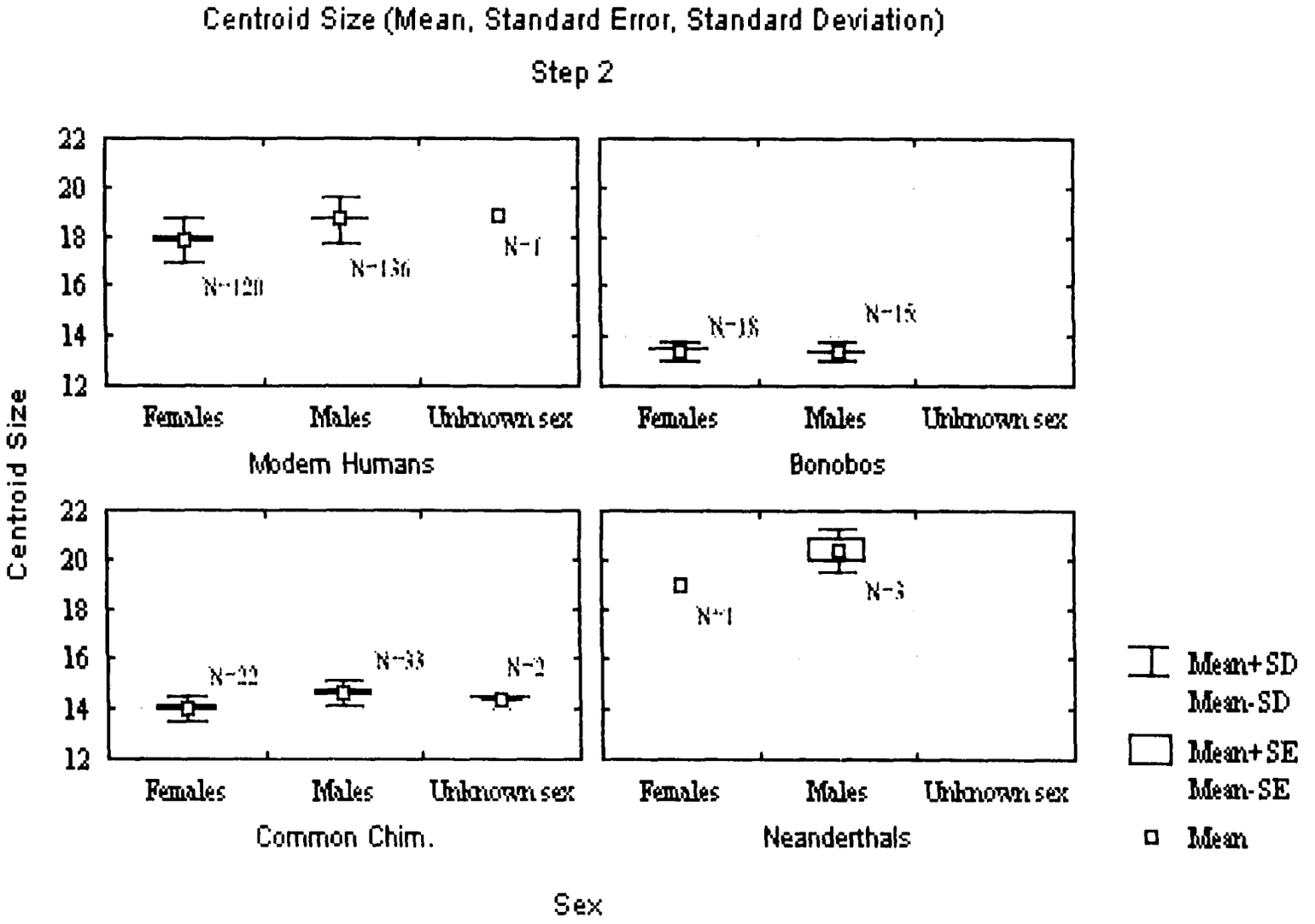

Figure 4.17: Centroid size mean, standard error and standard deviation, plotted by species and sex (Step 2).

mean value for modern human males, while Biache is close to the modern human mean. Skhul 5, Kanalda, and the Upper Paleolithic specimens again fall in the upper part of the modern human range. Unlike Step 1, the Epipaleolithic, whose sample is increased greatly here, have the largest mean value among modern human populations, although the Eskimo still show the highest upper limit in their range. The lowest values for both the mean and the upper limit are again those of the Andamanese.

Step 2A – Combined Sample

Principal Components Analysis: As in Step 1, this analysis fails to completely separate Neanderthals from modern humans. Even the tendency of Saccopastore 1 to fall at the extreme of the modern human range along PC 2 and 3 (Step 1A) is no longer clear. Table 4.16 summarizes the results of the PCA, while Table 4.17 shows the landmarks that influence most the first ten principal components.

Chimpanzees are separated from the humans only along PC 1 (58 % of the total variance, Fig. 4.18). All three chimpanzee taxa are significantly different in their mean scores on PC 1 from all human populations. This component is very similar to PC 1 of Step 1A. It is significant for genus, population and sex effects (0.0001). PC 1 also separates Kabwe from modern humans, as this specimen lies outside the modern human range and between the modern human and the chimpanzee clouds. Among chimpanzees, bonobos fall slightly closer to the human cloud, although they are not significantly different from common chimpanzees in their mean. None of the modern human populations are significantly different from each other along this component, although the Eskimo tend to extend furthest toward the chimpanzee cloud, while the Andamanese are the furthest away from it. Neanderthals are not significantly different from any of the modern human groups or from modern humans as a whole. Biache falls within the modern human variation and close to Shanidar 1 and La Ferrassie 1. Skhul 5 and the Upper Paleolithic specimens also fall well within the modern human range. When the mean scores on PC 1 for males and females are plotted by populations, the male means are more positive than the female means in the chimpanzees, and in most, but not all, human populations (Fig. 4.19).

Table 4.16: Summary of the PCA results, ANOVA and Correlation Analysis, PCs 1-10, Step 2A.

	Principal Components Analysis			ANOVA Pr > F			Correlation with Centroid Size	
	Eigenvalue	Proportion	Cumulative	Popul.	Sex	Interaction	Rho	Pr > F
PC 1	0.009055	0.579787	0.579787	0.0001	0.0001	0.3407	-0.78848	0.0001
PC 2	0.000956	0.061209	0.640996	0.0001	0.1265	0.0422	0.14861	0.0051
PC 3	0.00085	0.054419	0.695414	0.0001	0.1778	0.0796	-0.27688	0.0001
PC 4	0.000699	0.044778	0.740192	0.0001	0.1215	0.7735	-0.1236	0.0202
PC 5	0.000629	0.040279	0.780471	0.0001	0.9242	0.497	-0.04341	0.4162
PC 6	0.000426	0.027295	0.807766	0.0001	0.0055	0.8217	0.18483	0.0005
PC 7	0.000372	0.023839	0.831606	0.0001	0.0007	0.0026	-0.18042	0.0007
PC 8	0.000322	0.020632	0.852238	0.0001	0.4239	0.0047	0.11815	0.0264
PC 9	0.000251	0.016088	0.868326	0.0001	0.0001	0.3381	0.14674	0.0057
PC 10	0.000211	0.013522	0.881849	0.0002	0.0917	0.243	-0.04398	0.4101

Table 4.17: Squared roots of the sum of squares of the eigenvector coefficients for the three coordinates of each landmark. Step 2A.

	PC 1	PC 2	PC 3	PC 4	PC 5	PC 6	PC 7	PC 8	PC 9	PC 10
1. Inion	**0.34**	0.19	**0.35**	**0.19**	**0.51**	**0.34**	**0.48**	**0.35**	0.23	**0.50**
2. Asterion R	0.19	**0.34**	0.19	0.15	**0.27**	**0.42**	0.16	**0.33**	0.12	0.21
3. Asterion L	0.19	**0.29**	0.17	0.17	**0.27**	**0.40**	0.23	**0.32**	0.19	0.24
4. Lambda	**0.64**	**0.48**	0.24	**0.25**	**0.48**	**0.33**	0.15	0.24	0.15	0.18
5. Opisthion	0.03	0.08	0.20	0.18	0.21	0.08	0.19	**0.39**	0.16	**0.28**
6. Basion	0.03	0.23	0.15	0.11	0.15	0.17	0.08	0.09	0.12	0.20
7. Occ. Cond. R	0.14	0.16	**0.27**	0.17	0.06	0.19	**0.30**	0.16	**0.24**	0.03
8. Occ. Cond. L	0.15	0.10	**0.27**	0.15	0.06	0.18	**0.36**	0.11	**0.31**	0.07
9. Jugular F. Med. R	0.08	0.18	0.15	0.10	0.13	0.17	0.23	0.22	**0.50**	0.19
10. Jugular F. Lat. R	0.15	0.09	0.04	0.11	0.19	0.17	**0.34**	0.19	0.05	0.22
11. Jugular F. Med. L	0.10	0.18	0.15	0.13	0.12	0.18	0.24	0.17	**0.39**	0.16
12. Jugular F. Lat. L	0.17	0.07	0.07	0.11	0.20	0.18	**0.34**	0.08	0.05	0.24
13. Inf. Nuchal Line R	0.16	0.12	0.15	**0.60**	0.17	0.16	0.05	**0.31**	**0.31**	**0.39**
14. Inf. Nuchal Line L	0.15	0.10	0.14	**0.57**	0.13	0.17	0.13	0.27	**0.37**	**0.35**
15. Sup. Nuchal Line R	**0.34**	**0.44**	**0.46**	0.08	**0.27**	**0.24**	0.12	0.24	0.15	0.15
16. Sup. Nuchal Line L	**0.35**	**0.38**	**0.49**	0.09	**0.25**	**0.33**	0.17	0.24	0.10	0.15

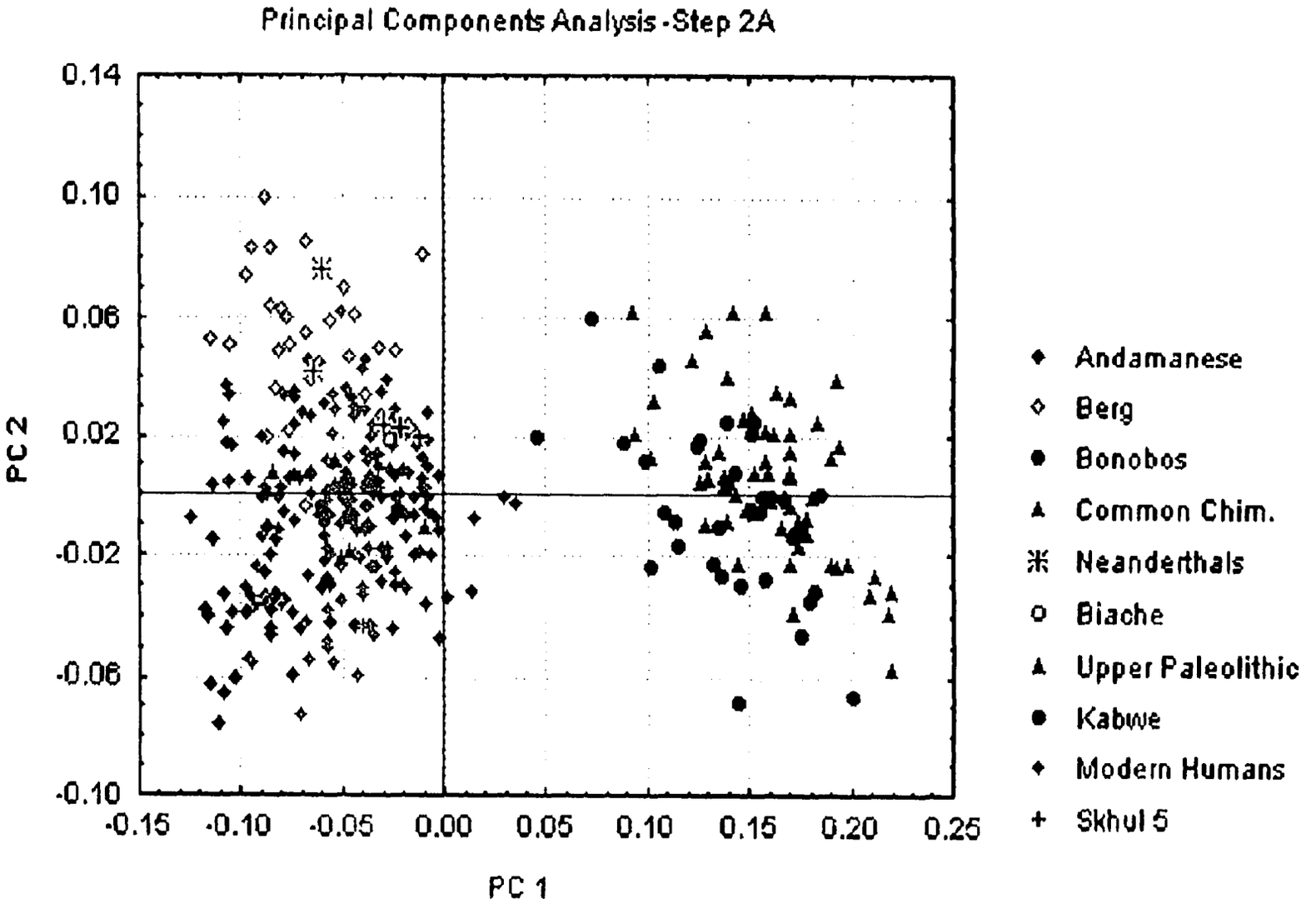

Figure 4.18: Principal Components Analysis, PCs 1 and 2 (Step 2A).

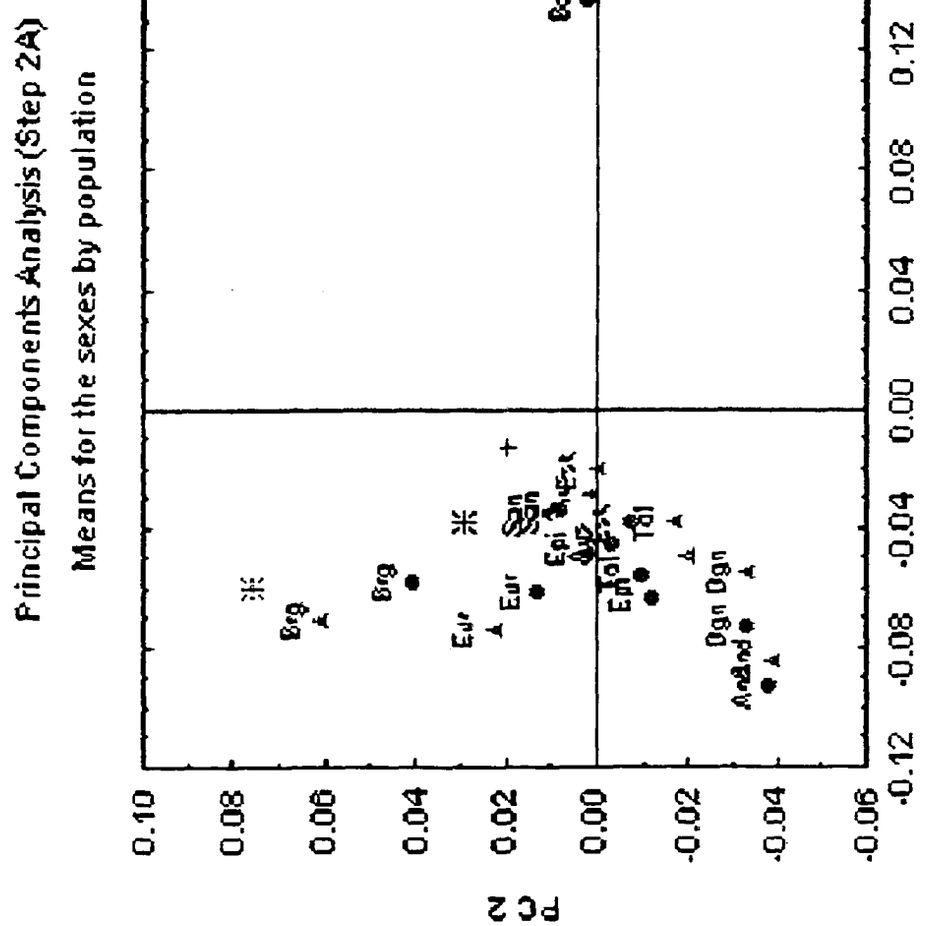

Figure 4.19: Principal Components Analysis (Step 2A), mean scores for the sexes plotted by population, PCs 1 and 2.

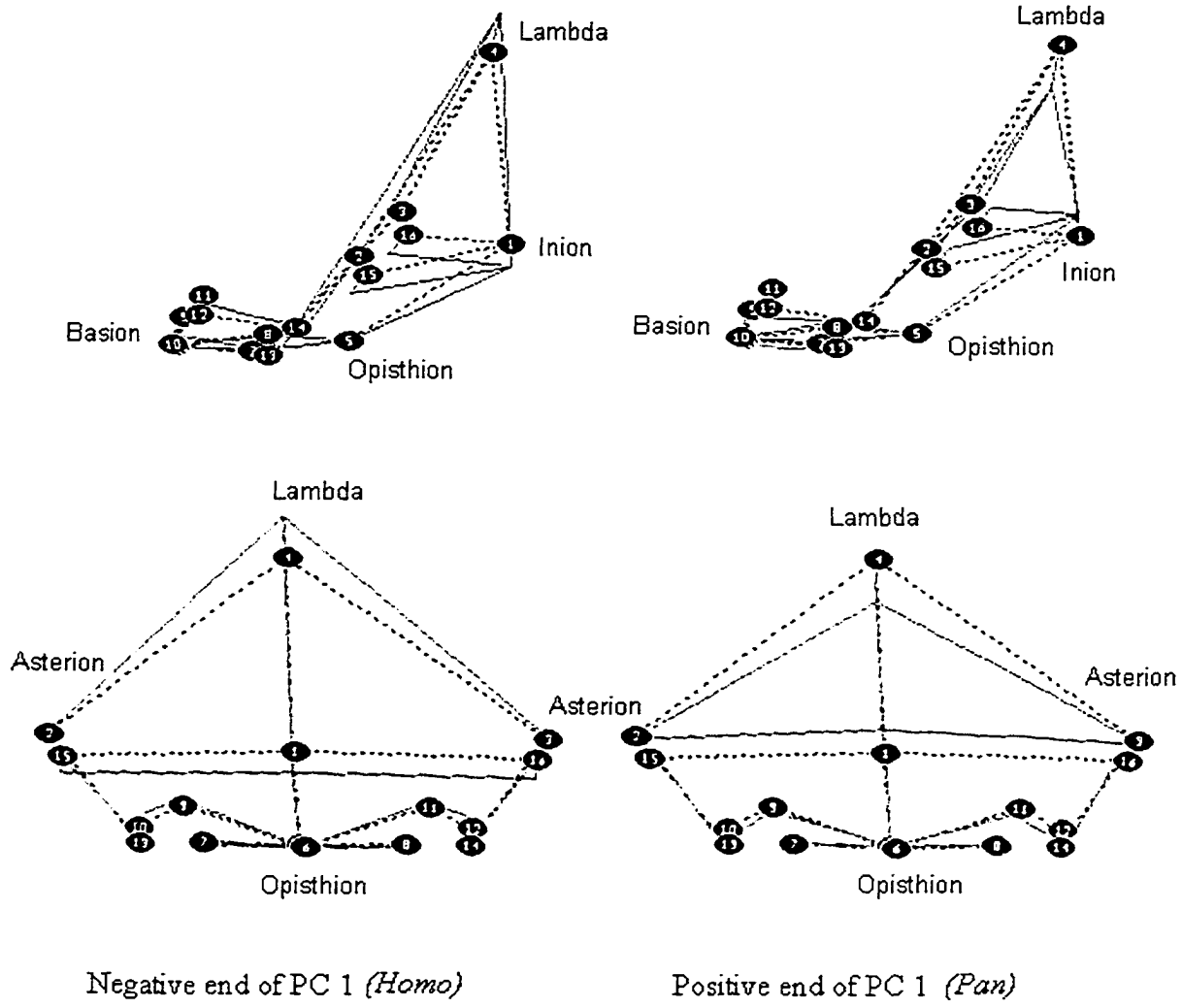

Negative end of PC 1 *(Homo)*

Positive end of PC 1 *(Pan)*

Figure 4.20: Shape variation along PC 1 (Step 2A). Lateral (top) and posterior views. The dotted line represents the consensus configuration.

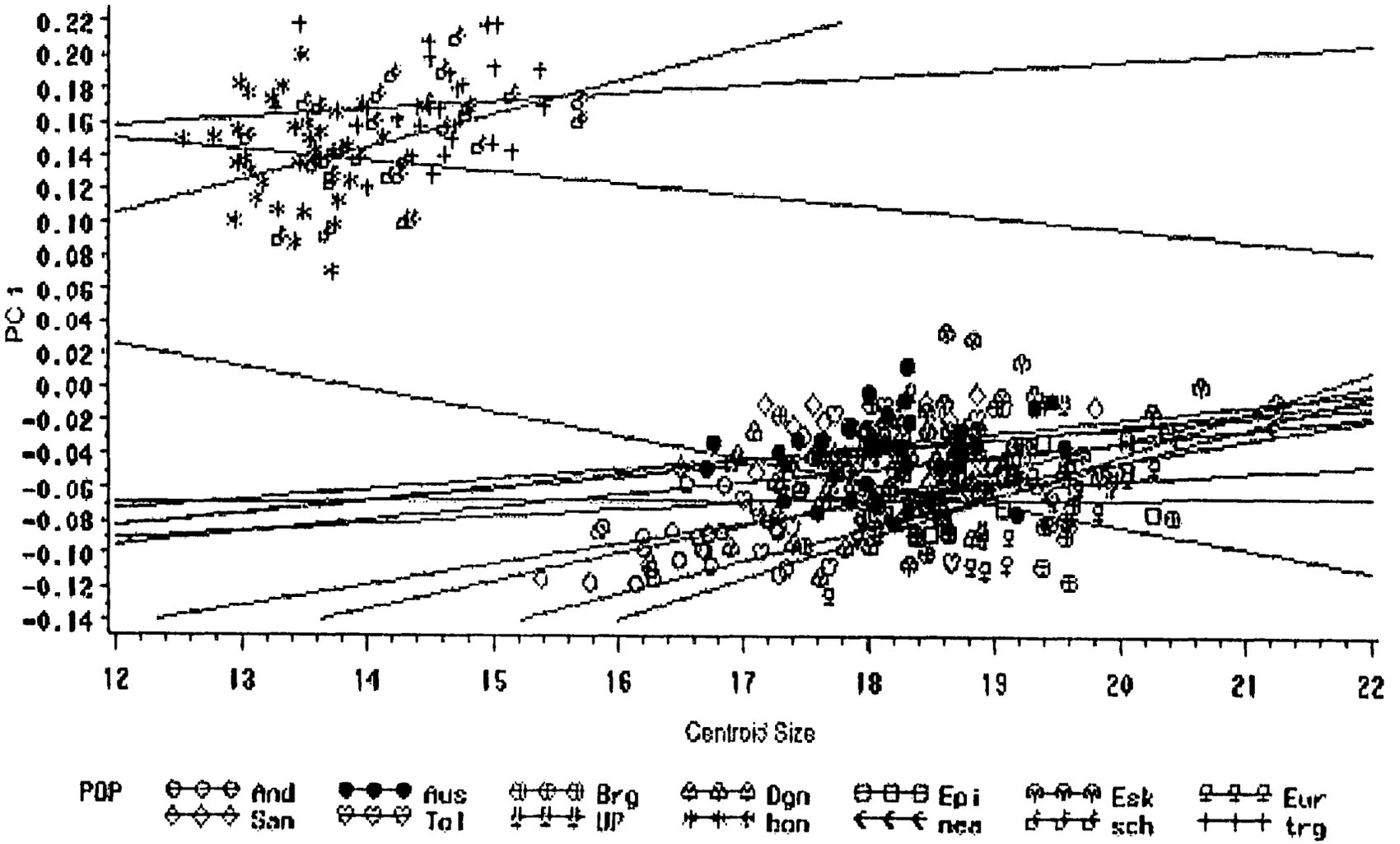

Figure 4.21: PC 1 plotted against centroid size, regression lines for populations fitted for each population (Step 2A).

Chimpanzees are separated from humans by a more inferiorly placed lambda (4), a more superior inion (1), and more superior lateral ends of the superior nuchal line (15, 16), reflecting a supero-inferiorly short occipital squama, and a relatively short occipital plane compared to the longer nuchal plane (Fig. 4.20). Kabwe is also characterized by these shape differences relative to the rest of the human sample, although to a lesser degree. These shape differences also tend to characterize males relative to females, although this trend is stronger among chimpanzees. As in Step 1A, PC 1 is relatively strongly correlated with centroid size. When PC 1 is plotted against centroid size the regression lines are not parallel across general and populations, as in Step 1A (Fig. 4.21).

PC 2 (6.1 % of the total variance, Fig. 4.18) is significant for population effects at the 0.0001 level, and for interaction effects at the 0.05 level. It separates modern human populations, with the Andamanese and the Dogon on one end and the Berg on the other end, and the remaining modern human groups in between. The Berg are significantly different from these two populations, but also from the Epipaleolithic, Eskimo, Upper Paleolithic and Tolai on this component. Neanderthals are not separated from the modern human range, but do fall on the positive side of this axis, mostly overlapping with the Berg. They are significantly different from modern humans when a one-way ANOVA is conducted for significant species effect. However, among modern human populations, Neanderthals are only significantly different from the Andamanese, the Dogon and the Tolai. Biache falls near the center of the modern human range, but again very close to Shanidar 1 and La Ferrassie 1, as do Kabwe and Skhul 5. The Upper Paleolithic group falls within the modern human cloud also. When the mean scores for PC 2 of males and females are plotted by population (Fig. 2.20), female means are more positive than males in the chimpanzee sample. The opposite trend is observed in most modern human populations, except in the Andamanese and Dogon, where the means for the two sexes are almost identical, and in the Tolai, where the female mean is more positive than the male. The mean for the male Neanderthal specimens is also more negative than the score of Saccopastore 1, the only female Neanderthal included here.

The shape differences (Fig. 4.22) that characterize the Berg, and to some degree Neanderthals also, include a more anteriorly and inferiorly placed lambda (4), a slightly more posterior and inferior inion (1), and more laterally placed asteria (2, 3) and lateral

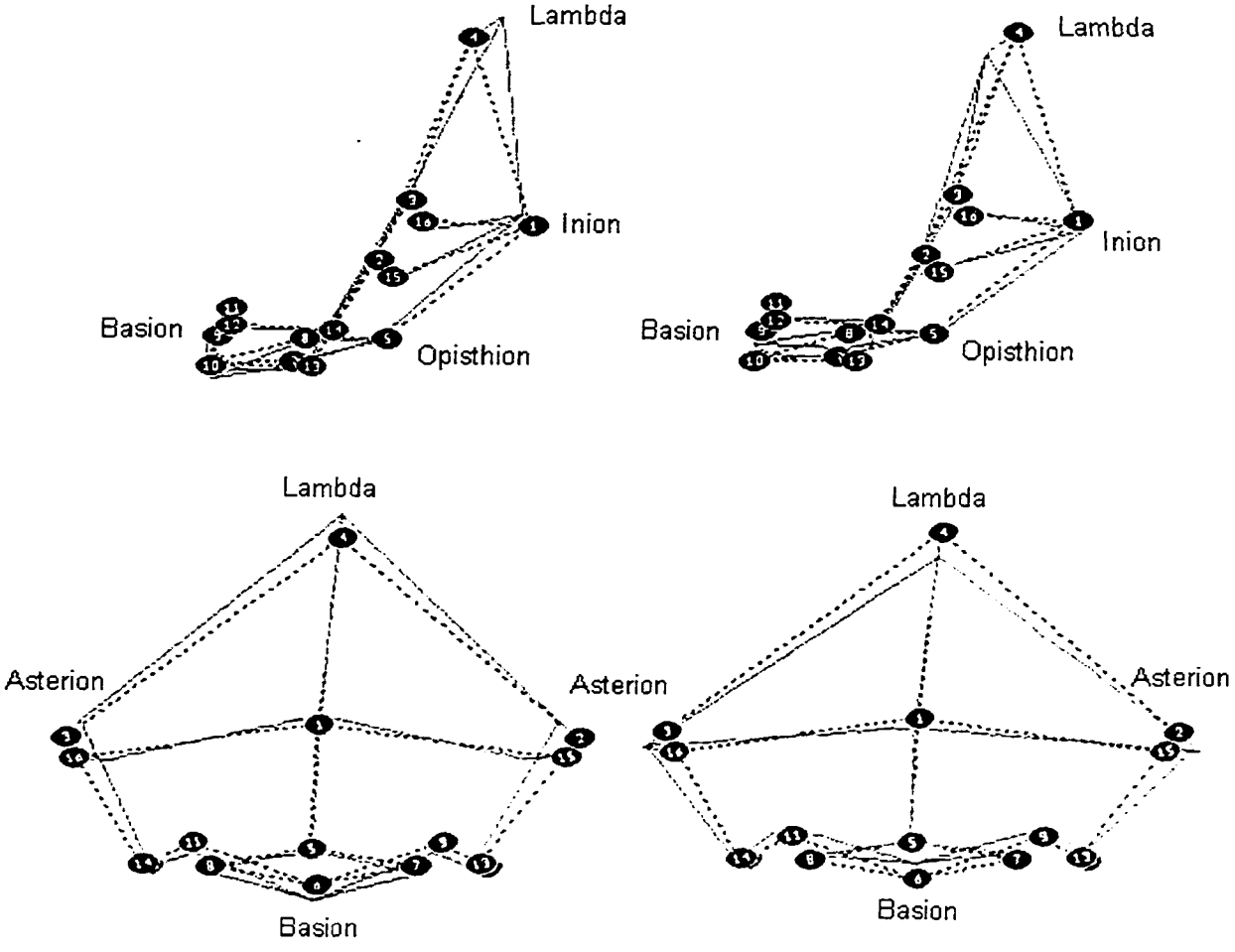

Negative end of PC 2 (Andamanese)

Positive end of PC 2 (Berg, Neanderthals)

Figure 4.22: Shape variation along PC 2 (Step 2A). Lateral (top) and posterior views. The dotted line represents the consensus configuration.

ends of the superior nuchal line (15, 16). They can be described as a supero-inferiorly short, medio-laterally wide and more posteriorly protruding occipital squama, with an antero-posteriorly longer and supero-inferiorly shorter occipital plane and a superior nuchal line that extends far laterally. These shape differences are consistent with the described Neanderthal morphology and are similar to those described in Step 1 for Saccopastore 1. However, this specimen is more extreme in the expression of these traits than the remaining Neanderthals included in this small sample. PC 2 (2.2 %) is only weakly correlated with centroid size.

PC 4 (4.5 %) separates Kabwe from modern humans, as this specimen falls just outside of the negative extreme of the human range. Bonobos also tend to have more positive scores than common chimpanzees on this component. Bonobos are significantly different in their means scores when compared to the common chimpanzees as a species, but not at the population level. The shape differences that drive the separation of Kabwe from the rest of the human sample along this component have to do mostly with its very anteriorly placed lateral ends of the inferior nuchal line (13, 14).

PC 6 (2.7 %) is significant for population (0.0001) and sex effects (0.01). This component is very similar to PC 6 of Step 1A. It separates Kabwe, Skhul 5 and the Upper Paleolithic specimens from modern humans, these specimens falling outside or at the extreme positive end of the modern human variation. The Upper Paleolithic group is significantly different in its mean score from all human populations except the Australians and Neanderthals. Neanderthals also fall on the positive side, but overlap with modern humans and are not significantly different from any modern human populations. When PC 6 is labeled by sex, females tend to have more negative scores than males, and this tendency is stronger in the human sample. When the mean scores for males and females are plotted by population, male means are more positive than female means in most modern human populations, except in the Andamanese, Dogon and Europeans. This trend is much weaker in the chimpanzees. The mean for the Neanderthal males is also more positive than the only female Neanderthal here, Saccopastore 1. This trend also holds for the Upper Paleolithic specimens. As Kabwe, Skhul 5, and three out of the five Upper Paleolithic specimens are male, they might be separated on the positive side of PC 6 as extreme males.

The shape differences that characterize Kabwe and the early modern human specimens at the positive end of PC 6 include more posteriorly, inferiorly and medially placed asteria (2, 3), a more posteriorly placed inion (1), a more superiorly and anteriorly placed lambda (4), and elevated and posterior lateral ends of the superior nuchal line (15, 16). These shape differences also tend to characterize males relative to females. They are similar to those shared by Kabwe and the Upper Paleolithic specimens in PC 6 of Step 1A. A small component of PC 6 (3.4 %, significant to the 0.001 level) is related to centroid size. When PC 6 is plotted against centroid size, however, only a weak relationship is observed.

Two additional components are significant for sex effects, PCs 7 and 9 (see Table 4.20). Along PC 7 (2.4 %) females tend to have more positive scores than males, but this trend is stronger in the chimpanzees. When the mean scores for males and females are plotted by population, the male means are more negative than the female means in most modern human groups. The Neanderthal male mean is also more negative than the score for Saccopastore 1, the only female Neanderthal specimen here. This trend is reversed in the European and the San populations, as well as in the Upper Paleolithic group. Bonobo The male means are much more positive than the female means in bonobos and *P. t. troglodytes*, but almost identical in *P. t. schweinfurthii*. PC 7 is also significant for population (0.0001) and species (0.001) effects. Biache falls at the extreme negative end of the modern human range on this component. The shape differences that characterize male chimpanzees relative to female chimpanzees, as well as Biache relative to most humans, include an elevated inion (1), occipital condyles (7, 8) that are more medially and inferiorly placed, and lateral ends of the jugular fossae (10, 12) that are more lateral and superior. These shape differences can be described as a supero-inferiorly shorter and more steeply inclined occipital plane, a supero-inferiorly long nuchal plane, more laterally projecting jugular processes and a medio-laterally narrow foramen magnum. They are similar to those described for males relative to females in Steps 1A and B. PC 7 is not related to centroid size.

PC 9 (1.6 %) is significant for sex and population effects at the 0.0001 level. Males tend to have more positive scores than females. When the mean scores for males and females are plotted by population, the male means are more positive than the female

means in all modern human groups except the Tolai and the Upper Paleolithic groups, where this trend is reversed. The male Neanderthal mean is also more positive than the score of Saccopastore 1. The same trend is present in bonobos and *P. t. schweinfurthii*, but not *P. t. troglodytes*. The shape differences at the positive end of PC 9 include a more anteriorly and inferiorly placed medial ends of the jugular fossae (9, 11), more medially placed lateral ends of the inferior nuchal line (13, 14), and more medially and posteriorly placed occipital condyles (7, 8).

Canonical Variates Analysis: A canonical variates analysis was conducted on the first 30 principal components (98.62 % of the total variance, Table 4.18). CaV 1 (82.07 % of the total variance, most highly influenced by PC 1, Fig. 4.23) separates the human from the chimpanzee sample. The mean scores of the three chimpanzee taxa are significantly different from those of all human groups. As with PC 1, and as in Step 1A, CaV 1 shows a relatively strong relationship to centroid size. The regression lines for each population, however, are not parallel across genera and across populations (Fig. 4.24). The shape differences along CaV 1 include, in the human end, a higher overall occipital squama with a supero-inferiorly taller occipital plane and a shorter nuchal plane. Chimpanzees are characterized by an overall shorter occipital squama, with a relatively taller supero-inferiorly nuchal plane and a shorter occipital plane. These shape differences are very similar to those described by PC 1 and those found for PC 1 and CaV 1 in Step 1A.

CaV 2 (4.7 % of the total variance, most highly influenced by PC 2, Fig. 4.23) separates bonobos from common chimpanzees, as well as the Berg on its negative end from the Andamanese on its positive end. The Andamanese are significantly different in their mean score from the Berg, San, European, Epipaleolithic, Eskimo, Upper Paleolithic and Neanderthal groups, while the Berg are significantly different from the Andamanese, Australian, Dogon and Tolai. Kabwe falls at the very end of the negative side of the modern human range and within the 95 % confidence ellipse of the Berg, as do the Neanderthals and Predmosti 3.

The shape differences that characterize the Berg, the Neanderthals and Kabwe on the negative end of CaV 2 (Fig. 4.25) include an overall supero-inferiorly short and posteriorly projecting occipital squama with a depressed lambda, a supero-inferiorly

Table 4.18: Summary of the CVA results and Correlation Analysis, CaV 1-5, Step 2A

	Canonical Variates Analysis			Correlation with Centroid Size	
	Eigenvalue	Proportion	Cumulative	Rho	Pr > F
CaV 1	46.6259	0.8207	0.8207	-0.9018	0.0001
CaV 2	2.6674	0.0469	0.8676	-0.33117	0.0001
CaV 3	2.43	0.0428	0.9104	-0.0919	0.0847
CaV 4	1.2216	0.0215	0.9319	0.00387	0.9423
CaV 5	0.9571	0.0168	0.9488	0.07596	0.1544

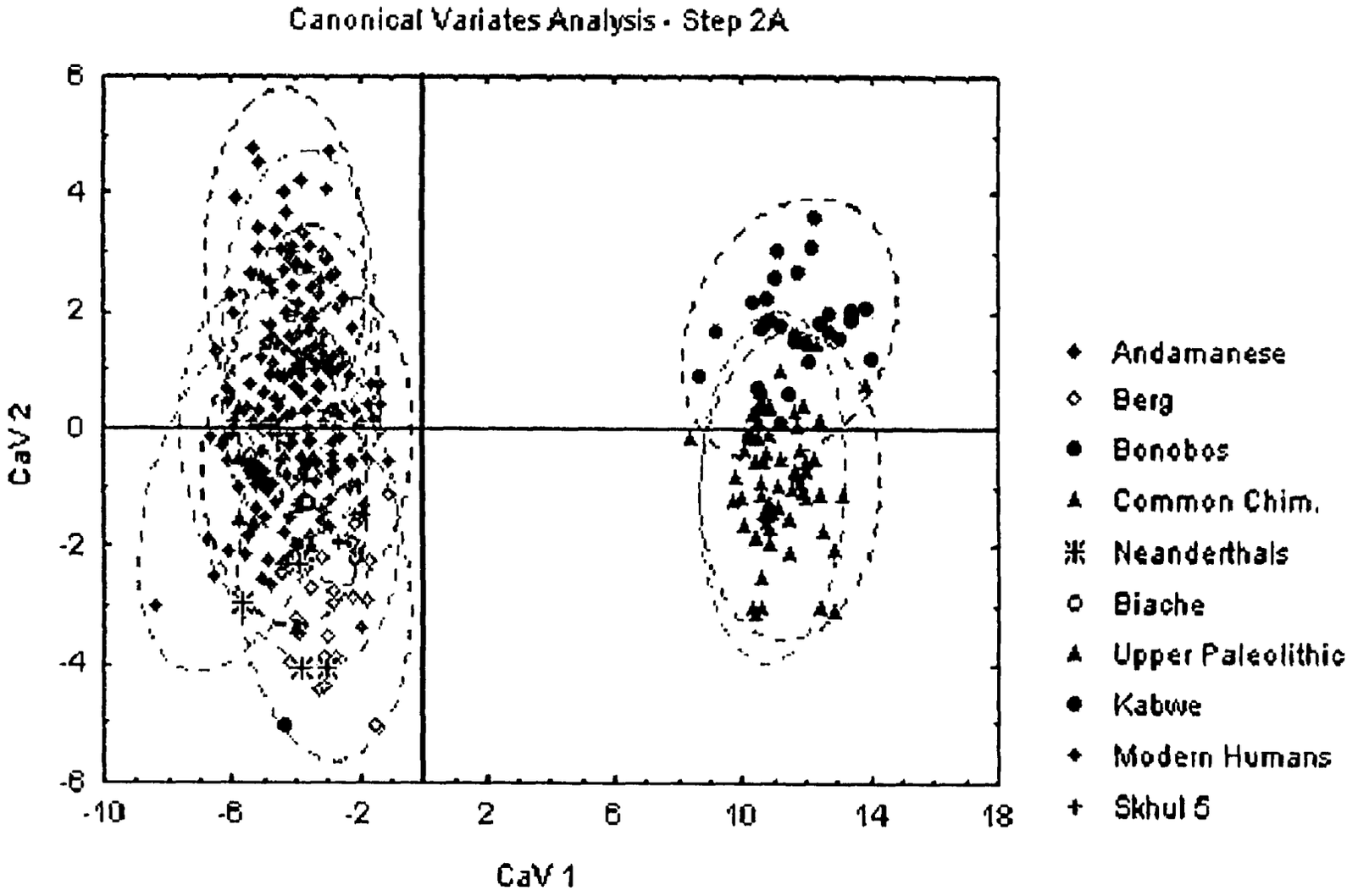

Figure 4.23: Canonical Variates Analysis (Step 2A) CaVs 1 and 2. Dotted lines represent the 95 % confidence ellipses for each group.

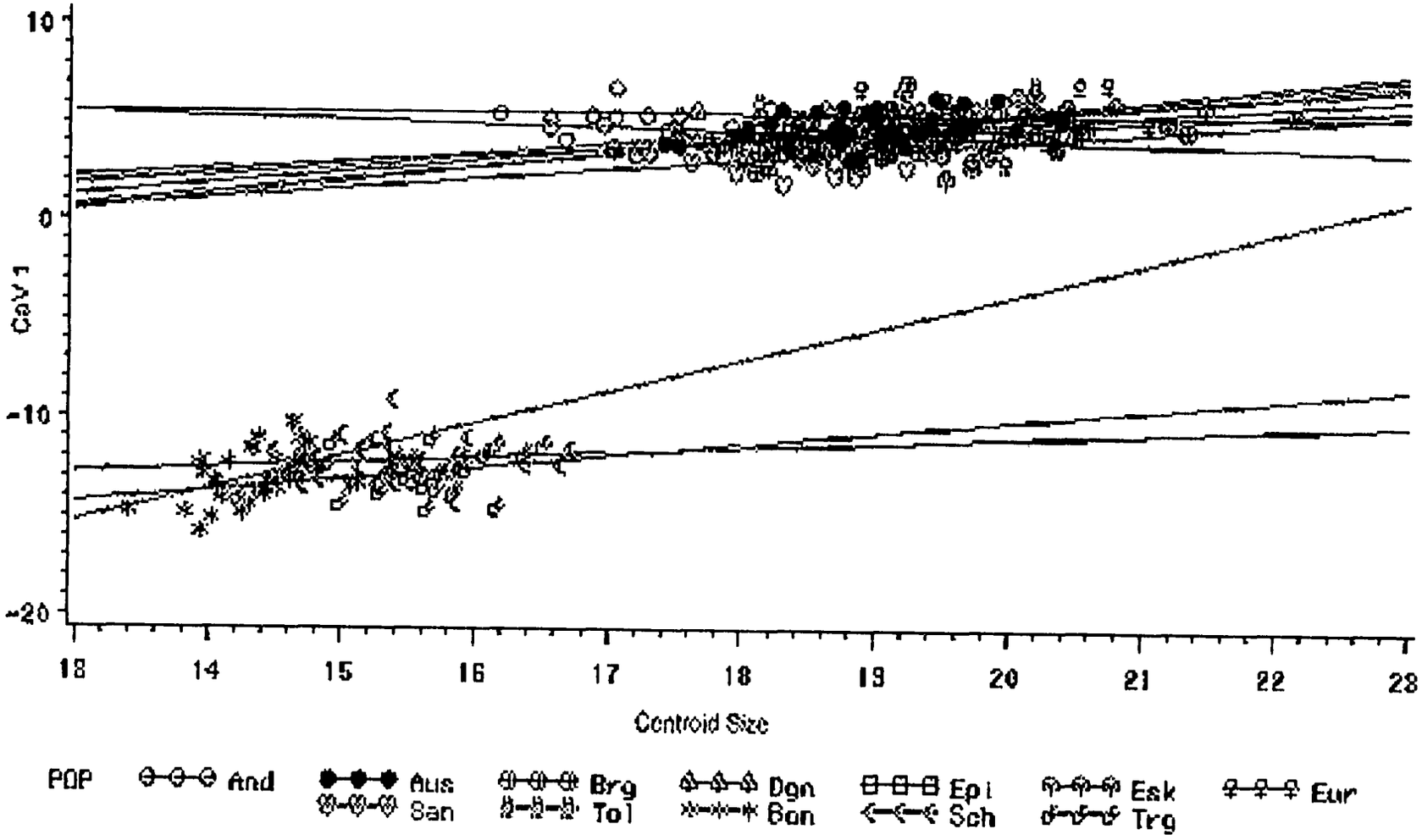

Figure 4.24: CaV 1 plotted against centroid size, with regression lines for populations fitted (Step 2A).

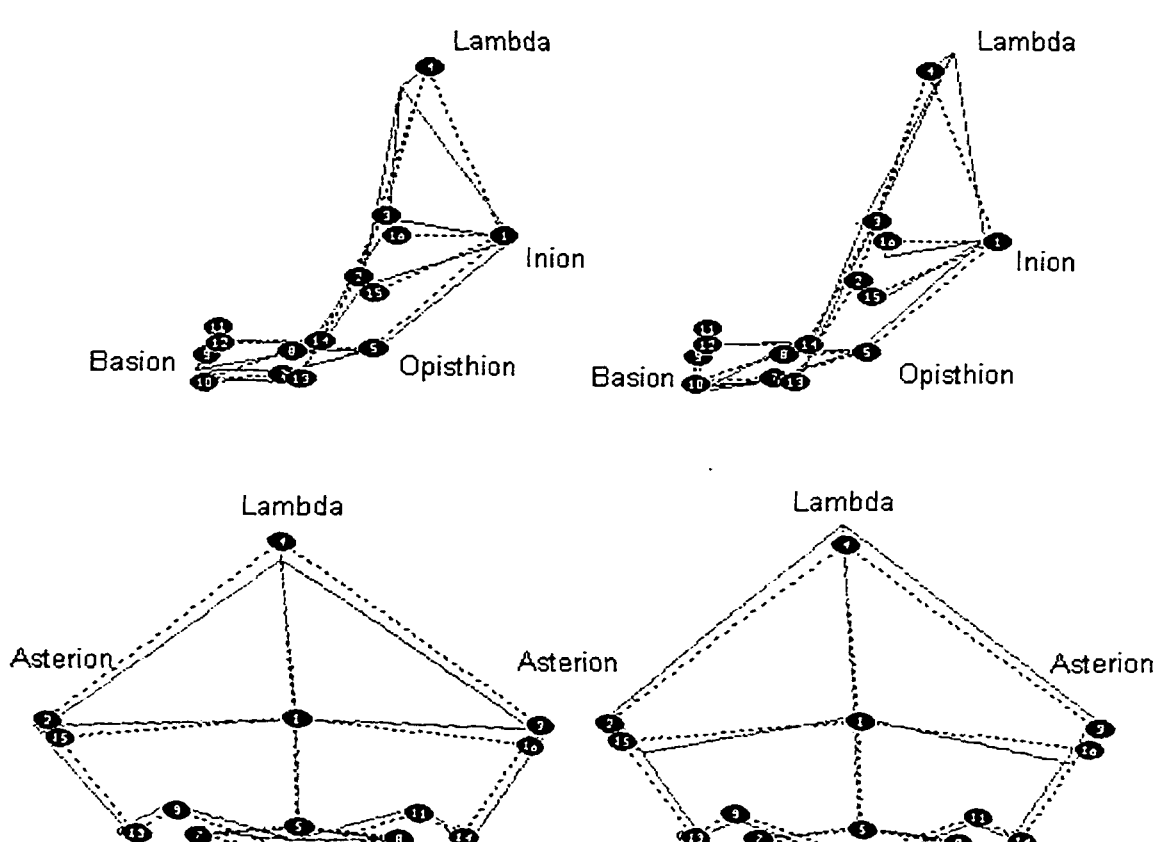

Negative end of CaV 2 (Berg, Neand.) Positive end of CaV 2 (Andamanese)

Figure 4.25: Shape variation along CaV 2 (Step 2A). Lateral (top) and posterior views. The dotted line represents the consensus configuration.

shorter and medio-laterally wider occipital plane, and a steeper angle between the occipital and the nuchal planes. This shape variation also differentiates between bonobos and common chimpanzees. It is similar to that described for PC 2. CaV 2 is only weakly correlated with centroid size (Table 4.18).

CaV 5 (1.8 %, most influenced by PCs 6 and 9, Fig. 4.26) separates Kabwe on its negative extreme from the rest of the human sample populations, this specimen falling outside the 95 % confidence ellipses of all modern human groups. The Upper Paleolithic specimens fall either outside or on the fringe of the modern human range on the negative side, where Shanidar 1 also falls. Cro Magnon 1 and Ein Gev fall outside the 95 % confidence ellipses of all modern human groups. The Upper Paleolithic population is significantly different from most human groups except the Neanderthal, Australian, Andamanese and Epipaleolithic populations. Neanderthals and Biache fall on the negative side of CaV 5, but well within the modern human range. The shape differences (Fig. 4.27) that characterize Kabwe and to a lesser extent, the Upper Paleolithic specimens, are similar to those found for CaV 5 in Step 1A, and include an elevated inion and superior nuchal line, as well as medially placed asteria, indicating a relatively short occipital plane and long nuchal plane and a medio-laterally narrow occipital squama.

Classification: Both Kabwe and Biache were classified as Neanderthals, with posterior probabilities of 0.99 and 0.97 respectively. Skhul 5 was classified as Berg (0.59) and Kanalda as Australian (0.81). All Upper Paleolithic specimens were placed correctly in their group.

The results of the cross-validation classification are shown in Table 4.19. They have improved in this analysis in comparison to those obtained in Step 1A. However, only two of the four Neanderthal specimens were classified correctly, one being classified as Berg and another as Epipaleolithic. No modern human specimen was classified as Neanderthal. Of the five Upper Paleolithic specimens, only 3 were classified correctly, the other two being classified as Australian and as Tolai. The highest correct classification rate overall was obtained for the bonobo sample (90.91 %), followed by the Australian and San groups (both 90 %). The lowest correct classification was obtained by the mixed European group (42.86 %) and the Tolai (75.86 %).

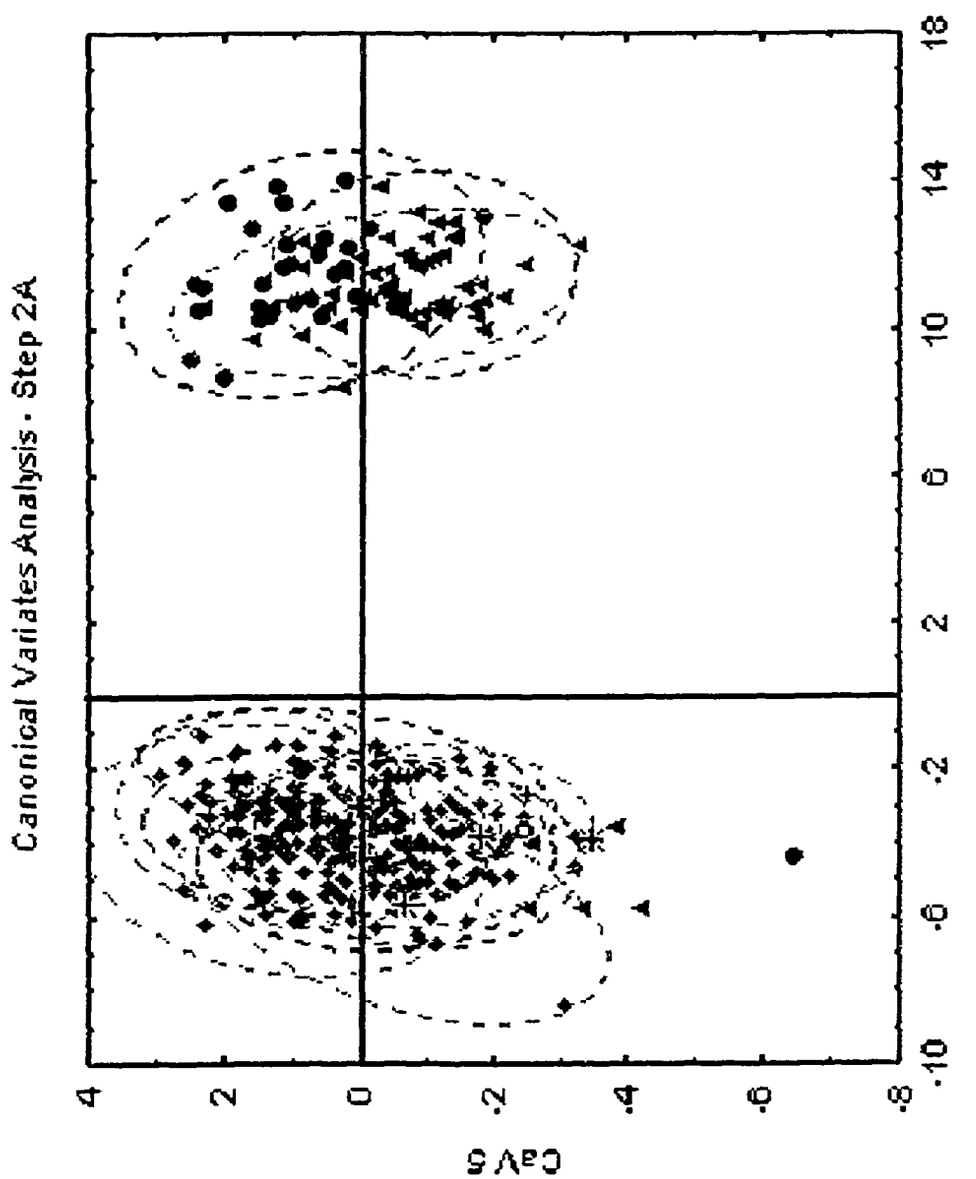

Figure 4.26: Canonical Variates Analysis (Step 2A) CaVs 1 and 5. Dotted lines represent the 95 % confidence ellipses for each group.

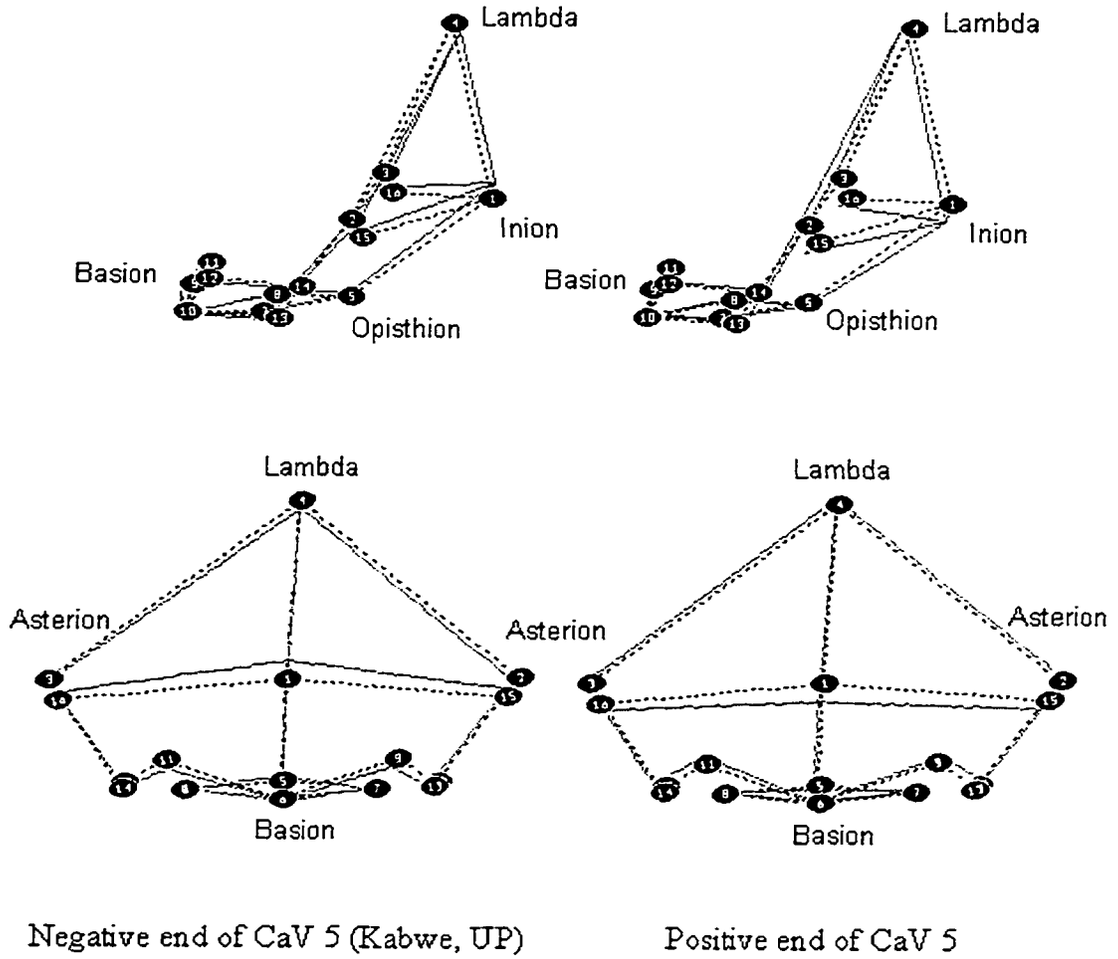

Negative end of CaV 5 (Kabwe, UP)

Positive end of CaV 5

Figure 4.27: Shape variation along CaV 5 (Step 2A). Lateral (top) and posterior view. The dotted line represents the consensus configuration.

Table 4.19: Cross-validation classification summary (percentages for each population in bold). Step 2A

	And	Aus	Brg	Dgn	Epi	Esk	Eur	San	Tol	UP	Bon	Nea	Sch	Trg	Total
And	24	2	0	1	0	0	1	0	1	0	0	0	0	0	29
%	**82.76**	6.9	0	3.45	0	0	3.45	0	3.45	0	0	0	0	0	100
Aus	0	27	0	0	0	1	1	1	0	0	0	0	0	0	30
%	0	**90**	0	0	0	3.33	3.33	3.33	0	0	0	0	0	0	100
Brg	0	0	24	0	0	1	5	0	0	0	0	0	0	0	30
%	0	0	**80**	0	0	3.33	16.67	0	0	0	0	0	0	0	100
Dgn	2	0	0	24	0	1	1	1	0	0	0	0	0	0	29
%	6.9	0	0	**82.76**	0	3.45	3.45	3.45	0	0	0	0	0	0	100
Epi	0	0	1	0	12	0	2	0	0	0	0	0	0	0	15
%	0	0	6.67	0	**80**	0	13.33	0	0	0	0	0	0	0	100
Esk	0	1	0	0	0	26	1	1	1	0	0	0	0	0	30
%	0	3.33	0	0	0	**86.67**	3.33	3.33	3.33	0	0	0	0	0	100
Eur	3	0	5	0	2	2	12	2	1	1	0	0	0	0	28
%	10.71	0	17.86	0	7.14	7.14	**42.86**	7.14	3.57	3.57	0	0	0	0	100
San	0	0	0	2	0	1	0	27	0	0	0	0	0	0	30
%	0	0	0	6.67	0	3.33	0	**90**	0	0	0	0	0	0	100
Tol	0	4	0	1	0	0	2	0	22	0	0	0	0	0	29
%	0	13.79	0	3.45	0	0	6.9	0	**75.86**	0	0	0	0	0	100
UP	0	1	0	0	0	0	0	0	1	3	0	0	0	0	5
%	0	20	0	0	0	0	0	0	20	**60**	0	0	0	0	100
Bon	0	0	0	0	0	0	0	0	0	0	30	0	2	1	33
%	0	0	0	0	0	0	0	0	0	0	**90.91**	0	6.06	3.03	100
Nea	0	0	1	0	1	0	0	0	0	0	0	2	0	0	4
%	0	0	25	0	25	0	0	0	0	0	0	**50**	0	0	100
Sch	0	0	0	0	0	0	0	0	0	0	0	0	24	5	29
%	0	0	0	0	0	0	0	0	0	0	0	0	**82.76**	17.24	100
Trg	0	0	0	0	0	0	0	0	0	0	2	0	3	23	28
%	0	0	0	0	0	0	0	0	0	0	7.14	0	10.71	**82.14**	100
Total	29	35	31	28	15	32	25	32	26	4	32	2	29	29	349
%	8.31	10.03	8.88	8.02	4.3	9.17	7.16	9.17	7.45	1.15	9.17	0.57	8.31	8.31	100

Mahalanobis D^2, Cluster Analysis and Mimimum Spanning Tree: The unbiased Mahalanobis distances were calculated (Table 4.20). Results are similar to those described for Step 1A. The distance between the chimpanzee species is equivalent to that between the more geographically distant modern human populations. It is slightly smaller than the smallest distance between Neanderthals and modern humans, as well as the smallest distance between the Upper Paleolithic group and modern humans. The Neanderthals are closest to the Berg and the Europeans and most distant from the Andamanese and the Dogon. The Upper Paleolithic group is found to be closest to the Epipaleolithic, confirming the findings of Step 1. They are most distant from the Dogon and the San. The Neanderthal and Upper Paleolithic samples are not particularly close to each other. The Upper Paleolithic group is more distant from four out of nine recent human groups than the Neanderthals are. As in Step 1, the greatest distance between any modern human group is that between the Andamanese and the San. Among the modern human groups that are geographically close, only the Berg and mixed Europeans both are nearest neighbors to the other.

A cluster analysis and a minimum spanning tree analysis were performed on the squared root of the unbiased D^2. As in Step 1A, the cluster diagram (Fig. 4.28) shows the chimpanzee species in a separate branch from the human groups, with the two common chimpanzee subspecies clustering very close to each other. Among the human groups, the Upper Paleolithic and the Neanderthal groups cluster together and are outliers to the other recent human groups. Their branch has a deeper split than the entire modern human branch. The geographic clustering of modern human populations breaks down even further than in Step 1. Although the Berg and Europeans still cluster closely together, neither the Australian-Melanesian, nor the sub-Saharan African geographic pairs cluster together. The minimum spanning tree shows the modern human populations far removed from the chimpanzee groups. The Upper Paleolithic group is shown to be closest to the Epipaleolithic population, while the Neanderthal group is closest to the Berg, with the distance between the latter pair being slightly smaller than that between the former pair. The Berg and the Europeans are linked, as expected, and so are the Australians and the Tolai, even though they neither of them is closest neighbor to the other. The San and the Dogon are not linked.

Table 4.20: Mahalanobis D^2 distances (Step 2A). All values significant to the 0.001 level except: NS = non-significant, * = 0.05 level, ** = 0.01 level.

	Kan	And	Aus	Bch	Brg	Dgn	Skh5	Epi	Esk
Kan	0.00	75.24	51.41	82.90*	73.16	73.18	104.01	61.01	62.94
And	75.24	0.00	30.49	67.72	35.01	15.83	56.24*	27.27	35.81
Aus	51.41	30.49	0.00	68.65	28.81	18.01	43.38	20.61	8.97
Bch	82.90*	67.72	68.65	0.00	58.36	75.01	69.91NS	64.96	73.38
Brg	73.16	35.01	28.81	58.36	0.00	31.22	41.00*	21.38	22.94
Dgn	73.18	15.83	18.01	75.01	31.22	0.00	64.56	27.13	20.34
Skh5	104.01	56.24	43.38*	69.91NS	41.00*	64.56	0.00	50.38*	56.93
Epi	61.01	27.27	20.61	64.96	21.38	27.13	50.38*	0.00	16.24
Esk	62.94	35.81	8.97	73.38	22.94	20.34	56.93	16.24	0.00
Eur	67.23	21.48	13.69	66.19	7.50	15.92	44.90*	11.09	11.85
Kbw	123.64	121.90	81.09	101.18	91.70	108.69	82.26*	71.03	70.22
San	74.92	39.51	10.83	80.07	26.45	17.09	48.13*	33.80	10.63
Tol	52.08	20.43	9.17	76.88	23.83	14.92	49.78*	19.99	12.57
UP	63.86	36.63	34.74	63.92	37.67	53.12	47.92*	25.94	35.01
Bon	291.20	254.06	230.19	281.68	227.49	237.73	243.42	298.79	251.10
Nea	90.66	53.66	41.57	49.15*	23.81	48.02	42.11NS	0.97	35.53
Sch	276.74	240.96	219.10	265.16	196.23	223.39	219.02	273.07	228.17
Trg	295.82	258.10	234.02	274.84	213.72	237.34	221.67	292.68	248.19

	Eur	Kbw	San	Tol	UP	Bon	Nea	Sch	Trg
Kan	67.23	123.64	74.92	52.08	63.86	291.20	90.66	276.74	295.82
And	21.48	121.90	39.51	20.43	36.63	254.06	53.66	240.96	258.10
Aus	13.69	81.09	10.83	9.17	34.74	230.19	41.57	219.10	234.02
Bch	66.19	101.18	80.07	76.88	63.92	281.68	49.15*	265.16	274.84
Brg	7.50	91.70	26.45	23.83	37.67	227.49	23.81	196.23	213.72
Dgn	15.92	108.69	17.09	14.92	53.12	237.73	48.02	223.39	237.34
Skh5	44.90*	82.26*	48.13*	49.78*	47.92*	243.42	42.11NS	219.02	221.67
Epi	11.09	71.03	33.80	19.99	25.94	298.79	30.97	273.07	292.68
Esk	11.85	70.22	10.63	12.57	35.01	251.10	35.53	228.17	248.19
Eur	0.00	91.14	18.01	8.57	29.83	243.01	25.69*	222.73	239.47
Kbw	91.14	0.00	78.09	97.55	65.19	344.07	48.34	294.92	302.23
San	18.01	78.09	0.00	16.25	52.90	197.74	44.11	180.90	196.09
Tol	8.57	97.55	16.25	0.00	35.41	222.46	41.20	212.27	230.74
UP	29.83	65.19	52.90	35.41	0.00	292.79	30.35	264.35	284.51
Bon	243.01	344.07	197.74	222.46	292.79	0.00	274.36	15.30	18.68
Nea	25.69	48.34*	44.11	41.20	30.35	274.36	0.00	241.31	253.79
Sch	222.73	294.92	180.90	212.27	264.35	15.30	241.31	0.00	6.10
Trg	239.47	302.23	196.09	230.74	284.51	18.68	253.79	6.10	0.00

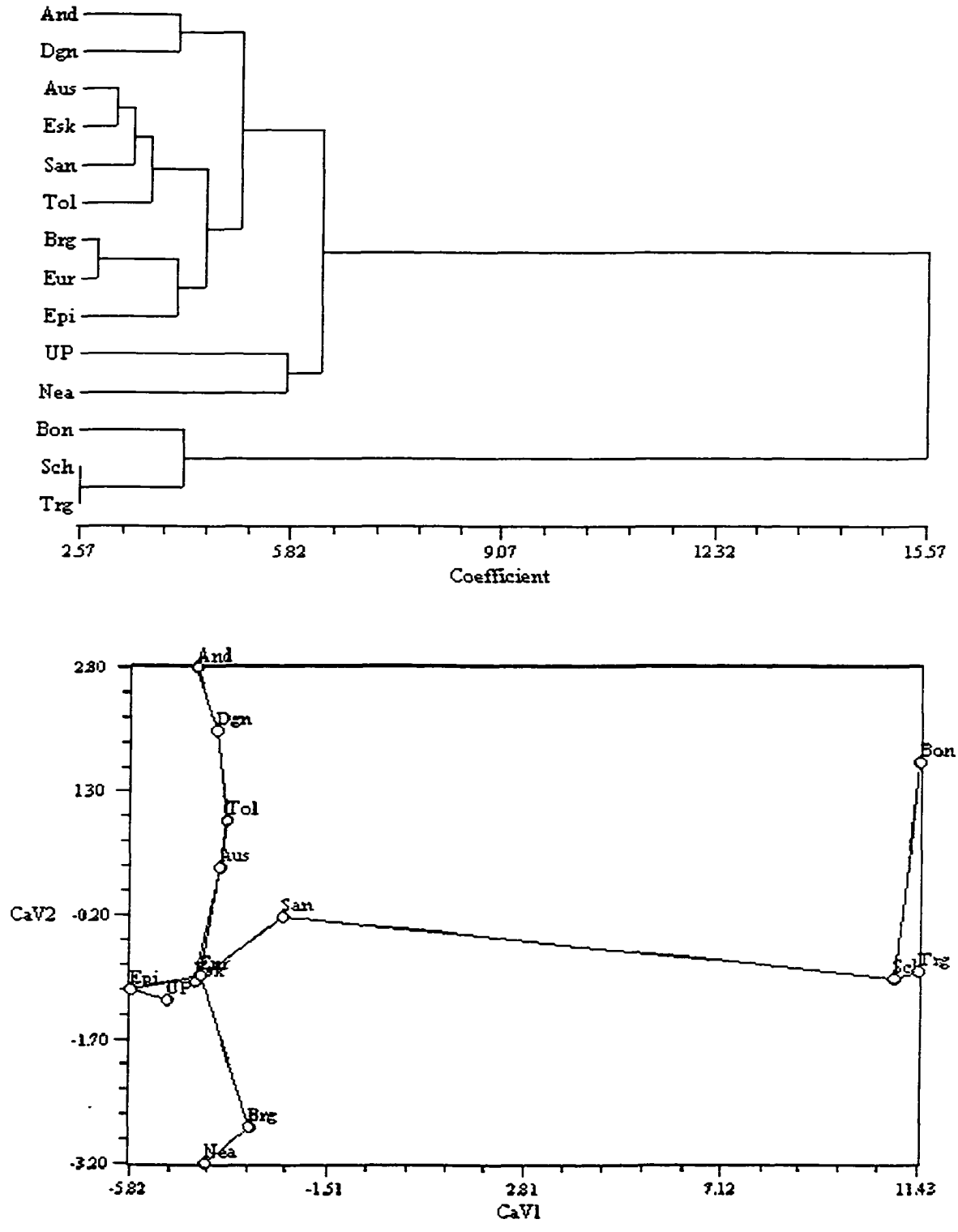

Figure 4.28: Cluster analysis (UPGMA, top) and minimum spanning tree (Step 2A).

Step 2B – Human sample only

Principal Components Analysis: These analyses (Tables 4.21 and 4.22) are similar to those found in Step 1B. Neanderthals fall on the positive side of the modern human range along PC 2 (14.2 %, Fig. 4.29), which also separates the Berg from other modern human groups, as in the previous analysis. In this component the Neanderthal mean score is significantly different only from the Andamanese and the Dogon. Neanderthals also fall mostly near the positive extreme of PC 3 (9 %, Fig. 4.30), where Kabwe, Skhul 5 and Ein Gev also fall. In PC 3 the Neanderthal mean score is significantly different only from the Eskimo and Epipaleolithic modern human population. When the ANOVA is conducted at the species level, however, the Neanderthal mean score significantly different from the mean score of all modern humans. The shape differences characterizing the Berg, and to a lesser extent Neanderthals, along PC 2, are similar to those found previously. They include a more posteriorly projecting inion, an anteriorly and inferiorly placed lambda, an elevated basion and a medio-laterally wide occipital plane. The shape differences that characterize Neanderthals, Kabwe, Skhul 5 and Ein Gev along PC 3 are a posteriorly projecting and elevated inion, an inferiorly placed lambda, a supero-inferiorly short and medio-laterally wide occipital plane and an elevated opisthion.

Kabwe also falls near the negative end of the modern human range along PC 1 (21.2 %), as in the previous analyses. The shape differences at the negative extreme of this component are a short occipital plane with a somewhat projecting inion, a long nuchal plane, elevated lateral ends of the superior nuchal line and a low angle between the occipital and nuchal planes. Kabwe, Skhul 5 and the Upper Paleolithic specimens are partially separated from recent humans along PC 4 (7.1 %) on its positive extreme. Of the five Upper Paleolithic individuals, Cro Magnon 1 and Predmosti 3 fall outside the modern human range. This group is significantly different in its mean score from the Australian, Dogon and San populations. Skhul 5 falls just at its fringe, near Kabwe. The shape differences that characterize the positive end of PC 4 include an anteriorly placed lambda, indicating and antero-posteriorly elongated occipital plane; asteria that are posteriorly placed, as are the lateral ends of the superior nuchal line; and a somewhat posteriorly projecting and elevated inion, indicating an elongated nuchal plane.

Table 4.21: Summary of the PCA results, ANOVA and Correlation Analysis, PCs 1-10, Step 2B.

	Principal Components Analysis			ANOVA, Pr > F			Correlation with Centroid Size	
	Eigenvalue	Proportion	Cumulative	Popul.	Sex	Interaction	Rho	Pr > F
PC 1	0.001596	0.211877	0.211877	0.0001	0.003	0.1029	-0.41873	0.0001
PC 2	0.001067	0.141579	0.353456	0.0001	0.0089	0.0436	0.40195	0.0001
PC 3	0.000676	0.08977	0.443226	0.0001	0.0006	0.5151	-0.00881	0.887
PC 4	0.000536	0.071134	0.514361	0.0001	0.001	0.4138	0.21774	0.0004
PC 5	0.000471	0.062498	0.576859	0.0001	0.5929	0.701	-0.09321	0.1316
PC 6	0.000405	0.05371	0.630569	0.0001	0.6128	0.5717	-0.03643	0.5564
PC 7	0.000327	0.04335	0.673919	0.0001	0.7818	0.2356	-0.05786	0.35
PC 8	0.00031	0.041188	0.715107	0.0057	0.1069	0.6578	-0.06504	0.2933
PC 9	0.000233	0.030983	0.746091	0.0001	0.0001	0.4214	0.25692	0.0001
PC 10	0.000191	0.025343	0.771433	0.0001	0.2508	0.2365	-0.0726	0.2407

Table 4.22: Summary of the CVA results and Correlation Analysis, CaV 1-5, Step 2B.

	Canonical Variates Analysis			Correlation with Centroid Size	
	Eigenvalue	Proportion	Cumulative	Rho	Pr > F
CaV 1	3.7613	0.29	0.29	-0.28512	0.0001
CaV 2	3.1222	0.2407	0.5307	0.57707	0.0001
CaV 3	1.6156	0.1246	0.6553	-0.32582	0.0001
CaV 4	1.0208	0.0787	0.734	-0.16761	0.0064
CaV 5	0.8256	0.0637	0.7976	0.20002	0.0011

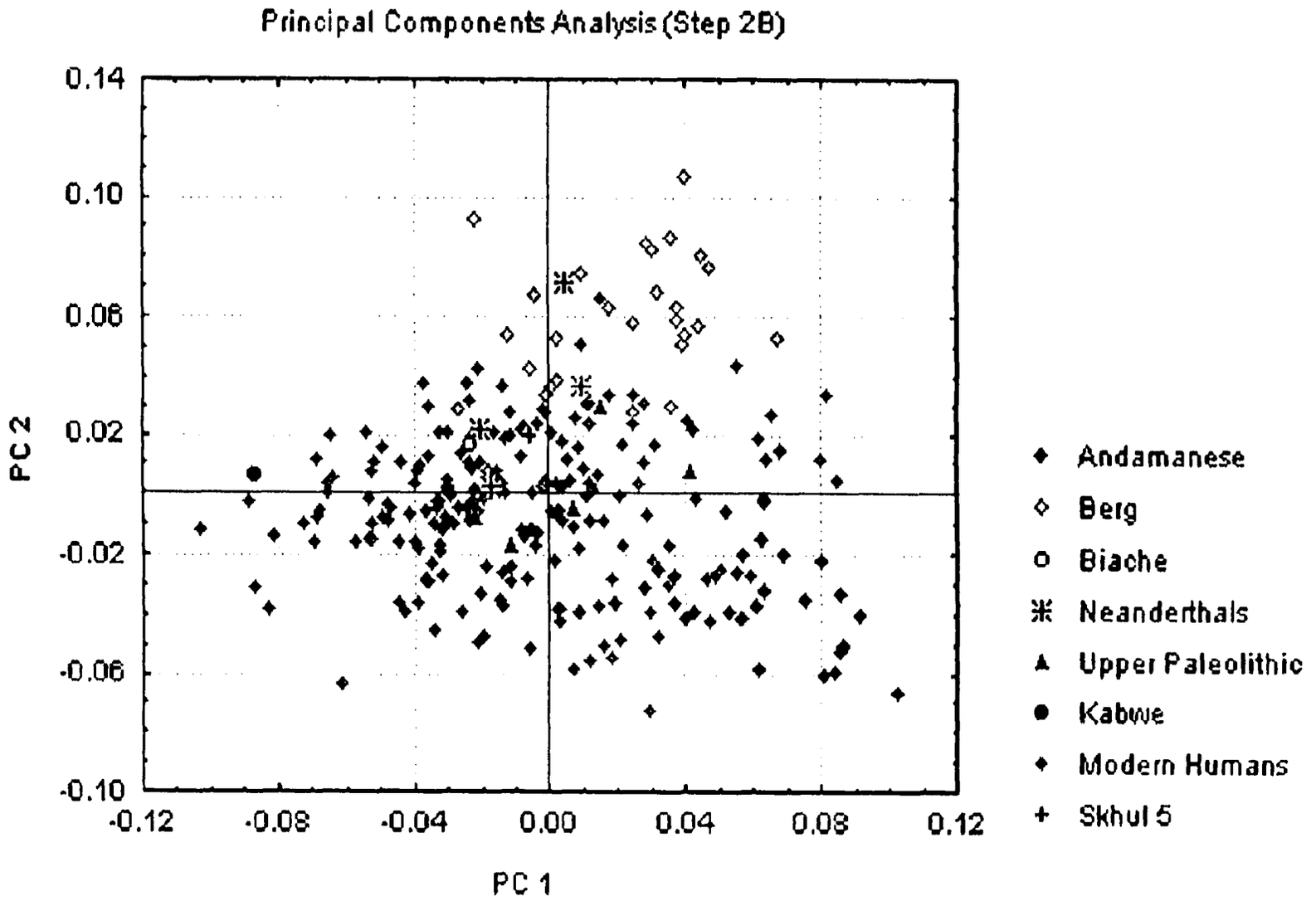

Figure 4.29: Principal Components Analysis (Step 2B), PCs 1 and 2.

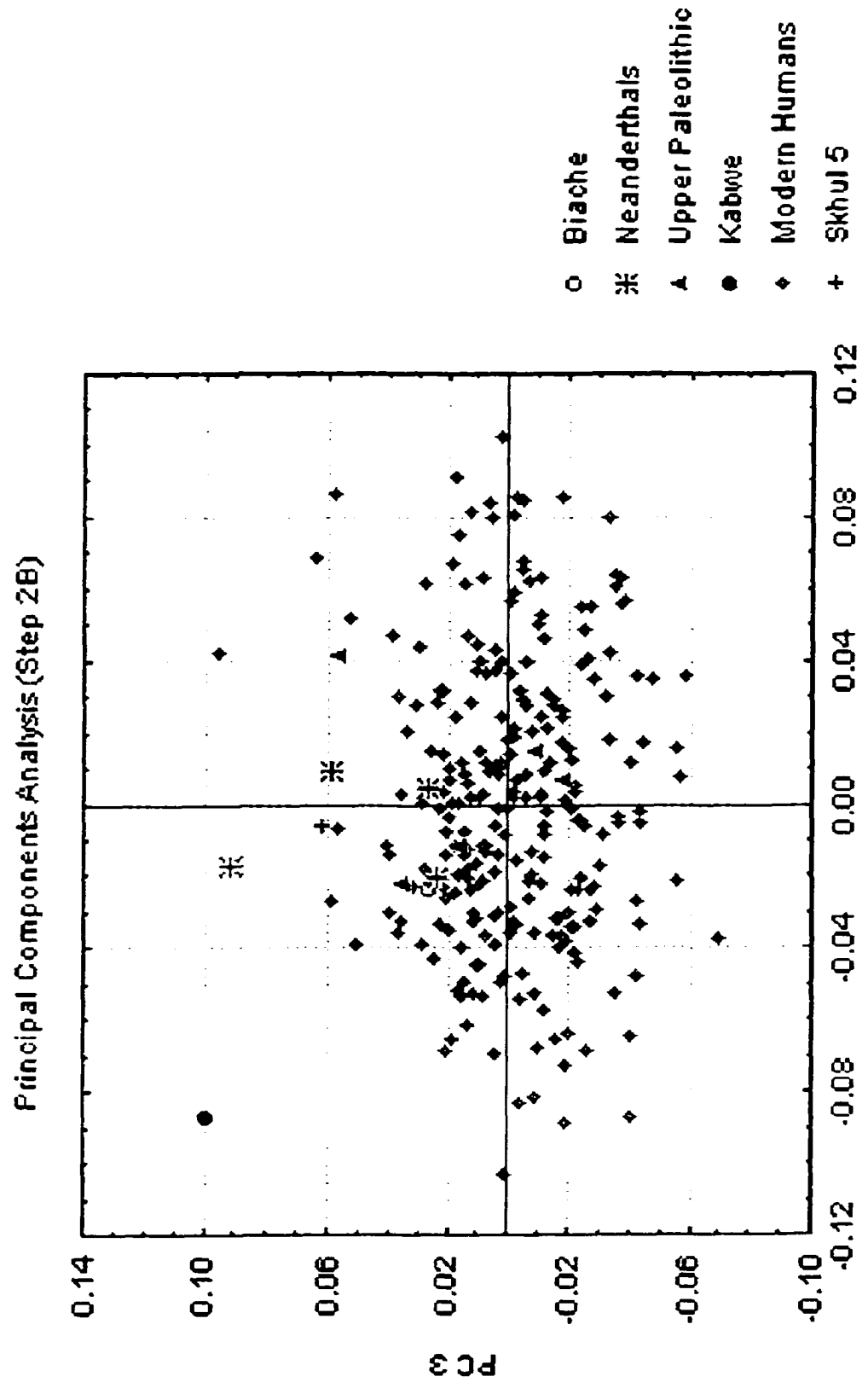

Figure 4.30: Principal Components Analysis (Step 2B), PCs 1 and 3.

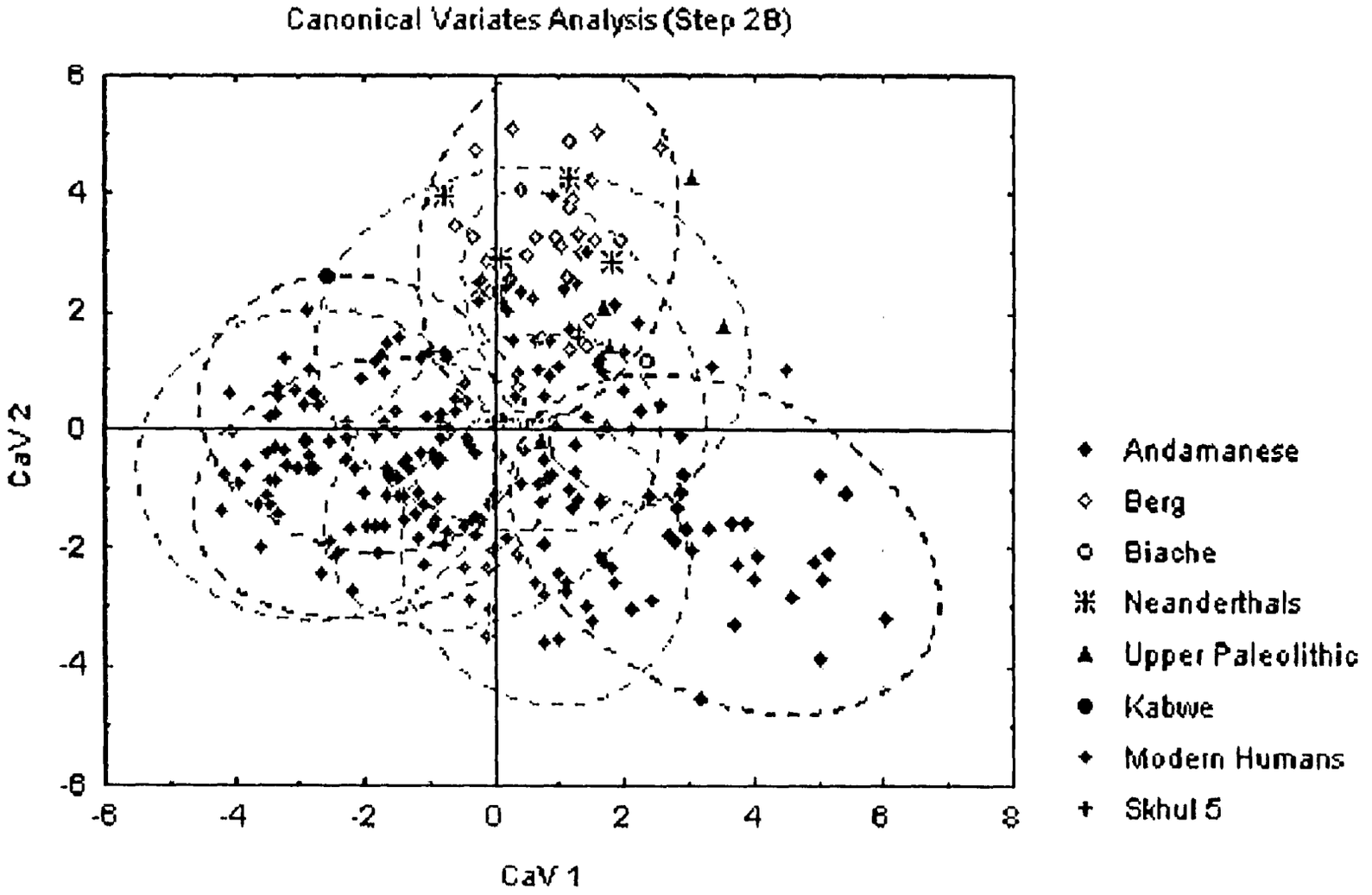

Figure 4.31: Canonical Variates Analysis (Step 2B), CaVs 1 and 2. Dotted lines represent the 95 % confidence ellipses for each group.

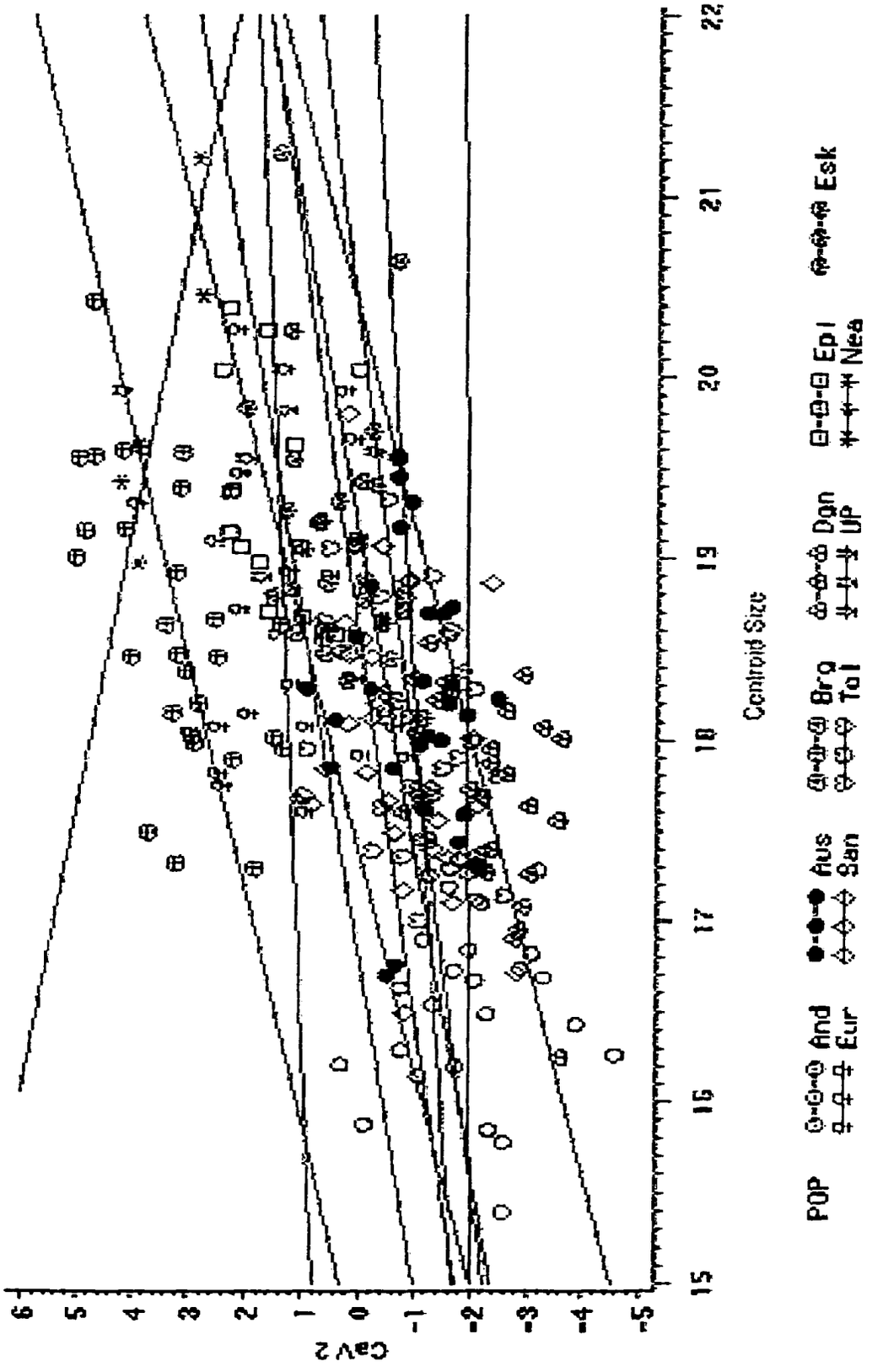

Figure 4.32: CaV 2 plotted against centroid size, with regression lines for populations fitted (Step 2B).

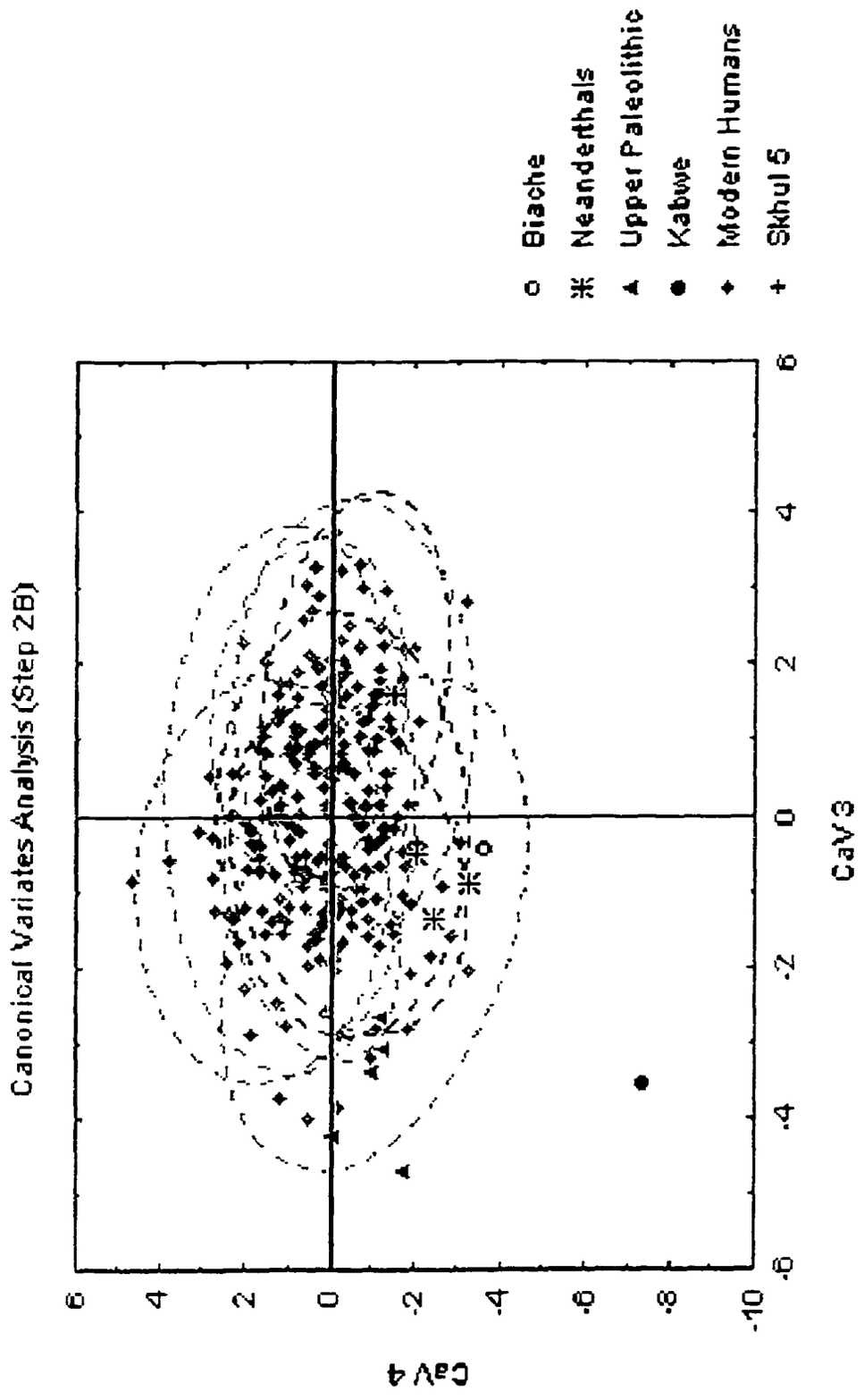

Figure 4.33: Canonical Variates Analysis (Step 2B), CaVs 3 and 4. Dotted lines represent the 95 % confidence ellipses for each group.

Several components are significant for sex effects. PCs 1 and 2 are significant to the 0.01 level for sex effects, but no pattern is apparent when the means for males and females are plotted by population. Along both PC 3 and PC 4 (sex effects significant to the 0.0001 level) male mean scores are more positive in all populations except in the European and Eskimo groups. Along PC 9 (sex effects significant to the 0.0001 level), male mean scores are more positive than female ones except in the Tolai and Epipaleolithic groups. No strong pattern, therefore, differentiates males from females across all modern human populations.

Canonical Variates Analysis: In the CVA, Neanderthals are again never completely separated from modern humans. As in Step 2A, they fall at the positive end of CaV 2 (24 %, mostly influenced by PC 1, Fig. 4.31), overlapping with the Berg population. As in CaV 2 of Step 2A, Predmosti 3 also falls close to the Neanderthals, as do also to a lesser extent Kabwe and Biache. The shape variation along this canonical axis is similar to that described in Steps 1A and 2A. At its positive end it includes an anteriorly and inferiorly placed lambda, an elevated and somewhat posteriorly projecting inion, and laterally placed asteria, indicating an antero-posteriorly elongated and medio-laterally wide occipital plane which is also flattened at lambda; as well as an elevated basion. CaV 2 is only weakly correlated with centroid size (Table 4.22, Fig. 4.32). These shape differences are consistent with the described Neanderthal morphology, which includes a wide occipital squama, a posteriorly projecting occipital plane with superiorly placed inion and lambdoid flattening (Boule 1911-1913; Thoma 1965, 1975; Heim 1974; Hublin 1978b; Sergi 1991; Condemi 1991; Dean et al. 1998; Wolpoff et al. 2001). However, in all of these characteristics, Neanderthals fall within the range of modern human variation. These results therefore would seem to agree with Spitery (1985), who found the occipital bone of Neanderthals to be within the modern human range in all its proportions. However, it must be noted that the lack of appropriate landmarks in the occipital squama make it impossible for the landmarks analysis to properly quantify features that may be more important, such as the occipital plane curvature.

CaV 3 (12.5 %, mostly influenced by PCs 9, 4 and 6, Fig. 3.33) partially separates the Upper Paleolithic specimens from recent humans on its negative end, Ein Gev falling

outside the 95 % confidence ellipse of all modern human populations. This group is significantly different in its mean score from Neanderthals and most recent human populations, except the Australians, Tolai and Epipaleolithic. Kabwe also falls at the negative extreme of the range of modern human variation. Neanderthals, Biache and Skhul 5 all fall near the center of the modern human cloud. The shape differences that characterize the Upper Paleolithic specimens and Kabwe are an elevated and posteriorly projecting inion, a superiorly placed superior nuchal line, an inferiorly placed opisthion and medially placed asteria, indicating an elongated nuchal plane relative to the occipital plane and a relatively narrow occipital squama. These differences are consistent with the morphology described for the 'Cro Magnon' group, which includes strong occipital protuberances and an elongated and flattened nuchal plane (Billy 1970; Genet-Varcin 1970; Gambier 1989; Smith 1982).

Kabwe is separated from the human sample on CaV 4 (7.9 %, influenced most by PCs 7, 5 and 19), falling far outside the 95 % confidence ellipse of all modern human groups. Neanderthals, Biache and, to a lesser extent, Skhul 5 fall at the negative end of the modern human range. The shape variation that drives the separation of Kabwe along this canonical axis includes an elevated position of opisthion, inion and the lateral ends of the superior nuchal line, as well as inferiorly placed medial ends of the jugular fossae.

Classification: The results of the posterior probability classification were similar to those obtained in Step 2A, with the exception of Skhul 5, which was classified as European (0.68) rather than Berg, and Kanalda, which was classified as Tolai (0.74) rather than Australian. All Neanderthals were successfully classified. The cross validation classification (Table 4.23) is also similar to that in Step 2A, but classification success is slightly lower. One modern human specimen (Epipaleolithic), was classified as Neanderthal. In addition to the European specimen previously misclassified as Upper Paleolithic, one Epipaleolithic specimen was also placed in this group.

Mahalanobis D^2, Cluster Analysis and Mimimum Spanning Tree: The Mahalanobis D^2 matrix is reported in Table 4.24. It is similar to that calculated in Step 2A. The Upper Paleolithic group appears even more distant from the recent human population, as it now is more distant than Neanderthals from five, rather than four, recent

Table 4.23: Cross-validation classification summary, (percentages for each population in bold). Step 2B.

	And	Aus	Brg	Dgn	Epi	Esk	Eur	San	Tol	UP	Nea	Total
And	24	0	1	2	1	0	1	0	0	0	0	29
%	**82.76**	0	3.45	6.9	3.45	0	3.45	0	0	0	0	100
Aus	0	26	0	0	0	1	1	0	2	0	0	30
%	0	**86.67**	0	0	0	3.33	3.33	0	6.67	0	0	100
Brg	0	0	26	0	0	0	4	0	0	0	0	30
%	0	0	**86.67**	0	0	0	13.33	0	0	0	0	100
Dgn	1	0	0	26	0	1	0	1	0	0	0	29
%	3.45	0	0	**89.66**	0	3.45	0	3.45	0	0	0	100
Epi	0	0	1	1	10	0	1	0	0	1	1	15
%	0	0	6.67	6.67	**66.67**	0	6.67	0	0	6.67	6.67	100
Esk	0	4	0	0	0	23	0	1	2	0	0	30
%	0	13.33	0	0	0	**76.67**	0	3.33	6.67	0	0	100
Eur	2	0	6	0	3	2	10	2	2	1	0	28
%	7.14	0	21.43	0	10.71	7.14	**35.71**	7.14	7.14	3.57	0	100
San	0	1	0	2	0	1	1	25	0	0	0	30
%	0	3.33	0	6.67	0	3.33	3.33	**83.33**	0	0	0	100
Tol	0	3	0	0	0	1	3	0	22	0	0	29
%	0	10.34	0	0	0	3.45	10.34	0	**75.86**	0	0	100
UP	0	1	0	0	0	0	0	0	1	3	0	5
%	0	20	0	0	0	0	0	0	20	**60**	0	100
Nea	0	0	1	0	1	0	0	0	0	0	2	4
%	0	0	25	0	25	0	0	0	0	0	**50**	100
Total	27	35	35	31	15	29	21	29	29	5	3	259
%	10.42	13.51	13.51	11.97	5.79	11.2	8.11	11.2	11.2	1.93	1.16	100

Table 4.24: Mahalanobis D^2 distances (Step 2B). All values significant to the 0.001 level except: NS = non-significant, * = 0.05 level, ** = 0.01 level.

	Kan	And	Aus	Bch	Brg	Dgn	Skh5	Epi	Esk	Eur	Kbw	San	Tol	UP	Nea
Kan	0.00	74.03	52.97**	93.78**	78.09	73.12	113.03	60.60	67.08	67.85	120.51	76.68	50.93**	61.73**	86.52
And	74.03	0.00	32.50	65.31	34.85	15.28	78.15	23.76	36.59	22.32	125.26	41.19	19.94	36.45	54.58
Aus	52.97**	32.50	0.00	74.36	30.95	20.12	78.31	24.95	9.99	16.39	92.01	11.27	10.37	41.11	44.32
Bch	93.78**	65.31	74.36	0.00	64.95	73.36	102.57**	66.75	79.93	72.56	113.78	85.37	80.61	75.22	60.94**
Brg	78.09	34.85	30.95	64.95	0.00	30.43	71.95	18.75	23.86	7.71	104.36	27.57	24.26	37.50	23.53
Dgn	73.12	15.28	20.12	73.36	30.43	0.00	85.29	24.82	21.52	17.40	113.25	18.30	14.41	52.77	46.52
Skh5	113.03	78.15	78.31	102.57**	71.95	85.29	0.00	72.30	89.40	68.80	107.84**	78.22	77.61	80.25	69.75
Epi	60.60	23.76	24.95	66.75	18.75	24.82	72.30	0.00	18.23	10.51	73.84	33.40	18.83	26.77	30.41
Esk	67.08	36.59	9.99	79.93	23.86	21.52	89.40	18.23	0.00	13.24	77.62	9.92	12.81	39.95	37.94
Eur	67.85	22.32	16.39	72.56	7.71	17.40	68.80	10.51	13.24	0.00	100.82	19.35	9.38	29.86	26.87
Kbw	120.51	125.26	92.01	113.78	104.36	113.25	107.84**	73.84	77.62	100.82	0.00	84.98	103.79	83.38	63.66**
San	76.68	41.19	11.27	85.37	27.57	18.30	78.22	33.40	9.92	19.35	84.98	0.00	17.66	58.13	45.13
Tol	50.93**	19.94	10.37	80.61	24.26	14.41	77.61	18.83	12.81	9.38	103.79	17.66	0.00	34.99	41.92
UP	61.73**	36.45	41.11	75.22	37.50	52.77	80.25	26.77	39.95	29.86	83.38	58.13	34.99	0.00	33.09
Nea	86.52	54.58	44.32	60.94**	23.53	46.52	69.75	30.41	37.94	26.87	63.66**	45.13	41.92	33.09	0.00

human populations. The UPGMA diagram and minimum spanning tree are identical to those obtained in Step 1A.

Step 2C - Chimpanzee sample only

Classification: A discriminant analysis was performed on the chimpanzee sample and a cross-validation classification obtained. Classification success was reduced for bonobos compared with Step 1C, but increased for the common chimpanzees. Five bonobos were misclassified, three as *P. t. schweinfurthii* and two as *P. t. troglodytes*. Two *P. t. schweinfurthii* and one *P. t. troglodytes* were misclassified as bonobos, a slightly better result than in Step 1C. The two common chimpanzee subspecies still show relatively high rates of misclassification among themselves, but these rates are lower than those found in Step 1.

Mahalanobis D^2: The unbiased Mahalanobis distances were calculated for the chimpanzee taxa (Table 4. 26). As in Step 1A, the distance between bonobos and the two common chimpanzee subspecies increases only slightly compared to the combined sample analysis, and is still equivalent the distances between some of the modern human populations in the combined sample and in the human sample analyses. It is still smaller than the distance between Neanderthals and all modern human populations, and smaller than that between the Upper Paleolithic specimens and all recent human groups. The distance between the two common chimpanzee groups is approximately doubled and is now equivalent to, and slightly larger than, the smallest distance among modern human populations in the combined sample and human sample analyses, that between the Berg and the Europeans.

Table 4.25: Cross-validation classification summary (percentages for each population in bold). Step 2C.

	Bon	Sch	Trg	Total
Bon	28	3	2	33
%	**84.85**	9.09	6.06	100
Sch	2	21	6	29
%	6.9	**72.41**	20.69	100
Trg	1	4	23	28
%	3.57	14.29	**82.14**	100
Total	31	28	31	90
%	34.44	31.11	34.44	100

Table 4.26: Mahalanobis D^2 distances (Step 2C). All values significant to the 0.001 level except: NS = non-significant, * = significant to the 0.05 level, ** = sigificant to the 0.01 level.

	Bon	Sch	Trg
Bon	0	18.28	22.39
Sch	18.28	0	13.16
Trg	22.39	13.16	0

Step 3

Eight additional landmarks were removed (opisthion, basion, occipital condyle right and left, medial end of jugular fossa right and left and lateral end of the jugular fossa right and left), so that only eight landmarks were used in this step (see Table 4.2). This increased the Neanderthal sample size to nine (Amud 1, La Chapelle 1. La Ferrassie 1, Guattari, La Quina, Saccopastore 1, Shanidar 1, Spy 2 and Tabun C1), the early anatomically modern human sample to two (Skhul 5 and Qafzeh 9), and allowed the inclusion of the fossil specimens Reilingen and Petralona. It also increased the Epipaleolithic sample to 28.

Centroid Size: Analysis of centroid size yielded results similar to those described in Steps 1 and 2 (Table 4.27, Fig. 4.34). Centroid size is significantly smaller in the chimpanzees relative to humans. It is also significant for sex (0.0001) and interaction effects (0.001).

Step 3A – Combined sample

Principal Components Analysis: The results of these analyses (Tables 4.28-4.29) were very similar to those obtained in the last two steps. Neanderthals are still not clearly separated from modern humans on any principal component despite the addition of five specimens. The separation is only slightly better in the CVA. Furthermore, and unlike the previous analyses, the Upper Paleolithic specimens are also not separated from modern humans on either the PCA or the CVA.

Neanderthals, Biache and Reilingen fall on the positive side of PC 2 (7.9 %, Fig. 4.35), mostly overlapping with the Berg. Neanderthals are significantly different only from the Dogon and Andamanese populations. However, when the ANOVA is conducted at the species level, they are significantly different from modern humans as a whole. While Amud 1 and Circeo 1 fall outside of the modern human range on the positive end of the axis, La Chapelle and La Quina 5 fall at the center of the modern human cloud. Petralona and Qafzeh 9 also fall at the positive extreme of the modern human range, while Reilingen, Biache and the Upper Paleolithic specimens fall near its center. The shape differences that characterize the Neanderthal end of the modern human

Table 4.27: Centroid size listed by genus, species, sex and population

	Mean	Range	St. Deviation	N
Homo	**14.45**	**11.97-17.15**	**0.87**	**286**
Males	14.77	12.62-17.15	0.85	154
Females	14.06	11.97-16.30	0.74	129
Modern	14.39	11.97-16.77	0.84	273
Males	14.70	12.62-16.77	0.80	145
Females	14.05	11.97-16.30	0.73	127
Neanderthals	15.66	14.72-17.15	0.75	9
Males	16.02	15.49-17.15	0.63	6
Females	15.05	14.77-15.32	0.39	2
Unknown sex	14.72	---	---	1
Kabwe	16.34	---	---	1
Petralona	16.04	---	---	1
Biache	14.39	---	---	1
Reilingen	15.50	---	---	1
Skhul 5	15.11	---	---	1
Qafzeh 9	14.47	---	---	1
Upper Paleolithic	15.00	14.71-15.35	0.24	5
Kanalda	15.37	---	---	1
Andamanese	13.08	11.97-13.75	0.45	30
Australian	17.19	12.97-15.48	0.60	30
Berg	17.79	13.38-16.00	0.71	30
Dogon	13.95	12.83-14.82	0.54	30
Epipaleolithic	15.22	14.07-16.30	0.60	28
Eskimo	14.91	14.08-16.77	0.63	30
European (mixed)	14.71	13.53-16.28	0.71	29
San	14.32	12.97-15.72	0.63	30
Tolai	14.17	13.35-15.06	0.58	29
Pan	**10.55**	**8.86 -12.20**	**0.69**	**92**
Males	10.66	9.01 -12.20	0.78	49
Females	10.39	8.86 -11.37	0.55	41
P. paniscus	9.93	8.86.-10.90	0.49	34
Males	9.76	9.01 -10.43	0.45	16
Females	10.08	8.86 -10.90	0.48	18
P. troglodytes	10.91	9.85 -12.20	0.51	58
Males	11.09	9.95 -12.20	0.46	33
Females	10.63	9.85 -11.37	0.48	23
P. t. schweinfurthii	10.77	9.95-12.20	0.54	30
P. t. troglodytes	11.06	10.86-11.70	0.43	28

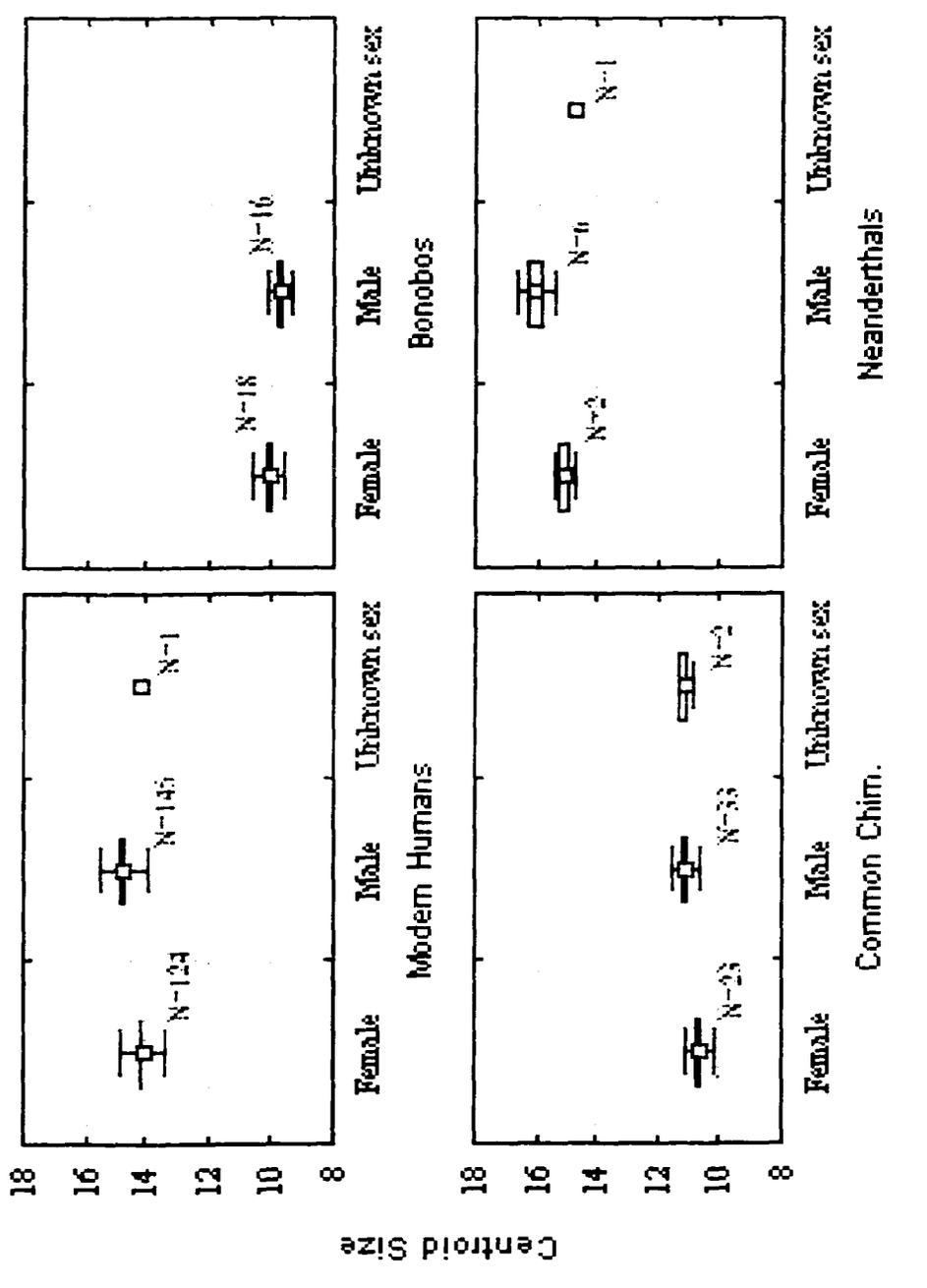

Figure 4.34: Centroid size mean, standard error and standard deviation, labeled by species and sex (Step 3).

range are laterally placed lateral ends of the superior nuchal line and asteria, superiorly placed lateral ends of the inferior nuchal line and a somewhat inferiorly positioned lambda. They reflect a medio-laterally wide occipital plane, with a superior nuchal line that extends far laterally and an elevated nuchal plane.

As in the previous steps, PC 1 (approx. 67 %, Fig. 4.35) separates humans from chimpanzees, the latter showing an occipital plane that is much shorter supero-inferiorly. The three chimpanzee taxa are significantly different in their mean scores from all human populations. PC 1 also separates Kabwe from the remaining human sample, this specimen falling between the human and the chimpanzee clouds. Reilingen, Petralona and Biache also fall near the end of the modern human range and close to Kabwe. This axis is also significant for sex effects, females having more negative scores than males in all chimpanzee taxa and in some, but not all human groups. PC 1 shows a relatively strong correlation with centroid size overall (Table 4.28). As in the previous steps, however, each population has a different relationship with centroid size along this component (Fig. 4.36).

Kabwe and Petralona also fall just outside the positive end the modern human range along PC 5 (3.8 %). Skhul 5, Reilingen and Ein Gev also fall at the positive extreme of the modern human range of variation, while one Neanderthal specimen, La Chapelle, also falls near it. The shape differences at the positive extreme of this axis include posteriorly and inferiorly placed asteria and lateral ends of the superior nuchal line, as well as elevated lateral ends of the inferior nuchal line and an anteriorly placed lambda. These differences reflect a sharper angle between the occipital and nuchal planes. In addition to PC 1, PCs 5 and 6 are significant for sex effects (0.001 and 0.05 respectively, the latter also being significant for interaction effects at the 0.0001 level). Along PC 5 (approx. 3.8 %), the mean scores for males are more positive than those for females in most human populations except the Eskimo and the Dogon. The male means are also more positive in bonobos and *P. t. troglodytes*, but not in *P. t. schweinfurthii*. Therefore, no clear pattern of sex differentiation emerges. PC 6 (2.8 %) shows a tendency for females to have more positive scores than males in the human sample. The opposite trend is present in the chimpanzee sample, where it is also stronger. Then mean scores of females in most human populations, except the Eskimo and the Upper

Table 4.28: Summary of the PCA results, ANOVA and Correlation Analysis, PCs 1-10, Step 3A.

	Principal Components Analysis			ANOVA, Pr > F			Correlation withCentroid Size	
	Eigenvalue	Proportion	Cumulative	Popul.	Sex	Interaction	Rho	Pr > F
PC 1	0.012004	0.671478	0.67148	0.0001	0.0001	0.3473	-0.77705	0.0001
PC 2	0.00141	0.078887	0.75037	0.0001	0.9063	0.8367	0.0882	0.0868
PC 3	0.000983	0.054986	0.80535	0.0001	0.8748	0.0466	0.22168	0.0001
PC 4	0.00085	0.04756	0.85291	0.0001	0.1041	0.4382	0.16559	0.0012
PC 5	0.000689	0.038525	0.89144	0.0001	0.0023	0.4135	0.15282	0.0029
PC 6	0.00051	0.028548	0.91999	0.0001	0.0205	0.0001	-0.11052	0.0317
PC 7	0.000353	0.019736	0.93972	0.0458	0.8667	0.0097	0.03294	0.5232
PC 8	0.000269	0.015067	0.95479	0.0001	0.7897	0.6972	0.06945	0.1779
PC 9	0.00016	0.008955	0.96374	0.0002	0.5533	0.2312	0.02245	0.6649
PC 10	0.000138	0.007706	0.97145	0.4667	0.5001	0.1119	0.02159	0.6757

Table 4.29: Squared roots of the sum of squares of the eigenvector coefficients for the three coordinates of each landmark, Step 3A

	PC 1	PC 2	PC 3	PC 4	PC 5	PC 6	PC 7	PC 8	PC 9	PC 10
1. Inion	**0.36**	0.18	**0.68**	**0.60**	0.17	**0.39**	**0.54**	**0.39**	**0.40**	0.10
2. Asterion R.	0.15	0.31	0.11	0.29	**0.46**	0.35	0.26	**0.46**	0.26	0.27
3. Asterion L.	0.14	0.28	0.11	0.33	**0.46**	0.32	0.28	**0.47**	0.34	0.11
4. Lambda	**0.69**	0.36	0.31	0.31	0.36	0.33	0.05	0.22	**0.58**	0.09
5. Inf. Nuchal Line R.	0.26	**0.43**	0.20	**0.37**	**0.43**	**0.40**	**0.48**	0.12	0.17	**0.54**
6. Inf. Nuchal Line L.	0.25	**0.37**	0.17	0.33	**0.42**	0.27	**0.49**	0.14	0.27	**0.67**
7. Sup. Nuchal Line R.	0.33	**0.44**	**0.40**	0.22	0.17	**0.38**	0.21	**0.46**	0.31	0.24
8. Sup. Nuchal Line L.	0.33	**0.39**	**0.43**	0.24	0.19	**0.37**	0.22	0.34	0.35	0.30

Table 4.30: Summary of the CVA results and Correlation Analysis, CaV 1-5, Step 3A.

	Canonical Variates Analysis			Correlation with Centroid Size	
	Eigenvalue	Proportion	Cumulative	Rho	Pr > F
CaV 1	16.5421	0.75	0.75	-0.78505	0.0001
CaV 2	1.9136	0.0868	0.8368	0.27792	0.0001
CaV 3	0.8543	0.0387	0.8755	0.12453	0.0154
CaV 4	0.6021	0.0273	0.9028	-0.07133	0.1664
CaV 5	0.5516	0.025	0.9278	-0.10142	0.0488

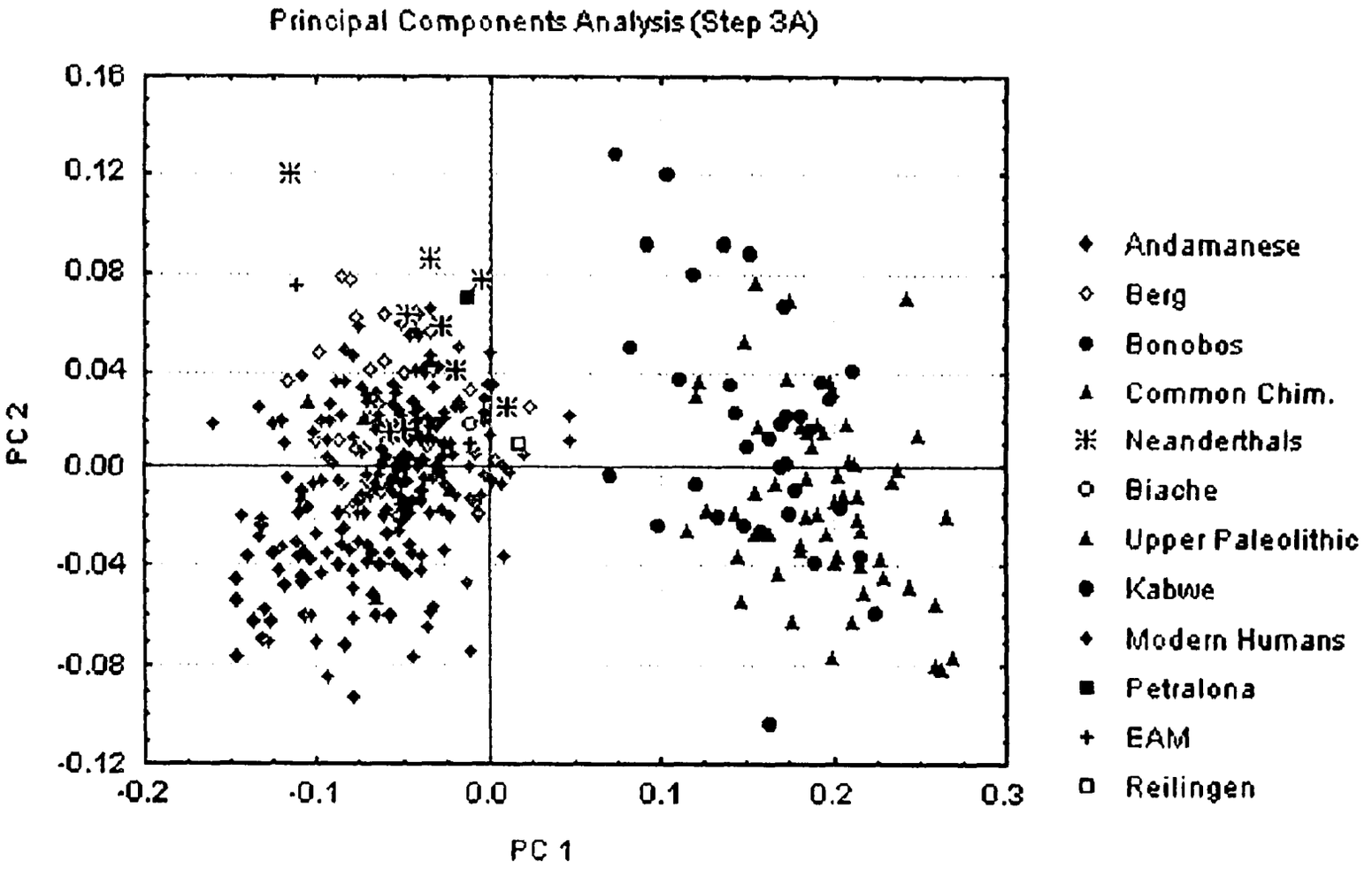

Figure 4.35: Principal Components Analysis (Step 3A). PCs 1 and 2.

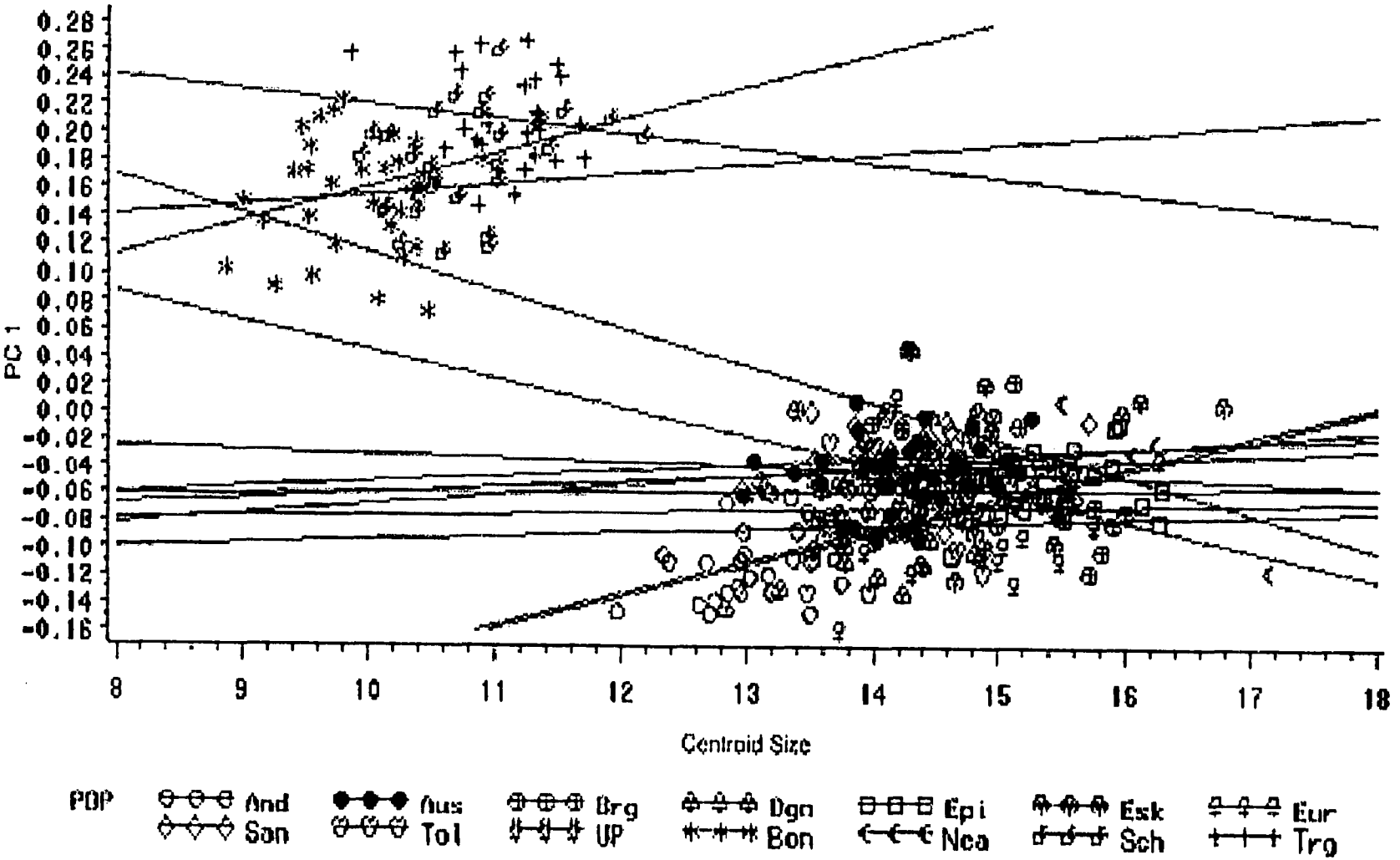

Figure 4.36: PC 1 plotted against centroid size, regression lines for populations fitted (Step 3A).

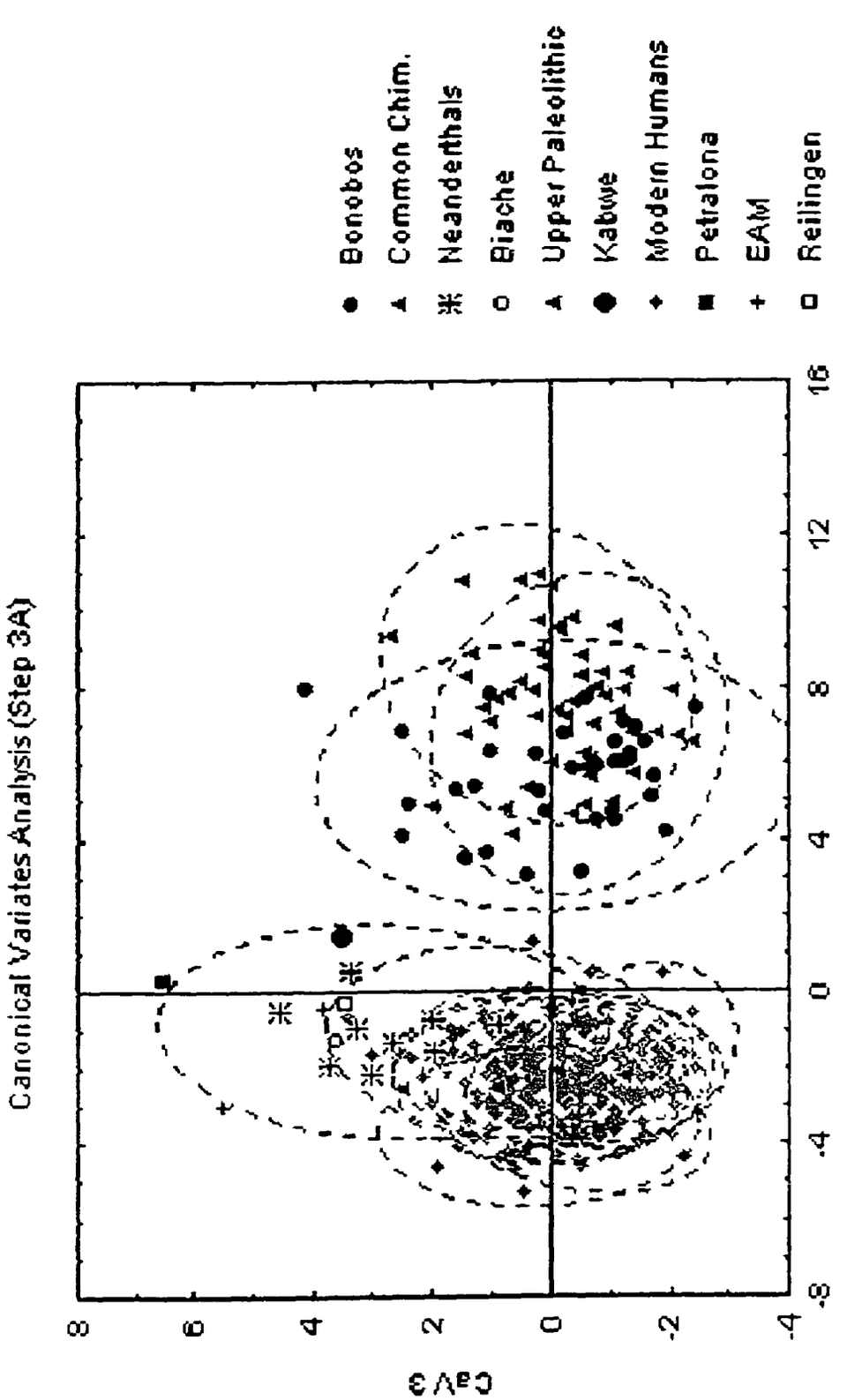

Figure 4.37: Canonical Variates Analysis (Step 3A). CaVs 1 and 4. Dotted lines represent the 95 % confidence ellipses for each group.

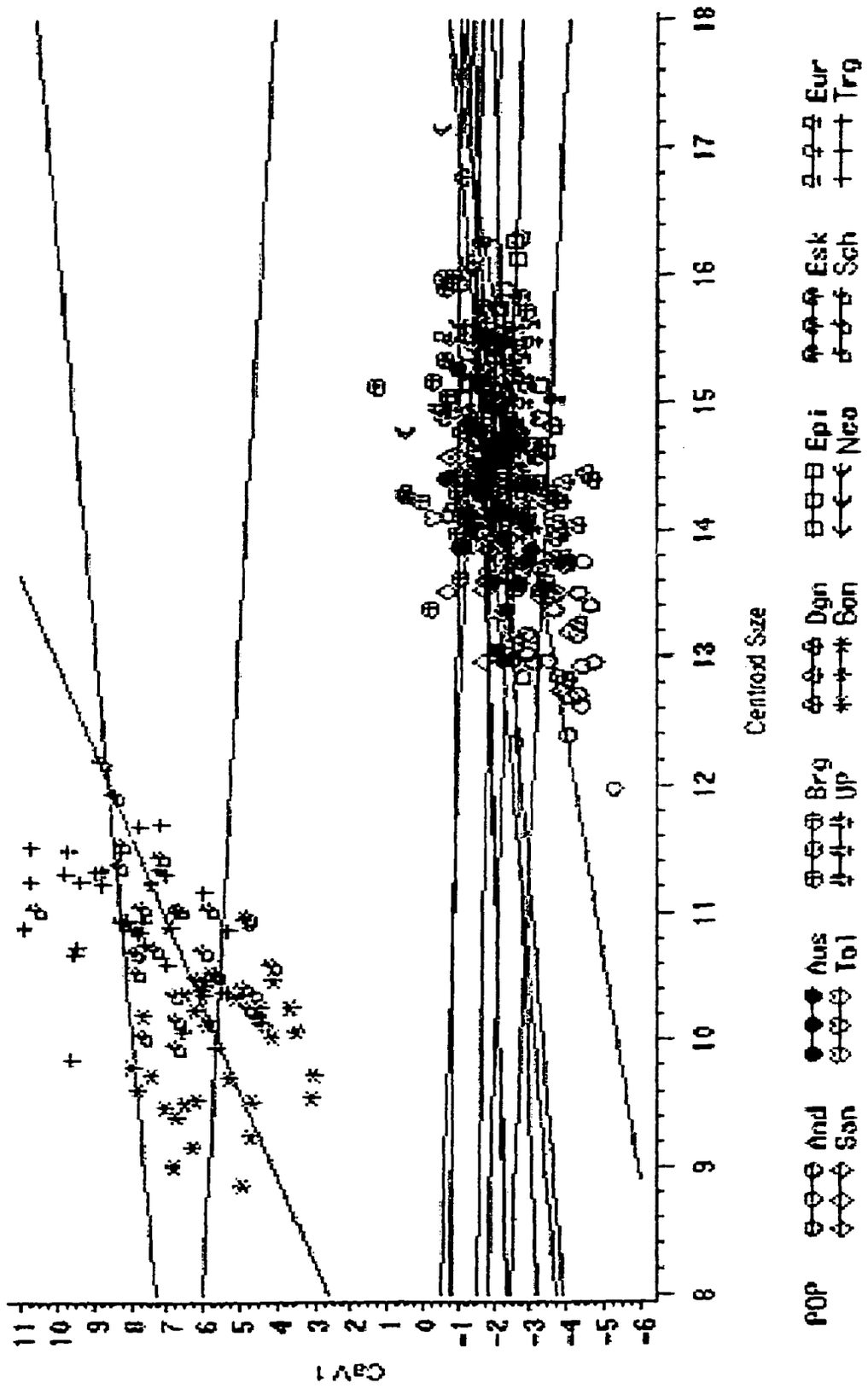

Figure 4.38: CaV 1 plotted against centroid size, regression lines for populations fitted (Step 3A).

Paleolithic groups, are more positive than the male means. The female means in all chimpanzee taxa are more negative than the male means. Human males, therefore, tend to be characterized by a posteriorly projecting inion, laterally and posteriorly placed lateral ends of the superior nuchal line, and an anteriorly placed lambda.

This component also separates Qafzeh 9 and, to a lesser extent, Amud 1 from the rest of the human sample on its positive side. Both these specimens exhibit a similar pattern of right-left asymmetry, which is evident in its much more inferiorly placed right asterion relative to the left and in its more laterally and posteriorly placed right lateral end of the inferior nuchal line. Skhul 5 also exhibits the same kind of asymmetry, which is, however, mostly limited to the asteria. PC 6 is unequally influenced by the right lateral end of the inferior nuchal line, as well as by the right asterion to a lesser extent. Therefore, the shape differences that separate Qafzeh 9 and Amud 1 along PC 6 probably partially reflect right-left asymmetry.

Canonical Variates Analysis: In the CVA, Neanderthals are partially separated from modern humans on the positive end of CaV 3 (3.9 %, mostly influenced by PCs 5 and 3, Fig. 4.37), although the Neanderthal 95 % confidence ellipse overlaps extensively with those of modern human populations, and particularly with the Berg. Neanderthals are significantly different from modern humans at the species level. At the population level, thet are significantly different from most, but not all, modern human populations (Upper Paleolithic, Europeans, Australians, Epipaleolithic, San, Dogon, Tolai and Eskimo). Saccopastore 1 is the specimen that falls furthest within the modern human range. Biache, Reilingen and Skhul 5 fall at the fringe of the Berg 95 % confidence ellipse and well within the Neanderthal one. Kabwe, Petralona and Qafzeh 9 fall at the fringe of the Neanderthal confidence ellipse, the latter two specimen placing at the positive extreme of CaV 3. The shape differences that characterize Petralona and Qafzeh 9, and to a lesser extent, Neanderthals include very laterally and inferiorly placed asteria and elevated lateral ends of the inferior nuchal line, reflecting a medio-laterally wide occipital plane, and a sharp angle between the occipital and nuchal planes.

As before, CaV 1 (75 %, mostly influenced by PC 1, Fig. 4.37) separates humans from chimpanzees. Kabwe, and to a lesser extent Petralona, are separated from modern humans, falling outside the 95 % confidence ellipse of all modern human populations, but

within the Neanderthal one. The shape differences that characterize chimpanzees relative to humans and these fossil specimens relative to most other human specimens include an inferiorly placed lambda and an elevated inion and lateral ends of the superior nuchal line. CaV 1 is relatively strongly correlated with centroid size overall overall, although each population behaves differently along this axis with regard to centroid size (Fig. 3.38).

Classification: Kabwe, Petralona, Biache and Reilingen were all classified as Neanderthal by posterior probability (1.00, 1.00, 0.83 and 0.94 respectively), as were also Qafzeh 9 (1.00) and Skhul 5 (0.98). Kanalda was classified as Epipaleolithic (0.63). All Upper Paleolithic and Neanderthal specimens were placed correctly in their group, with the exception of La Ferrassie 1, which was classified as Epipaleolithic. The cross-validation classification (Table 4.31) is less successful than in the previous steps of analysis, with most modern human groups showing much lower success rates. The highest success rate is achieved by the Dogon (80 %) and the lowest by the Australians (33.33 %). Only three Neanderthal specimens out of nine were classified correctly, the others being misclassified as Berg (3), Epipaleolithic (1), European (1) and Upper Paleolithic (1). Three modern human specimens (an Australian, a Berg and a European individual) were misclassified as Neanderthal, as was also one Upper Paleolithic specimen. None of the Upper Paleolithic crania were classified correctly. They were misclassified as Australian, Berg, Eskimo, Tolai and Neanderthal.

***Mahalanobis D^2, Cluster Analysis and Minimum Spanning Tree*:** The unbiased Mahalanobis D^2 matrix was calculated for all specimens including singletons (see Appendix), as well as excluding singletons (Table 4.39). The latter matrix was calculated excluding also the EAM population. This was done for two reasons: a. due to the small sample size of only two specimens and b. due to the high degree of left-right asymmetry present in both specimens, and particularly in Qafzeh 9, which undoubtedly affects their position relative to the rest of the human sample.

The most striking difference from the previous steps is the great reduction of the distances between the Upper Paleolithic group and the recent human populations. The distances between these specimens and five modern human populations are not significant, two of them are only significant to the 0.05 level and only two are significant

to the 0.001 level. The distance of this group to the Neanderthals is also reduced, and is only significant to the 0.01 level. The Upper Paleolithic sample now appears closest to the mixed Europeans and most distant from the Andamanese. The distances between Neanderthals and modern humans are also somewhat reduced, but are still significant to the 0.001 level at least. This group is now closest to the Australians and most distant from the Andamanese. None of the three geographic pairs of modern human populations are closest neighbors to the other, showing a further breakdown of the geographic clustering.

The cluster diagram (Fig. 4.39) shows the common branch of the Dogon and the Andamanese as the outlier of all other human groups, including Neanderthals. The latter are outliers to the remaining human populations. The Upper Paleolithic group clusters with the Berg within this larger branch. No geographic clustering is observed within the modern human populations. The minimum spanning tree (Fig. 4.39) shows Neanderthals linked to the Australians, and the Upper Paleolithic group to the San. None of the populations in the three geographic pairs is joined to its geographic neighbor.

Table 4.31: Cross-validation classification summary, (percentages for each population in bold), Step 3A.

	And	Aus	Brg	Dgn	Epi	Esk	Eur	San	Tol	UP	Bon	Nea	Sch	Trg	Total
And	18	0	0	8	0	0	0	1	1	2	0	0	0	0	30
%	**60**	0	0	26.67	0	0	0	3.33	3.33	6.67	0	0	0	0	100
Aus	0	10	0	0	1	2	3	12	1	0	0	1	0	0	30
%	0	**33.33**	0	0	3.33	6.67	10	40	3.33	0	0	3.33	0	0	100
Brg	0	3	15	0	3	0	2	1	1	4	0	1	0	0	30
%	0	10	**50**	0	10	0	6.67	3.33	3.33	13.33	0	3.33	0	0	100
Dgn	2	0	0	24	1	0	1	0	0	2	0	0	0	0	30
%	6.67	0	0	**80**	3.33	0	3.33	0	0	6.67	0	0	0	0	100
Epi	0	4	0	2	16	1	0	1	3	1	0	0	0	0	28
%	0	14.29	0	7.14	**57.14**	3.57	0	3.57	10.71	3.57	0	0	0	0	100
Esk	0	4	0	0	1	15	0	4	4	2	0	0	0	0	30
%	0	13.33	0	0	3.33	**50**	0	13.33	13.33	6.67	0	0	0	0	100
Eur	2	0	3	1	2	1	11	2	5	0	0	1	0	0	28
%	7.14	0	10.71	3.57	7.14	3.57	**39.29**	7.14	17.86	0	0	3.57	0	0	100
San	0	4	0	1	2	4	2	13	1	3	0	0	0	0	30
%	0	13.33	0	3.33	6.67	13.33	6.67	**43.33**	3.33	10	0	0	0	0	100
Tol	0	3	1	0	1	3	5	0	13	3	0	0	0	0	29
%	0	10.34	3.45	0	3.45	10.34	17.24	0	**44.83**	10.34	0	0	0	0	100
UP	0	1	1	0	0	1	0	0	1	0	0	1	0	0	5
%	0	20	20	0	0	20	0	0	20	**0**	0	20	0	0	100
Bon	0	0	0	0	0	0	0	0	0	0	26	0	6	2	34
%	0	0	0	0	0	0	0	0	0	0	**76.47**	0	17.65	5.88	100
Nea	0	0	3	0	1	0	1	0	0	1	0	3	0	0	9
%	0	0	33.33	0	11.11	0	11.11	0	0	11.11	0	**33.33**	0	0	100
Sch	0	0	0	0	0	0	0	0	0	0	6	0	16	8	30
%	0	0	0	0	0	0	0	0	0	0	20	0	**53.33**	26.67	100
Trg	0	0	0	0	0	0	0	0	0	0	2	0	6	20	28
%	0	0	0	0	0	0	0	0	0	0	7.14	0	21.43	**71.43**	100
Total	22	29	23	36	28	27	25	34	30	18	34	7	28	30	371
%	5.93	7.82	6.2	9.7	7.55	7.28	6.74	9.16	8.09	4.85	9.16	1.89	7.55	8.09	100

Table 4.32: Mahalanobis D^2 distances (Step 3A). All distances significant to the 0.001 level, except: NS = non-significant, * = 0.05 level, ** = 0.01 level.

	Kan	And	Aus	Bch	Brg	Dgn	EE	Epi	Esk	Eur	Kbw
Kan	0.00	41.34	35.34	28.31NS	23.73*	38.83	54.02	22.48*	34.58**	31.24**	57.57**
And	41.34	0.00	23.14	55.67	22.44	5.18	50.12	19.41	27.86	14.46	69.37
Aus	35.34**	23.14	0.00	33.72**	7.52	11.87	33.26	6.05	2.08**	3.80	28.73
Bch	28.31NS	55.67	33.72**	0.00	37.69	47.07	34.09*	39.66	42.90	38.11	20.83NS
Brg	23.73*	22.44	7.52	37.69	0.00	17.89	40.90	7.23	9.23	4.62	29.56
Dgn	38.83	5.18	11.87	47.07	17.89	0.00	41.83	9.41	15.82	8.71	57.22
EE	54.02	50.12	33.26	34.09*	40.90	41.83	0.00	35.16	47.06	33.87	42.08**
Epi	22.48*	19.41	6.05	39.66	7.23	9.41	35.16	0.00	6.93	5.65	36.99
Esk	34.58	27.86	2.08**	42.90	9.23	15.82	47.06	6.93	0.00	5.36	38.15
Eur	31.24	14.46	3.80	38.11	4.62	8.71	33.87	5.65	5.36	0.00	38.49
Kbw	57.57	69.37	28.73**	20.83NS	29.56	57.22	42.08**	36.99	38.15	38.49	0.00
Ptr	41.74*	74.83	53.46	34.92NS	42.74	71.46	27.70*	51.67	66.78	52.45	31.31NS
Rei	55.90	82.33	35.85	44.96*	46.39	64.99	7.84NS	37.43	40.39	44.41	15.55NS
San	36.08	23.24	0.45NS	39.11	5.57	14.16	38.96	6.47	2.09**	3.02	25.69*
Tol	29.25	14.19	4.55	42.00	8.80	8.54	41.24	5.66	4.26	2.87	43.88
UP	25.07*	17.45	3.74NS	35.52**	2.21NS	11.76	34.41	4.79*	4.88*	2.78NS	30.02*
Bon	67.83	93.62	57.89	81.07	53.17	84.09	85.85	59.88	57.24	63.92	46.36
Nea	32.23**	31.60	8.89	28.56**	10.09	24.41	20.59**	15.81	17.31	11.13	12.25NS
Sch	81.32	110.17	75.32	102.26	65.71	101.96	107.90	74.94	72.43	80.36	51.81
Trg	113.04	139.79	103.24	124.14	95.44	131.99	129.83	109.11	103.58	110.83	67.29

	Ptr	Rei	San	Tol	UP	Bon	Nea	Sch	Trg
Kan	41.74*	55.90**	36.08	29.25**	25.07**	67.83	32.23**	81.32	113.04
And	74.83	82.33	23.24	14.19	17.45	93.62	31.60	110.17	139.79
Aus	53.46	35.85**	0.45NS	4.55	3.74NS	57.89	8.89	75.32	103.24
Bch	34.92NS	44.96*	39.11	42.00	35.52**	81.07	28.56**	102.26	124.14
Brg	42.74	46.39	5.57	8.80	2.21NS	53.17	10.09	65.71	95.44
Dgn	71.46	64.99	14.16	8.54	11.76	84.09	24.41	101.96	131.99
EE	27.70*	7.84NS	38.96	41.24	34.41	85.85	20.59**	107.90	129.83
Epi	51.67	37.43	6.47	5.66	4.79*	59.88	15.81	74.94	109.11
Esk	66.78	40.39	2.09**	4.26	4.88*	57.24	17.31	72.43	103.58
Eur	52.45	44.41	3.02	2.87	2.78NS	63.92	11.13	80.36	110.83
Kbw	31.31NS	15.55NS	25.69*	43.88	30.02*	46.36	12.25NS	51.81	67.29
Ptr	0.00	26.58NS	52.43	58.56	53.73	71.22	24.38*	93.36	108.89
Rei	26.58NS	0.00	35.85**	48.33	31.00**	77.66	26.42*	86.47	114.60
San	52.43	35.85**	0.00	4.60	2.07NS	56.09	10.05	70.53	100.34
Tol	58.56	48.33	4.60	0.00	4.10NS	65.70	15.52	82.60	112.01
UP	53.73	31.00**	2.07NS	4.10NS	0.00	62.72	8.60**	72.02	102.67
Bon	71.22	77.66	56.09	65.70	62.72	0.00	54.25	6.36	14.10
Nea	24.38*	26.42*	10.05	15.52	8.60**	54.25	0.00	72.87	92.79
Sch	93.36	86.47	70.53	82.60	72.02	6.36	72.87	0.00	6.07
Trg	108.89	114.60	100.34	112.01	102.67	14.10	92.79	6.07	0.00

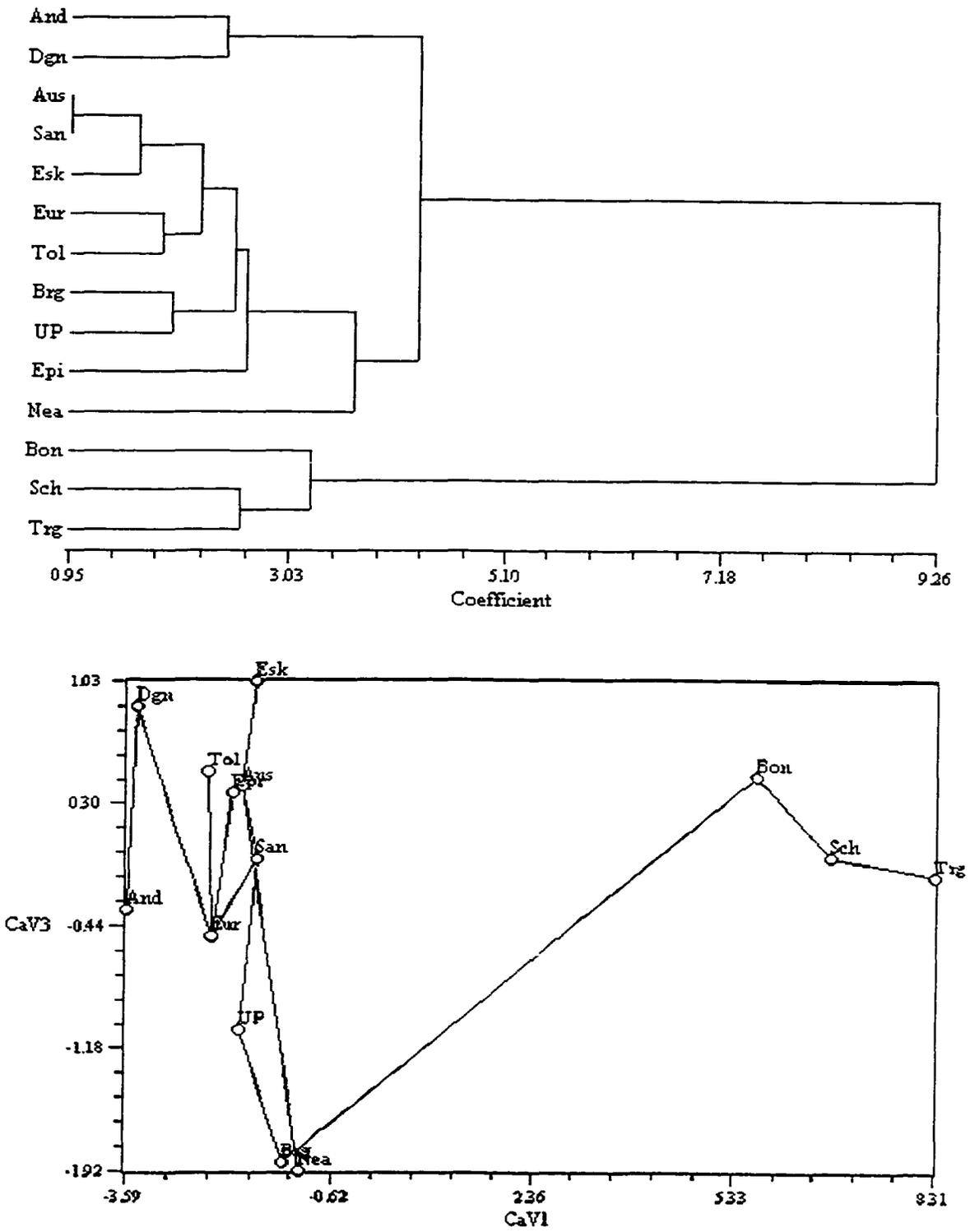

Figure 4.39: Cluster analysis (UPGMA, top) and minimum spanning tree, Step 3A.

Step 3B – Human sample only

***Principal Components Analysis*:** The analysis was repeated on the human sample only (Tables 4.33-4.34). The Upper Paleolithic specimens always fall well within the modern human range, while Neanderthals are again never completely separated from modern humans. They cluster near the positive end of PC 1 (30.3 %, Fig. 4.40), where Reilingen, Biache, Petralona and Skhul 5 also fall. Kabwe falls outside of the modern human range on the positive side of PC 1. Amud 1 is the only specimen that is separated from the Neanderthal sample, and it falls near the center of the human range on the negative side and close to Qafzeh 9. Although Neanderthals are significantly different from modern humans at the species level, at the population level they are only significantly different from the Andamanese on PC 1. The shape differences at the positive end of this axis are a supero-inferiorly short occipital plane and superiorly placed lateral ends of the superior nuchal line. Only Kabwe is outside the modern human range for these traits, however. PC 1 is also significant for sex effects, males tending to have more positive coefficients than females. However, when the male mean scores are plotted by population, the Berg, Europeans, San and Neanderthals show the opposite trend. PC 1 and is relatively weakly correlated with centroid size (Table 4.33).

Neanderthals also tend to fall on the negative side of PC 2 (14.9 %, Fig. 4.40) mostly overlapping with the Berg. Although Neanderthals are again significantly different in their mean score from modern humans at the species level, at the population level they are only significantly different from the Epipaleolithic and the Eskimo modern human populations. Amud 1 and Qafzeh 9 fall at the negative extreme of this axis and outside the range of modern human variation. The shape differences at the negative end of PC 2 are similar to those described for PC 2 in Step 3A and include a medio-laterally wide occipital plane and an elevated nuchal plane. The extreme position of Amud 1 and Qafzeh 9 along this axis is similar to that observed in PC 2 of Step 3A and may reflect the right-left asymmetries that are similar in these two specimens. Table 4.33 shows the unequal contribution of right versus left asterion and lateral end of the superior nuchal line to the variation along PC 2, indicating that some of the variation along this component reflects asymmetry.

Table 4.33: Summary of the PCA results, ANOVA and Correlation Analysis, PCs 1-10, Step 3B.

	Principal Components Analysis			ANOVA, Pr > F			Correlation with Centroid Size	
	Eigenvalue	Proportion	Cumulative	Popul.	Sex	Interaction	Rho	Pr > F
PC 1	0.002193	0.303501	0.3035	0.0001	0.0001	0.2497	0.42916	0.0001
PC 2	0.001076	0.14888	0.45238	0.0001	0.7706	0.3696	-0.05808	0.3277
PC 3	0.000957	0.132394	0.58478	0.0001	0.3332	0.1538	-0.23698	0.0001
PC 4	0.000675	0.093444	0.67822	0.0001	0.0002	0.0783	0.29652	0.0001
PC 5	0.000583	0.080742	0.75896	0.0001	0.2308	0.3675	-0.01483	0.8028
PC 6	0.000473	0.06551	0.82447	0.0001	0.018	0.1068	-0.09748	0.0999
PC 7	0.000319	0.044122	0.86859	0.0003	0.3259	0.0939	0.05624	0.3433
PC 8	0.000207	0.028688	0.89728	0.0001	0.8071	0.2884	0.10744	0.0696
PC 9	0.000158	0.021873	0.91916	0.008	0.5164	0.241	0.08791	0.1381
PC 10	0.000131	0.018067	0.93722	0.058	0.2202	0.5139	0.0441	0.4576

Table 4.34: Squared roots of the sum of squares of the eigenvector coefficients for the three coordinates of each landmark, Step 3A.

	PC 1	PC 2	PC 3	PC 4	PC 5	PC 6	PC 7	PC 8	PC 9	PC 10
1. Inion	0.26	0.04	**0.81**	0.33	0.13	0.52	0.46	0.50	0.35	0.26
2. Asterion R.	0.08	**0.40**	0.15	0.33	**0.49**	0.16	0.32	**0.48**	0.22	0.32
3. Asterion L.	0.10	**0.33**	0.19	0.31	**0.52**	0.13	**0.36**	**0.41**	0.29	0.23
4. Lamdba	**0.53**	0.27	**0.35**	**0.40**	**0.53**	0.24	0.07	0.16	**0.59**	0.05
5. Inf. Nuchal Line R.	0.17	**0.53**	0.22	**0.47**	**0.05**	**0.50**	**0.43**	0.03	0.28	**0.36**
6. Inf. Nuchal Line L.	0.19	**0.48**	0.20	**0.43**	0.11	**0.44**	**0.44**	0.15	**0.30**	**0.35**
7. Sup. Nuchal Line R.	**0.52**	**0.31**	0.20	0.25	0.25	**0.31**	**0.31**	**0.36**	**0.38**	**0.53**
8 Sup. Nuchal Line L.	**0.54**	0.24	0.20	0.25	**0.33**	**0.29**	**0.29**	**0.42**	**0.29**	**0.50**

Table 4.35: Summary of the CVA results and Correlation Analysis, CaV 1-5, Step 3B.

	Canonical Variates Analysis			Correlation with Centroid Size	
	Eigenvalue	Proportion	Cumulative	Rho	Pr > F
CaV 1	2.972	0.3724	0.3724	0.55244	0.0001
CaV 2	1.6482	0.2065	0.5789	0.18768	0.0014
CaV 3	0.8651	0.1084	0.6873	-0.06751	0.2552
CaV 4	0.5871	0.0736	0.7609	0.17649	0.0027
CaV 5	0.4378	0.0549	0.8157	0.03707	0.5324

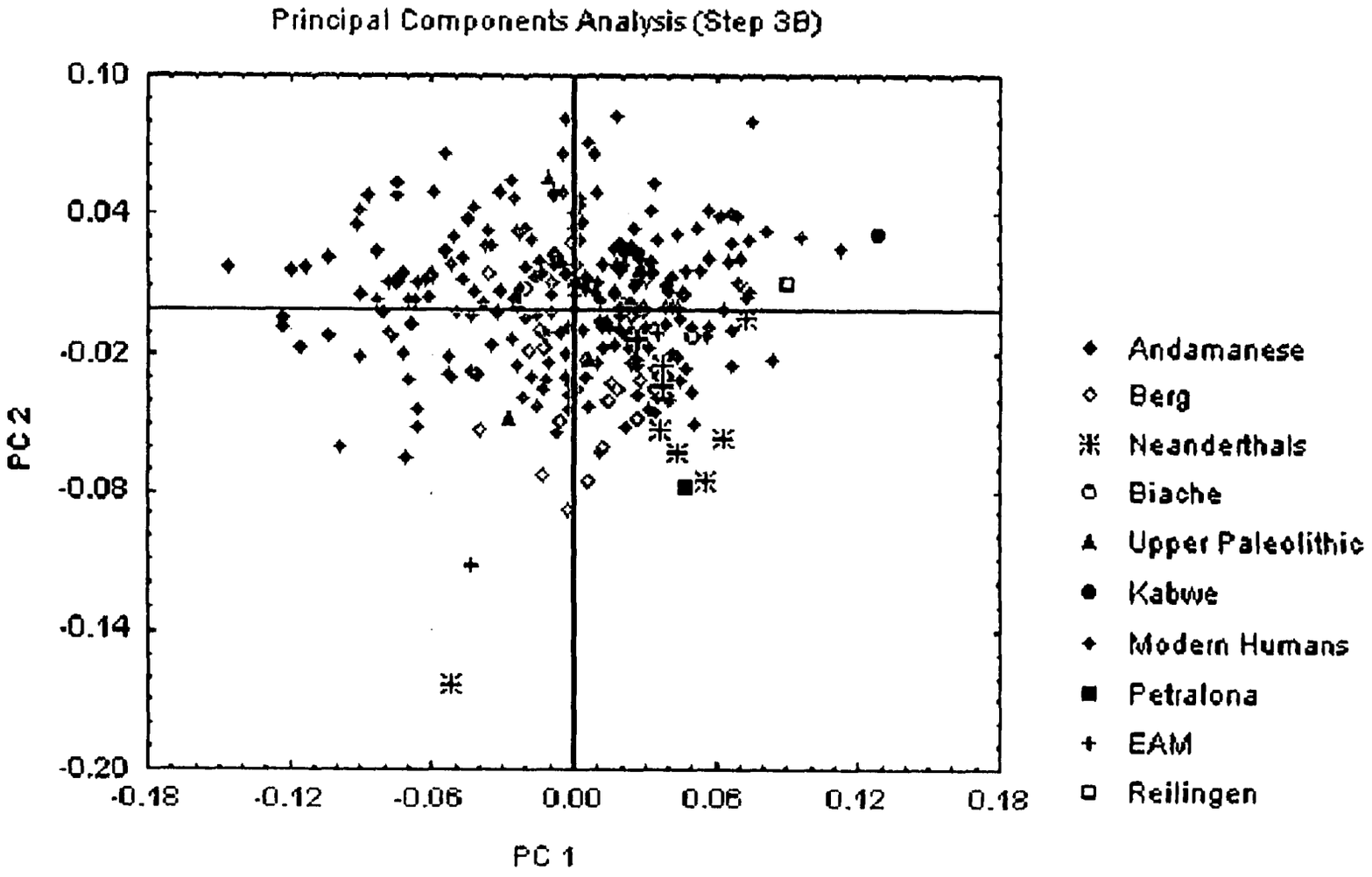

Figure 4.40: Principal Components Analysis (Step 3B), PCs 1 and 2.

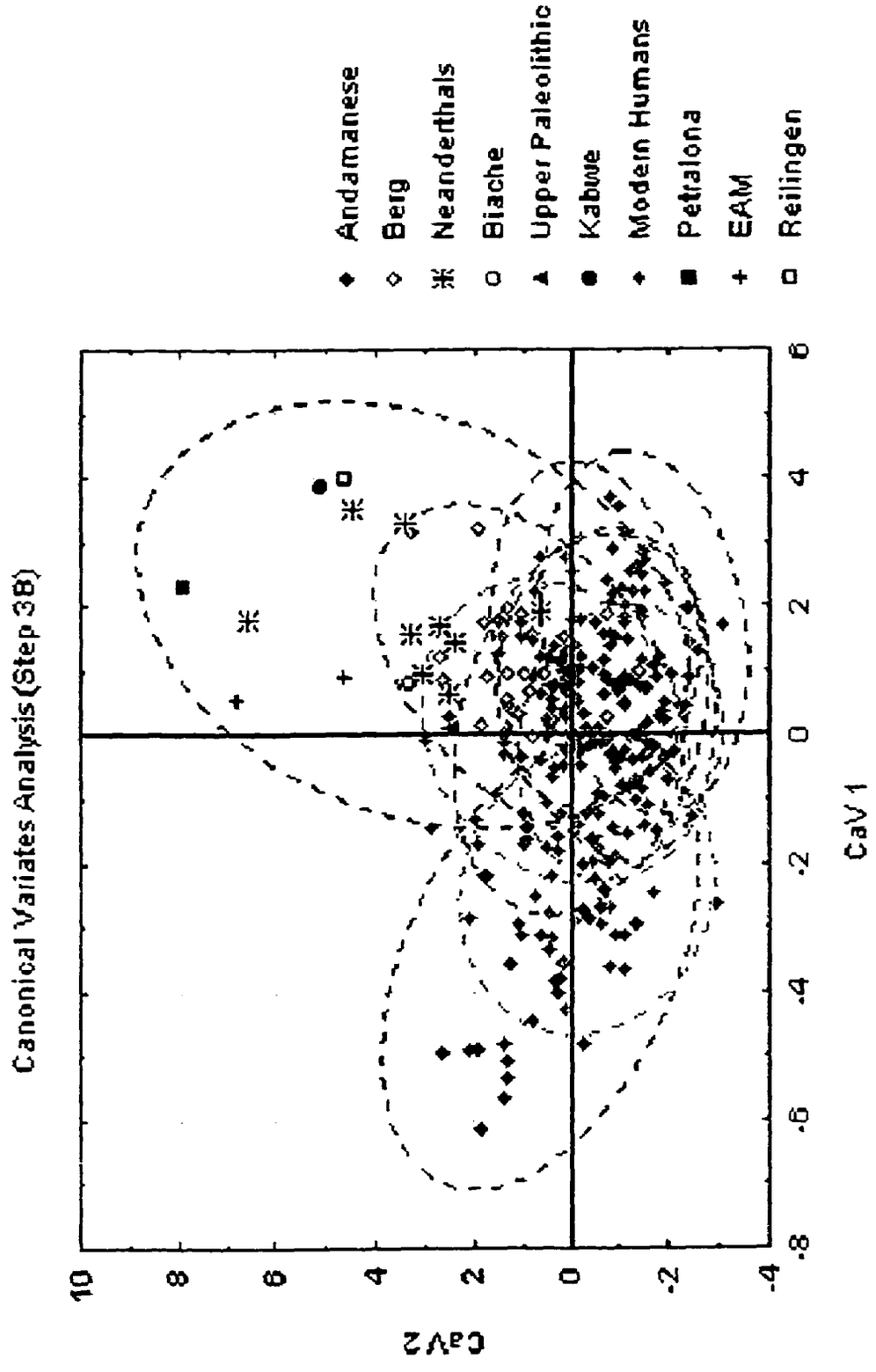

Figure 4.41: Canonical Variates Analysis (Step 3B), CaVs 1 and 2. Dotted lines represent the 95 % confidence ellipses for each group.

Kabwe, Petralona, and Skhul 5 fall on the positive extreme of PC 4 (9.3 %). Reilingen also falls near the positive extreme of the modern human range. The shape differences at the positive end include an anteriorly placed lambda, anteriorly and superiorly placed lateral ends of the inferior nuchal line and posteriorly placed inion, indicating a low angle between the occipital and nuchal planes, which are also antero-posteriorly elongated. This component is also significant for sex effects, males tending to have more positive scores than females. This pattern, however, does not hold across all modern human populations, as it is reversed among the Dogon and the Eskimo. PC 4 is weakly correlated with centroid size (Table 4.33).

Canonical Variates Analysis: The CVA also does not separate the Upper Paleolithic sample from modern humans. Neanderthals are partially separated along CaV 2 (20.6 %, mostly influenced by PCs 4, 2 and 6, Fig. 4.41). The Neanderthal ellipse partially overlaps with those of the modern human groups, particularly with that of the Berg. It also includes, at its positive end, Kabwe, Petralona, Reilingen, Skhul 5 and Qafzeh 9, while Biache falls in the overlap area with the Berg. At the species level the Neanderthal mean score is significantly different from that of modern humans on CaV 2, while at the population level it is significantly different from most modern human populations, including the European, Dogon, Australian, San, Tolai and Eskimo groups. The Neanderthal specimen that is most widely separated from the modern human cloud is Amud 1, while Saccopastore 1 falls near the center of the modern human range. The shape differences at the positive end of this axis are similar to those described for PC 2. The extreme position of Amud 1 and Qafzeh 9 along this axis may again partly reflect the strong right-left asymmetry present in these two specimens. CaV 1 is not strongly correlated with size (Table 4.35).

Neanderthals also cluster near the positive end of CaV 1 (37.2 %, mostly influenced by PC 1, Fig. 4.41). The shape variation along this axis is similar to that described for PC 1.

Classification: The results of the posterior probability classification are similar to those obtained in Step 3A. Here, however, La Ferrassie 1 is classified as Neanderthal (0.53) rather than Epipaleolithic, while Saccopastore 1 is classified as Berg (0.69) rather than Neanderthal. The cross-validation classification results (Table 4.36) are similar to

those obtained in Step 3A, but slightly worse for modern human groups. As in Step 3A, no Upper Paleolithic specimens were correctly classified, each of the five individuals being grouped instead with the Australians, Berg, San Tolai and Neanderthals. The classification success was slightly higher for Neanderthals. Four specimens were correctly classified compared to three in Step 3A. Three out of the remaining five individuals were placed with the Berg, one with the Epipaleolithic and one with the Upper Paleolithic group. One recent human specimen, a Berg, as well as an Upper Paleolithic individual, were classified as Neanderthal.

Mahalanobis D^2, Cluster Analysis and Minimum Spanning Tree: Results (Table 4.37) are similar to those obtained in Step 3A. The Upper Paleolithic group still shows non-significant distances from most modern human groups, whereas the distances between Neanderthals and all modern humans, including the Upper Paleolithic specimens, are significant at least to the 0.001 level. This group is now closest to the Andamanese, as in Steps 2A and 2B, and not to the Australians, as in Step 3A. Among the three geographic pairs of modern human populations only the Berg are closest neighbors to the European group, but not vice versa.

The cluster analysis (Fig. 4.42) is different from that obtained in Step 3A. Here Neanderthals are the outliers to all other human groups, while the Upper Paleolithic specimens cluster again with the Berg within a larger branch that includes the Epipaleolithic population. No geographic clustering is preserved. In the minimum spanning tree (Fig. 4.42) Neanderthals are joined to the Berg, while the Upper Paleolithic groups is joined to the Berg, the Epipaleolithic and the San. None of the geographic pairs of modern human populations are linked.

Table 3.36: Cross-validation classification summary (percentages for populations in bold), Step 3B.

	And	Aus	Brg	Dgn	Epi	Esk	Eur	San	Tol	UP	Nea	Total
And	18	0	0	9	0	0	0	0	1	2	0	30
%	**60**	0	0	30	0	0	0	0	3.33	6.67	0	100
Aus	0	10	0	0	1	2	5	12	0	0	0	30
%	0	**33.33**	0	0	3.33	6.67	16.67	40	0	0	0	100
Brg	0	3	15	0	3	0	2	0	1	5	1	30
%	0	10	**50**	0	10	0	6.67	0	3.33	16.67	3.33	100
Dgn	2	0	0	23	1	0	1	0	1	2	0	30
%	6.67	0	0	**76.67**	3.33	0	3.33	0	3.33	6.67	0	100
Epi	0	2	1	1	16	1	0	2	4	1	0	28
%	0	7.14	3.57	3.57	**57.14**	3.57	0	7.14	14.29	3.57	0	100
Esk	0	2	0	0	1	19	0	2	5	1	0	30
%	0	6.67	0	0	3.33	**63.33**	0	6.67	16.67	3.33	0	100
Eur	3	1	3	1	1	2	11	4	2	0	0	28
%	10.71	3.57	10.71	3.57	3.57	7.14	**39.29**	14.29	7.14	0	0	100
San	0	7	1	1	1	6	4	7	0	3	0	30
%	0	23.33	3.33	3.33	3.33	20	13.33	**23.33**	0	10	0	100
Tol	0	2	1	0	2	3	5	2	12	2	0	29
%	0	6.9	3.45	0	6.9	10.34	17.24	6.9	**41.38**	6.9	0	100
UP	0	1	1	0	0	0	0	1	1	0	1	5
%	0	20	20	0	0	0	0	20	20	**0**	20	100
Nea	0	0	3	0	1	0	0	0	0	1	4	9
%	0	0	33.33	0	11.11	0	0	0	0	11.11	**44.44**	100
Total	23	28	25	35	27	33	28	30	27	17	6	279
%	8.24	10.04	8.96	12.54	9.68	11.83	10.04	10.75	9.68	6.09	2.15	100

Table 4.37: Mahalanobis D^2 distances (Step 3B). All distances significant to the 0.001 level, except NS = non-significant, * = 0.05 level, ** = 0.01 level.

	Kan	And	Aus	Bch	Brg	Dgn	EE	Epi	Esk	Eur	Kbw	Ptr	Rei	San	Tol	UP	Nea
Kan	0.00	42.44	38.47**	29.84NS	25.61*	41.70	68.03	25.13*	40.85	34.79**	92.78	53.45*	71.45**	38.54**	34.21**	27.48*	36.78**
And	42.44	0.00	22.49	54.11	23.31	5.00	59.82	17.51	29.33	15.96	100.48	89.46	89.07	22.37	15.15	17.51	35.66
Aus	38.47	22.49	0.00	38.54**	8.50	11.86	49.00	7.01	3.93	3.83	73.79	76.99	53.93	0.57NS	4.55	4.77NS	15.74
Bch	29.84NS	54.11	38.54**	0.00	42.85	49.75	48.87**	43.42	51.16	42.75	63.84**	51.17*	64.85**	43.01	48.31	40.04**	36.61**
Brg	25.61*	23.31	8.50	42.85	0.00	18.45	53.21	7.91	12.23	5.21	74.37	63.07	61.79	6.97	10.33	2.71NS	14.64
Dgn	41.70	5.00	11.86	49.75	18.45	0.00	56.59	9.09	18.23	9.47	97.94	92.94	78.83	13.61	8.77	11.57	31.44
EE	68.03	59.82	49.00	48.87**	53.21	56.59	0.00	46.19	64.26	48.74	69.04	31.78NS	13.65NS	55.01	58.38	47.62	25.21
Epi	25.13*	17.51	7.01	43.42	7.91	9.09	46.19	0.00	9.31	6.57	73.54	69.21	48.88	7.16	6.25	4.84NS	19.98
Esk	40.85**	29.33	3.93	51.16	12.23	18.23	64.26	9.31	0.00	8.21	71.42	90.40	55.19	3.67	5.59	8.44*	23.27
Eur	34.79*	15.96	3.83	42.75	5.21	9.47	48.74	6.57	8.21	0.00	86.75	75.86	61.91	3.20	4.00	3.44NS	18.37
Kbw	92.78	100.48	73.79	63.84**	74.37	97.94	69.04	73.54	71.42	86.75	0.00	58.58*	30.40NS	70.67	86.61	74.36	37.77**
Ptr	53.45*	89.46	76.99	51.17*	63.07	92.94	31.78NS	69.21	90.40	75.86	58.58*	0.00	34.84NS	76.77	83.97	73.97	33.11**
Rei	71.45**	89.07	53.93	64.85**	61.79	78.83	13.65NS	48.88	55.19	61.91	30.40NS	34.84NS	0.00	54.06	65.24	47.14**	31.80*
San	38.54**	22.37	0.57NS	43.01	6.97	13.61	55.01	7.16	3.67	3.20	70.67	76.77	54.06	0.00	4.77	3.34NS	17.55
Tol	34.21**	15.15	4.55	48.31	10.33	8.77	58.38	6.25	5.59	4.00	86.61	83.97	65.24	4.77	0.00	5.46*	23.05
UP	27.48*	17.51	4.77NS	40.04**	2.71NS	11.57	47.62	4.84NS	8.44**	3.44NS	74.36	73.97	47.14	3.34NS	5.46*	0.00	14.68
Nea	36.78**	35.66	15.74	36.61**	14.64	31.44	25.21	19.98	23.27	18.37	37.77**	33.11**	31.80*	17.55	23.05	14.68	0.00

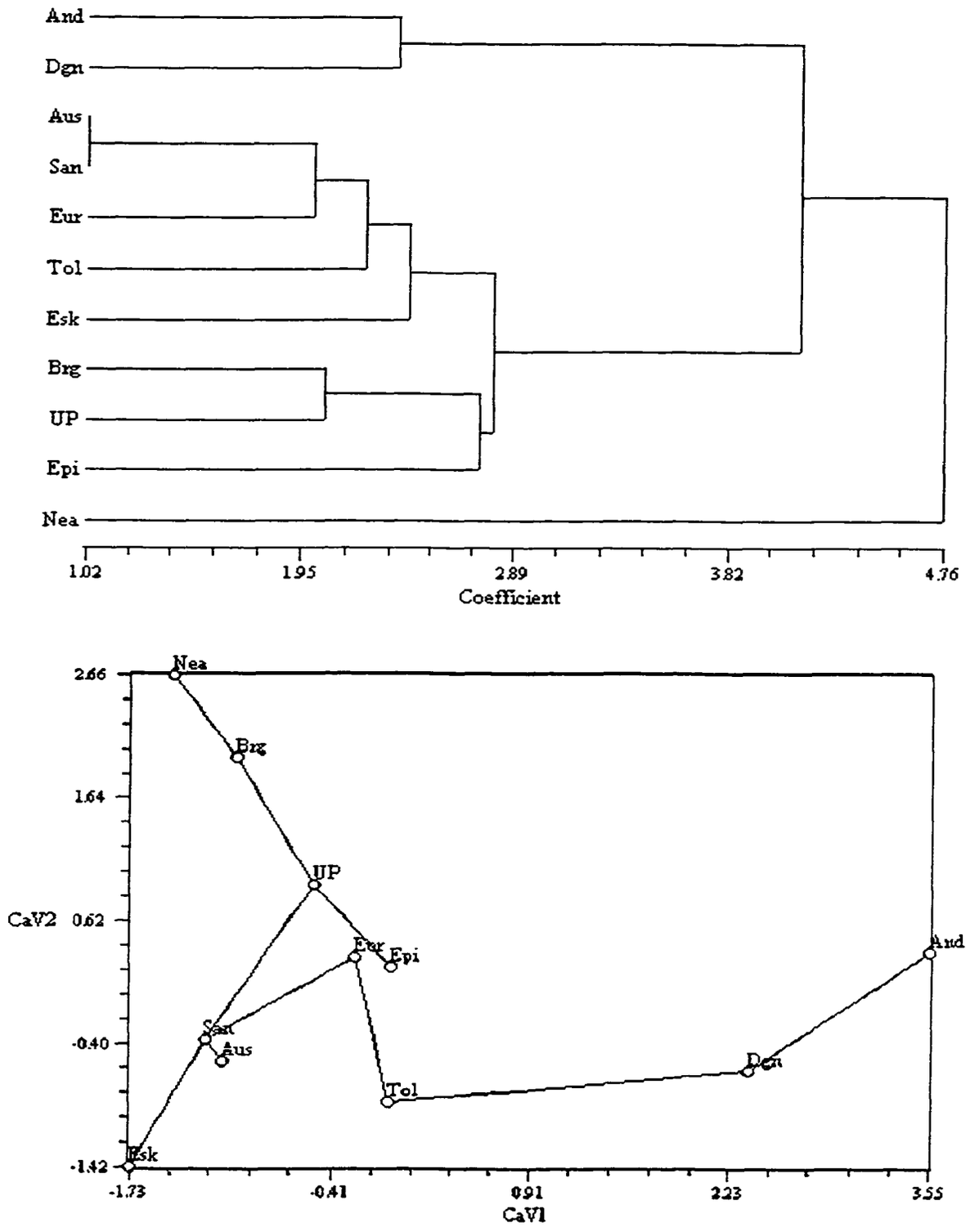

Figure 4.42: Cluster analysis (UPGMA, top) and minimum spanning tree, Step 3B.

Step 3C – Chimpanzee sample only

***Classification*:** The cross-validation classification here (Table 4.38) shows increased levels of misclassification between bonobos and *P. t. schweinfurthii.* Six bonobo specimens are classified as *P. t. schweinfurthii* and only one as *P. t. troglodytes.* Four *P. t. schweinfurthii* are classified as bonobos, while only one *P. t. troglodytes* is. On the other hand, the rates for misclassification between the two common chimpanzee subspecies are reduced. A high percentage of *P. t. troglodytes* (23.3 %) is still misclassified as *P. t. schweinfurthii,* but only two *P. t. schweinfurthii* (7.1 %) are classified as *P. t. troglodytes.*

***Mahalanobis D^2*:** The unbiased Mahalanobis distances were calculated (Table 4.39). The distances among the chimpanzee taxa are all significant to the 0.0001 level. They are similar to those obtained in the combined sample analysis (Step 3A), although slightly higher in all three cases. Bonobos are more distant to *P. t. schweinfurthii* than the two subspecies are from each other, but only marginally. The distance between bonobos and *P. t. troglodytes* is equivalent to the larger distances between some modern human populations, which were greatly reduced in this step. It is smaller than most, but not all, of the distances between Neanderthals and modern human populations, and it is larger than almost all the distances between the Upper Paleolithic specimens and recent human groups. The distance between the common chimpanzee subspecies is still small, but it is now equivalent or even larger than distances between several modern human groups, and those between the Upper Paleolithic group and most recent human populations (see Tables 4.32 and 4.37).

Table 3.38: Cross-validation classification summary (percentages for populations in bold), Step 3B.

	Bon	Sch	Trg	Total
Bon	27	6	1	34
%	**79.41**	17.65	2.94	100
Sch	4	19	7	30
%	13.33	**63.33**	23.33	100
Trg	1	2	25	28
%	3.57	7.14	**89.29**	100
Total	32	27	33	92
%	34.78	29.35	35.87	100

Table 4.39: Mahalanobis D^2 distances (Step 3B). All distances significant to the 0.001 level, except NS = non-significant, * = significant to the 0.05 level, ** = significant to the 0.01 level.

	Bon	Sch	Trg
Bon	0	8.54	16.8
Sch	8.54	0	7.4
Trg	16.8	7.4	0

Discussion

***Modern Humans*:** The mean human configuration shows a relatively rounded lateral profile from lambda to hormion, with a supero-inferiorly tall occipital plane relative to the nuchal plane and with a wide angle between the occipital and nuchal planes, both when compared to chimpanzees and to the fossil humans. As expected, it is most similar to the mean Upper Paleolithic configuration. There is wide variation in centroid size among modern human groups, the Andamanese being the smallest. Some geographic clustering is observed among modern human populations in Step 1, where two of the geographic pairs (the European and Australo-Melanesian pairs) are grouped together. After removal of hormion in Step 2, only the European pair clusters together. Even this relationship breaks down in Step 3, after removal of eight additional landmarks, and here only the Berg show the closest distance to the mixed European group, but not vice versa.

Within the modern human sample, females tend to have supero-inferiorly taller occipital squama, with relatively higher occipital plane and less posteriorly projecting inion, more posteriorly placed medial ends of the jugular fossae (probably indicating more antero-posteriorly restricted jugular fossae) and a medio-laterally wider foramen magnum.

***Chimpanzees*:** The greatest differences observed are between the mean configurations of modern humans and chimpanzees, as expected. Chimpanzees differ in having a supero-inferiorly shorter occipital squama, with a supero-inferiorly shorter occipital plane and a longer nuchal plane, and an antero-posteriorly longer clivus. In all steps they are separated from the human sample along the first principal component and canonical axis of the combined sample analysis. The axes separating chimpanzees from humans are invariably relatively strongly correlated with size. This correlation becomes much smaller when the chimpanzee sample is removed from the analysis. This would suggest that the differences between chimpanzee and human occipital bones are at least partly allometric. However, when PC 1 and CaV 1 of the combined analyses are regressed against centroid size and the regression lines calculated for each population, the regression lines across genera and across populations are not parallel to the average regression line or, in some cases, to each other. This pattern indicates that the different

populations behave in different ways along these axes relative to centroid size. Therefore, a correction for centroid size-related shape differences by regressing out centroid size cannot be attempted, as it would correct for shape differences along the average, meaningless, regression line. The shape differences between the chimpanzee occipital bones are probably not simply allometric. The strong correlation between centroid size and the axes separating humans from chimpanzees may instead reflect taxonomic differences, rather than simply size differences, since centroid size in the human sample is much greater than that in the chimpanzee sample.

Neanderthals: The mean modern human configuration differs from the mean Neanderthal configuration in having a slightly more inferiorly placed lambda, an elevated inion and lateral ends of the superior nuchal line, more laterally placed asteria and lateral ends of the superior nuchal line, and elevated basion and opisthion. These differences are consistent with previous descriptions of the Neanderthal occipital bone, which is sometimes described as supero-inferiorly compressed, and includes a medio-laterally broad and supero-inferiorly short occipital plane with a depressed lambda and superiorly placed inion and (McCown and Keith 1937; Heim 1974; Thoma 1975; Condemi 1992; Wolpoff et al. 2001). The elevated position of basion relative to hormion observed in Step 1 is also in agreement with the flat cranial base flexure observed in Neanderthals (Laitman and Heimbuch 1982; Lieberman 1989). However, only Saccopastore 1 is complete enough to be assessed in this fashion. Furthermore, additional landmarks, such as staphylion, are required for proper assessment of this trait.

Although these shape differences are found to characterize Neanderthals in both the principal component and the canonical variates analysis (e.g. PC 2 and CaV 2 of Step 1A, PCs 2 and 3 and CaV 2 of Step 2, and PC 2 and CaV 3 of Step 3), the Neanderthal sample is never clearly separated from modern humans, and Neanderthals are never significantly different from all modern human populations in their mean scores. This is perhaps not surprising, as the occipital landmarks analysis failed to quantify the aspects of the occipital bone morphology that are most diagnostic for Neanderthals, such as the occipital bun and the morphology of the occipital torus, due to the lack of appropriate landmarks in the occipital squama. Neanderthals are better separated from modern humans in Step 3, perhaps due to their increased sample size. However, the inclusion of

Amud 1, a highly asymmetric specimen may also have influenced this result. To test this hypothesis, the analysis was repeated without this specimen. The distances between Neanderthals and modern human population was slightly reduced, but not enough to change the position of this fossil group.

Neanderthals overlap most with the Berg population of Austria, and are closest to them in Mahalanobis distance. Relative to the other modern human groups the Berg are also characterized by an anterior and slightly inferior placement of lambda, as well as a medio-laterally wide occipital plane, shape differences that are also typical of the Neanderthal sample. Neanderthals are somewhat close to the Upper Paleolithic specimens (3rd closest in Step 2B and 3B). They are more distant from most modern human populations than modern groups are from one another, the smallest distance between Neanderthals and a modern human group being in the range of the largest distances among modern human populations. However, the Upper Paleolithic group is as distant, or slightly more distant, from the recent human populations in Steps 1 and 2. In Step 3 the distances between the Upper Paleolithic group and modern human populations are markedly reduced, and are in most cases not statistically significant (see below), while the distances between Neanderthals and modern humans remain similar to those in Steps 1 and 2.

The overlap between Neanderthals and modern humans is evident in the cross-validation classification results also, where only between two and four Neanderthals specimens were correctly classified. Classification success for these fossils increased somewhat in Step 3, probably due partly to their increased sample size, although it decreased for the modern human groups. Furthermore, in both Steps 2 and 3, with the exception of Step 2A, some modern human specimens were misclassified as Neanderthal. These misclassifications increased in Step 3 despite the better classification success for Neanderthals.

In the cluster diagrams of Step 2 Neanderthals cluster with the Upper Paleolithic group in a branch that is the outlier to all other modern human groups and that is relatively widely separated from them. This pattern is reversed in Step 3, where Neanderthals appear as the outliers to all other human groups and the Upper Paleolithic group clusters closely with the Berg population. Neanderthals are linked to the Berg

population as their closest neighbors in the minimum spanning trees.

Although Neanderthals appear quite distant from modern human groups in the Mahalanobis D^2 analysis, the great overlap observed here between them and modern humans differs from the results of previous analyses of cranio-facial measurements of distances, angles and indices (Stringer 1974a, 1992b; Bräuer and Rimbach 1990; Kidder et al. 1992; Turbón et al 1997), where a great separation was observed between Neanderthals and modern human individuals. This difference is probably due to the lack of representation of diagnostic anatomy. Aside from the occipital bun, occipital torus and suprainiac fossa morphology, which could not be assessed here due to the lack of appropriate landmarks, the Neanderthal occipital bone does not strongly differentiate this group from modern humans (Spitery 1985). Furthermore, the relatively small distance of Neanderthals to the European Berg population in this analysis also differs from these previous analyses, where Neanderthals were not shown to be consistently closer to modern Europeans relative to other modern human groups. As noted above, this similarity is limited to a single aspect of their cranial morphology, the width and height of the occipital plane of the occipital squama. The results of the present study are consistent with previous findings, however, in that Neanderthals are quite distant from the Upper Paleolithic sample.

***Kabwe*:** This specimen is very different from the mean modern human configuration in several ways. Lambda is more inferior and inion more posterior and superior, indicating a supero-inferiorly short occipital plane with a posteriorly projecting inion. In addition to inion, the lateral ends of the superior nuchal line are also elevated, reflecting again the small height of the occipital plane. Opisthion is placed superiorly, and the nuchal plane is elevated and long relative to the short occipital plane, and lies almost on the same plane as the foramen magnum. This configuration also shows a relatively sharp angle between the occipital and nuchal planes. Other differences include the more anterior placement of the lateral ends of the inferior nuchal line (marking the anterior extension of this line between the attachment sites of the rectus capitis posterior major and the superior oblique muscles) and the more anterior and inferior placement of the medial and lateral ends of the jugular fossae.

These differences are evident in the principal components and canonical variates analyses, where Kabwe falls at the extreme of, or outside, the modern human range and 95 % confidence ellipse along PC 1 in all steps, CaVs 2 and 5 (Steps 1A, 2A), CaVs 1 and 3 (Step 3A), CaV 4 (Steps 1B and 2B) and CaV 2 (Step 3B). This separation reflects its short occipital plane and a relatively long nuchal plane, its antero-posterior elongation of the occipital plane and posterior protrusion of inion, and its elongated nuchal plane relative to its short occipital plane.

Kabwe differs from the early anatomically modern humans and from the Upper Paleolithic specimens in the same ways that it differs from modern humans. Compared to the mean Neanderthal configuration, it shows again a supero-inferiorly shorter occipital plane, with an inferiorly placed lambda and an elevated inion and lateral ends of the superior nuchal line. This is in agreement with the finding that the height of the occipital plane increases relative to that of the nuchal plane through human evolution, Neanderthals falling at the lower end of the modern human range of variation for this trait (e.g. Condemi 1992). Inion is also more posteriorly projecting, and opisthion elevated in Kabwe, even though this landmark also appears elevated in Neanderthals relative to modern humans. When compare to Biache, the same kind of differences are apparent, although the difference in the height of the occipital plane is less strong. Petralona is very similar to Kabwe in the relative dimensions and orientation of the nuchal plane. Opisthion and inion are as elevated as in Kabwe, showing a similar elevated position of the nuchal plane and an orientation almost on the plane of the foramen magnum. Inion, however, projects posteriorly even more in Petralona, and the occipital plane is higher and much wider medio-laterally.

In the Mahalanobis D^2 analysis, Kabwe is closest to the Upper Paleolithic (Step 1A) and the Eskimo populations (Step 1B), although it is widely separated from all groups. In Step 2, where Neanerthals are included as a population, it is by far closest to the Neanderthal sample (Steps 2A and 2B). In Step 3 it is again closest to Neanderthals (Step 3A) and to Reilingen (Step 3B). Kabwe is also relatively close to Petralona and Biache in Step 3. It is classified as Eskimo by posterior probability in Step 1, and as Neanderthal in Steps 2 and 3. These results are consistent with the findings of Stringer (1974a, b), who, in a multivariate analysis of cranio-facial measurements of the Later

Pleistocene fossil hominid record, found Kabwe to be widely separated from modern human groups and the Upper Paleolithic specimens and to display some affinities to Neanderthals, although also relatively distant from them. The present study also found evidence for some similarities between Kabwe and Petralona, as noted in Stringer et al. (1979) and others (Stringer 1985; Vandermeersch 1985; Rightmire 1988, 1990).

Petralona: This specimen was only included in Step 3 due to its state of preservation. When compared to the mean modern human configuration, Petralona exhibits an elongated nuchal plane relative to the occipital plane and a relatively low angle between the two. Inion is elevated and posteriorly projecting, while the lateral ends of the superior nuchal line are slightly elevated, and posteriorly and laterally positioned. As in Kabwe, opisthion is also elevated, bringing the plane of the nuchal plane almost in a straight line with the plane of the foramen magnum. Furthermore, asteria are laterally placed, indicating a medio-laterally wide occipital squama. Petralona differs in very similar ways from the early anatomically modern and Upper Paleolithic specimens.

When compared to the mean Neanderthal configuration, it also differs from it in similar ways. The differences in the position of inion and asteria, however, are less pronounced, as Neanderthals also exhibit an elevated inion and laterally placed asteria relative to modern humans. The same holds for the comparison between Petralona and Biache. Petralona is most similar to Kabwe, although more extreme, in the posterior projection of inion. It is also similar in the relative dimensions and position of its nuchal plane, although its occipital plane is much wider medio-laterally and also relatively taller (see above). Similarities between these two fossil human specimens have been noted before (Kokkoros and Kanellis 1960; Stringer 1974a, b, 1985; Stringer et al. 1979; Rightmire 1988, 1990; Seidler et al. 1997), as well as the of the Petralona vault morphology to Neanderthals (Stringer 1974a, b, 1985; Vandermeersch 1985). These shape differences of Petralona from modern humans and Neanderthals are consistent with previous descriptions of this specimen (Stringer et al. 1979), where the elongation of the nuchal plane, the strong angulation between the nuchal and occipital planes, and the marked posterior projection of the iniac area were noted.

The same shape differences, and particularly its medio-laterally wide occipital plane, and a sharp angle between the occipital and nuchal planes, are responsible for the

separation of Petralona from modern humans along PC 2 and CaV 3 (Step 3A), the same axes that also tend to differentiate Neanderthals from modern humans. Petralona also falls near the extreme of the modern human range along PC 1 and CaV 1 near Kabwe in all analyses, and this similarity is due to mostly to the superior and posterior position of inion and the orientation of the nuchal relative to the occipital plane in the two specimens. In the Mahalanobis D^2 analysis, Petralona is closest to the Neanderthals (Step 3A) and to the Skhul 5 - Qafzeh 9 group (Step 3B). It is widely separated from modern human groups. These results are in agreement with the findings of Stringer's (1974) multivariate study, which found this specimen to show different degrees of resemblance to Neanderthals according to the subset of variables used. As in Stringer's analysis of the occipital and parietal variables, the distance between Petralona and Kabwe is non-significant. Petralona is classified as Neanderthal by posterior probability in all analyses of Step 3.

Biache: This specimen was only included in Steps 2 and 3. When compared to the mean modern human configuration, it shows a posteriorly and superiorly placed inion, an inferiorly placed lambda and a somewhat elevated opisthion. In all of these differences Biache appears intermediate between Neanderthals on one hand and Petralona and Kabwe on the other.

These shape characteristics separate Biache from modern humans along several axes (e.g. CaV 3, Step 3A, CaV 2 Step 3B), and the separation along both these axes is driven by the elevated and posteriorly projecting position of inion, the elevated opisthion, laterally placed asteria and the inferiorly placed lambda. In the Mahalanobis D^2 matrices this specimen is closest to Neanderthals in Step 2, while in Step 3 it is closest to Kanalda (non-significant distance) and to the Neanderthals. It is always classified as Neanderthal by posterior probability. These results are consistent with the Neanderthal affinities noted for this specimen (Vandermeersch 1985; Stringer 1985).

Reilingen: This specimen was only included in Step 3. When compared to the mean modern human configuration, Reilingen shows a much more posteriorly projecting and somewhat elevated inion and lateral ends of the superior nuchal line, with a slightly inferiorly placed lambda and laterally placed asteria. It differs from the Neanderthal average configuration in having a more posteriorly projecting inion. It differs from

Biache in its more posteriorly projecting inion and its medio-laterally wider occipital plane, and from Kabwe in its more inferiorly placed inion and higher occipital plane. It differs from Kabwe in having a slightly shorter and narrower occipital plane and a more superiorly placed inion. These differences are consistent with the morphological description of this specimen (Dean et al. 1998), which notes the large biasterionic breadth, the superior position of inion, the supero-inferiorly short occipital plane with lambdoid flattening, the presence of an incipient 'bun' and a suprainiac fossa. Dean and his co-authors found the external occipital morphology of this specimen to align it with Neanderthals.

In the present analysis, Reilingen is separated from the modern human range in the same axes that partially differentiate Neanderthals (CaV 3 of Step 3A and CaV 2 of Step 3B). The separation is due to the medio-laterally wide occipital plane, the sharp angle between the occipital and nuchal planes and the posterior projection of inion characterizing this specimen. In the Mahalanobis D^2 analysis, Reilingen is closest to the Skhul 5 - Qafzeh 9 group, as well as to Kabwe and Petralona (all three non-significant differences). It is classified as Neanderthal. These findings partially agree with the study of Dean et al. (1998), who found this specimen to be closest to Petralona, and classified it as Neanderthal based on general morphology and morphometric analysis of linear cranial measurements and three-dimensional ridge curves. The very small distance between this specimens and the early modern human group of Skhul and Qafzeh found in the present analysis, however, is unexpected.

Early anatomically modern humans: This group comprises only two specimens in this analysis, Skhul 5 (Steps 1-3) and Qafzeh 9 (Step 3). Compared to the mean modern human configuration, Skhul 5 shows a more posteriorly projecting and elevated inion, as well as an inferiorly placed lambda. The left asterion is also more laterally placed than the right one, showing a relatively high level of right - left asymmetry or warping (see also McCown and Keith 1937, p. 249 and Fig. 177). Compared to the mean Neanderthal configuration, this specimen again shows a more posterior placement of inion and a sharper angle between the lower occipital scale and the plane of the foramen magnum. These differences are consistent with the development of a robust occipital

torus and an external occipital protuberance and with the lambdoid flattening described for this specimen (McCown and Keith 1937; Vandermeersch 1981).

The configuration of Qafzeh 9 is very similar to the mean modern human configuration, showing only a slightly less posteriorly projecting inion and more posteriorly placed lambda. It differs from Neanderthals in having a higher occipital plane, a less posteriorly projecting inion, and a wider angle between the occipital and the nuchal plane. This specimen also exhibits strong warping, which is evident in the much more anterior, inferior and medial placement of the right asterion relative to the left. The right-left displacement of this crushed and heavily reconstructed specimen was also noted by Vandermeersch (1981), who described the dissimilarity in the two asterionic regions. The shape characteristics found here are similar to those previously reported for this specimen. Qafzeh 9 is described as having a rounded posterior cranial profile with no strong external occipital protuberance, no lambdoid flattening and a wide angle between the occipital and nuchal planes (Vandermeersch 1981).

Both of these specimens, and particularly Qafzeh 9, are separated from modern humans in the principal components and canonical variates analyses. Skhul 5 is separated along PC 6 in Step 2A, PC 1 and CaV 3 in Step 3A, CaV 4 in Step 3B, reflecting its anterior placement of lambda and posterior projection of inion. Qafzeh 9 is separated along PC 6 and CaV 3 of Step 3A, and PC 2 and CaV 2 of Step 3B. For both these specimens the right - left warping of their occipital bone contributes to some degree to their separation in these analyses. This is particularly true for Qafzeh 9, which does not otherwise exhibit substantial differences from the modern human mean configuration and is described as very modern and gracile in its occipital morphology.

In the Mahalanobis D^2 analysis, Skhul 5 is closest to the Berg (Step 1A, 2A and 2B) and the Europeans (Step 1B). The combined Skhul 5 and Qafzeh 9 group in Step 3 is closest to Reilingen (non significant distance). Skhul 5 is classified as Berg (Steps 1A and 2A) and European (Steps 1B and 2B) by posterior probability. Qafzeh 9 and Skhul 5 were both classified as Neanderthal in Step 3.

The results of Step 3 are contrary to the findings of the morphological descriptions of these specimens, which emphasize their similarities to modern humans rather than Neanderthals (McCown and Keith 1937; Vandermeersch 1981). They also

disagree with other multivariate analyses of the Late Pleistocene human fossil record, which, based on craniofacial measurements, have placed these specimens closer to modern human populations rather than to Neanderthals, although somewhat removed from modern human groups (Stringer 1974a,1992b; Howells 1989; Bräuer and Rimbach 1990; Brauer 1992; Turbón et al. 1997). Other multivariate analyses (Kidder et al. 1992), however, have placed these specimens outside the range of modern human variation based mainly on measurements of the neurocranium. As these results are inconsistent with those of Steps 1 and 2, the factors contributing to this change are either the addition of Qafzeh 9 and additional Neanderthal specimens, or the removal of particular landmarks. When the analysis was repeated with the fossil sample used in Step 2 and the landmark set used in Step 3, however, results were similar to Step 2. Step 3, therefore, is influenced by the warped nature of Qafzeh 9, which is probably aligning this group with other somewhat deformed fossil material. One Neanderthal specimen in particular, Amud 1, displays a pattern of warping very similar to that of Qafzeh 9.

Upper Paleolithic specimens: The sample used in this chapter comprised five Upper Paleolithic specimens, present in all three steps. The mean configuration of this group is very similar to that of modern humans, differing only in the slightly more posterior and superior projection of inion, more inferior placement of opisthion, the more anterior position of lambda, the somewhat more medial placement of asteria, and the more anterior placement of basion and the medial ends of the jugular fossae. These specimens differ from the mean Neanderthal configuration in similar ways as modern humans do: in their supero-inferiorly higher and medio-laterally wider occipital plane, the more posteriorly projecting inion, and the more inferior placement of opisthion and lower angle between the nuchal plane and the plane of the foramen magnum. Additionally, they also differ in the more anterior placement of basion.

These differences are consistent with the previous descriptions of these specimens as essentially modern in their morphology but very robust, exhibiting strong external occipital protuberances, a flattened and elongate nuchal plane, lambdoid flattening and occipital hemibuns (Ducros 1967; Jelinek 1969; Billy 1970; Genet-Varcin 1970; Vandermeersch 198; Smith 1982; Gambier 1989; Churchill and Smith 2000). The anterior position of the foramen magnum and anterior ends of the jugular fossae also

indicate a difference in the antero-posterior length of the condylar parts of the occipital bone.

These differences partially separate the Upper Paleolithic specimens from modern humans along several axes in Steps 1 and 2 (PC 6 and CaV 5 in Step 1A, PC 6, CaV 3 and 5 in Step 2A, CaVs 3 and 4 in Step 1B, PC 4 and CaV 3 in Step 2B). In the analyses of Steps 1 and 2 the separation between this group and modern humans is stronger than that between Neanderthals and modern humans. This is also observed in the Mahalanobis distances, where the Upper Paleolithic specimens are equally or more distant from the recent human groups than Neanderthals are. In both steps the Upper Paleolithic specimens are closest to the Epipaleolithic population. They are not close to the Neanderthals, but not the most distant group from them either. This situation is reflected in the cluster analysis, where the Upper Paleolithic group clusters with Neanderthals on a long branch that is the outlier to all recent human groups. In the minimum spanning trees this group is linked to the Epipaleolithic as their nearest neighbor in both Steps 1 and 2.

In Step 3, however, the Upper Paleolithic population is no longer separated from modern humans, and the Mahalanobis distances between it and most recent human groups are very small and not significant. Neanderthals are better separated in this step and are much more distant in Mahalanobis D^2 from the recent groups than the Upper Paleolithic specimens are, although the distances between Neanderthals and recent humans are also somewhat reduced. In the cluster analyses of Step 3 Neanderthals are outliers to all other human groups, while the Upper Paleolithic specimens fall within the modern human branch and cluster very closely with the Berg. Unlike Steps and 2, the Upper Paleolithic group occupies a central position in the minimum spanning trees of Step 3, being linked to the Berg and the San (Step 3A) or the Berg, Epipaleolithic and San (Step 3B).

This marked change in the position of the Upper Paleolithic group in Step 3 is the result of the removal of basion, opisthion and the landmarks on the anterior ends of the jugular fossae. It appears that these landmarks contribute greatly to the differentiation between these specimens and recent human populations. This is also reflected in the results of the cross-validation classification, which is most successful for the Upper

Paleolithic group in Step 2 (2-3 specimens classified correctly) and Step 1 (2 specimens classified correctly). None of the individuals in this sample was correctly placed in Step 3. Furthermore, the rate of misclassification of recent human specimens into this group also increased markedly in this step (16-17 specimens compared with 1-3 specimens in all analyses of Steps 1 and 2).

The Upper Paleolithic European specimens have been found to show morphological similarities to the Epipaleolithic specimens from North Africa (Ferembach 1962, 1985; Chamla 1978). These two groups have also shown affinities in metric studies using multivariate analyses of cranio-facial measurements (Turbón et al. 1997), while a strong resemblance has also been noted between the earlier North African specimen Dar –es Soltan 5 and Upper Paleolithic Europeans (Bräuer 1992; Bräuer and Rimbach 1990). Steps 1 and 2 of this analysis agree with these findings, as the Upper Paleolithic sample is placed nearest to the Afalou-Taforalt Epipaleolithic population from North Africa. The results of Step 3, however, place the Upper Paleolithic group closest to the European populations. This result is not consistent with the findings of previous craniometric studies, and may be due to the very small number of landmarks included in this step. Finally, in none of these analyses did this group exhibit particular affinities with the Neanderthal sample. Several morphological studies (Genet-Varcin 1970; Vlcek 1970; Smith 1984; Bräuer 1989; Wolpoff et al. 2001) see Neanderthal-like traits in the morphology of the occipital bone of this group, which is interpreted as evidence for continuity or interbreeding between these two populations. These affinities are thought to be stronger in the Central European Upper Paleolithic sample. A metrical study using multivariate statistical techniques on neurocranial measurements also found evidence for Neanderthal-like morphology in the subsample of Central Upper Paleolithic specimens (Kidder et al. 1992). No such evidence was found here, although the Western and Central European Upper Paleolithic specimens were combined in one sample in this analysis.

In summary, in the occipital bone landmark analysis Neanderthals show wide overlap with modern humans, consistent with previous analyses of measurements of the occipital bone, and also probably due to the lack of representation of the Neanderthal features of this area by the landmarks used. However, Neanderthals are still quite distant

from most modern human populations, except the European Berg group. The Upper Paleolithic specimens are also widely separated from recent human groups, but this distance greatly diminishes with the removal of most nuchal plane landmarks in Step 3. The separation between this group and recent humans is driven by the posterior projection of inion and the elongation of the nuchal plane in the antero-posterior dimension. Skhul 5 and Qafzeh 9 exhibited a high degree of asymmetry due to deformation. Not all geographic pairs of modern human populations cluster geographically in this analysis. Their geographic signal deteriorates with the removal of additional landmarks.

CHAPTER 5
Midline Ridge-Curves

Several of the traits thought to differentiate Neanderthals from modern humans and not included in the two landmarks analyses should be captured by the ridge curve from bregma to opisthion. The occipital 'bun', or chignon, encompasses the posterior projection of the occipital squama, and is associated with flattening at lambda and its adjacent area on the parietals and occipital. This trait has been cited widely as characteristic of Neanderthals (Boule 1911-1913; Thoma 1965; Hublin 1978b; Stringer et al. 1984; Sergi 1991; Condemi 1991; Dean et al. 1998), and has been claimed to be a Neanderthal autapomorphy (Hublin 1988a; Lieberman 1995; Dean et al. 1998), although this feature is difficult to assess and measure (Ducros 1967; Dean et al. 1998). The presence of a weak occipital bun or 'hemibun' in many Upper Paleolithic European specimens has also been seen as evidence of continuity or interbreeding between them and Neanderthals, particularly in the Central European fossil record (Jelinek 1969; Genet-Varcin 1970; Vlcek 1970; Smith 1982, 1984; Bräuer 1989; Gambier 1997; Churchill and Smith 2000; Wolpoff et al. 2001). However, the validity of the chignon as a Neanderthal derived trait and its usefulness in phylogenetic reconstruction has been questioned. Trinkaus and Le May (1982) saw it as a developmental featured shared by many other fossil and modern human specimens. In a study of the occipital morphology of fossil and modern humans, Spitery (1985) found the posterior projection of the occipital plane in Neanderthals, although strong, to be within the modern human range of variation. Yaroch (1996) concluded that this feature does not differentiate Neanderthals from modern humans. Other workers have suggested that the hemibuns present in many Upper Paleolithic European specimens are of a different shape than, and not homologous to, the occipital buns of Neanderthals (Ducros 1967; Lieberman 1995; Lieberman et. al 2000).

The suprainiac fossa, an oval depression above the occipital torus, is another proposed Neanderthal derived trait (Santa Luca 1978; Hublin 1978, 1988; Condemi 1991, 1992; Lieberman 1995). However, recent studies have found that it is the shape of this fossa, rather than simply its presence, that is a Neanderthal derived feature (Hublin 1988a; Bräuer and Broeg 1998). Finally, Neanderthal crania are described as platycephalic, with flat parietals and low vaults relative to modern humans (Boule and

Vallois 1957; Heim 1974, 1976; Stringer and Trinkaus 1981; Trinkaus 1983), a primitive condition. Some Neanderthal specimens, however, such as Shanidar 1 and 2, show a stronger curvature of the parietal, falling in this trait within the range of modern humans (Stringer and Trinkaus 1981; Trinkaus 1982, 1983).

As in the previous chapters, analysis was undertaken in steps so as to include as many ridge curve segments and as many specimens as possible (Table 5.1). The steps followed in this chapter are as follows: Step 1 includes three line segments forming a complete curve from bregma to opisthion. Step 2 includes two line segments, forming a line from lambda to opisthion, while Step 3 includes the two line segments from bregma to inion. No reconstruction of this ridge curve was undertaken, as it is a midline outline, and this study allowed only mirror imaging reconstruction of missing data. As described in Chapter 2, in each step the analysis was repeated A) on the combined chimpanzee and human sample; B) on the human sample only; and C) on the chimpanzee sample only.

Step 1 – Bregma-Opisthion

This step was conducted using all three line segments from bregma to opisthion. Four Neanderthal specimens were complete enough to be included: La Chapelle, La Ferrassie 1, Shanidar 1 and Saccopastore 1. Petralona, Biache, Singa and Kanalda were also included, as were Skhul 5 and four Upper Paleolithic specimens, Predmosti 3 and 4, Cro Magnon 1 and Ein Gev. Among modern human groups, the Epipaleolithic population is represented here by a reduced sample of 19 individuals (Table 5.1).

Centroid Size: An analysis of variance (ANOVA) was conducted on centroid size to test for significant effects for population and sex and interaction between the two. Both sex and population effects were significant to the 0.0001 level. A significant interaction effect was also found (0.01). A one-way ANOVA was also conducted to test for significant species and genus effects.

Chimpanzees are much smaller than humans in their mean centroid size and standard deviation, and this difference is even greater than that observed in the occipital bone landmarks analysis. The chimpanzee mean centroid size is significantly smaller than that of humans at the genus level. The mean values for all three chimpanzee taxa are

Table 5.1: Number of landmarks, semilandmarks and specimens in each step of analysis.

	Landmarks	Semilandmarks	Modern Human	Chimpanzees	Neanderthals	AMH	Other
Step 1	4 (Lambda, Inion, Opisthion, Bregma)	27	245	91	Saccopastore 1 La Chapelle La Ferrassie 1 Shanidar 1	Skhul 5 Cro Magnon 1 Predmosti 3 Predmosti 4 Ein Gev	Kanalda Petralona Biache Singa
Step 2	3 (Lamdba, Inion, Opisthion)	15	251	92	Saccopastore 1 La Chapelle La Ferrassie 1 Shanidar 1 Gibraltar 1	Skhul 5 Cro Magnon 1 Predmosti 3 Predmosti 4 Ein Gev	Kanalda Petralona Biache Singa
Step 3	3 (Lambda, Inion, Bregma)	25	249	92	Saccopastore 1 La Chapelle La Ferrassie 1 Shanidar 1 Amud 1 Circeo 1 La Quina 5 Tabun C1 Spy 1	Skhul 5 Cro Magnon 1 Predmosti 3 Predmosti 4 Ein Gev Cro Magnon 2 Mladec 1 Skhul 9	Kanalda Petralona Biache Singa Reilingen

Table 5.2: Centroid size by genus, species, sex and population, Bregma-Opisthion (Step 1).

	Mean	Range	St.Deviation	N
Homo	**32.73**	**27.68-37.49**	**1.81**	**259**
Males	33.28	29.66-37.49	1.72	136
Females	32.12	27.68-36.04	1.70	121
Modern	32.76	27.68-37.49	1.81	251
Males	33.32	29.66-37.49	1.72	130
Females	32.13	27.68-36.03	1.70	120
Neanderthals	32.52	30.72-35.12	1.97	5
Males	32.12	31.30-35.12	1.92	3
Females (Saccopastore 1)	30.72	---	---	1
Biache	29.32	---	---	1
Petralona	31.85	---	---	1
Skhul 5	33.12	---	---	1
Singa	32.29	---	---	1
Upper Paleolithic	34.36	33.72-35.29	0.69	4
Kanalda	35.99	---	---	1
Andamanese	31.10	28.38-34.64	1.43	29
Australian	32.59	30.08-35.81	1.65	29
Berg	32.90	29.66-35.29	1.37	29
Dogon	31.90	29.24-35.04	1.26	30
Epipaleolithic	35.13	33.08-37.49	1.24	19
Eskimo	33.92	30.67-37.17	1.49	29
European (mixed)	33.46	31.03-35.86	1.54	22
San	31.39	27.68-34.33	1.57	30
Tolai	33.21	31.81-35.76	1.00	28
Pan	**17.69**	**15.69-20.05**	**0.81**	**91**
Males	17.71	15.69-19.28	0.75	48
Females	17.72	15.81-20.05	0.85	41
P. paniscus	17.77	15.81-20.05	0.87	33
Males	17.70	16.66-19.28	0.72	15
Females	17.83	15.81-20.05	0.99	18
P. troglodytes	17.64	15.69-19.20	0.78	58
Males	17.70	15.69-19.06	0.77	33
Females	17.64	15.96-19.21	0.74	23
P. t. schweinfurthii	18.06	17.18-19.21	0.53	30
P. t. troglodytes	17.20	15.69-19.06	0.77	28

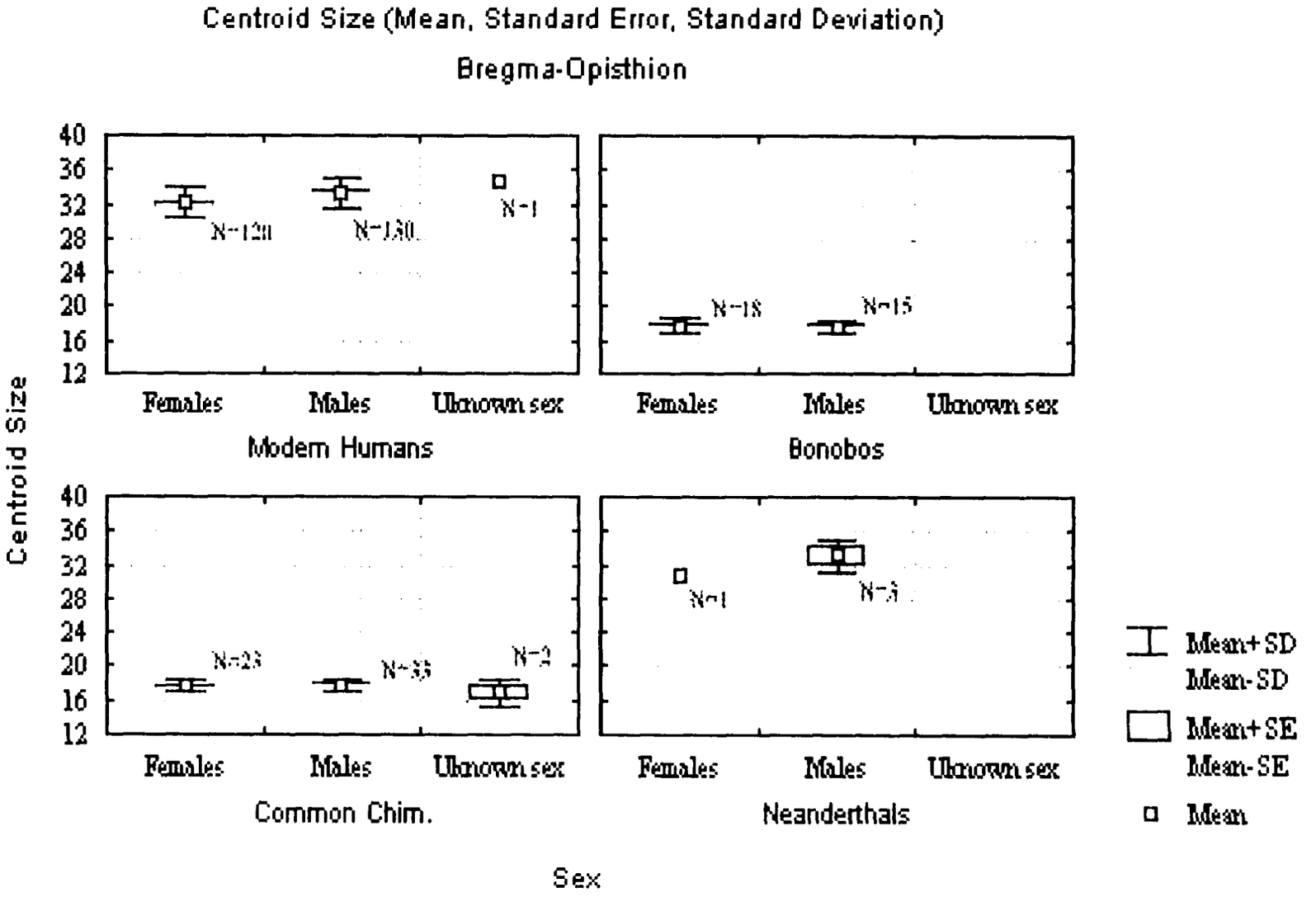

Figure 5.1: Centroid size mean, standard error and standard deviation, labeled by sex and species (Step 1).

also significantly smaller than those of all human groups at the population level.

Bonobos show a somewhat greater mean and standard deviation than common chimpanzees (Table 5.2, Fig.5.1), although the three chimpanzee taxa are not significantly different from each other in their mean centroid sizes both at the population and the species level. The mean centroid size for male chimpanzees is equivalent to that of females, while the standard deviation is greater in females. Among the two chimpanzee species, female bonobos show a higher mean and standard deviation than males. Common chimpanzees females, on the other hand, show a slightly smaller mean and standard deviation than males. Sexual dimorphism is very low in both chimpanzee species, females being slightly larger than males in bonobos, as was also found in the occipital bone landmarks analysis. At the population level, *P. t. schweinfurthii* has a larger mean value but a smaller standard deviation than *P. t. troglodytes*.

Among humans, Neanderthals show a mean centroid size value equivalent to that of modern humans and a slightly greater standard deviation. The mean value for the three Neanderthal male specimens is also larger than that of the only female Neanderthal included, Saccopastore 1. The centroid size for Petralona is relatively small, being smaller than the mean for modern human females. Biache is the smallest of the fossil specimens included here, being considerably smaller than the modern human female mean. The Upper Paleolithic specimens have a larger mean centroid size than modern humans but a much smaller standard deviation, indicating a high degree of homogeneity in centroid size in this group. Modern human females have smaller means than males, but their standard deviations are equivalent. Sexual dimorphism in modern humans is higher than in either chimpanzee species, males being larger than females.

At the population level, there is great variability in the means and standard deviations among modern human groups. The highest mean value is attained by the Epipaleolithic and the lowest by the Andamanese and the San. This result is consistent with centroid size analysis in the previous chapters. The Australians, the San and the mixed European groups have the largest standard deviation, perhaps reflecting the wide geographic origin in the case of the Australian and mixed European populations. The Melanesian Tolai population has the lowest standard deviation among all recent human groups, and is second only to the Upper Paleolithic group in the human sample.

Step 1A: Combined human and chimpanzee sample

Principal Components Analysis: A PCA was conducted on the variance-covariance matrix of the 93 coordinates. Table 5.3 summarizes the results of the PCA, as well as those of the ANOVA and Correlation Analysis. Table 5.4 shows the squared root of the sums of the squared three eigenvectors of each landmark or semilandmark, representing its three coordinates, for the first four principal components. As in the previous chapters, the landmarks and semilandmarks with the highest values for each principal component, presented here in bold, are discussed. They can be interpreted as driving the separation along that component. While the first principal component separates humans from chimpanzees, Neanderthals are only separated from the modern human sample on PC 3 and also partially on PC 4.

PC 1 (Fig. 5.2) explains 77.7 % of the total variance and is significant for population and sex effects (0.0001), as well as for interaction effects (0.01), but not for overall sex effects. It separates humans on its negative side from the chimpanzee sample on the positive side. All three chimpanzee taxa are significantly different in their mean scores from all modern human populations. PC 1 also partially separates bonobos from common chimpanzees, the former being closer to the human cloud, as well as *P. t. schweinfurthii* from *P. t. troglodytes*, although, at the population level, these three groups are not significantly different from one another in their mean scores. When the ANOVA is conducted at the species level, however, bonobos are significantly different from common chimpanzees. PC 1 does not separate Neanderthals, or any of the other fossil specimens, from modern humans, although Biache and Petralona fall towards the positive end of the modern human range of variation. Modern human populations overlap widely along this component, and are not significantly different from one another in their mean scores. When PC 1 is labeled by sex, females in both the human and chimpanzee samples tend to have more negative scores than males, but this tendency is stronger in the chimpanzee sample. When the mean scores for males and females are plotted by population (Fig. 5.3), the male means are more positive than the female ones in all three chimpanzee taxa, and in some modern human populations (but not in the San, Berg, European and Andamanese groups). The different trends among humans and chimpanzees are reflected in the significant interaction effect.

Table 5.3: Summary of the PCA results, ANOVA and Correlation Analysis for PCs 1-10, Step 1A.

	Principal Components Analysis			ANOVA, Pr > F			Correlation with Centroid size	
	Eigenvalue	Proportion	Cumulative	Popul.	Sex	Interaction	Rho	Pr > F
PC 1	0.006794	0.777272	0.777272	0.0001	0.0001	0.0051	-0.92508	0.0001
PC 2	0.000857	0.098022	0.875294	0.0001	0.0592	0.8345	0.00093	0.9861
PC 3	0.000386	0.044162	0.919456	0.0001	0.5085	0.248	0.03809	0.4781
PC 4	0.000314	0.035917	0.955373	0.0001	0.0195	0.0007	0.05218	0.3311
PC 5	0.000107	0.012268	0.967641	0.0001	0.8138	0.0172	0.0915	0.0879
PC 6	0.000047	0.0054	0.973041	0.0001	0.9149	0.0308	-0.1309	0.0144
PC 7	0.000039	0.004502	0.977543	0.0545	0.1286	0.0045	0.04063	0.4492
PC 8	0.00003	0.003394	0.980937	0.0005	0.5067	0.753	-0.03997	0.4567
PC 9	0.000023	0.00262	0.983557	0.0011	0.1355	0.7671	0.02344	0.6626
PC 10	0.000016	0.001844	0.985402	0.0002	0.2897	0.8476	0.00961	0.858

Table 5.4: Squared roots of the sum of squares of the eigenvector coefficients for the three coordinates of each semilandmark, Step 1A.

	PC 1	PC 2	PC 3	PC 4
Lambda (1)	0.19	**0.32**	0.09	0.16
Semilandmark 2	0.16	**0.26**	0.14	0.12
Semilandmark 3	0.14	0.20	0.19	0.10
Semilandmark 4	0.14	0.14	**0.22**	0.09
Semilandmark 5	0.16	0.08	**0.25**	0.10
Semilandmark 6	0.19	0.02	**0.27**	0.14
Semilandmark 7	**0.23**	0.04	**0.27**	**0.22**
Semilandmark 8	**0.28**	0.10	**0.24**	**0.30**
Inion (9)	**0.33**	0.16	0.18	**0.36**
Semilandmark 10	**0.24**	0.19	0.08	**0.25**
Semilandmark 11	0.18	0.19	0.05	0.14
Semilandmark 12	0.15	0.20	0.15	0.10
Semilandmark 13	0.16	**0.21**	**0.26**	0.18
Semilandmark 14	**0.22**	0.19	**0.36**	**0.26**
Opisthion (15)	**0.28**	0.17	**0.46**	**0.34**
Bregma (16)	**0.25**	**0.29**	0.09	**0.22**
Semilandmark 17	0.20	**0.26**	0.06	0.19
Semilandmark 18	0.16	**0.22**	0.03	0.17
Semilandmark 19	0.12	0.18	0.03	0.15
Semilandmark 20	0.08	0.14	0.06	0.13
Semilandmark 21	0.05	0.10	0.09	0.11
Semilandmark 22	0.03	0.07	0.12	0.08
Semilandmark 23	0.05	0.04	0.13	0.06
Semilandmark 24	0.08	0.03	0.14	0.05
Semilandmark 25	0.10	0.06	0.14	0.06
Semilandmark 26	0.12	0.10	0.14	0.09
Semilandmark 27	0.14	0.14	0.13	0.13
Semilandmark 28	0.16	0.17	0.11	0.16
Semilandmark 29	0.17	**0.21**	0.08	0.17
Semilandmark 30	0.18	**0.24**	0.04	0.18
Semilandmark 31	0.18	**0.28**	0.03	0.18

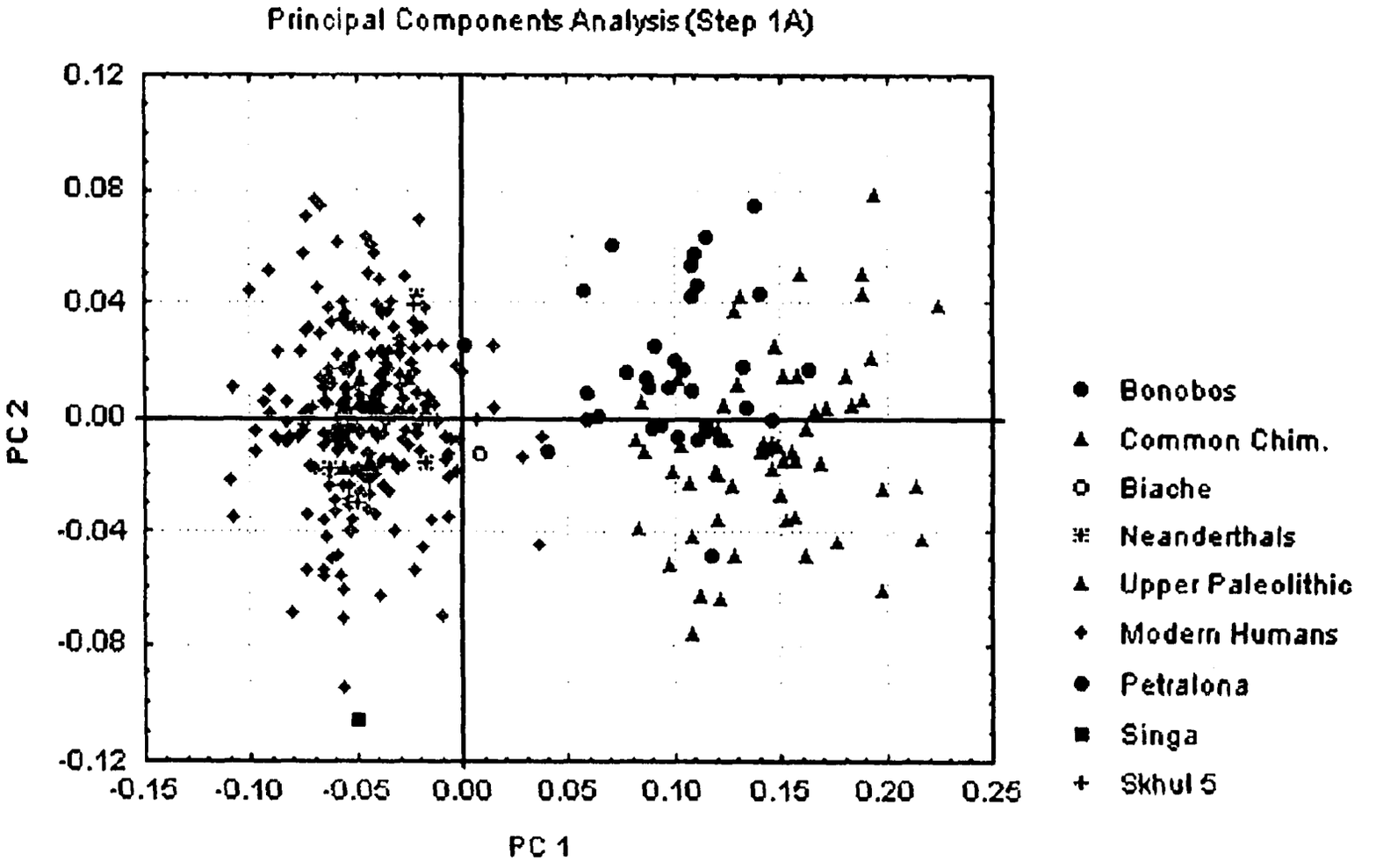

Figure 5.2: Principal Components Analysis (Step 1A), PCs 1 and 2.

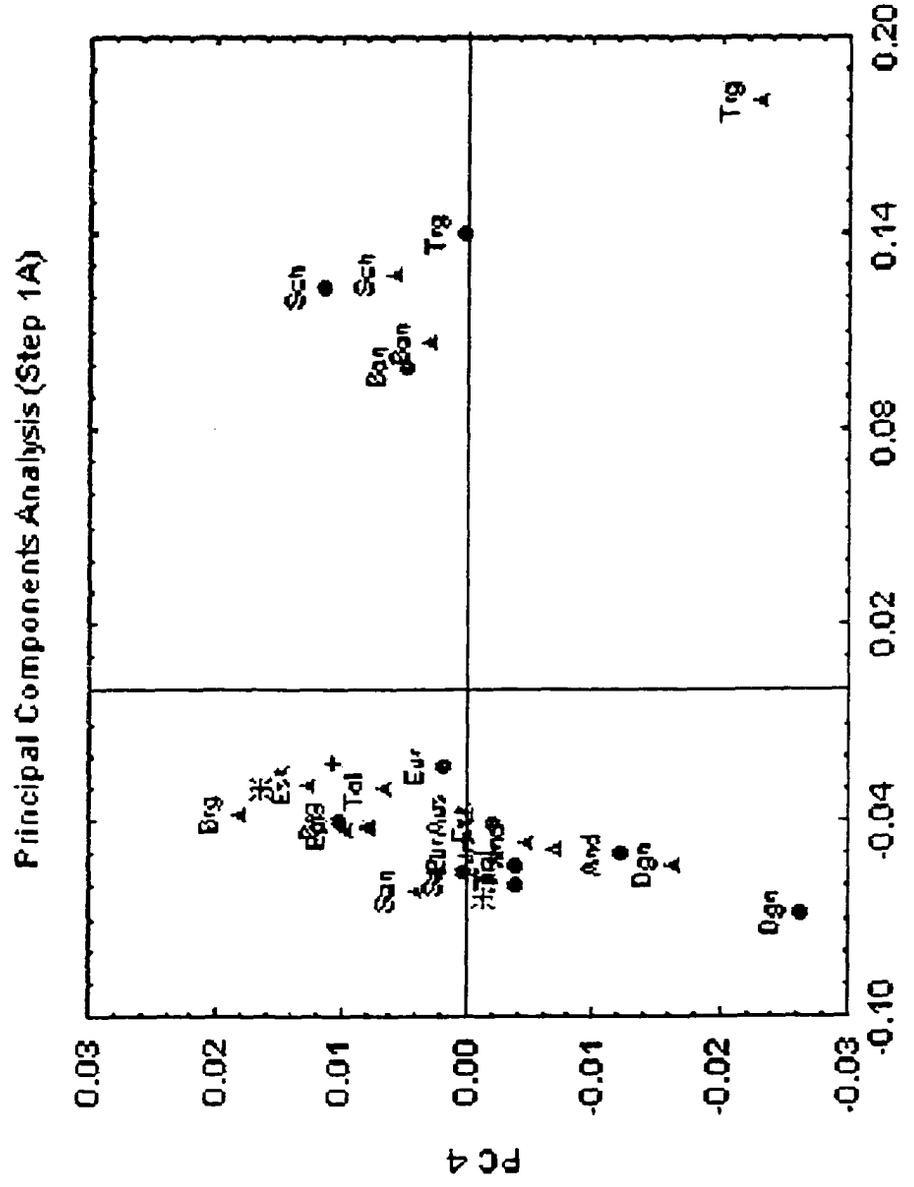

Figure 5.3: Principal Components Analysis (Step 1A), PCs 1 and 4, means for the two sexes plotted by population.

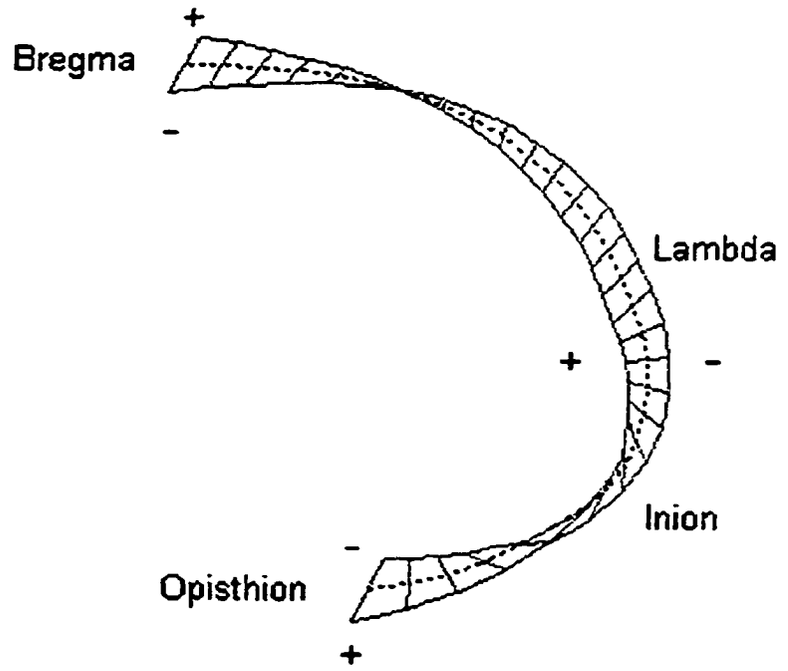

Figure 5.4: Shape variation along PC 1 (Step 1A). The dotted line represents the consensus configuration.

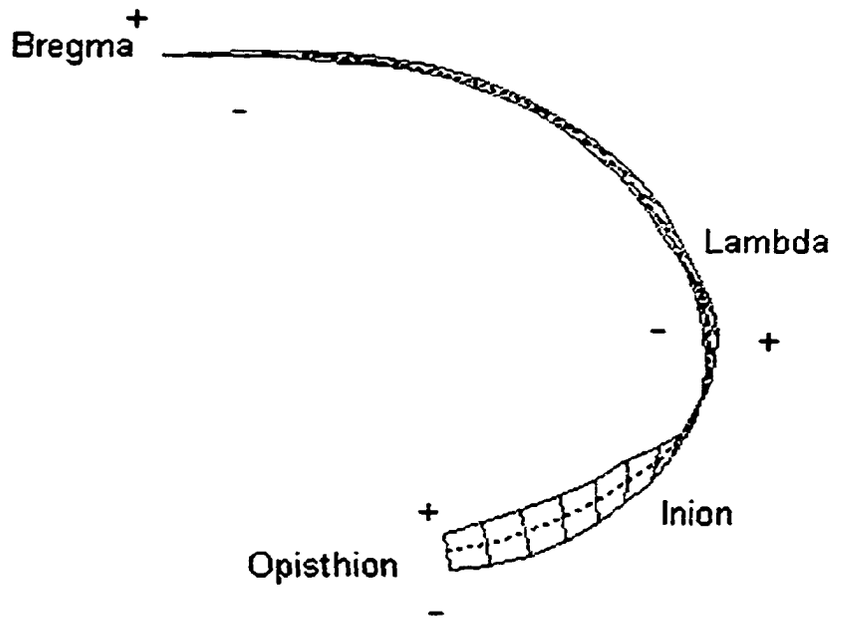

Figure 5.6: Shape variation along PC 2 (Step 1A). The dotted line represents the consensus configuration.

The most important shape differences driving the separation along PC 1 occur at landmarks or semilandmarks 9 (inion), 8, 15 (opisthion), 16 (bregma), 10, 7, 14 (Fig. 5.4). In the chimpanzee end, inion (9) and the semilandmarks around it (10, 8, 7) are elevated and posteriorly placed, while they are inferiorly and anteriorly placed in the human end; opisthion (15) and the semilandmarks around it (14) are more inferiorly placed in the chimpanzee end and elevated in the human end; and bregma (16) is elevated in the chimpanzee end and depressed in the human end. These differences can be described as humans having a supero-inferiorly taller and more rounded occipital plane, a more horizontally oriented nuchal plane and amore curved parietal, resulting in a more rounded posterior cranial profile. Furthermore, the human occipital plane and the lower parietal region project posteriorly compared to the chimpanzees, showing the expansion of the human cranium compared to that of the apes. They also tend to characterize females relative to males in the chimpanzee sample. As in the occipital landmarks analysis, PC 1 here is strongly correlated with centroid size (Table 5.3). However, and again as in Chapter 4, when PC 1 is plotted against centroid size and the regression lines fitted for each population, the slopes of the regression lines are not the same across genera or populations (Fig. 5.5).

PC 2 (Fig. 5.2) summarizes 9.8 % of the total variance and is significant for population effects at the 0.0001 level. In the human sample, PC 2 does not separate Neanderthals, Petralona, Biache, Skhul 5, Kanalda or the Upper Paleolithic specimens from modern humans. These specimens all fall near the center of the modern human range of variation. Neanderthals are not significantly different from modern humans either at the species or the population level, while none of the modern human populations are significantly different from one another. However, PC 2 does separate Singa from the rest of the human sample on its negative end. This component is not correlated with centroid size.

The most important shape differences driving the separation along this component (Fig. 5.6) occur at lambda (1) and the semilandmark just superior and inferior to it (31, 2, 30, 29), at bregma (16) and the semilandmarks posterior to it (17, 18), and in the nuchal plane (13). The shape differences that separate Singa from the rest of the human sample can be described as an elevated and anteriorly placed lambda (1) and semilandmarks

around it (2, 31), a more posteriorly placed bregma (16) and semilandmarks posterior to it (17, 18), and a more inferiorly placed the nuchal plane (12, 13). These changes can be described as a antero-posteriorly short parietal region, a supero-inferiorly tall occipital plane with a depression around lambda, and a very rounded nuchal plane that forms a continuous smooth curve with the occipital plane.

PC 3 (4.4 % of the total variance, significant for population effects at the 0.0001 level, Fig. 5.7) partially separates Neanderthals from the modern human sample on its negative end, although there is some overlap. Among these specimens, La Chapelle and Saccopastore 1 fall outside the modern human range, while La Ferrassie 1 and particularly Shanidar 1 fall within the modern human cloud. Petralona is separated from the modern human sample along PC 3 on its negative end, while Biache falls near the negative extreme of the modern human range. Skhul 5 and the four Upper Paleolithic specimens also fall on the negative side of PC 3 but within the modern human range, the specimen falling closest to the negative end of the range being Cro Magnon 1. Modern human populations overlap widely along PC 3. The Berg and Europeans, who were shown to overlap with Neanderthals in the occipital landmarks analysis, now tend to fall on the opposite end of PC 3 from the fossil group. Neanderthals are significantly different in their mean scores from modern humans at the species level. They are also significantly different from most human groups at the population level, except the Upper Paleolithic, San, Australian and Tolai groups.

The most important shape differences along PC 3 occur at opisthion (15) and the semilandmarks just posterior to it (14, 13), as well as in the occipital plane (4, 5, 6, 7 and 8) (Fig. 5.8). In the negative end of PC 3, where La Chapelle, Saccopastore 1 and Petralona fall, opisthion (15) and the semilandmarks around it (14, 13) are elevated and more anteriorly placed. The semilandmarks describing the lateral profile of the occipital plane between lambda and inion (4-8) are much more curved, posteriorly placed and slightly elevated as well. Furthermore, the semilandmarks on the posterior part of the parietal region above lambda are depressed. The shape differences can be described as an antero-posteriorly elongated and more horizontally oriented nuchal plane which angles relatively sharply to the occipital plane, a posteriorly projecting occipital plane and

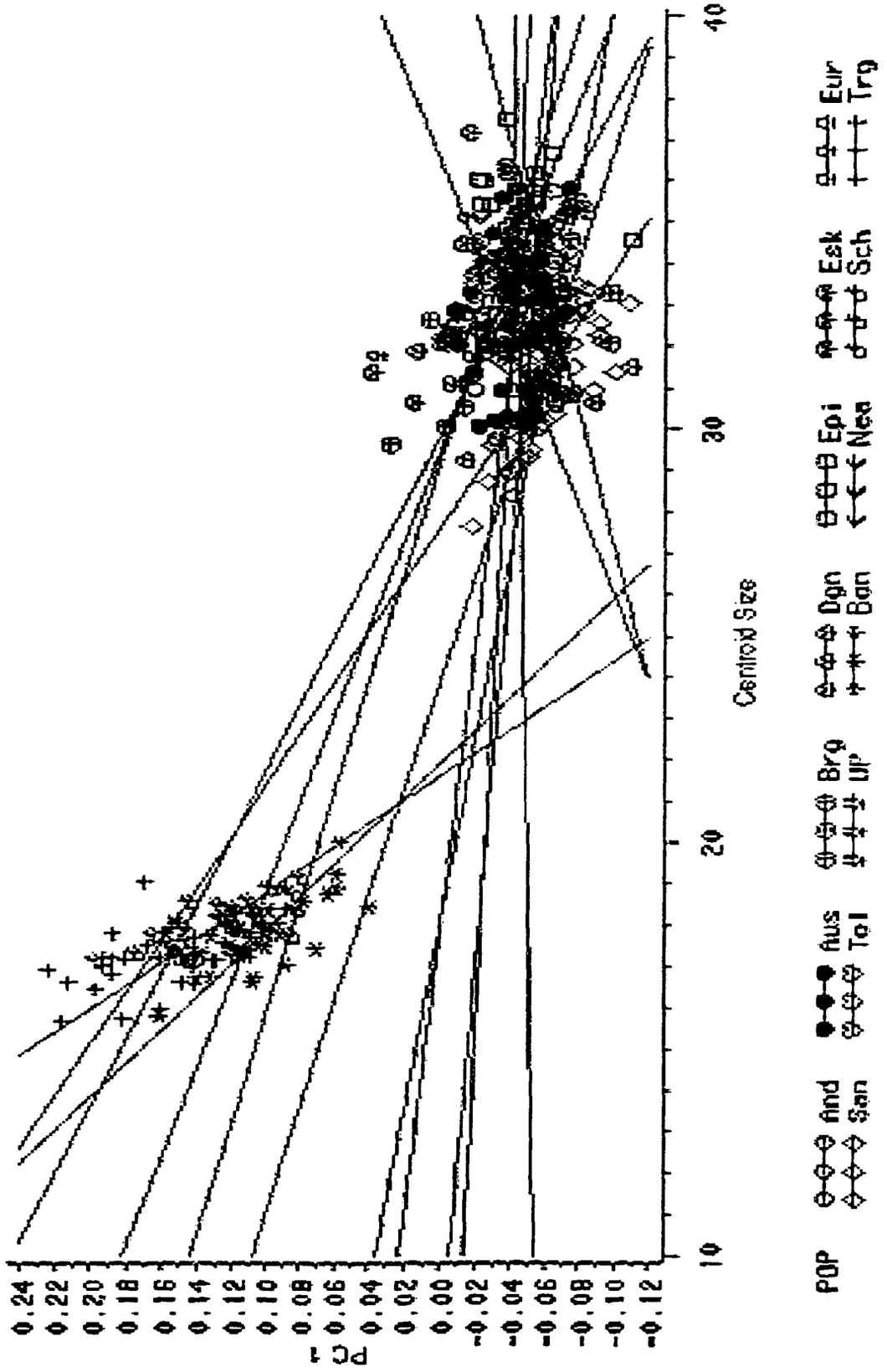

Figure 5.5: PC 1 (Step 1A) plotted against centroid size, regression lines fitted for each population.

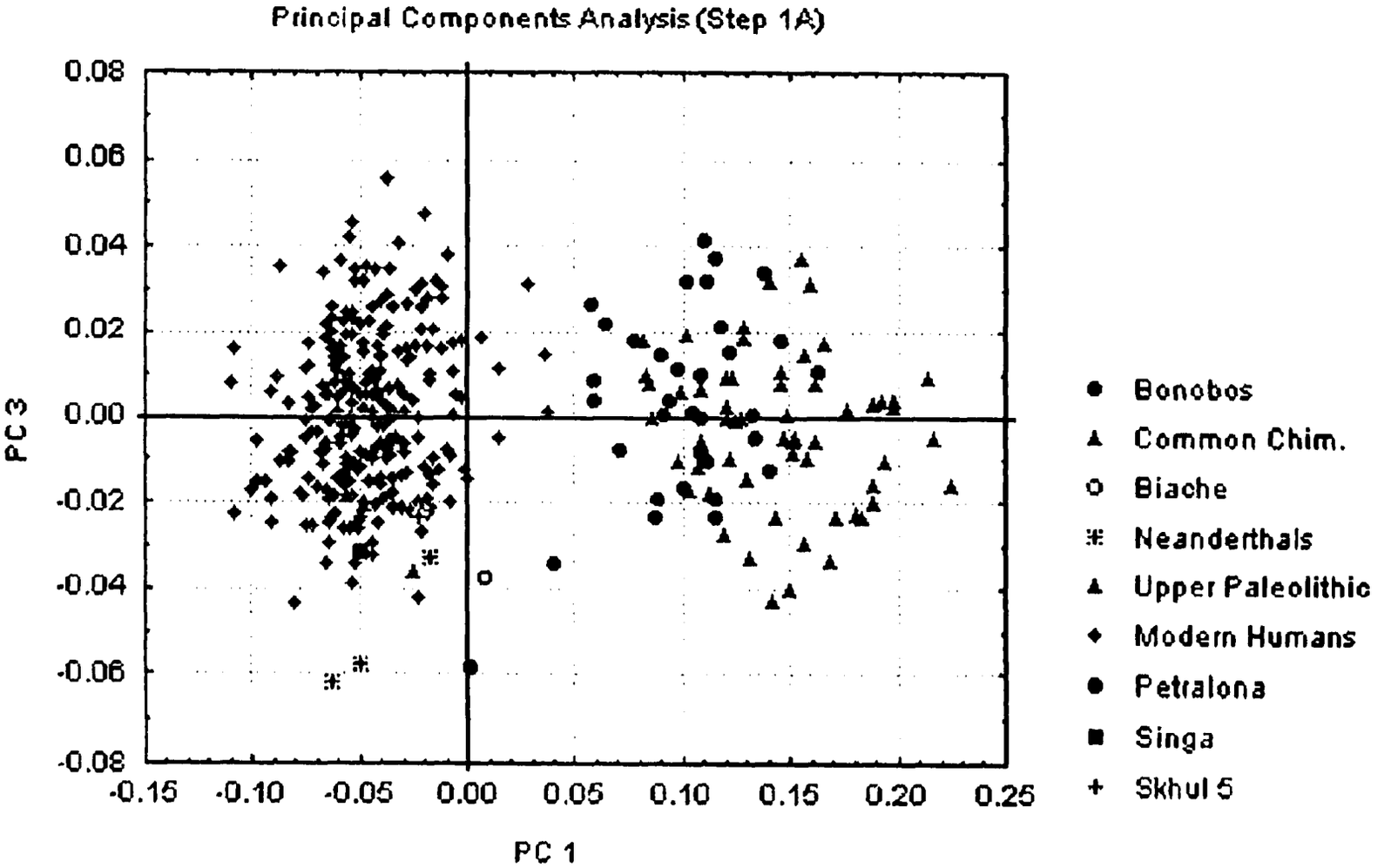

Figure 5.7: Principal Components Analysis, Step 1A, PCs 1 and 3.

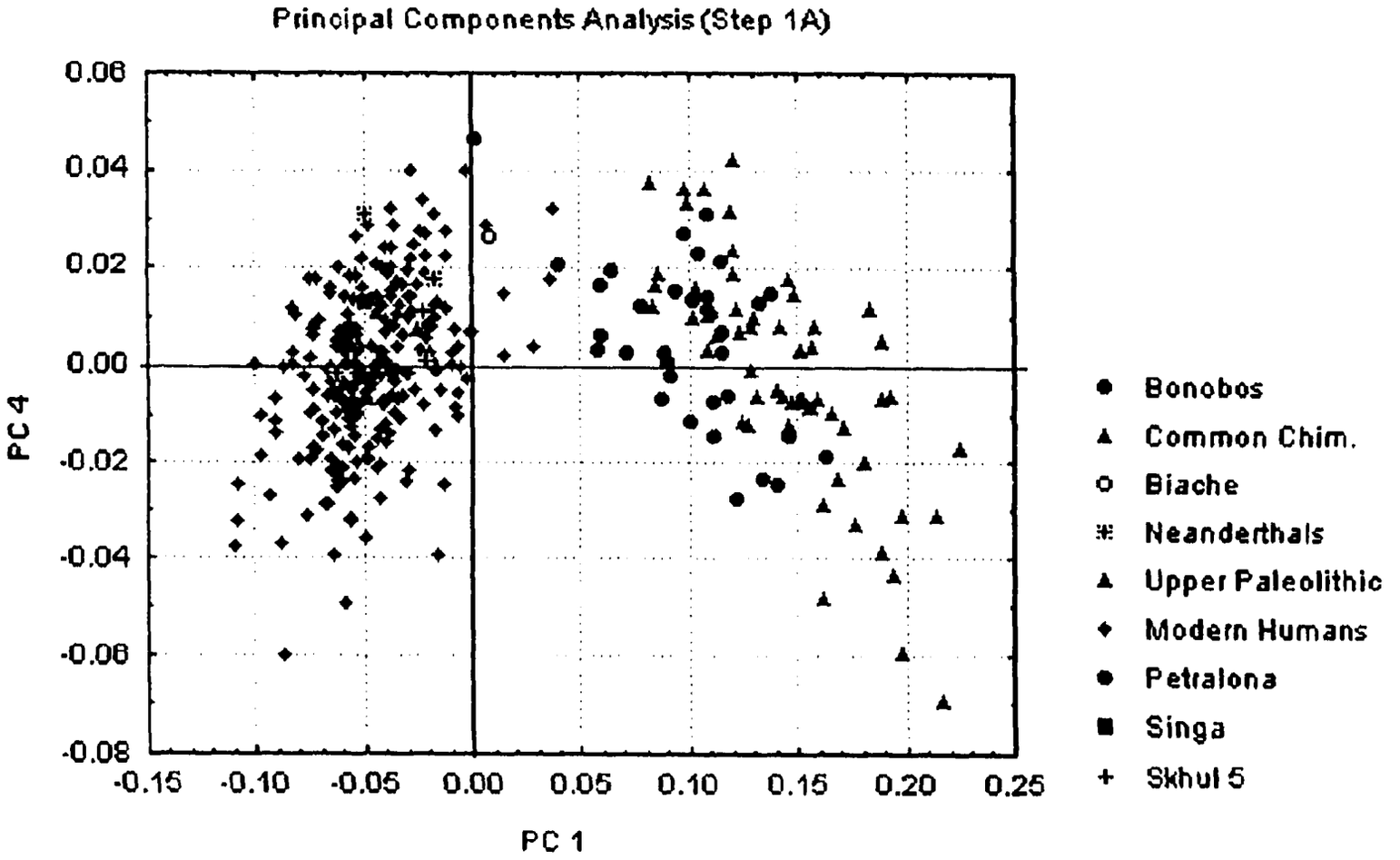

Figure 5.9: Principal Components Analysis, Step 1A, PCs 1 and 4.

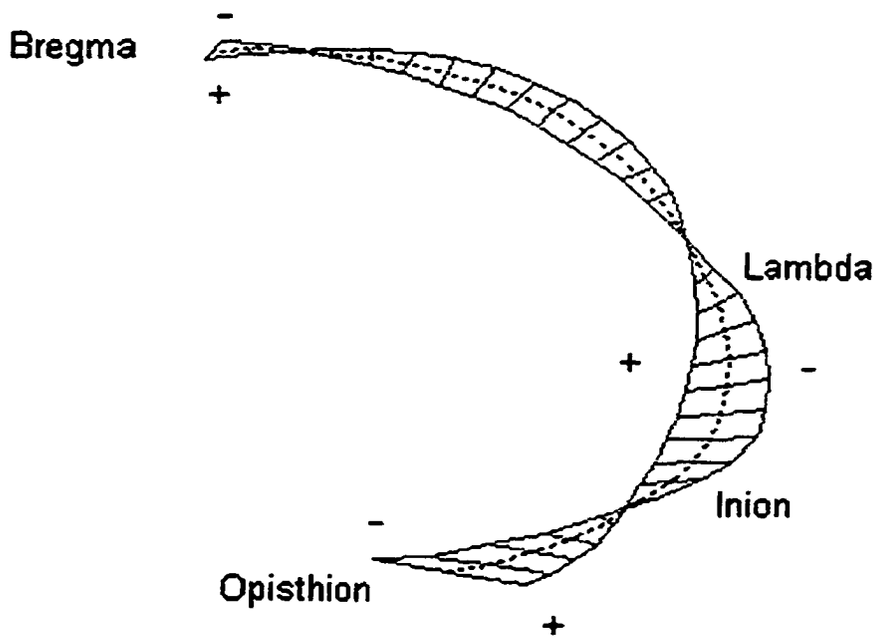

Figure 5.8: Shape variation along PC 3 (Step 1A). The dotted line represents the consensus configuration.

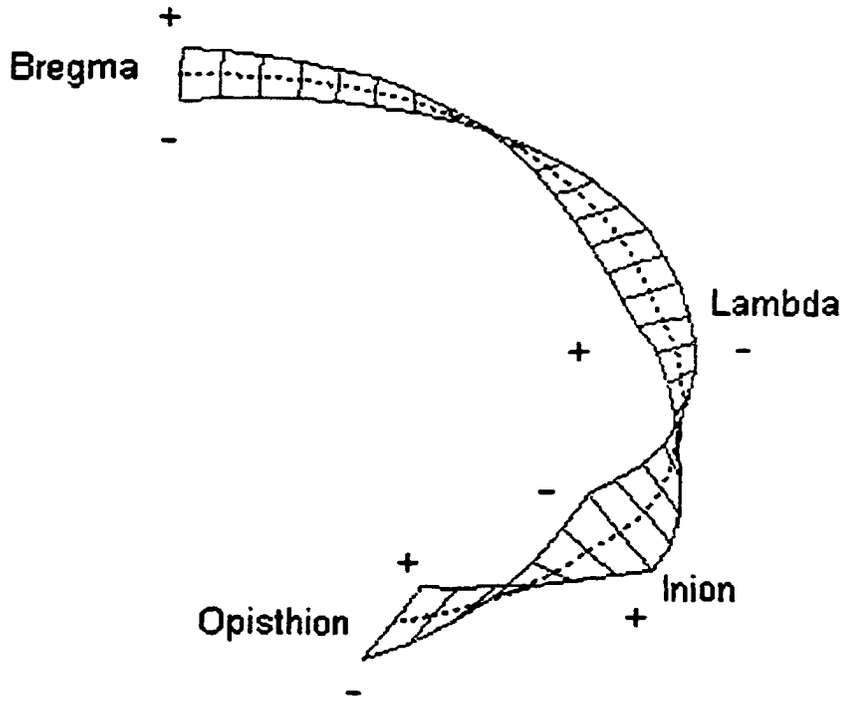

Figure 5.10: Shape variation along PC 4 (Step 1A). The dotted line represents the consensus configuration.

flattened parietal in Neanderthals, Biache and Petralona. A relatively sharp angle between the occipital and nuchal planes has been previously described for Petralona (Stringer 1979), but is not thought to be a general characteristic of Neanderthals (e.g. Hublin 1978). The posterior projection of the occipital plane found in the negative end of PC 3 is consistent with the Neanderthal morphology of the occipital 'bun', while the depression in the posterior parietal region reflects the flat Neanderthal parietal bone and their low vault. However, only two Neanderthal specimens, La Chapelle and Saccopastore 1, are outside the modern human range of variation in these traits, while Shanidar 1 falls well within the modern human range of variation. The position of this specimen probably reflects the more curved parietal and higher parietal vault found in this series of specimens and particularly in Shanidar 1 (Stringer and Trinkaus 1981).

Among the Upper Paleolithic specimens, Cro Magnon 1 also falls at the negative extreme of the range of modern human variation. This specimen has not been described as possessing a chignon (Trinkaus and LeMay 1982). Individual examination of the Cro Magnon 1 configuration shows that opisthion is more anteriorly placed and the lower part of the occipital plane above inion is more posteriorly projecting in this specimen than in the three other Upper Paleolithic specimens or Skhul 5. Predmosti 3 and 4, which both have been described as possessing 'buns' (Trinkaus and LeMay 1982), fall well within the modern human range along this component. The shape differences on the positive end of PC 3, where some Berg and European specimens fall, reflect a very rounded cranium, with a flattened occipital plane, an almost vertically oriented nuchal plane and a very wide angle between them, as well as a high and rounded parietal.

It is noted here that the posterior projection of the occipital plane in Neanderthals was not observed in the analysis of the occipital bone landmarks because, as shown in this analysis, the shape difference from modern humans in this area does not occur at inion (9) or lambda (1), landmarks included in the previous chapter, but at the semilandmarks between them. Furthermore, in the landmarks analysis, Neanderthals were found to be very similar to the Berg and mixed European populations among modern humans, due mostly to the great width of their occipital bone at the level of asteria. However, in this analysis, Neanderthals appear widely removed from the majority of the specimens belonging to the two European populations, which, in this case,

are characterized by exactly the opposite morphology.

PC 4 (3.4 % of the total variance, significant for population (0.0001), sex (0.05) and interaction effects (0.001), Fig. 5.9) separates Petralona from modern humans on its positive end. Biache, La Chapelle, and La Ferrassie 1 also fall on the positive side of PC 3, but within the range of modern human variation, while Shanidar 1 and Saccopastore 1 falling near its center. The Upper Paleolithic specimens and Skhul 5 fall near the center of the modern human range, as do Kanalda and Singa. Among modern human populations, the Dogon are partially separated from the remaining groups, falling on the negative end of the modern human range. The modern human group that extends furthest on the positive side of PC 4 is the Berg population. None of the modern human populations, however, is significantly different from the others. When PC 4 is labeled by sex, a strong tendency is observed for females to have more negative scores than males in the human sample, while the opposite tendency is observed in the chimpanzees. The human pattern also applies to the Neanderthal and the Upper Paleolithic specimens. When the means for the two sexes are plotted by population (Fig. 5.3), the male means for all human groups except the mixed European sample, are more positive than the female means, while the male means for all three chimpanzee taxa are more negative than the female ones.

The most important shape differences that drive the separation along PC 4 occur at inion (9) and the semilandmarks around it (7, 8 and 10), at opisthion (15) and the semilandmark just posterior to it (14) and at bregma (16) (Fig. 5.10). In the positive end of PC 4, where Petralona falls, inion (9) and its surrounding area projects posteriorly and inferiorly, while opisthion (15) and the anterior part of the nuchal plane are elevated and posteriorly placed. Bregma (16) and the semilandmark just behind it (17) are elevated, while the semilandmarks on the posterior parietal region again are depressed. These differences describe a relatively horizontally oriented nuchal plane, which angles sharply to the occipital plane, as in PC 3. Furthermore, they reflect a posteriorly and inferiorly protruding iniac region and lower part of the occipital plane, as well as a very flat parietal. A low angle between the two occipital scales is characteristic of Petralona. As discussed above, this specimen also possesses a posterior projection of the occipital plane, which is centered around inion and is not similar to the Neanderthal 'chignon'.

These traits also characterize to a lesser degree La Chapelle, La Ferrassie 1 and Biache, as well as human males in general relative to females, although in the chimpanzee sample they tend to characterize females. The position of Saccopastore 1 and Shanidar 1 near the center of the modern human range for this component may reflect the more curved parietal and higher parietal vault found in these specimens and particularly in Shanidar 1 (Stringer and Trinkaus 1981).

Canonical Variates Analysis: A canonical variates analysis was conducted on the first 30 principal components (99.8 % of the total variance). Neanderthals are separated on CaV 3, while the Upper Paleolithic specimens fall at the extreme of the modern human range on CaV 4. A correlation analysis of the first five canonical variates with centroid size was undertaken. The results of the CVA and the correlation analysis are reported in Table 5.5.

The first canonical axis (Fig. 5.11) summarizes 74.6 % of the total variance. It separates the human sample on the negative side from the chimpanzee sample on the positive side, Petralona and Biache falling at the extreme of the modern human range. Among the chimpanzees, CaV 1 also separates bonobos from *P. t. troglodytes*, with *P. t. schweinfurthii* falling between them and overlapping with both. CaV 1 is most highly influenced by PC 1. The shape differences driving the separation along CaV 1 and separating chimpanzees from humans are the similar to those described for PC 1. Furthermore, like PC 1, CaV 1 is strongly correlated with centroid size and the regression slopes across genera and populations are not the same (Fig. 5.12).

CaV 2 (5 % of the total variance, most highly influenced by PCs 2, 6 and 4, Fig. 5.11) separates Singa on the positive extreme from the rest of the human sample, this specimen falling outside the 95 % confidence ellipse of all modern human groups. Among modern human groups, CaV 2 separates the Berg on the positive side from the Dogon on the negative side, these two groups being significantly different from each other. The shape differences driving the separation along CaV 2 are similar to those described for PC 2. In addition to the antero-posteriorly short parietal region, the supero-inferiorly tall occipital plane and the rounded and inferiorly placed nuchal plane described for PC 2, Singa is also separated from the human sample along CaV 2 in showing a flattening in the posterior parietal region above lambda and a posterior

Table 5.5: Summary of the CVA results and Correlation Analysis for CaVs 1-5, Step 1A.

	Canonical Variates Analysis			Correlation with Centroid Size	
	Eigenvalue	Proportion	Cumulative	Rho	Pr > F
CaV 1	18.4298	0.7465	0.7465	-0.94538	0.0001
CaV 2	1.2473	0.0505	0.797	0.11085	0.0385
CaV 3	1.0019	0.0406	0.8376	-0.03956	0.4613
CaV 4	0.7713	0.0312	0.8688	0.01018	0.8497
CaV 5	0.5737	0.0232	0.8921	0.05135	0.3389

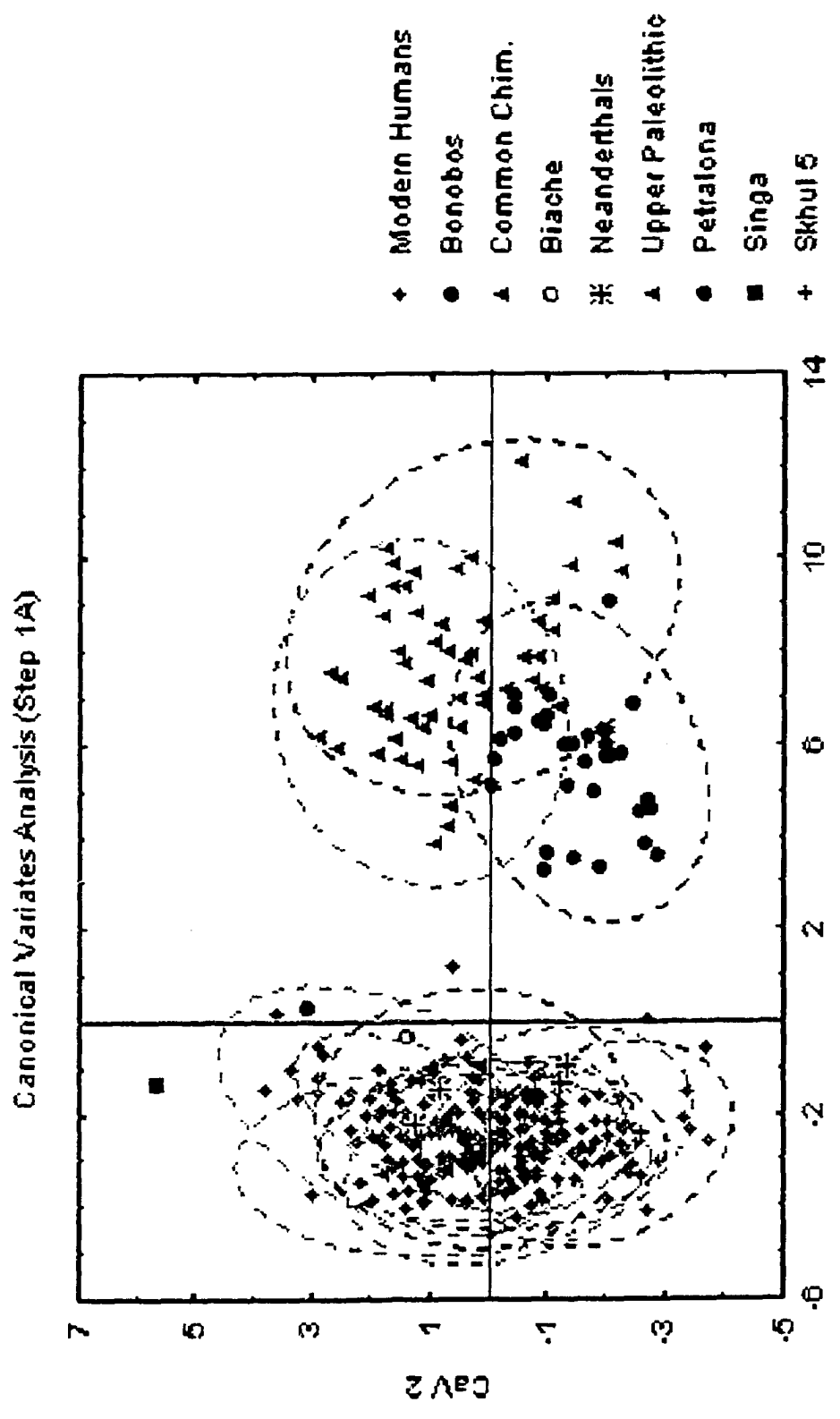

Figure 5.11: Canonical Variates Analysis (Step 1A), CaVs 1 and 2. Dotted lines represent the 95 % confidence ellipses for each group.

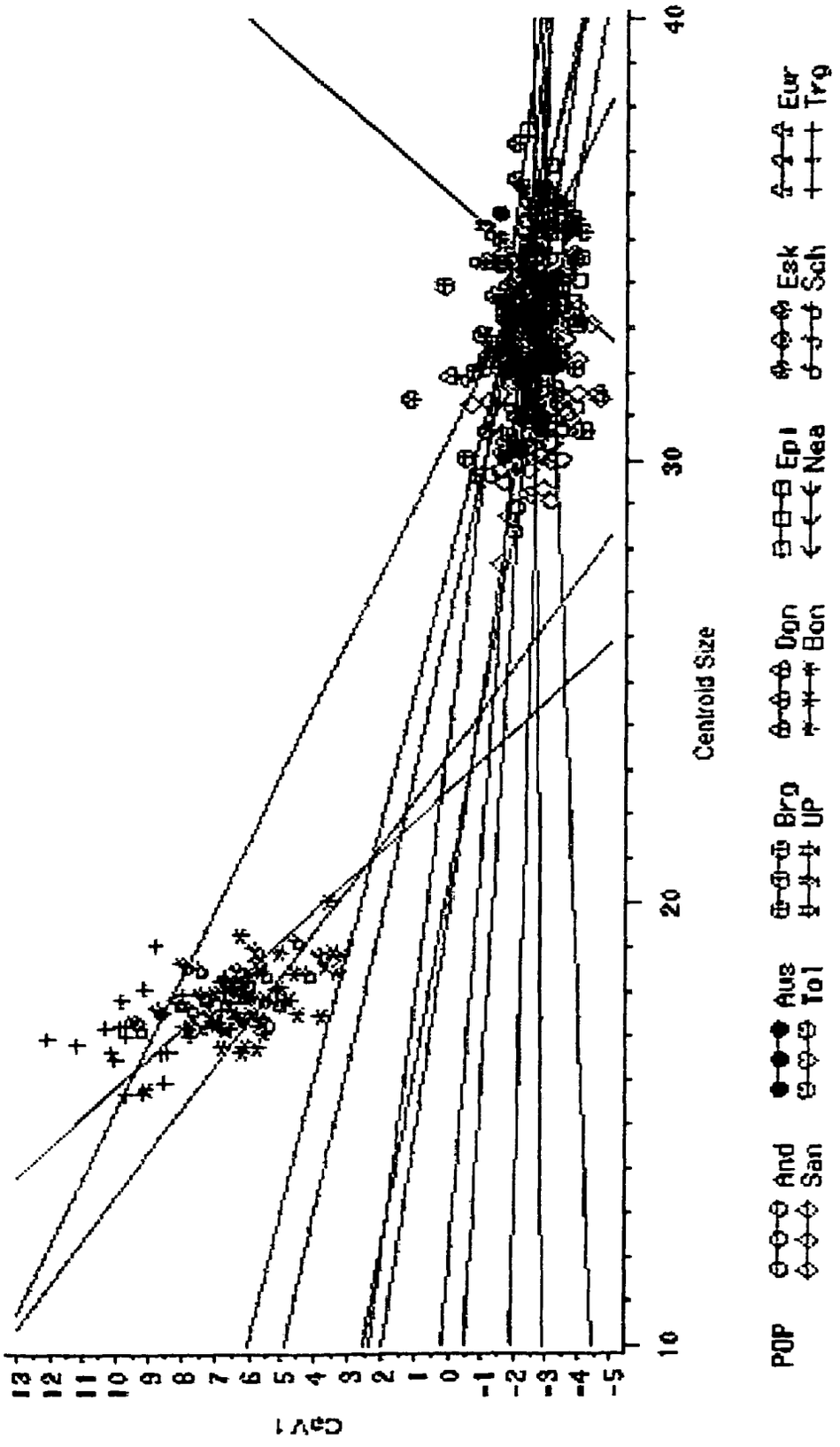

Figure 5.12: CaV 1 (Step 1A) plotted against centroid size, regression lines fitted for each population.

projection of the lower part of the occipital plane.

CaV 3 (4.1 % of the total variance, most highly influenced by PC 3, Fig. 5.13) partially separates Neanderthals on its negative end from modern humans. La Chapelle and Saccopastore 1 fall outside the 95 % confidence ellipses of all modern human populations along CaVs 1 and 3, while La Ferrassie 1 and Shanidar 1 fall at their fringe. Biache and Singa also fall in this end and in the area of overlap between Neanderthals and modern humans, while Petralona falls on the negative side close to the Neanderthal specimens, but within the modern human cloud. Neanderthals are significantly different from modern humans at the species level, as well from most modern human populations except the San, Dogon and Tolai groups, at the population level in their mean score.

The shape differences along CaV 3 (Fig. 5.14) are similar to those described for PC 3 and include a posteriorly projecting occipital plane, an elevated nuchal plane, flat parietals and a relatively low cranial vault. These shape differences are the expected ones for Neanderthals and are consistent with the described Neanderthal morphology of the posterior occipital projection and flat parietal area (see discussion above, p. 1, 9-11). Biache is also found to show these characteristics and to cluster with Neanderthals, consistent with the previous description of a large occipital bun for this specimen (Vandermeersch 1985; Trinkaus and LeMay 1982). However, no signal for the presence of a suprainiac fossa was picked up as separating Neanderthals from the modern human sample either in this or another canonical axis. The reason for this may be that this fossa is usually so shallow that it is not distinguished in the midsagittal profile. Another reason may be that the presence of a suprainiac fossa in the midline is not what distinguishes Neanderthals from modern humans, but rather its shape and lateral extent, as per Hublin (1988a; see also Bräuer and Broeg 1998).

CaV 4 (3.1 % of the total variance, most highly influenced by PCs 3 and 4, Fig. 5.15) separates Petralona on its positive end from the rest of the human sample, this specimen falling outside the 95 % confidence ellipses of all modern human populations along CaVs 1 and 4. The Upper Paleolithic specimens and Skhul 5 also fall at the positive extreme of the modern human range, although within the confidence ellipses of modern human groups. They are significantly different from the Dogon, Anndamanese and Europeans, but not from the other modern human groups. Neanderthals also fall on

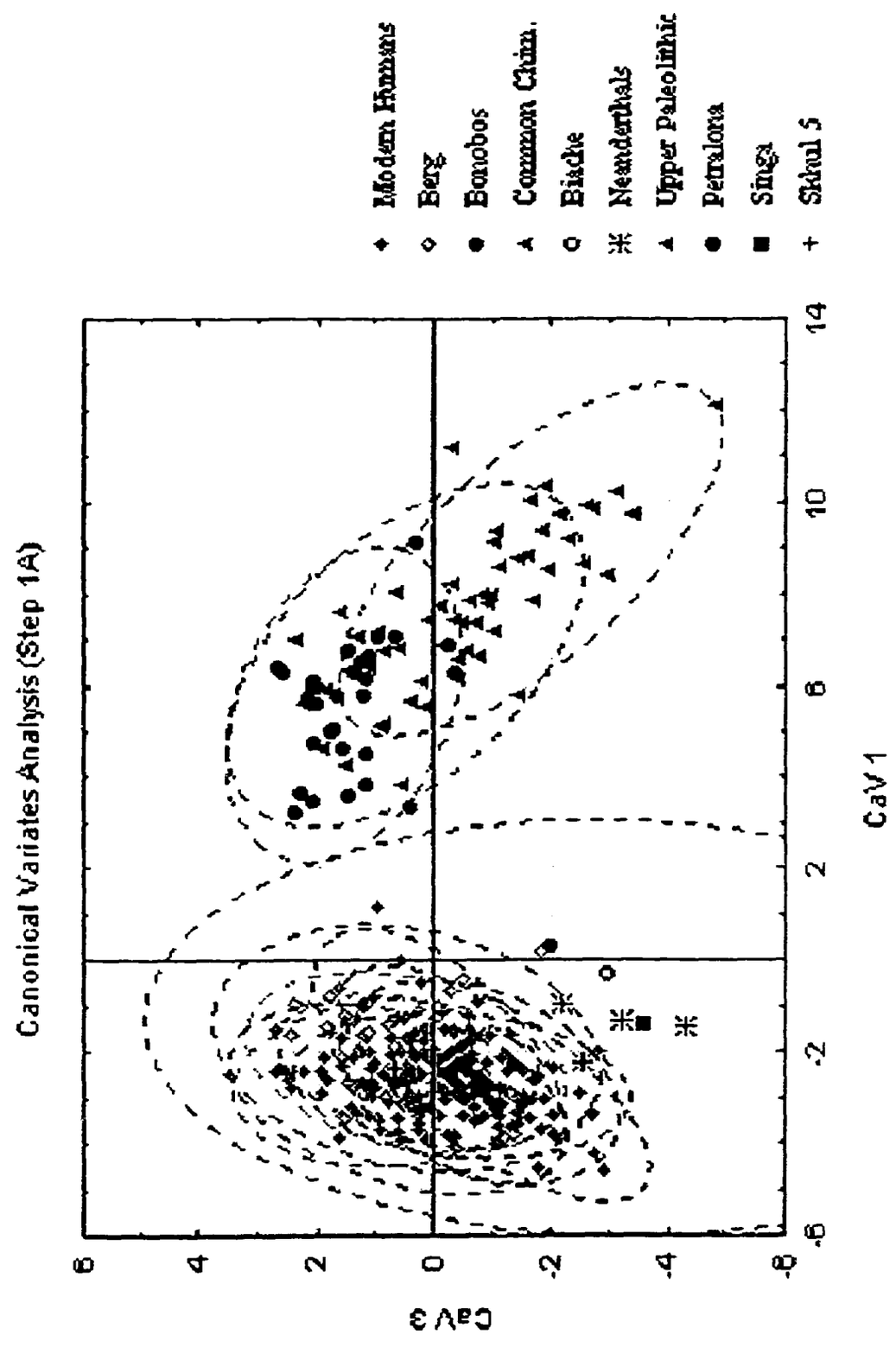

Figure 5.13: Canonical Variates Analysis (Step 1A), CaVs 1 and 3. Dotted lines represent the 95 % confidence ellipses for each group.

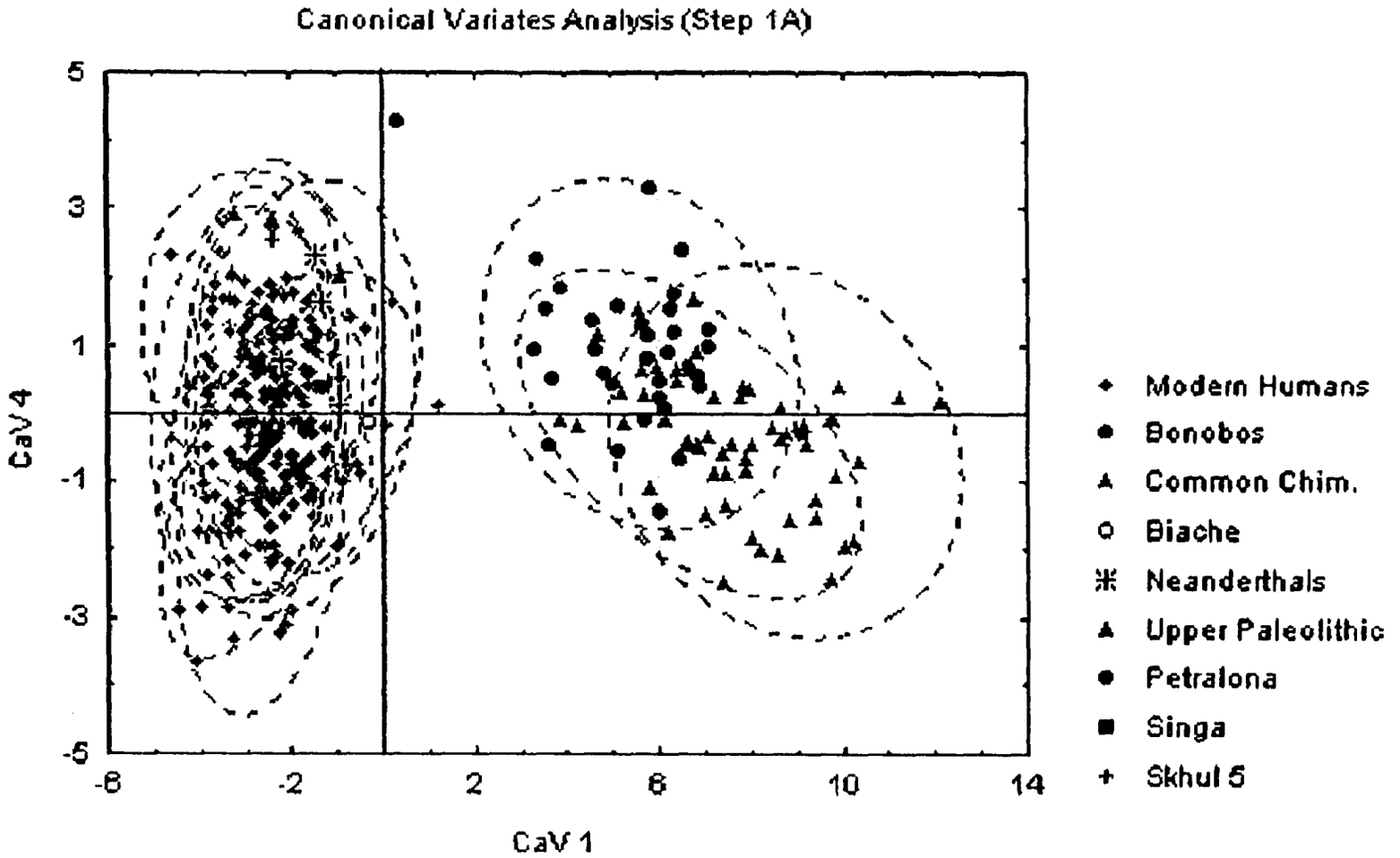

Figure 5.15: Canonical Variates Analysis (Step 1A), CaVs 1 and 4. Dotted lines represent the 95 % confidence ellipses for each group.

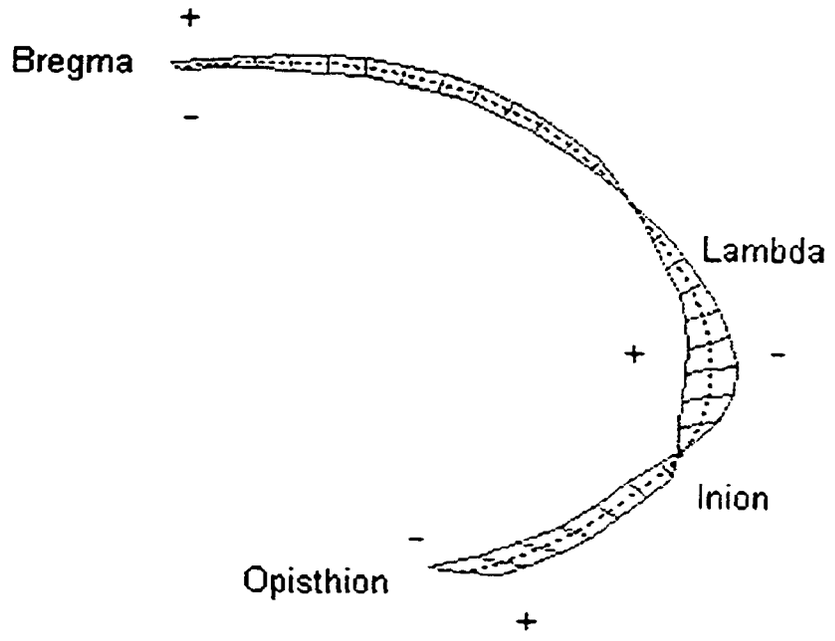

Figure 5.14: Shape variation along CaV 3 (Step 1A). The dotted line represents the consensus configuration.

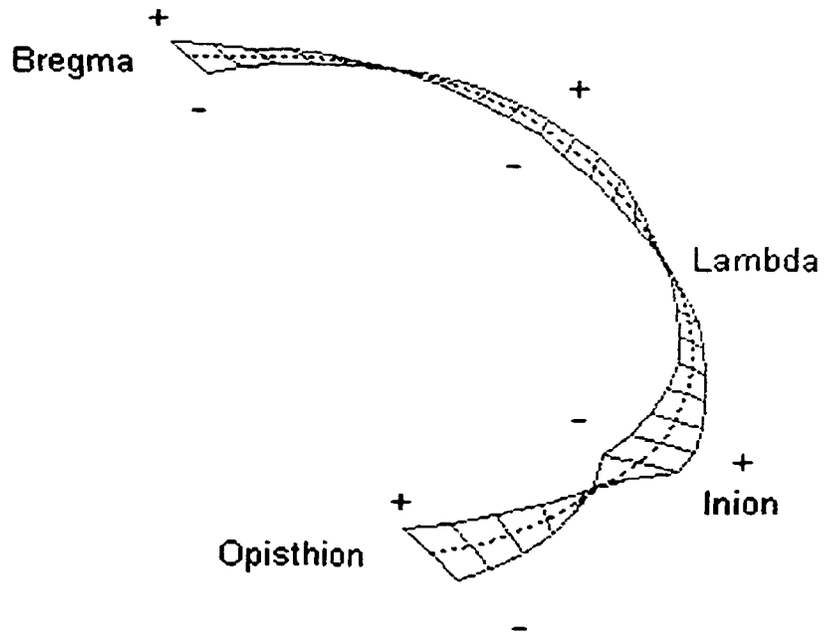

Figure 5.16: Shape variation along CaV 4 (Step 1A). The dotted line represents the consensus configuration.

mostly the positive side of CaV 4, La Chapelle being the most positive among them. Although the mean score for this group is significantly different from that of modern humans at the species level, it does not differ significantly from any of the modern human groups at the population level. The shape differences (Fig. 5.16) that characterize Petralona relative to the rest of the human sample are similar to those described for PCs 4 and 3. They include a posteriorly projecting inion and surrounding area, an elevated nuchal plane, which angles relatively sharply with the occipital plane, and an relatively flat parietal. They indicate that Skhul 5 and the Upper Paleolithic specimens, as well as Neanderthals to a lesser extent, exhibit a strong superstructure at the level of the superior nuchal lines, as well as a somewhat flattened parietal relative to most modern humans.

CaV 5 (2.3 % of the total variance, most highly influenced by PCs 29, 9 and 15, Fig. 5.17) separates Biache from the rest of the human sample, this specimen falling outside the negative extreme of the confidence ellipses of all modern human groups along CaVs 1 and 5. Singa also on the negative end of this axis and outside the confidence ellipses of modern humans, but is not as widely separated from them as Biache. The Neanderthal specimens fall within the confidence ellipses of modern humans at their negative end, La Chapelle and Shanidar 1 falling at the fringe of the modern human cloud. Although they are significantly different from modern humans at the species level, at the population level they are only significantly different from the Australian population. The Upper Paleolithic specimens fall near the center of the modern human cloud on this axis, while Skhul 5 falls at its positive extreme. Petralona also falls close to the center of the modern human range.

The shape differences at the negative extreme of CaV 5, where Biache and Singa fall, include a short and flat parietal with an elevated anterior part and a depressed posterior part, a posteriorly protruding and curved occipital plane and an inferiorly placed nuchal plane, reflecting a wide angle between the two occipital scales. The posterior end, where Skhul 5 lies, is characterized by a curved parietal with an elevated posterior part, a depression of the occipital plane above inion, and a slightly elevated nuchal plane, reflecting a relatively sharp angle between the upper and the lower occipital scale.

Classification: A discriminant analysis was performed excluding all singletons, which were treated as unknown specimens to be classified within one of the defined

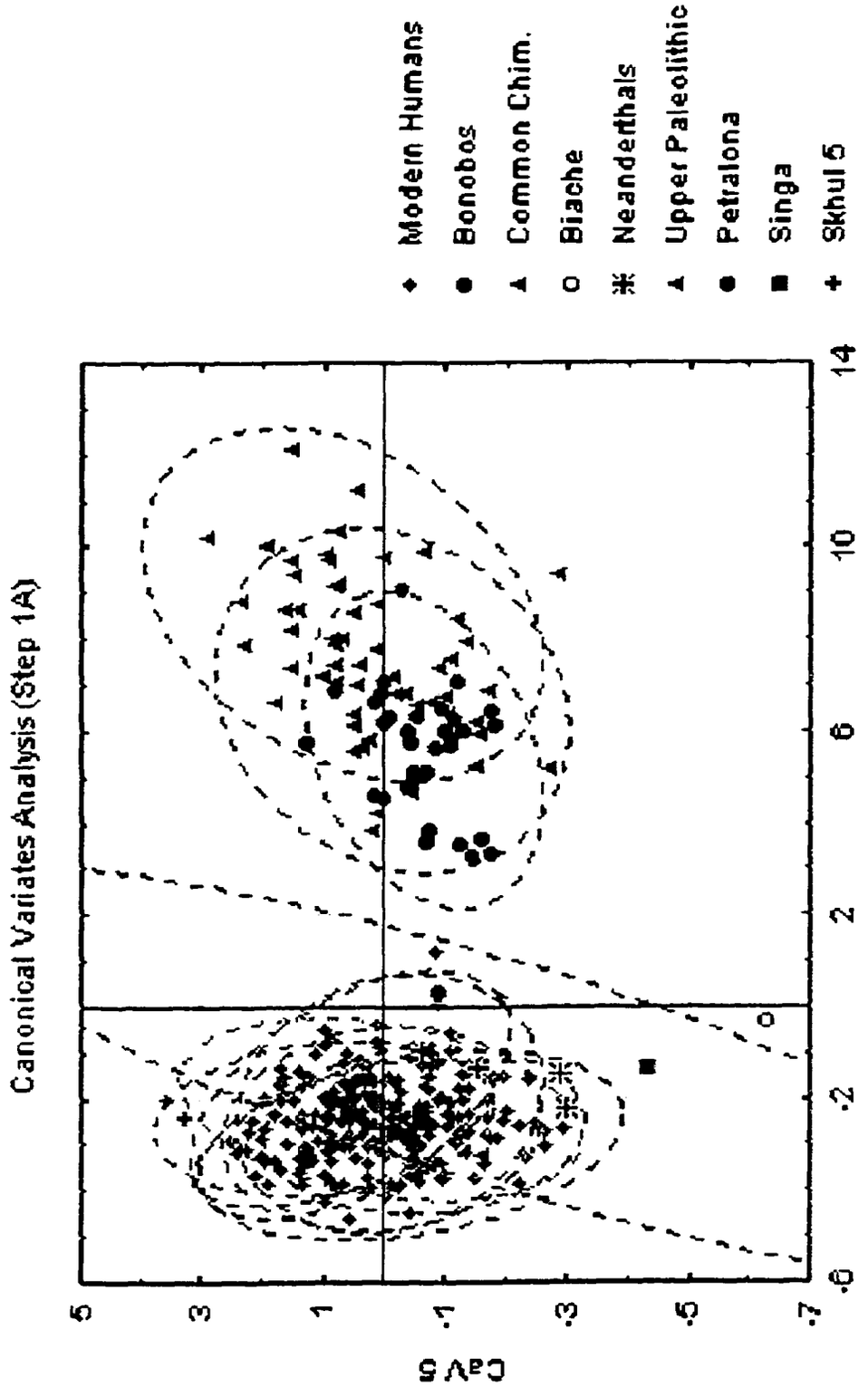

Figure 5.17: Canonical Variates Analysis (Step 1A), CaVs 1 and 5. Dotted lines represent the 95 % confidence ellipses for each group.

groups. A cross-validation classification was obtained for the remaining dataset (Table 5.6). All Neanderthals and all Upper Paleolithic European specimens were classified correctly by posterior probability. Biache was classified as Neanderthal with a posterior probability of 1.00, Petralona as Berg (0.82), and Kanalda as Australian (0.37), as was Skhul 5 (0.84). Singa was classified as Berg (0.79).

Classification success in the cross-validation classification was lower than in all previous chapters for all groups included. As before, no human specimens were classified as chimpanzees and vice versa. However, all Neanderthal specimens were misclassified, two as Eskimo and two as San. Two modern human specimens were misclassified as Neanderthal, one Berg and one Tolai. In the Upper Paleolithic group only one specimen was classified correctly, while two were misclassified as Australian and one as Epipaleolithic. Three recent human specimens were misclassified as Upper Paleolithic, including an Andamanese, an Australian and a European specimen.

The highest success rate overall was obtained for the bonobo population (87.88 %), followed by the *P. t. troglodytes* group (78.57 %). In the *P. t. schweinfurthii* group five specimens were misclassified as bonobos and six as *P. t. troglodytes*, while among the latter five specimens were misclassified as *P. t. schweinfurthii* and only one as bonobo. with the other common chimpanzee subspecies. Only four bonobos were misclassified, two as *P. t. schweinfurthii* and two as *P. t. troglodytes*. Among the modern human populations, the highest success rate was obtained for the Dogon (73.33 %) and the San (70 %),while the lowest success rates were obtained for the mixed European group (27.27 %), as in all other analyses and the Epipaleolithic (31.58 %). As in all other analyses, a very high percentage of the mixed European population (31.82 %) was misclassified as Berg, and vice versa (24.14 %).

Mahalanobis D^2, Cluster Analysis and Minimum Spanning Tree: The unbiased Mahalanobis distances among groups were calculated (Table 5.7). As before, the two chimpanzee species are very widely removed from the human groups. Here, however, and although bonobos are more distant from *P. t. troglodytes* than the two common chimpanzee subspecies are from each other, the distance between bonobos and *P. t. schweinfurthii* is slightly smaller than the distance between the two common chimpanzee subspecies *P. t. troglodytes* and *P. t. schweinfurthii*.

Table 5.6: Cross-validation classification summary (percentages for each population in bold), Step 1A.

	And	Aus	Brg	Dgn	Epi	Esk	Eur	San	Tol	UP	Bon	Nea	Sch	Trg	Total
And	15	1	2	2	2	1	3	0	2	1	0	0	0	0	29
%	**51.72**	3.45	6.9	6.9	6.9	3.45	10.34	0	6.9	3.45	0	0	0	0	100
Aus	3	15	0	2	0	1	0	1	6	1	0	0	0	0	29
%	10.34	**51.72**	0	6.9	0	3.45	0	3.45	20.69	3.45	0	0	0	0	100
Brg	2	2	10	0	2	2	7	2	1	0	0	1	0	0	29
%	6.9	6.9	**34.48**	0	6.9	6.9	24.14	6.9	3.45	0	0	3.45	0	0	100
Dgn	1	2	0	22	0	1	0	3	1	0	0	0	0	0	30
%	3.33	6.67	0	**73.33**	0	3.33	0	10	3.33	0	0	0	0	0	100
Epi	4	1	3	1	6	1	1	2	0	0	0	0	0	0	19
%	21.05	5.26	15.79	5.26	**31.58**	5.26	5.26	10.53	0	0	0	0	0	0	100
Esk	1	0	3	3	1	15	2	2	2	0	0	0	0	0	29
%	3.45	0	10.34	10.34	3.45	**51.72**	6.9	6.9	6.9	0	0	0	0	0	100
Eur	2	1	7	0	2	2	6	1	0	1	0	0	0	0	22
%	9.09	4.55	31.82	0	9.09	9.09	**27.27**	4.55	0	4.55	0	0	0	0	100
San	0	2	1	2	0	0	2	21	2	0	0	0	0	0	30
%	0	6.67	3.33	6.67	0	0	6.67	**70**	6.67	0	0	0	0	0	100
Tol	2	1	2	1	2	1	2	3	13	0	0	1	0	0	28
%	7.14	3.57	7.14	3.57	7.14	3.57	7.14	10.71	**46.43**	0	0	3.57	0	0	100
UP	0	2	0	0	1	0	0	0	0	1	0	0	0	0	4
%	0	50	0	0	25	0	0	0	0	**25**	0	0	0	0	100
Bon	0	0	0	0	0	0	0	0	0	0	29	0	2	2	33
%	0	0	0	0	0	0	0	0	0	0	**87.88**	0	6.06	6.06	100
Nea	0	0	0	0	0	2	0	2	0	0	0	0	0	0	4
%	0	0	0	0	0	50	0	50	0	0	0	**0**	0	0	100
Sch	0	0	0	0	0	0	0	0	0	0	5	0	19	6	30
%	0	0	0	0	0	0	0	0	0	0	16.67	0	**63.33**	20	100
Trg	0	0	0	0	0	0	0	0	0	0	1	0	5	22	28
%	0	0	0	0	0	0	0	0	0	0	3.57	0	17.86	**78.57**	100
Total	30	27	28	33	16	26	23	37	27	4	35	2	26	30	344
%	8.72	7.85	8.14	9.59	4.65	7.56	6.69	10.76	7.85	1.16	10.17	0.58	7.56	8.72	100

Table 5.7: Unbiased Mahalanobis D^2, Step 1A. All distances significant to the 0.001 level, except: NS = non-significant, * = significant to the 0.05 level, ** = significant to the 0.01 level.

	Kan	And	Aus	Bch	Brg	Dgn	Skh5	Epi	Esk	Eur
Kan	0.00	10.23NS	5.73NS	125.51	6.00NS	26.83NS	80.19**	7.25NS	17.77NS	8.52NS
And	10.23NS	0.00	8.16	73.06	9.44	8.02	89.46	7.10	6.38	4.69
Aus	5.73NS	8.16	0.00	86.27	8.22	7.75	74.10	7.14	6.55	7.11
Bch	125.51	73.06	86.27	0.00	83.53	82.91	173.53	76.25	72.69	74.52
Brg	6.00NS	9.44	8.22	83.53	0.00	15.61	83.11	8.36	4.52	1.84NS
Dgn	26.83NS	8.02	7.75	82.91	15.61	0.00	80.95	14.33	8.39	10.21
Skh5	80.19**	89.46	74.10	173.53	83.11	80.95	0.00	84.00	79.71	79.20
Epi	7.25NS	7.10	7.14	76.25	8.36	14.33	84.00	0.00	10.04	5.89
Esk	17.77NS	6.38	6.55	72.69	4.52	8.39	79.71	10.04	0.00	3.75
Eur	8.52NS	4.69	7.11	74.52	1.84NS	10.21	79.20	5.89	3.75	0.00
Ptr	89.34**	84.75	71.43	70.42	59.37	90.83	141.99	78.85	64.35	71.98
San	19.34NS	11.78	6.47	78.32	9.30	7.71	81.56	8.42	6.99	8.20
Sng	114.06	93.43	104.61	115.82	81.26	111.47	229.17	88.05	95.38	90.20
Tol	9.36NS	7.98	5.21	74.18	7.27	10.16	82.04	9.89	6.46	5.61
UP	29.74NS	30.22	19.91	83.22	24.60	31.94	99.71	23.81	28.72	24.08
Bon	70.84	72.44	67.16	113.17	65.04	73.23	132.83	80.32	64.11	66.03
Nea	57.06**	28.25	23.99	41.58**	25.53	22.46	89.08	26.86	16.97	22.16
Sch	87.39	87.29	82.92	114.56	71.06	92.43	167.60	92.58	75.47	76.62
Trg	138.50	130.94	123.52	147.63	114.99	128.78	195.56	138.73	117.00	119.20

	Ptr	San	Sng	Tol	UP	Bon	Nea	Sch	Trg
Kan	89.34**	19.34NS	114.06	9.36NS	29.74NS	70.84	57.06**	87.39	138.50
And	84.75	11.78	93.43	7.98	30.22	72.44	28.25	87.29	130.94
Aus	71.43	6.47	104.61	5.21	19.91	67.16	23.99	82.92	123.52
Bch	70.42*	78.32	115.82	74.18	83.22	113.17	41.58*	114.56	147.63
Brg	59.37	9.30	81.26	7.27	24.60	65.04	25.53	71.06	114.99
Dgn	90.83	7.71	111.47	10.16	31.94	73.23	22.46	92.43	128.78
Skh5	141.99	81.56	229.17	82.04	99.71	132.83	89.08	167.60	195.56
Epi	78.85	8.42	88.05	9.89	23.81	80.32	26.86	92.58	138.73
Esk	64.35	6.99	95.38	6.46	28.72	64.11	16.97	75.47	117.00
Eur	71.98	8.20	90.20	5.61	24.08	66.03	22.16	76.62	119.20
Ptr	0.00	66.63	127.77	65.10	77.83	97.25	60.49	98.23	130.70
San	66.63	0.00	86.71	7.22	25.08	72.51	14.44	90.50	128.56
Sng	127.77	86.71	0.00	94.81	91.36	159.01	80.75	144.41	180.39
Tol	65.10	7.22	94.81	0.00	25.62	74.67	19.63	88.96	128.40
UP	77.83	25.08	91.36	25.62	0.00	85.72	37.12	100.59	146.78
Bon	97.25	72.51	159.01	74.67	85.72	0.00	73.09	11.31	24.68
Nea	60.49	14.44	80.75	19.63	37.12	73.09	0.00	83.74	114.22
Sch	98.23	90.50	144.41	88.96	100.59	11.31	83.74	0.00	11.69
Trg	130.70	128.56	180.39	128.40	146.78	24.68	114.22	11.69	0.00

Unlike the temporal and occipital bone landmarks analysis, here the distances between the modern human groups are equivalent to or smaller than the distance between the two common chimpanzee populations. The greatest distance between any pair of recent human populations is that between the Dogon and the Berg, while the smallest one is that between the Berg and the Europeans. Of the three geographic pairs the European and Australian-Melanesian pairs are both closest to each other, but the San and the Dogon are not. Neanderthals are widely removed from the modern human groups, and the distances they show to most modern human groups are equivalent to that between bonobos and *P. t. troglodytes* (but much greater than that between bonobos and *P. t. schweinfurthii*). The smallest distance between Neanderthals and any modern human group (Neanderthals-San) is lower than the greatest distance between any two modern human populations (Berg-Dogon). Neanderthals are closest to the San and the Eskimo and most distant from the Andamanese. The proximity of these fossils to the San population may be due to the great curvature of the occipital bone of this modern human group, also noted by Tobias (1959). Neanderthals are not close to either of the European populations or to the Upper Paleolithic specimens, to which they show the greatest distance found in this analysis between any pair of human groups. The Upper Paleolithic specimens are very far removed from all modern human populations, in many cases showing greater distances to them than the Neanderthals do. They are closest to the Australians and the Epipaleolithic and most distant from the Dogon and the Andamanese.

The cluster analysis (Fig. 5.18) show the chimpanzee taxa to be widely separated from the human branch, with bonobos clustering with *P. t. schweinfurthii* rather than the two common chimpanzee subspecies clustering together, as in the two landmark analyses. Within the human cluster, the Upper Paleolithic group is an outlier to the remaining populations, including the Neanderthals, reflecting the great distances from all other human populations discussed above. Neanderthals are outliers to all recent human groups, and are also very widely separated from the recent populations. Unlike the previous analyses, the Dogon population is now an outlier to the remaining recent human groups. Some geographic clustering remains in that the two European populations cluster closely together, as do the Australian and Melanesian populations. As in the two

landmark analyses, the Epipaleolithic group falls within the cluster of the modern human groups, as also did the Afalou population in Howells (1989).

The minimum spanning tree (Fig. 5.18) shows the star-like configuration of the human populations greatly separated from the chimpanzee cluster. Neanderthals are placed within the human cluster, although on its second-longest branch, as in the occipital bone landmarks analysis, and unlike the analysis of temporal bone landmarks. The Upper Paleolithic group is also within the human cluster, but on its longest branch.

Step 1B – Human sample only

The analysis was repeated on the human sample only, in order to see whether this would clarify the differences between Neanderthals and the other fossil specimens and modern humans. Neanderthals were not separated more successfully from modern humans on the PCA. However, the canonical variates analysis did separate the fossil group slightly better than when the combined sample was used. Furthermore, the shape differences between Neanderthals and modern humans, as well as among the other fossil specimens, are clearer in this analysis.

Principal Components Analysis: The PCA was repeated on the human sample alone, in order to see whether this clarified the differences between Neanderthals and the other fossil specimens and modern humans. The results of this analysis were very similar to the combined sample analysis described above (Table 5.8). As in Step 1A, PC 1 Neanderthals are partially separated from modern humans along PC 3, with Shanidar 1 and La Ferrassie 1 falling at the negative extreme of the modern human range, where Biache and Singa also fall. On this component Neanderthals are significantly different in their mean score from most, but not all modern human populations, including the Andamanse, Epipaleolithic, European, Dogon and Berg groups. PC 3 also separates Petralona from the modern human cloud. The shape differences along it are similar to those found for PC 3 in Step 1A.

PC 2, PC 4 and PC 6 are significant for sex effects (0.01), females showing a tendency to have more negative scores than males in all three components. When the means for the two sexes are plotted by population, male means are more positive than female means on PC 2 for all populations except the mixed European group and the San,

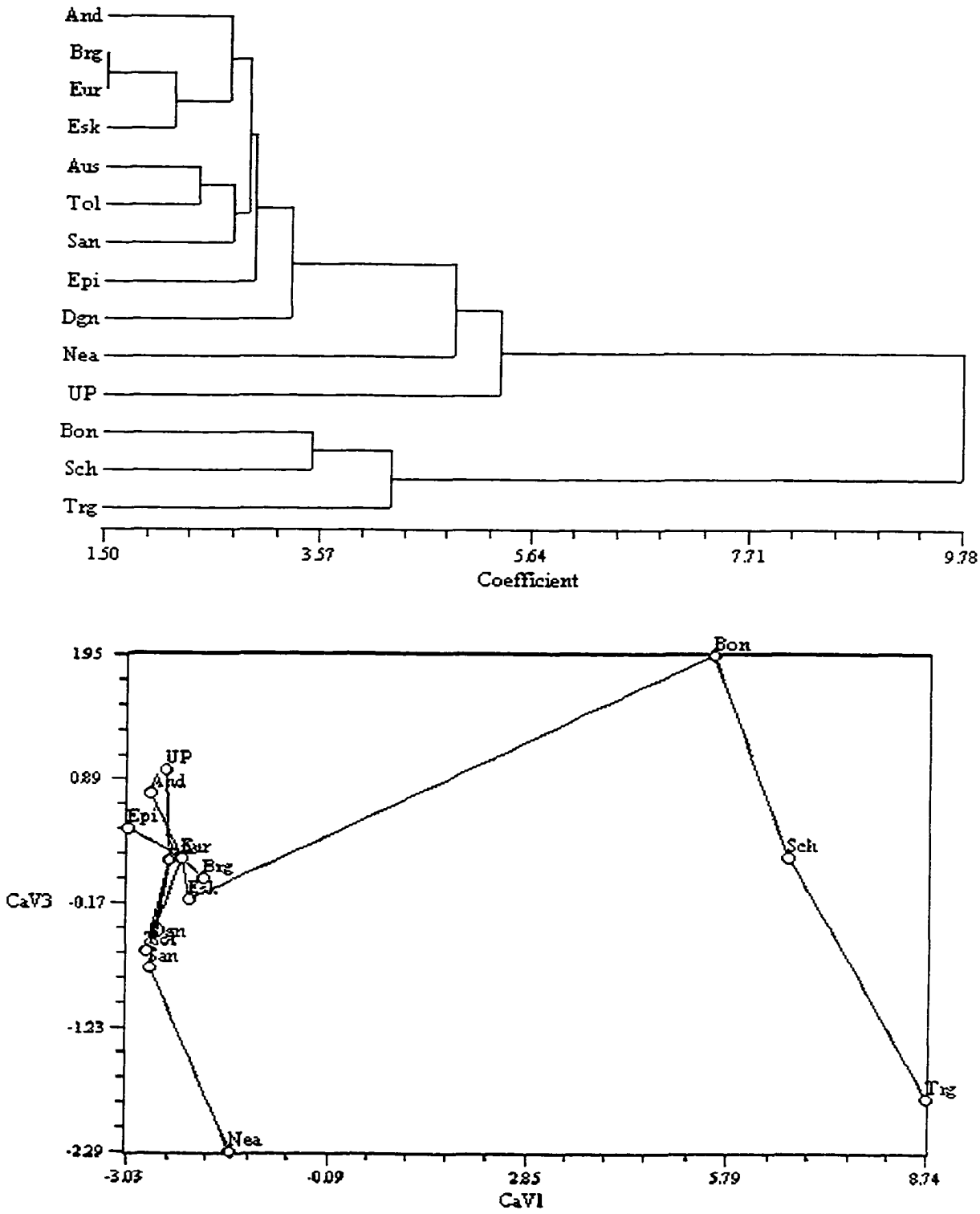

Figure 5.18: Cluster analysis (UPGMA) and minimum spanning tree (top, Step 1A).

Table 5.8: Summary of the PCA results, ANOVA and Correlation Analysis for PCs 1-10, Step 1B.

	Principal Components Analysis			ANOVA, Pr > F			Correlation with Centroid size	
	Eigenvalue	Proportion	Cumulative	Popul.	Sex	Interaction	Rho	Pr > F
PC 1	0.000795	0.325789	0.325789	0.0001	0.1267	0.7147	-0.01617	0.796
PC 2	0.000715	0.292924	0.618713	0.0001	0.0021	0.0106	-0.02733	0.6621
PC 3	0.000399	0.16363	0.782343	0.0001	0.689	0.3328	0.12785	0.0402
PC 4	0.000209	0.085462	0.867805	0.0001	0.004	0.6747	0.29337	0.0001
PC 5	0.000087	0.035784	0.903589	0.0001	0.2089	0.7844	0.23253	0.0002
PC 6	0.000042	0.017131	0.920719	0.3143	0.0046	0.2628	-0.03607	0.5641
PC 7	0.000033	0.013684	0.934403	0.0001	0.53	0.0049	-0.05819	0.3519
PC 8	0.000022	0.009109	0.943513	0.575	0.9383	0.7039	0.032	0.6089
PC 9	0.000019	0.007934	0.951447	0.0095	0.1495	0.1601	-0.11176	0.0731
PC 10	0.000016	0.006708	0.958155	0.0001	0.0002	0.0594	0.23119	0.0002

Table 5.9: Summary of the CVA results and Correlation Analysis for CaV 1-5, Step 1B.

	Canonical Variates Analysis			Correlation with Centroid size	
	Eigenvalue	Proportion	Cumulative	Rho	Pr > F
CaV 1	1.5625	0.1953	0.1953	0.24091	0.0001
CaV 2	1.3019	0.1628	0.3581	0.15157	0.0148
CaV 3	1.0056	0.1257	0.4838	0.2711	0.0001
CaV 4	0.7968	0.0996	0.5835	0.0553	0.3764
CaV 5	0.7169	0.0896	0.6731	0.01876	0.7643

and on PC 4 for all groups except the Tolai, and for all groups except the Dogon and the Andamanese on PC 6. The shape differences that tend to characterize females in most human populations include cases a rounder posterior cranial profile, while males are characterized by relatively flat parietals, strong posterior projection of the iniac region and a sharper angle between the two occipital scales.

Canonical Variates Analysis: The CVA was performed in the human sample only, so as to determine whether Neanderthals and the other fossil specimens were better separated from modern humans and whether classification success improved (Table 5.9). None of the canonical axes are strongly correlated with centroid size. CaV 1 (19.5 % of the total variance, most highly influenced by PCs 4, 2 and 1, Fig. 5.19) separates Singa on its positive end from the modern human range, this specimen falling outside the confidence ellipses of all modern human populations along CaVs 1 and 2. Among modern human groups, CaV 1 separates the Berg on the positive end from the Dogon on the negative end, these two groups being significantly different from each other in their mean scores. Petralona also falls on the positive CaV 1. The shape differences along this canonical axis are very similar to those described for CaV 2 in Step 1A, and include a short and flat parietal, a posteriorly and inferiorly projecting iniac region, and an inferiorly placed nuchal plane.

Neanderthals are separated from modern humans on CaV 2 (16. 3 % of the total variance, most highly influenced by PC 3, Fig. 5.19), which also separates Petralona, Biache and Singa from the modern human sample. All these specimens fall outside the 95 % confidence ellipses for all modern human populations, except for La Ferrassie 1. Neanderthals are significantly different in their mean score on CaV 2 from all modern human populations. Among modern human groups, the San and the Dogon fall mostly on the negative side of CaV 2 and closer to the Neanderthals. The shape differences along this canonical axis (Fig. 5.20) are consistent with the 'occipital bun' and the flat parietal morphology described for Neanderthals, and are similar to those found for CaV 3 in the combined sample analysis (Fig. 5.14). Here, however, the Neanderthal specimens show less overlap with the modern human sample.

On the third canonical axis (12.6 %, most influenced by PCs 12 and 1, Fig. 5.21) Skhul 5 and the Upper Paleolithic group fall at the positive extreme of the modern

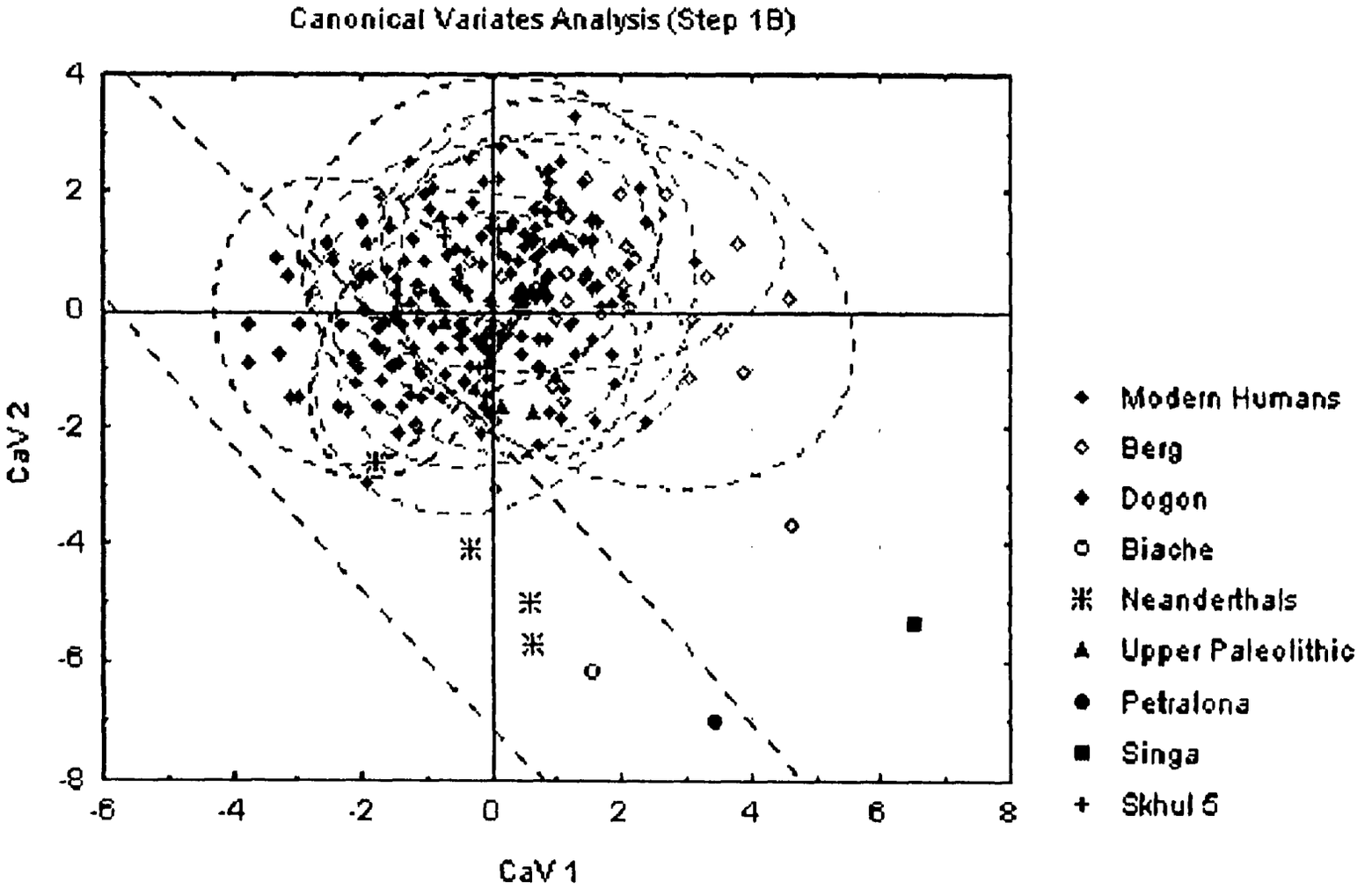

Figure 5.19: Canonical Variates Analysis (Step 1B), CaVs 1 and 2. Dotted lines represent the 95 % confidence ellipses for each group.

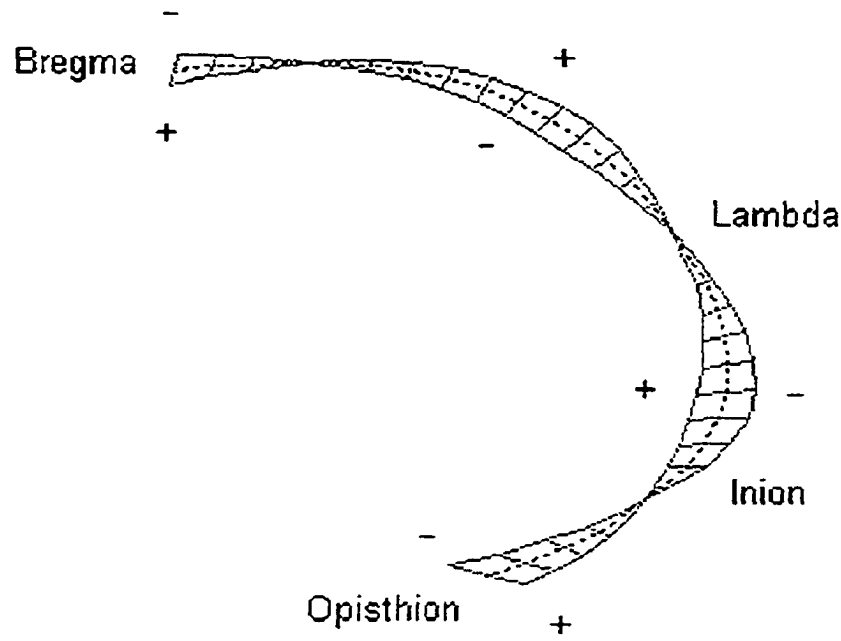

Figure 5.20: Shape variation along CaV 2 (Step 1B). The dotted line represents the consensus configuration.

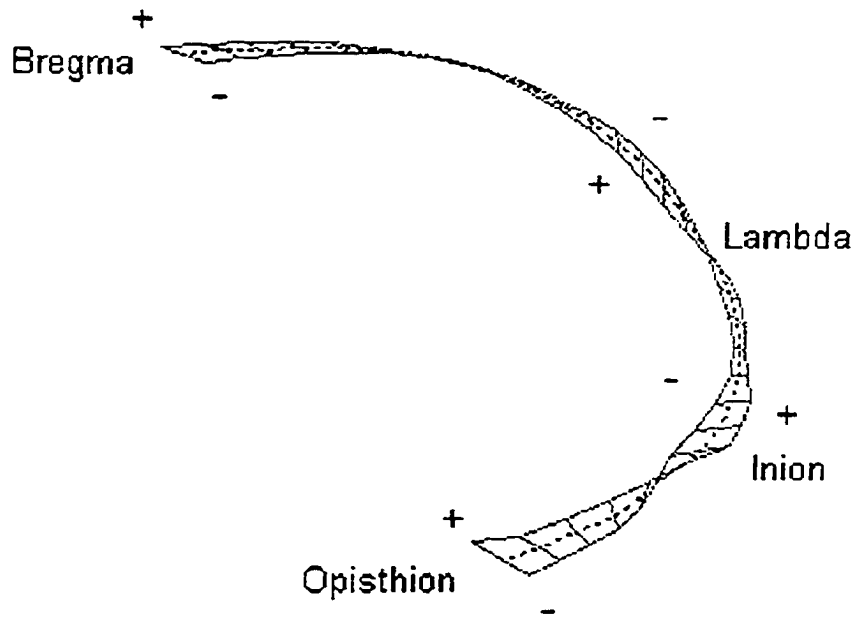

Figure 5.22: Shape variation along CaV 3 (Step 1B). The dotted line represents the consensus configuration.

human range, overlapping only with a few Australian and Tolai specimens, although these specimens are within the confidence ellipses for these populations. This population is significantly different from most modern human populations in their mean score, with the exception of the Australians, the Tolai and the Epipaleolithic. Singa and Biache fall at the negative extreme, while the Neanderthal specimens and Petralona fall near the center of the modern human range. The shape differences along this axis (Fig. 5.22) are similar to those found for CaV 4 in the combined sample (Fig. 5.16). In the positive end, they include a posteriorly projecting inion and semilandmarks around it (9, 10, 8), probably indicating strong superstructures at the level of the superior nuchal line. The posterior projection does not extend to the occipital plane above this area, as it does in Neanderthals, and therefore cannot be described as an occipital 'bun'. The shape differences that characterize the negative end, where Singa and Biache fall, include an inferiorly placed nuchal plane and an anteriorly positioned inion.

Classification: Removal of the chimpanzee sample resulted in some differences in classification. In the classification of singletons by posterior probability Petralona and Singa are now classified as Neanderthal (0.99 and 0.92 respectively) rather than Berg, and Kanalda is classified as Epipaleolithic (0.24) rather than Australian. The cross-validation classification (Table 5.10) is very similar to that obtained for the combined sample. However, in this analysis one Neanderthal specimen is classified correctly, while only one, rather than two, modern human specimen is misclassified as Neanderthal.

Mahalanobis D^2, Cluster Analysis and Minimum Spanning Tree: This analysis (Table 5.11) is very similar to that obtained for the combined sample. The Upper Paleolithic group is shown to be more distant than Neanderthals from all human groups except the Australian and Epipaleolithic populations. The greatest distance between the groups in the analysis is that between the Upper Paleolithic specimens and Neanderthals. The cluster analysis and minimum spanning trees (Fig. 5.23) are identical to those calculated from the combined sample.

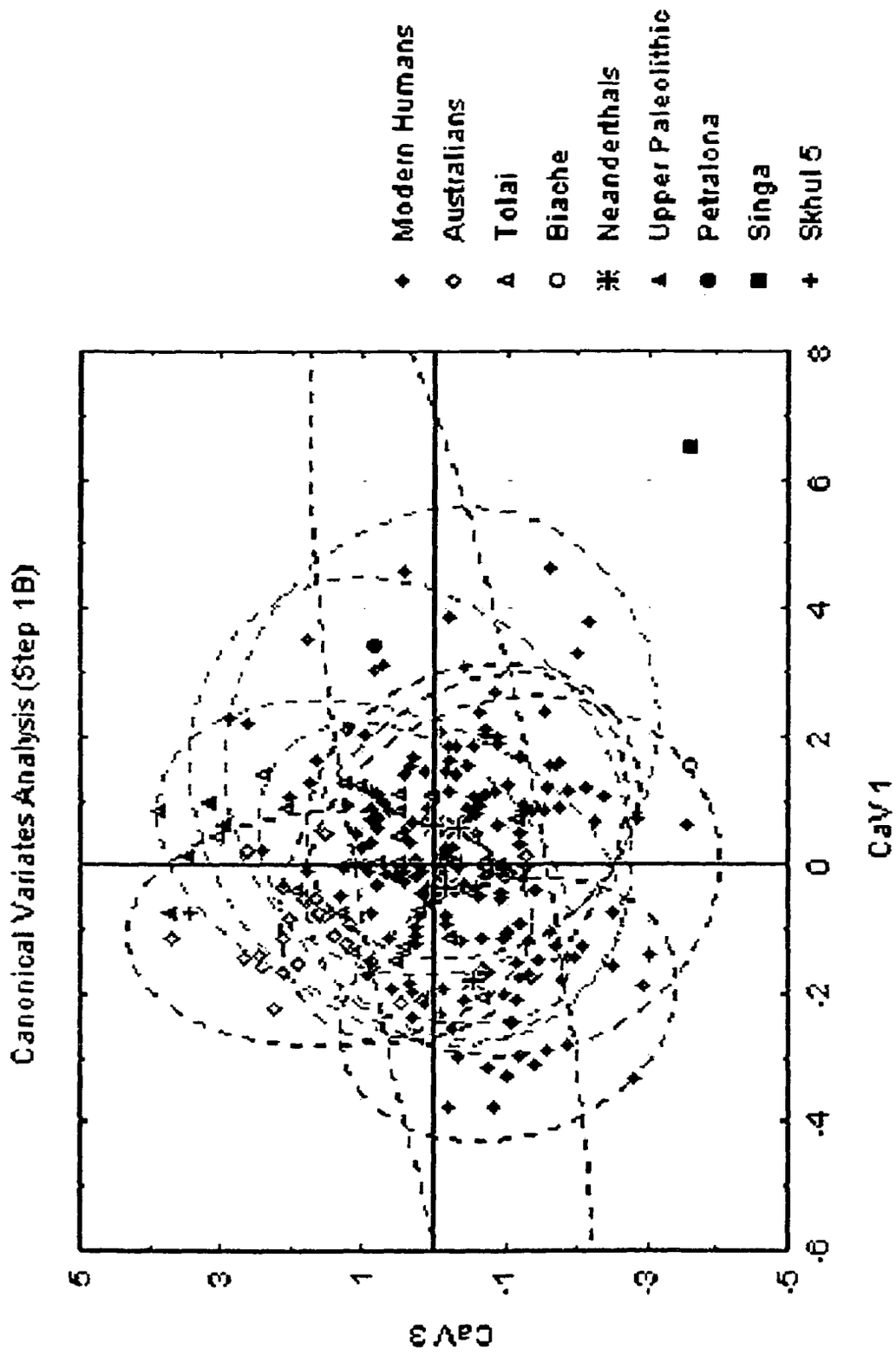

Figure 5.21: Canonical Variates Analysis (Step 1B), CaVs 1 and 3. Dotted lines represent the 95 % confidence ellipses for each group.

Table 5.10: Cross-validation classification summary (percentages for each population in bold), Step 1B.

	And	Aus	Brg	Dgn	Epi	Esk	Eur	San	Tol	UP	Nea	Total
And	14	1	1	2	2	2	4	0	2	1	0	29
%	**48.28**	3.45	3.45	6.9	6.9	6.9	13.79	0	6.9	3.45	0	100
Aus	2	16	0	3	0	2	0	1	4	1	0	29
%	6.9	**55.17**	0	10.34	0	6.9	0	3.45	13.79	3.45	0	100
Brg	1	1	13	0	2	3	5	3	1	0	0	29
%	3.45	3.45	**44.83**	0	6.9	10.34	17.24	10.34	3.45	0	0	100
Dgn	2	3	0	21	0	2	0	2	0	0	0	30
%	6.67	10	0	**70**	0	6.67	0	6.67	0	0	0	100
Epi	4	1	2	1	7	0	1	2	0	1	0	19
%	21.05	5.26	10.53	5.26	**36.84**	0	5.26	10.53	0	5.26	0	100
Esk	3	2	4	1	0	12	3	1	3	0	0	29
%	10.34	6.9	13.79	3.45	0	**41.38**	10.34	3.45	10.34	0	0	100
Eur	2	0	6	0	3	2	6	3	0	0	0	22
%	9.09	0	27.27	0	13.64	9.09	**27.27**	13.64	0	0	0	100
San	0	2	1	2	1	2	1	19	2	0	0	30
%	0	6.67	3.33	6.67	3.33	6.67	3.33	**63.33**	6.67	0	0	100
Tol	1	1	2	1	2	2	2	3	13	0	1	28
%	3.57	3.57	7.14	3.57	7.14	7.14	7.14	10.71	**46.43**	0	3.57	100
UP	0	2	0	0	0	0	0	0	1	1	0	4
%	0	50	0	0	0	0	0	0	25	**25**	0	100
Nea	0	0	0	1	0	1	0	1	0	0	1	4
%	0	0	0	25	0	25	0	25	0	0	**25**	100
Total	29	29	29	32	17	28	22	35	26	4	2	253
%	11.46	11.46	11.46	12.65	6.72	11.07	8.7	13.83	10.28	1.58	0.79	100

Table 5.11: Unbiased Mahalanobis D^2, Step 1B. All distances significant to the 0.001 level, except: NS = non-significant, * = 0.05 level, ** = 0.01 level.

	Kan	And	Aus	Bch	Brg	Dgn	Skh5	Epi	Esk	Eur	Ptr	San	Sng	Tol	UP	Nea
Kan	0.00	8.33NS	7.98NS	139.99	8.45NS	26.60NS	109.92	7.26NS	16.41NS	7.58NS	115.58	18.44NS	172.27	11.03NS	39.56NS	60.94**
And	8.33NS	0.00	9.38	90.49	9.91	8.93	119.03	7.19	6.65	4.27	109.12	11.10	144.47	7.95	38.03	33.52
Aus	7.98NS	9.38	0.00	102.89	12.21	8.83	108.84	9.26	6.82	9.26	93.89	8.31	156.71	7.03	24.44	25.64
Bch	139.99	90.49	102.89	0.00	96.70	94.18	228.51	96.48	88.20	88.85	70.68*	91.07	159.80	94.77	108.94	54.31**
Brg	8.45NS	9.91	12.21	96.70	0.00	17.24	112.91	8.86	5.55	2.62NS	83.84	9.19	126.90	8.01	35.96	30.59
Dgn	26.60NS	8.93	8.83	94.18	17.24	0.00	118.65	16.30	8.76	10.65	107.59	8.82	157.73	11.59	40.28	25.25
Skh5	109.92	119.03	108.84	228.51	112.91	118.65	0.00	110.44	114.79	113.11	220.90	108.98	305.36	111.34	154.14	123.43
Epi	7.26NS	7.19	9.26	96.48	8.86	16.30	110.44	0.00	10.02	6.35	107.42	9.00	135.16	11.03	32.48	32.69
Esk	16.41NS	6.65	6.82	88.20	5.55	8.76	114.79	10.02	0.00	3.97**	87.79	6.63	145.54	6.55	33.02	20.63
Eur	7.58NS	4.27	9.26	88.85	2.62NS	10.65	113.11	6.35	3.97	0.00	96.84	7.71	140.71	6.07	32.73	27.70
Ptr	115.58	109.12	93.89	70.68*	83.84	107.59	220.90	107.42	87.79	96.84	0.00	92.29	164.52	93.67	105.05	67.67
San	18.44NS	11.10	8.31	91.07	9.19	8.82	108.98	9.00	6.63	7.71	92.29	0.00	139.39	7.34	33.54	19.05
Sng	172.27	144.47	156.71	159.80	126.90	157.73	305.36	135.16	145.54	140.71	164.52	139.39	0.00	148.59	159.29	119.15
Tol	11.03NS	7.95	7.03	94.77	8.01	11.59	111.34	11.03	6.55	6.07	93.67	7.34	148.59	0.00	31.76	25.28
UP	39.56NS	38.03	24.44	108.94	35.96	40.28	154.14	32.48	33.02	32.73	105.05	33.54	159.29	31.76	0.00	46.47
Nea	60.94**	33.52	25.64	54.31**	30.59	25.25	123.43	32.69	20.63	27.70	67.67	19.05	119.15	25.28	46.47	0.00

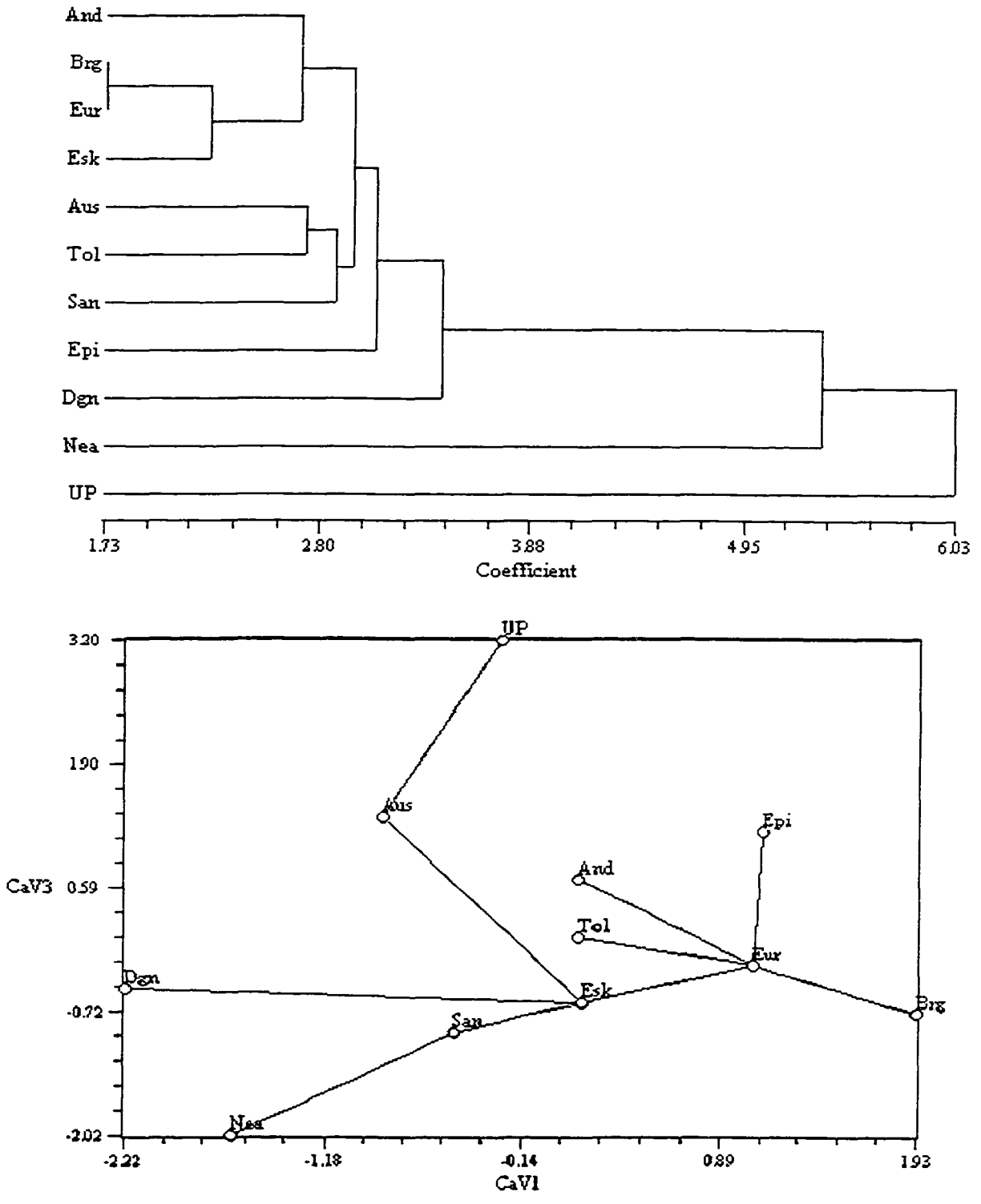

Figure 5.23: Cluster analysis (UPGMA) and minimum spanning tree (top, Step 1A).

Step 1C – Chimpanzee sample only

Classification: Classification success in the cross-validation classification for the chimpanzee sample is similar to that obtained in Step 1A. Twice as many specimens of *P. t. schweinfurthii* were misclassified as bonobos than *P. t. troglodytes*, a slight improvement to the results of Step 1A.

Mahalanobis D^2: The unbiased Mahalanobis distances were calculated for the chimpanzee taxa. The results differ from those found in Step 1A in that bonobos are more distant from both common chimpanzee subspecies than the two subspecies are from each other. Although bonobos were found to be closer to *P. t. schweinfurthii* than the two common chimpanzee subspecies were from each other in the combined sample analysis, the distances between the chimpanzee taxa can be underestimated due to the much greater variation in the human sample. The results of the chimpanzee sample analysis are consistent with the findings of both the temporal and occipital bone analyses.

The distance between the two chimpanzee species is greater than those among recent human populations. It is smaller than most of the distances between Neanderthals and modern humans, and equivalent to the smallest distance between Neanderthals and a modern human group (San). It is also smaller than all the distances between the Upper Paleolithic group and the recent human populations. The distance between the two common chimpanzee subspecies is equivalent to the highest distances between recent human populations.

Step 2 - Lambda-Opisthion

The analysis was repeated on the line segment from lambda to opisthion, describing the outline of the occipital bone in lateral view. This increased the Neanderthal sample only by one (La Chapelle, La Ferrassie 1, Shanidar 1, Saccopastore 1 and Gibraltar 1) and did not substantially change the results obtained in Step 1. Neanderthals were only partially separated in the PCA and CVA, although they were better separated when the human sample was analyzed alone. Classification success was similar to that in Step 1.

Table 5.12: Cross-validation classification summary (percentages for each population in bold), Step 1C.

	Bon	Sch	Trg	Total
Bon	30	1	2	33
%	**90.91**	3.03	6.06	100
Sch	4	20	6	30
%	13.33	**66.67**	20	100
Trg	2	7	19	28
%	7.14	25	**67.86**	100
Total	36	28	27	91
%	39.56	30.77	29.67	100

Table 5.13: Unbiased Mahalanobis D^2, Step 1C. All distances significant to the 0.001 level, except: NS = non-significant, * = 0.05 level, ** = 0.01 level.

	Bon	Sch	Trg
Bon	0	13.79	19.98
Sch	13.79	0	9.15
Trg	19.98	9.15	0

The Upper Paleolithic group remained equally or more distant from the modern human populations than the Neanderthals, as seen in the Mahalanobis D^2 matrices and the cluster and minimum spanning tree analyses. The shape differences separating Neanderthals from modern humans are similar to those described in Step 1 and include the posteriorly projecting and highly curved occipital plane, while those that characterize the Upper Paleolithic specimens relative to the modern groups involve the posterior projection of inion and the semilandmarks around it. The Mahalanobis distance matrices, cross-validation classification results, cluster analyses and minimum spanning trees are reported in the Appendix.

Step 3 - Bregma-Inion

The analysis was repeated on the two line segments from bregma to lambda and lambda to inion, defining the outline of the parietal and the upper scale of the occipital bone. The sample of Neanderthal specimens increased to nine specimens (La Chapelle, La Ferrassie 1, Shanidar 1, Saccopastore 1, Circeo 1, La Quina, Amud 1, Tabun C1 and Spy 1, see Table 5.1). This analysis also included six, rather than four, Upper Paleolithic specimens (Cro Magnon 1 and 2, Predmosti 3 and 4, Ein Gev and Mladec 1), as well as Skhul 5 and Skhul 9. Among the modern human groups, the Epipaleolithic sample increased to 22. The results of Step 3 differ from those obtained in the first two steps in that the Upper Paleolithic specimens are no longer widely separated from the recent human groups, while Neanderthals remain very distant and appear as outliers to all modern human groups in the cluster analyses. However, as in the first two steps, Neanderthals are not completely separated from modern humans in either the PCA or the CVA.

Centroid Size: Analysis of centroid size is very similar to that in Step 1 (Table 5.14, Fig. 5.24). Significant population and sex effects (0.0001) were observed, as well as interaction effects (0.01). As in Step 1, all three chimpanzee taxa are significantly smaller than all modern human populations in their mean centroid size values.

As in Step 1, bonobos have a larger mean centroid size than common chimpanzees, although the three chimpanzee taxa are not significantly different in their mean values. The standard deviations for the two species are equivalent. Among the two

Table 5.14: Centroid size listed by genus, species, sex and population, Bregma-Inion (Step 3).

	Mean	Range	St. Deviation	N
Homo	**25.97**	**21.89-30.00**	**1.55**	**271**
Males	26.42	23.25-30.00	1.38	143
Females	25.46	21.89-29.72	1.55	126
Modern	26.01	21.89-30.00	1.55	258
Males	26.47	23.25-30.00	1.38	135
Females	25.48	21.88-29.72	1.57	122
Neanderthals	25.44	24.08-28.17	1.35	9
Males	26.21	24.93-28.17	1.35	5
Females	24.61	24.08-25.26	0.53	4
Biache	22.95	---	---	1
Petralona	25.59	---	---	1
Reilingen	24.50	---	---	1
Skhul 5	26.61	---	---	1
Skhul 9	25.95	---	---	1
Singa	24.65	---	---	1
Upper Paleolithic	27.72	26.65-28.69	0.82	6
Kanalda	28.45	---	---	1
Andamanese	24.48	22.15-27.40	1.28	29
Australian	26.02	23.58-29.72	1.53	29
Berg	25.91	22.71-28.54	1.29	29
Dogon	25.36	22.80-28.23	1.20	30
Epipaleolithic	27.90	26.17-30.00	1.04	22
Eskimo	26.63	23.99-29.28	1.24	29
European (mixed)	26.27	23.74-28.47	1.41	23
San	25.20	21.88-28.03	1.41	30
Tolai	26.48	25.09-28.60	0.92	28
Pan	**13.16**	**10.60-15.67**	**0.83**	**91**
Males	13.10	10.60-14.81	0.79	49
Females	13.25	11.25-15.67	0.86	41
P. paniscus	13.51	11.64-15.67	0.80	33
Males	13.47	12.57-14.81	0.65	15
Females	13.54	11.65-15.67	0.93	18
P. troglodytes	12.96	10.60-14.71	0.78	59
Males	12.94	10.60-14.28	0.80	34
Females	13.03	11.25-14.71	0.75	23
P. t. schweinfurthii	13.34	12.05-14.71	0.60	30
P. t. troglodytes	12.57	10.60-13.89	0.76	29

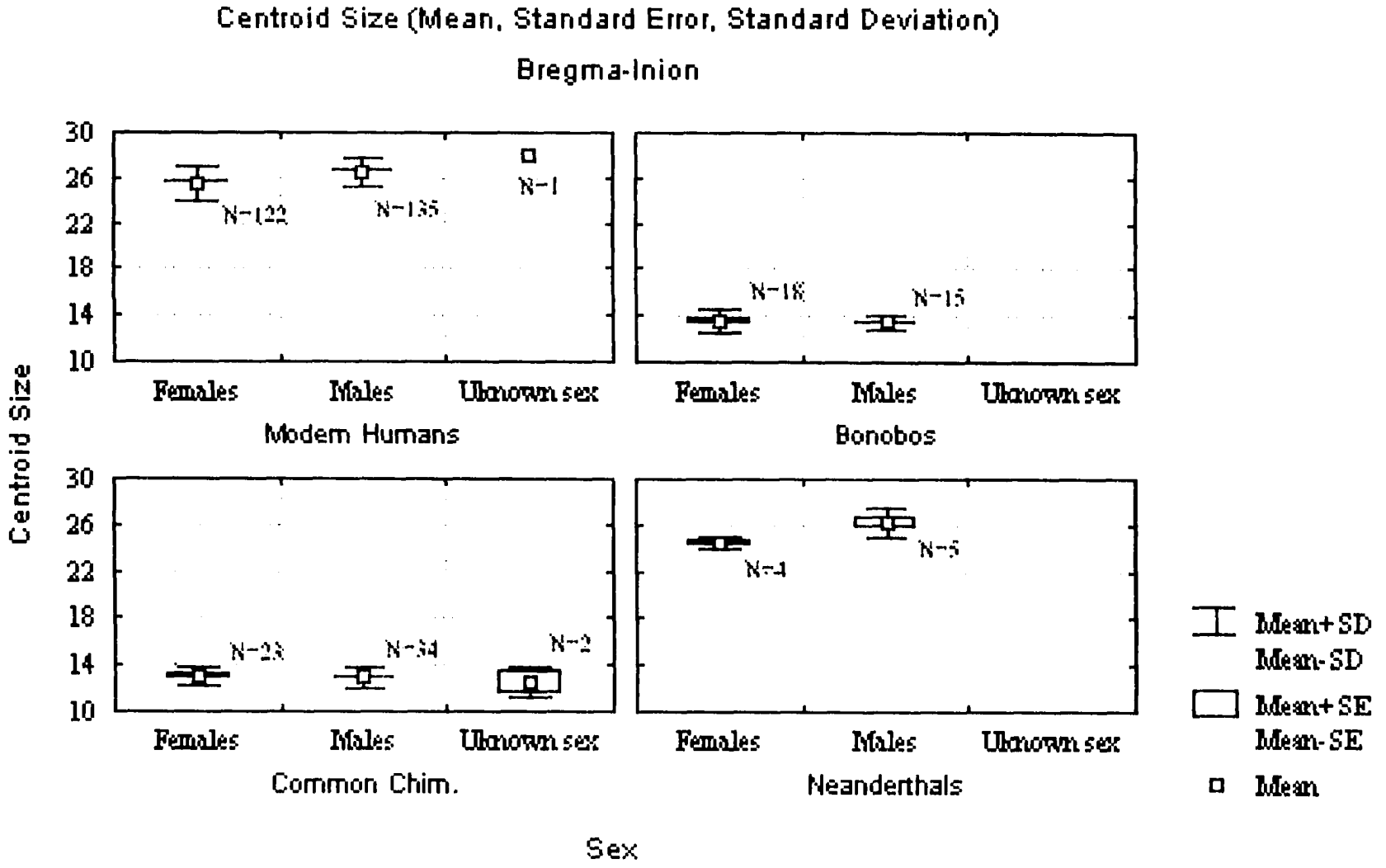

Figure 5.24: Centroid size mean, standard error and standard deviation, labeled by species and sex (Step 3).

subspecies, *P. t. schweinfurthii* show a higher mean value and a slightly smaller standard deviation than *P. t. troglodytes*. In both chimpanzee species females have slightly higher means than males, bonobo females also having a larger standard deviation. Both species show almost no sexual dimorphism, with females being slightly larger than males, suggesting that the removal of the nuchal plane decreases the degree of sexual dimorphism in centroid size at least among common chimpanzees.

Human females have a lower mean but a somewhat higher standard deviation than males. Modern humans still appear sexually dimorphic in centroid size, males being larger than females, although less so than in Step 1. The Neanderthal mean and standard deviation are somewhat lower than those of modern humans. Sexual dimorphism can be assessed in Neanderthals in this analysis, and is much more marked in this fossil group than in modern humans, males again being larger than females.

Among modern human groups, the Epipaleolithic population shows the highest mean centroid size, which is even higher than that of the Upper Paleolithic group in this analysis, and unlike Step 1. The Andamanese show the lowest mean value. The highest standard deviation is found in the Australian population, and the lowest in the Upper Paleolithic and Tolai groups.

Step 3A, Combined sample

Principal Components Analysis: The results of this analysis are similar to those obtained in Step 1 (Tables 5.15, 5.16). The first principal component (82.4 % of the total variance, Fig. 5.25) separates humans from chimpanzees. All three chimpanzee groups are significantly different from all modern human populations in their mean scores. Bonobos are also significantly different from *P. t. troglodytes*. The shape differences driving this separation are similar to those described for PC 1 and CaV 1 in Step 1A and include a much more rounded profile and a supero-inferiorly taller occipital plane in humans relative to chimpanzees. Both Petralona and Biache fall at the fringe of the human range, the former slightly overlapping with the bonobo range, reflecting the very flat parietals of these specimens. PC 1 is also significant for sex effects at the 0.0001 level, as well as for interaction effects (0.05). When the mean scores for the two sexes are plotted by population (Fig. 5.26), the male means of all three chimpanzee taxa are

Table 5.15: Summary of the PCA results, ANOVA and Correlation Analysis for PCs 1-10, Step 3A.

	Principal Components Analysis			ANOVA, Pr > F			Correlation with Centroid size	
	Eigenvalue	Proportion	Cumulative	Popul.	Sex	Interaction	Rho	Pr > F
PC 1	0.006743	0.824031	0.824031	0.0001	0.0001	0.0405	0.90334	0.0001
PC 2	0.000865	0.105761	0.929792	0.0001	0.677	0.1052	0.10179	0.0527
PC 3	0.000233	0.028444	0.958236	0.0001	0.0656	0.0021	-0.04662	0.3758
PC 4	0.00008	0.009742	0.967978	0.0001	0.4815	0.1228	-0.19534	0.0002
PC 5	0.00005	0.006137	0.974115	0.0001	0.387	0.6542	-0.08507	0.1056
PC 6	0.000038	0.00468 6	0.9788	0.0001	0.4349	0.8225	0.02141	0.6843
PC 7	0.000027	0.003297	0.982097	0.0009	0.0556	0.0053	-0.04825	0.3594
PC 8	0.000023	0.002751	0.984848	0.0001	0.027	0.8242	-0.02772	0.5986
PC 9	0.000017	0.002109	0.986957	0.3583	0.985	0.4231	0.00258	0.9609
PC 10	0.000016	0.002011	0.988968	0.4732	0.8569	0.4097	-0.01043	0.843

Table 5.16: Squared roots of the sum of squares of the eigenvector coefficients for the residuals of the three coordinates for each landmark and semilandmark, Step 3A.

	PC 1	PC 2	PC 3
Lambda (1)	**0.24**	**0.25**	0.19
Semilandmark 2	0.17	0.17	**0.24**
Semilandmark 3	0.10	0.10	**0.27**
Semilandmark 4	0.06	0.06	**0.25**
Semilandmark 5	0.09	0.11	**0.21**
Semilandmark 6	0.17	0.18	0.10
Semilandmark 7	**0.26**	**0.25**	0.10
Semilandmark 8	**0.36**	**0.31**	**0.33**
Inion (9)	**0.46**	**0.37**	**0.50**
Bregma (10)	**0.28**	**0.32**	**0.21**
Semilandmark 11	**0.22**	**0.26**	0.16
Semilandmark 12	0.17	0.19	0.09
Semilandmark 13	0.12	0.13	0.03
Semilandmark 14	0.08	0.09	0.06
Semilandmark 15	0.03	0.05	0.13
Semilandmark 16	0.02	0.06	0.18
Semilandmark 17	0.06	0.08	0.20
Semilandmark 18	0.10	0.12	0.21
Semilandmark 19	0.13	0.14	0.20
Semilandmark 20	0.15	0.17	0.18
Semilandmark 21	0.18	0.20	0.13
Semilandmark 22	0.20	**0.22**	0.11
Semilandmark 23	0.22	0.23	0.05
Semilandmark 24	0.23	0.23	0.03
Semilandmark 25	0.23	0.23	0.11

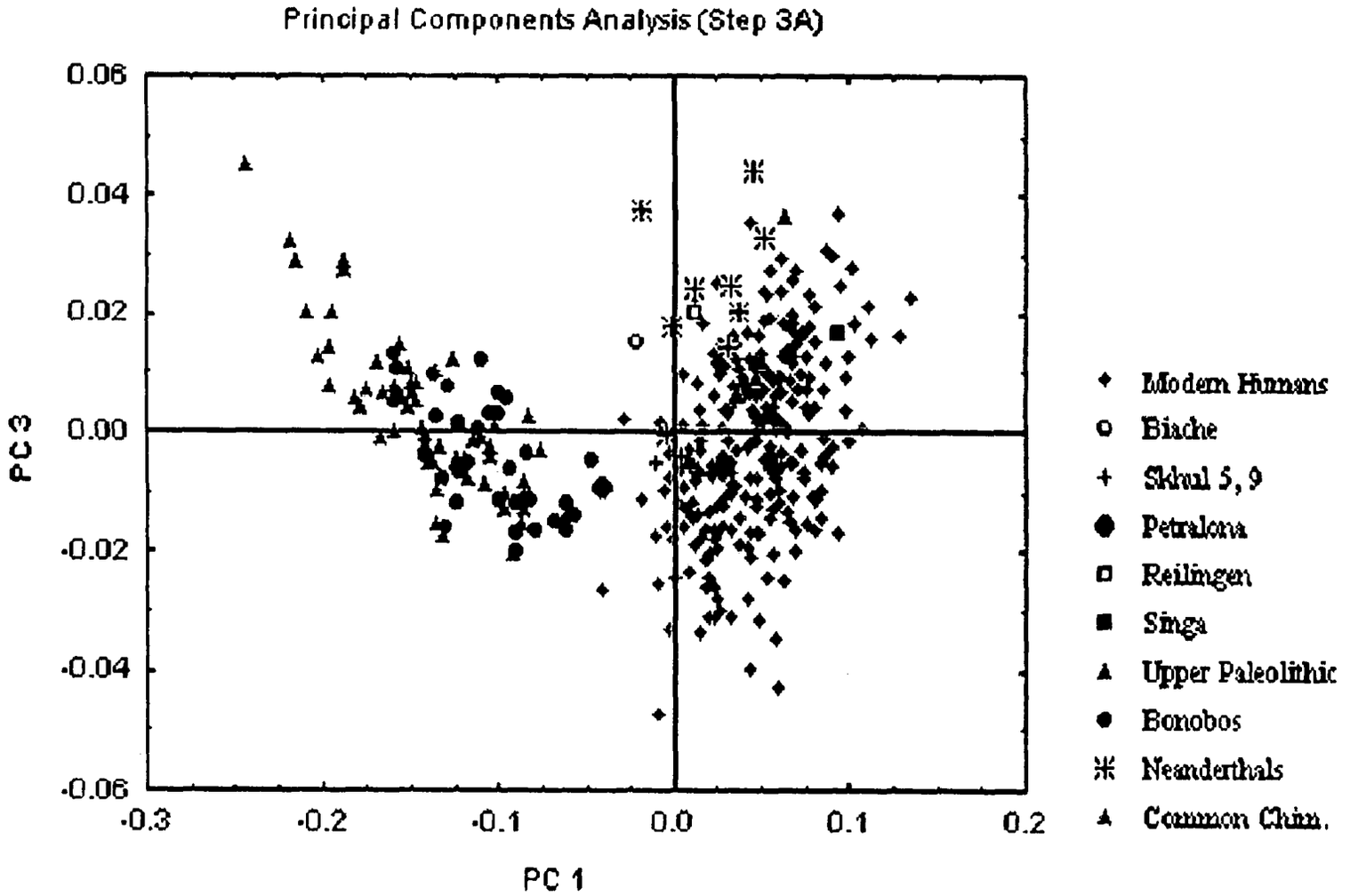

Figure 5.25: Principal Components Analysis, PC 1 and PC 3 (Step 3A).

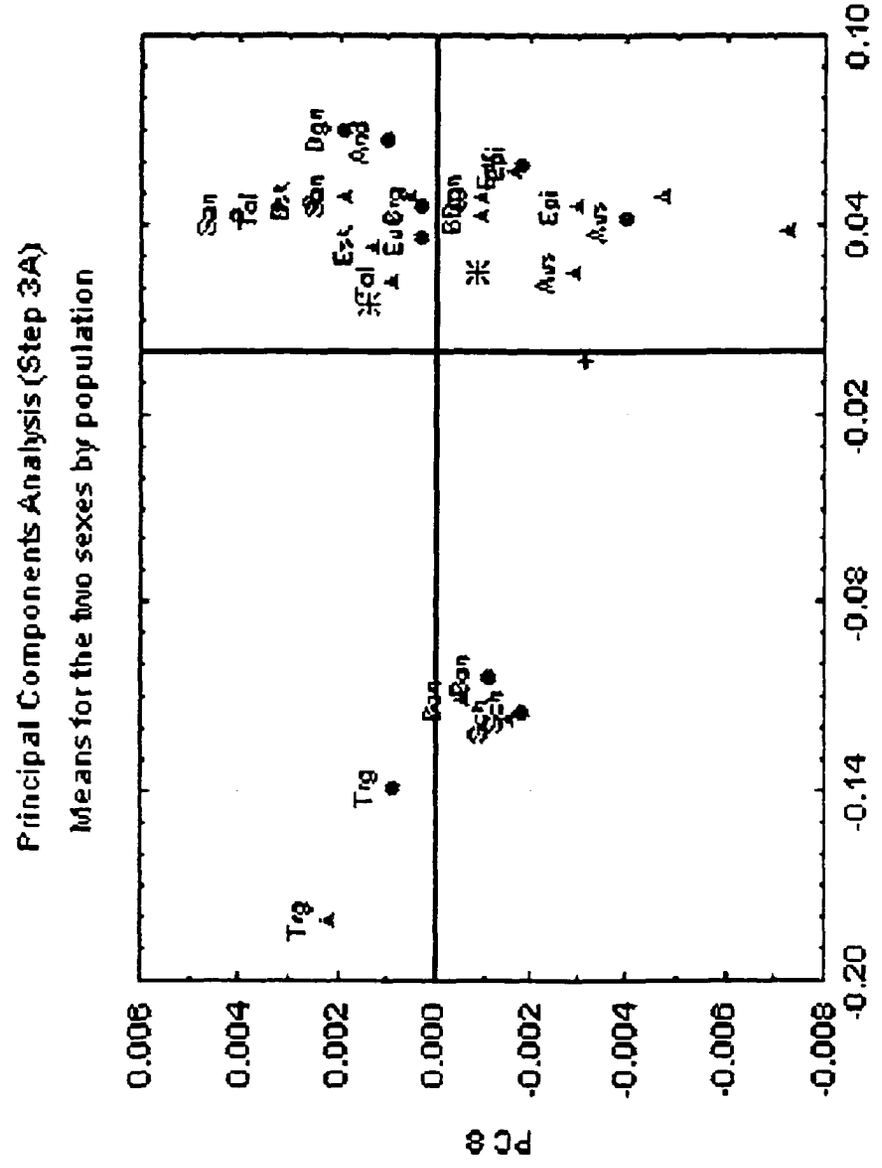

Figure 5.26: Principal Components Analysis (Step 3A), PCs 1 and 8, means for the two sexes plotted by population.

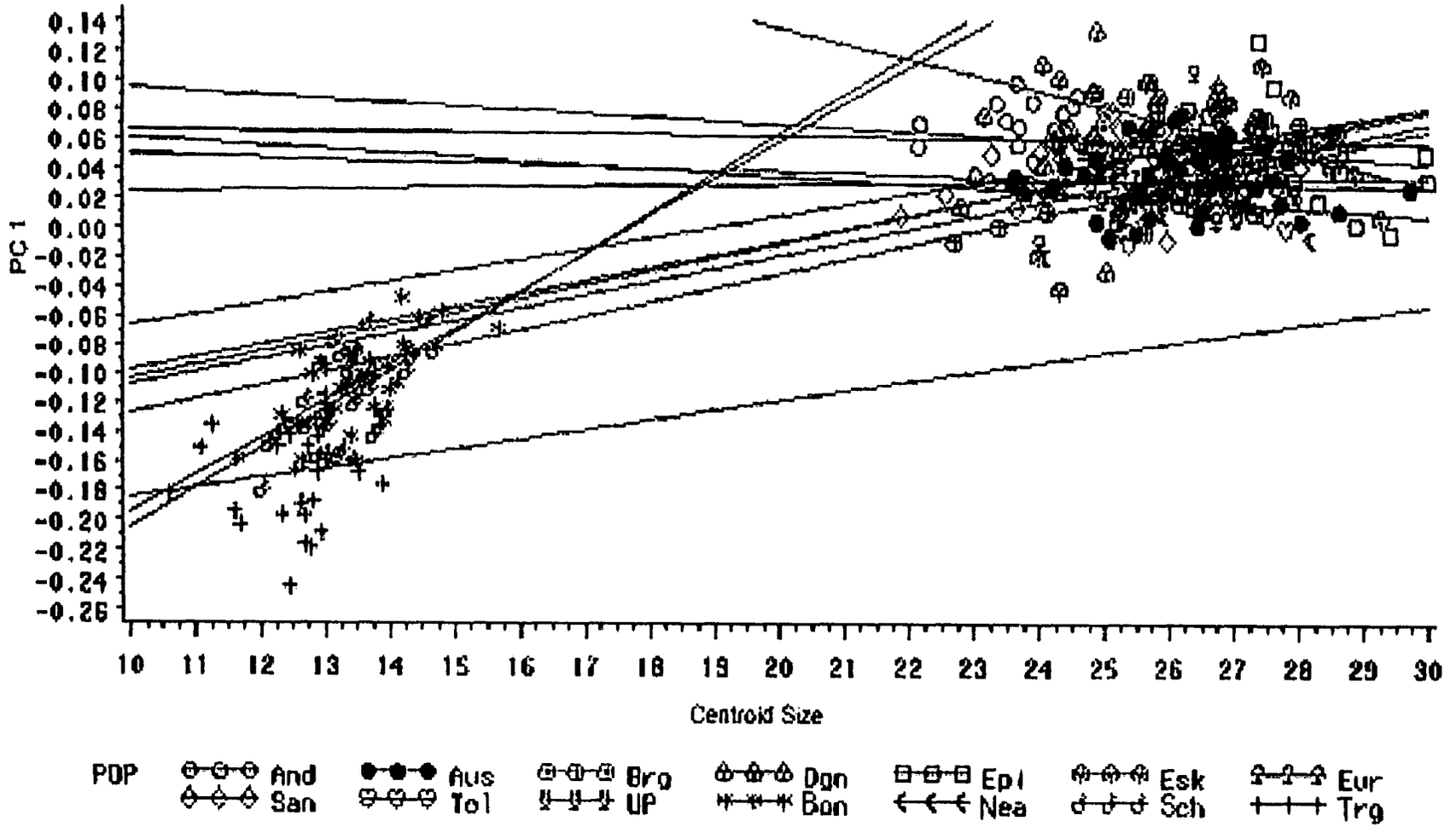

Figure 5.27: PC 1 (Step 3A) plotted against centroid size, regression line fitted for each population.

more negative than those of the females. Most, but not all, modern human groups also show more negative means, although the difference is much less pronounced. No such tendency is observed in the human sample. PC 1 is strongly correlated with centroid size (Table 5.15). When plotted by centroid size, however, and regression lines are fitted for each population, the slopes shown across the groups are not the same (Fig. 5.27), as was also found in Step 1A.

PC 2 (10.6 % of the total variance) separates Singa from modern humans on the negative side. Neanderthals also cluster at the negative extreme of the modern human range, with the exception of Shanidar 1 and Tabun C1, which fall near its center. They are not significantly different in their mean score from any modern human group. The shape differences along this component include a flat and antero-posteriorly short parietal and posteriorly projecting and inferiorly placed inion and lower part of the occipital plane. Tabun C1 and particularly Shanidar 1 are characterized by more curved parietals and less posteriorly and inferiorly projecting lower part of the occipital plane. Amud 1 also has a less posteriorly projecting lower part of the occipital plane, however it shows a very flat parietal. This specimen falls within the modern human cloud, but at the end of the modern human range and close to other Neanderthal specimens.

PC 3 (2.8 %, Fig. 5.24) partially separates Neanderthals on its positive end from modern humans. This group, however, is only significantly different from the Berg and European populations in its mean score. Mladec 1 also falls at the positive extreme of the modern human range, as do also Reilingen and Biache. Shanidar 1 is the only Neanderthal specimen that is widely separated from the others, falling at the center of the modern human range and near Skhul 5 and 9. The shape differences along this component include, at the positive end, a flat parietal, a posteriorly projecting upper part of the occipital plane and an anteriorly and superiorly placed inion. The position of Shanidar 1 is probably due again to its curved parietal and its flat occipital plane relative to all other Neanderthal specimens included here. Among the other specimens, Tabun C1, which also shows a somewhat curved parietal bone and a weak occipital 'bun', falls furthestin the modern human range. Amud 1, however, falls outside the modern human range along PC 3, due to its very flat parietal region and anteriorly and superiorly placed inion.

Canonical Variates Analysis: A CVA was conducted on the first 30 principal components (Table 5.17). CaV 1 (73.5 %, most highly influenced by PC 1, Fig. 5.28) separates humans from chimpanzees. The shape differences along this component are similar to those found for PC 1, and include a more rounded profile and a higher occipital plane in humans. Petralona falls outside the 95 % confidence ellipses of all modern human populations along CaV 1. As in the PCA, CaV 1 is strongly correlated with centroid size. The regression lines for each population show that the groups are behaving differently with regard to centroid size along this axis (Fig. 5.29).

Neanderthals, Biache and Reilingen cluster at the positive end of the modern human range along CaV 2 (5.9 %, most highly influenced by PCs 3 and 6, Fig. 5.28), while Singa falls just outside negative end of the modern human cloud and just at the border of the confidence ellipses of the modern human populations along CaVs 1 and 2. Although Neanderthals overlap with modern humans, they are significantly different in their mean score from several modern human groups, including the Andamanese, Tolai, Epipaleolithic, European and Berg groups. The shape differences along this canonical axis in the positive end, where Neanderthals fall, include an anteriorly and superiorly placed inion and a posteriorly projecting occipital plane. In the negative end, where Singa falls, they include an inferiorly and posteriorly placed inion and a less posteriorly projecting upper part of the occipital scale.

Neanderthals are partially separated from modern humans along CaV 3 (4.6 %, most highly influenced by PCs 2 and 4, Fig. 5.30). However, they are only significantly different in their mean score from the Australian modern human population. Most Neanderthal specimens, Biache, Singa and Reilingen fall outside the modern human range, although the confidence ellipse of Neanderthals overlaps widely with those of modern humans, and two modern human outliers (a European and a Berg) fall within the Neanderthal range. Three Neanderthals (Tabun C1, Shanidar 1 and Saccopastore 1) fall at the fringe of the confidence ellipses of most modern human populations, and near Skhul 9 and Mladec 1. Biache, Singa and Reilingen fall within the Neanderthal confidence ellipse. Amud 1 is the most widely removed Neanderthal specimen from modern humans. The shape differences at the negative end of CaV 3, where

Table 5.17: Summary of the CVA results and Correlation Analysis for CaV 1-5, Step 3A.

	Canonical Variates Analysis			Correlation with Centroid size	
	Eigenvalue	Proportion	Cumulative	Rho	Pr > F
CaV 1	15.9596	0.7355	0.7355	0.94137	0.0001
CaV 2	1.2836	0.0592	0.7946	-0.05258	0.3178
CaV 3	0.9933	0.0458	0.8404	-0.05196	0.3235
CaV 4	0.6843	0.0315	0.8719	-0.03149	0.5498
CaV 5	0.5749	0.0265	0.8984	0.05396	0.3052

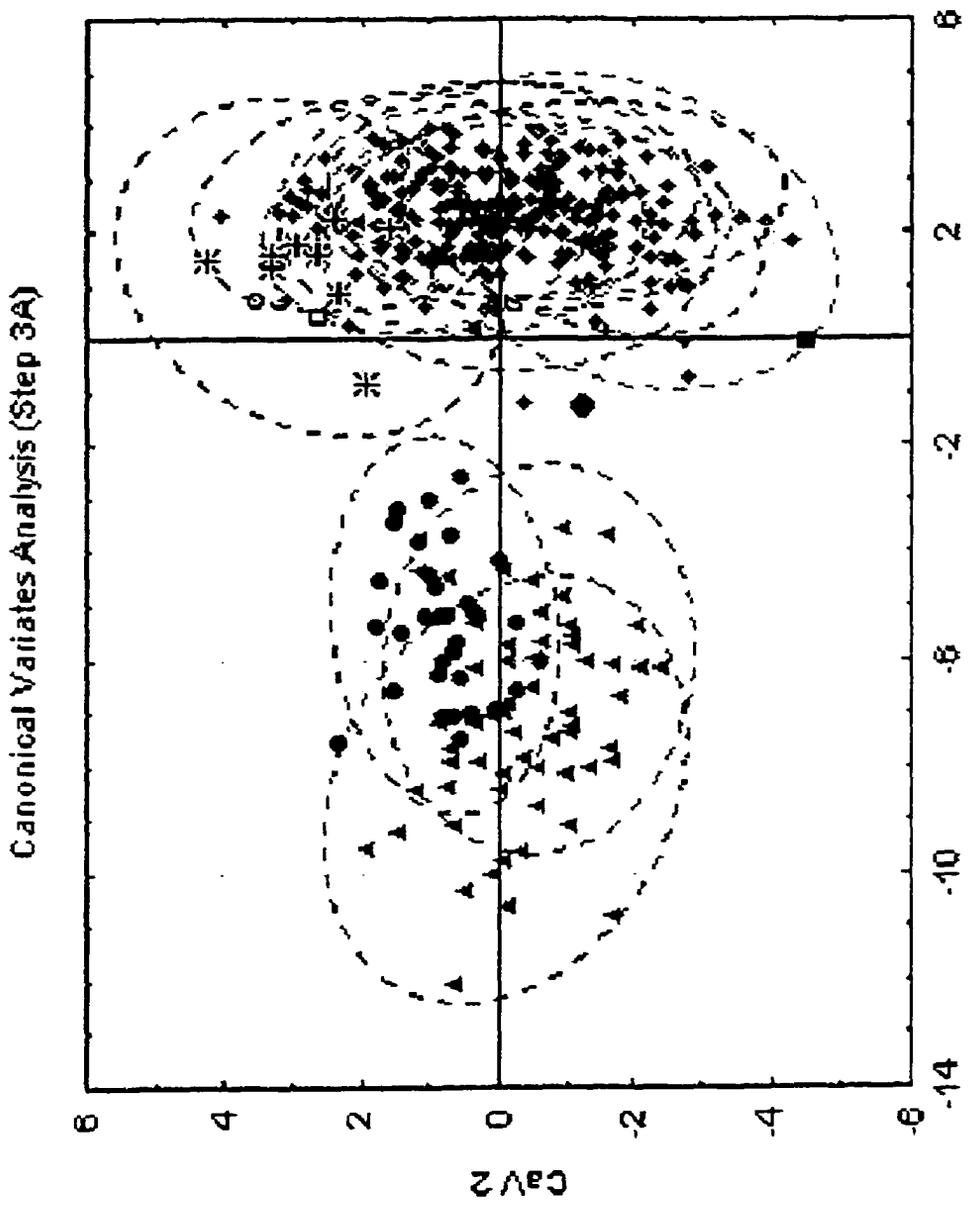

Figure 5.28: Canonical Variates Analysis (Step 3A), CaVs 1 and 2. Dotted lines represent the 95 % confidence ellipses for each group.

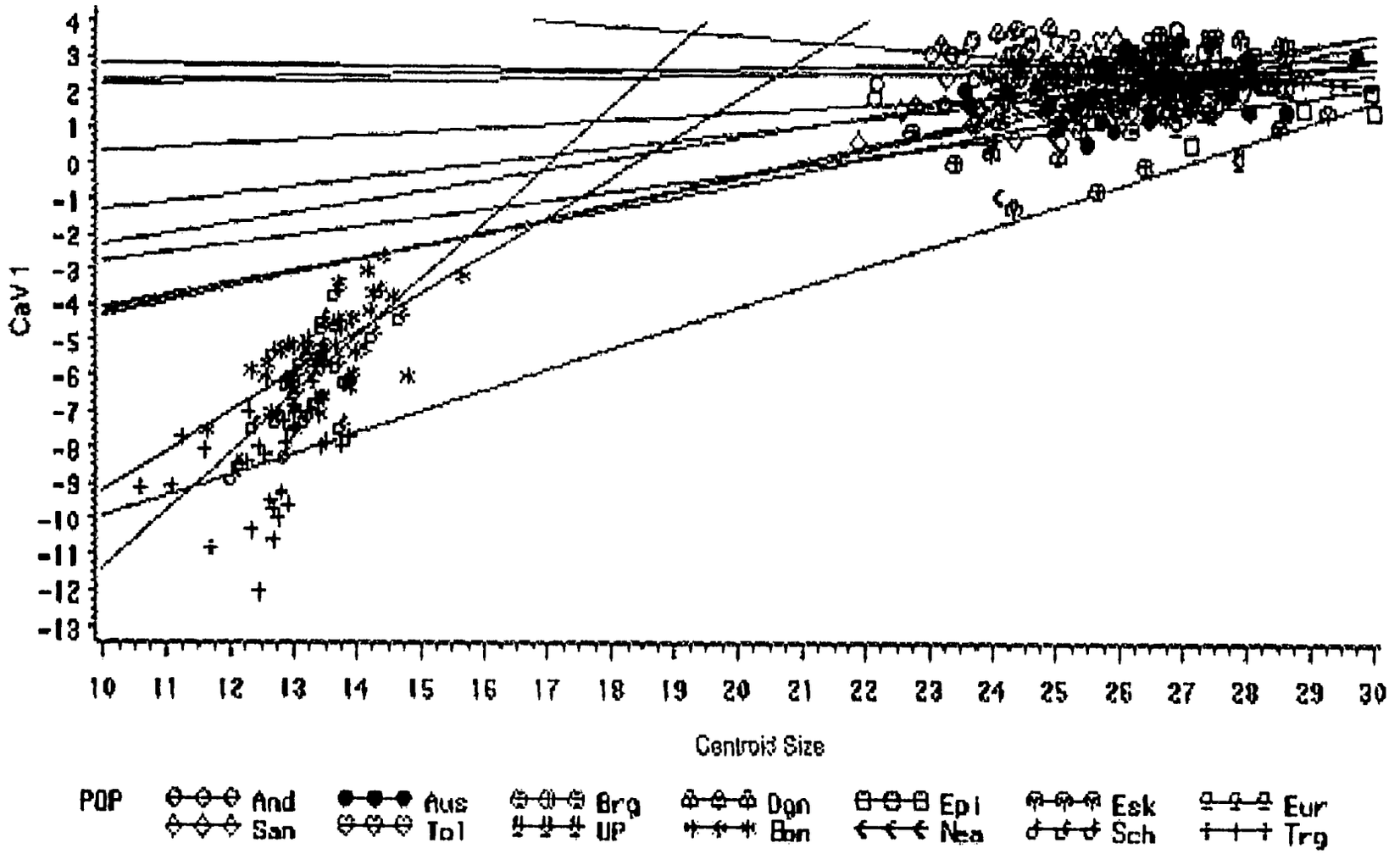

Figure 5.29: CaV 1 (Step 3A) plotted against centroid size, regression lines fitted for each population.

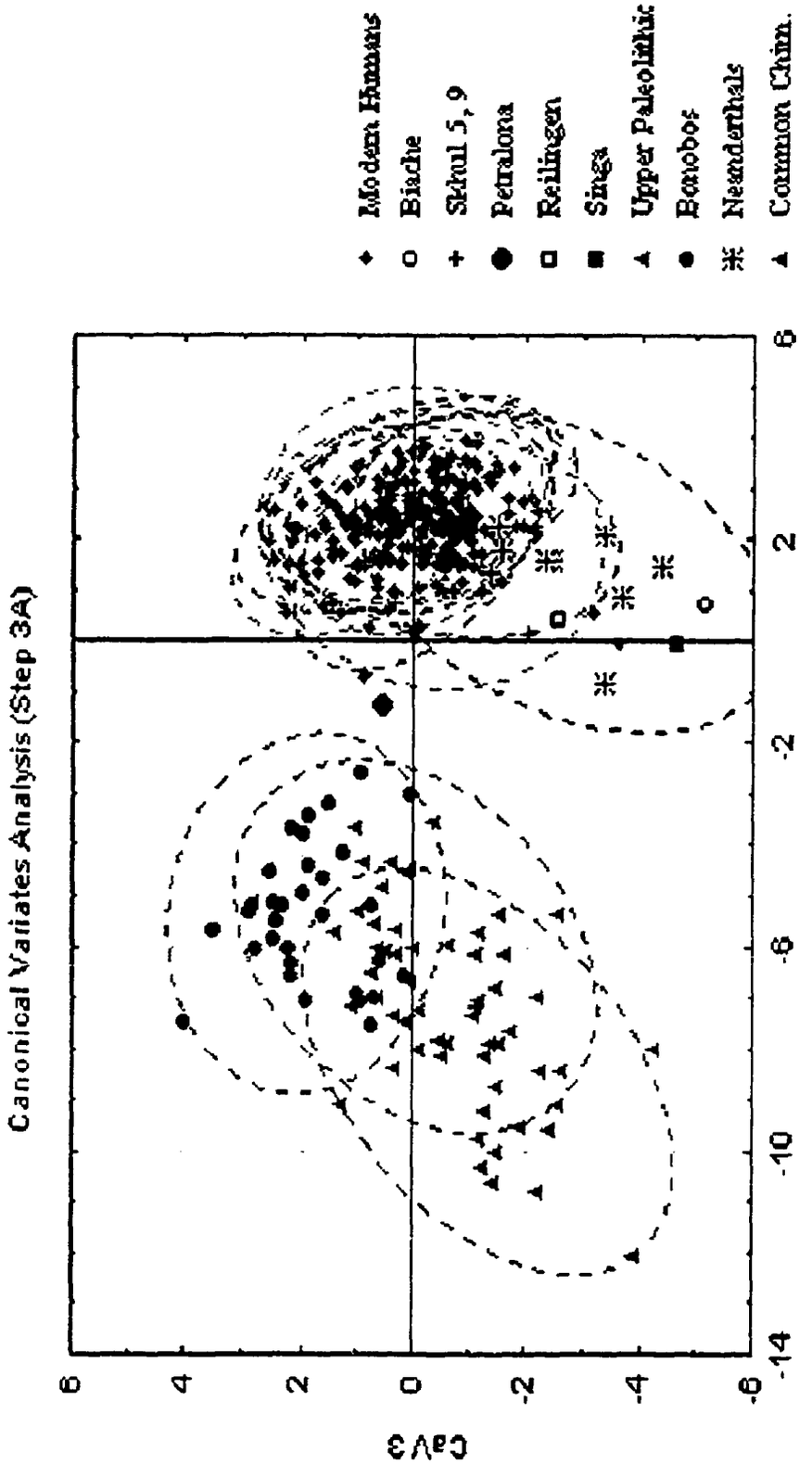

Figure 5.30: Canonical Variates Analysis, CaVs 1 and 3 (Step 3A). Dotted lines represent the 95 % confidence ellipses for each group.

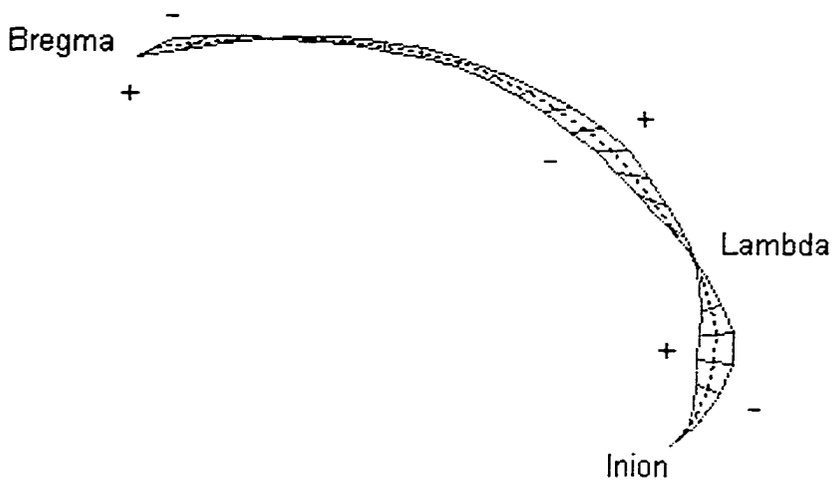

Figure 5.31: Shape variation along CaV 3 (Step 3A). The dotted line represents the consensus configuration.

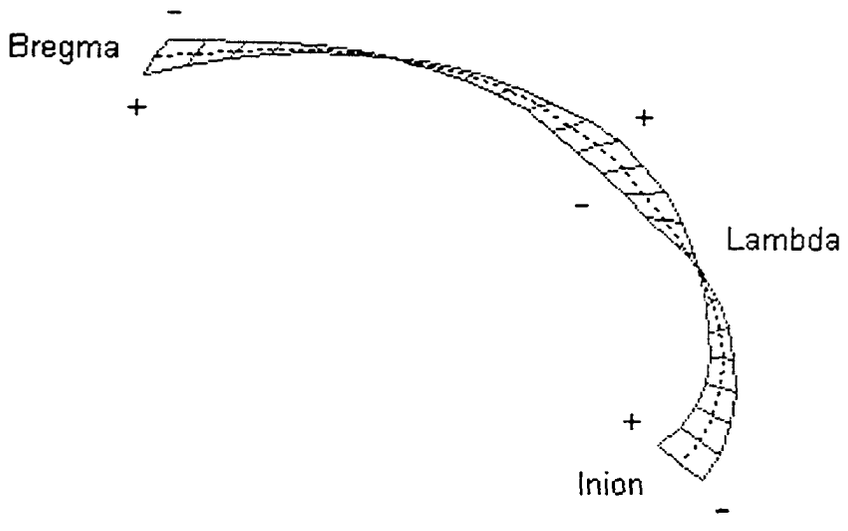

Figure 5.33: Shape variation along CaV 4 (Step 3A). The dotted line represents the consensus configuration.

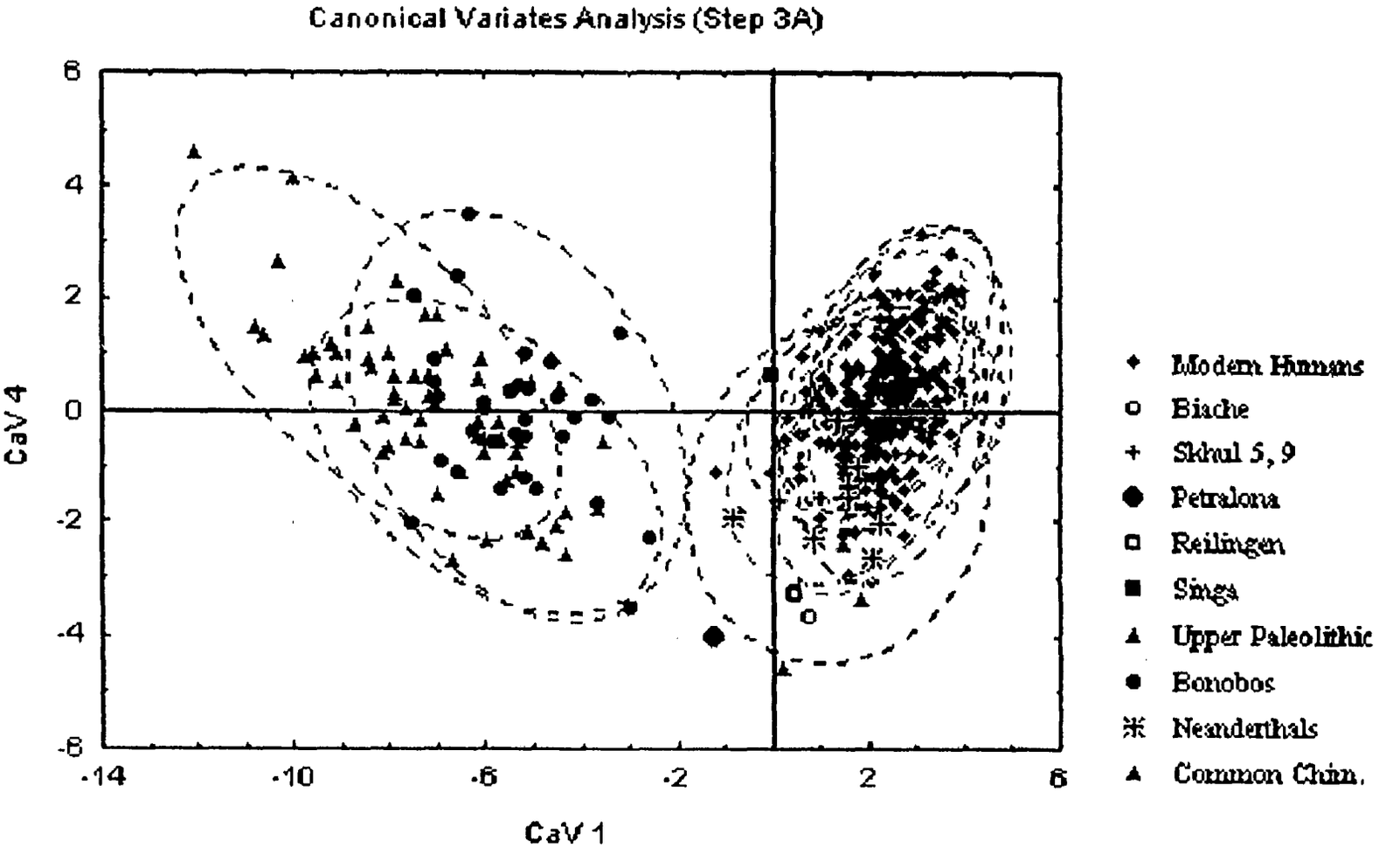

Figure 5.32: Canonical Variates Analysis (Step 3A), CaVs 1 and 4. Dotted lines represent the 95 % confidence ellipses for each group.

Neanderthals fall, include a posteriorly projecting occipital plane and a flat parietal (Fig. 5.31). These shape characteristics, as well as those described in CaV 2, and PCs 2 and 3, are consistent with the occipital bun morphology of the posteriorly projecting upper occipital plane, lambdoid flattening, flat parietal area and low cranial vault described for Neanderthals (Boule 1911-1913; Thoma 1965; Hublin 1978b; Dean et al. 1998). Again, the position of Shanidar 1, Tabun C1 and Saccopastore is due to their more curved parietal areas also previously described for these specimens, as well as their relatively weak occipital buns (i.e. Stringer and Trinkaus 81).

CaV 4 (3.1 %, most influenced by PCs 8 and 2, Fig. 5.32) separates Petralona, Biache, Reilingen, Predmosti 3 and Cro Magnon 1 from modern humans on its negative extreme, these specimens falling outside the 95 % confidence ellipses of all modern human populations along CaVs 1 and 4. The remaining Upper Paleolithic specimens and Skhul 5 and 9 fall near the negative end of the modern human cloud, with the exception of Cro Magnon 2, which falls near the center of the modern human range. The shape differences at its negative end include a flat parietal with a marked depression above lambda and a posteriorly and inferiorly projecting iniac area (Fig. 5.33). These characteristics are similar to those found for Petralona and the Upper Paleolithic group in Step 1, and indicate the combination of a flat parietal with strong iniac superstructures.

Classification: A discriminant analysis was performed treating the fossils as unknown specimens to be classified by posterior probability into one of the defined groups. A cross-validation classification was calculated for the rest of the dataset. Petralona was classified as Upper Paleolithic (0.92), Biache as Neanderthal (1.00), Reilingen as Upper Paleolithic (0.81), Singa as European (0.80), Skhul 5 and 9 both as European (0.44 and 0.85 respectively) and Kanalda as Epipaleolithic (0.49). All Neanderthal specimens were classified correctly by posterior probability, as were three Upper Paleolithic specimens. However, Cro Magnon 2 was classified as Eskimo (0.26), Ein Gev as European (0.55) and Mladec 1 as Neanderthal (0.79).

The cross-validation classification was not very successful and it was similar to those obtained in Steps 1 and 2. The highest success rate was achieved by bonobos (72.73 %), and, among modern human groups, by the Dogon (63.33 %). However, and unlike steps 1 and 2, Neanderthals show a high success rate, six out of nine specimens

Table 5.18: Cross-validation classification summary (percentages for each population in bold), Step 3A.

	And	Aus	Brg	Dgn	Epi	Esk	Eur	San	Tol	UP	Bon	Nea	Sch	Trg	Total
And	11	0	2	1	4	2	2	1	6	0	0	0	0	0	29
%	**37.93**	0	6.9	3.45	13.79	6.9	6.9	3.45	20.69	0	0	0	0	0	100
Aus	2	13	1	0	2	3	1	3	2	2	0	0	0	0	29
%	6.9	**44.83**	3.45	0	6.9	10.34	3.45	10.34	6.9	6.9	0	0	0	0	100
Brg	2	2	10	0	2	2	8	1	2	0	0	0	0	0	29
%	6.9	6.9	**34.48**	0	6.9	6.9	27.59	3.45	6.9	0	0	0	0	0	100
Dgn	2	3	0	19	1	1	0	4	0	0	0	0	0	0	30
%	6.67	10	0	**63.33**	3.33	3.33	0	13.33	0	0	0	0	0	0	100
Epi	3	1	1	0	7	2	2	3	1	2	0	0	0	0	22
%	13.64	4.55	4.55	0	**31.82**	9.09	9.09	13.64	4.55	9.09	0	0	0	0	100
Esk	2	2	5	1	0	9	3	2	5	0	0	0	0	0	29
%	6.9	6.9	17.24	3.45	0	**31.03**	10.34	6.9	17.24	0	0	0	0	0	100
Eur	1	0	7	0	3	1	9	1	0	1	0	0	0	0	23
%	4.35	0	30.43	0	13.04	4.35	**39.13**	4.35	0	4.35	0	0	0	0	100
San	2	0	0	2	2	7	2	15	0	0	0	0	0	0	30
%	6.67	0	0	6.67	6.67	23.33	6.67	**50**	0	0	0	0	0	0	100
Tol	4	1	3	1	3	2	3	1	9	1	0	0	0	0	28
%	14.29	3.57	10.71	3.57	10.71	7.14	10.71	3.57	**32.14**	3.57	0	0	0	0	100
UP	0	3	0	0	0	1	1	0	0	0	0	1	0	0	6
%	0	50	0	0	0	16.67	16.67	0	0	**0**	0	16.67	0	0	100
Bon	0	0	0	0	0	0	0	0	0	1	24	0	5	3	33
%	0	0	0	0	0	0	0	0	0	3.03	**72.73**	0	15.15	9.09	100
Nea	0	0	0	0	0	1	0	2	0	0	0	6	0	0	9
%	0	0	0	0	0	11.11	0	22.22	0	0	0	**66.67**	0	0	100
Sch	0	0	0	0	0	0	0	0	0	0	7	0	17	6	30
%	0	0	0	0	0	0	0	0	0	0	23.33	0	**56.67**	20	100
Trg	0	0	0	0	0	0	0	0	0	0	0	0	7	22	29
%	0	0	0	0	0	0	0	0	0	0	0	0	24.14	**75.86**	100
Total	29	25	29	24	24	31	31	33	25	7	31	7	29	31	356
%	8.15	7.02	8.15	6.74	6.74	8.71	8.71	9.27	7.02	1.97	8.71	1.97	8.15	8.71	100

(66.67%) being classified correctly, two being classified as San and one as Eskimo. Furthermore, no recent human specimen was misclassified as Neanderthal, again unlike the previous analyses. None of the Upper Paleolithic specimens were correctly classified, an even worse performance than that observed in Steps 1 and 2. Three of these specimens were classified as Australian, one as Eskimo, one as European and one as Neanderthal. Two Australians, two Epipaleolithic specimens, one European and one Tolai were misclassified as Upper Paleolithic, as was one bonobo. This is the first time that a chimpanzee is classified as human.

Mahalanobis D^2, Cluster Analysis and Minimum Spanning Tree: The unbiased Mahalanobis D^2 matrix was calculated. As in Steps 1 and 2, *P. t. schweinfurthii* are closer to bonobos to than to *P. t. troglodytes*. Neanderthals are more distant from all modern human groups than any of the chimpanzee groups are to each other. As in the two previous analyses, Neanderthals are closest to the San population and most distant from the Berg, unlike Step 1 (Upper Paleolithic) and Step 2 (Andamanese). Neither the mixed European nor the Upper Paleolithic groups are close to the Neanderthal sample. Unlike the previous analyses, where the Upper Paleolithic group was equally or more distant from most recent human groups than Neanderthals were, here they are much closer to all recent human populations than Neanderthals. They are most distant from Neanderthals, and, among recent humans, from the Tolai population. The greatest distance among recent human groups is that between the Berg and the Dogon. Of the three geographic pairs, both the European pair as well as the sub-Saharan African pair are closest to each other.

The cluster analysis (Fig. 5.34) reflects these relationships. *P. t. schweinfurthii* cluster with bonobos. In the human branch, Neanderthals are outliers to all other groups, while the Upper Paleolithic population is the outlier to the recent human groups, rather than the reverse, as in steps 1 and 2. Furthermore, the Upper Paleolithic group is much closer to the recent human populations than the Neanderthals are, unlike steps 1 and 2. Both the European populations and the sub-Saharan African populations cluster together. The minimum spanning tree (Fig. 5.34) shows the Neanderthals on the longest branch off the human cluster and linked to the San, while the Upper Paleolithic group is linked to the Australians.

Table 5.19: Unbiased Mahalanobis D^2, Step 3A. All distances significant to the 0.001 level, except: NS = non-significant, * = 0.05 level, ** = 0.01 level.

	Kan	And	Aus	Bch	Brg	Dgn	EE	Epi	Esk	Eur
Kan	0.00	8.84NS	5.91NS	139.04	1.89NS	25.85NS	34.59NS	1.35NS	15.47NS	7.40NS
And	8.84NS	0.00	6.66	104.39	5.89	6.80	37.41	4.90	4.93	3.73
Aus	5.91NS	6.66	0.00	104.12	8.56	8.26	34.29	6.37	5.59	8.75
Bch	139.04	104.39	104.12	0.00	102.70	93.19	109.69	95.88	90.51	99.13
Brg	1.89NS	5.89	8.56	102.70	0.00	14.34	24.18	4.80	4.37	1.15NS
Dgn	25.85NS	6.80	8.26	93.19	14.34	0.00	37.36	11.17	7.80	11.40
EE	34.59NS	37.41	34.29	109.69	24.18	37.36	0.00	25.52	28.32	19.98**
Epi	1.35NS	4.90	6.37	95.88	4.80	11.17	25.52	0.00	7.79	4.68
Esk	15.47NS	4.93	5.59	90.51	4.37	7.80	28.32	7.79	0.00	4.08
Eur	7.40NS	3.73	8.75	99.13	1.15NS	11.40	19.98**	4.68	4.08	0.00
Ptr	35.26NS	49.62	29.47*	99.48	30.94*	50.99	50.01*	39.26**	28.38*	38.37**
Rei	79.54**	80.51	66.80	97.06	79.62	62.00	79.59	70.27	74.60	78.92
San	18.27NS	5.44	6.23	92.17	8.35	4.29	26.71	7.02	4.52	6.35
Sng	93.53	99.06	108.31	251.54	85.92	110.38	71.95	95.97	97.95	83.49
Tol	9.47NS	2.96**	6.45	98.93	4.34	7.71	31.27	6.70	3.16	4.28
UP	15.71NS	15.43	7.09	97.64	12.27	14.42	31.09	9.97	13.27	12.07
Bon	66.86	68.50	57.01	142.41	61.85	66.31	63.50	66.53	58.53	61.67
Nea	61.03	25.17	26.95	65.98	29.38	20.79	42.07	29.51	18.64	24.81
Sch	70.65	76.59	64.69	132.42	62.53	77.93	62.01	70.90	64.45	64.71
Trg	122.43	121.70	111.48	168.54	108.40	119.59	104.09	118.62	109.67	109.70

	Ptr	Rei	San	Sng	Tol	UP	Bon	Nea	Sch	Trg
Kan	35.26NS	79.54**	18.27NS	93.53	9.47NS	15.71NS	66.86	61.03	70.65	122.43
And	49.62	80.51	5.44	99.06	2.96**	15.43*	68.50	25.17	76.59	121.70
Aus	29.47*	66.80	6.23	108.31	6.45	7.09	57.01	26.95	64.69	111.48
Bch	99.48	97.06	92.17	251.54	98.93	97.64	142.41	65.98	132.42	168.54
Brg	30.94*	79.62	8.35	85.92	4.34	12.27	61.85	29.38	62.53	108.40
Dgn	50.99	62.00	4.29	110.38	7.71	14.42	66.31	20.79	77.93	119.59
EE	50.01*	79.59	26.71	71.95	31.27	31.09	63.50	42.07	62.01	104.09
Epi	39.26**	70.27	7.02	95.97	6.70	9.97	66.53	29.51	70.90	118.62
Esk	28.38*	74.60	4.52	97.95	3.16	13.27	58.53	18.64	64.45	109.67
Eur	38.37**	78.92	6.35	83.49	4.28	12.07	61.67	24.81	64.71	109.70
Ptr	0.00	101.70	43.85**	128.09	40.15**	19.85NS	45.92**	49.62**	39.04**	81.24
Rei	101.70	0.00	73.78	148.54	77.32	56.40	110.15	65.77	101.43	140.72
San	43.85**	73.78	0.00	97.83	6.61	11.71	59.50	16.77	68.94	112.58
Sng	128.09	148.54	97.83	0.00	104.20	91.81	142.10	115.00	118.91	148.76
Tol	40.15**	77.32	6.61	104.20	0.00	16.93	62.75	25.67	68.83	114.86
UP	19.85NS	56.40	11.71	91.81	16.93	0.00	59.06	23.07	60.63	108.08
Bon	45.92**	110.15	59.50	142.10	62.75	59.06	0.00	68.19	6.68	22.35
Nea	49.62**	65.77	16.77	115.00	25.67	23.07	68.19	0.00	70.92	110.53
Sch	39.04**	101.43	68.94	118.91	68.83	60.63	6.68	70.92	0.00	11.45
Trg	81.24	140.72	112.58	148.76	114.86	108.08	22.35	110.53	11.45	0.00

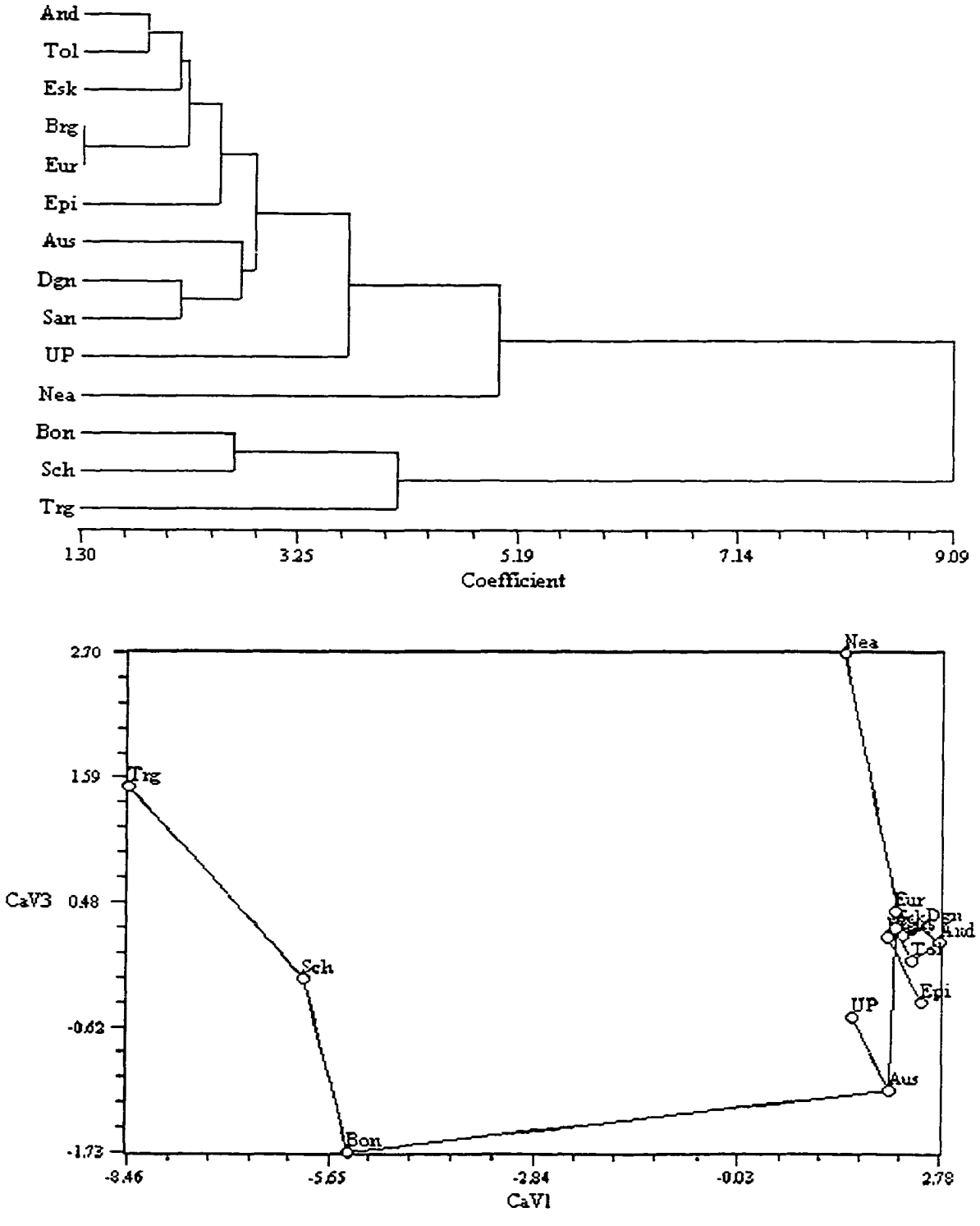

Figure 5.34: Cluster analysis (UPGMA) and minimum spanning tree (top, Step 3A)

Step 3B – Human sample only

Principal Components and Canonical Variates Analyses: The analysis was repeated on the human sample alone (Tables 5.20, 5.21). Results were similar to those obtained in Step 3A. Neanderthals were partially separated along PC 3 (10.8 % of the total variance) and PC 2 (33.1 %), Shanidar 1 and Tabun C1 overlapping with modern humans (Fig. 5.35). However, Neanderthals are only significantly different in their mean score from the Dogon (PC 2) and the European, Berg and Andamanese populations (PC 3). In the CVA, Neanderthals are separated form modern humans along CaV 1 (28.2 %, most highly influenced by PC 3, Fig. 5.36). They are significantly different from all modern human populations in their mean scores on this axis. All Neanderthal specimens fall outside the 95 % confidence ellipses for all modern human populations along CaV 1 and 2, although the Neanderthal confidence ellipse overlaps slightly with those of the modern human groups. Biache, Reilingen, as well as Mladec 1, fall outside the ellipses of all modern human groups and within that of Neanderthals. The shape differences that drive this separation include a posteriorly projecting and curved occipital plane and a flat parietal, as also found is Step 3A. Singa and Petralona fall outside all modern human confidence ellipses along CaV 1and CaV 2 (17.7 %, most influenced by PC 2, Fig. 5.36). The shape differences at the negative end of CaV 2 include a short and flat parietal, an posteriorly projecting occipital plane and an posteriorly and inferiorly placed iniac region.

Classification: With a few exceptions, the results of this analysis (Table 5.22) are very similar to those of Step 3A. Petralona is now classified as Eskimo (0.46) and Reilingen as Neanderthal (0.47). The classification success was lower for modern human groups in this analysis than in Step 3A. However, eight out of the nine Neanderthal specimens were classified correctly, compared to six in the previous analysis, achieving the highest success rate for human populations in the midline ridge-curve analysis (88.89 %). The one misclassified Neanderthal was classified as Eskimo. One Upper Paleolithic specimen, as well as one Dogon and one Eskimo, were misclassified as Neanderthal. No Upper Paleolithic was correctly classified, three being misclassified as Australian, one as Eskimo, and one as European.

Table 5.20: Summary of the PCA results, ANOVA and Correlation Analysis for PCs 1-10, Step 3B.

	Principal Components Analysis			ANOVA, Pr > F			Correlation with Centroid size	
	Eigenvalue	Proportion	Cumulative	Popul.	Sex	Interaction	Rho	Pr > F
PC 1	0.000973	0.430443	0.430443	0.0005	0.0032	0.2258	-0.00568	0.9258
PC 2	0.000772	0.341634	0.772077	0.0001	0.0176	0.2707	0.15197	0.0123
PC 3	0.000234	0.103678	0.875755	0.0001	0.036	0.4063	0.09361	0.1242
PC 4	0.000067	0.029591	0.905346	0.3939	0.1485	0.0536	-0.16278	0.0072
PC 5	0.000038	0.016634	0.921979	0.0656	0.5123	0.5524	-0.09729	0.11
PC 6	0.000032	0.01418	0.93616	0.0014	0.6351	0.2809	0.01292	0.8323
PC 7	0.000026	0.011438	0.947598	0.0001	0.0012	0.7	-0.17186	0.0045
PC 8	0.000017	0.007434	0.955032	0.0009	0.462	0.2237	-0.11351	0.062
PC 9	0.000014	0.006211	0.961244	0.0082	0.3682	0.2028	-0.07738	0.2041
PC 10	0.000014	0.006011	0.967254	0.0574	0.0381	0.3986	-0.09249	0.1288

Table 5.21: Summary of the CVA results and Correlation Analysis for CaV 1-5, Step 3B.

	Canonical Variates Analysis			Correlation with Centroid size	
	Eigenvalue	Proportion	Cumulative	Rho	Pr > F
CaV 1	1.7432	0.2371	0.2371	-0.20735	0.0006
CaV 2	1.2982	0.1766	0.4137	-0.0347	0.5695
CaV 3	0.8753	0.1191	0.5327	-0.23586	0.0001
CaV 4	0.7209	0.0981	0.6308	-0.03259	0.5932
CaV 5	0.5987	0.0814	0.7122	-0.05493	0.3677

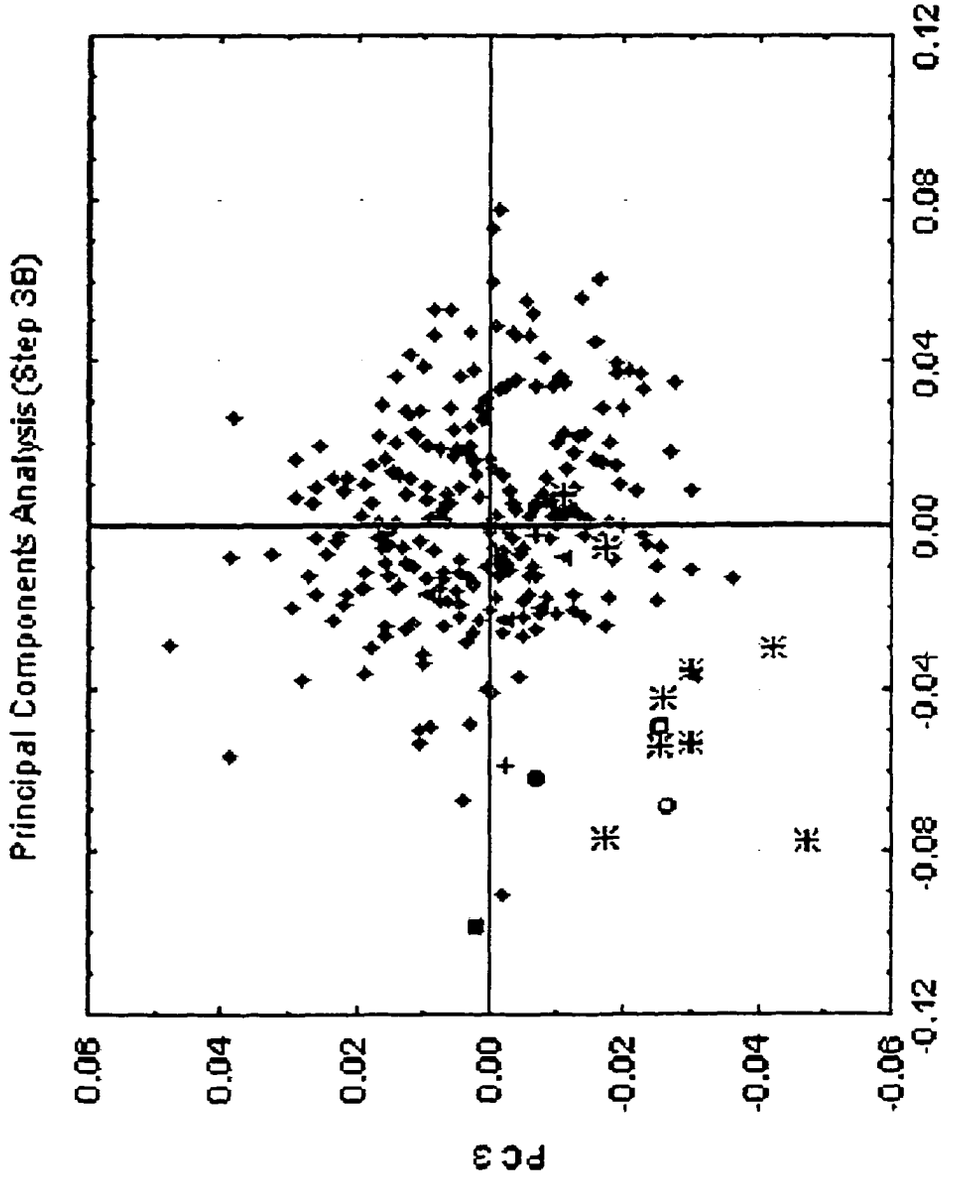

Figure 5.35: Principal Components Analysis (Step 3B), PCs 2 and 3.

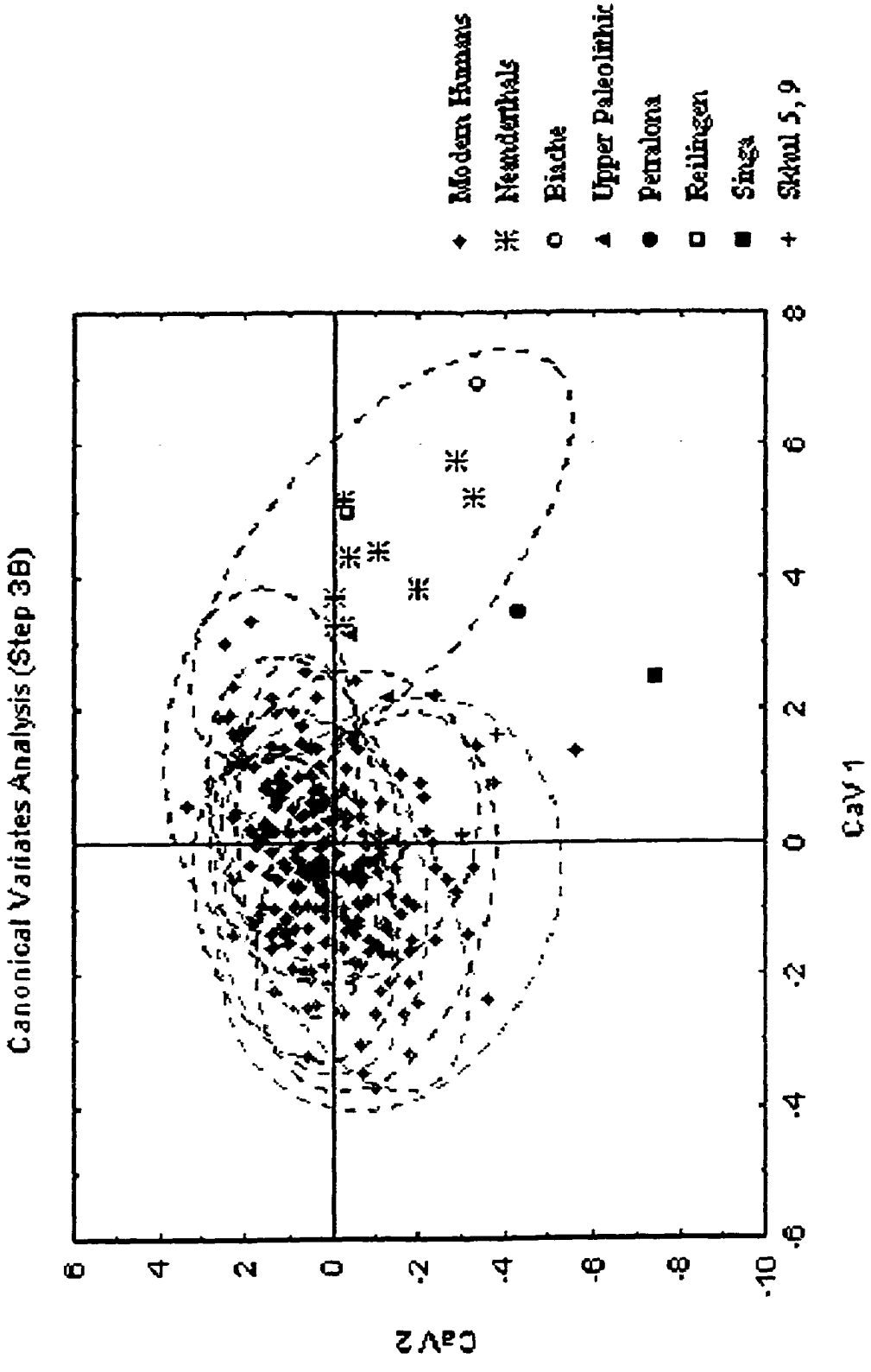

Figure 5.36: Canonical Variates Analysis, CaV 1 and 2 (Step 3B). Dotted lines represent the 95 % confidence ellipses for each group.

Table 5.22: Cross-validation classification summary (percentages for each population in bold), Step 3B.

	And	Aus	Brg	Dgn	Epi	Esk	Eur	San	Tol	UP	Nea	Total
And	11	0	2	2	5	1	2	0	6	0	0	29
%	**37.93**	0	6.9	6.9	17.24	3.45	6.9	0	20.69	0	0	100
Aus	2	14	1	1	2	3	1	0	2	3	0	29
%	6.9	**48.28**	3.45	3.45	6.9	10.34	3.45	0	6.9	10.34	0	100
Brg	3	2	11	0	2	4	5	0	2	0	0	29
%	10.34	6.9	**37.93**	0	6.9	13.79	17.24	0	6.9	0	0	100
Dgn	2	4	0	16	1	1	0	5	0	0	1	30
%	6.67	13.33	0	**53.33**	3.33	3.33	0	16.67	0	0	3.33	100
Epi	3	1	1	1	6	2	3	3	0	2	0	22
%	13.64	4.55	4.55	4.55	**27.27**	9.09	13.64	13.64	0	9.09	0	100
Esk	2	2	5	0	0	9	3	2	4	1	1	29
%	6.9	6.9	17.24	0	0	**31.03**	10.34	6.9	13.79	3.45	3.45	100
Eur	2	0	7	0	2	2	6	2	1	1	0	23
%	8.7	0	30.43	0	8.7	8.7	**26.09**	8.7	4.35	4.35	0	100
San	3	0	0	3	0	5	2	17	0	0	0	30
%	10	0	0	10	0	16.67	6.67	**56.67**	0	0	0	100
Tol	5	1	4	1	3	3	3	1	7	0	0	28
%	17.86	3.57	14.29	3.57	10.71	10.71	10.71	3.57	**25**	0	0	100
UP	0	3	0	0	0	1	1	0	0	0	1	6
%	0	50	0	0	0	16.67	16.67	0	0	**0**	16.67	100
Nea	0	0	0	0	0	1	0	0	0	0	8	9
%	0	0	0	0	0	11.11	0	0	0	0	**88.89**	100
Total	33	27	31	24	21	32	26	30	22	7	11	264
%	12.5	10.23	11.74	9.09	7.95	12.12	9.85	11.36	8.33	2.65	4.17	100

Table 5.23: Unbiased Mahalanobis D^2, Step 3B. All distances significant to the 0.001 level, except: NS = non-significant, * = 0.05 level, ** = 0.01 level.

	AA	And	Aus	Bch	Brg	Dgn	EE	Epi	Esk	Eur	Ptr	Rei	San	Sng	Tol	UP	Nea
AA	0.00	13.39NS	11.73NS	167.34	7.79NS	29.77NS	38.08NS	5.42NS	20.40NS	10.54NS	77.85*	103.50	20.25NS	160.16	12.42NS	17.86NS	71.22
And	13.39NS	0.00	7.31	154.19	6.30	7.93	36.92	5.91	5.53	4.90	81.74	88.23	5.87	159.05	3.07**	16.45	31.06
Aus	11.73NS	7.31	0.00	143.61	8.00	7.85	32.81	6.98	5.56	9.17	53.47	71.84	6.28	159.26	6.99	6.15NS	28.86
Bch	167.34	154.19	143.61	0.00	143.45	136.55	137.72	134.77	132.78	140.32	124.72	165.13	134.72	290.60	143.08	132.49	102.38
Brg	7.79NS	6.30	8.00	143.45	0.00	13.72	23.22**	5.78	3.99	1.70NS	57.16	84.85	7.84	137.65	4.18	11.46	29.62
Dgn	29.77NS	7.93	7.85	136.55	13.72	0.00	34.43	11.89	8.05	12.80	69.02	68.21	4.86	153.48	8.54	15.87	23.40
EE	38.08NS	36.92	32.81	137.72	23.22**	34.43	0.00	24.76**	26.81	18.93*	66.10**	91.41	25.67**	108.74	29.66**	28.62**	37.22
Epi	5.42NS	5.91	6.98	134.77	5.78	11.89	24.76**	0.00	8.32	6.01	66.16	80.35	7.94	152.68	6.50	10.16**	34.46
Esk	20.40NS	5.53	5.56	132.78	3.99	8.05	26.81**	8.32	0.00	4.55	53.52	81.16	4.81	150.91	3.46	12.46	20.63
Eur	10.54NS	4.90	9.17	140.32	1.70NS	12.80	18.93*	6.01	4.55	0.00	70.20	89.14	6.04	142.41	4.74	10.85	29.18
Ptr	77.85*	81.74	53.47	124.72	57.16	69.02	66.10**	66.16	53.52	70.20	0.00	109.59	72.24	141.24	69.33	55.12**	58.30
Rei	103.50	88.23	71.84	165.13	84.85	68.21	91.41	80.35	81.16	89.14	109.59	0.00	83.24	183.72	86.73	64.44	65.37
San	20.25NS	5.87	6.28	134.72	7.84	4.86	25.67**	7.94	4.81	6.04	72.24	83.24	0.00	154.93	6.69	10.73	22.83
Sng	160.16	159.05	159.26	290.60	137.65	153.48	108.74	152.68	150.91	142.41	141.24	183.72	154.93	0.00	157.07	154.05	144.89
Tol	12.42NS	3.07**	6.99	143.08	4.18	8.54	29.66	6.50	3.46	4.74	69.33	86.73	6.69	157.07	0.00	17.13	30.31
UP	17.86NS	16.45	6.15NS	132.49	11.46	15.87	28.62**	10.16**	12.46	10.85	55.12**	64.44	10.73	154.05	17.13	0.00	28.67
Nea	71.22	31.06	28.86	102.38	29.62	23.40	37.22	34.46	20.63	29.18	58.30	65.37	22.83	144.89	30.31	28.67	0.00

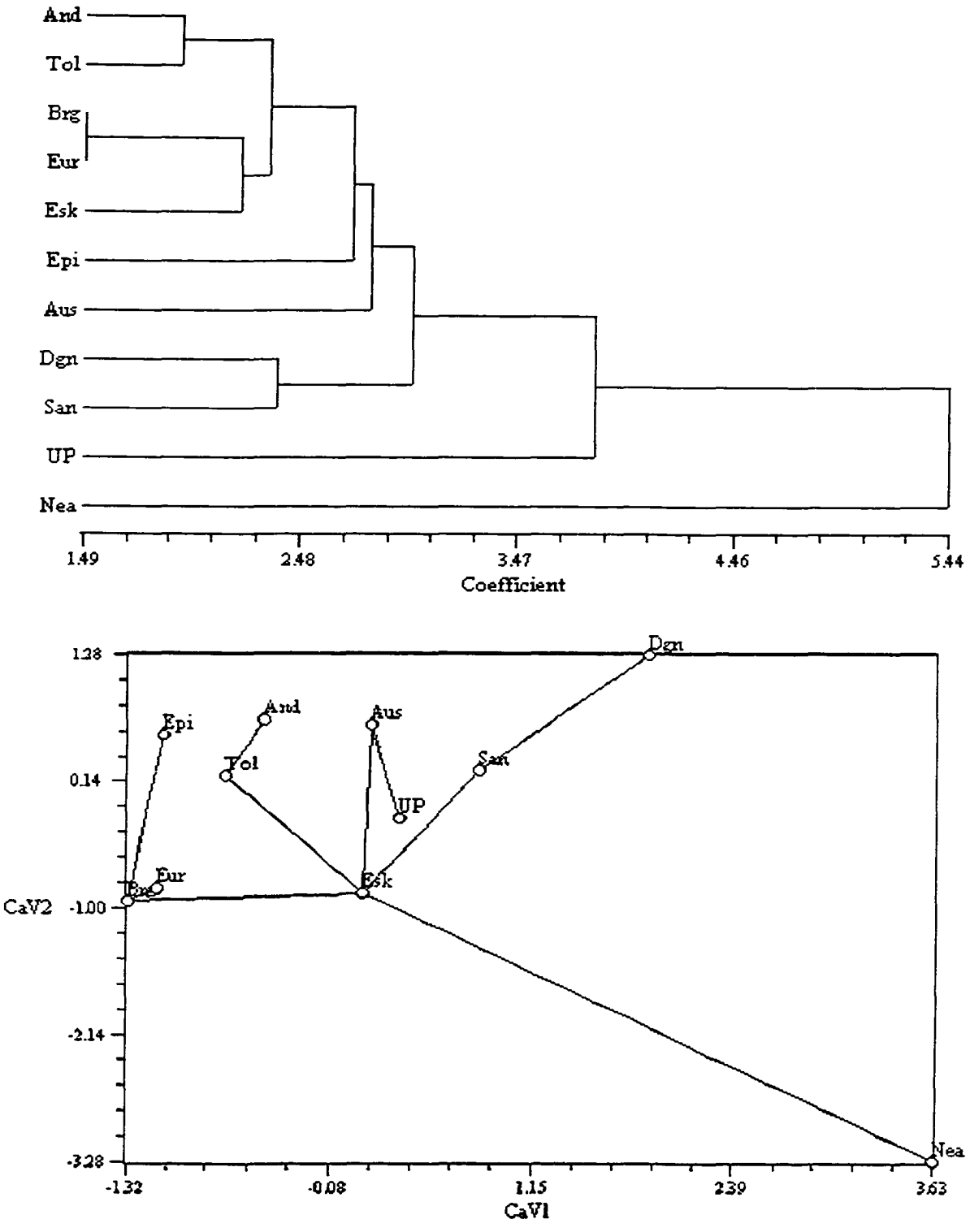

Figure Fig. 5.37: Cluster analysis (UPGMA) and minimum spanning trees (top, Step 3B).

Mahalanobis D^2, Cluster Analysis and Minimum Spanning Tree: The unbiased Mahalanobis D^2 matrix is reported in Table 5.23. It differs from that obtained in Step 3A in that Neanderthals are closest to the Eskimo rather than to the San and most distant from the Epipaleolithic rather than the Berg among the modern human groups. No affinities of either the recent European groups or the Upper Paleolithic group are observed. The Upper Paleolithic group is most distant from the Neanderthals and closest to the Australians. The European geographic pair still show the shortest distances to each other, while only one of the sub-Saharan African pair is closest neighbor to the other. The cluster analysis (Fig. 5.37) is similar to that obtained in Step 3A, differing only in the position of the Eskimo and the Australian populations within the modern human cluster. The minimum spanning tree (Fig. 5.37) shows Neanderthals on the longest branch linked to the Eskimo, while the Upper Paleolithic group is linked to the Australians.

Step 3C – Chimpanzee sample only

Classification: The cross-validation classification is similar in this analysis to that obtained in Step 3A. Misclassification rates are higher between bonobos and *P. t. schweinfurthii* than those between bonobos and *P. t. troglodytes*. Misclassification is also very high between the two common chimpanzee subspecies, as in all other analyses. The lowest classification success is achieved by *P. t. schweinfurthii*.

Mahalanobis D^2: The unbiased Mahalanobis distances were calculated for the three chimpanzee taxa (Table 5.25). They are similar to those obtained in Step 1C in that bonobos are more distant from both common chimpanzee subspecies than the two subspecies are from one another (and unlike both Step 1A and 3A). The distances between bonobos and the common chimpanzee subspecies are greater than those found in Step 3A, while the distance between the two common chimpanzee subspecies is greater.

The distances between bonobos and the two common chimpanzee subspecies are somewhat greater than, or equivalent to the greater distances among modern human groups in steps 3A and 3B, but lower than those between Neanderthals and modern humans or the Upper Paleolithic group and recent human populations. The distance between the two common chimpanzee subspecies is equivalent to those among modern human groups.

Table 5.24: Cross-validation classification summary (percentages for each population in bold), Step 3B.

	Bon	Sch	Trg	Total
Bon	24	7	2	33
%	**72.73**	21.21	6.06	100
Sch	5	17	8	30
%	16.67	**56.67**	26.67	100
Trg	1	7	21	29
%	3.45	24.14	**72.41**	100
Total	30	31	31	92
%	32.61	33.7	33.7	100

Table 5.25: Unbiased Mahalanobis D^2, Step 3C. All distances significant to the 0.001 level, except: NS = non-significant, * = 0.05 level, ** = 0.01 level.

	Bon	Sch	Trg
Bon	0.00	9.83	15.67
Sch	9.83	0.00	6.60**
Trg	15.67	6.60**	0.00

Discussion

***Modern humans*:** The modern human mean configuration shows a very rounded posterior cranial profile, both in comparison to chimpanzees and to the fossil specimens included here. Of the other groups, the Upper Paleolithic mean configuration is the most similar one to the mean modern human configuration. The small Mahalanobis distances among modern human populations indicates that the modern human groups are relatively homogeneous in their posterior cranial profile. Within the modern human sample, females tend to be characterized by a rounder cranial profile and weaker development of the nuchal superstructures in most populations (PCs 1 and 4, Step 1A).

Chimpanzees: By far the greatest shape differences observed in the posterior cranial profile are those between modern humans and chimpanzees. When the mean chimpanzee configuration is directly compared to the mean modern human configuration, chimpanzees are shown to have a longer and more inferiorly placed nuchal plane and a shorter and flatter occipital plane, as also shown in the occipital landmarks analysis, as well as a very flat parietal bone. These shape differences are responsible for the separation along PC 1 and CaV 1 in the combined sample analyses. As in the occipital landmarks analysis, these axes are strongly correlated with size, but may reflect taxonomic rather than simply size-related differences.

In all combined analyses of the midsagittal ridge-curves, *P. t. schweinfurthii* is closer to *P. paniscus* in Mahalanobis D^2 than it is to *P. t. troglodytes*. However, this situation is reversed in the chimpanzee sample analyses (Steps 1C and 3C), where the two common chimpanzee subspecies are closer to each other than either is to bonobos.

Neanderthals: The occipital 'bun' and the suprainiac fossa, are among the most frequently discussed Neanderthal characteristics, often considered derived for the Neanderthal lineage (Santa Luca 1978; Hublin 1977, 1978a, b; Condemi 199; Lieberman 1995; Dean et al. 1998; Lieberman et al. 2000). One of the objectives of the analysis of the posterior cranial profile was to evaluate these traits, as this ridge curve was designed to capture the relevant morphology. A comparison between the mean Neanderthal configuration and the mean modern human configuration shows that Neanderthals are characterized by a greater posterior projection and curvature of the occipital plane, a flat parietal bone, and a slight elevation of the nuchal plane, reflecting a more horizontal

lower scale of the occipital bone. Although no indication of the presence of a suprainiac fossa was detected, these shape differences are consistent with previous descriptions of this anatomical region in Neanderthals and with the presence of a 'chignon' (Boule 1911-1913; Thoma 1965; Heim 1974; Hublin 1978b, 1988a; Stringer and Trinkaus 1981; Stringer et al. 1984; Sergi 1991; Dean et al. 1998).

Although the occipital bun and the parietal flattening are present and responsible for the separation observed in the principal components and canonical variates analyses, there is overlap between Neanderthals and modern humans in steps 1 and 2 and in both the PCA and the CVA (e.g. Step 1A PC 3 and CaV 3, Step 1B PC 3, CaV 2). A stronger separation is achieved in Step 3, in part due to the greatly increased Neanderthal sample (Step 3A PC 3, CaV 3, Step 3B PC 2 and CaV 1). The overlap between Neanderthals and modern humans is reflected in the cross-validation classification results, where correct classification for the Neanderthal fossils ranges from 0 to 2 out of four (Steps 1 and 2), but greatly improves (6-8 out of 9) in Step 3. In all steps, however, some modern human specimens were misclassified as Neanderthals.

In all steps the specimens showing the greatest similarity to modern humans are Shanidar 1, Tabun C1 and Saccopastore 1. Shanidar 1 and Tabun C1 have been described as exhibiting very weak occipital buns (McCown and Keith 1937; Trinkaus 1983) and this was also observed in their individual configurations relative to the mean Neanderthal configuration in the present analysis. The high convexity of the Shanidar 1 parietal, also noted previously (Trinkaus, 1983; Stringer and Trinkaus 1981; Stringer et al. 1984), is also observed here and contributes to the overlap of this specimen with modern humans. Although striking, this feature may in fact be due to artificial deformation of this cranium (Trinkaus 1982). Amud 1, the third Eastern Neanderthal included in this analysis, is quite distant from modern humans, indicating variability within the Eastern Neanderthal group. Finally, Saccopastore 1 consistently falls near Shanidar 1 and Tabun C1 in the PCA and CVA. The similarities of this specimen to the Eastern Neanderthals have been noted by Condemi (1992), and include a weak occipital bun and a relatively high cranium. Some similarities were also found between the Saccopastore specimens and Eastern Neanderthals by Stringer (1990), who considered them to reflect retention of primitive conditions in both groups.

These findings are in keeping with previous observations of geographic and temporal variability within the Neanderthal sample. The Eastern Neanderthals are often considered to exhibit less pronounced Neanderthal features than the 'classic' European Neanderthals (Thoma 1965, 1975; Stringer and Trinkaus 1981; Vandermeersch 1989; Dean et al. 1998), a pattern which has been suggested by some authors to be intermediate to the morphology of the early anatomically modern humans (Thoma 1965, 1975). The variable expression of these similarities, furthermore, is also consistent with the mosaic pattern observed by some authors in the Late Pleistocene hominid evolution of Western Asia (Trinkaus 1984; Trinkaus and Smith 1985). These results also support the observations of similarities between the Saccopastore specimens and the Eastern Neanderthal sample (Condemi 1992; Vandermersch 1989).

In all analyses Neanderthals are far more distant from modern humans in Mahalanobis D^2 than either the two chimpanzee species or the two common chimpanzee subspecies are from one another. They are also much more distant from modern humans than any two modern human groups are from each other. Unlike either landmarks analysis, modern human populations appear very close to each other in Mahalanobis D^2, suggesting that variation in the shape of the posterior cranial profile is limited among modern groups. The two populations that are widely separated from the modern human groups are the Neanderthals and the Upper Paleolithic specimens. The distance between Neanderthals and recent human populations is equal to or slightly lower than that between the Upper Paleolithic specimens and recent human populations in Steps 1 and 2. In Step 3, however, after removal of the nuchal plane landmarks and semilandmarks, the Upper Paleolithic specimens are much closer to the recent populations than Neanderthals are. This difference may be due in part to the increase in both the Neanderthal as well as the Upper Paleolithic sample in this analysis. It may, however, also be related to the exclusion of the nuchal plane of the occipital, as this region is not directly involved in the morphology of the 'chignon'. In order to test these hypotheses, Step 3A was repeated using only the Neanderthal and Upper Paleolithic specimens available in Step 1. The Upper Paleolithic group was not as widely separated from modern humans as in Step 1, but more so than in Step 3. This indicates that both the addition of further specimens, as well as the focus on the most relevant morphology, were important in Step 3.

Neanderthals are closest to the South African San and the Eskimo populations in Mahalanobis D^2. Similarity to the San is perhaps not surprising, as this group has been previously described as exhibiting a highly curved and posteriorly elongated occipital bone (Tobias 1959). A flatness of the parietal, described for 'bushman' crania by Broom (1912), may also contribute to this similarity. Unlike the occipital landmarks analysis, Neanderthals do not exhibit any similarities in their posterior cranial profile either to the recent European populations or to the Late Paleolithic European specimens included here. In fact, in Step 1 the greatest Mahalanobis D^2 distance in the human sample is that between Neanderthals and the Upper Paleolithic group. This distance is somewhat reduced in Step 3, probably due in part to the addition of Mladec 1 to the Upper Paleolithic sample. This specimen falls very close to the Neanderthals in all analyses of Step 3 and is always classified as Neanderthal.

The results of this analysis indicate that only the profile of inion to bregma differentiates Neanderthals well from both recent humans and the Upper Paleolithic European specimens included here. This profile includes the described morphology of the occipital 'bun' (posterior projection and great curvature of the occipital plane in combination with lambdoid flattening), as well as the primitive condition of the flat parietals. The inclusion of the nuchal plane of the occipital bone confounds the analysis through a combination of too little and too much information. On the one hand, very few Neanderthal and Upper Paleolithic specimens can be included; on the other hand, the nuchal plane is not involved in the Neanderthal morphology described for this area. The inclusion of this morphology, therefore, appears to be swamping the analysis with information that is not relevant to differentiating Neanderthals from modern humans. This is not true, for instance, in the case of Petralona, where the orientation of the nuchal plane relative to the occipital is very different to that observed in modern humans and diagnostic (see below). The misclassification of some modern human specimens as Neanderthals even in Step 3, however, suggests that this morphology can occasionally occur in modern humans.

The failure of the analysis to detect the presence of a suprainiac fossa may be due to the inability of the three-dimensional geometric morphometric method used to capture a very subtle and shallow depression. Furthermore, as has been previously claimed, the

simple presence of such a fossa in the midsagittal plane is not limited to Neanderthals, but also often appears in modern human specimens. If this trait indeed distinguishes this fossil group from modern humans, it is in its lateral extent and particular form, rather than its simple presence (Hublin 1988a; Bräuer and Broeg 1998).

Petralona: This specimen shows marked differences from the mean modern human configuration, as well as to the mean Neanderthal configuration, although these differences are more pronounced in Step 1 than they are in Step 3. Petralona is similar to Kabwe in the occipital bone landmarks analysis in that lambda is more inferior, inion posterior and superior and opisthion more anterior than in modern humans, indicating a supero-inferiorly short occipital plane and an antero-posteriorly elongated nuchal plane. Furthermore, relative to the mean modern human configuration, Petralona shows a very strong posterior projection of the lower part of the occipital plane, at and above inion, indicating strong superstructures at the level of the nuchal torus; a strongly depressed posterior parietal and elevated bregma and anterior parietal region, indicating a very flat parietal bone; and a more anteriorly and superiorly placed opisthion and anterior part of the nuchal plane, reflecting a sharper angle between the upper and lower scales of the occipital bone. These shape differences are more pronounced than those between Neanderthals and modern humans. Petralona differs from the Neanderthal specimens in having an even flatter parietal bone, a more posteriorly projecting inion and surrounding area, a much less curved occipital plane and a lower angle between the occipital scales. These shape differences are consistent with the previous description of this specimen by Stringer et al. (1979), who noted the strong angulation of the occipital bone, the markedly posteriorly projecting iniac region and lower part of the occipital plane and the flatness of the parietal bones in lateral view.

Petralona falls outside the range of modern human variation on PCs 3 and 4 and CaV 4 in Steps 1A and 3A, indicating that it falls outside the modern human range in the posterior projection of its occipital plane, and particularly inion and the area immediately above it, in the flatness of its parietal bone, and in the sharp angle between the upper and lower occipital scales. It also falls at the extreme of the modern human range along PC 1 and CaV 1 in both Steps 1 and 3, reflecting a relatively short occipital plane, a flat

parietal and an elongated nuchal plane, and along CaV 2, indicating again a flat parietal region.

In the Mahalanobis D^2 analysis, Petralona is closest to the Berg population in Step 1A and to Neanderthals in Step 1B. It is closest to the Upper Paleolithic in Step 3A and to the Australian population in Step 3B. It generally shows very large distances both to Neanderthals and to the modern human groups, although the distances between Petralona and the modern human populations are generally somewhat greater than that between it and Neanderthals. This result is consistent with previous analyses based on cranial measurements (Stringer 1974a, b), where this specimen was found to be relatively distant from both modern humans and Neanderthals. Petralona is classified as Berg by posterior probability in Step 1A, and as Neanderthal in Step 1B. In Step 3A it is classified as Upper Paleolithic, and as Eskimo in Step 3B.

Biache: Like Petralona, this specimen also shows strong shape differences from the modern human mean configuration. It differs from the modern human mean configuration in its very flat parietal region and in the posterior projection and strong curvature of its occipital plane. It differs from Neanderthals in having a flatter parietal and a more inferiorly placed opisthion and anterior part of the nuchal plane, although it shows a similar degree of posterior projection and curvature of the occipital plane. Biache also differs markedly from Petralona. Although both have a flattened parietal bone, Biache shows a much less posteriorly projecting inion and surrounding area, and a much more inferior opisthion. These differences reflect weaker superstructures at the attachment site of the nuchal musculature and a wider angle between the two occipital scales in this specimen. The weak development of the nuchal torus and the similarity of the sagittal profile of this specimen to Neanderthals have also been noted by Stringer et al. (1984).

In Step 1A Biache is separated from the modern human sample along PCs 1 and 3, as well as along CaVs 3 and 5, while in Step 3A along PC1, CaV 3 and CaV 4. The shape differences driving this separation are the same as those described above. The same shape differences drive the separation of Biache in the human sample analysis (Step 1B: CaVs 1, 2 and 3; Step 3B: CaV 1). In the Mahalanobis D^2 analysis, Biache is by far closest to the Neanderthals, confirming its previously described similarities to this group

(Stringer et al. 1984; Vandermeersch 1985; Dean et al. 1998). In all analyses Biache is classified as Neanderthal with a posterior probability of 1.00.

Singa: The Singa cranium from Sudan has in the past been considered a terminal Pleistocene modern human specimen with probable affiliations with the San of South Africa or with Mesolithic African populations (Woodward 1938; Brothwell 1963; Stringer 1979; Bräuer 1984; Rightmire 1984). However, archaic, and even 'Neanderthaloid', affinities have also been proposed for this specimen (Stringer 1979). A craniometric analysis by Stringer (1979), found that it is most similar to 'archaic *H. sapiens*' from Africa and Europe. Recent U-Th dating of the matrix on the specimen, as well as ESR dating of associated animal teeth, have placed Singa at a minimum age of 133 ± 2 ka (Grün and Stringer 1991; McDermott et al. 1996), confirming its suspected great antiquity. Furthermore, a pathology of the right temporal bone and diploic thickening at the parietals were also recently documented (Spoor et al. 1998), probably indicating some form of anemia. Spoor and his co-authors report that the morphology of the bony labyrinth of the left, normal, temporal bone, does not resemble that exhibited by Neanderthals, and conclude that Singa does not have affinities to this hominid group.

The configuration of Singa differs from the modern human mean configuration in its antero-posteriorly short and relatively flat parietal, its posteriorly and inferiorly bulging lower part of the occipital plane and its inferiorly placed nuchal plane. It differs from the mean Neanderthal configuration in having an antero-posteriorly shorter parietal which is also somewhat more flattened, and a more inferiorly placed inion, lower part of the occipital plane and nuchal plane. When compared to Petralona, it shows again a very short parietal antero-posteriorly, which is also slightly more curved, a much more inferiorly placed nuchal plane, reflecting a much wider angle between the two occipital scales, and a smaller posterior projection at inion. The configuration of Singa most closely resembles that of Biache, differing from it only in a slightly more curved and antero-posteriorly shorter parietal bone, and a more inferior placement of inion and the nuchal plane. When compared to the Upper Paleolithic specimens, Skhul 5, the Epipaleolithic population from North Africa and the South African San group, Singa differs from all in the same aspects that differentiate it from the modern human mean

configuration, in a very short and flat parietal, a more inferiorly projecting lower part of the occipital plane and a more inferiorly placed nuchal plane.

These shape characteristics separate Singa from modern humans in Step 1A along PC 2 and CaV 2, in Step 1B along PC 1 and CaV 1, in Step 3A in PC 2 and CaV 2, and in Step 3B in PC 2 and CaV 2. Its highly curved occipital plane also places it within the Neanderthal range of variation and at the fringe of the modern human range along PC 3 in Steps 1A, along CaV 2 in Step 1B, CaV 3 in Step 3A. Its inferiorly placed nuchal plane also places it at the extreme of the modern human range along CaV 3 in Step 1B. In the Mahalanobis D^2 analysis, Singa is closest to the Neanderthals and to the Berg population in Step 1. In Step 3, however, it is by far closest to the two early anatomically modern humans, Skhul 5 and 9, even though it is very distant from Skhul 5 in Step 1. Singa was classified as Berg by posterior probability in Step 1A, and as Neanderthal in Step 1B. In Steps 3A and 3B it was classified as European.

The results of this analysis are in agreement with those of Stringer (1979), who also noted a very short and flat parietal arch and a protruding occipital bone. Stringer considered Singa as a late 'archaic *H. sapiens*' specimen with morphological similarities to African and European archaic specimens and even with Neanderthals. The present study also did not find any affinities between the Singa calvarium and the San population, the Mesolithic North African group, or Skhul 5, although a relatively strong affinity was observed between it and the group of two early anatomically modern human specimens (Skhul 5 and 9) in the bregma-inion line segment. This similarity is probably due to the antero-posteriorly short parietal bone in Skhul 9, which is only included in Step 3. The very distant placement of Singa to any of the groups in this analysis is also probably due to the unusual antero-posterior shortening of the parietal. The very short parietal and unusual vault morphology of this specimen were also noted by Bräuer (1984), while Stringer (1979) suggested that the unusually short bregma-lambda chord of this specimen may be pathological. However, although pathologies involving the temporal and parietal bones in this specimen have been documented (Spoor et al. 1998), they do not seem to directly affect the shortening of the parietal vault. Furthermore, contra Spoor et al. (1998), but in agreement with Stringer (1979), the present analysis of the posterior cranial

profile of this specimens found some similarities to the Neanderthals, but only when the entire posterior profile is considered (Step 1).

Reilingen: This specimen was only included in Step 3. Its configuration differs from the mean modern human configuration in the same general way as Neanderthals. It exhibits a flat parietal, a posteriorly projecting occipital plane, and a posteriorly protruding inion. It differs from Neanderthals in having a slightly more posteriorly protruding inion, as well as a somewhat deeper depression above lambda. It is very similar to Biache, differing from it only in the slightly more curved parietal and more posteriorly projecting upper part of the occipital plane. It differs from Petralona in having a more curved parietal, a more posteriorly projecting occipital plane, and a less posteriorly protruding inion and surrounding area. Finally, it differs from Singa in its antero-posteriorly longer parietal and its much less inferiorly placed inion and iniac region.

Reilingen is separated from modern humans and falls within the Neanderthal range in CaV 3 of Step 3A and CaV 1 in Step 3B. The shape differences driving this separation are similar to the shape differences that separate Neanderthals from modern humans. In the Mahalanobis D^2 analysis, Reilingen is closest to the Upper Paleolithic specimens and is classified as such in Step 3A by posterior probability, despite the apparent similarities between it and Neanderthals. It is classified as Neanderthal in Step 3B. The similarities of this specimen to Neanderthals have been previously noted by Dean and his co-authors (1998), who classified it as an early Neanderthal based on both general morphology and a metric analysis.

Skhul 5 and Skhul 9: Steps 1 and 2 included only Skhul 5, while Step 3 also included Skhul 9. When examined individually, Skhul 5 differs from the mean modern human configuration in its sightly flatter parietal, depression in the posterior parietal region, more posteriorly protruding inion and surrounding area and slightly elvated opisthion and nuchal plane. The same differences are observed when the mean of Skhul 5 and 9 is compared to the mean modern human configuration in Step 3. When the two specimens are compared, Skhul 9 shows an even flatter and anter-posteriorly shorter parietal, as well as a more posteriorly projecting occipital plane. These differences are consistent with the well developed occipital torus and external occipital protuberance in

these specimens, as well as the low vault of Skhul 9, described by McCown and Keith (1937).

In the Mahalanobis D^2 analysisof Step 1, Skhul 5 is very distant from all modern human populations, as well as Neanderthals and other fossils. However, this may partly be an effect of the sample size of one. It is closest to the mixed European population and is most distant from Singa in Step 1A, while it is closest to the San and again most distant from Singa in Step 1B. It is classified as Australian in Steps 1A and 1B. In Step 3, the two specimens are treated as a group, and again they are very distant from both modern humans and Neanderthals. They are closest to the Epipaleolithic in Step 3A, and to the Berg in Step 3B, and are most distant from Singa. Skhul 5 and 9 were both classified as European by posterior probability in both Steps 3A and B. These findings are consistent with those of previous studies (Stringer 1974a, 1992; Bräuer and Rimbach 1990; Bräuer 1992; Kidder et al. 1992; Turbón et al. 1997), where these specimens were found to be distant from both Neanderthals and modern humans, but closer to modern humans.

Upper Paleolithic specimens: While three males and one female are included in Steps 1 and 2, Step 3 comprises six specimens, three of which are female (Predmosti 4, Mladec 1 and Cro Magnon 2). The mean configuration of the Upper Paleolithic group in Step 1 differs from the mean modern human configuration in having a slight lambdoidal depression, a slight posterior projection of the occipital plane, and iniac region, and an antero-posteriorly long and relatively elevated nuchal plane. They differ from Neanderthals in having a more curved parietal, a less posteriorly projecting and curved occipital plane, a slightly more posteriorly placed inion, and a slightly more inferiorly placed nuchal plane. The addition of the two female specimens in Step 3 results in a slightly reduced posterior projection of inion.

These differences are consistent with the morphology previously described for the Cro Magnon 'type' of Western Europe. This includes greater robusticity, an elongated cranium with lambdoid flattening and an occipital 'bun', often termed 'hemibun', a strong iniac region with a projecting occipital protruberance, and a flat and antero-posteriorly long nuchal plane (Billy 1970; Genet-Varcin 1970; Gambier 1989, 1997; Churchill et al. 2000), although great variability has also been noted in this group (Stringer et al. 1984). An elongated cranium and 'hemibun', as well as greater robusticity, have also been

described for the Central European Upper Paleolithic specimens (Vlcek 1970; Smith 1982, 1984; Gambier 1989; Churchill and Smith 2000). In the case of both Western and Central European specimens, these traits have been interpreted as evidence for at least some continuity and interbreeding between the Upper Paleolithic modern humans and Neanderthals (Genet-Varcin 1970; Vlcek 1970; Smith 1981, 1984; Bräuer 1989; Churchill and Smith 2000; Wolpoff et al. 2001). Other authors, however, find evidence for 'hemibuns' in many modern human and fossil specimens, and do not consider this trait indicative of continuity with Neanderthals (Trinkaus and LeMay 1982; Gambier 1989; Bräuer and Broeg 1998). The 'hemibuns' found in the Upper Paleolithic specimens have also been considered as the result of different developmental processes than in Neanderthals and not homologous to the Neanderthal occipital buns (Lieberman 1995; Lieberman et al. 2000).

In both Step 1 and 3 the Upper Paleolithic group was placed at the extreme of the modern human range in CaV 4 (Steps 1A and 3A), and CaV 3 (Steps 1B and 3A-3B). The shape differences that drive the separation along all of these canonical axes include the posterior projection of inion and the iniac region and a relatively low angle between the occipital and nuchal planes, consistent with the description of strong external occipital protuberances and robust nuchal areas. These specimens are not separated from the modern human range along the principal components and canonical variates that separate Neanderthals from modern humans, where the separation is driven by the occipital 'bun' morphology. However, Mladec 1, and, to a lesser extent, Predmosti 3, fall at the extreme of the modern human range and very close to Shanidar 1 and Tabun C1 along CaV 2 of Step 3A and CaV 1 of Step 3B. It is interesting that this specimen, a female, is closer to Neanderthal specimens in this respect, as the archaic features of this population are thought to be less accentuated in females (Stringer 1982; Gambier 1989). The Mladec males, specimens 5 and 6, who were not included here, are thought to show stronger occipital bunning than Mladec 1.

In the Mahalanobis D^2 analysis, the Upper Paleolithic group is widely separated from both Neanderthals and modern humans in Step 1, and it is slightly more distant from modern humans than Neanderthals are. It is closest to the Australian population and most distant to the Neanderthals. Only one Upper Paleolithic specimen is classified correctly

in the cross-validation classification, while the other three are mislcassified as Australian and Epipaleolithic or Tolai. In Step 3 the distances between the Upper Paleolithic population and the modern human groups diminish. Although they are still mostly somewhat larger than those between pairs of recent human populations, they are much smaller than those separating Neanderthals from the same recent groups. They are still closest to the Australian population and most distant from Neanderthals. None of the Upper Paleolithic specimens were correctly classified in the cross-validation classification in Step 3, being grouped instead with the Australian, Eskimo, European and San populations. One specimen, however, Mladec 1, is consistently classified as Neanderthal. This failure in classification shows perhaps a high degree of heterogeneity in the sample (Stringer et al. 1984). As discussed above, the reduced separation of the Upper Paleolithic specimens from recent humans in Step 3 relative to Step 1 is due both to the increased sample, which now included more females, as well as to the removal of the nuchal plane in Step 3. The first of these factors reduces the robusticity of the iniac area, a feature very important in setting this group apart in Step 1, while the second removes part of the morphology involved in the posterior protrusion of this region. The wide separation between this group and modern humans in Step 1, therefore, is probably due to the small sample size and the extreme robusticity present in a group of robust individuals that are mostly male.

The great separation between the Upper Paleolithic European specimens and Neanderthals is in agreement with the results of previous studies based on cranial measurements (Stringer 1974a, 1989, 1992; Bräuer and Rimbach 1990; Bräuer 1992; Kidder et al. 1992; Turbón et al. 1997). However, the position of Mladec 1 supports the findings of Kidder et al. (1992) and of non-metric studies (Jelinek 1969; Smith 1982, 1984; Churchill and Smith 2000), who have noted some similarities of the Central European, and particularly the Mladec, Upper Paleolithic specimens to Neanderthals. Furthermore, it refutes the results of Bräuer and Broeg (1998), who found no occipital bunning in this specimen.

In summary, the posterior cranial profile does differentiate Neanderthals from modern humans, particularly when only the ridge-curve segments from bregma to inion are considered, although there is some overlap between the two groups. The Neanderthal

specimens that show strongest similarities to modern humans are Shanidar 1, Tabun C1 and Saccopastore 1, all previously described as showing less pronounced Neanderthal features as a result of either geographic or temporal variation within the Neanderthal lineage. The Upper Paleolithic specimens are also quite widely separated from recent humans, but only when the nuchal plane is included in the analysis. They appear extreme among recent humans in the strong development of their nuchal superstructures. With the exception of Mladec 1, the Upper Paleolithic specimens are not similar to Neanderthals in their 'hemibuns', and, as a group, show a great Mahalanobis distance to them. No similarities are observed between the Neanderthal posterior cranial profile and those of Skhul 5 and 9, although the latter are quite distant from recent humans also.

CHAPTER 6

Discussion

The objectives of this study are two-fold. The first objective is the quantitative evaluation of traits thought to differentiate Neanderthals and modern humans. This study focused on the morphology of the temporal, occipital and parietal bones, which are considered highly diagnostic for Neanderthals. Furthermore, the traits analyzed are difficult to measure directly linearly (Ducros 1967; Trinkaus 1983; Martínez et al. 1997; Dean et al. 1998). Their quantification, therefore, was made possible by the use of three-dimensional geometric morphometrics and the employment of landmark and ridge-curve analyses. The second objective is the development of models of variation, so that the level of variation both within and among closely related species can be assessed. These models would then be applied to a comparison between modern humans and Neanderthals, in order to shed light on the question of specific or subspecific differentiation between the two. Two such models were developed, one based on modern human populations (within-species variation) and one based on the two species of chimpanzee and their subspecies (within- and between-species variation).

The analysis proceeded in three units defined by restricted anatomical areas: the temporal bone, the occipital bone and the posterior cranial profile. These units of analysis also differed in that the first two used landmarks, while the last one used landmarks and semilandmarks, defining ridge-curve segments. The results of each regional analysis were extensively presented and briefly discussed in Chapters 3-5. This chapter will integrate the findings of the three regional analyses and will interpret them in light of the predictive hypotheses outlined in Chapter 1.

A. Evaluation of proposed Neanderthal traits

Temporal Bone

Several traits of the temporal bone were found to separate Neanderthals from modern humans. These include the morphology of the occipito-mastoid area, the tympanic crest, the supramastoid crest and the position of the external auditory meatus relative to the zygomatic process. Furthermore, a strong signal of geographic clustering

among modern human groups is present in this analysis, suggesting that the morphology of this region is under genetic control and reflects phylogenetic relationships.

Occipito-mastoid area: The Neanderthal occipito-mastoid area is described as showing a large juxtamastoid eminence relative to a small mastoid process, traits often considered as derived Neanderthal features (Boule 1911-1913; Boule and Vallois 1957; Santa Luca 1978; Hublin 1978b; Stringer et al. 1984; Vandermeersch 1985; Condemi 1991, 1992; Dean et al. 1998). However, this region is highly variable in modern humans (Taxman 1963; McKee and Helman 1991; also personal observation), and considerable confusion exists in the literature over the terminology used to describe it (see Hublin 1978a), while the homology of the structure interpreted as the juxtamastoid eminence in different fossil specimens has been questioned (Schwartz and Tattersall 1996b). This study follows Hublin (1978a) in his definition of the juxtamastoid eminence as the crest on the medial border of the digastric fossa, which may or may not straddle the occipito-mastoid suture. It is formed by the insertion of the digastric muscle on the lateral side and can be continuous or to some extent merge with the line formed by the attachment of the superior oblique muscle postero-medially (Hublin 1978a; McKee and Helman 1991).

Authors also disagree over the relative contribution of the mastoid process and the juxtamastoid eminence to the subequal height of the two structures in Neanderthals. Trinkaus (1983) found that, when measured from the Frankfurt plane or from the parietal notch, the height of the Neanderthal mastoid process falls within the range of modern humans. Trinkaus found the great development of the juxtamastoid eminence to contribute more to the appearance of the equal height of the two structures. Vandermeersch (1981) noted that it is inappropriate to measure the height of the mastoid process from the Frankfurt horizontal, as the external auditory meatus, one of the points used to define this line, is slightly elevated in Neanderthals relative to modern humans. He followed the Zoja technique in measuring the mastoid process from the deepest point of the digastric fossa, and found Neanderthal mastoids to be much smaller than those of modern humans. Finally, Martínez et al. (1997) measured the mastoid process from the parietal notch. They found the Neanderthal mastoid process height average to be much lower the modern human mean, and also to fall in the lower parts of the range for Middle

Pleistocene specimens and *H. erectus*. These authors proposed that the small mastoid process in Neanderthals is a derived condition.

In this study the position of the tip of the mastoid was found to be more important in separating Neanderthals from modern humans than the tip of the juxtamastoid eminence in the PCA and the CVA, suggesting that a reduction in the height of this process is actually present in this fossil group. The only specimen with a mastoid process comparable to that in modern humans is Amud 1. This specimen is less well separated from modern humans in the temporal bone analysis due to the large size of this structure. The position of the tip of the juxtamastoid eminence was also found to separate modern humans and Neanderthals. This position, however, often involved a more medial placement, rather than a larger size, in Neanderthals. This medial position of the juxtamastoid eminence reflects a medio-laterally wide digastric fossa in Neanderthals, also described by Vallois (1969). The Upper Paleolithic specimens exhibit a fully modern pattern, with the possible exception of Mladec 2, which shows a small mastoid and larger juxtamastoid eminence, as in Neanderthals, combined with a posterior placement of the lateral origin of the tympanic plate and a sagittal orientation of this plate, as in modern humans (see discussion below). Although this specimen never falls outside the modern human range in the principal components and canonical variates analysis, and is not misclassified as Neanderthal, its position is interesting given the claims for Neanderthal-like traits in the Mladec specimens (Jelinek 1969; Vlcek 1970; Smith 1982, 1984, 1992; Bräuer 1989; Wolpoff 1992; Churchill and Smith 2000; Wolpoff et al. 2001). It is also interesting that Predmosti 3 and 4, also from Central Europe, both exhibit completely modern temporal bone landmark configurations.

Tympanic area: The tympanic area in Neanderthals is thought to retain the primitive condition also found in *H. erectus*. Neanderthals are described as showing a tympanomastoid fissure, a trait often thought to characterize Asian *H. erectus* (Andrews 1984; see also Delson et al. 2001), as the tympanic crest separates their tympanic into an anterior and a posterior area (Vallois 1969; Trinkaus 1983; Vandermeersch 1985; Elyaqtine 1995a; Dean et al. 1998; Minugh-Purvis et al. 2000). This crest is thought to have an anteriorly placed lateral origin in Neanderthals, at the most inferior point of the tympanic tube. In modern humans, on the other hand, this crest is described as

originating laterally from the root of the mastoid process with no tympanomastoid fissure. The medial continuation of this crest forms a tall and plate-like vaginal plate of the styloid process, and slopes obliquely to its termination at the carotid canal, showing an orientation that approaches the sagittal, rather than the coronal, plane (Schwartz and Tattersall 1996; Martínez et al. 1997). Neanderthals are thought to show a more coronal orientation of this crest and a supero-inferiorly shorter and less plate-like vaginal plate of the styloid process. The expression of this trait in Neanderthals is also somewhat disputed, as some authors consider the orientation of the petro-tympanic crest in these hominids to also be sagittal, rather than coronal (Weidenreich 1943; Stringer 1984).

This analysis confirmed previous observations of a more anterior placement of the lateral origin of the petro-tympanic crest, as well as the more coronal orientation of this crest, in Neanderthals relative to modern humans. The tympanic crest landmarks, and particularly the landmark marking its lateral origin, were also very important in separating these two groups in both the PCA and the CVA. A coronal orientation of the tympanic crest was also observed in the Sima de los Huesos Middle Pleistocene fossils by Martínez et al. (1997), and was observed here in Reilingen, but not in Kabwe (as also found by Martínez et al. 1997). Furthermore, Kabwe does not show a tympanomastoid fissure (Elyaqtine 1995a; Delson et al. 2001). The modern affinities of the temporal bone of this specimen was also noted by Santa Luca (1978). If the sagittal orientation of the petro-tympanic crest and the absence of a tympanomastoid fissure represent derived conditions in modern humans, their presence in Middle Pleistocene African fossil hominids implies a direct relationship between modern humans and the latter fossil group to the exclusion of the European lineage, as has previously been suggested (Hublin 1978b; Stringer 1974a, 1989, 1992).

Supramastoid crest: The Neanderthal supramastoid crest has been described as variable in its expression but strong relative to that of modern humans (Boule and Vallois 1957; Vallois 1969; Heim 1976; Elyaqtine 1995a). In this analysis the lateral position of auriculare in Neanderthals, reflecting a strong supramastoid crest, was found to contribute to the separation of the two groups in both the PCA and the CVA.

Position of the external auditory meatus: An elevated position of the external auditory meatus relative to the zygomatic process and to the floor of the glenoid fossa has

previously been described for Neanderthals (Vallois 1969; Vandermeersch 1985; Hublin 1988b; Elyaqtine 1995a, 1995b). This feature was more difficult to assess, due to the reduced Neanderthal sample that preserved the zygomatic process. Where the zygomatic suture landmarks were included, an inferior position of the floor of the glenoid fossa and, to a lesser extent, of the inferior aspect of the zygomatic suture, contributed to the separation of Neanderthals from modern humans. As was also found by Yaroch (1996), it is the more inferior placement of these structures relative to porion that results in an apparent elevated position of the external auditory meatus relative to the glenoid fossa and the zygomatic arch in Neanderthals. Although present, this shape difference between Neanderthals and modern humans is not as strong as the features described above, and was no longer observed when the two zygomatic suture landmarks were removed.

Occipital Bone

The occipital bone landmarks analysis failed to separate Neanderthals from modern humans, suggesting that, as found by Spitery (1985), Neanderthals fall within the modern human range in all the dimensions of this bone. Due to the absence of landmarks on the occipital squama, however, this analysis was unable to quantify such proposed Neanderthal traits as the occipital bun and the suprainiac fossa. The geographic clustering of modern human groups is not as strong as in the temporal bone landmark analysis, and breaks down further with the removal of landmarks.

Neanderthals were characterized by a medio-laterally wide and supero-inferiorly low occipital squama, and particularly by a low occipital plane relative to modern humans. As previously described, lambda is depressed and inion is superiorly placed (McCown and Keith 1937; Heim 1974, 1976; Thoma 1975; Condemi 1992; Wolpoff et al. 2001). However, Neanderthals fall within the range of modern human variation in all of these features. Kabwe and Petralona differ more and were separated from modern humans, showing a supero-inferiorly short occipital plane and antero-posteriorly elongated nuchal plane, with a strong posterior projection of inion.

Posterior cranial profile

The posterior cranial profile analysis was expected to capture the morphology of the occipital bun and suprainiac fossa, often described as derived Neanderthal features (Boule 1911-1913; Hublin 1978a, 1978b, 1988a, 1988b; Stringer et al. 1984; Vandermeersch 1985; Condemi 1991, 1992; Lieberman 1985; Bräuer and Broeg 1998; Dean et al. 1998). Furthermore, the presence of similar morphology, described as a 'hemibun', in the posterior cranial profile of some Upper Paleolithic European specimens has been interpreted as evidence for interbreeding, or even continuity, between them and Neanderthals (Jelinek 1969; Genet-Varcin 1970; Vlcek 1970; Smith 1982, 1984, 1992; Bräuer 1989; Churchill and Smith 2000; Wolpoff et al. 2001). As with the temporal bone traits, there is some disagreement about the validity, as well as the definition of these traits, and particularly of the occipital bun. This analysis is similar to the occipital bone analysis, in that the geographic clustering of recent human groups is not complete and deteriorates with the removal of landmarks.

Occipital bun and parietal contour: The occipital bun is described variably as a posterior projection of the occipital squama or a great convexity of the occipital plane, and is often associated with the presence of a depression of the area around lambda on the occipital and parietals. This trait, however, is very difficult to define or to measure, and the term 'occipital bun' has been applied to a range of morphological patterns (Ducros 1967; Dean et al. 1998). Using a complicated method for measuring the depth of the lambdoid depression, Ducros (1967) concluded that the occipital 'bun' morphology shown by Neanderthals is of a different kind from that found in certain modern human crania, including the Upper Paleolithic specimens. He found that the Neanderthal bun describes a relatively smooth curve on the parietal and occipital and is formed by a general antero-posterior elongation of the cranium and of the occipital bone. The occipital plane seems to be pointing backwards, as it is delimited superiorly by a flat parietal and inferiorly by a flat nuchal plane. The modern human occipital bun, on the other hand, including the morphology shown by the Upper Paleolithic European specimens, is characterized by a 'saddle-like' depression of the posterior cranial profile in the area surrounding lambda (Ducros 1967). Furthermore, as Churchill and Smith note (2000), the Neanderthal occipital bun differs from those seen in modern humans by

extending further laterally. However, these authors see similarities with the Neanderthal condition in the early modern human specimens from Mladec, and consider them as evidence for Neanderthal contribution in the modern human gene pool.

Trinkaus and LeMay (1982) disputed the distinction between Neanderthal and modern human occipital bunning. They suggested that its formation is related to the prolongation of the posterior growth of the brain relative to the development of the vault bones, questioning the validity of this trait as a phylogenetic character. Lieberman (1995; Lieberman et al. 2000) accepted that the formation of a bun in modern humans is related to the rate of posterior brain growth relative to the formation of the vault, and proposed that bunning is especially pronounced in large-brained individuals with narrow cranial bases. As Neanderthals exhibit very marked occipital buns and have large brains but wide cranial bases, these authors considered modern human 'bunning' as convergent to the Neanderthal condition, which was accepted as a derived Neanderthal feature. Although Lieberman and his co-authors noted the relatively strong projection of the occipital plane in some Upper Paleolithic European specimens, they proposed that it is not homologous to the Neanderthal condition. However, as these authors cautioned, they did not include the Mladec specimens in their analysis and therefore could not test the hypothesis that these individuals possess Neanderthal-like morphology in their occipital contours.

Finally, Yaroch (1996), using the geometric morphometric method of thin plate splines based on two-dimensional landmarks (collected in lateral view), found that Neanderthals do not show marked occipital plane curvature relative to modern humans. According to Yaroch, the Neanderthal occipital bun morphology is part of the overall antero-posterior elongation of the Neanderthal cranium. What little occipital plane curvature she did observe was not found to be significantly different from some recent human groups.

The geometric morphometric ridge curve analysis and multivariate statistics employed here allows for direct comparison and quantification of shape differences between Neanderthal, Upper Paleolithic and modern human posterior cranial profiles in an effort to resolve these issues. This approach is superior to a landmark-based analysis, such as Yaroch's (1996), as the lack of landmarks on the occipital plane aside from

lambda and inion preclude appropriate evaluation of this feature. The difference between the results of the occipital landmark analysis and of the ridge curve analysis in this study are indicative of the limitations of the former (although Yaroch did use one additional landmark on the occipital plane).

Neanderthals were found to differ from modern humans in the greater posterior projection and curvature of their occipital plane, their flat parietal and the more horizontal orientation of their nuchal plane. As described by Ducros (1967), the curve of the parietal and the occipital plane is smooth and continuous, without a pronounced lambdoid depression. Neanderthals are mostly, although not completely, separated from modern humans in these traits in the PCA and CVA. The occipital bun morphology, therefore, does characterize this fossil group and does differentiate them from modern humans, although incompletely. However, the derived nature of this feature for Neanderthals cannot be properly evaluated until the African and Asian fossil specimens thought to show an occipital bun (Jebel Irhoud, Laetoli H 18, Jinniushan, see Trinkaus and LeMay 1982; Bräuer and Broeg 1998) are included in this analysis. As the occipital bun of Neanderthals is also considered different in its great lateral expansion (Churchill and Smith 2000), analysis of the parasagittal profile of the posterior vault in the future may shed more light on this question.

The Neanderthal specimens that tend to overlap the most with the modern human range of variation are the Eastern Neanderthal specimens Shanidar 1 and Tabun C1, as well as the early Neanderthal Saccopastore 1. Shanidar 1 was found here to possess a very curved parietal bone, as also previously described (Stringer and Trinkaus 1981; Trinkaus 1983), which may be due to artificial deformation (Trinkaus 1982). This specimen and Tabun C1 also show relatively weak occipital buns (Trinkaus 1983), as does Saccopastore 1 (Condemi 1992). Amud 1, the other Eastern Neanderthal included here, is well separated from modern humans and shows a flat parietal and a strong occipital bun. This specimen fell within the modern human range of variation in its mastoid process morphology in the temporal bone analysis.

The variable expression of Neanderthal traits in the Eastern Neanderthal sample is consistent with the view of a geographically differentiated Neanderthal population and of a mosaic pattern in the evolution of this group in Western Asia. (Thoma 1965, 1975;

Stringer and Trinkaus 1981; Trinkaus 1984; Trinkaus and Smith 1985; Vandermeersch 1989; Dean et al. 1998). The similarities of Saccopastore 1 with these specimens in its posterior cranial profile support previous observations of the affinities of the Saccopastore crania and Eastern Neanderthals (Vandermeersch 1989; Condemi 1992), although they can be interpreted as retentions of more primitive conditions (Stringer 1990).

The Upper Paleolithic specimens fall at the extreme of the modern human range of variation in the PCA and CVA of the posterior cranial profile analysis but do not show affinities to the Neanderthals, except the case of Mladec 1. The Mahalanobis distance between these two groups is very large, reflecting their different cranial profile morphology. The shape differences that separate the Upper Paleolithic specimens from most modern humans include a more posterior projection of inion and the iniac region and an elongated and relatively horizontally oriented nuchal plane. A strong projection of inion is consistent with previous descriptions of strong external occipital protuberances, occipital tori and great cranial robusticity in these specimens (Billy 1970; Genet-Varcin 1970; Smith 1984; Gambier 1989, 1997; Churchill and Smith 2000; Churchill et al. 2000). Mladec 1 consistently falls within the Neanderthal range of variation in its posterior cranial profile shape and is characterized by a somewhat weak expression of the same shape differences that separate Neanderthals from modern humans. Furthermore, this specimen is consistently misclassified as Neanderthal and is the only Upper Paleolithic specimen that approaches the Neanderthal occipital bun condition. These findings disagree with those of Bräuer and Broeg (1998), who found the hemibun shown by Mladec 1 not to be similar to the Neanderthal condition in the degree of its expression.

The Central European Upper Paleolithic specimens, and particularly the Mladec series, are considered by many authors to exhibit several similarities to Neanderthals, despite their undisputedly modern overall morphological pattern. These similarities are seen as evidence of continuity or interbreeding with this fossil group (Jelinek 1969; Vlcek 1970; Smith 1982, 1984, 1992; Bräuer 1989; Wolpoff 1992; Churchill and Smith 2000; Wolpoff et al. 2001). The position of Mladec 1 in the posterior profile analysis, as well as the presence of some similarities between Mladec 2 and Neanderthal temporal

bone landmark configurations, lend some support to previous observations of affinities between these early Central European Upper Paleolithic specimens and Neanderthals. They also refute the possibility that these similarities are due to the robusticity exhibited by the male specimens, as suggested by Stringer (1982), since both specimens included here are female. Evidence for possible limited gene flow in the form of similarities of individual specimens to Neanderthals has been previously reported from multivariate analyses of cranio-facial measurements. Stringer (1989) found that Predmosti 3 and Dolni Vestonice 3, but not the Mladec or Cro Magnon specimens, were more similar to Neanderthals in some of his analyses. Kidder et al. (1992) found similarities between Mladec 5 and Neanderthals. The present findings may be interpreted as weakly supporting the hypothesis of limited gene flow between Neanderthals and Central European Upper Paleolithic specimens. The inclusion of the male specimens Mladec 5 and 6, which have been claimed to show stronger affinities with Neanderthals, but which were not measured here, would shed further light on this issue.

The possibility of limited gene flow between Neanderthals and early modern humans raises questions about species hypotheses, as reproductive isolation is the criterion for species definition according to the biological species concept and the underlying premise in the use of analogy to living biospecies to define species in paleontology. Despite this criterion, however, there are several instances under which interbreeding between biological species can occur (Mayr 1970). Separate species are indicated by two populations showing distinct epiphenotypes with no intermediates, or with only occasional hybridization, in the area of sympatry, while the existence of complete intergradation between the two epiphenotypes throughout the sympatric zone indicates two populations of the same species (Stringer 1992). Even if the similarities between the two Mladec specimens and Neanderthals are the result of gene flow, this evidence indicates at most sporadic interbreeding, rather than a zone of intergradation, between Neanderthals and modern humans. The different species hypothesis, therefore, is not refuted. Further investigation of additional Central European Upper Paleolithic specimens will help resolve this issue.

Petralona is separated from modern humans by its extremely flat parietal profile, in which it is similar to, but more extreme than, the Neanderthals, in the posterior

projection of its iniac region, and in the sharper angle between the two occipital scales. Its position in this analysis is consistent with the described morphology of a very flat and low cranial vault and lack of occipital bunning (Jelinek 1969; Trinkaus and LeMay 1982). The early anatomically modern human specimens Skhul 5 and 9 also show no occipital bunning, but retain a flat parietal contour in combination with a strongly posteriorly projecting iniac region. A well developed occipital torus and external occipital protuberance, as well as a lack of occipital bunning, is also described by McCown and Keith (1937) for these specimens.

Suprainiac fossa: This feature is widely discussed as a Neanderthal derived trait (Santa Luca 1978; Hublin 1978a; 1978b; 1988a; 1988b; Condemi 1991, 1992; Lieberman 1995; Dean et al. 1998). This analysis failed to separate Neanderthals on the basis of this feature, and it also failed to even detect its presence. As noted in Chapter 5, this failure is most likely due to the inability of the method used to capture a very subtle and shallow depression. Furthermore, the simple presence of such a fossa in the midsagittal plane is not limited to Neanderthals, but also often appears in modern human specimens (see Bräuer and Broeg 1998). Therefore, if this trait distinguishes Neanderthals from modern humans, it is in its lateral extent and particular form, rather than its simple presence (Hublin 1988a; Bräuer and Broeg 1998).

B. Models of Variation

The pattern of morphological variation of Neanderthals relative to modern humans was assessed using two models of variation. The modern human model can be used only to assess within species variation, although it is the most appropriate model for Neanderthals given the very close phylogenetic relationship between the two. The chimpanzees provided a model for inter-, as well as intra-specific variation, although this model is less appropriate phylogenetically and ecologically than the modern human one.

Two predictive hypotheses were outlined in Chapter 1: *A*) Neanderthals and modern humans represent two different species, and Neanderthals did not contribute to the evolution of modern humans; and *B*) Neanderthals and modern humans represent populations of the same species, and Neanderthals did contribute to the evolution of modern humans. Hypothesis *A* predicts that Neanderthals would be more distant from

modern human populations than any pair of modern human groups are from each other and more distant than the two common chimpanzee species are from each other. The distance between Neanderthals and modern humans would be approximately as great as that between the two chimpanzee species. Neanderthals would show no affinities to the Upper Paleolithic European specimens or to recent Europeans. Hypothesis *B* predicts that the distance between Neanderthals and modern humans would be equivalent to the distances among modern human populations, or to that between the two common chimpanzee subspecies. This distance would be smaller than that present between the two chimpanzee species. Furthermore, Neanderthals would show affinities to the Upper Paleolithic European specimens and possibly also to recent European specimens.

The patterns of variation between Neanderthals and modern humans revealed in this study differ from one regional anatomical analysis to the next. However, one finding is consistent across all three regional analyses: the great separation of Neanderthals from recent human populations. The smallest distance between Neanderthals and modern human populations is greater than that between any pair of modern human groups in the temporal bone and the posterior cranial profile analysis. In the occipital bone analysis, the smallest distances between Neanderthals and a modern human population fall in the range of distances among modern human groups. Even in this analysis, however, most distances between Neanderthals and recent human groups are much greater than those among modern human populations. This general dichotomy between Neanderthals on one hand, and recent human populations on the other, is consistent with the findings of several studies using multivariate analyses of cranial measurements (Stringer 1974, 1992; Howells 1989; Bräuer and Rimbach 1990; Bräuer 1992; Kidder et al. 1992) and fits the predictions of hypothesis *A*.

The results of the chimpanzee model are more interesting, as they provide a measure of morphological differentiation between two closely related species, as well as between two populations of the same species. The distance between Neanderthals and modern human populations is always much greater than that between the two chimpanzee species, bonobos and common chimpanzees. This finding strongly supports hypothesis *A*, suggesting that the morphological differences observed between Neanderthals and modern humans are greater than those present between the two chimpanzee species. It is

similar to the finding recently reported by Schillaci and Froelich (2001), who found Neanderthals to be more distant from Upper Paleolithic Europeans than macaque species are from each other based on cranial measurements. The two chimpanzee species, however, appear in all analyses to be as close to each other than some modern human population pairs are. The finding of somewhat reduced morphological variability among chimpanzees relative to modern humans is somewhat surprising in light of new evidence of reduced genetic variability in modern humans relative to chimpanzees and to great apes in general (Kaessmann et al. 2001). This pattern may be due to the small geographic range sampled in the two groups of common chimpanzee included in this study relative to the much wider geographical, temporal and ecological range represented by the modern human groups. It may also be affected by the lack of differentiation between chimpanzee species on the basis of the morphological features selected here to best differentiate between Neanderthals and modern humans. The anatomical areas examined here may not be the most successful in discriminating between bonobos and common chimpanzees, although the two chimpanzee species are consistently more distant from each other than the two common chimpanzee subspecies are. Finally, the chimpanzee may not be the most appropriate model, as this genus is not similar to hominids ecologically.

Neanderthals do not show affinities to the Upper Paleolithic specimens in any of the regional analyses, with the exception of Mladec 1, and possibly also Mladec 2 (see discussion above). The distances between the two groups are either the largest, or among the largest, distances among all human groups in the posterior cranial profile analysis. Neanderthals also do not show affinities to recent Europeans in either the temporal or the cranial profile analyses. They are closest to the Austrian Berg population in the analysis of occipital bone landmarks, and this resemblance is based on the medio-laterally wide occipital squama exhibited by both groups. However, no similarities were found between Neanderthals and Upper Paleolithic Europeans in this analysis, which are expected to be much stronger than those between Neanderthals and recent Europeans if Neanderthals contributed to the modern European gene pool (Relethford 2001a). These findings therefore generally fit with the predictions of hypothesis ***A***. As discussed above, however, the position of Mladec 1 in the posterior cranial profile analysis, as well as the similarities of the Mladec 2 temporal to Neanderthals, however, lend some support to the

suggestion of some genetic exchanges between Neanderthals and Upper Paleolithic Europeans in Central Europe. This matter warrants further investigation, particularly in the male specimens of the Mladec series.

The position of the Upper Paleolithic specimens relative to modern humans is more problematic. While these specimens are very close to the recent human groups in the temporal bone analysis, in agreement with previous studies (Stringer 1974, 1992; Bräuer and Rimbach 1990; Kidder et al. 1992) they are very distant from recent humans in both the occipital landmarks and the cranial profile analyses. In both these cases, they are often as removed from recent humans as Neanderthals are. As the modern status of this fossil human group is not disputed, if it is as distant from recent human populations as Neanderthals then the case for specific status of the latter cannot be made.

These large distances are influenced mostly by the posterior projection of the iniac area and the elongation of the nuchal plane, and are drastically reduced with the removal of most landmarks on the nuchal plane (Step 3) in the occipital bone analysis, and with the removal of the nuchal plane (also Step 3) in the cranial profile analysis. The importance of the nuchal plane in separating these specimens from recent humans is clear, and consistent with previous descriptions of these specimens. Although quite variable (Stringer et al. 1984), Upper Paleolithic specimens are often described as robust, with strong occipital protuberances, occipital tori and elongated and flat nuchal planes (Jelinek 1969; Billy 1970; Genet-Varcin 1970; Vlcek 1970; Smith 1984; Gambier 1989, 1997; Churchill and Smith 2000; Churchill et al. 2000). A combination of a robust nuchal torus and an antero-posteriorly elongated nuchal plane may be the factor driving the separation between recent humans and Upper Paleolithic Europeans in the two analyses involving the occipital bone. These results are similar to those reported by Pearson (2000), who, in a multivariate analysis of postcranial measurements, found the Upper Paleolithic specimens to be greatly separated from modern humans due to a pattern of overall robusticity, rather than to individual distinguishing features.

Only the results of the temporal bone analysis, therefore, are entirely consistent with the predictions of hypothesis *A* with respect to the Upper Paleolithic specimens. However, the separation observed between this group and recent humans may be the result of their great robusticity, indicating behavioral rather than phylogenetic patterns.

The affinities of the Upper Paleolithic specimens to recent humans are also of interest. Ferembach (1985) has proposed that the Upper Paleolithic Europeans originated from the North African Aterians around 50 ka and that a 'Cromagnoid' group, probably an Epigravettian Italian population, gave rise to the Mesolithic populations of Northern Africa, represented here by the Afalou/Taforalt sample. Similarities between these two groups would also support an African origin for modern humans in Europe (Turbón et al. 1997). Affinities between the Upper Paleolithic European specimens and the North African Mesolithic material have been noted in the past both from general morphology (Ferembach 1962; Chamla 1978; Lahr 1996) and from multivariate analyses of facial measurements (Turbón et al. 1997). In the present study, the Upper Paleolithic group is closest to the North African Epipaleolithic sample only in the occipital bone analysis. It is closest to the Austrian Berg in the temporal bone analysis, and to the Australian population in the posterior cranial profile analysis. No particular affinities of the Upper Paleolithic specimens can therefore be claimed to the Epipaleolithic group based on the measurements used here.

The early modern human specimens Skhul 5, Skhul 9 and Qafzeh 9 were included in different sets of analyses. Due to the very small sample size for this group (1-2 specimens in each analysis), and, in the case of the occipital bone analysis, also due to postmortem distortion, the distances between it and all other groups are probably inflated. These specimens are found to be very distant from both modern humans and Neanderthals, but closer to the former. Again, this is in keeping with previous metric studies of both cranial and postcranial measurements (Stringer 1974, 1992; Bräuer and Rimbach 1990; Bräuer 1992; Kidder et al. 1992; Pearson 2000). The position of the early anatomically modern human specimens is interpreted as due to their having retained primitive conditions, and therefore perhaps representing an intermediate form between archaic and modern humans, as has been suggested by Stringer (1992).

Conclusions

The results of each regional analysis differed in how successfully they separated Neanderthals from modern humans, as well as modern human geographic populations and chimpanzee species and subspecies. The temporal bone landmark analysis has the

lowest rates of misclassification of Neanderthals as modern humans and vice versa, and it shows the strongest geographic clustering among modern human populations. The posterior cranial profile is also relatively successful in separating the two groups, although the rates of misclassification on both sides are higher. Finally, the occipital bone landmark analysis does not separate Neanderthals from modern humans, in part due to the lack of landmarks in the occipital plane.

The temporal bone analysis may preserve the strongest phylogenetic signal. This analysis consistently shows the strongest geographic clustering among recent human populations. Furthermore, it includes the highest number of unpaired landmarks, as only one side was used, as opposed to the occipital bone landmarks, which include midline and both right and left homologous points. The temporal bone landmarks are also located almost entirely on the basicranium, a region that has long been considered very conservative and little affected by epigenetic factors (see discussion in Olson 1981). Further research is needed to confirm basicranial conservatism. If true, however, the temporal bone landmarks may represent the most appropriate characters for phylogenetic analysis relative to the other two anatomical regions.

Neanderthals are consistently very widely separated from modern humans in Mahalanobis D^2, more so than any pair of modern human groups, and more than the two chimpanzee species are from each other, although they do overlap widely with modern humans in the occipital bone landmarks analysis. They do not show affinities to the Upper Paleolithic specimens in any regional analysis, with the possible exception of the two specimens from Mladec. They also do not show affinities to the recent European groups, except in the occipital bone landmark analysis. However, stronger similarities should be observed under hypothesis *B* between Neanderthals and Upper Paleolithic Europeans than between Neanderthals and recent Europeans. Relethford (2001a) recently argued that no similarities should be expected between Neanderthals and recent Europeans based on accumulated ancestry. None of the regional analyses, therefore, supports continuity and a strong ancestral-descendant relationship between Neanderthals and modern humans. The Skhul/Qafzeh sample might represent an intermediate condition between archaic and modern humans, although they are very distant from both Neanderthals and modern humans in all three analyses. These specimens, however,

appear to preserve primitive features and not Neanderthal characters along with their modern morphological pattern, and hence they do not represent evidence for continuity or interbreeding between Neanderthals and early modern humans.

The consistently great distance of Neanderthals to modern human populations in all analyses is similar to the consistent separation between bonobos and common chimpanzees despite some overlap between the two. This distance is also consistently greater than that observed between the two chimpanzee species. These observations support the placement of this fossil hominid group in a different species. The great distance of the Upper Paleolithic specimens from recent humans in the occipital bone and cranial profile regional analyses can probably be attributed to the robusticity of this group. Unlike the pattern exhibited by Neanderthals, this separation is not consistent, but tends to diminish with increased sample sizes and removal of the idiosyncratic nuchal areas from the analysis. Furthermore, no great separation is observed in the temporal bone analysis, which may be preserving the strongest phylogenetic signal.

Although Neanderthals are consistently and widely separated from modern humans and do not show affinities to the Upper Paleolithic group, some evidence was found for similarities between individual Upper Paleolithic specimens and Neanderthals. Mladec 1 shows a posterior profile shape similar to that found in Neanderthals, while Mladec 2 does not completely conform to the modern human temporal bone configuration, showing limited similarities to the Neanderthal configuration. Such instances of individual similarities have also been reported in previous multivariate analyses of cranio-facial measurements (Stringer 1989; Kidder et al. 1992), and may represent evidence for limited gene flow between Neanderthals and early modern Europeans.

In summary, all of the analyses support the hypothesis that Neanderthals represent a separate species from modern humans. However, this support is not unequivocal. No evidence for continuity or significant contribution to the evolution of modern Europeans was found. The limited similarities between Neanderthals and the Mladec specimens, however, may be indicative of occasional interbreeding. Investigation is warranted into the possible similarities of additional Central European Upper Paleolithic European specimens with Neanderthals, into the nature of the morphological differences between

the Upper Paleolithic Europeans and recent humans, and into the position of the Skhul/Qafzeh sample relative to both the Upper Paleolithic specimens and recent humans. A more extensive study of archaic and *H. erectus* fossils is also necessary, in order to better assess the polarity of the traits used in this study.

APPENDIX – Chapter 5, Step 2

Cross-validation classification summary (percentages for each population in boldStep 2A.

	And	Aus	Brg	Dgn	Epi	Esk	Eur	San	Tol	UP	Bon	Nea	Sch	Trg	Total
And	17	2	2	2	2	0	2	0	2	0	0	0	0	0	29
%	**58.62**	6.9	6.9	6.9	6.9	0	6.9	0	6.9	0	0	0	0	0	100
Aus	1	13	2	1	2	1	1	2	4	2	0	1	0	0	30
%	3.33	**43.33**	6.67	3.33	6.67	3.33	3.33	6.67	13.33	6.67	0	3.33	0	0	100
Brg	0	1	13	3	0	4	3	2	3	0	0	0	0	0	29
%	0	3.45	**44.83**	10.34	0	13.79	10.34	6.9	10.34	0	0	0	0	0	100
Dgn	1	1	0	20	0	2	3	3	0	0	0	0	0	0	30
%	3.33	3.33	0	**66.67**	0	6.67	10	10	0	0	0	0	0	0	100
Epi	3	1	0	2	10	2	2	3	0	0	0	0	0	0	23
%	13.04	4.35	0	8.7	**43.48**	8.7	8.7	13.04	0	0	0	0	0	0	100
Esk	1	4	3	3	1	13	4	1	0	0	0	0	0	0	30
%	3.33	13.33	10	10	3.33	**43.33**	13.33	3.33	0	0	0	0	0	0	100
Eur	2	0	3	4	2	5	4	2	0	0	0	0	0	0	22
%	9.09	0	13.64	18.18	9.09	22.73	**18.18**	9.09	0	0	0	0	0	0	100
San	0	0	5	2	1	0	1	13	4	0	0	4	0	0	30
%	0	0	16.67	6.67	3.33	0	3.33	**43.33**	13.33	0	0	13.33	0	0	100
Tol	3	4	3	2	0	4	1	2	7	1	0	1	0	0	28
%	10.71	14.29	10.71	7.14	0	14.29	3.57	7.14	**25**	3.57	0	3.57	0	0	100
UP	0	2	0	0	0	0	0	1	0	1	0	0	0	0	4
%	0	50	0	0	0	0	0	25	0	**25**	0	0	0	0	100
Bon	0	0	0	0	0	0	0	0	0	0	23	0	7	4	34
%	0	0	0	0	0	0	0	0	0	0	**67.65**	0	20.59	11.76	100
Nea	0	0	0	0	0	0	0	3	2	1	0	0	0	0	6
%	0	0	0	0	0	0	0	50	33.33	16.67	0	**0**	0	0	100
Sch	0	0	0	0	0	0	0	0	0	0	8	0	16	6	30
%	0	0	0	0	0	0	0	0	0	0	26.67	0	**53.33**	20	100
Trg	0	0	0	0	0	0	0	0	0	0	0	0	7	21	28
%	0	0	0	0	0	0	0	0	0	0	0	0	25	**75**	100
Total	28	28	31	39	18	31	21	32	22	5	31	6	30	31	353
%	7.93	7.93	8.78	11.05	5.1	8.78	5.95	9.07	6.23	1.42	8.78	1.7	8.5	8.78	100

Cross-validation classification summary (percentages for each population in bold), Step 2B.

	And	Aus	Brg	Dgn	Epi	Esk	Eur	San	Tol	UP	Nea	Total
And	15	3	0	4	2	1	2	0	2	0	0	29
%	**51.72**	10.34	0	13.79	6.9	3.45	6.9	0	6.9	0	0	100
Aus	1	18	1	1	2	2	1	0	2	2	0	30
%	3.33	**60**	3.33	3.33	6.67	6.67	3.33	0	6.67	6.67	0	100
Brg	0	2	13	3	0	3	4	4	0	0	0	29
%	0	6.9	**44.83**	10.34	0	10.34	13.79	13.79	0	0	0	100
Dgn	2	1	0	20	0	3	3	1	0	0	0	30
%	6.67	3.33	0	**66.67**	0	10	10	3.33	0	0	0	100
Epi	2	1	1	2	9	2	2	4	0	0	0	23
%	8.7	4.35	4.35	8.7	**39.13**	8.7	8.7	17.39	0	0	0	100
Esk	1	4	3	1	1	12	5	1	2	0	0	30
%	3.33	13.33	10	3.33	3.33	**40**	16.67	3.33	6.67	0	0	100
Eur	2	0	2	3	2	7	3	2	0	1	0	22
%	9.09	0	9.09	13.64	9.09	31.82	**13.64**	9.09	0	4.55	0	100
San	0	0	5	2	1	1	2	13	3	0	3	30
%	0	0	16.67	6.67	3.33	3.33	6.67	**43.33**	10	0	10	100
Tol	2	3	1	2	0	5	1	2	9	2	1	28
%	7.14	10.71	3.57	7.14	0	17.86	3.57	7.14	**32.14**	7.14	3.57	100
UP	0	1	0	0	0	0	0	1	1	1	0	4
%	0	25	0	0	0	0	0	25	25	**25**	0	100
Nea	0	0	0	0	0	0	0	2	1	1	2	6
%	0	0	0	0	0	0	0	33.33	16.67	16.67	**33.33**	100
Total	25	33	26	38	17	36	23	30	20	7	6	261
%	9.58	12.64	9.96	14.56	6.51	13.79	8.81	11.49	7.66	2.68	2.3	100

Unbiased Mahalanobis D^2, Step 2A. All distances 0.001 significance level except: NS = non-significant, * = 0.05 level, ** = 0.01 level.

	Kan	And	Aus	Bch	Brg	Dgn	Skh5	Epi	Esk	Eur
Kan	0.00	27.52NS	24.79NS	100.99	18.27NS	41.28**	102.35	18.17NS	28.17NS	23.83NS
And	27.52NS	0.00	8.47	45.73**	10.54	5.49	76.65	7.31	6.57	5.09
Aus	24.79NS	8.47	0.00	47.69	6.34	8.52	74.17	8.09	4.61	4.58
Bch	100.99	45.73**	47.69	0.00	46.05**	34.97*	75.11**	49.32	38.84**	38.57**
Brg	18.27NS	10.54	6.34	46.05**	0.00	10.66	84.57	8.50	2.82**	1.78NS
Dgn	41.28**	5.49	8.52	34.97*	10.66	0.00	86.17	11.06	5.76	4.41
Skh5	102.35	76.65	74.17	75.11**	84.57	86.17	0.00	82.00	85.63	78.00
Epi	18.17NS	7.31	8.09	49.32	8.50	11.06	82.00	0.00	8.47	4.38
Esk	28.17NS	6.57	4.61	38.84**	2.82	5.76*	85.63	8.47	0.00	0.81NS
Eur	23.83NS	5.09	4.58	38.57**	1.78NS	4.41	78.00	4.38	0.81NS	0.00
Ptr	118.03	101.45	78.98	120.10	73.79	102.69	157.04	103.07	83.08	88.57
San	31.67*	11.23	6.76	32.17*	5.21	7.73	80.89	5.85	4.63	3.60**
Sng	61.51*	35.32*	33.11*	70.61*	28.76NS	36.99*	91.50**	24.84NS	36.65*	30.85*
Tol	23.51NS	8.99	3.87	35.23*	4.12	7.10	77.94	7.96	2.65**	2.04NS
UP	25.50NS	24.82	8.42*	57.04**	16.44	23.45	81.42	19.83	19.25	16.94
Bon	55.15	46.85	40.91	67.91	40.32	48.46	102.77	57.57	40.79	39.55
Nea	43.73**	25.02	15.44	24.97NS	16.54	18.07	74.96	20.90	14.04	12.74
Sch	61.07	50.02	44.16	68.12	40.97	50.79	116.09	61.60	41.07	41.90
Trg	104.45	89.15	81.73	96.17	76.00	87.40	142.95	98.91	77.20	77.23

	Ptr	San	Sng	Tol	UP	Bon	Nea	Sch	Trg
Kan	118.03	31.67*	61.51*	23.51NS	25.50NS	55.15	43.73**	61.07	104.45
And	101.45	11.23	35.32*	8.99	24.82	46.85	25.02	50.02	89.15
Aus	78.98	6.76	33.11*	3.87	8.42*	40.91	15.44	44.16	81.73
Bch	120.10	32.17*	70.61*	35.23**	57.04**	67.91	24.97NS	68.12	96.17
Brg	73.79	5.21	28.76NS	4.12	16.44	40.32	16.54	40.97	76.00
Dgn	102.69	7.73	36.99*	7.10	23.45	48.46	18.07	50.79	87.40
Skh5	157.04	80.89	91.50**	77.94	81.42	102.77	74.96	116.09	142.95
Epi	103.07	5.85	24.84NS	7.96	19.83	57.57	20.90	61.60	98.91
Esk	83.08	4.63	36.65*	2.65**	19.25	40.79	14.04	41.07	77.20
Eur	88.57	3.60**	30.85*	2.04NS	16.94	39.55	12.74	41.90	77.23
Ptr	0.00	80.45	118.91	77.30	79.06	80.11	99.18	79.46	96.45
San	80.45	0.00	19.77NS	3.44	17.41	51.76	9.08**	53.77	86.56
Sng	118.91	19.77NS	0.00	34.32*	47.25**	96.99	26.87NS	95.91	119.82
Tol	77.30	3.44	34.32*	0.00	12.49**	37.00	8.73**	38.68	73.22
UP	79.06	17.41	47.25**	12.49**	0.00	51.24	17.75**	60.53	96.47
Bon	80.11	51.76	96.99	37.00	51.24**	0.00	54.04	5.54	17.19
Nea	99.18	9.08**	26.87NS	8.73**	17.75	54.04	0.00	53.11	81.90
Sch	79.46	53.77	95.91	38.68	60.53	5.54	53.11	0.00	14.49
Trg	96.45	86.56	119.82	73.22	96.47	17.19	81.90	14.49	0.00

Unbiased Mahalanobis D^2, Step 2B. All distances 0.001 significance level except: NS = non-significant, * = 0.05 level, ** = 0.01 level.

	Kan	And	Aus	Bch	Brg	Dgn	Skh5	Epi	Esk	Eur	Ptr	San	Sng	Tol	UP	Nea
Kan	0.00	37.54*	38.93*	117.58	33.78NS	53.63**	114.39	33.25NS	41.60*	37.61*	209.81	45.64**	87.36**	35.46*	43.95*	54.43**
And	37.54*	0.00	8.83	50.52**	10.89	6.54	78.33	7.62	6.59	5.53	161.54	11.51	47.31**	8.61	25.57	28.28
Aus	38.93*	8.83	0.00	54.39**	6.46	7.81	71.96	7.39	4.55	4.46	143.70	6.35	43.61**	3.84	10.50*	17.17
Bch	117.58	50.52**	54.39**	0.00	49.93**	41.69*	71.10*	52.94**	43.53**	43.23**	189.11	38.70*	74.51*	43.19**	68.31	30.70NS
Brg	33.78NS	10.89	6.46	49.93**	0.00	9.43	82.48	8.57	3.06**	2.17NS	132.00	5.07	37.93*	4.54	16.31	16.82
Dgn	53.63**	6.54	7.81	41.69*	9.43	0.00	85.48	10.39	5.41	4.19	153.60	6.62	47.47**	6.45	21.83	19.76
Skh5	114.39	78.33	71.96	71.10*	82.48	85.48	0.00	77.42	82.53	75.73	227.47	78.06	91.57**	77.72	87.87	71.57
Epi	33.25NS	7.62	7.39	52.94**	8.57	10.39	77.42	0.00	8.02	4.12**	159.74	5.94	35.70*	8.03	20.43	22.39
Esk	41.60*	6.59	4.55	43.53**	3.06**	5.41	82.53	8.02	0.00	0.99NS	147.65	4.63	47.52**	2.72*	19.29	16.44
Eur	37.61*	5.53	4.46	43.23**	2.17NS	4.19	75.73	4.12**	0.99NS	0.00	151.09	3.66**	42.09*	2.34NS	16.98	15.31
Ptr	209.81	161.54	143.70	189.11	132.00	153.60	227.47	159.74	147.65	151.09	0.00	134.47	147.64	140.99	141.75	147.98
San	45.64**	11.51	6.35	38.70*	5.07	6.62	78.06	5.94	4.63	3.66**	134.47	0.00	30.51NS	3.33**	16.90	10.68**
Sng	87.36**	47.31**	43.61**	74.51*	37.93*	47.47**	91.57**	35.70*	47.52**	42.09*	147.64	30.51NS	0.00	47.10**	59.01**	32.08NS
Tol	35.46*	8.61	3.84	43.19	4.54	6.45	77.72	8.03	2.72*	2.34NS	140.99	3.33**	47.10**	0.00	13.33**	12.37**
UP	43.95*	25.57	10.50*	68.31	16.31	21.83	87.87	20.43	19.29	16.98	141.75	16.90	59.01**	13.33**	0.00	22.66**
Nea	54.43**	28.28	17.17	30.70NS	16.82	19.76	71.57	22.39	16.44	15.31	147.98	10.68**	32.08NS	12.37**	22.66**	0

REFERENCES

Adcock G. J., Dennis E.S., Easteal S., Huntley G. A., Jermin L. S., Peacock W. J. and Thorne A. 2001. Mitochondrial DNA sequences in ancient Australians: implications for modern human origins. *Proc. Natl. Acad. Sci. USA* 98: 537-542.

Ahlström T. 1996. Sexual dimorphism in medieval human crania studied by three-dimensional thin-plate spline analysis. In L. F. Marcus, M. Corti, A. Loy, G. J. P. Naylor and D. E. Slice (eds.): Advances in Morphometrics. New York: Plenum Press.

Albrecht G. H. and.Miller. M. A. 1993. Geographic variation in primates: A review with implications for interpreting fossils. In W. H. Kimbel and L. B. Martin (eds.): Species, Species Concepts and Primate Evolution. New York: Plenum Press, pp. 123-161.

Andrews P. 1984. An alternative interpretation of characters used to define *Homo erectus*. *Cour. Forsch. Inst. Seckenberg* 69: 167-175.

Armour J. A. L., Anttinen T., May C. A., Vega E. E ., Sajantila A., Kidd J. R., Kidd K. K., Bertranpetit J., Pääbo S. and Jeffreys A. J. 1996. Minisatellite diversity supports a recent African origin for modern humans. *Nature Genetics* 13: 154-160.

Arsuaga J.-L., Martínez I., Gracia A., Carretero J.-M. and Carbonell E. 1993. Three new human skulls from the Sima de los Huesos Middle Pleistocene site in Sierra de Atapuerca, Spain. *Nature* 362: 534-537.

Bermudez de Castro J. M., Arsuaga J. L., Carbonell E., Rosas A., Martinez I. and Mosquera M. 1997. A hominid from the Lower Pleistocene of Atapuerca, Spain: Possible ancestor to Neandertals and modern humans. *Science* 276: 1392-1395

Billy G. 1970. Définition du type de Cro-Magnon "sensu stricto". In G. Camps and G. Olivier (eds): L'Homme de Cro-Magnon. Paris: Arts et Métiers Graphiques, pp. 23-32.

Bock W. J. 1986. Species concepts, speciation, and macroevolution. In K. Iwatsuki, P. H. Raven and W. J. Bock (eds.): Modern Aspects of Species. Tokyo: Tokyo University Press, pp. 31-54.

Bookstein F. L. 1990. Introduction to methods for landmark data. In F. J Rohlf and F. L. Bookstein (eds.): Proceedings of the Michigan Morphometrics Workshop. Ann Arbor: The University of Michigan Museum of Zoology, pp.216-225.

Boule M. 1911-1913. L'homme fossile de la Chapelle-aux-Saints. *Annales de Paleontologie* 6: 11-172; 7: 21-56; 8: 1-70.

Boule M. and Vallois H. V. 1957. Fossil Men. New York: Dryden Press.

Bräuer G. 1984. A craniological approach to the origin of anatomically modern *H. sapiens* in Africa and implications for the appearance of modern Europeans. In F. Smith and F. Spencer (eds.): The origins of modern humans. New York: Alan Liss, pp. 327-410.

Bräuer G. 1989. The evolution of modern humans: A comparison between the African and non-African Evidence. In C. Stringer and P. Mellars (eds.): The Human Revolution. Princeton: Princeton University Press, pp. 123-154.

Bräuer G. 1992. Africa's place in the evolution of *Homo sapiens*. In G. Bräuer and F. H. Smith (eds.): Continuity or Replacement: Controversied in *Homo sapiens* Evolution. Rotterdam: A. A. Balkema, pp. 83-98.

Bräuer G. and Rimbach K. W. 1990. Late archaic and modern *Homo sapiens* from Europe, Africa and Southwest Asia: Craniometric comparisons and phylogenetic implications. *Journal of Human Evolution* 19: 789-807.

Bräuer G. and H. Broeg. 1998. On the degree of Neandertal-modern continuity in the earliest Upper Paleolithic crania from the Czech Republic: Evidence from non-metrical features. In K. Omoto and P. V. Tobias (eds): Recent Advances in Human Biology vol. 3, The Origins and Past of Modern Humans: Towards Reconciliation. Singapore: World Scientific, pp. 106-125.

Broom R. 1912. A contribution to the craniology of the yellow-skinned races of South Africa. *Journal of the Royal Anthropological Institute of Great Britain and Ireland,* 53: 132-149.

Brothwell D. R. 1963. Evidence of early population change in Central and Southern Africa: Doubts and problems. *Man* 63: 101-104.

Cann R. L., Stoneking M. and Wilson A. C. 1987. Mitochondrial DNA and human evolution. *Nature* 325: 31-36.

Chamla M. C. 1978. Le peuplement de l'Afrique du Nord de l'Épipaleolithique à l'époque actuelle. *L 'Anthropologie*, 82: 385-430.

Churchill S. E., Formicola V, Holliday T. W., Holt B. M. and Schuman B. A. 2000. The Upper Paleolithic population of Europe in an evolutionary perspective. In: W. Roebroeks, M. Mussi, J. Svoboda and K. Fennema (eds.) Hunters of the Golden Age: The Mid Upper Paleolithic of Eurasia 30,000-20,000 BP. Leiden: University of Leiden, pp. 31-57.

Churchill S. E. and Smith F. H. 2000. Makers of the Early Aurignacian of Europe. *American Journal of Physical Anthropology (Yrbk)* 43: 61-115.

Condemi S. 1991. Circeo I and variability among classic Neanderthals. In: M. Piperno and G. Scichilone (eds.) The Circeo 1 Neanderthal skull; Studies and documentation. Rome: Instituto Poligrafico e Zecca dello Stato, pp. .

Condemi S. 1992. Les Hommes Fossiles de Saccopastore et Leurs Relations Phylogénétiques. Cahiers de Paléoanthropologie, Paris: CNRS Éditions.

Cracraft J. 1983. Species concepts and speciation analysis. *Current Ornithology* 1: 159-187.

Cramer D. L. 1977. Craniofacial morphology of *Pan paniscus*: A morphometric and evolutionary appraisal. *Contributions to Primatology* vol. 10.

Dean D. 1993. The middle Pleistocene *Homo erectus / Homo sapiens* transition: New evidence from space curve statistics. Ph.D. Dissertation, City University of New York, New York.

Dean D., Marcus L. F. and Bookstein F. L. 1996. Chi-square tests of biological space curve affinities. In L. F. Marcus, M. Corti, A. Loy, G. J. P. Naylor and D. E. Slice (eds.): Advances in Morphometrics. NATO ASI Series. New York: Plenum Press, pp. 235-251.

Dean D., Hublin J.-J., Holloway R. and R. Ziegler. 1998. On the phylogenetic position of the pre-Neanderthal specimen from Reilingen, Germany. *Journal of Human Evolution*, 34:485-508.

Delson E. 1989. Commentary on: Human fossil history and evolutionary paradigms. In: M. K. Hecht (ed.) Evolutionary Biology at the Crossroads, pp.141-145, Queens College Press, New York.

Delson E., Harvati K., Reddy D., Marcus L. F., Mowbray K., Sawyer G. J., Jacob T. and Marquez S. 2001. Sambungmachan 3 *Homo erectus* calvaria: A comparative morphometric and morphological analysis. *Anatomical Record* 262: 380-297.

Duarte C., Mauricio J., Pettitt P. B., Souto P., Trinkaus E., van der Plicht H. and Zilhao J. 1999. The early Upper Paleolithic human skeleton from the Abrigo do Lagar Velho (Portugal) and modern human emergence in Iberia. *Proc. Natl. Acad. Sci. USA* 96: 7604-7609.

Ducros A. 1967. Le chignon occipital, mesure sur le squelette. *L'Anthropologie* 71: 75-96.

Eldredge N. 1971. The allopatric model and phylogeny in Paleozoic invertebrates. *Evolution* 25 :156-267.

Eldredge N. 1993. What, if anything, is a species? In W. H. Kimbel and L. B. Martin (eds.): Species, Species Concepts and Primate Evolution. New York: Plenum Press, pp. 3-20.

Eldredge N. and Cracraft J. 1980. Phylogenetic Patterns and Evolutionary Process. Method and Theory in Comparative Biology. New York: Columbia University Press.

Elyaqtine M. 1995a. Variabilité et évolution de l'os temporal chez *Homo sapiens*. Comparaisons avec *Homo erectus*. Thèse, Université Bordeaux I, n° d'ordre 1321, 215.

Elyaqtine M. 1995b. Situation du méat auditif par rapport au processus zygomatique chez *Homo erectus* et *Homo sapiens*: Implications biomécaniques et phylogénétiques. Comptes Rendus de l'Académie des Sciences de Paris, 321 (serie IIa): 347-352.

Elyaqtine M. 1996. L'os temporal chez *Homo erectus* et *Homo sapiens*: Variabilité et évolution. *Revue d'Archaeometrie* 20: 5-22.

Ferembach D. 1962. La Nécropole Épipaléolithique de Taforalt (Maroc Oriental). Étude des Squelettes Humains. Avec la collaboration de J. Dastugue et M. J. Poitrat-Targowla. Casablanca: Edita.

Ferembach D. 1985. On the origin of the Iberomaurusians (Upper Paleolithic: North Africa). A new hypothesis. *Journal of Human Evolution* 14: 393-397.

Frayer D. W. 1992. The persistence of Neanderthal features in post-Neanderthal Europeans. In G. Bräuer and F. H. Smith (eds.): Continuity or Replacement: Controversies in *Homo sapiens* Evolution. Rotterdam: A. A. Balkema, pp. 179-188.

Frayer D. W., Wolpoff M. H., Thorne A.G., Smith F. H. and Pope G.G. 1993. Theories of modern human origins: The paleontological test. *American Anthropologist* 95: 14-50.

Frost S. F., Marcus L. F., Delson E. and Reddy D. 1998. Quantification of facial variation in the Papionini (Cercopithecinae, Cercopithecidae). Abstract. *American Journal of Physical Anthropology.*

Gambier D. 1989. Fossil hominids from the early Upper Paleolithic (Aurignacian) of France. In: C. Stringer and P. Mellars (eds.) The Human Revolution. Princeton: Princeton University Press, pp. 194-211.

Gambier D. 1997. Modern humans at the beginning of the Upper Paleolithic in France, anthropological data and perspectives. In G. A. Clark and C. M. Willermet (eds.): Conceptual Issues in Modern Human Origins Research. New York: Aldine de Gruyter, pp.117-131.

Genet-Varcin E. 1970. Considérations morphologiques sur l'homme de Cro-Magnon. In G. Camps and G. Olivier (eds): L'Homme de Cro-Magnon. Paris: Arts et Métiers Graphiques, pp. 33-35.

Genoves S. 1954. The problem of the sex of certain fossil hominids, with special reference to the Neanderthal skeletons from Spy. *Journal of the Royal Anthropological Institute of Great Britain and Ireland* 84: 131-144.

Gonder M. K., Oates J. F., Disotell T. R., Forstner M. R. J., Morales J. C. and Melnick D. J. 1997. A new west African chimpanzee subspecies? *Nature* 388: 337.

Grün R. and Stringer C. B. 1991. ESR dating and the evolution of modern humans. *Archaeometry* 23:153-199.

Harpending H. C., Batzer M. A., Gurven M., Jorde L. B., Rogers A. R. and Sherry S. T. 1998. Genetic traces of ancient demography. *Proc. Natl. Acad. Sci. USA,* 95: 1961-2967.

Harpending H. C. and Relethford J. 1997. Population perspectives on human origins research. In G. A. Clarck and C. M. Willermet (eds.): Conceptual Issues in Modern Human Origins Research. New York: Aldine de Gruyter, pp. 361-368.

Heim J.-L. 1974. Les hommes fossiles de la Ferassie (Dordogne) et le problème de la définition des Néanderthaliens classiques. *L'Anthropologie* 78:312-378.

Heim J.-L. 1976. Les Hommes Fossiles de la Ferassie. Tome 1, Mem. 35. Archives de l'Institut de Paléontologie Humaine. Paris: Masson.

Howells W. W. 1973. Cranial Variation in Man: A Study by Multivariate Analysis of Patterns of Difference Among Recent Human Populations. Papers of the Peabody Museum of Archaeology and Ethnology, Harvard University, Vol. 67.

Howells W. W. 1989. Skull Shapes and the Map: Craniometric Analyses in the Dispersion of Modern *Homo*. Papers of the Peabody Museum of Archaeology and Ethnology, Harvard University, Vol. 79.

Hublin J.-J. 1978a. Le torus occipital transverse et les structures associées: Évolution dans le genre *Homo*. Thèse, Université Pierre et Marie Curie, Paris VI.

Hublin J.-J. 1978b. Quelques caractères apomorphes du crâne néanderthalien et leur interprétation phylogénique. *C. R. Acad. Sc. Paris* 287:923-926.

Hublin J.-J. 1988a. Caractères derivés de la region occipitomasto-dienne chez les Néandertaliens. *L'Anatomie*, L'Homme de Néandertal, vol.3: 67-73.

Hublin J.-J. 1988b. Les plus ancients répresentants de la lignée prénéandertalienne. *L'Anatomie*, L'Homme de Néandertal, vol.3: 81-94.

Jelinek J. 1969. Neanderthal man and *Homo sapiens* in Central and Eastern Europe. *Current Anthropology* 10: 475-503.

Kaessmann H., Wiebe V., Weiss G. and S. Pääbo. 2001. Great ape DNA sequences reveal a reduced diversity and an expansion in humans. *Nature Genetics* 27: 55-56.

Kidder J. H., Jantz R. L. and Smith F. H. 1992. Defining modern humans: A multivariate approach. In G. Bräuer and F. H. Smith (eds.): Continuity or Replacement: Controversied in *Homo sapiens* Evolution. Rotterdam: A. A. Balkema, pp. 157-177.

Kimbel W. H and Rak Y. 1993. The importance of species taxa in paleoanthropology and an argument for the phylogenetic concept of the species category. In W. H. Kimbel and L. B. Martin (eds.): Species, Species Concepts and Primate Evolution. New York: Plenum Press, pp. 461-484.

King W. 1864. The reputed fossil man of the Neanderthal. *Quarterly Journal of Science* 1: 88-97. Reprinted in W. E. Meikle and S. T. Parker (eds.): 1994. Naming our ancestors: An anthology of hominid taxonomy. Prospect Heights: Waveland Press, pp. 22-35.

Kokkoros P. and Kanellis A. 1960. Découverte d'un crâne d'homme paléolithique dans la péninsule Chalchidique. *L'Anthropologie* 64: 438-446.

Krings M., Stone A., Schmitz R. W., Krainitzki H., Stoneking M. and Päabo S. 1997. Neandertal DNA sequences and the origin of modern humans. *Cell* 90: 19-30.

Krings M., Geisert H., Schmitz R. W. Krainitzki H. and S. Pääbo. 1999. DNA sequence of the mitochondrial hypervariable region II from the Neandertal type specimen. *Proc. Natl. Acad. Sci. USA,* 96: 5581-5585.

Krings M., Capelli C., Tschentscher F., Geisert H., Meyer S., von Haessler A., Crossschmidt K., Possnert G., Paunovic M. and Päabo S. 2000. A view of Neandertal genetic diversity. *Nature Genetics* 26: 144-146.

Lahr M. M. 1996. The evolution of modern human diversity: A study of cranial variation. Cambridge: Cambridge University Press.

Laitman J. T. and Heimbuch R. C. 1982. The basicranium of Plio-Pleistocene hominids as an indicator of their upper respiratory systems. *American Journal of Physical Anthropology* 59:323-344.

Lieberman D. E. 1995. Testing hypotheses about recent human evolution from skulls: Integrating morphology, function, development and phylogeny. *Current Anthropology* 36: 159-197.

Lieberman D. E., Pearson O. M. and Mowbray K. M. 2000. Basicranial influence of overall cranial shape. *Journal of Human Evolution* 38: 291-315.

Lieberman P. 1989. The origins of some aspects of human language and cognition. In C. Stringer and P. Mellars (eds.): The Human Revolution. Princeton: Princeton University Press, pp. 391-414.

Lynch J. M., Wood C. G. and Luboga S. A. 1996. Geometric morphometrics in primatology: Craniofacial variation in *Homo sapiens* and *Pan troglodytes*. *Folia Primatologica* 67: 15-39.

Marcus L. F. 1990. Traditional morphometrics. In F. J. Rohlf and F. B. Bookstein (eds.): Proceedings of the Michigan Morphometrics Workshop, Special Publication, The University of Michigan Museum of Zoology, Ann Arbor, pp. 77-122.

Martínez I. and Arsuaga J. L. 1997. The temporal bones from Sima de los Huesos middle Pleistocene site (Sierra de Atapuerca, Spain). A phylogenetic approach. *Journal of Human Evolution* 33: 283-318.

Mayr E. 1940. Speciation phenomena in birds. *American Naturalist* 74: 249-278.

Mayr E. 1959. Species concepts and definitions. In E. Mayr (ed.): The Species Problem. pp.1- 22, publication no. 50 of the American Association for the Advancement of Science.

Mayr E. 1970. Populations, Species, and Evolution. Cambridge: Harvard University Press.

Mayr E. 1976. Evolution and the Diversity of Life. Cambridge: Harvard University Press.

McCown T. D. and Keith A. 1937. The Stone Age of Mount Carmel Vol. II: Fossil Human Remains from the Levalloiso-Mousterian. Oxford: Clarendon Press.

McDermott F., Stringer C., Grün R., Williams C. T., Din V.K. and Hawkesworth C.J. 1996. New Late Pleistocene uranium-thorium and ESR dates for the Singa hominid (Sudan). *Journal of Human Evolution* 31: 507-516.

McKee J. K. and Helman S. B. Variability of the hominid juxtamastoid eminence and associated basicranial features. 1991. *Journal of Human Evolution* 21: 275-281.

Mellars P. 1989. Technological changes across the Middle-Upper Palaeolithic transition: Economic, social and cognitive perspectives. In C. Stringer and P. Mellars (eds.): The Human Revolution. Princeton: Princeton University Press, pp. 338-365.

Mellars P. and Stringer C. 1989. Introduction. In C. Stringer and P. Mellars (eds.): The Human Revolution. Princeton: Princeton University Press, pp. 1-14.

Minugh-Purvis N., Radov i J. and F. H. Smith. 2000. Krapina 1: A juvenile Neandertal from the early Late Pleistocene of Croatia. *American Journal of Physical Anthropology* 111: 393-424.

Morin P. A., Moore J. J., Chakraborty R., Jin L., Goodall J. and Woodruff D. S. 1994. Kin selection, social structure, gene flow, and the evolution of chimpanzees. *Science* 365: 1193-1201.

Oakley K. P., Campbell B. G. and Molleson T. I. 1971. Catalogue of Fossil Hominids, Part II: Europe. Kettering: Staples Printers Limited.

O'Higgins P. 2000. The study of morphological variation in the hominid fossil record: biology, landmarks and geometry. *Journal of Anatomy* 197:103-120.

Olson T. R. 1981. Basicrania and evolution of the Pliocene hominids. In C. B. Stringer (ed.): Aspects of Human Evolution. London: Taylor and Francsis, pp. 99-128.

Olson T. R. 1985. Cranial morphology and systematics of the Hadar Formation hominids and *"Australopithecus" africanus*. In E. Delson (ed.): Ancestors: The Hard Evidence. New York: Liss, pp.102-119.

Ovchinnikov I. V., Götherström A., Romanova G. P., Kharitonov V. M., Lindén K and Goodwin W. 2000. Molecular analysis of Neandertal DNA from the Northern Caucasus. *Nature* 404:490-493.

Oxnard C. 1997. Time and place of modern human origins, implications from modeling. In G. A. Clarck and C. M. Willermet (eds.): Conceptual Issues in Modern Human Origins Research. New York: Aldine de Gruyter, pp. 369-391.

Paterson H. E. H. 1985. The recognition concept of species. In E. S. Vrba (ed.): Species and speciation. *Transvaal Museum Monographs* 4: 21-29.

Pearson O. M. 2000. Postcranial remains and the origin of modern humans. *Evolutionary Anthropology* 9: 229-247.

Radcliffe-Brown A. R. 1948. The Andaman Islanders. Illinois: The Free Press.

Radovcic J., Smith F. H., Trinkaus E. and Wolpoff M. H. 1988. The Krapina Hominids: An Illustrated Catalog of Skeletal Collection. Zagreb: Croatian Natural History Museum.

Rak Y. 1993. Morphological Variation in *Homo neanderthalensis* and *Homo sapiens* in the Levant: A biogeographic model. In W. H. Kimbel and L. B. Martin (eds.): Species, Species Concepts and Primate Evolution. New York: Plenum Press, pp. 523 -536.

Relethford J. H. 2001a. Absence of regional affinities of Neanderthal DNA with living humans does not reject multiregional evolution. *American Journal of Physical Anthropology*, 115: 95-98.

Relethford J. H. 2001b. Ancient DNA and the origin of modern humans. *Proc. Natl. Acad. Sci. USA* 98: 390-391.

Rightmire P. G. 1984. *Homo sapiens* in Sub-Saharan Africa. In F. H. Smith and F. Spencer: The Origins of Modern Humans: A World Survey of the Fossil Evidence. New York: Liss, pp. 295-325.

Rightmire P. G. 1988. *Homo erectus* and later Middle Pleistocene humans. *Annual Review of Anthropology* 17: 239-59.

Rightmire P. G. 1990. The evolution of *Homo erectus*; Comparative Anatomical Studies of an Extinct Human Species. Cambridge: Cambridge University Press.

Rightmire G. P. 1995. Diversity within the genus *Homo*. In E. S. Vrba, G. H. Denton, T. C. Partridge and L. H. Burkle (eds.): Paleoclimate and Evolution, with Emphasis on Human Origins. New Haven: Yale University Press, pp. 483-492.

Rohlf J. F. 1986-1998 (Copyright). NTSYSpc, version 2.02k.

Rohlf J. F. 1990. Rotational fit (Procrustes) methods. In F. J Rohlf and F. L. Bookstein (eds.): Proceedings of the Michigan Morphometrics Workshop. Ann Arbor: The University of Michigan Museum of Zoology, pp. 227-236.

Rohlf J. F. 1998 (Copyright). TpsSmall, version 1.18.

Rohlf J. F. 2000. Statistical power comparisons among alternative morphometric methods. *American Journal of Physical Anthropology* 111: 463-478.

Rohlf J. F. and Marcus L. F. 1993. A revolution in morphometrics. *Trends in Ecology and Evolution* 8: 129-132.

Santa Luca A. P. 1978. A re-examination of presumed Neanderthal-like fossils. *Journal of Human Evolution* 7:619-636.

Sarmiento E. E. and Marcus L. F. 2000. The os navicular of humans, great apes, OH 8, Hadar and Oreopithecus: Function, phylogeny and multivariate analyses. American Museum Novitates n. 3288: 1-38.

Schillaci M. A. and Froelich J. W. 2001. Nonhuman primate hybridization and the taxonomic status of Neanderthals. American Journal of Physical Anthropology 115: 157-166.

Schwartz J. H. and Tattersall I. 1996a. Significance of some previously unrecognized apomorphies in the nasal region of *Homo neanderthalensis*. *Proc. Natl. Acad. Sci. USA* 93: 10852-10854.

Schwartz J. H. and Tattersall I. 1996b. Toward distinguishing *Homo neanderthalensis* from *Homo sapiens*, and vice versa. *L'Anthropologie* 34: 79-88.

Schwartz J. H. and Tattersall I. 2000. The human chin revisited: what is it and who has it? *Journal of Human Evolution* 38: 367-409.

Seidler H., Falk D., Stringer C., Wilfing H., Müller G. B., zur Neden D., Weber G., Reicheis W. and Arsuaga J. L. 1997. A comparative study of stereolithigraphically modelled skulls of Petralona and Broken Hill: Implications for future studies of Middle Pleistocene hominid evolution. *Journal of Human Evolution* 33: 691-703.

Sergi S. 1991. The Neanderthal cranium of Monte Circeo (Circeo 1). In M. Piperno and G. Scichilone (eds.): The Circeo 1 Neanderthal skull; Studies and documentation. Rome: Instituto Poligrafico e Zecca dello Stato.

Shea B. T. and Coolidge H. J. Jr. 1988. Craniometric differentiation and systematics in the genus *Pan*. *Journal of Human Evolution* 17: 671-685.

Shea B. T., Leigh, S. T. and Groves C. P. 1993. Multivariate craniometric variation in chimpanzees: Implications for species identification. In W. H. Kimbel and L. B. Martin (eds.): Species, Species Concepts and Primate Evolution. New York: Plenum Press, pp. 265 -296.

Simmons T. and Smith F. H. 1991. Human population relationships in the Late Pleistocene. *Current Anthropology* 32: 623-627.

Simpson G. G. 1951. The species concept. *Evolution* 5: 285 - 298.

Slice D. E. 1992, 1994 (Copyright). GRF-ND: Generalized rotational fitting of n-dimensional landmark data.

Slice D. E. 1994-1999 (Copyright). Morheus et al.

Slice D. E. 1996. Three-dimensional generalized resistance fitting and the comparison of least-squares and resistant fit residuals. In L. F. Marcus, M. Corti, A. Loy, G. J. P. Naylor and D. E. Slice (eds.): Advances in Morphometrics. NATO ASI Series. New York: Plenum Press, pp.179-199.

Slice D. E. 2001. Landmark coordinates aligned by Procrustes analysis do not lie in Kendall's shape space. *Systematic Biology* 50: 141-149.

Smith F. H. 1980. Sexual differences in European Neanderthal crania with special reference to the Krapina remains. *Journal of Human Evolution* 9: 359-375.

Smith F. H. 1982. Upper Pleistocene Hominid Evolution in South-Central Europe: A review of the evidence and analysis of Trends. *Current Anthropology* 23: 667-703.

Smith F. H. 1984. Fossil hominids from the Upper Pleistocene of Central Europe and the origin of modern Europeans. In F. H. Smith and F. Spencer: The Origins of Modern Humans: A World Survey of the Fossil Evidence. New York: Liss, pp. 211-250.

Smith F. H. 1992. The role of continuity in modern human origins. In G. Bräuer and F. H. Smith (eds.): Continuity of Replacement: Controversies in *Homo sapiens* Evolution, A. A. Balkema, Rotterdam, pp. 145-156.

Smith F. H., Simek J. F. and Harrill M. S. 1989. Geographic variation in supraorbital torus reduction during the later Pleistocene (*c.* 80 000-15 000 BP). In P. Mellars and C. Stringer (eds.): The Human Revolution, Princeton University Press, Princeton, pp. 62-108.

Spoor F., Stringer C. and Zonneveld F. 1998. Rare temporal bone pathology of the Singa calvaria from Sudan. *American Journal of Physical Anthropology* 107: 41-50.

Spitery E. 1985. Principaux caractères évolutifs de l'os occipital chez les hominidés fossiles. *L'Anthropologie* 89:75-91.

Steele G. D. and C. A. Bramblett. 1988. The Anatomy and Biology of the Human Skeleton. College Station: Texas A&M University Press.

Stringer C. B. 1974a. Population relationships of Later Pleistocene hominids: A multivariate study of available crania. *Journal of Archaeological Science* 1: 317-142.

Stringer C. B. 1974b. A multivariate study of the Petralona skull. *Journal of Human Evolution* 3: 397-404.

Stringer C. B. 1979. A re-evaluation of the fossil human calvaria from Singa, Sudan. *Bull. Br. Mus. Nat. Hist. (Geol.)* 32:77-83.

Stringer C. B. 1982. Comment to Smith. F. H.: Upper Pleistocene hominid evolution in South-Central Europe: A review of the evidence and analysis of trends. Current Anthropology 23: 690-691.

Stringer C. B. 1984. The definition of *Homo erectus* and the existence of the species in Africa and Europe. *Cour. Forsch. Inst. Seckenberg* 69: 131-143.

Stringer C. B. 1985. Middle Pleistocene hominid variability and the origin of Late Pleistocene humans. In E. Delson (ed.): Ancestors: The Hard Evidence. New York: Liss, pp. 289-295.

Stringer C. B. 1989. The origin of early modern humans: a comparison of the European and non-European evidence. In C. Stringer and P. Mellars (eds.): The Human Revolution. Princeton: Princeton University Press, pp. 232-244.

Stringer C. B. 1990. A metrical study of the Guattari and Saccopastore crania. *Quaternaria Nova* 1: 621-638.

Stringer C. B. 1992a. Replacement, Continuity and the origin of *Homo sapiens*. In G. Bräuer and F. H. Smith (eds.): Continuity or Replacement: Controversied in *Homo sapiens* Evolution. Rotterdam: A. A. Balkema, pp. 9-24.

Stringer C. B. 1992b. Reconstructing recent human evolution. *Philosophical Transactions: Biological Sciences*, Vol. 337, Issue 1280, The Origin of Modern Humans and the Impact of Chronometric Dating: 217-224.

Stringer C. B. 1994. Out of Africa - A personal history. In: M.H. Nitecki and D. V. Nitecki (eds.) Origins of Anatomically Modern Humans, pp. 149-172, Plenum Press, New York.

Stringer C. B., Howell F.C., and Melentis J. 1979. The significance of the fossil hominid skull from Petralona, Greece. *Journal of Archaeological Science* 6: 235-253.

Stringer C. B. and E. Trinkaus. 1981. The Shanidar Neanderthal crania. In C. B. Stringer (ed.): Aspects of Human Evolution. London: Taylor and Francsis, pp. 129-165.

Stringer C. B., Hublin J. J. and Vandermeersch B. 1984. The origin of anatomically modern humans in Western Europe. In F. H. Smith and F. Spencer: The Origins of Modern Humans: A World Survey of the Fossil Evidence. New York: Liss, pp. 51-135.

Stringer C. B. and Andrews P. 1988a. Genetic and fossil evidence for the origin of modern humans. *Science* 239: 1263-1268.

Sullivan L. R. 1921. A few Andamanese skulls with comparative notes on negrito craniometry. Anthropological Papers of the American Museum of Natural History, Vol. XXIII, Part IV, pp. 177-201.

Suzuki H. and Takai F. 1970. The Amud Man and His Cave Site. Tokyo: Academic Press of Japan.

Szalay F. S. 1993. Species concepts: The tested, the untestable and the redundant. In W. H. Kimbel and L. B. Martin (eds.): Species, Species Concepts and Primate Evolution. New York: Plenum Press, pp. 523-535.

Tattersall I. 1986. Species recognition in human paleontology. *Journal of Human Evolution* 15: 165-175.

Tattersall I. 1992. Species concepts and species identification in human evolution. *Journal of Human Evolution* 22: 341-349.

Tattersall I. 1993. Speciation and morphological differentiation in the genus *Lemur*. In W. H. Kimbel and L. B. Martin (eds.): Species, species concepts and primate evolution. New York: Plenum Press, pp. 163-176.

Tattersall I. 1996. Paleoanthropology and preconception. In W. E. Meikle. F. C. Howell and N. G. Jablonski (eds.): Contemporary Issues in Modern Human Evolution.

Tattersall I. 2000. Paleoanthropology: The last half-century. Evolutionary Anthropology 9: 2-16.

Taxman R. M. 1963. Incidence and size of the juxtamastoid eminence in modern crania. *American Journal of Physical Anthropology* 21: 153-157.

Templeton A. R. 1997. Testing the Out of Afria replacement hypothesis with mirochondrial DNA data. In G. A. Clarck and C. M. Willermet (eds.): Conceptual Issues in Modern Human Origins Research. New York: Aldine de Gruyter, pp. 329-360.

Thoma A. 1965. La définition des Néanderthaliens et la position des hommes fossiles de Palestine. *L'Anthropologie* 69:519-534.

Thoma A. 1975. Where the Spy fossils evolutionary intermediates between classic Neanderthal and modern man? *Journal of Human Evolution* 4:387-410.

Tischkoff S. A., Dietzsch E., Speed W., Pakstis A. J., Kidd J. R., Cheung K., Bonne-Tamir B., Santachiara-Benerecetti A. S., Moral P., Krings M., Pääbo S., Watson E., Risch N., Jenkins T. and Kidd K. K. 1996. Global patterns of linkage disequilibrium at the CD4 locus and modern human origins. *Science* 271: 1380-1387.

Tobias P. V. 1959. Studies on the occipital bone in Africa. V: The occipital curvature in fossil man and the light it throws on the morphogenesis of the Bushman. *American Journal of Physical Anthropology* 17:3-11.

Trinkaus E. 1982. Artificial deformation in the Shanidar 1 and 5 Neanderthals. *Current Anthropology* 23: 198-199.

Trinkaus E. 1983. The Shanidar Neanderthals. New York: Academic Press.

Trinkaus E. 1984. Western Asia. In F. H. Smith and F. Spencer (eds.): The Origin of Modern Humans. New York: Liss pp. 251-293.

Trinkaus E. and M. LeMay. 1982. Occipital bunning among Later Pleistocene hominids. *American Journal of Physical Anthropology*, 57:27-35.

Trinkaus E. and Smith F. H. 1985. The fate of the Neanderthals. In E. Delson (ed.): Ancestors: The Hard Evidence. New York: Liss, pp. 325-333.

Trinkaus E. and Shipman P. 1992. The Neanderthals. New York: Vintage Books.

Trinkaus E. and Shipman P. 1993. Neanderthals: Images of ourselves. *Evolutionary Anthropology* 1: 194-201.

Turbón D., Pérez-Pérez A. and Stringer C. B. 1997. A multivariate analysis of Pleistocene hominids: Testing hypotheses about European origins. *Journal of Human Evolution* 32: 449-468.

Valeri C. J. Cole T. H. III, Lele S. and Richtsmeier J. T. 1998. Capturing data from three-dimensional surfaces using fuzzy landmarks. American Journal of Physical Anthropology 107: 113-124.

Vallois H. V. 1969. Le temporal Néanderthalien H 27 de La Quina. Étude anthropologique. *L'Anthropologie* 73: 524-400.

Vandermeersch B. 1981. Les Hommes Fossiles de Qafzeh (Israel). Cahiers de Paléontologie, Paris: CNRS Éditions.

Vandermeersch B. 1985. The origin of the Neanderthals. In E. Delson (ed.): Ancestors: The Hard Evidence. New York: Liss, pp. 306-309.

Vandermeersch B. 1989. The evolution of modern humans: Recent evidence from Southwest Asia. In C. Stringer and P. Mellars (eds.): The Human Revolution. Princeton: Princeton University Press, pp.155-171.

Van Valen L. 1976. Ecological species, multispecies, and oaks. *Taxon* 25: 233-239.

van Vark G. N. 1995. The study of hominid skeletal remains by means of statistical methods. In N. T. Boaz and L. D. Wolfe (eds.): Biological Anthropology: The State of the Science, Bend, Oregon: International Institute for Human Evolutionary Research, pp. 71-90.

Vlcek E. 1970. Relations morphologiques des types humains fossiles de Brno et Cro-Magnon au Pleistocene Supérieur d'Europe. In G. Camps and G. Olivier (eds): L'Homme de Cro-Magnon. Paris: Arts et Métiers Graphiques, pp. 59-72.

Weidenreich F. 1943. The skull of *Sinanthropus pekinensis*: A comparative study. *Paleontologica Sinica New Series D* 10: 1-484.

Wiley E. O. 1978. The evolutionary species concept reconsidered. *Systematic Zoology* 27: 17-26.

Willmann R. 1989. Evolutionary or biological species? *Abh. naturwiss. Ver. Hamburg* 28: 95-110.

White T. D. and Folkens P. A. 1991. Human Osteology. San Diego: Academic Press.

Wolpoff M. H. 1989. Multiregional evolution: The fossil alternative to Eden. In P. Mellars and C. Stringer (eds.): The Human Revolution. Princeton: Princeton University Press, pp. 62-108.

Wolpoff M. H. 1992. Theories of modern human origins. In G. Bräuer and F. H. Smith (eds.): Continuity or Replacement: Controversies in *Homo sapiens* Evolution. Rotterdam: A. A. Balkema, pp. 25-63.

Wolpoff M. H., Thorne A. G., Jelinek J. and Yinyun Z. 1994. The case for sinking *Homo erectus*. 100 years of *Pithecanthropus* is enough! *Courier Forschungs-Institut Seckenberg* 171: 341-361.

Wolpoff M. H., Smith F. H. and Frayer D. W. 1997. Neandertals are a race of *Homo sapiens*.(Abs.) *Journal of Human Evolution* 32: A25.

Wolpoff M. and Caspari R. 1997. What does it mean to be modern? In G. A. Clarck and C. M. Willermet (eds.): Conceptual Issues in Modern Human Origins Research. New York: Aldine de Gruyter, pp. 28-44.

Wolpoff M. H., Hawks J., Frayer D. and Hunley K. 2001. Modern human ancestry at the peripheries: A test of the replacement theory. *Science* 291: 293-297.

Wood B. 1992. Origin and evolution of the genus *Homo*. *Nature* 355: 783-790.

Wood C. G. and Lynch J. M. 1996. Sexual dimorphism in the craniofacial skeleton of modern humans. In L. F. Marcus, M. Corti, A. Loy, G. J. P. Naylor and D. E. Slice (eds.): Advances in Morphometrics. New York: Plenum Press.

Woodward A. S. 1938. A fossil skull of an ancestral bushman from the Anglo-Egyptian Sudan. *Antiquity* 12: 190-195.

Yaroch L. A. 1996. Shape analysis using the Thin-Plate Spline: Neanderthal cranial shape as an example. *American Journal of Physical Anthropology (Yearbook)* 39: 43-89.

Zollikofer C. P. E., Ponce De Leon M. S. and Martin R. D. 1998. Computer-assisted paleoanthropology. *Evolutionary Anthropology* 6: 41-54.